Stromal Cell Diversity Drives Pathogenic Mechanisms in Rheumatoid Arthritis and Pre-Disease Onset

Brianne Ellen Barker, M.Sc. (Hons)

Feb 2025

Thesis submitted to Trinity College Dublin in fulfilment of the requirement for the degree of Doctor in Philosophy (PhD) in Clinical Medicine

Under the Primary supervision of Prof. Ursula Fearon

Co-supervisor: Dr Mary Canavan

Department of Molecular Rheumatology

Trinity Biomedical Science Institute

School of Medicine, Trinity College Dublin

Head of School: Professor Colin Doherty

Declaration of Authorship

I, Brianne Ellen Barker, declare that this thesis has not been submitted as an exercise for a degree at this or any other university and it is entirely my own work.

I agree to deposit this thesis in the University's open access institutional repository or allow the library to do so on my behalf, subject to Irish Copyright Legislation and Trinity College Library conditions of use and acknowledgement. I consent to the examiner retaining a copy of the thesis beyond the examining period, should they so wish (EU GDPR May 2018).

Signed: **February 2025**

Table of Contents

Declaration of Authorship ii
List of Figures vii
List of Tables xi
Abstract xii
Acknowledgements xiv
Publications xvi
Published Abstracts and Presentations xvi
Awards Received xviii
Abbreviations xix

1.0 General Introduction 1
1.1 A Brief History of Rheumatoid Arthritis 2
1.2 Global Prevalence 3
1.3 Classification of RA 4
1.4 Pre-Clinical RA and Individuals-At-Risk 6
1.5 Autoantibodies 7
1.6 Genetic and Epigenetic Risk Factors 9
1.7 Environmental Risk Factors 11
1.8 Infection and Malignancy 13
1.9 Cardiovascular Comorbidity 15
1.10 Economic Burden 17
1.11 Normal Synovial Joint 19
1.12 Inflamed Joint Microenvironment 20
1.13 Angiogenesis 21
1.14 Infiltrating Immune Cells 25
1.15 Inflammatory Cytokines and Chemokines 29
1.16 Synovial Fibroblasts 30
1.17 Overview of Cellular Metabolism 32
1.18 Hypoxia, Metabolism, and RA 35
1.19 Immunometabolism 36
1.20 Fibroblast Metabolism 38
1.21 Current Treatments for RA 40
1.22 Disease Modifying Anti-Rheumatic Drugs (DMARDs) 40
1.23 Biological DMARDs 41
1.24 JAK-STAT Inhibitors 43
1.25 Personalised Medicine 44

2.0 The Mammalian Target of Rapamycin Contributes to Synovial Fibroblast Pathogenicity in Rheumatoid Arthritis **46**
2.1 Introduction 47
2.2 Specific Aims for this Chapter 49
2.3 Materials & Methods 50
2.3.1 Patient Recruitment *50*
2.3.2 Arthroscopy and Sample Collection *50*
2.3.3 Isolation of Primary Fibroblasts *50*
2.3.4 Bulk RNA Sequencing Analysis *51*

2.3.5 Flow Cytometry *52*
2.3.6 Cellular Bioenergetic Functional Analysis *53*
2.3.7 mRNA Extraction and cDNA Synthesis *54*
2.3.8 RT PCR Analysis *54*
2.3.9 Chemokine Measurements *55*
2.3.10 Migration Assay *55*
2.3.11 MMP Detection via Multiplex ELISA *56*
2.3.12 Transwell Invasion Assay *56*
2.3.13 Protein Isolation and Western Blot Analysis *56*
2.3.14 Statistical Analysis 57
2.4 Results 58
2.4.1 Dysregulated Expression of the mTOR Pathway in RA Synovial Tissue *58*
2.4.2 Targeting the mTOR Pathway in RA FLS Alters Cellular Bioenergetics *62*
2.4.3 mTOR Inhibition in RA FLS Decreases Cellular Migration *67*
2.4.4 RA FLS Cellular Invasion is Decreased by mTOR Inhibition *67*
2.4.5 Crosstalk Between Dysregulated Hippo-YAP and mTOR Pathways Mediates RA FLS Invasion 74
2.5 Discussion 79

3.0 Identification and Characterisation of PRIME Cells in the Circulation and at the Site of Inflammation in Patients with Rheumatoid Arthritis and Individuals-At -Risk. **84**
3.1 Introduction 85
3.2 Specific Aims for this Chapter 88
3.3 Materials and Methods 89
3.3.1 Patient Recruitment and Sample Collection *89*
3.3.2 Obtaining Synovial Tissue and Blood Samples *89*
3.3.3 Synovial Tissue Digestion *91*
3.3.4 Peripheral Blood Mononuclear Cell Isolation *91*
3.3.5 Flow Cytometry *91*
3.3.6 Statistical Analysis *93*
3.4 Results 94
3.4.1 Identification of PRIME Cells in the Circulation of RA Patients *94*
3.4.2 Inflammatory Profiling of RA PRIME Cells Compared to HC *97*
3.4.3 Differential FLS Marker Expression on RA PRIME Cells Compared to HC *98*
3.4.4 PRIME Cells are Present and Increased Prior to Clinical Onset of Disease and in IAR *105*
3.4.5 Pro-inflammatory Phenotype of PRIME Cells is Altered in the Pre-clinical Stage *105*
3.4.6 Differential Frequency of CD45-CD31-PDPN+ Cells in RA Peripheral Blood and Synovial Tissue *111*
3.4.7 Differential Fibroblast Marker Expression in RA Synovial Tissue Compared to Peripheral Blood *111*
3.4.8 Functional and Metabolic Profiles of RA PDPN+ Cells Differ Between the Circulation and the Joint *115*
3.5 Discussion 118

4.0 Distinct Homeostatic and Inflammatory FLS Signatures between RA and HC Synovial Tissue **124**
4.1 Introduction 125
4.2 Specific Aims for this Chapter 128
4.3 Materials and Methods 129
4.3.1 Patient Recruitment and Sample Collection *129*
4.3.2 Obtaining Synovial Tissue Samples *129*
4.3.3 Synovial Tissue Digestion for Flow Cytometry Analysis *129*
4.3.4 Isolation of Primary FLS for Functional Experiments *130*
4.3.5 Histology Scoring *130*
4.3.6 Flow Cytometry of Synovial Tissue Biopsies *131*
4.3.7 TSNE Analysis of Flow Cytometry Data *133*
4.3.8 Single-Cell (sc)RNA Sequencing *134*
4.3.9 mRNA Extraction and cDNA Synthesis *135*
4.3.10 RT-PCR Analysis *136*
4.3.11 Statistical Analysis *137*
4.4 Results 138
4.4.1 Histological Differences and Identification of FLS in the Synovial Tissue in HC vs RA *138*
4.4.2 Differential FLS Marker Expression on RA PDPN+ FLS Compared to HC *144*
4.4.3 Inflammatory Profiling of RA FLS Compared to HC *148*
4.4.4 Frequency of PDPN+ FLS and their Inflammatory Profile are Associated with High Disease Activity *156*
4.4.5 Frequency of THY-1 FAPα Populations of FLS Differ Between HC, RA+, and RA- *158*
4.4.6 Identification and Comparison of Activated LL and SL FLS Subset Frequencies in HC vs RA *161*
4.4.7 Pro-inflammatory Profile of Synovial PDPN+ FLS is Altered Prior to Disease Onset *166*
4.4.8 FLS Subset Frequencies are Altered in IAR Prior to Onset of Clinical Symptoms *173*
4.4.9 Frequency of Pro-inflammatory Markers Varies Between FLS Subsets Regardless of Disease Status *178*
4.4.10 Single-cell Transcriptomic Analysis of Synovial Tissue FLS from Health to Disease *182*
4.4.11 Identification of Upregulated Signaling Pathways in FLS Clusters Enriched in RA *188*
4.4.12 DAPT Inhibition of Notch Signaling Pathway in RA FLS *194*
4.5 Discussion 196

5.0 Circulating Endothelial Cells and Epithelial Progenitor Cells in Circulation of Patients with Rheumatoid Arthritis and Individuals-At-Risk **201**
5.1 Introduction 202
5.2 Specific Aims for this Chapter 205
5.3 Materials and Materials 206
5.3.1 Patient Recruitment and Sample Collection *206*
5.3.2 Peripheral Blood Mononuclear Cell Isolation *206*
5.3.3 Serum Isolation and Preparation *207*

5.3.4 Flow Cytometry *207*
5.3.5 MSD Multiplex Assay *210*
5.3.6 Principal Component Analysis (PCA), Bi-plot and String analysis *212*
5.3.7 Statistical Analysis *212*
5.4 Results 213
5.4.1 Identification of CECs in the Circulation of RA Patients *213*
5.4.2 CECs have the Capacity to Proliferate Further and are Metabolically Active *216*
5.4.3 RA CECs have a Pathogenically Activated Phenotype *220*
5.4.4 Identified CECs are Microvasculature Derived *220*
5.4.5 Identification of EPCs from the Circulation of RA Patients *226*
5.4.6 RA CEC and EPC Frequency Differ Across Disease Activity and can be Found Prior to Disease Onset *226*
5.4.7 Hierarchical Clustering Analysis and Protein-Protein Interactions of CEC Cellular Markers *232*
5.4.8. Serum Profiling Across Disease States *235*
5.4.9. Hierarchical Clustering Analysis and Protein-Protein Interactions of Serum Markers 242
5.5 Discussion 244

6.0 General Discussion and Future Directions **249**
6.1 General Discussion 250
6.2 Future Directions 256
Bibliography **260**
Appendix **316**

List of Figures

Figure 1.1: X-rays of Hand and Feet from Normal vs Rheumatoid Arthritis Joint 5
Figure 1.2: Representative Macroscopic Images of the Synovium 7
Figure 1.3: Schematic Overview of Comorbidities in Rheumatoid Arthritis 16
Figure 1.4: CVD Comorbidities in Rheumatoid Arthritis and Circulatory Endothelial Cells 17
Figure 1.5: The Healthy Joint vs the Inflamed Synovium 21
Figure 1.6: Representative Macroscopic Images of Synovial Blood Vessels 22
Figure 1.7: Schematic of General NOTCH Signaling Pathway 24
Figure 1.8: Synovial Fibroblast Function in Health and Disease 32
Figure 1.9: Pathways of Cellular Metabolism 34
Figure 1.10: Effect of 'Immunometabolites' on Specific Cell Subsets within the Inflamed Synovial Joint 36
Figure 2.3.1: Representative Seahorse Cell Mito-Stress Test Assay 54
Figure 2.1: Genes Involved in mTOR Pathway are Dysregulated in RA Synovial Tissue 59
Figure 2.2: Differential Expression of mTOR Pathway Between HC and RA Synovial Tissue 60
Figure 2.3: mTOR Genes are Dysregulated Prior to Disease Onset and Throughout Disease Progression 61
Figure 2.4: mTOR Pathway is Upregulated in RA FLS 64
Figure 2.5: Inhibition of mTOR in RA FLS Alters Cellular Metabolism 65
Figure 2.6: Metabolic Shift with Inhibition of mTOR Mirrored with Decreased Expression of Metabolic Genes 66
Figure 2.7: Inhibition of mTOR has Selective Effect on Expression of Chemokine Receptors on RA FLS 68
Figure 2.8: mTOR Inhibition Reduces Chemokine Production by RA FLS 69
Figure 2.9: Rapamycin Decreases Expression of Adhesion Molecules in RA FLS 70
Figure 2.10: mTOR Inhibition in RA FLS Decreases Cellular Migration 71
Figure 2.11: Rapamycin Inhibition of mTOR Alters Expression of MMPs in RA FLS 72
Figure 2.12: RA FLS have Diminished Invasive Capabilities as a Result of mTOR Inhibition 73
Figure 2.13: Genes Involved in Hippo-YAP Pathway are Upregulated in RA Compared to HC and may Interact with mTOR 76
Figure 2.14: Genes Involved in Hippo-YAP Pathway are Dysregulated Prior to Disease Onset and Throughout Disease Pathogenesis 77
Figure 2.15: Crosstalk Between Dysregulated Hippo-YAP and mTOR Pathways Mediates RA FLS Invasion 78
Figure 2.16: Summary of Therapeutic Effects of Rapamycin on TNFα-Stimulated RA FLS 83
Figure 3.1: Peripheral Blood PRIME Cell (CD45-CD31-PDPN+) Gating Strategy 95
Figure 3.2: Identification of PRIME Cells in the Peripheral Blood of HC and RA 96
Figure 3.3: Immunoregulatory Marker Expression on PRIME Cells in RA vs HC Peripheral Blood 100
Figure 3.4: Differential Expression of Adhesion Molecules VCAM-1 and ICAM-1 on PRIME Cells 101
Figure 3.5: Increase in Adhesion Molecules CD61 and CD44 on RA PRIME Cells 102
Figure 3.6: Differential Expression of Functional and Metabolic Markers on PRIME Cells Across Disease States 103
Figure 3.7: Analysis of Frequency of Common FLS Subset Markers (THY-1, CD34, CD55, FAPα) on PRIME Cells Across Disease States 104
Figure 3.8: PRIME Cells are Present in Pre-clinical Disease 107

Figure 3.9: Differential Frequency and Expression of Immunoregulatory and Adhesion Molecules Observed Prior to Disease Onset 108
Figure 3.10: Differential Expression of Metabolic and Functional Markers in IAR and ART 109
Figure 3.11: FLS Subset Markers Present on PRIME Cells Prior to Clinical Onset 110
Figure 3.12: PRIME Cell (CD45-CD31-PDPN+) Gating Strategy Applied to Synovial Tissue 112
Figure 3.13: CD45-CD31-PDPN+ Cells Differ in Frequency and Size Between Circulation and Site of Inflammation 113
Figure 3.14: FLS Marker Expression Differences on PDPN+ Cells from RA Peripheral Blood Compared to Synovial Tissue 114
Figure 3.15: Phenotypic Characterisation of RA Peripheral Blood PDPN+ Cells Compared to Synovial Tissue 116
Figure 3.16: Differential Metabolic Profiles and Cellular Growth Profiles of RA PDPN+ Cells Between Peripheral Blood and Synovial Tissue 117
Figure 3.17: Summary of PRIME Cell Phenotype and Function 123
Figure 4.1: Histologic Differences can be Observed Across Disease States 140
Figure 4.2: PDPN+ Synovial Tissue Biopsy FLS Gating Strategy 141
Figure 4.3: Frequency of Non-immune Cells (Stromal Cells) Differ Between HC and Seropositive RA Samples 142
Figure 4.4: Frequency of PDPN+ FLS Increased in RA Synovial Tissue Compared to HC 143
Figure 4.5: Differential FLS Subset Marker Expression Identification by Unsupervised Clustering 145
Figure 4.6: Altered Frequency of Classic FLS Subset Markers on RA FLS Compared to HC 146
Figure 4.7: FLS in Synovial Tissue are Activated and are Increased in RA+ 147
Figure 4.8: FLS Phenotypic Profiling by Unsupervised Clustering 150
Figure 4.9: Immunoregulatory Marker Expression on FLS in RA vs HC Synovial Tissue 151
Figure 4.10: Differential Expression of Adhesion Molecules ICAM-1 and VCAM-1 on Synovial FLS 152
Figure 4.11: Differential Frequency of FLS Positive for Adhesion Molecules CD61 and CD44 on Synovial FLS 153
Figure 4.12: RA FLS Demonstrate Reduced Expression for Proliferation and Cytoskeletal Rearrangement 154
Figure 4.13: Differential Expression of Functional and Metabolic Markers on FLS Across Disease States 155
Figure 4.14: FLS Frequency and Functional Phenotype are Associated with High RA Disease Activity 157
Figure 4.15: THY-1 FAPα Subsets Differ in Proportion for HC, RA+, and RA- FLS 159
Figure 4.16: Comparison of Each THY-1 FAPα Subset Between Disease States 160
Figure 4.17: Activated LL and SL FLS Subset (CD55 THY-1 FAPα) Gating Strategy for Synovial Tissue 163
Figure 4.18: CD55 THY-1 FAPα Subsets Differ in Proportion for HC, RA+, and RA- FLS 164
Figure 4.19: Comparison of each CD55 THY-1 FAPα Subset Between Disease States 165
Figure 4.20: Changes in FLS Frequency Prior to Disease Onset 168
Figure 4.21: Differential FLS Subset Marker Expression Identification by Unsupervised Clustering Between HC, IAR, and RA+ 169
Figure 4.22: FLS Phenotypic Profiling by Unsupervised Clustering Between HC, IAR, and RA+ 170
Figure 4.23: Comparison of Immunoregulatory and Adhesion Markers Across Disease Progression 171
Figure 4.24: Comparison of Proliferation, Invasive, and Metabolic Markers Across Disease Progression 172
Figure 4.25: Frequency of THY-1 FAPα Subsets Differ in HC, IAR, and RA+ Tissue 174

Figure 4.26: Comparison of each THY1 FAPα Subset Across Disease Progression 175
Figure 4.27: CD55 THY-1 FAPα Subsets Differ in Proportion for HC, IAR, and RA+ FLS 176
Figure 4.28: Comparison of each CD55 THY-1 FAPα Subset Across Disease Progression 177
Figure 4.29: Immunoregulatory and Adhesion Marker Expression Differ Between FLS Subsets 180
Figure 4.30: Functional Markers Differ Across FLS Subsets 181
Figure 4.31: scRNA-sequencing Defines Synovial Tissue FLS Heterogeneity from Health to Disease 185
Figure 4.32: scRNA-seq Transcriptional Profiling of Identified Synovial Tissue FLS Clusters 186
Figure 4.33: scRNA-seq Transcriptional Profiling of FLS Cluster identified LL, SL and Intermediate Subsets 187
Figure 4.34: scRNA-seq Analysis of Metabolism Associated Gene Modules in Synovial Tissue FLS 190
Figure 4.35: Upregulated Signaling Pathways in SL Clusters Enriched in RA 191
Figure 4.36: Genes within the NOTCH Pathway are Upregulated in RA 192
Figure 4.37: Receptor-ligand Interactions and Downstream Targets for Cluster 3 (POSTN+COL3A1+) 193
Figure 4.38: NOTCH Signaling Mediates FLS Function 195
Figure 4.39: Summary of RA FLS Subsets and Therapeutic Effects of NOTCH Pathway Blockade 200
Figure 5.1: Peripheral Blood Circulating Endothelial Cell (CEC) Gating Strategy 214
Figure 5.2: Identification of CECs in RA Peripheral Blood Compared to HC 215
Figure 5.3: CECs Retain the Capacity to Proliferate 217
Figure 5.4: Proportion of CECs Retain Metabolic Activity 218
Figure 5.5: HC and RA CECs Differ in their Capacity for Wound Healing 219
Figure 5.6: RA CECs are Pathogenically Activated 222
Figure 5.7: Immunoregulatory Marker Expression on CECs in RA vs HC PBMCs 223
Figure 5.8: Differential Expression of Adhesion Molecules on CECs 224
Figure 5.9: Majority of Identified CECs come from the Microvasculature of HC and RA Individuals 225
Figure 5.10: Peripheral Blood Endothelial Progenitor Cell (EPC) Gating Strategy 228
Figure 5.11: Identification of EPCs in the Peripheral Blood of HC and RA 229
Figure 5.12: CEC and EPC Frequencies Differ Across Disease Activity and Between Sexes 230
Figure 5.13: CECs and EPCs are Present in Altered Numbers in Circulation Prior to Clinical Onset of Disease 231
Figure 5.14: Correlation of Marker Expression on CECs varies between RA and HC 233
Figure 5.15: CECs Form Distinct Clusters Based on Phenotypic Marker Expression 234
Figure 5.16: Minimal Levels of Pro-inflammatory Cytokines Expressed in Serums from HC, Pre-Disease, and RA Patients 237
Figure 5.17: Elevated Levels of Soluble Adhesion Molecules and Markers of Vascular Injury Across Disease States 238
Figure 5.18: Elevated Levels of Soluble Markers for Tissue Injury Observed in Serums Across Disease States 239
Figure 5.19: Differential Expression of Soluble Metabolic Markers in Serum Across Disease States 240
Figure 5.20: Expression of Soluble Metabolic Markers in Serum Across Disease States 241
Figure 5.21: Soluble Marker Expression Forms Distinct Serum Cluster Profiles for RA+ Patients 243

Figure 5.22: Summary of CEC Phenotype and Function in RA **248**
Figure 7.1: Verteporfin did not affect FLS viability **317**
Figure 7.2: Effects of TNFα on % Frequency of mTOR in Cultured FLS **318**
Figure 7.3: Additional Markers Analysed on PRIME Cells **319**
Figure 7.4: Frequency of CD200R1+ FLS in HC, RA+, and RA- **320**

List of Tables

Table 1.1: 2010 ACR/EULAR Classification Criteria. 6
Table 2.1: Patient Demographics for RA Patients Utilised in FLS Functional Experiments 51
Table 2.2: Panel of Fluorochrome Antibodies Used for Flow Cytometry Analysis 53
Table 2.3: Designed Primer Sequences Used for RT-PCR Analysis 55
Table 3.1: Patient Demographics for RA Synovial Tissue Biopsies used for Flow Cytometry Analysis 90
Table 3.2: Patient Demographics for RA PBMC used for Flow Cytometry Analysis 90
Table 3.3: Demographics for HC donor PBMCs used for Flow Cytometry Analysis 91
Table 3.4: Panel of Fluorochrome antibodies used for Flow Cytometry Analysis of PRIME cells in PBMC and Synovial Tissue Biopsy Samples 93
Table 4.1: Patient Demographics for RA Synovial Tissue Biopsies used for Flow Cytometry 130
Table 4.2: Demographics for HC Synovial Tissue Biopsies used for Flow Cytometry 130
Table 4.3: Panel of Fluorochrome Antibodies used for Flow Cytometry Analysis of FLS in Synovial Tissue Biopsy Samples 133
Table 4.4: Patient Demographics for RA Synovial Tissue Biopsies used for scRNA Sequencing Analysis 135
Table 4.5: Demographics for HC Synovial Tissue Biopsies used for scRNA Sequencing 135
Table 4.6: Patient Demographics of RA Patient Samples Utilised for FLS Functional Experiments 136
Table 4.7: Designed Primer Sequences used for RT-PCR. 137
Table 5.1: Patient Demographics for RA PBMCs used for Flow Cytometry Analysis. 207
Table 5.2: Demographics for HC PBMCs used for Flow Cytometry Analysis 207
Table 5.3: Panel of Fluorochrome Antibodies used for Flow Cytometry Analysis of CEC and EPC in PBMC Samples. 209
Table 5.4: Patient demographics for RA serums used for MSD analysis 211
Table 5.5: Demographics for HC serums used for MSD analysis 211

Abstract

Rheumatoid Arthritis (RA) is a chronic, progressive, inflammatory autoimmune disease primarily characterised by joint damage and disability and is frequently associated with comorbidities including diabetes and cardiovascular disease (CVD). In the last two decades, targeted biotherapeutics have proven successful in the treatment of RA, leading to significantly improved outcomes. Recent research has also focused on 'individuals at-risk' (IAR) of developing RA, an approach that may provide important insights into the evolution of RA. Despite these advances in therapies and early intervention, a significant proportion of patients experience suboptimal responses, no response, or suffer adverse events that limit therapeutic impact. Currently, it is difficult to predict who will respond to treatment or who will develop severe, erosive disease. This difficulty arises from the complex microenvironment of the joint, where interactions between immune and stromal cells drive pro-inflammatory responses. Furthermore, recent studies have suggested that based on autoantibody status and differential cellular predominance in the synovium, that several different pathotypes exist under the umbrella of RA. One such pathotype is associated with a predominance of synovial fibroblasts (FLS), key stromal cells involved in immune regulation, metabolic re-wiring, and invasive mechanisms within the joint. Indeed, studies suggest that this pathotype may be refractory to current treatments. However, little is known about their phenotype or transcriptional profile in health and disease, particularly in relation to autoantibody status. Therefore, the aim of this thesis is to functionally characterise distinct FLS populations in RA patients (autoantibody positive vs autoantibody negative), the findings of which may have implications for treatment strategies.

In Chapter 2, the role of the mammalian target of Rapamycin (mTOR) in mediating RA FLS activation and function was examined. Transcriptomic analysis of healthy donor and RA synovial tissue revealed dysregulated expression of several key components of the mTOR pathway in RA. Moreover, the expression of phospho-ribosomal protein S6 (pS6), a major downstream target of mTOR, was increased in RA FLS compared to HC FLS. In the presence of TNFα, RA FLS displayed heightened phosphorylation of pS6 and were responsive to mTOR inhibition via Rapamycin. Rapamycin effectively altered RA FLS cellular bioenergetics by inhibiting glycolysis and the expression of rate-limiting glycolytic enzymes. Furthermore, mTOR signaling was shown to mediate RA FLS migratory and invasive mechanisms, with these functions abrogated in the presence of Rapamycin. Finally, transcriptomic analysis identified a significant upregulation in several genes involved in the Hippo-Yes-associated protein (YAP) pathway in RA synovial tissue, with predicted convergence on the mTOR pathway identified. Crosstalk between the mTOR and YAP pathways was shown to mediate RA FLS invasive mechanisms. Together these data identify mTOR as a key driver of RA FLS pathogenic mechanisms, effects that were, in part, mediated via crosstalk with the Hippo-YAP pathway.

In Chapter 3, the phenotypic characterization of the recently identified circulatory 'pre-inflammatory mesenchymal' (PRIME) cells was examined in RA and IAR as potential systemic cellular biomarkers of disease. Additionally, site-specific functional differences in PRIME cells were also investigated. The frequency of PRIME cells (CD45-CD31-PDPN+) was increased in RA->RA+ compared to HC. An increase in the frequency of RA+ PRIME cells positive for immunoregulatory markers CD200+ and HLA-DR+ was observed compared to HC. Enhanced adhesive capacity of PRIME cells was observed in RA, reflected by the increased expression of ICAM-1, CD44, VCAM-1 and CD61. RA PRIME cells also displayed increased expression of established FLS subset/sub-lining markers THY-1, CD34, and FAPα. Similar to RA, in IAR, increases in HLA-DR+ and ICAM-1+ PRIME cells were observed, as were the THY-1+, FAPα+ and CD34+ subsets. Site-specific analysis demonstrated that PDPN+ cells were significantly more abundant in synovial tissue compared to circulation. These PDPN+ cells demonstrated greater frequency of CD61, ICAM-1, CD200R1, CD200, pmTOR and pS6 in peripheral blood compared to synovial tissue, while their expression of CD44, HLA-DR, and pAKT was enriched in the synovial tissue. In summary, PRIME cells could function as a potential cellular biomarker in IAR and as indicators of disease severity in RA.

Moreover, further investigation comparing the characteristics of circulating PRIME cells to PDPN+ cells in the joint may provide insight into which specific FLS subsets arise from these circulating mesenchymal precursors as opposed to a tissue-resident origin. Finally, additional research is required to better understand the origins of PRIME cells to elucidate the early stages of joint inflammation and joint spreading.

In Chapter 4, FLS diversity was further examined focusing on the site of inflammation—the synovium. PDPN+ FLS were enriched in RA+<RA-<HC. Analysis of FLS-specific subset markers demonstrated that CD55+ (lining layer marker) FLS were significantly increased in RA- compared to RA+ and HC, while THY1+ (sub-lining) and FAPα+ (activation) FLS were increased in RA+ compared to HC. An increased frequency of HLA-DR+ and ICAM-1+ FLS was observed for RA+ patients compared to HC, whereas CD61+ and pAKT+ FLS were associated with RA- patients. RA+ demonstrated increased frequency of the activated SL subset (CD55-THY1+FAPα+), while RA- were associated with the activated LL subset (CD55+THY1-FAPα+). CD55+THY1-FAPα+ subsets demonstrated increased expression of Ki67+ and pAKT+, while CD55+THY1+FAPα+ subsets demonstrated increased expression of VCAM-1+, CD61+, CD44+, and YAP+ cells. The CD55-THY1+FAPα+ sub-lining subset was associated with increased expression of HLA-DR, CD200, ICAM-1, CD34, and pS6. Finally, CD55-THY1-FAPα+ demonstrated increased frequency of CD200R1+, ICAM-1+, Cadherin 11+, PDGFRα+, and pmTOR+ cells compared to the other subsets. Enrichment of these subsets and specific activation markers were also observed in IAR. In parallel, scRNA-seq identified 14 FLS clusters between HC and RA synovial tissue. Cluster 3 (POSTN+COL3A1+), a sub-lining cluster was enriched in RA compared to HC and was characterised by genes involved in collagen and ECM reorganization, as well as key signaling pathways NFκB, TGF-β, and NOTCH. Receptor-ligand interaction analysis for this cluster identified interactions with macrophage- and T cell-derived ligands including IL-1β, VEGF and TGF-β. Functional assays demonstrated IL-1β-induced expression of the NOTCH ligands DLL4 and JAG-1, with addition of the NOTCH inhibitor DAPT abrogating NOTCH-induced pro-inflammatory responses. Identification of differential FLS subsets and their associated function in the HC vs IAR vs RA synovium will better facilitate our understanding of their contribution to RA disease pathogenesis. Furthermore, stratifying RA patients by seropositivity will give better insight into the pathogenic differences between these two disease cohorts, with the potential for better tailored treatments.

RA is associated with several comorbidities including the development of CVD. Therefore, in Chapter 5, circulatory endothelial dysfunction and serum biomarkers associated with inflammation and cardiovascular/metabolic processes were analysed. Circulating endothelial cells (CECs) were found to be elevated in both RA and IAR compared to HC. Most CECs identified originated from the microvasculature with a majority positive for CD36 expression. RA CECs demonstrated impaired capacity for wound healing with decreased expression of PDGFRα and YAP compared to HC. CECs have a pathogenically activated phenotype, evident by increased expression of FAPα and THY-1. RA CECs demonstrated trending increases in immunoregulatory and adhesive markers. Analysis of serum biomarkers demonstrated increases in inflammatory, metabolic, and tissue injury soluble mediators in RA, some of which were also increased in IAR. Analysis of circulatory CECs and serum biomarkers could act as potential biomarkers in IAR and RA patients for disease onset and progression but may also have implications for those at greater risk of developing a cardiovascular comorbidity, further contributing to disease pathogenesis.

In conclusion, the data outlined in this thesis provide a significant in-depth analysis of FLS subsets and a better understanding of the unique phenotypic function of FLS that may differ in RA pathotypes. Moreover, the data indicate a role for metabolic reprogramming of FLS in inducing the resolution of inflammation. Finally, cellular and soluble markers in the circulation may be useful predictive markers of RA disease onset and progression, in addition to associated CVD. Taken together, the data in this thesis significantly enhance our understanding of RA disease pathogenesis, with implications for biomarker discovery and the development of new therapeutic approaches for difficult-to-treat patients with RA.

Acknowledgements

I don't think I'll be able to adequately convey just how grateful I am to everyone that has helped me through this journey, but I will try my best. The past three and a half years have been some of the most difficult and challenging, yet most rewarding of my life. Through all the failed experiments, analysis frustrations, eureka moments, small everyday joys of chatting and laughing in lab, and the excitement of participating in research that sparks curiosity and joy, I wouldn't have been able to experience or make it through any of it without the extraordinary people in my life. To all the members of the Fearon Lab, past and present, thank you. Your teachings, advice, chats, and laughs have been invaluable throughout this entire journey.

First, and foremost, I truly cannot express the depth of my gratitude and appreciation to my incredible supervisor Ursula Fearon. Ursula, I am so grateful you gave me the opportunity to stay on for a PhD after doing the master's research project in your lab. You have been, and are, an incredible supervisor, mentor, and inspiration for the type of researcher and leader I hope to become in the future. I truly could not have asked for a better lab or mentor to have done my PhD in. Thank you for all your guidance, support, and excitement for my research. No matter how I felt about work or progress going into a meeting with you, I always left feeling better and more confident. I've loved all the office chats, karaoke, and lab drinks. Thank you for all the kind words, and all the hugs! Through all the stressful moments and tears (especially towards the end of the writing process) you were always there to help see me through and I couldn't be more grateful. I admire you so much and I am sad to be leaving but hope to stay in touch. I hope I have made you proud.

To Mary, my lovely co-supervisor who was there from the very start when I just began for my master's project. Your kindness was unwavering and your excitement for the data never failed to put a smile on my face. Thank you for all the words of support and encouragement, whether it be in your office or during early morning kitchen chats. We've had some wonderful milestone moments like our first paper together!! It has truly been a pleasure, and I can't thank you enough!

Vivi, thank you for the hugs and the reading room chats, I'll miss being able to say to you (a little too loudly) 'the sun is shining, the birds are chirping, it's a wonderful day!' during mornings of conferences. Thank you for all the advice, pep talks, and for always being so kind. Alyssa, thank you for all the help with the PCRs, especially at the end (I am truly grateful), and for the rest of the advice you have provided over the years, I appreciate it. Conor, the R genius, thank you for all your hard work and help on the scRNAseq. Thank you for the fun reading room chats and for the infamous Christmas Tinsel War of 2024, you are a great scientist and friend (workplace acquaintance, haha). Siobhan, how funny that you have bookended my time in the Fearon lab haha! Thank you for all your help in the beginning with teaching me new lab techniques like ELISAs and always being so kind when I came to you with a problem. Thank you for helping me across the finish line with all your help with the thesis (I owe you a mocha from Honey Truffle). To everyone else in the Fearon Lab (past and present) and in the Molecular Rheumatology family, thank you. Thank you for the reading room chats, the coffee breaks, the advice on experiments, and the help and support during the final writing push at the end, you've made the experience a memorable and enjoyable one.

To the LGALS: Hannah, Aoife, Niamh, Aenea, and Órla, you girls have gotten me through. I have especially loved our monthly supper clubs; it always gave me something to look forward to and was always to fun hanging with you all. To my fellow Canavan Lab girlies: Hannah, you've never failed to offer a kind word of support, thank you my fellow Swiftie. Aoife, thank you for being my Drumcondra jogging buddy and for letting me ask you a million questions about flow. Niamh, my fellow lab fairy, from our early mornings in the reading room to spamming each other

with funny Insta reels, to surprise little treats and coffees, you have been such a kind and supportive friend. Aenea, from becoming friends during the masters, to lab mates, to housemates, you've been there for the whole journey! The cat memes, the kitchen chats, and all the laughs we've had (hehe, hihi, haha), I have appreciated them all. To my other lovely friends from the master's that have continued being there throughout this journey, Megan, Kate, Lucy, and Nicole, thank you all so much.

To Órla, my lab twin, I don't even know where to begin. I couldn't have done this without you. We've been a part of each other's PhD journeys since the very beginning when we happened to serendipitously meet and become lab buddies during the few overlapping weeks of our respective research projects, and now here we are, you Dr Órla Tynan (I am so proud), and hopefully soon to be Dr Brianne Barker, lifelong friends at the end of this incredible and sometimes stressful journey. Every peptalk, coffee, brunch, conference, venting session, victory, and everything else in between, you have been there, and I am so incredibly grateful. I truly can't thank you enough, but I am so glad we got to do this together.

To my friends back home Alison, Carolyn, and Jessica. You have all been amazing and supportive friends while I have been abroad these past four and a half years. Alison and Carolyn, thank you for all the Facetime catch ups, constant Instagram memes, and words of encouragement and support. Your stray cat thanks you and is coming home soon! Miss Jessica, you've known all phases of me and have never wavered. Thank you for all the snapchats of Ollie, the ramblings about Gilmore Girls, and for our voice note 'Ted Talks'. They have all helped see me through this and I cannot tell you how thankful I am to call you my friend and for everything you have done for me. Sadie, now Dr Sadie, I am so grateful we saw each other through our PhD journeys. The daily snapchats, Instagram memes, hours long brunch Facetimes, to our adventures singing Abba karaoke in Ireland and seeing the Eras Tour in Switzerland together, have all meant so much to me. Thank you for being the 'idiotic fool' to my 'godforsaken mess'.

To Kyle, thank you for being my rock. Every late-night stressed-out phone call, venting session, virtual date night, and everything in between you've completely changed this whole experience. Thank you for staying by my side through the long-distance and stress of this journey, words cannot even express how much it means. Thank you for always making the time for chats and for coming all the way over to visit me. I am so happy I got to share Ireland and my life over here with you. I love you. To my family, my unfailing support system, words cannot express my gratitude. Aunt Debbie, Grandpa, Dad, Kathy, Bill, Grandpa Carl, Auntie, Uncle, Kyle, Jakey, Eric, Aisling, and now little Ronan, you have all been so supportive and I can't thank you enough, love you all!

Mama, I couldn't have done this without you. You know me better than anyone and always know the right thing to say when I am stressed or freaking out. From the very beginning you were always so supportive and excited for me to do my PhD in Ireland. I will never forget when I called you with the news and you saying, without hesitation, that I absolutely had to do this, and I needed to go accept the position immediately. Every phone call to you, no matter what we talked about, brightened my day even on the bad ones. You have always been so supportive, and I don't know how to repay you for everything you have done for me, but I will do everything I can to try to. This is for you Mom, for everything you have taught me, for everything you have done for me, I owe it all to you.

To everyone that has been a part of my life during this journey, thank you for being my village!

Publications

Metabolites as Drivers and Targets in Rheumatoid Arthritis

Hanlon, M.M., Canavan, M., **Barker, B.E.** and Fearon, U., 2022. *Clinical and experimental immunology*, *208*(2), pp.167-180.

The Mammalian Target of Rapamycin Contributes to Synovial Fibroblast Pathogenicity in Rheumatoid Arthritis

Barker, B.E., Hanlon, M.M., Marzaioli, V., Smith, C.M., Cunningham, C.C., Fletcher, J.M., Veale, D.J., Fearon, U. and Canavan, M., 2023. *Frontiers in medicine*, *10*, p.1029021.

Loss of Synovial Tissue Macrophage Homeostasis Precedes Rheumatoid Arthritis Clinical Onset

Hanlon, M.M., Smith, C.M., Canavan, M., Neto, N.G., Song, Q., Lewis, M.J., O'Rourke, A.M., Tynan, O., **Barker, B.E.**, Gallagher, P. and Mullan, R., 2024. *Science advances*, *10*(39), p.eadj1252.

Published Abstracts and Presentations

Examining the inhibitory effects of Rapamycin on the invasive and metabolic profiles in Rheumatoid Arthritis IL-1β-stimulated stromal cells

Barker, BE., Canavan, M., Fearon, U. Irish Society for Rheumatology Autumn Meeting (2021) **(Poster Presentation)**

Examining the inhibitory effects of Rapamycin on the inflammatory, invasive, and metabolic capabilities of IL-1β stimulated synovial fibroblasts in Rheumatoid Arthritis

Barker, BE., Canavan, M., Fearon, U. UCD SVHG Translational Medicine Symposium (2021) **(Poster Presentation)**

Molecular interplay between Mammalian Target of Rapamycin (mTOR) and the Hippo-Yap pathway mediates RA synovial fibroblast activation

Barker, BE., Hanlon, M, Wade, S., Veale, DJ., Fearon, U., Canavan, M. 41st European Workshop for Rheumatology Research (2022) **(Poster Presentation)**

Metabolic reprogramming of IL-1β stimulated Rheumatoid Arthritis synovial fibroblasts reduces their inflammatory and invasive capability

Barker, BE., Hanlon, M., Wade, S., Veale, DJ., Canavan, M., Fearon, U. 41st European Workshop for Rheumatology Research (2022) **(Poster Presentation)**

Rapamycin inhibits IL-1β induced RA synovial fibroblast activation, an effect associated with alteration in their metabolic profile

Barker, BE., Hanlon, MM., Wade, S., Veale, DJ., Canavan, M., Fearon, U. Annual European Congress of Rheumatology (2022) **(Electronic Abstract Book)**

Identification of Homeostatic and Inflammatory Synovial Fibroblast Signatures in Healthy Control and RA Patients Synovial Tissue Biopsies

Barker BE, Smith CM, Floudas A, Orr C, Canavan M, Veale DJ, Fearon U. 42nd European Workshop for Rheumatology Research (2023) **(Poster Presentation)**

Comparison of inflammatory and homeostatic synovial fibroblast phenotypes within the synovium of patients with Rheumatoid Arthritis and Healthy Control

Barker BE, Smith CM, Tynan Ó, O'Rourke A, Anton D, Orr C, Canavan M, Veale DJ, Fearon U. Irish Society of Rheumatology (2023). **(Premium Poster Presentation)**

Identification of Homeostatic and Inflammatory Synovial Fibroblast Signatures in Synovial Tissue Biopsies of Healthy Controls and Patients with Rheumatoid Arthritis

Barker BE., Smith CM., Tynan Ó., Anton D., Orr C., Canavan M., Veale DJ., Fearon U. American College of Rheumatology Convergence (2023) **(Poster Presentation)**

Characterization of Circulating Endothelial Cells in Patients with Rheumatoid Arthritis Compared to Healthy Control

Barker BE., Canavan M., Anton D., O'Rourke A., Orr C., Veale DJ., Fearon U. 43rd European Workshop for Rheumatology Research (2024) **(Oral Presentation)**

Identification and Characterization of PRIME Cells in Circulation of Patients with Rheumatoid Arthritis Compared to Healthy Control

Barker BE., Tynan Ó., Anton D., O'Rourke A., Orr C., Veale DJ., Canavan M., Fearon U. 43rd European Workshop for Rheumatology Research (2024) **(Poster Presentation)**

Presence and Characterization of Circulating Endothelial Cells in Individuals-At-Risk and Patients with Rheumatoid Arthritis

Barker BE., Canavan M., Anton D., O'Rourke A., Orr C., Veale DJ., Fearon U. 7th European Congress of Immunology (2024). **(Oral Presentation)**

Characterization of PRIME Cells Identified in Circulation of Individuals-At-Risk and Patients with Rheumatoid Arthritis

Barker BE., Tynan Ó., Anton D., O'Rourke A., Orr C., Veale DJ., Canavan M., Fearon U. 7th European Congress of Immunology (2024). **(Poster Presentation)**

Identification and Characterization of Circulating Endothelial Cells and Endothelial Progenitor Cells in Patients with Rheumatoid Arthritis Compared to Healthy Control

Barker BE., Canavan M., Anton D., O'Rourke A., Orr C., Veale DJ., Fearon U. Irish Society of Rheumatology (2024) **(Poster Presentation)**

Characterization of PRIME Cells Identified within Circulation and Site of Inflammation of Patients with Rheumatoid Arthritis Compared to Healthy Control

Barker BE., Tynan Ó., Anton D., O'Rourke A., Orr C., Veale DJ., Canavan M., Fearon U. Irish Society of Rheumatology (2024) **(Poster Presentation)**

Awards Received

Best Regular Poster (1st) for:

Examining the inhibitory effects of Rapamycin on the invasive and metabolic profiles in Rheumatoid Arthritis IL-1β-stimulated stromal cells

Barker, BE., Canavan, M., Fearon, U. Irish Society for Rheumatology Autumn Meeting (2021) **(Poster Presentation)**

Best Poster Prize for:

Characterization of PRIME Cells Identified in Circulation of Individuals-At-Risk and Patients with Rheumatoid Arthritis

Barker BE., Tynan Ó, Anton D, O'Rourke A, Orr C, Veale DJ, Canavan M, Fearon U. 7th European Congress of Immunology (2024). **(Poster Presentation)**

Travel Bursaries Granted

Awarded EULAR Travel Bursary for 41st EWRR Congress, Vienna, Austria. (2022)

Abbreviations

3PO	(3-(3-pyridinyl)-1-(4-pyridinyl)-2-propen-1-one)
4EBP	eukaryotic translation initiation factor 4E binding protein 1
A-SAA	Acute-phase Serum Amyloid A Protein
ACL	anterior cruciate ligament
ACPA	Anti-citrullinated Protein
ACR	American College of Rheumatology
AIA	Adjuvant Induced Arthritis
AMP	Accelerating Medicines Partnership
AMPK	AMP-activated Protein Kinase
Ang	Angiopoietin
ANOVA	Analysis of Variance
APC	Antigen-presenting Cell
ApoA1	Apolipoprotein A-I
ApoC3	Apolipoprotein C-3
ARA	American Rheumatism Association
ART	Arthralgia
AS	Ankylosing Spondylitis
ASIR	Age-standardised Incidence Rate
ATP	Adenosine Triphosphate
BAFF	B cell-activating factor
BCA	Bicinchoninic Acid Assay
BCR	B Cell Receptor
bDMARD	Biological Disease Modifying Anti-Rheumatic Drug
bFGF	Basic Fibroblast Growth Factor
BSA	Bovine Serum Albumin
CAD11	Cadherin-11
CADM1	Cell Adhesion Molecule 1
cDNA	Complementary Deoxyribonucleic Acid
CEC	Circulating Endothelial Cell
CIA	Collagen Induced Arthritis
CLEC3b	C-Type Lectin Domain Family 3 Member B
CLIC5	Chloride Intracellular Channel 5
CRP	C Reactive Protein
csDMARD	Conventional Synthetic Disease Modifying Anti-Rheumatic Drug
Ct	Comparative Threshold
CTAP	Cell Type Abundance Phenotype
CTAP-F	Cell Type Abundance Phenotype - Fibroblasts
CTAP-TF	Cell Type Abundance Phenotype - T cells+ Fibroblasts
Ctrl	Control
CV	Cardiovascular

CVD	Cardiovascular Disease
D2T	Difficult to Treat
DAS28	Disease Activity Score
DC	Dendritic Cell
DEG	Differentially Expressed Gene
DKK3	Dickkopf WNT Signaling Pathway Inhibitor 3
DMARD	Disease-Modifying Anti-Rheumatic Drug
DMEM	Dulbecco's Modified Eagle Medium
DMSO	Dimethylsulfoxide
DNA	Deoxyribonucleic Acid
EBV	Epstein Barr Virus
EC	Endothelial Cells
ECAR	Extracellular Acidification Rate
ECM	Extracellular Matrix
ELISA	Enzyme-linked Immunosorbent Assay
EMP	endothelial microparticles
EMT	epithelial-to-mesenchymal transition
EPC	Endothelial Progenitor Cell
ERK1/2	Extracellular Signal-regulated Kinase1/2
ESR	Erythrocyte Sedimentation Rate
ETC	Electron Transport Chain
EULAR	European League Against Rheumatism
FACS	Fluorescence-Activated Cell Sorting
FADH	Flavin Adenine Dinucleotide
FAPα	Fibroblast Activation Protein α
FBS	Fetal Bovine Serum
FCCP	Trifluorocarbonylcyanide Phenylhydrazone
FcγR	Fc-gamma receptor
FLIP	FLICE-like inhibitory protein
FLS	Fibroblast
FMO	Fluorescent Minus One
FMO	Fluorescence minus one
FSC	Forward Scatter
G6PD	Glucose-6-Phosphate Dehydrogenase
GCA	Giant Cell Arteritis
GEO	Gene Expression Omnibus
GIP	Gastric Inhibitory Peptide
GLP-1	Glucagon-like peptide-1
GLS1	Glutaminase
GLUT1	Glucose Transporter 1
GM-CSF	Granulocyte-Macrophage Colony-Stimulating Factor
GP	General Practitioner

GSK3β	Glycogen Synthase Kinase 3
H&E	Haematoxylin and Eosin
HA	Hyaluronan
HAS1	Hyaluronan Synthase 1
HC	Healthy Control
HIF	Hypoxia Inducible Factor
HK2	Hexokinase 2
HLA	Human Leukocyte Antigen
HLA-DR	Human Leukocyte Antigen – DR isotype
IA	Inflammatory Arthritis
IAR	Individuals-At-Risk
ICAM-1	Intracellular Adhesion Molecule 1
IFN	Interferon
IgSF	Immunoglobulin Superfamily
IL	Interleukin
ITGAD	Integrin Subunit Alpha D
JAK	Janus Kinase
JNK	Jun N-terminal Kinase
KIM-1	Kidney-injury molecule 1
LCN2	Lipocalin-2
LDH	Lactate Dehydrogenase
LL	Lining Layer
LMIC	Lower-Middle Income Country
lncRNA	Long non-coding RNAs
LPS	Lipopolysaccharide
LUM	Lumican
M-CSF	Macrophage Colony Stimulating Factor
MCP	Monocyte Chemoattractant Protein
MCT4	Monocarboxylate Transporter 4
MFI	Mean Fluorescence Intensity
MHC	Major histocompatibility complex
miRNA	microRNA
MMP	Matrix Metalloproteinase
MSD	Mesoscale Discovery
mtDNA	Mitochondrial DNA
mTOR	Mammalian Target of Rapamycin
mTORC1	Mammalian Target of Rapamycin Complex 1
mTORC2	Mammalian Target of Rapamycin Complex 2
MTX	Methotrexate
NAD	Nicotinamide Adenine Dinucleotide
NCAM	Neural Cell Adhesion Molecule
NF-κB	Nuclear Factor kappa B

NGAL	Neutrophil gelatinase-associated lipocalin
NK	Natural Killer Cell
NKT	Natural Killer T Cell
NLRP3	NLR Family Pyrin Domain Containing 3
NO	Nitric Oxide
NOTCH	Neurogenic locus notch homolog protein
NSAID	Non-Steroidal Anti-Inflammatory Drug
OA	Osteoarthritis
OCR	Oxygen Consumption Rate
OGN	Osteoglycin
OPN	Ostepontin
OSM	Oncostatin M
OXPHOS	Oxidative Phosphorylation
PADs	Peptidyl-arginine Deiminases
PB	Peripheral blood
PBMC	Peripheral Blood Mononuclear Cells
PBS	Phosphate Buffered Saline
PCA	Principle Component Analysis
PDGF	Platelet Derived Growth Factor
PDGFRα	Platelet-derived growth factor receptor A
PDH	Pyruvate Dehydrogenase
PDK1	3-phosphoinositide-dependent kinase 1
PDPN	Podoplanin
PFA	Paraformaldehyde
PFKFB3	6-Phosphofructo-2-kinase/fructose-2,6-biphosphatase 3 Enzyme
PI3K	Phosphoinositide 3-kinase
PKM2	Pyruvate Kinase M2
pmTOR	Phospho-mTOR
PP	Pancreatic polypeptide
PPP	Pentose Phosphate Pathway
PRG4	Proteoglycan 4
PRIME	Pre-Inflammatory Mesenchymal
pS6	Phospho-ribosomal Protein S6
PsA	Psoriatic Arthritis
PTPRC	Protein Tyrosine Phosphatase Receptor Type C
RA	Rheumatoid Arthritis
RA-	Seronegative Rheumatoid Arthritis
RA+	Seropositive Rheumatoid Arthritis
RANK	Receptor Activator of Nuclear Factor kappa-B
RANKL	Receptor Activator of Nuclear Factor kappa-B Ligand
RANTES	Regulated on Activation, Normal T Cell Expressed and Secreted
RBP4	Retinol Binding Protein 4

RF	Rheumatoid Factor
RIPA	Radioimmunoprecipitation Assay
RNA	Ribonuclease Acid
ROS	Reactive Oxygen Species
RT	Room Temperature
RT-PCR	Real-time Polymerase Chain Reaction
RTX	Rituximab
SCFA	Short-chain Fatty Acid
SCID	Severe Combined Immunodeficiency Disease
scRNA-seq	Single-cell RNA-sequencing
SDS	Sodium Dodecyl Sulfate
SEM	Standard Error of the Mean
SJC	Swollen Joint Count
SL	Sublining layer
SLE	Systemic Lupus Erythematosus
SNP	Single Nucleotide Polymorphism
SSc	Systemic Sclerosis
ST	Synovial Tissue
STAT	Signal Transducers and Activators of Transcription
SVUH	St. Vincent's University Hospital
TB	Tuberculosis
TBS	Tris-buffered Saline
TCA	Tricarboxylic Acid Cycle
TCZ	Tocilizumab
TFF3	Trefoil factor 3
Tfh	T Follicular Helper
TGF-β	Transforming Growth Factor Beta
Th	T Helper
TIMP	Tissue Inhibitor of Metalloprotease
TJC	Tender Joint Count
TLR	Toll Like Receptor
TNF	Tumour Necrosis Factor
TNFi	Tumour Necrosis Factor Inhibitor
Tregs	Regulatory T cells
TSC2	TSC complex subunit 2
TSP1	Thrombospondin-1
UA	Undifferentiated Arthritis
UCSC	University of California Santa Cruz
UMAP	Uniform Manifold Approximation and Projection
VAS	Visual Analogue Scale
VCAM-1	Vascular Cell Adhesion Molecule 1
VEGF	Vascular Endothelial Growth Factor

CHAPTER ONE:

General Introduction

1.1 A Brief History of Rheumatoid Arthritis

Rheumatoid Arthritis (RA) is a chronic autoimmune disease characterised by systemic polyarthritis and synovial inflammation of the diarthrodial joints, particularly of the hands and feet, but can affect larger joints as well (Gerlag *et al.*, 2012; McInnes and Schett, 2011). It was first described clinically by French physician Augustin Jacob Landré-Beauvais in his dissertation in 1800. Referring to it as 'asthenic gout,' he differentiates it from ordinary gout (already known at the time) by describing distinct features such as having a predominance in female patients, severe pain in multiple joints, and a thickening of cellular tissue (Landré-Beauvais, 2001). However, affliction of the joints had been described as early as 1616 by Guillaume de Baillou, known as the 'Father of Rheumatism' who, in his posthumous publication, was the first to use the word 'rheumatism' in a way that we use today as referring to polyarthritis, and classified rheumatic disease into the categories of classical type gout, acute and chronic polyarthritis, and 'rheumatism' which was considered separate from gout (Garrod AE, 1980; Copeman, 1971). In his 1890 'Treatise on Rheumatism and Rheumatoid Arthritis,' Archibald Garrod coined the term 'Rheumatoid Arthritis' to more accurately reflect how the disease afflicted the body, building upon the observations of Landré-Beauvais and his own father, Alfred Garrod, who in 1859 was the first to distinguish gout from other arthritic conditions (Entezami 2011).

Although Landré-Beauvais is credited with the first clinical description of RA, the earliest observations were noted in ancient literature and art. Hippocrates described a 35-year-old patient having arthritis that spread from their hand and feet to other joints within the body (Entezami 2011). The 1638 painting 'The Three Graces' by Peter Paul Rubens shows disfigurement of the right hand of one of the Graces, reflective of what would be described as progressive RA today. Rubens was known for realism in his paintings which gives more weight to the hypothesis that the disfigurement depicted in the hand could be attributed to a rheumatologic disease. Similarly, the Renaissance painting 'The Temptation of St. Anthony' by an unknown artist depicts a beggar with deformity in his right hand, particularly dislocation of the wrist, again reflective of a severe form of arthritis (Entezami 2011). Palaeopathological evidence identified in the bones from skeletons of Egyptians of the Ptolemaic period, of Norse Vikings, found in a Roman sarcophagus, and those found in the ruins of Pompeii all showed characteristic changes typical of RA and/or ankylosing spondylitis, suggesting the antiquity of rheumatic diseases (Short, 1974).

1.2 Global Prevalence

Currently, RA has a global prevalence of about 0.1-2.0% depending on geographical location, with a 2-3-times higher prevalence in females compared to males (Cross *et al*., 2014; Almutairi *et a*l., 2020). Though onset of disease can occur at any age, incidence increases with age with a peak incidence between 60-70 years (Jeffery, 2014). Previous studies have mainly focused on Western European countries and found a prevalence of 0.5%-1% in the Caucasian population (Smolen *et al*., 2018). However, the highest occurrence of RA is observed within Native American populations, such as the Prima Indians and the Chippewa Indians, with a prevalence of 5.3% and 6.8%, respectively (Silman and Pearson, 2002). Industrialised counties have a higher prevalence of RA specifically within urban settings, which could be attributed to urbanization factors including but not limited to, pollution as a potential main factor for RA development (Almutairi *et al*., 2020; Finckh *et al.*, 2022). For example, within the United States the lifetime risk of developing an inflammatory autoimmune rheumatic disease is 8.4% for women (1 in 12) and 5.1% for men (1 in 20). Lifetime risk for developing RA was calculated to be 3.6% for women (1 in 28) and 1.7% for men (1 in 59) (Crowson *et al.*, 2011). Prevalence of RA in Spain between 2016 and 2017 was approximately 0.82% with the mean age of 60.48 years, having a higher frequency in women (61.5%) and in those living in urban areas (74.4%) (Silva-Fernández *et al.*, 2020).

Interestingly, a study conducted in Taiwan from 2001 to 2011 demonstrated increasing prevalence each year across both sexes with the highest prevalence identified in suburban and rural areas especially amongst those with a lower socioeconomic status (Yang *et al.*, 2018). Similarly, the prevalence of RA was significantly higher in women from low-to-middle income countries (LMIC) than males at 0.75% compared to 0.16%, respectively. However, in LMIC, there was no significant difference in prevalence between urban and rural areas (Rudan *et al.*, 2015).

A global analysis conducted by Almutairi *et al.* calculated the global prevalence of RA to be 0.46% between the years of 1980 to 2018 with a 95% prediction interval, thus expanding prevalence anywhere between 0.06%-1.27%. Geographical location impacted the observed RA prevalence with the highest prevalence identified in North America, specifically in Cuba with 2.7% (Almutairi et al, 2020). Safiri *et al.* examined the burden of RA on a national, regional, and global level, between the years of 1990 and 2017 across 195 countries. In total, 20 million prevalent cases were identified globally. Incidence and prevalence rates increased globally, especially in Guatemala, Paraguay, and Canada. At a regional level, the highest age-standardised prevalence was in high income areas of North America, Western Europe, and the Caribbean. The lowest age-standardised rates were in lower income regions of Oceania, Southeast Asia, and Western Sub-Saharan Africa, with similar incidence rate observations (Safiri *et al.*, 2019). Updated Global

Burden of Disease Studies found similar results: from 1990 to 2019, there were approximately 18.5 million cases of RA globally with incident cases per year reaching 1.07 million by the year 2019. Incidence rate and prevalent cases of RA were higher in females. In 2019, the global age-standardised incidence rate (ASIR) peaked in the 60-64 and 65-69 age cohorts for females and males respectively and overall, the ASIR was higher in females and increased with age. The most significant increases of ASIR of RA were in Andean Latin America, closely followed by Southern Latin America, and Central Asia. Specifically in 2019, high-income North America had the highest ASIR with 21.46 per 100,000. RA numbers have increased over the past 30 years and are predicted to continue increasing with a 1.4-fold increase in incident cases by 2040 (Shi *et al.,* 2023) and about 31.7 million people predicted to be living with RA by 2050 (GBD 2021 Rheumatoid Arthritis Collaborators, 2023).

Focusing on Ireland specifically, a population-based survey conducted in Dublin in 1995 found a prevalence rate of 5 per 1000 (Power *et al.,* 1999). More recently, it has been estimated that up to 15% of the Irish population is affected by arthritis, with inflammatory arthritis, specifically RA and Psoriatic Arthritis (PsA), affecting approximately 2% (Arthritis in Ireland, 2018). A recent estimate from Arthritis Ireland suggests that roughly 40,000 individuals suffer from RA in Ireland, with approximately 70% of these individuals being women (Arthritis Ireland, 2023).

1.3 Classification of RA

In 1956, diagnostic criteria for RA were first introduced by the American Rheumatism Association (ARA) comprising of 11 disease manifestations which resulted in two diagnostic categories "definite" and "probable" RA (Mitchell and Fries, 1982). However, these criteria were not specifically designed for routine use in clinical practice, and it was not until 1987 when RA was officially classified by Arnett *et al.* on behalf of the ARA, now known as the American College of Rheumatology (ACR) (Arnett *et al.*, 1988). These comprised of seven criteria for classification, some adopted from the ARA criteria with more specified definitions. For a patient to be diagnosed with RA they had to satisfy four out of the seven listed criteria, with criteria one through four required to be present for at least six weeks (Arnett *et al.*, 1988).

The 1987 Criteria relied heavily on radiographic imaging evidence of rheumatoid nodule development and erosions (van der Heijde, 1996; van der Heijde, 2000). Clinical assessments criticised this classification system's lack of sensitivity for diagnosing patients with RA particularly at an early stage of disease (Levin *et al.*, 1996; Harrison *et al.*, 1998; Sugimoto *et al.*, 2000; Saraux *et al.*, 2001). Indeed, while recent onset of early RA involves joint swelling, radiographic assessments in many cases are normal, therefore more sensitive criteria were required. Circulating autoantibodies, such as anti-citrullinated protein antibodies (ACPA), were found to be

increasingly helpful in identifying patients with early RA and predicting disease progression but were not included in the 1987 classification criteria (Meyer *et al*., 2003; Panchagnula *et al.*, 2006; Liao *et al.*, 2008). This, along with several studies showing the benefits of drug intervention at the earlier stages of RA resulted in published editorials highlighting the need for a revision of the current classification system (van der Heide *et al.*, 1996; van Jaarsveld *et al.*, 2000, Aletaha *et al.*, 2005). In 2010, ACR in collaboration with the European League Against Rheumatism (EULAR) updated the classification criteria to facilitate the diagnosis and study of early RA (Aletaha *et al.*, 2010). This classification is now used in standard clinical practice. For a "definite RA" classification, the presence of synovitis in at least one joint is required with no alternative diagnosis to explain the synovitis. Additionally, a diagnosis of RA requires a score of $\geq$6 across four domains as highlighted in Table 1.1 (Aletaha *et al.*, 2010). These new criteria successfully address the concerns regarding the diagnosis and study of early RA (van der Linden *et al.*, 2011).

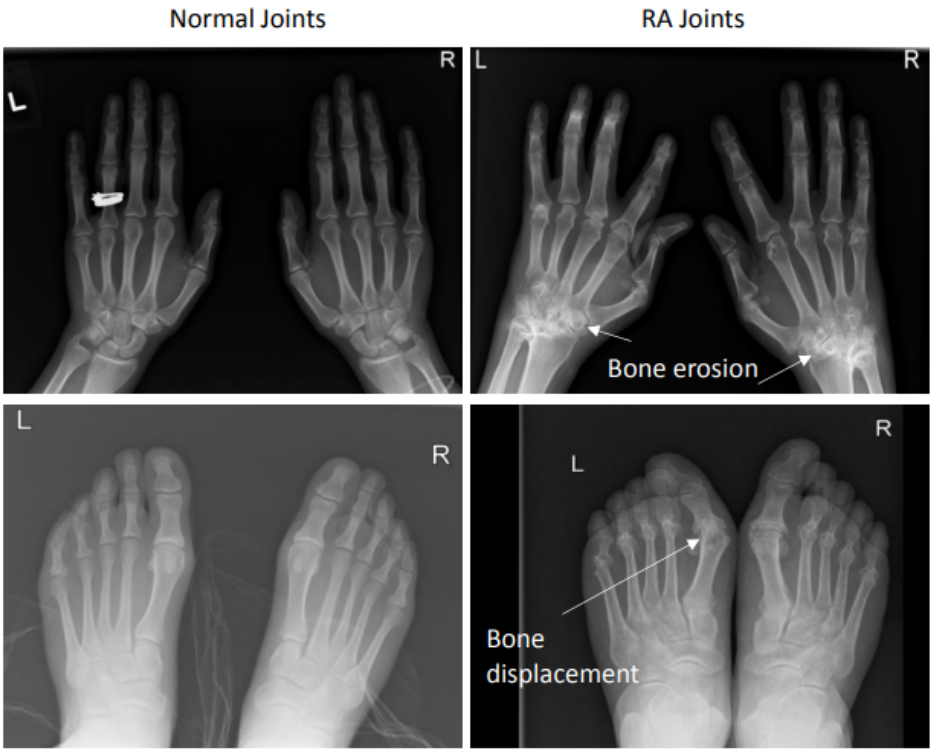

Figure 1.1: X-rays of Hand and Feet from Normal Joints vs Rheumatoid Arthritis Joint.
Radiographic images of hands (top panel) and feet (bottom panel) in an individual without RA (left panels), and with RA (right panels). Extensive erosive destruction of the carpal bones and proximal interphalangeal joints, as well as significant joint collapse in the metatarsal-phalangeal joints can be seen in radiographs of the individual with RA as indicated by the white arrows. (Images provided by St Vincent's University Hospital Rheumatology Department).

	Criteria	Score
Joint Involvement	1 large	0
	2-10 large	1
	1-3 small (w/o large)	2
	4-10 small (w/0 large)	3
	>10 (w/at least 1 small)	5
Serology	(-) RF **and** (-) ACPA	0
	(+) RF **or** (+) ACPA (LOW)	2
	(+) RF **or** (+) ACPA (HIGH)	3
Acute-Phase Reactants	Normal CRP **and** ESR	0
	Abnormal CRP **or** ESR	1
Symptom Duration	<6 weeks	0
	≥6 weeks	1

Table 1.1: 2010 ACR/EULAR Classification Criteria.
Joint involvement refers to swollen or tender joints upon examination. "Large" joints refer to ankles, knees, hips, elbows, and shoulders. "Small" joints refer to metacarpophalangeal, proximal interphalangeal, second through fifth metatarsophalangeal, thumb interphalangeal, and wrist joints (distal interphalangeal, first carpometacarpal, and first metatarsophalangeal joints are excluded). RF: Rheumatoid Factor; ACPA: Anti-citrullinated protein antibody; CRP: C-reactive protein; ESR: erythrocyte sedimentation rate. Symptom duration refers to patient self-report of duration of signs/symptoms of synovitis (e.g., pain, swelling, tenderness) of joints involved at time of assessment (Adapted from (Aletaha *et al.*, 2010)).

1.4 Pre-Clinical RA and Individuals-At-Risk

RA can be classified into stages: pre-clinical, early, and established RA. The pre-clinical stage occurs prior to disease onset before signs of clinical symptoms are apparent. Individuals in this stage are seropositive for associated autoantibodies such as RF and ACPAs and present with general aches and arthralgia, yet do not exhibit clinical signs of synovitis (Smolen *et al.*, 2018). They are therefore referred to as 'individuals-at-risk' (IAR) of developing RA. To better identify individuals in this cohort, first degree relatives of patients with RA are often assessed for the presence of RA-associated autoantibodies. Individuals that present with musculoskeletal symptoms are also referred on to rheumatologists for further assessment (Jutley *et al.*, 2017; van Steenbergen *et al.*, 2018). IAR have reported experiencing fatigue, weak or total loss of motor control, sleeping difficulties, and joint redness (Jutley *et al.*, 2017). These individuals have an increased positive predictive risk of developing RA within four years. However, not all individuals in this cohort progress to a clinical diagnosis of RA, with the conversion rates varying between 30-70% (van Boheemen *et al.*, 2019; Cunningham *et al.*, 2021). As such, characteristics of this pre-

clinical cohort are not completely indicative of disease development and further research needs to be conducted to better identify progressors versus non-progressors. Established tissue and blood biomarkers have yet to be identified in IAR, however, recent studies suggest circulating immune cells may already be primed in these 'at risk' individuals. Studies have shown differences in circulatory CD4 and CD8 T cells in arthralgia patients (Lübbers *et al.*, 2016). It has been demonstrated that *ex vivo* monocytes from the periphery are hypermetabolic and hyperinflammatory with increases observed in 'pre-RA' arthralgia patients (Hanlon *et al.*, 2022). In addition, T cells in 'pre-RA' demonstrate altered metabolic pathways, inducing a hyperproliferative phenotypic profile (Chang *et al.*, 2016). Studies of synovial tissue in IAR are limited, showing either no abnormality or early T cell infiltration and altered gene signatures (de Hair *et al.*, 2014; de Hair *et al.*, 2015; de Jong *et al.*, 2022). More recent bulk-RNA-seq analysis of synovial tissue has demonstrated that plasma/plasmablast cells and CD40-CD40L pathway gene signatures are increased at different stages of disease progression including in patients defined as 'at-risk', suggesting pre-existing autoimmune dysregulation (Guo *et al.*, 2017; Cole *et al.*, 2018).

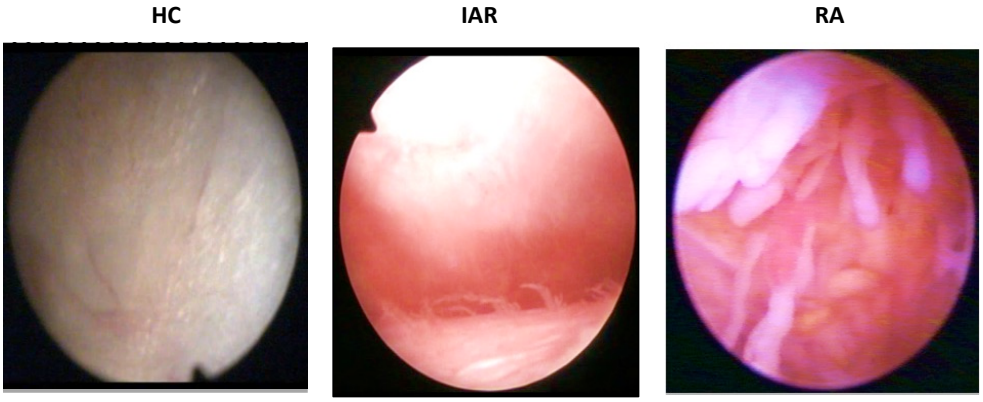

Figure 1.2: Representative Macroscopic Images of the Synovium.
Macroscopic images of the joint from a healthy control (HC), 'individual-at-risk' (IAR), and patient with RA obtained under direct visualisation using key-hole video arthroscopy. HC synovium is translucent and acellular contrasting to the inflammation observed in RA. (Images obtained from SVUH clinical team).

1.5 Autoantibodies

The presence of autoantibodies has been well-documented over the years and has gained significant importance in the diagnosis and pathogenesis of RA. The first autoantibody to be described in RA was RF, an autoantibody targeting the Fc region of IgG molecules (Waaler, 2007). RF is present in the sera of 50-80% of patients and its presence is associated with worsened prognosis for RA (Masi *et al.*, 1976; Mannik, Nardella, and Sasso, 1988; Waaler, 2007). However, RF can also be detected in healthy elderly individuals as well as those with infectious diseases, therefore diminishing its predictive value alone in diagnosing RA due to its lack of specificity

(Schellekens *et al.*, 2000). Though still taken into consideration, ACPA has since superseded RF, having a higher specificity for RA diagnosis and association with disease severity (Nishimura *et al.*, 2007). ACPA are autoantibodies that target proteins that have undergone a post-translational modification in which their arginine residue has been replaced by citrulline. These citrullination reactions are catalysed by a family of enzymes known as peptidyl-arginine deiminases (PADs) (Vossenaar *et al.*, 2003). Approximately two thirds of RA patients are seropositive for ACPA, and detection of this autoantibody often occurs before onset of disease supporting the proposed "two-hit hypothesis" where neo-antigen presentation initially may occur in the lung or lymph node while the second hit may take place within the joint resulting in citrullination of synovial proteins (Rantapaa-Dahlqvist *et al.*, 2003; Nielen *et al.*, 2004; van de Sande, de Hair *et al.*, 2011; Alivernini *et al.*, 2017). The presence of ACPA has been associated with more extra-articular manifestations, earlier onset of erosions, a more erosive phenotype, and overall, more destructive disease (Kroot *et al.*, 2000; Jansen *et al.*, 2003; van der Heim-van Mil *et al.*, 2005; Machold *et al.*, 2007; Syversen *et al.*, 2008; Aubart *et al.*, 2011; Lopez-Longo, Sanchez-Ramon, and Carreno, 2009; Orr *et al.*, 2017). ACPA is also associated with increased mortality, mainly linked with cardiovascular events (Gorman *et al.*, 2004; Ajeganova et al, 2016).

There are differences in immune cell profiles between ACPA+ and ACPA- RA with higher frequencies of peripheral TNFα expressing cells and an increased CD4 T cell pro-inflammatory cytokine profile observed in ACPA+ compared to ACPA- (Floudas *et al.*, 2021). Frequency of circulatory memory T cells, and CCR6+ Th cells is higher in ACPA+ patients, whereas circulatory naïve and Tregs are lower (Hunt *et al.*, 2015; Paulissen *et al.*, 2015; Anderson *et al.*, 2016; Pieper *et al.*, 2018; Ponchel *et al.*, 2020). In addition, higher IL-6-driven STAT signaling within circulating CD4+ lymphocytes is associated with ACPA positivity (Anderson *et al.*, 2016). Accumulation of ACPA producing B cells in the RA joint has been observed and synovial B cell lymphoid aggregates are significantly increased in ACPA+ RA (Amara *et al.*, 2013, Orr *et al.*, 2017). Mechanisms by which this occurs are unclear, however, chemokine-dependent mechanisms have been implicated (Krishnamurthy *et al.*, 2016). Indeed, recent studies have shown through RNA-seq analysis, distinct synovial tissue gene signaling pathways in ACPA+ vs ACPA- demonstrating differences in the usage of chemokine receptors CXCR3, CCR7, and CCR2 (Floudas *et al.*, 2021). Furthermore, studies have shown that ACPA titre levels may determine the response to specific therapies with some suggesting that ACPA positivity and the presence of synovial B cell, particularly synovial B cell lymphoid aggregates, may predict responsiveness to B cell therapies (Teng *et al.*, 2007; Humby *et al.*, 2009; Bugatti *et al.*, 2014). Other studies have demonstrated that differences in T cell expression are associated with ACPA positivity, in addition to the development of chronic arthritis

(van Oosterhout *et al.*, 2008; de Hair *et al.*, 2014). Orr *et al.* (2017) demonstrated that the number of CD19+ B cell lymphoid aggregates was associated with ACPA positivity, however they also found that the EULAR response in these patients was significantly associated with CD3+ T cells and CD68+ macrophages. Additionally, studies have shown that high ACPA+ titres are predictive of response to abatacept evident by a greater reduction in DAS28-CRP (Sokolove *et al.*, 2016; Harrold *et al.*, 2021). For these reasons, with the development of the 2010 ACR/EULAR classifications, criteria for RA diagnosis were revised to take such autoantibodies into consideration (Aletaha *et al*., 2010).

Studies have suggested that several RA genetic factors are likely to be functionally related to RA through modulation of the production of citrullinated proteins or the antibodies that target them (Venrooij, Vossenaar, and Zendman, 2004). In fact, healthy relatives of ACPA+ RA patients can have an increased ACPA positivity incidence rate of up to 19%, which is significantly higher than that observed in the general population (Ioan-Facsinay *et al.*, 2008). Interestingly, while relatives have increased risk of ACPA positivity, studies have demonstrated that ACPA isotypes differ between healthy relatives and their family member with RA (Ioan-Facsinay *et al.,* 2008). Furthermore, ACPAs specific for anti–CEP-1, anti–vimentin 60–75, and anti– fibrinogen β 573 are more predictive for the risk of developing of RA (de Hair *et al.*, 2014).

Other autoantibodies have also been identified in patients with RA, many of which are associated with worse disease outcomes, such as those directed against ribosomal proteins (anti-RA33) and carbamylated proteins (anti-CarP) (Hassfeld *et al.*, 1989; Epitope *et al.*, 1997; Shi *et al.*, 2011). Anti-CarP antibodies have been identified prior to disease onset and can be detected even in patients seronegative for RF and ACPA making it an interesting potential biomarker for RA diagnosis (Shi *et al.*, 2011; Shi *et al.*, 2013; Jiang *et al.*, 2014; Gan *et al.*, 2015). Furthermore, anti-nuclear antibodies (ANA) target nuclear antigens and testing for such antibodies is often used in the screening process for autoimmune connective tissue diseases and in the case of RA, can be detected in approximately 45% of patients (Shiel Jr and Jason 1989; Slater, Davis, and Shmerling, 1996).

1.6 Genetic and Epigenetic Risk Factors

Understanding the exact cause of RA, as well as accurately determining who will develop the disease, has proven to be a difficult task. Indeed, it has become increasingly evident that there are multiple contributing risk factors for the development of RA. While familial risk of RA is low in comparison to other autoimmune diseases, there is still a two to five factor increase in the risk of developing RA for first-degree relatives of patients with RA (Gravallese and Firestein, 2023). Familial and twin studies have identified a strong genetic risk association (Hemminki *et al.*, 2009; Smolen *et al.*, 2018). Although twin concordance for disease development is only about 12-15%,

overall, RA heritability is approximately 60% with a slightly higher percentage observed in seropositive patients (65%) compared to seronegative patients (Aho *et al.*, 1986; Silman *et al.*, 1993, MacGregor *et al.*, 2000, Stahl *et al.*, 2012, Frisell *et al.*, 2016). Frequency differences in risk alleles, specifically within the human leukocyte antigen (HLA) region, close to the HLA-DRB1 locus, have been observed between ACPA+ vs ACPA- individuals (Padyukov *et al.*, 2011). The HLA-DR isotype (HLA-DR) locus on chromosome six and the 'shared epitope' (SE) hypothesis is implicated in the development of RA, where studies have shown that specific sequences within the hypervariable region of the HLA-DRβ chain are associated with an enhanced risk of an individual developing RA (Holoshitz, 2010; Padyukov, 2022). SNPs within the HLA locus have been demonstrated to be associated with genetic risk (at least 30%) including HLA-DRB1 alleles HLA-DRB1*01 and HLA-DRB1*04 (Nepom, Hansen and Nepom, 1987; Gregersen, Silver, and Winchester, 1987; Raychaudhuri *et al.*, 2012; Smolen *et al.*, 2018, Dedmon, 2020; Karami *et al.*, 2019). Other non-HLA genes associated with RA include protein tyrosine phosphatase non-receptor type 22 (PTPN22), IL23R, BLK, ANKRD55, TNFAIP3, IL6ST, PADI4, STAT4, PRKCQ, KIF5A, TRAF1, C5, and IL2RB (Suzuki *et al.*, 2003; Begovich *et al.*, 2004; Plenge *et al.*, 2007; Remmers *et al.*, 2007; Barton *et al.*, 2008; Smolen *et al.*, 2018; Karami *et al.*, 2019; Demon, 2020).

Though genetics play a prominent role, they do not solely account for RA incidence. Sex differences, as well as epigenetic modifications have also been established as associated risk factors. For example, RA affects at least twice as many women as men, with a peak incidence age of 50 years (however disease can occur at any age) (van der Woude and van der Helm-van Mil, 2018). However, this difference in occurrence between sexes was not observed in familial risk studies suggesting that genetics cannot account for why RA is more prevalent in women (Frisell *et al.*, 2016). It is logical then to assume hormone imbalances, specifically with oestrogen, progesterone, and androgens potentially increase the risk of RA. Indeed, progesterone and androgens have been reported to have anti-inflammatory effects, whereas oestrogens can be pro- or anti-inflammatory depending on concentration and cell type (anti-inflammatory effects on T cells) (Raine and Giles, 2022). Due to this, there is an increased risk of RA particularly in early menopause when levels of these hormones decrease (Pikwer *et al.*, 2011; Wong *et al.*, 2015).

Additionally, some epigenetic disturbances associated with RA risk include DNA methylation, histone acetylation, and altered expression of certain microRNAs (miRNAs) and long non-coding RNAs (LncRNAs) (Liu *et al.*, 2013; Kolarz and Majdan, 2017; Taheri *et al.*, 2020). These biological risk factors occur during the early stage of disease development, either asymptomatic or very early symptomatic (van der Woude and van der Helm-van Mil, 2018).

1.7 Environmental Risk Factors

It is now understood that the initiation of RA disease progression requires two 'hits'. There are various lifestyle and environmental triggers that can contribute to the initial insult. Then, in those that are genetically susceptible, a subsequent or second insult which includes further environmental triggers or transient infectious agent-dependent pathways induces development of RA (Firestein and McInnes, 2017). While there are many environmental risk factors implicated, smoking has been shown to have the strongest association with RA development, with a twofold higher risk amongst men and 1.3 times higher risk in female smokers compared to non-smokers (Sugiyama *et al.*, 2009). Studies have suggested that smoking accounts for approximately 20-30% of the environmental risk for RA (Deane *et al.*, 2017). Studies have also demonstrated that smoking increases the levels of ACPA in a dose dependent manner in the circulation suggesting a causal relationship, with the working hypothesis that smoking triggers protein citrullination in which an arginine amino acid is exchanged with citrulline, increasing the presence of autoantigens, and thus increasing the propensity of developing ACPA positivity (Klareskog *et al.*, 2006; Verpoort *et al.*, 2007, Lee, *et al.*, 2009, Catrina *et al.*, 2016; Catrina *et al.*, 2016). Smoking is associated with worse disease progression and is strongly linked to anti-ACPA-positive RA and those who have the HLA-DRB1 shared epitope (Saag *et al.*, 1997; Másdóttir *et al.*, 2000; Lu *et al.*, 2014). In individuals who are genetically susceptible, citrullination increases their affinity for the MHC molecules, resulting in enhanced activation of autoreactive CD4+ T cells, subsequently initiating an autoimmune response (Hill *et al.*, 2003; Klareskog *et al.*, 2006; Källberg *et al.*, 2011). Exposure to silica dust has also been linked to an increased risk in ACPA-positivity (Stolt *et al.*, 2010).

Poor diet and obesity have also been connected to risk of RA. Studies have reported an 18-31% increased risk of developing obesity and associated cardiovascular risk in RA, which were associated with worse disease activity and reduced quality of life (Michaud and Wolfe, 2007; Armstrong *et al.*, 2006; Naranjo *et al.*, 2008, Ajeganova *et al.*, 2013; Sandberg *et al.*, 2014). The implication of obesity is further emphasised in studies demonstrating a reduced response to biological treatments in patients with RA who are overweight, with several studies showing increased levels of adipokines in the blood of patients with RA which in turn can induce pro-inflammatory responses (Otero *et al.*, 2006; Fantuzzi, 2008, Gremese *et al.*, 2013). Some studies demonstrated that increased risk is associated with higher consumption levels of red meat, caffeine, and high-refined carbohydrates, however, these associations remain controversial due to contradicting results (Pattinson *et al.*, 2004, Guan and Beg, 2023). Conversely, studies examining the protective effects of certain dietary measures have proven to yield more consistent results. For example, moderate alcohol consumption has been shown to have anti-inflammatory

effects (Guan and Beg, 2023) and multiple studies demonstrated an association between moderate consumption and a decrease in RA risk and severity of diseases (Voigt *et al.*, 1994; Källberg *et al.*, 2008; Maxwell *et al.*, 2010; Lu *et al.*, 2014). Similarly, long-term follow up studies found that long-term adherence to a healthy dietary pattern (i.e. less red meat, moderate alcohol consumption) resulted in better disease outcomes (Geusens *et al.*, 1994; Kjeldsen-Kragh, 1999; Di Giuseppe *et al.*, 2013; Schönenberger *et al.*, 2021). Restricting calorie intake can dampen inflammation by inhibiting the NLRP3 inflammasome and IL-β production (Vandanmagsar *et al.*, 2011). Furthermore, fish consumption has been shown to have a protective effect against RA development (Fakhri *et al.*, 2023). Indeed, omega-3 fatty acids and Vitamin D are associated with decreasing RA disease activity, with *in vitro* studies demonstrating that omega-3 fatty acids can inhibit pro-inflammatory responses in macrophages (Naughton *et al.*, 1993; Volker *et al.*, 2000; L'homme *et al.*, 2013, Tedeschi and Costenbader, 2016). The 'Mediterranean diet' which is rich in olive oil, fruits and vegetables, fish, and reduced quantities of red meat, was demonstrated to improve disease activity in two separate intervention trials (Sköldstam, Hagfors and Johansson, 2003; McKellar *et al.*, 2007). Furthermore, short chain fatty acids (SCFA) have been shown to alter the induced anti-inflammatory function in innate immune cells, in addition to increased frequency and function of Tregs (Trompette *et al.*, 2014). Genistein, an isoflavone found in soybeans, inhibited the growth of RA FLS and reduced their expression of MMP-2 and MMP-9 (Zhang *et al.*, 2011).

The human gut microbiome and its influence on health and disease has recently become a field of interest. Current studies have focused on characterizing the gut microbiome populations in specific disease states, in addition to observing temporal changes over the course of a disease (Cho and Blaser, 2011). In the context of autoimmune disease, it is appreciated that the presence of a particular microbe may be required to or help trigger an autoimmune response in genetically susceptible individuals (Chervonsky, 2009). For example, one study demonstrated how the colonization of the commensal microbe, segmented filamentous bacterium (SFB), in the small intestine of mice was sufficient to induce the appearance of Th17 cells within the lamina propria (Ivanov *et al.*, 2009). Within the healthy gut, there is a balance between Th1, Th17, and Treg cells working with epithelial cells, DCs, and B cells to maintain equilibrium of a basal state of physiological mucosal inflammation preventing commensal bacteria from causing damage to the host. However, lifestyle and diet changes can lead to dysbiosis (an imbalance of the microbial community) in the gut, eliciting a pro-inflammatory response (Scher and Abramson, 2011; Gioia *et al.*, 2020). Distinct microbial DNA was observed in the bloods of RA patients and subsequent blood draws post-treatment demonstrated a modulated microbiome in some patients, especially

seronegative RA (Hammad *et al.*, 2020). Patients with Early RA were found to have significantly less bacteria of the Bacteroides-Porphyromonas-Prevotella group, B. fragilis subgroup, and bifidobacteria compared to those with fibromyalgia (Vaahtovuo *et al.*, 2008). Despite these studies however, the exact role the gut microbiota plays in RA pathogenesis is still unclear.

1.8 Infection and Malignancy

The proposal that bacteria and other microorganisms are associated with RA development is not new. Indeed, in 1900, the oral sepsis hypothesis was introduced implicating the bacteria in oral infections as a contributing factor in the cause of other diseases (Hunter, 1900; Scher and Abramson, 2011). It was once believed that RA was caused by streptococci found in milk (Scher and Abramson, 2011). However, it is now apparent that no one single organism has been consistently implicated as being responsible for the cause of RA (Symmons and Harrison, 2000), but rather multiple organisms have been proposed as possible triggers. The Epstein-Barr virus (EBV), Mycobacterium tuberculosis, and Escherichia coli (E. coli) have been implicated as triggers via induction of an immune cell response through molecular mimicry (Albani *et al.*, 1992; Auger and Roudier, 1997; Newkirk *et al.*, 2005, Blaschke *et al.*, 2000; Kanagawa *et al.*, 2015, Sherri *et al.*, 2024).

The oral microbiome is the second largest bacterial reservoir in humans and has been implicated in RA pathogenesis (Yeoh *et al.*, 2013). Periodontitis is an inflammatory oral disease caused by bacterial infection of the periodontal tissue resulting in destruction of the periodontal ligament and alveolar bone (Saini *et al.*, 2009). Periodontal disease has been associated as a potential risk factor identified pre-disease onset of RA (Potempa *et al.*, 2017; Kobayashi and Bartold, 2023). The bacterial species Prevotella intermedia and other Prevotella sp. (Lopez-Oliva *et al.*, 2019), Proteus sp.(Senior *et al.*, 1995; Newkirk *et al.*, 2005), A. actinomycetemcomitans (Konig *et al.*, 2016), Filifactor alocis, and Leptotrichia spp., collectively constitute microbes that are not only associated with periodontal diseases but have also been implicated in RA development as potential initiating triggers (Ogrendik, 2009; Saini *et al.*, 2009; Detert *et al.*, 2010; de Smit *et al.*, 2015; Chen *et al.*, 2018; Ayala Herrera *et al.*, 2019).

Porphyromonas gingivalis (P. gingivalis), the main causative agent of periodontal disease, can secrete the enzyme Peptidyl Arginine Deiminase 4 (PAD4) which catalyses the citrullination of arginine on native host peptides, an ability lacking in other oral cavity bacteria (Wegner *et al.*, 2010, Bernardoni *et al.*, 2024). Subsequently, this secretion of systemic immunogens leads to the production of rheumatoid factor-containing complexes promoting a humoral response and provoking inflammation (Rosenstein *et al.*, 2004). Antibodies against P. gingivalis are higher in RA patients and are strongly associated with ACPA+ patients suggesting immune responses against

these bacteria may aid in breaking immune tolerance to citrullinated antigens (Hitchon *et al.*, 2010). DNA of P. gingivalis can also be detected in the synovial fluid of some RA patients (Reichert *et al.*, 2013). Infection is not only considered as a risk factor for developing RA, but infection susceptibility due to RA treatment is also a concern. For example, patients undergoing anti-TNF treatments are at a greater risk for reactivating latent tuberculosis (TB), highlighting the need for prior TB screening and alternative treatment strategies to be implemented to reduce the incidence of TNF inhibitor-associated TB infections (Winthrop, 2006, Salgado and Gómez-Reino, 2011).

In addition to infections, risk of malignancy amongst RA patients is an area of concern. There is a moderate risk of 5-10% across malignancies, with a greater risk for lymphoma and lung cancer observed in RA patients (Simon *et al.*, 2015). The increased risk of some cancers, for example lung cancer, is potentially due to shared risk factors (like smoking) (De Cock and Hyrich, 2018). Lymphoma risk was associated with RA disease severity, with an 8-fold increase observed with moderate disease activity and a 70-fold increase observed for high disease activity (Baecklund *et al.*, 2006).

Malignancy risk is elevated further in RA patients that are on biological DMARDs due to a disruption of normal immunosurveillance as a result of directly modifying immunologic signaling pathways (Kim *et al.*, 2019). Anti-TNF treatments specifically, have been a point of concern as they appear to increase malignancy risk 2-to-3 fold in patients, however it is important to note that these were short-term studies conducted on small cohorts (De Cock and Hyrich, 2018). Other safety trials investigating the risk of treatments found little to no increased risk of malignancy as a result of tofacitinib treatment compared to TNF inhibitors while others have observed an increased risk of malignancy with tofacitinib and other JAK inhibitors, though malignancy was still considered a rare event (Khosrow-Khavar *et al.*, 2023, Russell *et al.*, 2023). There have been conflicting studies with some stating no increased risk of malignancy observed with biologic DMARD (bDMARD) use (Sepriano *et al.*, 2023). Because of this, it is important to continuously monitor RA patients on DMARD treatment to minimise the risk of malignancy development.

Interestingly, in some cases RA has been associated with a reduced risk of specific cancers including colorectal cancer compared to the general population due to immune-mediated inflammation (Li *et al.*, 2024). This decrease in risk of colorectal malignancy has been attributed to the use of NSAIDs and aspirin which have been known to decrease risk (Kauppi *et al.*, 1996; Din *et al.*, 2010; Hamoya *et al.*, 2016). Similarly, multiple studies identified a decreased risk of breast cancer in RA patients (De Cock and Hyrich, 2018).

1.9 Cardiovascular Comorbidities

Patients with RA are at higher risk of developing comorbidities. RA has the highest multimorbidity rate (26.6%) for three or more comorbidities compared to other forms of inflammatory arthritis such as PsA (16.8%) and axSpA (10.6%) (Gula *et al.*, 2024). In fact, cardiovascular disease (CV) (including stroke, myocardial infarction, and congestive cardiac failure, etc.), is the most common comorbidity, with a 48% increased incidence risk of suffering a CV event in patients with RA compared to the general population (Avina-Zubieta *et al.* 2012). However, other studies report this risk to be increased anywhere from 30-60% (Watson, Rhodes and Guess, 2003; Han *et al.*, 2006). As a result of CV comorbidity, mortality rates in RA patients are higher than in the general population (Solomon *et al.*, 2003; Boer *et al.* 2004; Hall and Dalbeth 2005). For patients with RA, CV events tend to occur earlier in disease (usually within the first seven years) compared to the general population in which cardiovascular disease is more associated with increasing age (Ajeganova *et al.*, 2013). Increased risk of CV in RA patients is independent of traditional CV risk factors (i.e. smoking, obesity, etc.) (Meyer *et al.*, 2018). Studies have implicated chronic subclinical inflammation as the mechanistic model for the development of CV in RA patients as it often precedes atherosclerosis and large artery dysfunction (Anyfanti *et al.*, 2024). Lipid metabolism abnormalities have also been demonstrated to accelerate atherosclerosis and increase CV risk and have been increasingly linked to RA pathogenesis (Lei *et al.*, 2023). In the general population, lipid profile levels are directly correlated with elevated risk of CV, however, lipoprotein levels are reduced in RA, yet CV risk is still increased, creating what is known as the 'lipid paradox' (Robertson *et al.*, 2013; Lei *et al.*, 2023). A longitudinal population-based study conducted on patients with RA reported nearly 50% of deaths (176/354) in this cohort (603 total patients), listing the primary cause as cardiovascular disease (Maradit-Kremers *et al.*, 2005). Higher ESR values and swelling of large joints at the time of RA onset were significant predictors. Over time, RF positivity, rheumatoid nodules, destructive changes on radiographs, and corticosteroid treatment, also increased the likelihood of death by cardiovascular disease. These markers are all indicative of systemic inflammation as well as RA disease severity (Maradit-Kremers, *et al.* 2005). Additionally, high levels of Acute Serum Amyloid A (A-SAA) can predict CV events over the course of long-term follow-up (Mullan *et al.*, 2010). Further serum proteomic profiling in both newly diagnosed and established RA patients demonstrated altered cardiometabolic and CV profiles with increased levels of CTSL-1 (endosomal enzyme involved in ECM degradation), SORT1 (regulator of lipid metabolism), SAA-4, TNFRSF10A, ST6GAL1 (sialyltransferase enzyme), and CCL18 observed in both cohorts (Cuesta-López *et al.*, 2024).

Due to a convergence of implicated inflammatory pathways (for example, IL-1 and IL-6 pathways) in RA and CV, controlling disease activity through treatment is imperative (Weber *et al.*, 2023). RA patients on DMARDs or TNF inhibitors had a decreased risk of both morbidity and mortality for CV (Micha *et al.*, 2011; Low *et al.*, 2017; Weber *et al.*, 2023). Therefore, proactive screening for subclinical CV as well as collaboration of care between rheumatologists and cardiologists are required for optimal management of CV risk in RA patients (Crowson *et al.*, 2014).

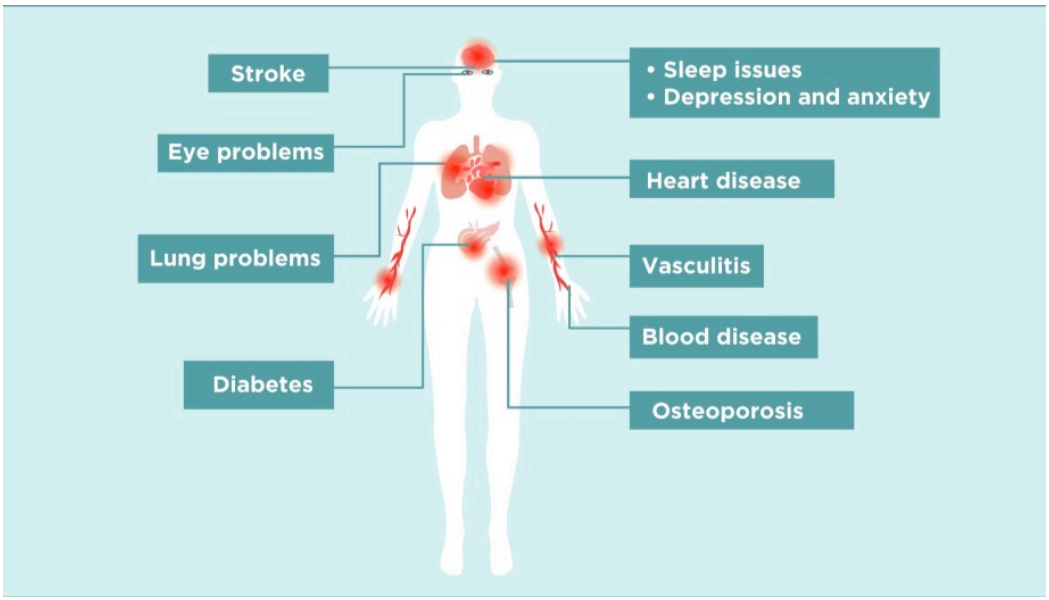

Figure 1.3: Schematic Overview of Comorbidities in Rheumatoid Arthritis.
List of common comorbidities associated with RA and the relative organs/locations that they affect. Cardiovascular disease (CVD) is the most common comorbidity associated with RA. (Image adapted from CreakyJoints.org).

CV is associated with endothelial dysfunction and arterial stiffness as a result of inflammation (Meyer *et al.*, 2018). Endothelial dysfunction, characterised by oxidative stress, inflammation, and nitric oxide (NO) dysregulation, plays an important role in CV and heart failure through the impairment of the vascular endothelium to perform normally (Premer *et al.*, 2019). Several biological markers have been previously proposed as indicators of endothelial dysfunction such as soluble sICAM-1, sVCAM-1, sE-selectin, and von Willebrand factor (Constans and Conri, 2006). However, the most well documented and established indicator of vascular damage is the increased presence of circulating endothelial cells (CECs) (Blann *et al.*, 2005; Goon, Boos, and Lip, 2005; Erdbruegger, Haubitz, and Woywodt, 2006; Wu, Chen, and Hu, 2007). CECs are mature ECs that have detached from the vessel wall, often due to a pathological insult or injury, and have entered the circulation (Blann *et al.* 2005; Boos, Lip, and Blann, 2006). Though CECs can be found in healthy individuals, EC shedding, and the renewal of the endothelial layer takes place at a low

replication rate of about 0-1% per day (Erdruegger, Haubitz, and Woywodt, 2006). CECs have now become more appreciated for their role as a biomarker for CV (Boos, Lip, and BLann, 2006; Farinacci *et al.*, 2018; Aulak *et al.*, 2024). In addition to CV, due to their association with endothelial injury, CECs have also been examined in other diseases associated with vascular dysfunction such as systemic sclerosis (SSc), systemic lupus erythematosus (SLE), septic shock, inflammatory vasculitis, and multiple cancers (Mutunga *et al.*, 2001; Woywodt *et al.*, 2003; Beerepoot *et al.*, 2004; Rajagopalan *et al.*, 2004; Boos, Lip, and Blann *et al.*, 2006; Di Martino *et al.*, 2021). Studies of CECs in the context of RA is limited and whether they have a role in RA pathogenesis independent of CV risk and involvement has yet to be determined.

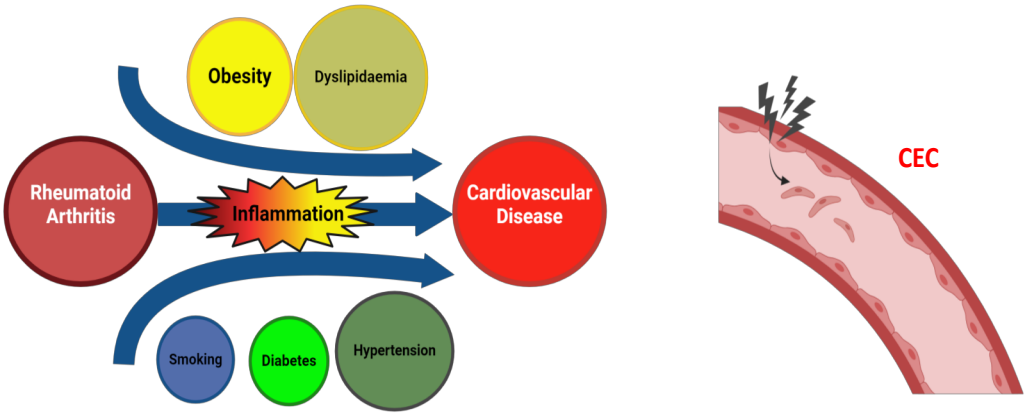

Figure 1.4: CVD Comorbidities in Rheumatoid Arthritis and Circulatory Endothelial Cells.
RA patients have an increased risk of developing CVD in part due to the chronic systemic inflammation observed within the disease. CVD often leads to vascular damage resulting in the shedding of endothelial cells into the circulation. Circulating endothelial cells (CECs) have become established indicators of vascular damage and considered a biomarker for CVD risk. (Image created using BioRender 2025).

1.10 Economic Burden

RA constitutes a substantial economic burden in the form of societal and medical costs. When estimating the total financial burden of illness, one must take into consideration direct costs (costs of medications and required monitoring when using), indirect costs such as loss of productivity (i.e. absenteeism, presenteeism, and/or unemployment) due to uncontrolled disease, and intangible costs (effects of pain and impact on quality of life) (Smolen *et al.*, 2018). RA results in higher average direct healthcare costs, out of pocket expenditures, and indirect costs of productivity reduction compared to other rheumatic diseases such as Ankylosing Spondylitis (AS) (Boonen and Mau, 2009). According to a 2009 study, the estimated annual excess health care costs of RA patients in the US was $8.4 billion with an additional $10.9 billion cost from additional

RA consequences (totalling $19.3 billion) with 33% of costs allocated to employers, 28% to patients, 20% to the government, and 19% to caregivers (Birnbaum *et al.*, 2010). Annual direct and indirect costs of the management of RA for over 2.3 million people in Europe is estimated to be over €45 billion (Lundkvist, Kastang, and Kobelt, 2008). Specifically, in Portugal, the economic impact of RA increased over the course of 10 years with annual costs amounting to an estimated €119,525,000 (Miranda *et al.*, 2012). In Ireland, in 2014, the combined estimated annual cost of OA and RA is €13.6 million (Doherty and O'Neill, 2014). More recently, a report from Arthritis Ireland estimated the average personal expenditure was €3,538 over a 12-month period (Sorensen *et al.*, 2024).

Absence from work due to RA can be significant during active disease but can occur in the early stages as well. The average number of absent days from work due to RA can range from 2.7-30 days/per annum (Cooper, 2000). Once RA patients have progressed to a point in the disease where they have reached an unemployed work state, the ability to return to work becomes even more difficult (Boonen and Severens, 2011). Indeed, results of 12 cross-sectional studies demonstrated that there is an increased risk for RA patients of having no paid employment or losing said employment within the first two years of diagnosis (Boonen and Severens, 2011). Similarly, cross-sectional and longitudinal studies observed that rates of work disability increased with disease duration, especially in US studies (Verstappen *et al.*, 2004). A recent sibling study aimed to examine the earnings of patients before and after diagnosis utilizing recent data along with sibling comparisons and observed that during the first five years after receiving a diagnosis, RA patients were found to earn 5.4% less annually compared to same-sexed siblings (Miller *et al.*, 2024). In Ireland, a survey found 70% of responders under current employment reported a loss of €3,111 in annual income due to arthritis (Sorensen *et al.*, 2024). In both studies, this discrepancy increased in older individuals.

The financial burden is even higher in non-responder patients cycling through different treatments, increasing the health care costs and the number of physician visits (Davis, 2019; Dalén *et al.*, 2020). One study, spanning three years, reported the cost of biologic therapies to be nearly three times the cost of non-biologic agents (Michaud *et al.*, 2003). However, some studies report that patients on anti-TNF therapies (i.e. adalimumab) had reduced workplace costs resulting from RA compared to other therapies ($9,071 compared to $16,335) (Birnbaum *et al.*, 2010). Early identification and referral models show promise in their ability to save the Irish health-care system an estimated €237,547 over a five-year period due to reductions in the number of general practitioner (GP) visits and diagnostic tests (Kelleher *et al.*, 2020). This alleviation of RA associated health costs is just one more example highlighting the importance of early detection for patients.

1.11 Normal Synovial Joint

A healthy synovial joint is a specialised structure composed of two bones encased within the joint capsule that facilitates frictionless and stable movement. Synovial fluid is produced within the joint to deliver nourishment to the cartilage, in addition to lubricating the inner surface of the capsule to help ensure frictionless movement (Smolen *et al.*, 2018; Veale DJ and Firestein GS, 2024). It contains hyaluronan (HA) which gives the fluid the required viscosity for its lubricating function (Tamer, 2013). Additionally, the articular surfaces of the opposing bones are covered by a layer of smooth cartilage. This is an avascular connective tissue in the form of a dense matrix composed of type II collagens and various proteoglycans (O'Connor, Orford, and Gardner, 1988; Martel-Pelletier *et al.*, 2008; Tamer, 2013; Veale DJ and Firestein GS, 2024). Externally, the synovial joint is surround by a fibrous capsule, which in addition to joint ligaments and muscle tendon insertions, serves to provide strength and flexibility support to the joint (Betts *et al.*, 2013).

The synovium is a thin tissue membrane that lines the non-articular surface of the joint comprised of the intimal lining layer (LL) spanning approximately 1-3 cells thick and the sub-lining layer (SL) (Smith *et al.*, 2003; Chu *et al.*, 2020; Veale DJ and Firestein GS, 2024). The lining layer is composed of two cell types: macrophages (Type A synoviocytes) and fibroblast-like synoviocytes (FLS) (Type B synoviocytes), which together through the expression of CX_3CR1 provide a protective barrier for the healthy joint from potential insults (McInnes and Schett, 2011; Firestein and McInnes, 2017, Culemann et al, 2019; Hanlon et al, 2024). Both cell types play an important role in maintaining synovial homeostasis, with the macrophages phagocytosing cellular debris in the intra-cellular space, while FLS secrete Lubricin and HA facilitating joint lubrication (Firestein *et al.*, 2016; Kurowska-Stolarska and Alivernini, 2017; Lee *et al.*, 2018; Hannemann, Apparailly, and Courties, 2021). Furthermore, the FLS also secrete fibronectin, laminin, proteoglycans, and collagens, key components of the extracellular matrix (ECM), thus playing a key role in physiological remodelling of the joint (Kular, Basu, and Sharma, 2014). Beneath the LL, is the SL (or intima layer) which contains a rich vascular capillary network embedded in a loose stromal matrix comprised of fibrous and adipose tissue (Walsh and Pearson 2001; Kennedy *et al.*, 2010; Ng *et al.*, 2010; Kennedy *et al.*, 2011; Smith, 2011; Kemble and Croft, 2021; Veale DJ and Firestein, 2024). This mature capillary network supplies nutrients directly to the LL and cartilage and maintains the appropriate oxygenation levels within the joint for cellular function (Ng et al, 2010; Kennedy et al, 2010/2011; Veale DJ and Firestein GS, 2024). FLS, however, can be found in both the LL and SL layers of the synovial tissue and studies have shown that they express key adhesion molecules such as cadherin 11 (Cad11), which helps maintain the dynamic structure of the tissue (Bottini and Firestein, 2013; Pap *et al.*, 2020). Due to its continuous exposure to weight bearing

stress and minor trauma, the bones within the joint are under constant degradation and remodelling to maintain the dynamic homeostatic structure (Iwanaga *et al.*, 2000; Kurowska-Stolarska and Alivernini, 2017).

1.12 Inflamed Joint Microenvironment

A fundamental feature of RA pathology is inflammation of the synovial joint. The inflamed joint is a dramatically different microenvironment compared to the healthy synovium and is the basis of joint damage, pain, and systemic manifestations in the disease. One of the earliest events contributing to synovial inflammation is the increased and dysregulated neo-angiogenesis (new blood vessel formation) facilitating the persistent influx of immune cells (monocytes, T cells, B cells, Dendritic cells (DCs), Natural Killer (NK) cells, mast cells, and neutrophils) into the synovial SL through a coordinated series of interactions including chemokine homing gradients and EC adhesion molecules, resulting in synovial expansion (Tak and Bresnihan, 2000; Walsh and Pearson, 2001; Smolen, Aletaha and McInnes, 2016; Orr *et al.*, 2017; Firestein and McInnes, 2017). The influx of immune cells leads to complex cell-cell interactions and the release of pro-inflammatory mediators, which in turn activate the LL FLS and other resident cells which together shape the formation of a tumour-like 'pannus' (Pillinger and Abramson, 1995; Tak and Bresnihan, 2000; Fearon *et al.*, 2003; Firestein and McInnes, 2017; Fearon and Szekanecz, 2020).

It was initially hypothesised that in the LL, FLS underwent active local proliferation, however, more recent studies have indicated that synovial FLS change from quiescence to semi-transformed, invasive cells with a more aggressive phenotype that are resistant to apoptotic mechanisms and play a central role in RA pathogenesis (Qu *et al.*, 1994, Muller-Ladner *et al.*, 1996; Ospelt *et al.*, 2004; Korb *et al.*, 2009; Filer, 2013; Ospelt, 2017; Marsh *et al.*, 2021). FLS in turn invade adjacent cartilage through the release of matrix metalloproteinases, and release bone degrading mediators such as RANKL, which when bound to its receptor on osteoclasts leads to the erosion of bone (Pap *et al.*, 2000; Goldring, 2003; Rengel *et al.*, 2007; Lefèvre *et al.*, 2009). In addition, FLS can also secrete pro-inflammatory mediators that can further potentiate pathogenic immune responses within the synovium and stimulate differentiation of infiltrating monocyte progenitors into osteoclasts to expedite bone reabsorption, thus further augmenting the inflammatory response within the joint resulting in debilitating and irreversible damage (Pap *et al.*, 2000; Gravellese *et al.*, 2000; Mor *et al.*, 2005; Mullan *et al.*, 2007; Tu *et al.*, 2018).

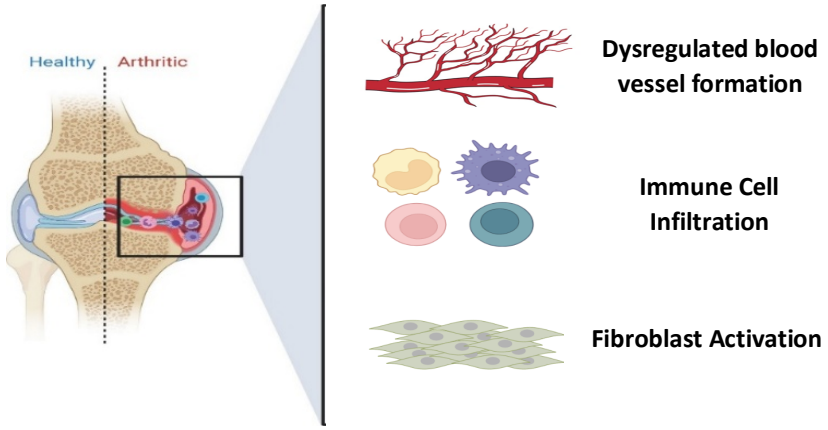

Figure 1.5: The Healthy Joint vs the Inflamed Synovium.
The inflamed joint microenvironment is due to an increase in dysregulated neoangiogenesis and blood vessel formation, facilitating the infiltration of immune cells from the circulation into the synovium where they then activate the tissue-resident FLS leading to cartilage destruction and bone erosion. (Image created in BioRender 2025).

1.13 Angiogenesis

Angiogenesis is the outgrowth and development of new blood vessels from pre-existing ones and is one of the earlier events in RA development (Balogh *et al.*, 2019). This facilitates the sufficient delivery of oxygen and nutrients to the synovial tissue however, when uncontrolled, allows the infiltration of pathogenic immune cells from the periphery into the inflamed joint microenvironment, thus promoting disease progression (Folkman *et al.*, 1989; Tas *et al.*, 2016; Markham *et al.*, 2006; Szekanecz *et al.*, 2010; Kennedy *et al.*, 2010; Fearon *et al.*, 2024). Distinct vascular patterns can be observed at the macroscopic level between RA and other arthropathies including PsA (Veale and Fearon, 2015). For example, the synovial vasculature in RA is comprised of straight regular branching vessels contrasting with the tortured, elongated, dilated vessels observed in PsA (Reece *et al.*, 1999; Fraser et al 2001; Fiocco *et al.*, 2001; Fearon *et al.*, 2003).

Under homeostatic conditions, the endothelial cells (EC) lining the blood vessel are in a quiescent state until they are activated by pro-angiogenic mediators leading to EC differentiation, proliferation, and migration (Potente *et al.*, 2011; Geudens and Gerhardt, 2011; Fearon *et al.*, 2024). In general, there are three EC subsets including, the tip cell, stalk cell, and phalanx cell, all of which have distinct cellular fates and functions (migration, proliferation and quiescence) (Dorrell *et al.*, 2002; Gerhadt *et al.*, 2003; Gerhardt and Betsholtz, 2005; Carmeliet *et al.*, 2009; Eelen *et al.*, 2013). Their distinct function is critical to the development of a proper functioning vessel, which is dependent on their spatial patterns and interactions within the inflamed

microenvironment. In this context, all three EC subtypes must "know" the phenotypic status of their neighbouring EC, which in turn determines their function.

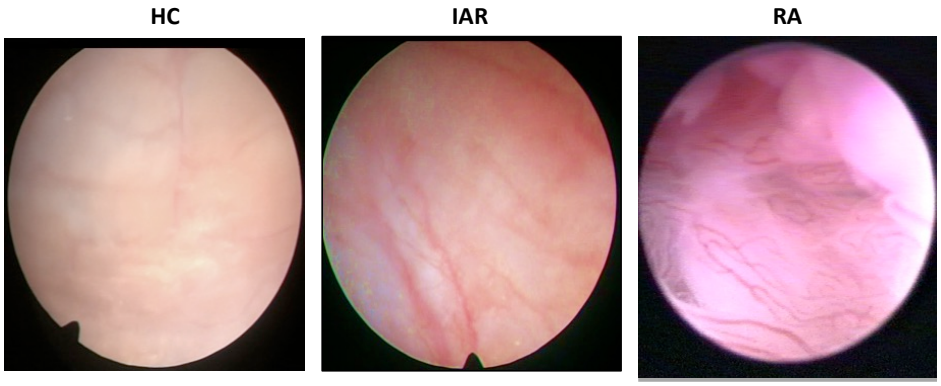

Figure 1.6: Representative Macroscopic Images of Synovial Blood Vessels.
Images obtained under direct visualisation using key-hole video arthroscopy. The minimal vessels observed in healthy control (HC) synovium nourish and oxygenate the joint. An increase in synovial blood vessels is observed in individual-at-risk (IAR). Increased angiogenesis is observed for Rheumatoid Arthritis (RA) evident by the straight regular branching vessels that typifies the morphology of blood vessels in RA. (Images courtesy of SVUH clinical team).

Vascular Endothelial Growth Factor (VEGF) is thought to be the 'master' regulator of sprouting angiogenesis, and studies have shown that it is increased in RA synovial fluid, and in the RA synovium both in the LL and SL (Fearon *et al.*, 1999; Reece *et al.*, 1999; Fraser, 2001; Fearon *et al.*, 2003; Coultas *et al.*, 2005; Fink *et al.*, 2007). Differential expression of other key angiogenic factors have also been demonstrated in the RA joint including angiopoietins (Ang1, Ang2), basic Fibroblast Growth Factor (bFGF), TNFα, IL-8, Transforming Growth Factor β (TGFβ), IL-18, and IL-1β (Creamer *et al.*, 1997; Fearon *et al.*, 1999; Fraser *et al.*, 2001; Fearon *et al.*, 2003; Kennedy *et al.*, 2010; Szekancez *et al.*, 2010; Volin and Koch, 2011).

The stability of blood vessels is of critical importance to maintaining the nutrient supply and oxygenation required for tissue function (Helfrich and Schadendorf, 2011). In healthy tissue, the pericytes confer vessel stability to ECs through tight-junctional complexes and an intact basement membrane (Fearon *et al.*, 2024). The tight alignment between ECs and pericytes is mediated by numerous growth factors and signaling pathways including platelet-derived growth factor (PDGF), Ang1, NOTCH signaling, Rho GTPases, and neural cellular adhesion molecule (NCAM) (Lindblom *et al.*, 2003; Bergers and Song, 2005; Xian *et al.*, 2006; Gerhardt and Semb, 2008; Kennedy *et al.*, 2010 Fearon *et al.*, 2024). The growth factors that the EC sense within the tissue microenvironment dictate the stability of the blood vessel, and key to this is the interactions between VEGF, Ang1, and Ang2. Activation of new blood vessel formation occurs in the presence of high levels of VEGF and Ang2 which interact to induce sprouting angiogenesis, a process that is

highly reliant on the NOTCH signaling pathway and tip-stalk cell lateral inhibition (Gao *et al.*, 2013). These blood vessels are immature and vulnerable as they lack pericyte coverage, thus if the levels of VEGF and Ang2 are inhibited the vessel will undergo regression through EC apoptosis. However, as the vessel matures, it becomes less dependent on VEGF, and instead Ang1, along with PDGF-B/PDGFR-β and TGFβ, signals the recruitment of pericytes to surround the EC wall. Intact junctional complexes and close EC-pericyte alignment are also regulated by NCAM (Xian *et al.*, 2006; Kennedy *et al.*, 2010).

Several studies have demonstrated a mixture of mature (with pericytes) and immature (without pericytes) blood vessels within the RA synovium, which is associated with differential growth factor expression (VEGF, Ang1 , Ang2, PDGF, TGFβ and NCAM), joint hypoxia, and increased oxidative damage (Creamer *et al.*, 1997; Fraser *et al.*, 2001; Fearon *et al.*, 2003; Izquierdo *et al.*, 2009, Szekanecz *et al.*, 2010; Kennedy *et al.*, 2010; Ng *et al.*, 2010; Volin and Koch, 2011;Biniecka *et al.*, 2014; Fearon *et al.*, 2024). These data suggest that synovial blood vessels are in a constant state of simultaneous angiogenesis, maturation, and regression depending on growth factor gradients sensed by ECs in the surrounding synovial microenvironment. The expanding synovium (due to the influx of immune cells) outpaces the dysfunctional vascular supply leading to a hypoxic microenvironment, with studies showing levels as low as 0.46% in the inflamed RA joint (Ng *et al.*, 2010). In turn, hypoxia further exacerbates angiogenesis, immune extravasation, and FLS expansion, perpetuating pannus expansion and joint destruction (Pugh and Ratcliffe, 2003; Ng *et al.*, 2010; Szekanecz *et al.*, 2010; Gao *et al.*, 2013; Gao *et al.*, 2015; Balogh *et al.*, 2019; Fearon *et al.*, 2016). Furthermore, these key growth factors and hypoxia can induce complex interactions between key signaling pathways including NFκB, mTOR, glycolysis, HIF1α, JAK/STAT, and NOTCH-DLL4 that regulate not only blood vessel function but also other cell types within the joint. Inhibition of these pathways reduce both angiogenesis and inflammatory mechanisms (Gao *et al.*, 2013; Gao *et al.*, 2015; Maracle *et al.*, 2017; McGarry *et al.*, 2018; Wade *et al.*, 2019). Finally, studies have shown that successful anti-TNF treatment promotes vessel stabilisation paralleled by decreases in cellular infiltrates, which are associated with improved clinical disease activity scores (Izquierdo *et al.*, 2009; Kennedy *et al.*, 2010).

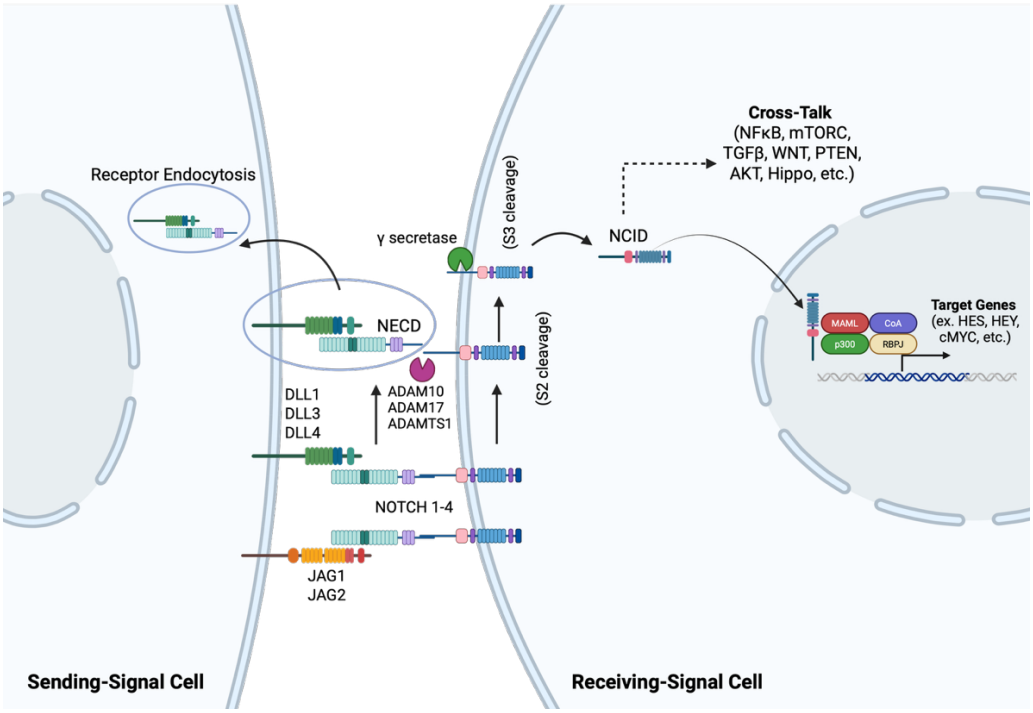

Figure 1.7: Schematic of General NOTCH Signaling Pathway.
Overview of the NOTCH signaling pathway. NOTCH Receptors are activated in the signal-receiving cell by binding to a ligand found on a neighboring cell (known as transactivation). The NOTCH ligands are then endocytosed by the signal-sending cell which results in cleavage of the extracellular portion of the NOTCH receptor exposing the S2 site for subsequent cleavage by ADAM metalloproteases (either ADAM10, 17, or TS1). The remaining portion of the NOTCH receptor in the membrane is further cleaved by γ secretase, releasing NICD into the cytoplasm where it then translocates to the nucleus. Within the nucleus it binds to RBPJ, facilitating further binding to transcriptional Co-A, MAMLs, and histone acetyltransferase p300 to activate transcription of target genes. NICD can also remain in the cytoplasm and crosstalk with other signaling pathways. NCID, NOTCH intracellular domain; MAML, mastermind-like; Co-A, coactivators; NECD, NOTCH extracellular domain. (Figure created using BioRender 2025; Adapted from (Zack et al., 2024)).

Leukocyte extravasation into the synovium is a multi-step process which involves cell 'rolling', activation, adhesion, and prolonged survival (Raza *et al.*, 2006; Schnoor *et al.*, 2015). Initially, weak adhesion or 'rolling' occurs within 1-2 h, mediated through the adhesion molecules P-selectin and L-selectin expressed on EC and their ligands. Subsequently, leukocytes are activated through their interactions with chemokine receptors (Szekanecz *et al.*, 2016; Tas *et al.*, 2016). This leads to stable intercellular adhesion, paralleled by chemokine secretion, and subsequent chemokine homing gradients. Finally, trans-endothelial diapedesis takes place where the secreted chemokines bind to heparin sulphate glycosaminoglycans expressed on EC. Leukocyte-EC adhesion is mediated through numerous cellular adhesion molecules (CAMs) which are subdivided into groups based on their structural properties; integrins, selectins, and the immunoglobulin gene superfamily (IgSF) CAMs and chemokines (Veale *et al.*, 1993; Koch, 2003; Klimiuk *et al.* 2009

). Once in the joint, leukocytes promote pro-inflammatory responses through cell-cell interactions, secretion of pro-inflammatory mediators, and cellular differentiation into more pathogenic phenotypes (Burman *et al.*, 2005).

1.14 Infiltrating Immune Cells

Cellular infiltrates include both innate and adaptive immune cells. The majority of innate immune cells involved in synovial inflammation are monocytes, DCs, and macrophages. Monocytes represent ~10% of the total circulatory leukocytes and are key players involved in the initiation of inflammation in RA (Italiani and Boraschi, 2014). They are characterised as a phenotypically heterogenic population of immune cells that have numerous key functions including: (i) the ability to phagocytose cellular debris and invading pathogens, (ii) the capacity to secrete a plethora of pro-inflammatory mediators, and (iii) the ability to differentiate into macrophages, DCs, and osteoclasts depending on which environmental cues they receive within the inflamed joint (Sudoł-Szopińska *et al.*, 2012; Rana *et al.*, 2018; Marzaioli *et al.*, 2020; Xue *et al.*, 2020). Monocytes have been shown to be metabolically rewired to support pro-inflammatory responses in RA and positively correlate with RA disease activity and treatment responses (Luo *et al.*, 2018; Zeisbrich *et al.*, 2018; Marzaioli *et al.*, 2020; McGarry *et al.*, 2021; Hanlon *et al.*, 2023). Furthermore, studies have shown that differentiated macrophages maintain the pro-inflammatory and metabolic memory bias of their precursor monocyte phenotype, a profile that is even present pre-disease onset in IAR (Zeisbrich *et al.*, 2018; Hanlon *et al.*, 2023). Studies have also demonstrated that RA monocytes may display priming properties that define the route of differentiation into DCs, macrophages, or osteoclasts (Guo *et al.*, 2017; Marzaioli *et al.*, 2017; Zeisbrich *et al.*, 2018; Marzaioli *et al.*, 2020; Marzaioli *et al.*, 2022; Hanlon *et al.*, 2023). In addition, Mo-DC priming and activation are regulated by specific therapeutic treatments, being sensitive to JAK/STAT inhibition, but not TNFα inhibition (Marzaioli *et al.*, 2020; Marzaioli *et al.*, 2022). Single-cell technology of cellular subsets has significantly advanced in recent years, however, the majority of studies have focused on three main monocyte subsets based on the expression of CD14 and CD16, which characterises monocytes into three main subsets: classical monocytes (CD14+CD16-), intermediate monocytes (CD14+CD16+), and non-classical monocytes (CD14dimCD16+) (Kapellos *et al.*, 2019). The classical CD14+CD16- compartment are thought to display enhanced phagocytosis properties and to be the circulating precursors of DC and osteoclasts responsible for bone erosion in the RA joints (Komano *et al.*, 2006; Yang *et al.*, 2014; Boyette *et al.*, 2017). The intermediate subgroup is thought to skew towards a more pro-inflammatory phenotype and are potent producers of many pro-inflammatory cytokines (Rossol *et al.*, 2012; Klimek *et al.*, 2014; Yang *et al.*, 2014; Tsukamoto *et al.*, 2017). Finally, non-classical monocytes account for between

5-10% of total monocytes and patrol the vascular endothelium at the time of tissue injury, but studies have also suggested they are primed to differentiate into anti-inflammatory macrophages (Misharin *et al.*, 2014; Thomas *et al.*, 2015; Boyette *et al.*, 2017). Finally, analysis of circulatory monocytes has demonstrated increased levels early in RA disease, correlation with disease activity, and response to therapy (Coulthard *et al.*, 2012; Lou *et al.*, 2018; Marzaioli *et al.*, 2020; McGarry *et al.*, 2021).

Macrophages are essential regulators in RA due to their presence in large numbers in the inflamed synovium and their decrease following patient response to treatment, underpinning their importance in the pathogenesis of RA (Mulherin *et al.*, 1996; Smolen and Steiner, 2003; Haringman *et al.*, 2005). Macrophages are the key producers of the most crucial RA-associated cytokines – TNFα, IL-1β, and IL-6. In addition to the production of cytokines, macrophages release matrix-degrading enzymes, present antigen, phagocytose, and drive bone resorption (Szekanecz and Koch, 2007; Drexler *et al.*, 2008; McInnes & Schett, 2011). Indeed synovial SL frequency of macrophages has been shown to be the only synovial cellular biomarker to date that correlates with treatment response, independent of what treatment is utilised (Haringman *et al.*, 2005; Bresnihan *et al.*, 2007; Bresnihan *et al.*, 2009). However, it is now clear that macrophage phenotypes within the joint are more complex than this simplistic view, displaying remarkable plasticity and diversity in response to environmental cues, giving rise to different macrophage populations that lie between these two terminals (Culemann *et al.*, 2019; Kuo *et al.*, 2019; Alivernini *et al.*, 2020; Kemble and Croft, 2021; Hanlon *et al.*, 2024). An eloquent study conducted by Culemann et al (2019), demonstrated that depletion of CX_3CR1+ lining macrophages in mouse-models of arthritis resulted in the breakdown of the synovial macrophage-FLS protective barrier, which is further supported by a recent study in humans which demonstrated that breakdown of this protective barrier preceded clinical manifestations of disease in RA (Hanlon et al 2024). Studies by our group and others have identified distinct macrophage phenotypes in RA associated with disease activity (CD163+CD206+CD40+), acute and chronic inflammation (SLAMF7+macrophages) and remission (MerTK+) (Alivernini *et al.*, 2020, Simmons *et al.*, 2022, Huang *et al.*, 2021; Hanlon *et al.*, 2024).

Dendritic cells (DC) are the major professional antigen-presenting cell (APC) which, following their activation, differentiate and migrate to lymphoid tissues where they display antigens to naïve T cells, which in turn activates the adaptive immune response (Gierut *et al.* 2010). DC subsets are classified based on specified function, origin, and their maturation profile (Shortman and Liu, 2002). In the immature state, DCs display enhanced phagocytic and migratory capacity but express low levels of key costimulatory markers, CD80, CD86, and CD40. However,

following DC activation and maturation, DCs secrete high levels of pro-inflammatory mediators, and express high levels of costimulatory markers and the chemokine receptors CCR7 and CXCR3, which induce DC migration and homing to lymph nodes and inflamed tissues (Dalod *et al.*, 2014). The main DC subsets identified to date include: CD141+ DCs (cDC1), CD1c+ DCs (cDC2), and DC3 which are phenotypically and functionally distinct (Breton *et al.*, 2016; Canavan *et al.*, 2018; Collin and Bigley, 2018; Rhodes *et al.*, 2019; Bourdely *et al.*, 2020; Canavan *et al.*, 2021). Few studies have analysed DC subsets within the blood or tissue of RA patients due to their low frequency and complexity. In the context of RA, CD1c+ DCs have been described in the peripheral blood of early and established RA patients where their diminished frequency is inversely correlated with disease activity (Cooles *et al.*, 2018; Canavan *et al.*, 2021). Increased frequency of CD1c+ DCs in RA SF have been identified, with enhanced frequencies observed in the RA synovium compared to osteoarthritis (Jongloed *et al.*, 2006, Moret *et al.*, 2013). Segura *et al.* also identified enrichment of a novel inflammatory DC subset in the SF of RA patients (Segura *et al.*, 2013). Furthermore, CD1c+ DC frequency is increased in the inflamed IA synovium where they are present in a distinct poly-maturational state compared to circulatory CD1c+ DC (Canavan *et al.*, 2021). Distinct transcriptional signatures have been demonstrated for joint specific CD1c+ DCs and CD141+ DC (Canavan *et al.*, 2021). Furthermore, synovial CD141+ DC induce CD4+ and CD8+ T cell responses, and can activate synovial FLS, inducing adhesive and invasive pathogenic mechanisms (Canavan *et al.*, 2018). A novel monocyte-DC intermediate subset (CD209/CD14+ DCs) is significantly enriched in RA compared to HC and display unique chemokine homing receptors and higher cytokine producing capabilities, effects that are mediated through NOX5-dependent ROS signaling and reversed by JAK-STAT inhibition (Marzaioli *et al.*, 2020, Marzaioli *et al.*, 2022). Finally, the synovial joint microenvironment induces Mo-DC to become more activated, a phenotype that is accompanied by an altered metabolic profile (Canavan *et al.*, 2020).

The RA inflamed synovium also contains adaptive immune cellular infiltrates. These are mainly T cells and B cells composing between 30-50% and 5%, respectively (Duke *et al.*, 1982). Lymphoid aggregates are easily identified in perivascular regions of inflamed synovial tissue, though T and B cells are also found scattered throughout the synovial tissue (Iguchi & Ziff, 1986; Baeten *et al.*, 2005; Orr *et al.*, 2017; Rivellese *et al.*, 2022). Several studies have shown large follicular lymphocyte aggregates are associated with higher disease severity compared with diffusely infiltrated synovial tissue and may be a predictor of a poorer response to therapy (Cañete *et al.*, 2009; Klimiuk *et al.*, 2003; Humby *et al.*, 2019; Lliso-Ribera *et al.*, 2019; Rivellese *et al.*, 2020). Indeed, recent studies have shown T cells and B cells are associated with partial disease pathotype,

defined as cell-type abundance phenotypes (CTAPs), which were associated with cytokines levels, risk genes, histology, serology metrics, and treatment response (Zhang *et al.*, 2023).

Numerous T cell subsets have now been identified including Type 1 helper T cells (Th1), natural killer T cells (NKT), regulatory T cells (Tregs), Th17 helper cells (Th17), and ex Th17 (Lubberts *et al.*, 2005; Fletcher *et al.*, 2009; Miossec *et al.*, 2009; Raychaudhuri *et al.* 2012; Basdeo *et al.*, 2015; Basdeo *et al.*, 2017). Using global transcriptomic analysis, our group identified five synovial T cell clusters, with enriched frequencies of CD4+ clusters in RA, consistent with previous studies (Costello P *et al.*, 1999, Floudas *et al.*, 2022). A significant reduction in CD4+ T cells in TNFi responders has been observed, with minimal change demonstrated for CD8+ T cells (Choy *et al.*, 1996; Veale *et al.*, 1999; Mason *et al.*, 2002). This is consistent with the hypothesis that CD4+ T cells are crucial in initiating and driving specific immune responses (Choy *et al.*, 1996; Veale *et al.*, 1999; Mason *et al.*, 2002). A subset of PD1hiCXCR5-CD4+ T cells have been identified in the RA synovium and periphery, which drive B cell responses and antibody production (Rao *et al.*, 2017). Furthermore, CD69 and/or CD103 expressing T cells, which are defined as tissue-resident memory T cells, have also been identified in the RA joint and display different immune functions compared to that of PsA (Masopust and Soerens, 2019; Povoleri *et al.*, 2023). While studies have shown enrichment of Th17 T cells in the RA joint and shown increased expression their IL-17 receptors, RA does not respond to anti-IL17A therapies. This may be due to heterogeneity in expression patterns across patients, but also the observed enrichment of ex-Th17 cells in RA (Van Barsen *et al.*, 2014; Basdeo *et al.,* 2017). Finally, a recent study by Floudas *et al.*, demonstrated increased plasticity of Tfh cells and CD4 T cell polyfunctionality in RA synovial tissue, which are also present pre-disease onset, with implications for therapeutic intervention in early in disease (Floudas *et al.*, 2022).

Furthermore, B cells within the joint are mainly localised to B cell aggregates. These cells are responsible for the production of antibodies. Previous studies have indicated that seropositivity for ACPA and synovial B cells may be a predictor of chronic inflammation and relate to changes observed in radiographic erosion (Teng *et al.*, 2007; Gerlag *et al.*, 2012; Orr *et al.*, 2017). The interplay between B cells and its chemoattractant CXCL13 have also been studied; indeed, CXCL13 redistributes B cells into the inflamed tissue and enhances BCR-mediated activation (Corsiero *et al.*, 2012). Development of B cell targeted therapies, like rituximab (anti-CD20), were based on investigations in animal models where decreased expression of B cells reduced severity of disease (Hamel *et al.*, 2008), and through identification of the antigen presenting properties of B cells which may be important in T cell activation in inflamed joints (Takemura *et al.* 2001).

1.15 Inflammatory Cytokines and Chemokines

Cytokines are soluble or membrane bound proteins that are transmitted between cells and have broad functionality including the regulation of cell replication, differentiation, cell survival and death, and tissue repair and fibrosis (Choy and Panayi, 2001; McInnes and Schett, 2007; Alunno *et al.*, 2017). Cytokines can be pleotropic (having multiple biological properties) depending on the context and target, however, generally they can broadly be classified into pro-inflammatory and anti-inflammatory and finding the balance between the two is crucial in therapeutically targeting disease (Lubberts and van den Berg, 2003).

The interleukin-1 (IL-1) family of cytokines is more closely linked to innate immunity more than any other cytokine and was the first to be identified in RA synovial fluid in 1982 (Fontana *et al.*, 1982). In addition to IL-1β, the other key cytokine associated with RA pathogenesis is TNFα (Kay and Calabrese, 2004; McInnes and Schett, 2007). Both cytokines are potently produced by macrophages and play an integral role in the communication between the multiple cell types within the joint (Ruschen *et al.*, 1989; McInnes and Schett, 2007; Agbanoma et a., 2012). IL-1β, for example, can act as an angiogenic factor and is responsible for upregulating CAMs on ECs, as well as the production of numerous chemokines, thus aiding in immune cell infiltration into the joint (Proudman *et al.*, 1999; Honorati *et al.*, 2004; Dinarello, 2009; Guo *et al.*, 2018). Furthermore, IL-1β stimulates synovial FLS and chondrocytes to release MMPs resulting in cartilage degradation and induces the secretion of additional pro-inflammatory cytokines (i.e. IL-6) through various signaling pathways (Deon *et al.*, 2001; Kay and Calabrese, 2004; Fearon *et al.*, 2006; Yeon-Ah *et al.*, 2012). TNFα promotes inflammation by acting as an autocrine stimulator and paracrine inducer of other inflammatory cytokines such as IL-1, IL-6, IL-8, and granulocyte-monocyte colony-stimulating factor (GM-CSF) (Hanlon *et al.*, 2019; McInnes and Schett, 2007). Like IL-1β, TNFα can also stimulate FLS, promoting cytokine, chemokines, MMP secretion, adhesion molecule expression, and osteoclast activation markers. Other pro-inflammatory cytokines that have been identified in the RA synovium are IL-6, IFNγ, M-CSF, GM-CSF, and IL-17 amongst others (Hopkins and Meager, 1988; Firestein *et al.*, 1988; Xu *et al.*, 1989; Chabaud *et al.*, 1999; Choy and Panayi, 2001; Wood *et al.*, 2008; McInnes, Buckley and Isaacs, 2016).

Anti-inflammatory cytokines are also present within the inflamed synovium, with IL-10 regarded as the most potent with an ability to inhibit Th1 cell activity by suppressing IFNγ expression (Lubberts and van den Berg, 2003). Additionally, IL-4 and IL-13 are also immunomodulatory cytokines. Studies have shown that IL-4 can inhibit Th1 cells and decrease the production of IL-1β, TNFα, IL-6, and IL-8 (Levings and Schrader, 1999; Raingeaud *et al.*, 2005; López-Bravo *et al.*, 2013; Onderdijk *et al.*, 2015). TGFβ has also been identified within the

synovium, with studies demonstrating its ability to both perpetuate and dampen the immune response. Floudas *et al.* (2022), demonstrated a synergistic pro-inflammatory effect in RA FLS when stimulated with both IL-1β and TGFβ. However, TGFβ can also suppress autoimmunity via its influence on Tregs (Marie *et al.*, 2005).

Chemokines are chemoattractant cytokines responsible for leukocyte chemotaxis and migration through the endothelial barrier (Chen, Oppenheim, and Howard, 2004). Chemokine receptors are noted as either CXCR, CCR, CR, or CX_3CR and their ligands as CXCL, CCL, CL, and CX_3CL based on their cysteine residue location (Bacon *et al.*, 2002; Murayama *et al.*, 2023).

Multiple chemokines have been identified in the synovial tissue, fluid, and sera of patients with RA (Hosaka *et al.*, 1994; Kraan *et al.*, 2000; McKinney *et al.*, 2008; Endres *et al.*, 2010; Huang *et al.*, 2019; Aldridge *et al.*, 2021; Murayama *et al.*, 2023). Some studies have demonstrated the correlation of serum levels of chemokines to disease activity, suggesting their potential as a possible biomarker (Kuan *et al.*, 2010; Pandya *et al.*, 2017; Bechman *et al.*, 2020). Resident synovial macrophages, FLS, and ECs are all major producers of chemokines (Szekanecz *et al.*, 2010; Murayama *et al.*, 2023). Chemokines aid in cellular infiltration and migration, cellular adhesion, cytoskeleton rearrangement, and angiogenic processes (Middleton *et al.*, 1997; Szekanecz *et al.*, 2010; Cambier *et al.*, 2023). Two key chemokines involved in inflammatory arthritis are CXCL8 and CXCL1 which promote neutrophil recruitment to the site of inflammation (Brennan *et al.*, 1990; Koch *et al.*, 1991; Hou *et al.*, 2020; Li *et al.*, 2023). In addition, CXCL12 has been implicated as an important chemokine in the synovium and in RA FLS subsets, and actives FLS pathogenic and survival pathways (Bradfield *et al.*, 2003; Yang *et al.*, 2018; Kuang *et al.*, 2020; Smith *et al.*, 2023). Monocyte chemoattractant protein 1 (MCP-1/CCL2) and Regulated upon Activation Normal T Cell Expressed and Secreted (RANTES/CCL5) are common chemokines found within the RA synovium and attract monocytes, NK cells, and T cells (Deshmane *et al.*, 2009; Szekanecz *et al.*, 2010; Pavkova Goldvergova *et al.*, 2012). Finally, CXCR13 has been implicated in B cell recruitment and associated with the presence of B cell lymphoid aggregates and worse disease activity in RA (Orr *et al*., 2017).

1.16 Synovial Fibroblasts

Fibroblast-like synoviocytes (FLS) are the resident mesenchymal cells of the synovium and were first described as a key cell-type within the inflamed synovium in 1983 by Fassbender *et al.*, (1983). These resident stromal cells, identified by their expression of vimentin and various collagens, are normally found within the healthy joint as part of the thin lining layer along with resident macrophages. They help build the structural framework of the tissue by producing extracellular matrix components and assist in its maintenance by secreting HA and lubricin for lubrication

(Bartok and Firestein, 2010). However, studies have demonstrated that in RA, FLS adopt an aggressive, invasive phenotype and are key active drivers of joint destruction in RA (Müller-Ladner *et al.*, 1996; Seemayer *et al.*, 2003; Lefèvre *et al.*, 2009; Ospelt, 2017).

RA FLS are active drivers of joint destruction due to their ability to produce pro-inflammatory cytokines, MMPs, and invade collagen and articular cartilage (Bartok and Firestein, 2010; Ospelt, 2017). Indeed, RA FLS secrete multiple pro-inflammatory mediators such as VEGF, IL-6, IL-8, MCP-1, GM-CSF, and RANKL further amplifying and perpetuating joint inflammation (Nanki *et al.*, 2001; Mor, Abramson, and Pillinger, 2005; Ryu *et al.*, 2006; Darrieutort-Laffite *et al.*, 2014; Kim *et al.*, 2015). Specifically, RA FLS and resident macrophages can modulate one another in a positive feedback loop via paracrine and autocrine networks, thus exacerbating and perpetuating their inflammatory effects (Sweeney and Firestein, 2004; Ospelt, 2017). Furthermore, studies have demonstrated RA FLS display increased frequency of the cell-surface expression of adhesion molecules (i.e. ICAM-1, VCAM-1, cadherin 11, integrins) and an ability to secrete MMPs (Morales-Ducret *et al.*, 1992; Müller-Ladner *et al.*, 1996; Rinaldi *et al.*, 1997; Tolboom *et al.*, 2002; Valencia *et al.*, 2004; Køster *et al.*, 2021).

In recent years, with the advances of single-cell technologies, it has become apparent that RA FLS are not a homogenous cell population as previously thought. Studies have identified and begun to characterise distinct FLS subsets within the RA synovium (Croft *et al.*, 2016; Mizoguchi *et al.*, 2018; Croft *et al.*, 2019; Zhang *et al.*, 2019; Wei *et al.*, 2020; Floudas *et al.*, 2022; Smith *et al.*, 2023; Zhang *et al.*, 2023). Particularly within the SL layer, multiple unique FLS subsets have been identified with some exhibiting a more pro-inflammatory and/or invasive phenotype, while others appear to be involved in the resolution of inflammation (Mizoguchi *et al.*, 2018; Croft *et al.*, 2019; Wei *et al.*, 2020; Kemble and Croft, 2021; Marsh *et al.*, 2021; Floudas *et al.*, 2022; Smith *et al.*, 2023; Rauber *et al.*, 2024). Furthermore, perivascular FLS subsets co-localising with ECs have demonstrated increased expression of NOTCH3, believed to be involved in driving FLS identity and differentiation (Wei *et al.*, 2020; Smith et a., 2023). Additionally, synovial FLS from different anatomical locations demonstrate specific transcriptomic and epigenetic signatures which result in site-specific phenotypes (Chang *et al.*, 2002; Frank-Bertoncelj *et al.*, 2017; Korsunsky *et al.*, 2022; Buckley and Ospelt, 2021).

Despite the tissue residency of these cells, studies have demonstrated the ability of human RA FLS to migrate substantial distances through the vasculature. Indeed, studies conducted in SCID mice chimera models have demonstrated the ability of RA FLS to migrate through the circulation to directly invade and degrade contralaterally located cartilage (Lefèvre *et al.*, 2009). A study in the New England Journal of Medicine recently identified circulating 'pre-

inflammatory mesenchymal' (PRIME) cells in the vasculature of RA patients just before a disease flare. RNA-seq identified a gene signature within these cells, characteristic of FLS (Orange *et al.*, 2019). Their increased numbers just before symptom flare and subsequent decrease suggest that these PRIME cells may be entering into the joint, perpetuating disease progression.

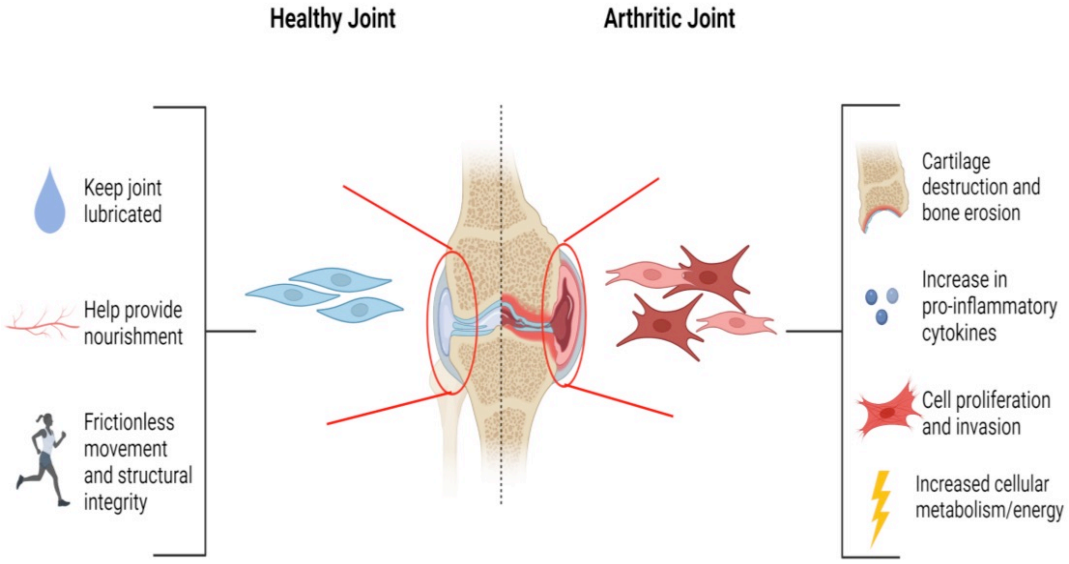

Figure 1.8: Synovial Fibroblast Function in Health and Disease.
FLS are one of the main tissue resident cells found within the synovium. In health, these cells are responsible for lubrication, nourishment, and frictionless movement; however, within the inflamed RA joint, FLS adopt a more aggressive phenotype marked by an increase in cellular metabolism, cellular proliferation and invasion. RA FLS also secrete pro-inflammatory cytokines and mediators such as RANKL which activate osteoclasts, resulting in synovial inflammation, cartilage destruction and bone erosion. (Image created in BioRender 2025).

1.17 Overview of Cellular Metabolism

Cellular metabolism can be broadly defined as the sum of all biochemical processes involving the production, consumption, or use of energy by living organisms (Zhu and Thompson, 2019). These processes encompass several hundred simultaneous reactions and numerous metabolites (Judge and Dodd, 2020). At its core, metabolism can be simplified into pathways utilizing essential nutrients including carbohydrates, amino acids, and fatty acids, all of which are crucial for the synthesis of macromolecules and energy homeostasis (DeBerardinis and Thompson, 2012).

Two main metabolic pathways currently at the forefront of research are glycolysis and oxidative phosphorylation (OXPHOS). The utilisation of these pathways is dependent on intrinsic and extrinsic factors such as oxygen availability and environmental stress. Glycolysis commences

with the uptake of glucose from the surrounding environment and is subsequently irreversibly phosphorylated into glucose-6-phosphate (G6PD). Each molecule is then further oxidised through a series of anaerobic steps resulting in the generation and release of two molecules of pyruvate and two molecules of ATP. Under normoxic conditions where sufficient oxygen is present, pyruvate molecules are then decarboxylated by pyruvate dehydrogenase (PDH) before entering the tricarboxylic acid (TCA) cycle within the mitochondrial matrix. Next, the electron carriers, nicotinamide adenine dinucleotide (NADH) and flavin adenine dinucleotide-2 ($FADH_2$), being major products of the TCA cycle, transfer electrons to the electron transport chain (ETC). Other metabolites such as succinate and oxidated fatty acids also enter the ETC. This complex is composed of five large protein structures that are embedded into the inner mitochondrial membrane and are referred to as Complex I-VI and ATP synthase (Complex V). Electrons are shuttled across the complexes in the ETC creating a proton gradient which ATP synthase then utilises to produce 36 ATP molecules. Reactive oxygen species (ROS), CO_2, and H_2O are additional byproducts of this process, collectively known as OXPHOS (Chaban, Boekema and Dudkina, 2014; O'Neill, Kishton, and Rathmell, 2016; Fearon *et al.*, 2019).

When oxygen is not present, OXPHOS cannot occur, and the cell must solely rely on anaerobic glycolysis. The two pyruvate molecules generated at the end of glycolysis are directed away from the TCA cycle and instead converted into lactate via lactate dehydrogenase (LDH) in the cytosol of the cell, resulting in a net yield of just two ATP molecules. Glycolysis is often regarded as an inefficient means for ATP production compared to OXPHOS; however, anaerobic glycolysis allows for rapid energy generation even during environmental stress or conditions where oxygen is low or not present (Senyilmaz and Teleman, 2015). Another benefit of glycolysis is that it produces multiple intermediate metabolites that can be used in parallel with biosynthetic growth pathways to further support anabolic growth of the cell. G6PD, for example, can be used by the pentose phosphate pathway to generate amino acids, NADPH, and ribose for nucleotide synthesis (Buchakjian and Kornbluth, 2010; García-Domínguez *et al.*, 2022). Additionally, glycolytically reduced NADH (an important cofactor) can be recycled back into NAD+ maintaining glycolytic flux, thus resulting in pyruvate being reduced to lactate (O'Neill, Kishton and Rathmell, 2016).

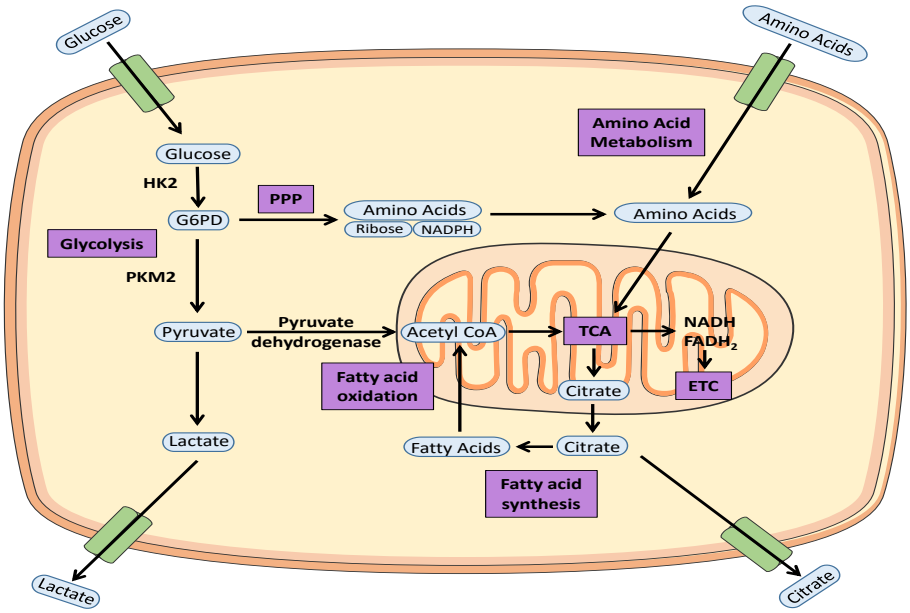

Figure 1.9: Pathways of Cellular Metabolism.
Glucose enters the cell via glucose transporters and enters the glycolytic pathway. Hexokinase 2 (HK2) converts glucose into glucose 6-phosphate dehydrogenase (G6PD). Glycolysis generates pyruvate from glucose with the help of pyruvate kinase M2 (PKM2). This process generates energy in the form of adenosine triphosphate (ATP). Pyruvate is then either converted to lactate and secreted out of the cell or decarboxylated by pyruvate dehydrogenase and converted to acetyl CoA, which enters the tricarboxylic acid (TCA) cycle. The TCA cycle generates nicotinamide adenine dinucleotide (NADH), flavin adenine dinucleotide (FADH2) to feed into the electron transport chain (ETC), which produces 36 molecules of ATP. Glycolysis also feeds into the pentose phosphate pathway (PPP) to produce ribose, NADPH and amino acids. Amino acid metabolism can also feed into the TCA cycle to drive ATP production by the ETC. TCA intermediate citrate drives fatty acid synthesis, while fatty acid oxidation drives the TCA cycle further by generating acetyl CoA. (Figure taken from Fearon et al. Clinical Experimental Immunology 2019).

Other metabolic pathways are also used by the cell to ensure sufficient energy levels for proper function. As previously mentioned, the pentose phosphate pathway (PPP) takes place within the cell cytosol and utilises glycolytic intermediate metabolites to produce nucleotide precursors and amino acids, both essential for cell proliferation and growth. Multiple metabolic pathways utilise amino acids as substrates highlighting the importance of amino acid metabolism. In addition, fatty acid synthesis is needed to produce cellular lipids and is linked to the mammalian target of Rapamycin (mTOR), a master regulator of cellular metabolism (O'Neill, Kishton, and Rathmell, 2016). After synthesis, fatty acids can then take part in the fatty acid oxidation pathway where they are converted, via the mitochondria, into acetyl CoA, NADH, and additional cofactors needed for further energy production. Significant cross communication between metabolic pathways and their metabolites occurs, leading to complex pathway interactions. For example, the PPP and TCA cycles produce NADPH and citrate, respectively, which can be utilised in fatty acid synthesis. Fatty acid oxidation can drive the ETC by providing NADH and $FADH_2$. Products from

amino acid metabolism can feed into the TCA cycle and specifically, the amino acid glutamine can act as a source of citrate for additional fatty acid synthesis (O'Neill, Kishton, and Rathmell, 2016).

1.18 Hypoxia, Metabolism, and RA

Despite the increase in angiogenesis and new vasculature in the inflamed joint, the combination of dysregulated architecture of the microvasculature, an influx of immune cells and proliferation of resident stromal cells leads to an oxygen-deprived, hypoxic environment (Kennedy *et al.*, 2010; Biniecka *et al.*, 2016; Fearon *et al.*, 2016). Hypoxia can be defined as an imbalance between the supply and demand for oxygen, which varies depending on the specific organ or tissue in the body (McGarry *et al.*, 2018). It has been previously demonstrated that a correlation exists between oxidative damage and inflammation of synovial tissue and the hypoxic joint environment (Biniecka *et al.*, 2010; Biniecka *et al.*, 2014). Increased expression of hypoxia-inducible factor-1 alpha (HIF1α), a master regulator of hypoxia, has been demonstrated in both the lining and sub-lining cells of the joint (Giatromanolaki *et al.*, 2003; Guo and Chen, 2020). It is possible that a hypoxic gradient may exist within the inflamed synovium, the extent of which would depend on the distance of synovial cells in the tissue from the blood vessels (McGarry *et al.*, 2018). In the inflamed joint, this hypoxic environment correlates with disease activity, increased number of immune cells (T cells and macrophages), and with mtDNA mutations (Ng *et al.*, 2010; Kennedy *et al.*, 2011; Biniecka *et al.*, 2011; Biniecka *et al.*, 2011; Biniecka *et al.*, 2016). Furthermore, hypoxia altered immune cell responses, induces cytokine levels, ROS, and mitochondrial dysfunction in FLS and ECs *in vitro*, effects that are mediated by key signaling pathways including HIF1α, NOTCH, and JAK-STAT (Biniecka *et al.*, 2011; Gao *et al.*, 2012; Gao *et al.*, 2013; Gao *et al.*, 2015; Wade *et al.*, 2019).

This increase in metabolic activity within the joint is evidenced by increased levels of metabolic intermediates including lactate, succinate, glutamine, and itaconate (Treuhaft and McCarty, 1971; James, Cleland, and Rofe, 1992; Kim *et al.*, 2014; Michopoulos *et al.*, 2016). These in turn have the capacity to activate synovial cells, further perpetuating disease (Biniecka et al 2016: McGarry *et al.*, 2018; Ahmed *et al.*, 2023; Pucino *et al.*, 2023). Lactic acid for example, enhances the secretion of IL-6 and IL-23 from monocytes and macrophages, increases IL-17 production, while simultaneously inhibiting T cell motility, and facilitates RA FLS invasiveness (Shime *et al.*, 2008; Samuvel *et al.*, 2009; Witkin *et al.*, 2011; Haas *et al.*, 2015; McGarry *et al.*, 2018; Caslin *et al.*, 2021). Additionally, activated ECs heavily rely on glycolysis and further contribute to elevated lactate levels within the joint (De Bock *et al.*, 2013; Cruys *et al.*, 2016). Elevated lactic acid levels within the joint are also correlated to increased levels of cytokines, FLS invasive mechanisms, and disease activity scores (Troughton, *et al.*, 1996; Biniecka M et al 2016; Kvacskay *et al.*, 2021; Hanlon *et al.*, 2022). Studies have demonstrated succinate's ability to

activate macrophages and stimulate IL-1β secretion (Tannahill *et al.*, 2013; Mills *et al.*, 2016). In addition, succinate can promote the expression of growth factors as well as invasive mechanisms in RA FLS and in conjunction with the NLRP3 inflammasome can activate RA FLS in a HIF1α dependent way (Biniecka *et al.*, 2016; Li *et al.*, 2016). Glutamine, a key component of the TCA cycle, has been shown to regulate the balance between Tregs, Th1 and Th17 cells, with Th17 cells being more reliant on glutaminolysis (Klysz *et al.*, 2015; Araujo *et al.*, 2017; Xu *et al.*, 2017; Johnson *et al.*, 2018). Itaconate, interestingly, has immunomodulatory effects, regulating levels of succinate in activated macrophages and reducing the secretion of inflammatory cytokines in these cells (Lampropoulou *et al.*, 2016; McGarry *et al.*, 2018; Mills *et al.*, 2018; Hanlon *et al.*, 2022).

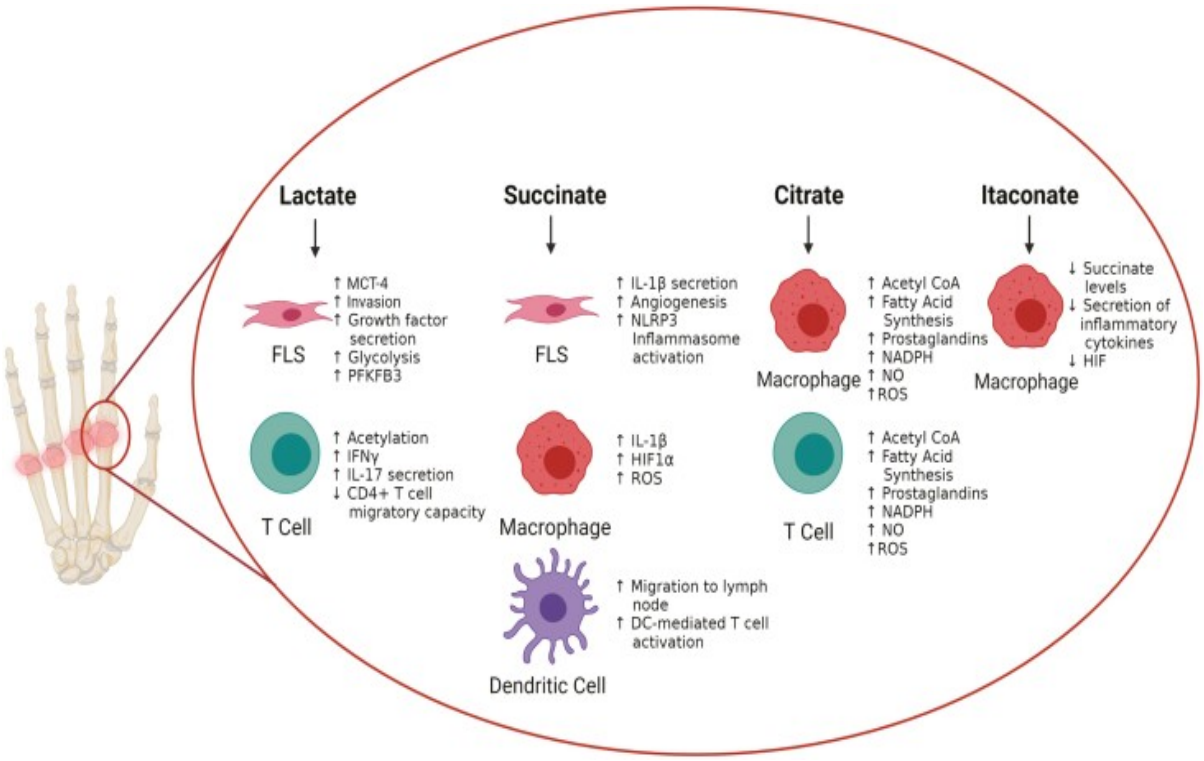

Figure 1.10: Effect of 'Immunometabolites' on Specific Cell Subsets within the Inflamed Synovial Joint. Metabolites are no longer regarded as simply by-products of metabolism, but rather can influence and further potentiate the immune and inflammatory response. During the inflammatory process at the site of inflammation, stromal and immune cells sense and respond to elevated levels of metabolites such as lactate, citrate, succinate, and itaconate, which in turn alters their function (Figure taken from Hanlon et al. Clinical Experimental Immunology 2022).

1.19 Immunometabolism

Cellular metabolism, especially in the context of immunology, has garnered a new appreciation with the observation that perturbations in metabolism consequently disrupt normal physiology resulting in disease (Trowell, 1975; Trowell, 1982; DeBerardinis and Thompson, 2012). This new,

fast-moving field, termed immunometabolism, focuses on the concept that metabolic pathways can regulate the phenotype and function of cells in addition to providing energy (Chi, 2022). Though the interest has only emerged over the last 15 years, the link between human disease and metabolism can date back thousands of years. For example, over 2,000 years ago, Celsus observed rich food and beverages exacerbated gout symptoms. Similarly, Indian physicians noticed that curiously, urine from diabetic patients attracted ants while urine from a healthy individual did not (Trowell, 1982; DeBerardinis and Thompson, 2012).

Immune cells receive a combination of intrinsic and extrinsic signals directing them to reprogram their metabolism to aid in providing the necessary energy and biological intermediates needed for a quick and robust immune response (Mathis and Shoelson, 2011; Ganeshan and Chawla, 2014). Normally, glycolysis is considered to be a less efficient means of ATP production compared to the TCA cycle in OXPHOS (McGettrick and O'Neill, 2013). However, in certain contexts, activated immune and stromal cells will favour glycolysis for their ATP production to better suit their energy demands (Fearon *et al.*, 2019). Engaging in OXPHOS requires mitochondrial biogenesis, which is a lengthy and complex process. Therefore, when cells require faster generation of ATP, switching to glycolysis becomes the more favourable option due to the faster turnover per cycle (O'Neill, Kishton, and Rathmell, 2016). This phenomenon, termed the 'Warburg Effect' was observed by Otto Warburg in the 1900's where he noted how cancer cells preferred glycolysis, even in the presence of oxygen, as a means of generating energy over OXPHOS (Warburg, 1956). Warburg proposed that switching to glycolysis could account for cancer cells tolerance to extreme hypoxia within the local environment and aid in their ability to compete with normal cells under normoxia (Warburg, 1956).

Immune cells have adopted this ability where, when activated, they can switch from OXPHOS to aerobic glycolysis, similar to what has been observed in tumour cells (Krawczyk *et al.*, 2010; Van den Bossche, O'Neill,and Menon, 2017; Kim *et al.*, 2022; Hu et a., 2024). Indeed, in addition to rapid generation of ATP, aerobic glycolysis provides the activated immune cells with intermediate metabolites that can be used by other biosynthetic pathways and provide the molecules needed for proliferation (Palsson-McDermott and O'Neill, 2013; Wang and Patti, 2023). For example, the pentose phosphate pathway (PPP) can utilise G6PD to produce NADPH, purines and pyrimidines, and amino acids needed for cell growth and proliferation (Buchakjian and Kornbluth, 2010; McGettrick and O'Neill, 2013; O'Neill, Kishton, and Rathmell, 2016). Tumour and immune cells are not the only cell types to take advantage of this metabolic switch. Increasing evidence has demonstrated stromal cells have this ability as well (de Bock *et al.*, 2013; Eelen *et*

al., 2013; Ahn *et al.*, 2016; Balogh *et al.*, 2018; Eelen *et al.*, 2018; Aghakhani, Zerrouk, and Niarakis, 2020).

1.20 Fibroblast Metabolism

As stated previously, metabolism impacts cellular function, and in the context of FLS in the inflamed joint, numerous studies have demonstrated the link between metabolic rewiring of the cell and the pathogenic function of FLS (Ahn *et al.*, 2016; Biniecka *et al.*, 2016; Garcia-Carbonell *et al.*, 2016; Bustamente *et al.*, 2017; McGarry *et al.*, 2017; Hanlon *et al.*, 2019; de Oliveira *et al.*, 2019; Petrasca *et al.*, 2020; Pucino *et al.*, 2023). Indeed, metabolism is a key contributor to the FLS pathogenic phenotype in RA. These cells demonstrate increased sugar metabolism, specifically glycolysis and PPP, amino acid metabolism, and a reliance on glutamine metabolism (Ahn *et al.*, 2016; Garcia-Carbonell *et al.*, 2016; Bustamante *et al.*, 2017; Fearon *et al.*, 2019).

RA FLS have been shown to be hyper glycolytic, expressing increased levels of glucose transporter 1 (GLUT1) and hexokinase 2 (HK2), which in turn mediate their invasive phenotype (Garia-Carbonell *et al.*, 2016; Bustamante *et al.*, 2018; McGarry and Fearon, 2019; Koedderitzsch *et al.*, 2021). Furthermore, when compared to OA FLS, RA FLS produce significantly higher levels of lactate (Biniecka *et al.*, 2016; Kvacskay *et al.*, 2021). Indeed, when cultured with conditioned media from T cells, RA FLS metabolically switch to aerobic glycolysis and increase lactate production (Kvacskay *et al.*, 2021). Furthermore, RA FLS express the lactate transporter MCT4, blockade of which promotes RA FLS apoptotic mechanisms and thus FLS pathogenic function, in addition, MCT4-knockdown reduces disease activity scores in CIA mouse models of arthritis (Fujii et a., 2015). When cultured with lactate itself, RA FLS secreted growth factors and increased their invasive capabilities (Biniecka *et al.*, 2016). In RA mouse models, succinate has also been shown to induce IL-1β expression through activation of the NLRP3 inflammasome and can promote synovial angiogenesis via a VEGF-dependent HIF1α pathways (Li *et al.*, 2016; Li *et al.*, 2018). Lipid metabolism also contributes to RA FLS pathogenesis. For example, the choline kinase CHoKα is upregulated in TNFα-stimulated FLS, with inhibition of this kinase resulting in decreased resistance to apoptosis and cell migration (Guma *et al.*, 2015). The amino acid, glutamine, provides carbons to the TCA cycle through a process called glutaminolysis and has been shown to be elevated in the synovial fluid of RA patients (Wise *et al.*, 2010; Kim *et al.*, 2014). RA FLS have increased levels of the enzyme Glutaminase 1 (GLS1), a key enzyme involved in glutaminolysis (Takahashi *et al.*, 2017). Inhibition of GLS1 has been shown to reduce FLS proliferation in murine models of RA, and it has been proposed that RA FLS may be 'addicted to glutamine' similar to what has been observed in cancer cells (Wise *et al.*, 2010; Takahashi *et al.*, 2017).

In the context of the joint microenvironment, numerous studies have shown that key pro-inflammatory mediators, hypoxia, and oxidative stress, all promote a metabolic switch in RA FLS towards glycolysis, evident by the increased expression of HK2, PFKFB3, PKM2, and GLUT1, key glycolytic enzymes (Biniecka *et al.*, 2016; McGarry *et al.*, 2017; Balogh *et al.*, 2018; Bustamante *et al.*, 2018; Hanlon *et al.*, 2019). This is associated with increased mitochondrial dysfunction and enhanced pathogenic function of RA FLS (Biniecka *et al.*, 2011; McGarry *et al.*, 2017).

Multiple studies have identified increased accumulation of HIF1α/2α in the lining layer and sub-lining layer of the synovium which are associated with increased inflammation (Giatromanolaki *et al.*, 2003; Brouwer *et al.*, 2009). TNFα and IL-17 synergistically induce a HIF1α-dependent invasive phenotype in RA FLS (Hot *et al.*, 2012). HIF1α signaling can also mediate RA FLS function induced by TLR activation (Hu *et al.*, 2014). Furthermore, under hypoxic conditions, increased expression of MMPs, chemokines, and pro-inflammatory cytokines, and decreased expression of the tissue inhibitor of metalloproteinase 1 (TIMP-1) were observed in RA FLS (Hitchon *et al.*, 2002; Charbonneau *et al.*, 2007; Cha *et al.*, 2003; Ahn *et al.*, 2008; Petrasca *et al.*, 2020). Crosstalk between HIF1α and members of the JAK-STAT pathway further perpetuate the invasive phenotype of RA FLS (Gao *et al.*, 2015). Activation of STAT3 mediates hypoxia-induced invasive and migratory mechanisms in RA FLS which can be mitigated with HIF1α silencing (Goa *et al.*, 2015). STAT3 also differentially regulates the metabolic and functional activity of RA FLS and human endothelial cells (HUVEC) (Hanlon *et al.*, 2019).

The mammalian target of Rapamycin (mTOR) is involved in various signaling pathways and is one of the master regulators of cellular metabolism (Shao *et al.*, 2017). Indeed, mTOR has been implicated in autoimmune diseases, including RA, with inhibition of this pathway leading to a reduction in synovial inflammation in RA patients (Suto *et al.*, 2020). Multiple studies have suggested a role for mTOR signaling in driving erosive disease in RA via regulation of proliferation and invasion of RA FLS (Laragione and Gulko, 2010; Dai *et al.*, 2018). For example, IL-1β induces the amino acid transporter SLC7A5 in RA FLS, thus promoting secretion of MMP-3 and MMP-13 via NF-kB and mTOR-P70S6K signaling (Xu *et al.*, 2020). TNFα can 'co-opt' the mTOR pathway in RA FLS, inducing IFNγ responses via differential STAT1 and NF-kB signaling (Karonitsch *et al.*, 2018).

Alteration and/or blockade of metabolic pathways can potentially inhibit the pathogenic capacity of FLS directly or indirectly via other cellular pathways. Indeed, several studies have shown that metabolic blockade reduces the invasive capacity of RA FLS (Biniecka *et al.*, 2016; Garcia-Carbonell *et al.*, 2016; Takahashi *et al.*, 2017; Karonitsch *et al.*, 2018). For example, studies have demonstrated that blockade with PFKFB3-inhibitor 3-(3-pyridinyl)-1-(4-pyridinyl)-2-propen-1-one (3PO) and HK2-inhibitor (BrPA), significantly decreased RA FLS proliferation, invasion, and

migration capacity (Zou *et al.*, 2017; Biniecka *et al.*, 2016: Bustamante *et al.*, 2018). This highlights the importance of fully understanding RA FLS metabolism in connection to RA pathogenesis.

1.21 Current Treatments for RA

Before the introduction of corticosteroids in the 1950s, the only treatment options for patients were non-steroidal anti-inflammatory drugs (NSAIDs), aspirin for example, to help alleviate their pain and reduce inflammation (Hyndman, 2017). However, these did nothing to treat the disease progression itself or slow down the debilitating effects from cartilage destruction and bone erosion. Treatment options over the last two decades have greatly improved outcomes for patients with RA. The recognition that early, aggressive treatment aimed specifically at reducing pro-inflammatory responses in a target–driven manner has revolutionised treatment approaches (Emery 2006; van der Linden *et al.,* 2010; Nell *et al.,* 2004; Quinn and Cox 2005; Raza, 2009; Smolen, *et al.,* 2010; Bergman *et al.,* 2010; Pierreisnard *et al.*, 2013; Nam *et al.,* 2014).

Currently, rheumatologists have a range of biologic therapies that can be utilised in the clinic to treat patients with RA, these include molecules that target specific cytokines such as TNFα, IL-6 and IL-1β, cell-based therapies like rituximab (B cell depletion) and abatacept (T cell deactivation), and more recently, small molecular weight molecules targeting downstream signaling pathways, namely the JAK-STAT pathway (Curtis and Singh, 2011). While these targeted biotherapeutics have significantly improved outcomes of RA, responses may be sub-optimal or associated with adverse events. Studies have shown that if introduced early, the right treatment consistently produce better long-term outcomes (Demoruelle and Deane, 2013). However, currently it is impossible to predict what the right treatment is for that specific patient at onset of disease, in addition, we cannot predict who will develop severe, erosive disease. This 'trial-and-error' approach impacts on patient outcomes and is not a cost-effective strategy. Safe effective drugs to prevent disease progression in individuals with RA are required.

1.22 Disease Modifying Anti-Rheumatic Drugs

Disease modifying anti-rheumatic drugs (DMARDs) utilised in the treatment of RA include methotrexate (MTX), sulfasalazine, cyclosporine A, and leflunomide. Traditionally, MTX is considered the first choice DMARD globally, and is used by rheumatologists as a monotherapy or in combination with other DMARDs or biologics when inadequate response is achieved (Landewé *et al.*, 2002; Smolen *et al.*, 2009; Gossec *et al.*, 2020; Smolen *et al.*, 2023). MTX, is a folate antimetabolite and functions through the inhibition of folate dependent enzymes, thus interfering with cell proliferation (Purcell and Ettinger, 2003). In addition, MTX inhibition results in the release of adenosine from cells which in the extracellular space can bind to their receptors on synovial

cells and induce anti-inflammatory mechanisms, with suppressive effects on T cells, B cells, and FLS, with subsequent inhibition of pro-inflammatory cytokines, MMPs, and osteoclast RANKL observed (Genestier *et al.*, 1998; Hobl *et al.*, 2011; Lee *et al.*, 2004; Chan and Cronstein, 2010; Shervington *et al.*, 2018; Misra *et al.*, 2021). However, despite MTX use as a first-line treatment, it is estimated that a significant non–response rate of 30-45% for patients is observed, leading to patients requiring further treatment strategies (Nikiphorou *et al.*, 2014).

1.23 Biological DMARDs

For patients with active RA that are refractory to conventional DMARDs, such as MTX, there are five main anti-TNF drugs available: infliximab (chimeric mouse/human monoclonal antibody), entanercept (fusion protein of TNF receptors with Fc fragment of human IgG1), adalimumab (completely humanised monoclonal antibody), certolizumab pegol, and golimumab (Ma and Xu, 2013). These were found to be effective and safe, however, prolonged use increased the risk of susceptibility to tuberculosis infections in some patients (Toussirot and Wendling, 2005). The importance of the cytokine TNFα in RA was first identified following elegant experiments performed in human RA synovial explants *ex vivo* models (Feldmann, Brennan, and Maini, 1996; Feldmann *et al.*, 2004). These models reflect the *in vivo* joint microenvironment and maintain the architecture and cell-cell contact of synovial cells, therefore an ideal model for testing potential therapeutic targets. Brennan *et al.*, demonstrated that treatment of synovial explants with anti-TNFα led to significant inhibition of downstream pro-inflammatory mediators, and demonstrated that TNFα was in the hierarchy of key pro-inflammatory cytokines involved in driving RA pathogenesis (Brennan *et al.*, 1989). Subsequent studies confirmed these results in mouse models of arthritis (collagen induced arthritis), thus together, these studies provided the first *ex vivo* and *in vivo* evidence for TNFα as a potential target (Williams, Feldmann, and Maini 1992). Studies have demonstrated that more than 70% of patients respond to treatment, nearing 80% if treated early (Emery *et al.*, 2003; Quinn and Emery, 2003; Quinn *et al.*, 2005). Furthermore, 30-40% of patients achieve clinical remission out as far as 12 years (Murray *et al.* 2021).

Tocilizumab (TCZ) is an approved recombinant humanised anti-IL-6 receptor monoclonal antibody that targets the key cytokine IL-6, which is highly expressed in the joint of patients with RA (Mihara, Ohsugi, and Kishimoto, 2011). Macrophages, FLS and ECs are potent produces of IL-6 within the joint, and IL-6 itself acts on a wide range of cells, activating pathogenic function of T cells, B cells, neutrophils, FLS, and osteoclasts (Gabay, 2006; Srirangan and Choy, 2010). TCZ demonstrates comparative effects with anti-TNF therapies for DAS28, SJC, and TJC, and TCZ has shown significant benefit in patients that are inadequate responders to TNF inhibitors (Song *et al.*, 2013; Tanaka *et al.*, 2014). Furthermore, TCZ is effective in achieving rapid and sustained

improvements in combination with MTX in RA patients who failed TNFi (Emery *et al.*, 2008; Tak and Kalden, 2011; Kaly and Rosner, 2012). TCZ has demonstrated efficacy either as a monotherapy or in combination with DMARDs for patients with moderate to severe RA (Al-Shakarchi, Gullick and Scott, 2013). Furthermore, TCZ was shown to be the highest performing second-line biologic agent in TNF-inadequate responders compared to three other current biologic agents (Lee *et al.*, 2015). Pathologically, TCZ reduces systemic inflammation and synovial inflammation, in addition to cartilage/bone damage (Conaghan *et al.*, 2014; Chen *et al.*, 2017; Ruiz-Limón *et al.*, 2017).

B cells play a key role in RA pathogenesis. Rituximab is a monoclonal antibody against CD20, a receptor found on the surface of B cells (but not pro-B cells or plasma cells) (Mok, 2013). Rituximab has shown high efficacy in RA and used generally following inadequate response to at least one TNFi, however does not work in other forms of inflammatory arthritis such as PsA patients (Rossi *et al.*, 2015; Veale and Fearon, 2015; Alivernini, Firestein, and McInnes, 2022). This could be due in part to the more central role that B cells and their autoantibodies play in RA pathogenesis. Indeed, studies have shown that RTX is less effective in RA patients that are seronegative for ACPA and RF (Edwards, Leandro, and Cambridge, 2004; Cohen *et al.*, 2006; Sellam *et al.*, 2011; Isaacs *et al.*, 2013).Rituximab results in B cell depletion, reduced autoantibody production, and subsequent inhibition of antigen presentation to T cells (Di Gaetano *et al.*, 2003; Liossis and Sfikakis, 2008). Rituximab treatment in RA patients was shown to reduce naïve memory B cells and follicular B cells within the lymph node (Ramwadhdoebe *et al.*, 2019). Studies using rituximab have also shown depletion in synovial B cells with an indirect decrease in macrophages, T cells, and plasma cells at the time of the clinical response (Teng *et al.* 2007; Kavanaugh *et al.* 2008; Thurlings *et al.* 2008; Walsh et al 2008; Orr et al 2017).

Next line treatment is abatacept, which targets T cell activation through the blockade of T cell co-stimulatory molecules. T cell activation requires two cognate interactions, one between the T cell receptor and the MHC antigen presentation and a second co-stimulatory signal between CD28 and CD80/CD86. Abatacept interrupts the interaction between CD80/CD86 and CD28 thereby disrupting the second signal and thus T cell activation (Buch, Vital, and Emery, 2008; Bonelli and Scheinecker, 2018). Studies have demonstrated the efficacy of abatacept in reducing disease activity in inadequate responders to MTX or TNFi (Schiff *et al.*, 2011; Genovese *et al.*, 2012). Interestingly, even though B cells produce ACPAs, studies have shown that high ACPA titres are predictive of response to abatacept (Sokolove *et al.*, 2016; Harrold *et al.*, 2018). Finally, a recent study by Cope *et al.* (2024), treated individuals in the pre-clinical phase of RA with abatacept (APIPPRA) trial, and demonstrated at 12 months that there was a significant reduction

in progression to RA, with evidence of sustained efficacy beyond the treatment period, and importantly with no significant adverse events (Cope *et al.*,2024).

1.24 JAK-STAT Inhibitors

Highlighted throughout the introduction, is that the synovium is the target of interplay for many pro-inflammatory cytokines with key circulating mediators controlling cell traffic from peripheral blood into the underlying tissue. More recent approaches have been to target downstream signaling with small-molecular anti-rheumatic agents targeting specifically the JAK-STAT pathway (O'Shea, Laurence and McInnes, 2013). The JAK-STAT signaling pathway mediates the action of a vast array of cytokines involved in driving inflammatory processes in RA and other inflammatory forms of arthritis. These include IL-6, OSM, IFNγ, IFNα, IFNβ, IL-21, IL-12, IL-23 GM-CSF, and IL-9 to name a few. The cytokine signal defines the specific JAKs that interact and subsequent homodimers or heterodimer of STAT proteins that form (Fragoulis, McInnes, and Siebert, 2019). Activated JAKs recruit and activate signal transducer and activator of transcription (STATs), which in turn translocate to the nucleus and drive gene transcription (Morris, Kershaw, and Babon, 2018). There are four JAK isoforms: JAK1, JAK2, JAK3 and TYK2, which depending on their cytokine stimulus, induce the phosphorylation of different STAT (1-6) proteins (Morris, Kershaw, and Babon, 2018).

Numerous studies have demonstrated the efficacy of JAK-STAT blockade for both RA and PsA, with particular emphasis on the use in RA patients with inadequate responses or intolerance to MTX (Lee *et al.*, 2014; Strand *et al.*, 2016; Wallenstein *et al.*, 2016; Nash *et al.*, 2020). Tofacitinib, baricitinib, upadacitinib, peficitinib, delgocitinib, and filgotinib are all FDA-approved JAKis that have distinct properties and indications for treating a range of autoimmune illnesses, including RA (Potlabathini *et al.*, 2024; Szekanecz *et al.*, 2024). At the cellular/molecular level many studies have shown the effects of JAK-STAT inhibition in synovial cells, including inhibition of FLS invasive mechanisms, monocyte differentiation, and pro-inflammatory response in T cells in both RA and PsA (Fiocco *et al.*, 2014; Gao *et al.*, 2016; McGarry *et al.*, 2018; Diller *et al.*, 2019; O'Brien *et al.*, 2021; Marzaioli *et al.*, 2022). Interestingly, studies have also shown that TNFα is capable of indirectly activating the JAK-STAT pathway through induction of type I interferons in RA FLS, thus further implications for the use of these inhibitors in inadequate responders (Rosengren *et al.*, 2012). Other studies have shown JAK-STAT decreases the T cell stimulatory capability of DCs through the suppression of type-I-IFN signaling and suppresses enthesitis in a $A20^{myelKO}$ animal model (Fiocco *et al.*, 2014; Kubo *et al.*, 2014; Gao *et al.*, 2016; De Wilde *et al.*, 2017). Finally, JAK-STAT signaling through complex positive and negative feedback loops interacts with key

transcriptional signaling pathways implicated in driving pro-inflammatory responses in the RA synovium including NFκB, HIF1α, PI3K, and NOTCH (Gao *et al.*, 2015).

1.25 Personalised Medicine

Despite the significant progress made over the past couple of decades in treatment, there is still an unmet need for effective treatments. Clinicians are still seeing a cohort of patients that respond sub-optimally or not at all, with only one quarter of patients reaching remission. Because of this, it is imperative to find new targets for treatment to help patients that currently don't respond, but also to develop biomarkers that will help predict treatment response from disease onset (Tak and Kalden, 2011; Tak, 2012). What works in one patient may not work in the next, therefore, there is a focus in the field to develop more personalised medicine approaches where treatments are tailored specifically to each individual (Wang *et al.*, 2021). However, this has proven difficult. Indeed, while a vast array of genome-wide association studies, transcriptomics, proteomics, epigenetics, and metabolomics studies have been performed on large cohorts, serological status remains the only diagnostic test for RA stratification in the clinic (Wang *et al.*, 2021). Many patients are still categorised as 'difficult-to-treat' (D2T) which means they are still symptomatic even after failing targeted DMARDs or biologics. Some reasons for this can be comorbidities or non-adherence. There is also a cohort of patients that are considered to have refractory RA (subgroup of D2T RA) in which the DMARDs/biologics are ineffective or result in unacceptable side effects (Roodenrijs *et al.*, 2022).

Clinical studies have shown that rituximab, which targets B cells, may be more efficacious in seropositive RA patients over seronegative patients since there is a greater involvement of autoantibodies (Alivernini *et al.*, 2017; Courvoisier *et al.*, 2021). Furthermore, studies have suggested that the presence of B cell lymphoid aggregates in the joint may be predictive also of rituximab response (Sellam *et al.*, 2011; Orr et al 2017; Humby *et al.*, 2019). However, contrary to this, high titre levels of ACPA have been shown to be predictive of response to abatacept, thus it is difficult to determine in these patients whether rituximab or abatacept is the best first line treatment from the onset of disease (Sokolove *et al.*, 2016; Harrold *et al.*, 2018).

More recently, studies have started to focus specifically on the synovium, the key tissue at the site of inflammation. Indeed, the patients' heterogeneity and their clinical responses may be driven by differences in cellular/molecular pathology in the synovium. Transcriptomic analysis of synovial tissue is emerging as a clinically significant methodology of identifying disease biomarkers. Advances in arthroscopic biopsy and ultrasound-guided synovial biopsies, with advances in single-cell technologies, will hopefully allow for detailed profiling of RA synovial tissue

to uncover the heterogeneous manifestations of the disease (Romão *et al.*, 2017). Studies have shown differences in cellular profiles in ACPA+ vs ACPA- RA suggesting that treatment strategies should differ (Padyukov *et al.*, 2011; Paulissen *et al.*, 2015; Floudas *et al.*, 2021; Wu *et al.*, 2021). A study by Lliso-Ribera *et al.* (2019), demonstrated three different synovial pathotypes (lympho-myeloid, diffuse-myeloid or pauci-immune), and demonstrated at 12 months a significantly higher proportion of patients defined by the lympho-myeloid pathotype required biological therapy (Lliso-Ribera *et al.*, 2019). However, patients with a pauci-immune pathotype demonstrated inadequate responses to TNFα blockade compared to lympho-myeloid and diffuse-myeloid (Nerviani *et al.*, 2020). Furthermore, an eloquent paper in Nat Medicine, demonstrated that synovial endotypes predicted response to rituximab vs TCZ (Rivellese *et al.*, 2022). Our group recently performed global single cell analysis and demonstrated distinct stromal and immune cell interactions that defined RA from PsA (Floudas *et al.*, 2022). Finally, a large multicentre consortium (AMP), performed scRNA-seq analysis on 79 RA patients and stratified tissues into six groups, which they defined as cell-type abundance phenotypes (CTAPs). CTAPs were associated with disease-relevant states, histology and serology metrics, and thus possibly may predict treatment response (Zhang *et al.*, 2023).

While this highlights the clinical utility of classifying RA synovial phenotypes and the need to understand patients' molecular patterns at the site of disease, ultimately, we need to be able to translate this to a blood correlate, as the vast majority of rheumatology clinics do not perform biopsy analysis. However, we first need to have better understanding of the site of inflammation if we are to definitively translate this to meaningful blood biomarkers in the clinic.

We hypothesise that stromal cells (FLS, PRIME, and CECs) play a key role in driving pathogenic mechanisms in RA disease progression, effects that are altered prior to disease onset. Therefore, this thesis aims to

(i) examine the effect of metabolic re-programming on RA FLS function
(ii) characterise the phenotype and function of distinct FLS populations in RA patients (autoantibody positive vs autoantibody negative), compared to IAR and HC
(iii) characterise differences in circulating stromal cell populations between HC, IAR, and RA, with implications for diagnostic biomarkers.

CHAPTER TWO:

The Mammalian Target of Rapamycin Contributes to Synovial Fibroblast Pathogenicity in Rheumatoid Arthritis

2.1 Introduction:

RA is characterised by dysregulated blood vessel formation facilitating infiltration of leukocytes leading to synovial proliferation and activation of FLS, ultimately leading to joint destruction and functional disability (McInnes and Schett, 2011). RA FLS are resistant to apoptosis with an increased capacity to proliferate (McInnes and Schett, 2011). Moreover, they are potent producers of pro-inflammatory cytokines, chemokines, and matrix-degrading enzymes, resulting in a highly invasive phenotype that contributes to bone erosion (Bottini and Firestein, 2012; Filer, 2013). Current treatment approaches target innate and adaptive immune cells, in addition to their secreted cytokines (Chaudhari *et al.*, 2016). However, there is now strong evidence to suggest that a synovial phenotype dominated by RA FLS may also exist which is refractory to current conventional treatments (Nerviani *et al.*, 2020; Rivellese *et al.*, 2022, Zhang *et al.,* 2023). This underpins the need to understand the molecular signatures and pathways which govern the RA FLS phenotype to improve treatment outcomes for difficult-to-treat or refractory RA.

The synovial microvasculature in RA is highly dysregulated with the formation of immature blood vessels, which lack efficacy in providing a robust oxygen supply to the joint (Kennedy *et al.*, 2010). Additionally, the increased metabolic demands of highly proliferative and inflammatory cells outpace the vascular supply of oxygen, thus resulting in a profoundly hypoxic microenvironment (Fearon *et al.*, 2016). Hypoxia itself has been previously shown to drive mitochondrial dysfunction in RA FLS, thereby altering cellular bioenergetics and promoting a shift toward glycolysis in the joint (Fearon *et al.*, 2016; Biniecka *et al.*, 2011; Biniecka *et al.*, 2011; Balogh *et al.*, 2018). This, in conjunction with the complexity of the synovial microenvironment itself, can alter metabolic dynamics in immune cells (Canavan *et al.*, 2020). The mammalian target of Rapamycin (mTOR) pathway is an evolutionarily conserved pathway known for its non-redundant role in cellular metabolism (Saxton and Sabatini, 2017). Accumulating evidence now exists confirming the involvement of master regulators of metabolism, like mTOR, in controlling the metabolically demanding processes involved in innate and adaptive immune cell activation (Powell *et al.*, 2012; Weichhart *et al.*, 2015). However, the contribution of mTOR signaling to fibroblast activation and function is still not fully elucidated, with only a handful of studies to date exploring this pathway in RA FLS. Indeed, globally in the RA synovium, the contribution of mTOR to synovial joint inflammation is also unknown. Previous studies have demonstrated that TNFα induces mTOR activation, potentiating the RA FLS phenotype, while mTOR inhibition limits synovial FLS invasion and prevents actin reorganization in both DA rat and RA human FLS (Laragione and Gulko, 2017; Karonitsch *et al.*, 2018). Moreover, inhibition of mTOR via curcumin

results in reduced inflammation, synovial hyperplasia, and a reduction in pro-inflammatory cytokine secretion in CIA rats (Dai *et al.*, 2018).

The Hippo-YAP pathway is another evolutionarily conserved signaling pathway that regulates cell survival, proliferation, differentiation, tissue development and homeostasis, and control of organ size (Caire *et al.*, 2021). Yes-associated-protein (YAP) along with PDZ-binding motif transcriptional coactivator, TAZ, are key downstream effectors within this pathway and are important regulators for actin cytoskeleton polymerization and rearrangement, as well as cell motility (Qiao *et al.*, 2017; Zhou *et al.*, 2020). To date, a large body of evidence exists on the role of the Hippo-YAP pathway in multiple forms of human cancer (Johnson and Halder, 2013), however, its role in autoimmune disease, particularly RA, is yet to be extensively studied. In parallel, limited data exists on the role of Hippo-YAP on RA FLS activation and pathogenicity. Recent literature has reported increased expression of YAP in the RA synovium (Symons *et al.*, 2022), while enriched epigenetic modifications within components of the Hippo pathway have also been reported in RA FLS compared to OA (Bottini *et al.*, 2019). Furthermore, inhibition of YAP using its specific inhibitor, verteporfin, reduced synovial FLS invasion, arthritis severity, and MMP-13 production in mice (Symons *et al.*, 2022; Bottini *et al.*, 2019). Moreover, evidence exists showing crosstalk between the Hippo-YAP and mTOR pathways as demonstrated by increased expression of YAP via mTORC1 signaling in mouse and human epithelial cell tumours (Liang *et al.*, 2014), while the YAP pathway itself is also capable of promoting mTOR signaling via increased amino acid uptake (Park *et al.*, 2016; Hansen *et al.*, 2015).

At present, it is unknown what role mTOR plays in RA FLS metabolism and pathogenicity and whether crosstalk exists with the Hippo-YAP pathway in mediating these effects. This chapter focuses on exploring the role the mTOR pathway plays in RA FLS metabolism and pathogenic functions, and whether inhibition of this pathway mitigates this pro-inflammatory phenotype. It further aims to determine whether signaling through the Hippo-YAP pathway contributes to these effects. Finally, this chapter assesses if there is crosstalk between the mTOR and Hippo-YAP pathways, where targeting this signaling may ameliorate their dual downstream pathogenic effect.

2.2 Specific Aims for this Chapter:

- To investigate whether the mTOR pathway is dysregulated in RA synovial tissue compared to HC tissue.
- To determine whether mTOR dysregulation is present within the tissue prior to disease onset.
- To investigate whether TNFα signals through the mTOR pathway in RA FLS.
- To understand the functional role of the mTOR pathway in RA FLS activation, metabolism, migration, and invasiveness.
- To elucidate whether inhibition of the mTOR pathway via Rapamycin alleviates the pathogenicity of RA FLS.
- To establish whether there is molecular crosstalk between the mTOR and Hippo-YAP pathway in RA FLS activation.
- To explore the role of the YAP pathway in RA FLS activation.

2.3 Materials and Methods:

2.3.1 Patient Recruitment

RA patients were recruited from the Department of Rheumatology at St Vincent's University Hospital, Dublin, Ireland. All patients provided fully informed written consent for the use of biological samples and medical information approved by the St Vincent's University Hospital, Ethics and Medical Research Committee prior to inclusion. Patients fulfilling the revised ACR/EULAR classification criteria were included (Aletaha *et al.*, 2010). Research and experiments were performed in accordance with the guidelines and regulations of the Declaration of Helsinki. Patient assessment included same-day tender and swollen joint count (TJC/SJC), ESR, CRP, and global health visual analogue scale (VAS) (Aletaha *et al.*, 2010). Additionally, patients were assessed for the presence of rheumatoid factor (RF) and anti-citrullinated protein antibody (ACPA). RA patients with an actively inflamed knee joint as well as those that fulfilled the revised ACR/EULAR criteria were included (Aletaha *et al.*, 2010).

2.3.2 Arthroscopies and Sample Collection

Arthroscopy of the inflamed knee was performed under local anaesthetic, using a 2.7 mm needle arthroscope (Richard Wolf, IL, USA). Macroscopic synovitis was assessed and scored under direct visualization at video arthroscopy by the clinician performing the procedure as previously described (Veale *et al.*, 1999; Ng *et al.*, 2010). Biopsies were utilised for the isolation and culture of primary RA synovial fibroblasts (RA FLS).

2.3.3 Isolation of Primary Fibroblasts

RA synovial tissue biopsies were digested with 1 mg/mL collagenase type II (Worthington Biochemical, Freehold, NJ, USA) in RPMI-1640 (Gibco-BRL, Paisley, UK) and incubated for 4 h at 37°C in humidified air with 5% CO_2. Dissociated cells were grown to confluency in RPMI-1640, 10% fetal bovine serum (FBS) (Gibco-BRL), 10 mL of 1 mmol/L HEPES (Gibco-BRL), penicillin (100 units/mL; Bioscience), streptomycin (100 units/mL; Bioscience) and fungizone (0.25 µg/mL; Bioscience) before passaging. Cells were used between passages 3-8. Clinical information for RA patients utilised for functional FLS experiments are described in Table 2.1.

Characteristics	Number or Average	Percent or Range
Age (years)	51.9	24-77
Female	19	54.3% (19/35)
Seropositive		
RF and ACPA positive	19	54.3% (19/35)
RF positive only	4	11.4% (4/35)
ACPA positive only	3	8.6% (3/35)
Seronegative	9	25.7% (9/35)
Disease Duration (years)	7.8	<1-42
DAS28 Score	3.95	1.49-8.22
On DMARD	10	28.6% (10/35)
On Biologic	11	31.4% (11/35)
Naïve to Treatment	14	40% (14/35)

Table 2.1: Patient demographics of RA patients utilised in FLS functional experiments.
Anti-citrullinated protein (ACPA), Rheumatoid Factor (RF), Disease Activity Score (DAS28), C-Reactive Protein (CRP) Disease Modifying Anti-Rheumatic Drugs (DMARD).

2.3.4 Bulk RNA Sequencing Analysis

Transcriptomic analysis was conducted on our previously published synovial tissue bulk RNA-seq dataset (Guo *et al.*, 2017). The quality of the RNA was assessed using an Agilent bioanalyzer followed by RNA sequencing by Q2 Solutions (Morrisville, NC, USA). The Illumina Ribo-Zero protocol was utilised to prepare sequencing libraries on Truseq stranded total RNA. The pooled libraries were sequenced on an Illumina HiSeq 2000 and FastQC evaluated the raw read quality. Raw reads were trimmed based on sequence quality and adaptors leading to an average number of clusters per sample of 8.9×10^7. Reads were then aligned to the human reference genome b37.3 using Star v2.4 (Dobin *et al.*, 2013). Quantification of aligned reads was performed using RSEM 1.2.14 with the University of California Santa Cruz (UCSC) transcriptome model that included lncRNAs from Ensembl v75. Aligned data were subjected to evaluation of quality using several metrics including mapping rate, coverage, and deviation from PCA. Counts were converted to log2 counts per million, quantile normalised, and precision weighted.

Healthy controls (HC), individuals-at-risk (IAR), Undifferentiated Arthritis (UA), early RA and established RA, used in this bulk RNA-seq analysis have been previously described (Guo *et al.*, 2017). Synovial biopsies were obtained from 28 HC (14 male, 14 female) with no evidence of arthritis upon examination or history of arthritis. IAR within this cohort (n= 10) were defined as

individuals with symptoms of aches and pains, without clinical signs of synovitis or significantly raised C-reactive protein, but positive for RF and ACPA. UA patients (n=6) were defined as individuals presenting with clinical signs of synovitis but failed to meet the 2010 ACR criteria for RA. Early RA (n=57) was defined as within 12 months of diagnosis without prior treatment. For this cohort, the mean disease duration was five months. Established RA patients (n=95) had an average disease duration of 68 months, and all patients were diagnosed greater than one year before sample collection. All established RA patients had received disease-modifying anti-rheumatic drugs (DMARDs) or anti-TNFα treatments.

2.3.5 Flow Cytometry

RA FLS were seeded into 6-well plates at a concentration of 1 x 10^5 cells per well and left to adhere and grow to confluence. Following this, cells were incubated in serum-free (1% FBS) RPMI-1640 for 24 h and subsequently pre-treated for 2 h with Rapamycin (100 nM) or Verteporfin (50 nM), where indicated, before being stimulated with TNFα (1 ng/mL) for another 24 h. Viability of cells treated with Verteporfin was also assessed via flow cytometry as demonstrated in Appendix Figure 7.1. Cells were enzymatically removed from the 6-well plates using Accutase (Sigma-Aldrich) and washed twice with phosphate buffered saline (PBS) and centrifuged at 1400 rpm for 5 min. To exclude dead cells, samples were resuspended in Live/Dead Zombie Near IR (NIR) (Biolegend) and left to incubate for 30 min in the dark at 4°C. To eliminate non-specific binding of monoclonal antibodies to the Fc-gamma receptors (FcγR), samples were blocked for 10 min with human FcγR-binding inhibitor (TruStain FcX Receptor blocking solution; Biolegend) prior to antibody staining. Subsequently, cells were stained with the extracellular antibodies listed in Table 2.2 for 30 min in the dark at 4°C. Samples were washed with fluorescence-activated cell sorting (FACS) buffer ((Dulbecco's PBS without Mg^{2+} or CA^{2+} (Sigma-Aldrich), 2% heat-inactivated FBS (Biosciences), 0.05% sodium azide (Sigma-Aldrich), and 0.5 M EDTA pH 8.0 (Ambion)) and fixed in 1% paraformaldehyde (PFA) (Thermo Fisher Scientific, USA) for 30 min at 4°C. Samples were washed and resuspended in 200 µL of FACS buffer. Samples were acquired using the LSR Fortessa (BD) cytometer and analysed using FlowJo software (Treestar Inc.). To adjust for spectral overlap between detectors, compensation was applied using single-stained compensation plus beads (BD). Cells were gated based on forward and side scatter, and doublets and dead cells were excluded. Fluorescence Minus One (FMO) controls were used to determine gating boundaries.

Antibody	Fluorochrome	Clone	Company
Phospho-S6	PE	5316S	Cell Signaling Technology
ICAM-1	BV605	HA58	BD Biosciences
mTOR	AF647	O21-404	BD Biosciences
CXCR3	PE	G025H7	Biolegend
CXCR4	PE-CF594	12G5	Biolegend
CXCR5	BV786	J252D4	Biolegend

Table 2.2: Panel of fluorochrome antibodies used for flow cytometry analysis.

2.3.6 Cellular Bioenergetic Functional Analysis

Oxygen consumption rate (OCR) and extracellular acidification rate (ECAR), reflecting oxidative phosphorylation and glycolysis respectively, were measured before and after treatment with oligomycin (2 µg/mL) (Seahorse Biosciences, UK), trifluorocarbonylcyanide phenylhydrazone (FCCP) (5 µM) (Seahorse Biosciences, UK), antimycin A (2 µM) (Seahorse Biosciences, UK)), and rotenone (2 µM) (Seahorse Biosciences, UK) using the Seahorse XF96-analyser (Agilent Technologies, USA). RA FLS were seeded at a density of 15,000 cells per well in a 96-well XF-microplate (Agilent Technologies) and allowed to adhere overnight in RPMI. Following this, cells were pre-treated with Rapamycin (100 nM) for 2 h before being stimulated with TNFα (1 ng/mL) for 24 h. After 24 h, cells were rinsed with assay medium (unbuffered Dulbecco's Modified Eagle's medium (DMEM) supplemented with 10 mM glucose, pH 7.4) before incubation with assay medium for 30 min at 37°C in a non-CO_2 incubator.

Four baseline OCR and ECAR measurements were obtained over 28 min before injection of specific metabolic inhibitors. Moreover, to challenge the metabolic capacity of RA FLS, three OCR and ECAR measurements were obtained over 15 min following injection with oligomycin (ATP-synthase-inhibitor), FCCP (mitochondrial uncoupler), antimycin A (complex-III inhibitor) and rotenone (complex-I inhibitor). The maximal respiratory capacity and maximal glycolytic capacity were calculated by averaging the three OCR or ECAR measurements following FCCP and oligomycin injection, respectively. The spare respiratory capacity was calculated by subtracting the baseline OCR from the maximal respiratory capacity OCR, and ATP synthesis was calculated by subtracting the post-oligomycin OCR from the baseline OCR. Finally, the extent of proton leakage was calculated by subtracting non-mitochondrial respiration from the minimum rate measurement after oligomycin injection, while the coupling efficiency was determined by dividing the ATP synthesis rate by baseline OCR x 100 (as depicted in Figure 2.3.1).

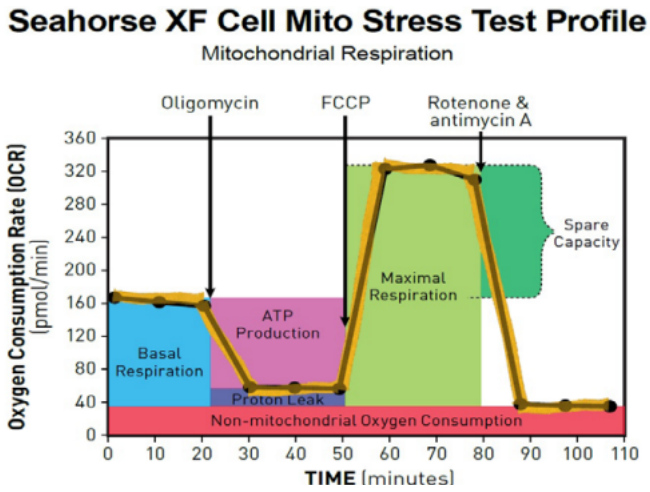

Figure 2.3.1: Representative Seahorse Cell Mito stress Test assay including calculable parameters.

2.3.7 mRNA Extraction and cDNA Synthesis

To assess the effects of TNFα stimulation in the presence or absence of Rapamycin on specific metabolic and inflammatory genes, RA FLS were seeded into 6-well plates at a concentration of 1 x 10^5 cells per well and allowed to grow to confluence. Cells were then incubated in serum-free (1% FBS) RPMI-1640 for 24 h and subsequently pre-treated, where indicated, with Rapamycin (100 nM) for 2 h before stimulation with TNFα (1 ng/mL). Total RNA was isolated using the miRNeasy Mini Kit (Qiagen, Germany) according to the manufacturer's protocol. The integrity of the RNA was assessed using a NanoDrop 2000 spectrophotometer. Samples with a 260:280 nm ratio of 1.8 and above were used in subsequent experiments. Isolated RNA was stored at -80°C. Total RNA (100 ng) was reverse transcribed to complementary DNA (cDNA) using a high-capacity cDNA reverse transcription kit (Applied Biosystems, Cheshire, UK) and stored at -20°C until further use.

2.3.8 RT-PCR Analysis

Gene expression data were quantified by Real Time (RT)-PCR using the Quant Studio 5 Thermal Cycler (Applied Biosystems, Lewes, UK). Reaction mixtures contained 1 µL of cDNA, 10 µM of specifically designed forward and reverse primers (Table 2), SYBR green II Universal Master Mix (Thermo Fisher Scientific, USA) and RNase-free water. Samples lacking multiscribe reverse transcriptase acted as negative controls to ensure target-specific quantification. Data were analysed using the comparative threshold cycle (Ct) method with normalization to the expression of the housekeeping genes *RPLP0* and *HPRT1* as endogenous controls. Reactions were performed in duplicate in a 96-well plate format. Thermal cycling conditions were as recommended by the manufacturer (Applied Biosystems).

Gene Name	Forward Primer	Reverse Primer
RPLP0	5′ GCGTCCTCGTGGAAGTGACATCG 3′	5′ TCAGGGATTGCCACGCAGGG 3′
HPRT1	5′ ATGGACAGGACTGAACGTCTTG 3′	5′ GGCTACAATGTGATGGCCTC 3′
HK2	5′ TTCTTGTCTCAGATTGAGAGTGAC 3′	5′ TTGCAGGATGGCTCGGACTTG 3′
G6PD	5′ CGTCACCAAGAACATTCACGAG 3′	5′ ATGCGGTTCCAGCCTATCTG 3′
GLUT-1	5′ GCCGGCGGAATTCAATGCTG 3′	5′ AGCATCTCAAAGGACTTGCCCA 3′
VCAM-1	5′ GTAAAAGAATTGCAAGTCTACATATCAC 3′	5′ GATGGATTCACAGAAATAACTGTATTC 3′
ICAM-1	5′ AACCAGAGCCAGGAGACACTC 3′	5′ GCGCCGGAAAGCTGTAGATG 3′
MMP-1	5′ GCTAACAAATACTGGAGGTATGATG 3′	5′ ATTTTGGGATAACCTGGATCCATAG 3′
MMP-3	5′ CGGTTCCGCCTGTCTCAAG 3′	5′ CGCCAAAAGTGCCTGTCTT 3′

Table 2.3: Designed primer sequences used for real-time PCR analysis.

2.3.9 Chemokine Measurements

To assess the effect of TNFα in the presence or absence of Rapamycin on pro-inflammatory mediators, RA FLS were seeded in 48-well plates at a density of 3 x 10^4 and allowed to adhere overnight. Cells were incubated in serum-free (1% FBS) RPMI-1640 for 24 h and subsequently pre-treated for 2 h with Rapamycin (100 nM) or Verteporfin (50 nM) where indicated before being stimulated with TNFα (1 ng/mL) for 24 h. Supernatants were collected and levels of IL-8, MCP-1, and RANTES were measured by specific ELISAs (IL-8, RANTES: R&D Systems, UK; MCP-1: eBiosciences, USA) according to manufacturer's conditions. IL-8 (min detection range of 31.2 pg/mL and standard range of 31.2-2000 pg/mL), MCP-1 (min detection of 7 pg/mL and standard range of 7-1000 pg/mL) and RANTES (min detection range of 3 pg/mL and standard range of 7.8-500 pg/mL).

2.3.10 Migration Assay

RA FLS were seeded into 48-well plates at a density of 2 x 10^4 for 24 h and serum starved as described in section 2.3.9. A single scratch wound was induced through the middle of each well with a sterile pipette tip and cells were subsequently pre-treated with Rapamycin (100 nM), where indicated, for 2 h followed by stimulation with TNFα (1 ng/mL) for 24 h. RA FLS migration across the wound margins was assessed and photographed using a phase-contrast microscope (Nikon TMS microscope connected to a Canon S70 camera). Semi-quantitative analysis of cell repopulation of the wound was assessed. Briefly, cells were fixed with 4% PFA, stained with 0.1%

crystal violet (Cruinn Diagnostics, Ireland) and the number of migrating cells across the time zero margin was assessed.

2.3.11 MMP Detection via Multiplex ELISA

RA FLS were seeded in 48-well plates at a density of 3 x 10^4 and allowed to adhere overnight. Cells were incubated in serum-free (1% FBS) RPMI-1640 for 24 h and subsequently pre-treated with Rapamycin (100 nM) or Verteporfin (50 nM) for 2 h, where indicated, before stimulation with TNFα (1 ng/mL) for 24 h. Supernatants were collected and used to measure MMP-1 and MMP-3 by multiplex ELISA (Meso Scale Discovery) as per the manufacturer's instructions. Briefly, 25 µL of supernatants were added to precoated multiplex wells for 2 h at room temperature (RT) under constant shaking. Simultaneously, an eight-point standard curve was added to the plate with a lower limit of detection of 11 pg/mL (MMP-1) and 2.1 pg/mL (MMP-3). The plate was subsequently washed three times using PBS/Tween, after which 25 µL of Detection antibody was added for 2 h at RT under constant shaking. Finally, after three washes, 150 µL of Read Buffer was added and the plate was analysed using Meso Sector S600 Imager.

2.3.12 Transwell Invasion Assay

Biocoat Matrigel™ Invasion Chambers (Corning) were used to assess RA FLS invasion. Cells were seeded at a density of 3 x 10^4 RA FLS cells per well in the migration chamber on 8 µM membranes precoated with Matrigel. Cells were pre-treated with Rapamycin (100 nM) or Verteporfin (50 nM) for 2 h and subsequently stimulated with TNFα (1 ng/mL) for 48 h. non-migrating cells were removed from the upper surface by gentle scrubbing. Migrating cells attached to the lower membrane were fixed with 4% PFA and stained with 0.1% crystal violet. Cells from five random high-power fields for each view were counted to assess the average number of invading cells.

2.3.13 Protein Isolation and Western Blot Analysis

RA FLS were seeded into 6-well plates at a concentration of 1 x 10^5 cells per well and allowed to grow to confluence. Once confluent, cells were incubated in serum-free (1% FBS) RPMI-1640 for 24 h and subsequently pre-treated, where indicated, with Rapamycin (100 nM) before being stimulated with TNFα (1 ng/mL) for 24 h. Cells were lysed and protein extracted from RA FLS samples using 100 µL of ice-cold Radio-Immunoprecipitation Assay (RIPA) Buffer (Sigma-Aldrich) containing 10 µg/mL phosphatase inhibitor cocktail 3 (Sigma-Aldrich) and 10 µg/mL protease inhibitor cocktail (Sigma-Aldrich). A BCA assay (Pierce Chemical Co., Thermo Scientific, Rockford, IL, USA) was used to quantify protein concentration as per manufacturer's instructions. Protein (5 µg) was resolved by SDS-Acrylamide (4% stacking, 10% resolving) gels and were then transferred

onto nitrocellulose blotting membranes (Amersham Protran 0.2 µM NC, Cytiva) prior to blocking for 1 h with wash buffer (Tris-buffered saline (TBS) with 0.1% Tween-20 (Sigma-Aldrich,) containing 5% bovine serum albumin (BSA) with gentle agitation at RT. Membranes were incubated with rabbit monoclonal anti-YAP (Cell Signaling Technology, 4912S) diluted at 1:1000 in 5% BSA in TBS-Tween-20 at 4°C overnight with gentle agitation. Following three 5 min washes, membranes were incubated with horseradish peroxidase-conjugated anti-rabbit secondary antibody (Cell Signaling Technology, 7074S) diluted at a 1:5000 dilution in 1% BSA in TBS-Tween-20 for 1 h in the dark at RT with gentle agitation. β-actin was used as a loading control and identified using monoclonal anti-β-actin-peroxidase antibody (Sigma-Aldrich) diluted at 1:60,000 in 3% BSA in TBS-Tween-20 incubated at RT in the dark for 1 h with gentle agitation. The signal was detected using Immobilon® Western Chemiluminescent HRP Substrate (Millipore). Band densities were imaged using the ChemiDoc MP Imaging System (Bio-Rad, USA) and quantified using ImageJ software (Version 1.8.0, National Institutes of Health, USA).

2.3.14 Statistical Analysis

Statistical analyses were performed using Prism 8 software. Paired Wilcoxon Signed-Rank test, paired Friedman ANOVA with Dunn's Multiple Comparisons, unpaired Mann-Whitney U test and Kruskal-Wallis was used for analysis of non-parametric data. p-values of less than 0.05 ($p<0.05$) were determined as statistically significant.

2.4 Results:

2.4.1 Dysregulated Expression of the mTOR Pathway in RA Synovial Tissue

Transcriptomic analysis of bulk RNA-Seq data on synovial tissue biopsies from HC donors (n=28) and RA patients (n=152) (GEO database GSE89408) (Guo *et al.*, 2017) revealed enrichment in several key components in the mTOR pathway (Figure 2.1). Specifically, a significant increase in the expression of MTORC1 activators, LAMTOR2 ($p<0.01$), LAMTOR3 ($p<0.0001$), LAMTOR5 ($p<0.01$) was demonstrated between RA synovial tissue compared to HC donor tissue. SLC38A9, an arginine sensor for mTORC1, was also significantly increased in RA compared to HC donors ($p<0.0001$), while genes involved in MTORC1 re-localization (RRAGC and STRADB) were also significantly increased in RA ($p<0.0001$ and $p<0.05$, respectively) compared to that of HC (Figure 2.1). Furthermore, a significant decrease in the expression of AKT1 and AKT2, in addition to LAMTOR1 (all $p<0.0001$) was observed in RA synovial tissue compared to HC (Figure 2.1). Dysregulation of these genes is further demonstrated in heatmaps illustrating the differences in expression between HC and RA (Figure 2.2 (A)). STRING analysis identified any known and predicted interactions between the dysregulated genes depicted in Figure 2.2 (B).

As there has been growing interest in identifying how early pathological changes occur in RA, next the expression differences in the aforementioned genes in IAR were investigated (n=10) (Figure 2.3). A significant enrichment in IAR of LAMTOR2 ($p<0.001$), LAMTOR3 ($p<0.0001$), LAMTOR5 ($p<0.01$), SLC38A9 ($p<0.0001$), and STRADB ($p<0.05$) compared to HC (Figure 2.3) was demonstrated. Concomitantly, a significant decrease in the expression of AKT1 ($p<0.0001$) and AKT2 ($p<0.0001$) in IAR compared to HC along with a decrease in LAMTOR1 in IAR compared to controls was observed, though not significant (Figure 2.3), thus indicating that mTOR dysregulation may occur within the synovium before clinical manifestations of the disease develop.

Moreover, patients were stratified into early versus established disease, with early RA being defined as within 12 months of disease diagnosis without prior small or large molecule disease modifying anti-rheumatic drugs (DMARDs) usage, while established RA had received small molecule DMARDs or anti-TNFα treatments. Following stratification, a significant dysregulation of several mTOR components in both early (n=57) and established RA (n=95) (LAMTOR3, SLC38A9, RRAGC, AKT1, AKT2, and LAMTOR1) (Figure 2.3) was demonstrated. Collectively, this reported dysregulation of components of mTOR signaling in RA synovial tissue suggests involvement of the mTOR pathway in RA disease pathogenesis.

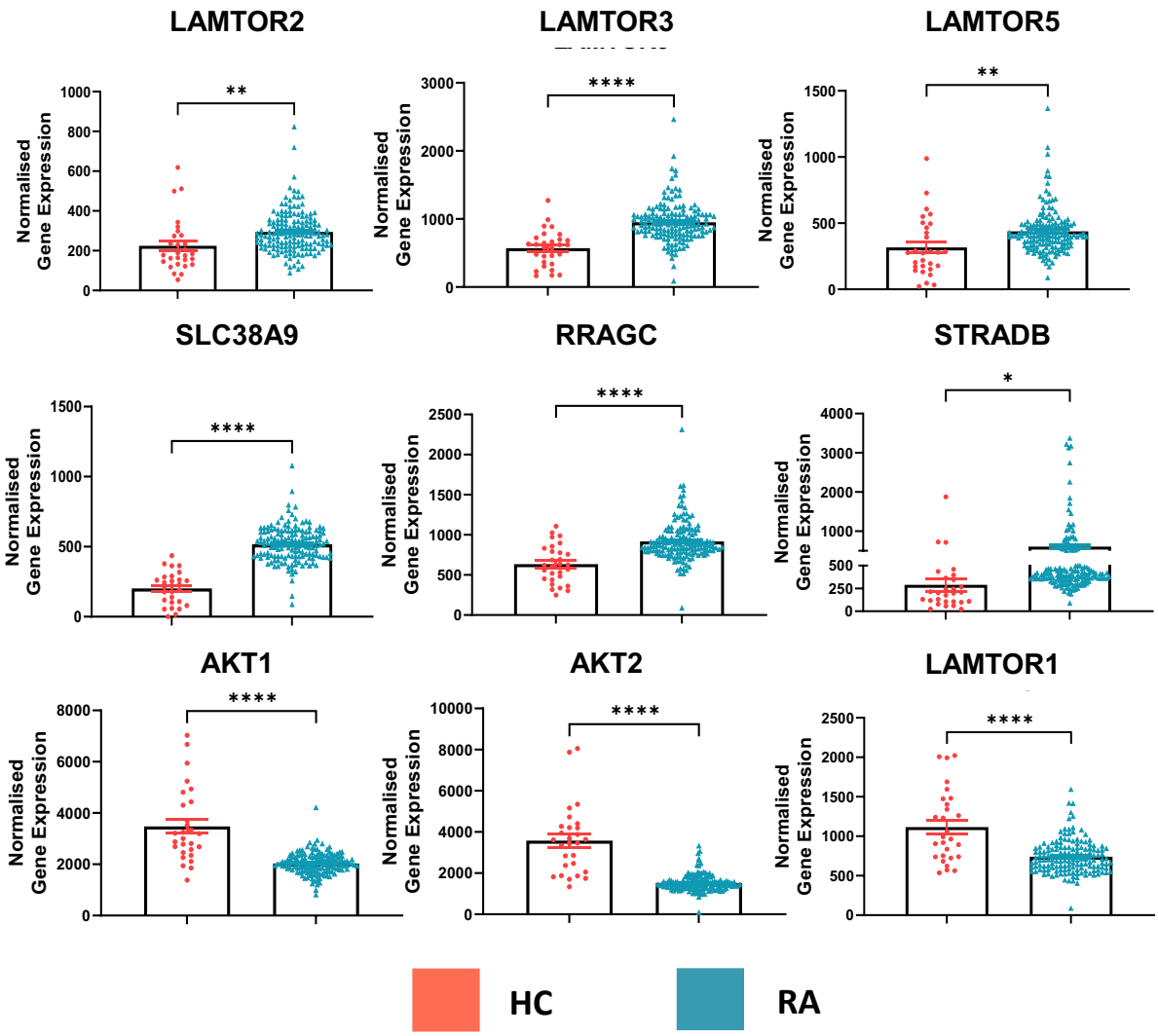

Figure 2.1: Genes involved in mTOR pathway are dysregulated in RA synovial tissue.

Bar graphs depicting normalised gene expression of key components of the mTOR pathway: LAMTOR2, LAMTOR3, LAMTOR5, SLC38A9, RRAGC, STRADB, AKT1, AKT2, and LAMTOR1 via transcriptomic analysis of bulk RNA-Seq (GEO database GSE89408) on synovial tissue biopsies from HC (n=28) and RA (n=152). Data represented as mean ± SEM with each symbol representing an individual sample. Statistical analysis performed using unpaired nonparametric Mann-Whitney U test with *p<0.05, **p<0.01, ***p<0.001, and ****p<0.0001 being significantly different from HC.

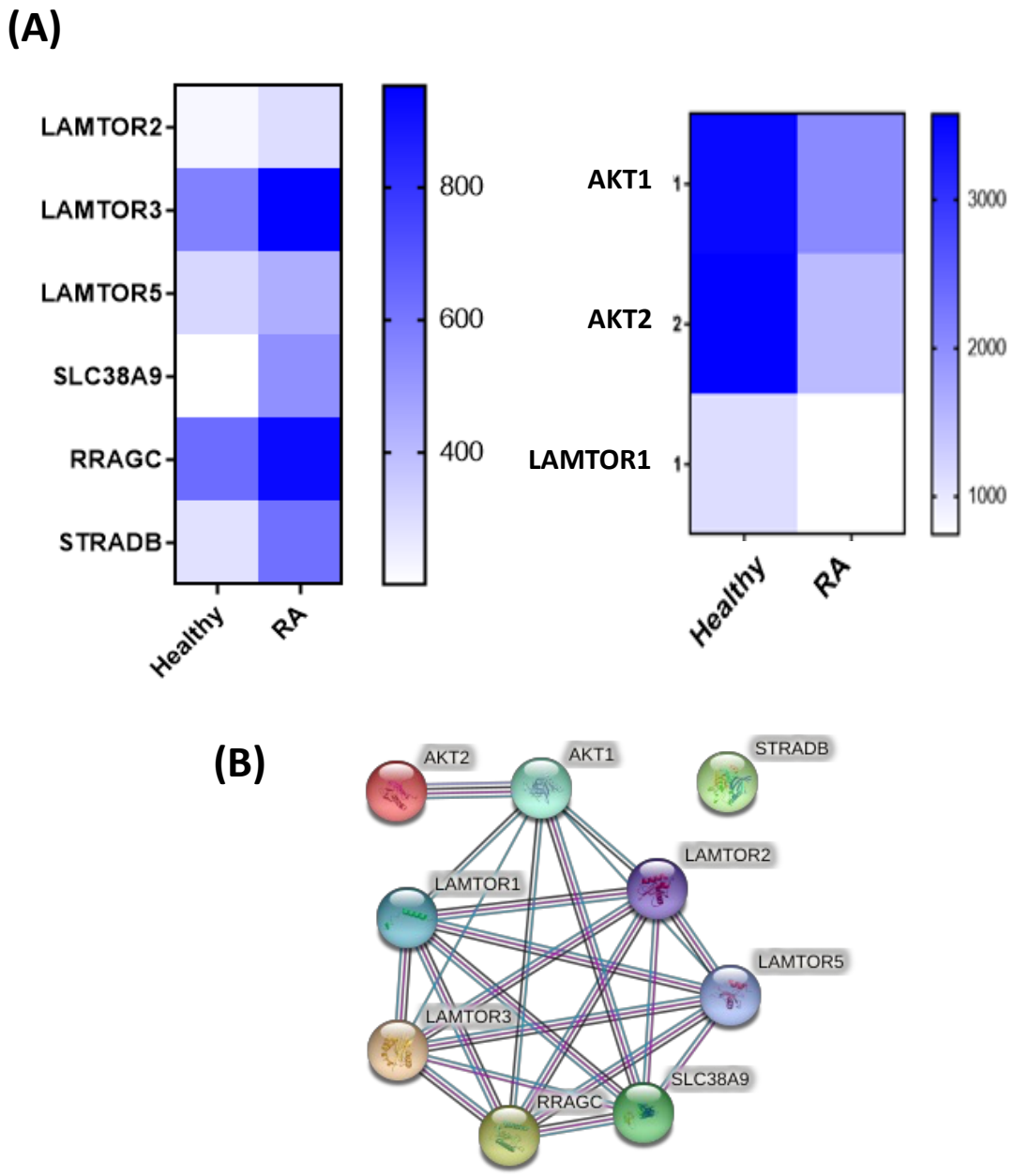

Figure 2.2: Differential expression of mTOR pathway between HC and RA synovial tissue.

(A) Clustered heatmaps representing DEG involved in metabolism (mTOR pathway) from RA compared to HC. (B) STRING analysis plot of known and predicted interactions of dysregulated genes in mTOR pathway.

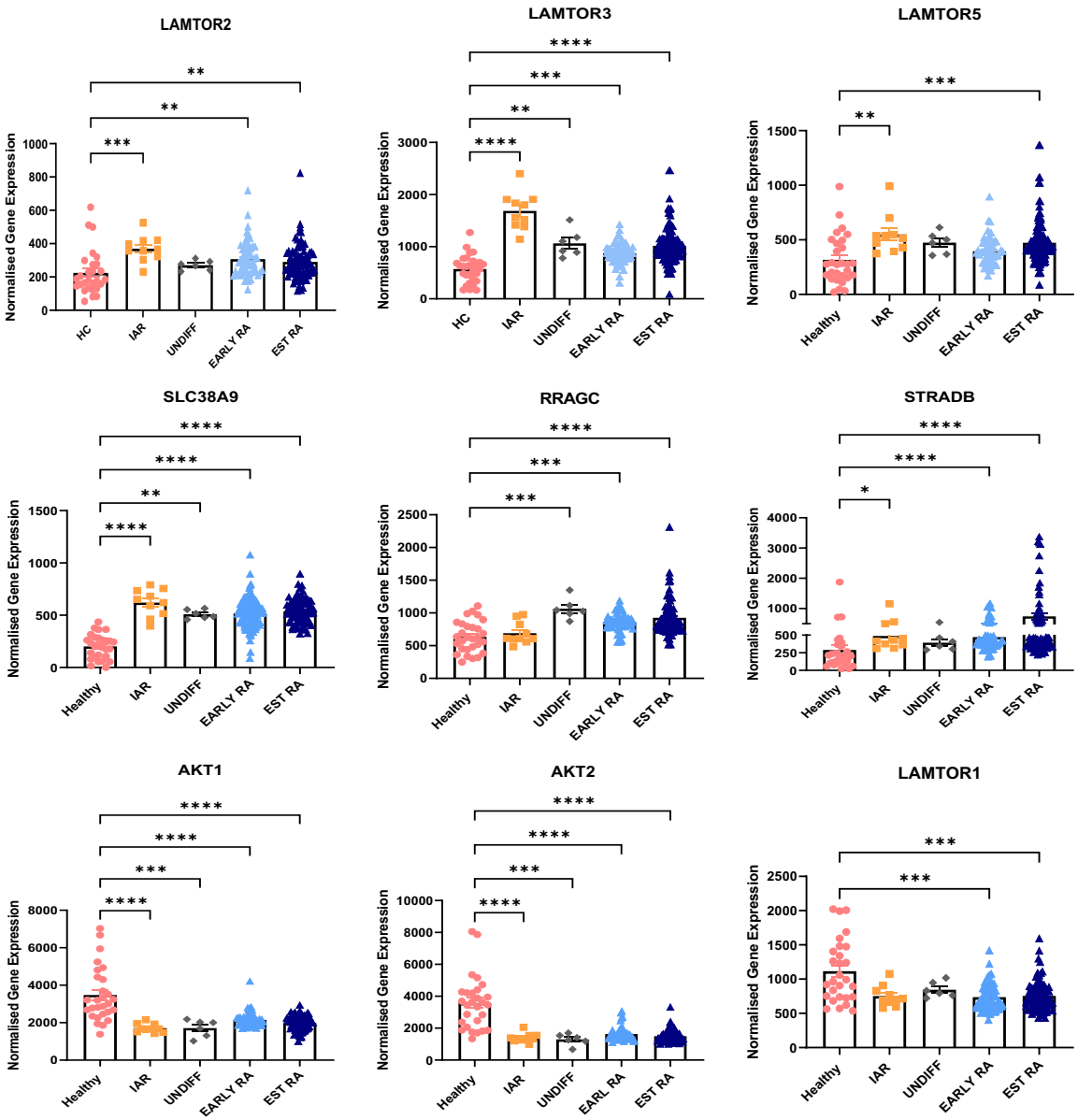

Figure 2.3: mTOR genes are dysregulated prior to disease onset and throughout disease progression.

Dot plot bar graphs demonstrating normalised gene expression of key components of the mTOR pathway (LAMTOR2, LAMTOR3, LAMTOR 5, SLC38A9, RRAGC, STRADB, AKT1, AKT2, and LAMTOR1) stratified by disease status. Data generated via transcriptomic analysis of bulk RNA-sequencing data (GEO database GSE89408) on synovial tissue biopsies from HC donors (n=28), individuals-at-risk (IAR) (n=10), undifferentiated arthritis (n=6), early RA (n=57) and established RA (n=95). Data represented as mean ± SEM. Kruskal-Wallis ANOVA utilised for statistical analysis with *p<0.05, **p<0.01, ***p<0.001, and ****p<0.0001 being significant.

2.4.2 Targeting the mTOR Pathway in RA FLS Alters Cellular Bioenergetics

Bulk RNA-sequencing demonstrated dysregulation of the mTOR pathway in RA synovial tissue, therefore, the cellular source of this dysregulation was next examined. RA FLS isolated from synovial tissue biopsies displayed increased expression of phospho-ribosomal protein S6 (pS6), the major downstream target and effector of the mTOR pathway, in respect to HC ($p=0.0714$; Figure 2.4 (A)). This is further illustrated by the representative histogram depicting a shift in the MFI expression of pS6 on RA FLS compared to HC FLS (Figure 2.4 (A)). Furthermore, we recapitulated this phenotype in cultured FLS stimulated with TNFα. While there was no significant increase observed in the % frequency of mTOR expressing RA FLS following stimulation with TNFα compared to control (Ctrl) (Appendix Figure 7.2), a marked increase in the MFI expression of phosphorylation of S6 was demonstrated ($p=0.0625$; Figure 2.4 (B)). This is further demonstrated in the representative MFI histogram plot depicted in Figure 2.4 (B). Increased S6 phosphorylation in RA FLS is indicative of an increase in mTOR signaling. Moreover, evaluation of the specificity of Rapamycin to abrogate mTOR signaling in TNFα-stimulated RA FLS demonstrated a reduction in TNFα-induced pS6 in the presence of Rapamycin (Figure 2.4 (C)).

As a master regulator of cellular metabolism, the effect of mTOR inhibition on RA FLS cellular metabolism was investigated. Using Seahorse XF96 Technology, simultaneous measurement of the two major cellular energy pathways, oxidative phosphorylation and glycolysis was performed via a Mito Stress test to allow for multiple parameters of mitochondrial function to be measured. Figure 2.5 (A) demonstrates the average bioenergetic traces for ECAR and OCR in RA FLS before and after injections of the mitochondrial inhibitors oligomycin, trifluorocarbonylcyanide phenylhydrazone (FCCP), antimycin A and rotenone following TNFα stimulation in the presence or absence of Rapamycin. RA FLS demonstrated a significant increase in baseline glycolysis following stimulation with TNFα ($p<0.001$), which was significantly abrogated in the presence of Rapamycin ($p<0.05$) (Figure 2.5 (B)). Though baseline OXPHOS levels were comparable between TNFα-stimulated RA FLS and controls, a significant reduction was observed in the presence of Rapamycin compared to TNFα alone ($p<0.001$) and to controls ($p=0.0522$) (Figure 2.5 (B)).

Oligomycin acts as an inhibitor to ATP synthase and is used to evaluate the maximal glycolytic capacity. FCCP which acts as a mitochondrial uncoupler was injected to evaluate the maximal respiratory capacity. Interestingly, ATP synthesis demonstrated a significant stepwise decrease from control to TNFα alone to TNFα in the presence of Rapamycin (Ctrl vs TNFα $p<0.05$; TNFα vs TNFα + Rap $p<0.01$) (Figure 2.5 (C)). Taken together, these reported changes in glycolysis and oxidative phosphorylation suggest a distinct metabolic shift toward glycolysis following TNFα

stimulation, which shifts back towards oxidative phosphorylation following mTOR inhibition as illustrated by the cell energy phenotype profile in Figure 2.5 (D). In support of this, significant changes in the expression of several glycolytic genes in response to Rapamycin was demonstrated. Specifically, a significant decrease in the expression of TNFα-induced HK2 and G6PD (both $p<0.05$; Figure 2.6) in the presence of Rapamycin was observed, while also demonstrating a significant reduction in the expression of TNFα-induced GLUT-1—the main glucose transporter in RA FLS ($p<0.001$; Figure 2.6). Collectively, these data suggest that mTOR inhibition decreases cellular glycolysis and oxidative phosphorylation in RA FLS.

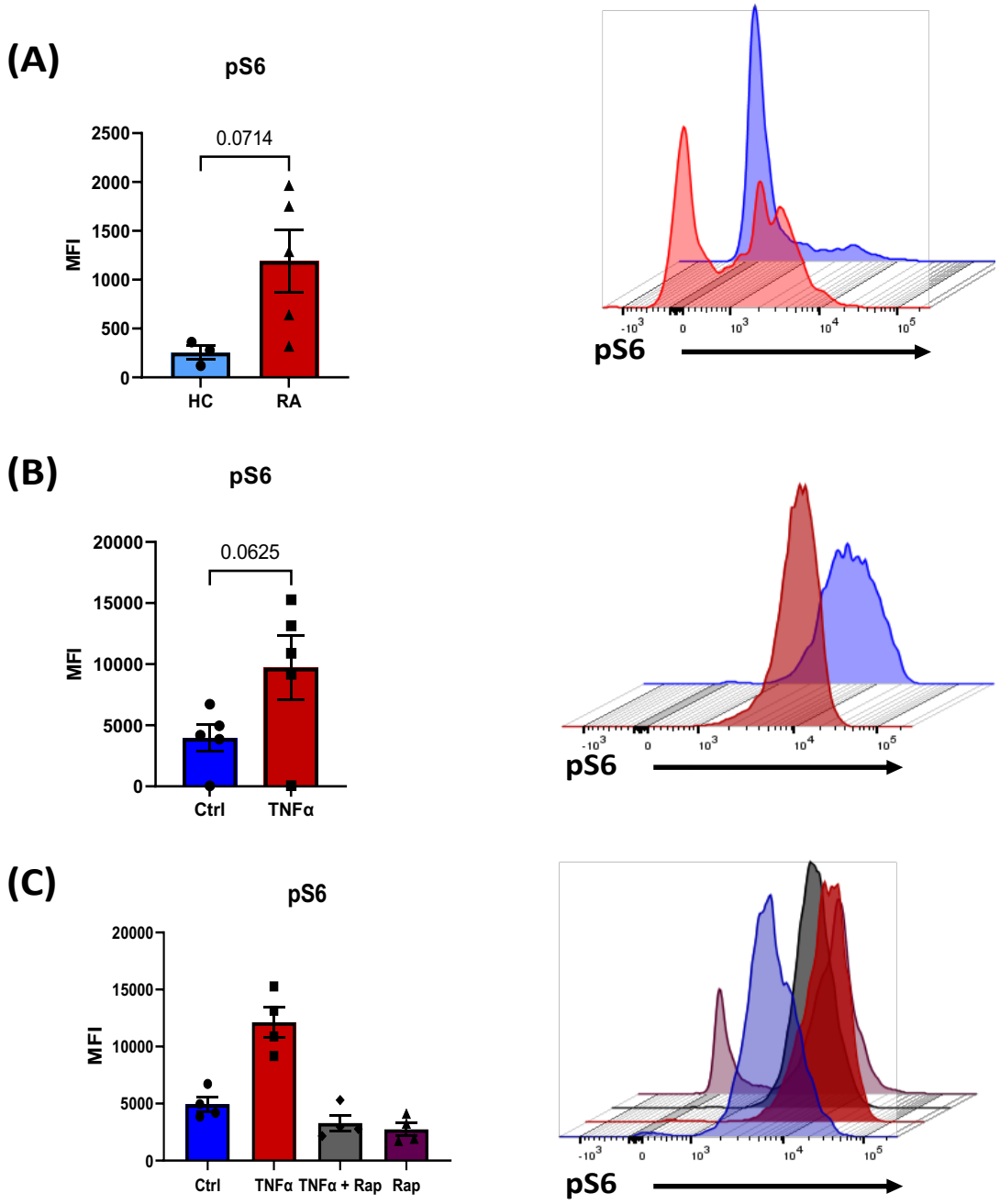

Figure 2.4: mTOR pathway is upregulated in RA FLS.

Bar graphs and representative stacked histograms demonstrating MFI expression of downstream mTOR marker pS6 in (A) *ex vivo* FLS from synovial tissue biopsies of HC (n=3) and RA (n=5), (B) RA FLS (n=5) stimulated with TNFα (1 ng/mL) for 24 hr compared to basal control, and (C) RA FLS (n=4) treated with TNFα (1 ng/mL) and Rapamycin (100 nM) alone or in combination for 24 hr. Data represented as mean ± SEM. Statistical analysis performed using unpaired nonparametric Mann-Whitney U test for comparisons between HC and RA. Wilcoxon Signed-Rank test utilised for RA FLS conditions with *p<0.05 being statistically significant.

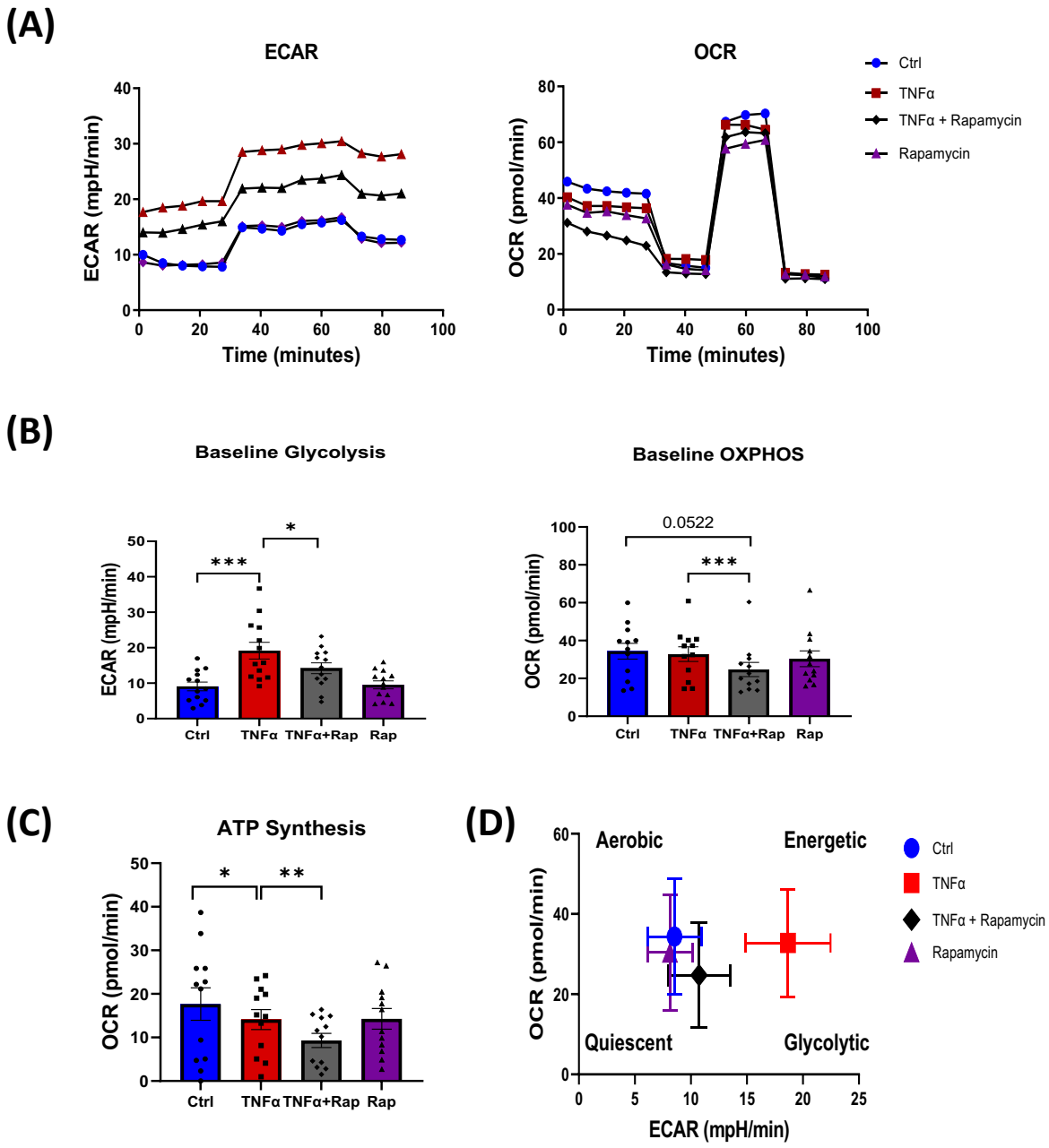

Figure 2.5: Inhibition of mTOR in RA FLS alters cellular metabolism.

(A) Average seahorse profiles demonstrating extracellular acidification rate (ECAR) (representative of glycolysis) and oxygen consumption rate (OCR) (representative of oxidative phosphorylation), before and after injections of oligomycin, FCCP, and antimycin A and rotenone in RA FLS. Dot plot bar graphs demonstrating (B) baseline glycolysis and baseline OXPHOS (oxidative phosphorylation) and (C) ATP synthesis in RA FLS treated with TNFα (1ng/mL) and Rapamycin (100 nM) alone or in combination for 24 h (n=12-13). (D) Cell energy phenotype profiles of RA FLS representing the metabolic changes in response to TNFα (1ng/mL) and Rapamycin (100 nM) alone or in combination for 24 h. Data expressed as mean ± SEM. Wilcoxon Signed-Rank test (*) utilised for comparisons between conditions with *p<0.05, **p<0.01, ***p<0.001 being statistically significant.

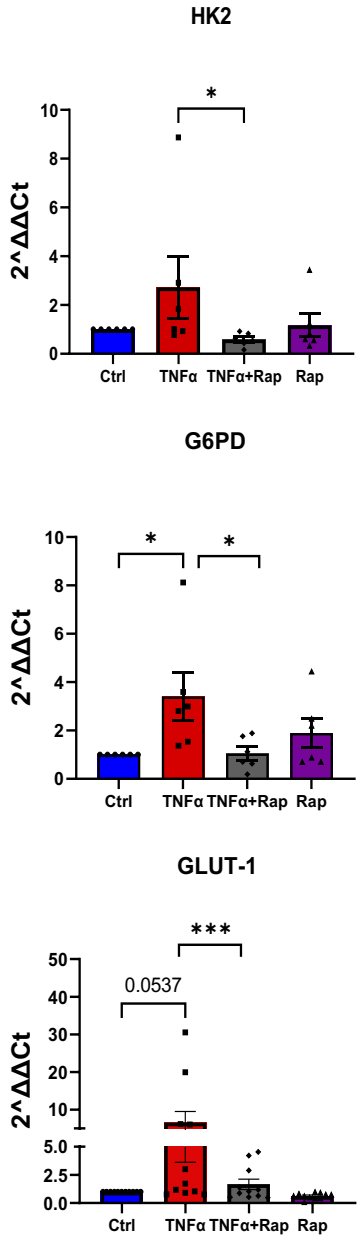

Figure 2.6: Metabolic shift with inhibition of mTOR mirrored with decreased expression of metabolic genes.

Bar graphs depicting mRNA gene expression of hexokinase 2 (HK2), glucose-6-phosphate dehydrogenase (G6PD), and glucose transporter 1 (GLUT-1) in RA FLS (n= 6-11). Data represented as fold increase compared to endogenous controls (RPLPO and HPRT1). Values expressed as mean ± SEM. Wilcoxon Signed-Rank test (*) utilised for comparison between conditions. *p<0.05, **p<0.01, ***p<0.001 statistically significant.

2.4.3 mTOR Inhibition in RA FLS Decreases Cellular Migration

It is now widely appreciated that cellular metabolism is intrinsically linked to cellular function. Given that one of the most potent and pathogenic functions of RA FLS is to migrate to the articular cartilage and invade bone, we next assessed if altered metabolism via mTOR inhibition would have functional effects for RA FLS migration. Firstly, the presence of the chemokine receptors CXCR3, CXCR4, and CXCR5 on RA FLS were examined (Figure 2.7). TNFα stimulation significantly increased the % frequency of RA FLS expressing all three receptors (all $p<0.05$; Figure 2.7 (A)), however, the effect of Rapamycin varied depending on the specific receptor. For example, Rapamycin reduced the % frequency of TNFα-stimulated CXCR5-positive RA FLS ($p=0.0781$), whereas it had no effect on CXCR4, and interestingly significantly increased % frequency of TNFα-stimulated CXCR3-positive RA FLS ($p<0.05$) (Figure 2.7 (A)). These responses are further demonstrated in the representative flow dot plots in Figure 2.7 (B).

However, Rapamycin significantly decreased TNFα-induced MCP-1 and RANTES chemokine secretion ($p<0.01$ and $p<0.05$, respectively) from RA FLS while simultaneously potentiating the secretion of TNFα-induced IL-8 ($p<0.05$) (Figure 2.8). Moreover, while no changes were observed for VCAM-1 gene expression, a significant decrease in TNFα-induced gene expression of the adhesion molecule ICAM-1 in the presence of Rapamycin was observed ($p<0.05$) (Figure 2.9 (A)). This was further demonstrated at the protein level, with TNFα-induced ICAM-1 MFI expression significantly decreased in the presence of Rapamycin ($p<0.05$) (Figure 2.9 (B)). Additionally, alterations in RA FLS cellular migration in the presence of Rapamycin was observed. Figure 2.10 (A) displays representative images of RA FLS migration with quantification shown in Figure 2.10 (B), demonstrating a significant reduction in TNFα-induced migration in the presence of Rapamycin ($p<0.05$).

2.4.4 RA FLS cellular Invasion is Decreased by mTOR Inhibition

Following migration to the articular cartilage, RA FLS produce matrix degrading enzymes such as MMPs which facilitate the invasion of RA FLS into adjacent bone, resulting in bone destruction and joint damage. Rapamycin reduced the expression and significantly reduced secretion of TNFα-induced MMP-1 in RA FLS ($p<0.05$), with minimal change observed for MMP-3 secretion (Figure 2.11 (A-B)). Functionally, assessment of RA FLS invasion via Transwell invasion chambers demonstrated a significant reduction in TNFα-induced cell infiltration in the presence of Rapamycin as depicted by the representative images (Figure 2.12 (A)) and accompanying quantitative bar graph ($p<0.05$; Figure 2.12 (B)). Collectively, these data suggest that mTOR inhibition can reduce the migration and invasiveness of RA FLS.

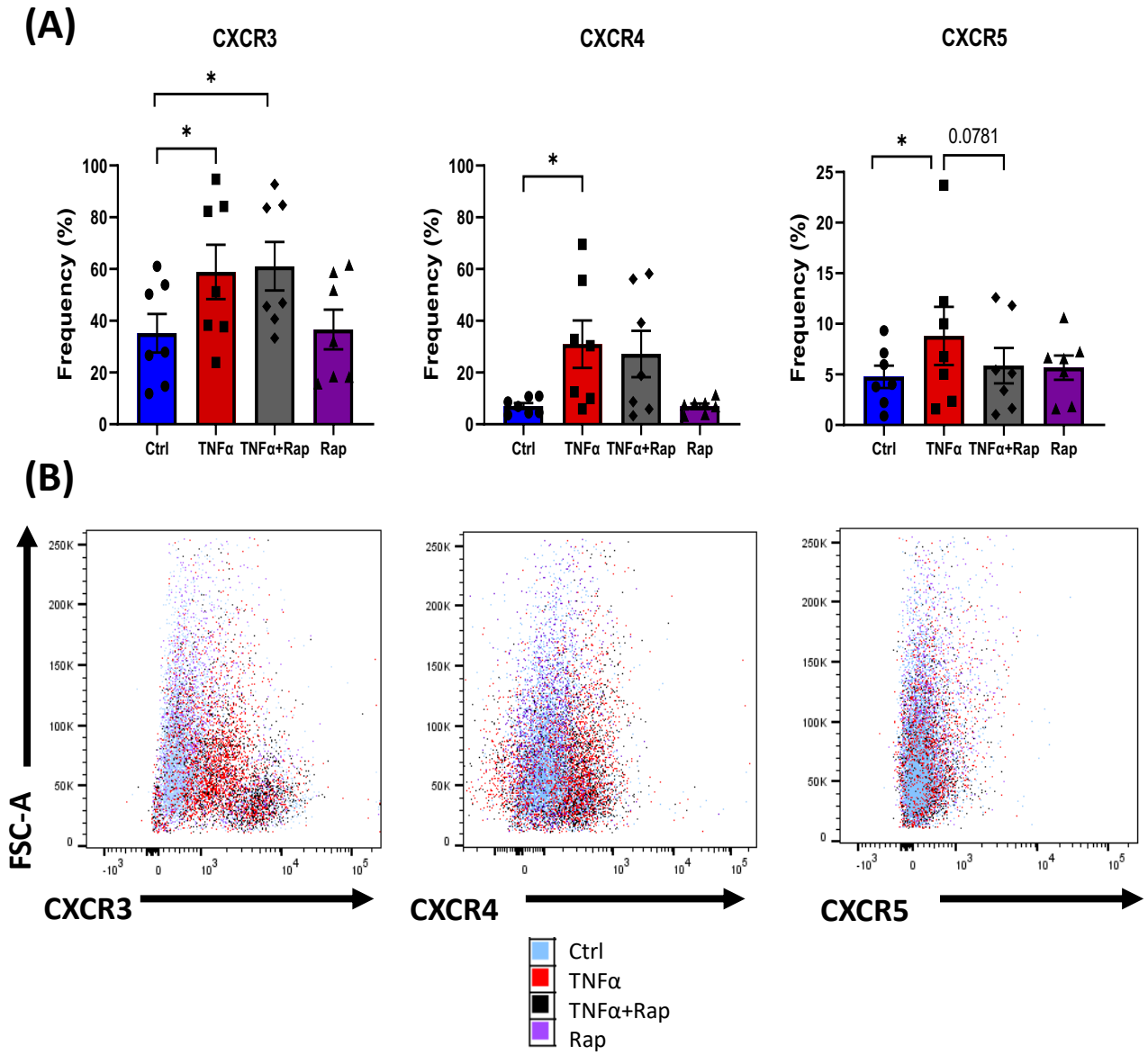

Figure 2.7: Inhibition of mTOR has selective effect on expression of chemokine receptors on RA FLS.

(A) Bar graphs demonstrating percentage frequency of CXCR3, CXCR4, and CXCR5 positive RA FLS treated with TNFAα (1 ng/mL) and Rapamycin (100 nM) alone or in combination for 24 h (n=7). (B) Representative flow cytometric dot plots overlaying Ctrl (Blue), TNFAα (1 ng/mL) (Red), TNFAα (1 ng/mL) in the presence of Rapamycin (100 nM) (Black), and Rapamycin alone (100 nM) (Purple). Data represented as mean ± SEM. Statistical analysis performed using Wilcoxon Signed-Rank test with *p<0.05 statistically significant.

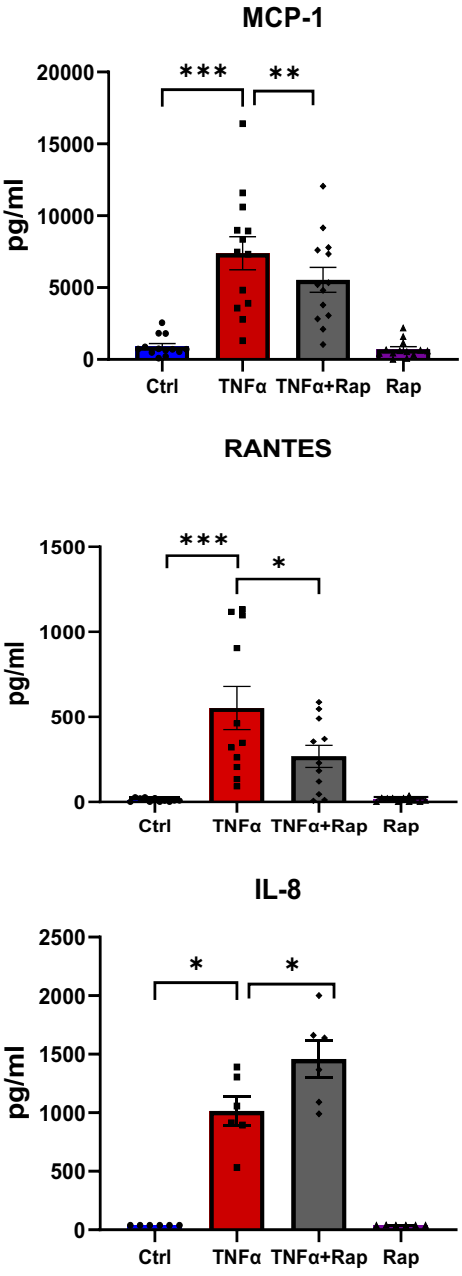

Figure 2.8: mTOR inhibition reduces chemokine production by RA FLS.

Bar graphs demonstrating the measured secretion of MCP-1, RANTES, and IL-8 from RA FLS (n= 6-13) stimulated with TNFα (1ng/mL) and Rapamycin (100 nM) alone or in combination for 24 h. Data represented as mean ± SEM and Wilcoxon Signed-Rank test utilised to determine statistical significance with *p<0.05, **p<0.01, and ***p<0.001.

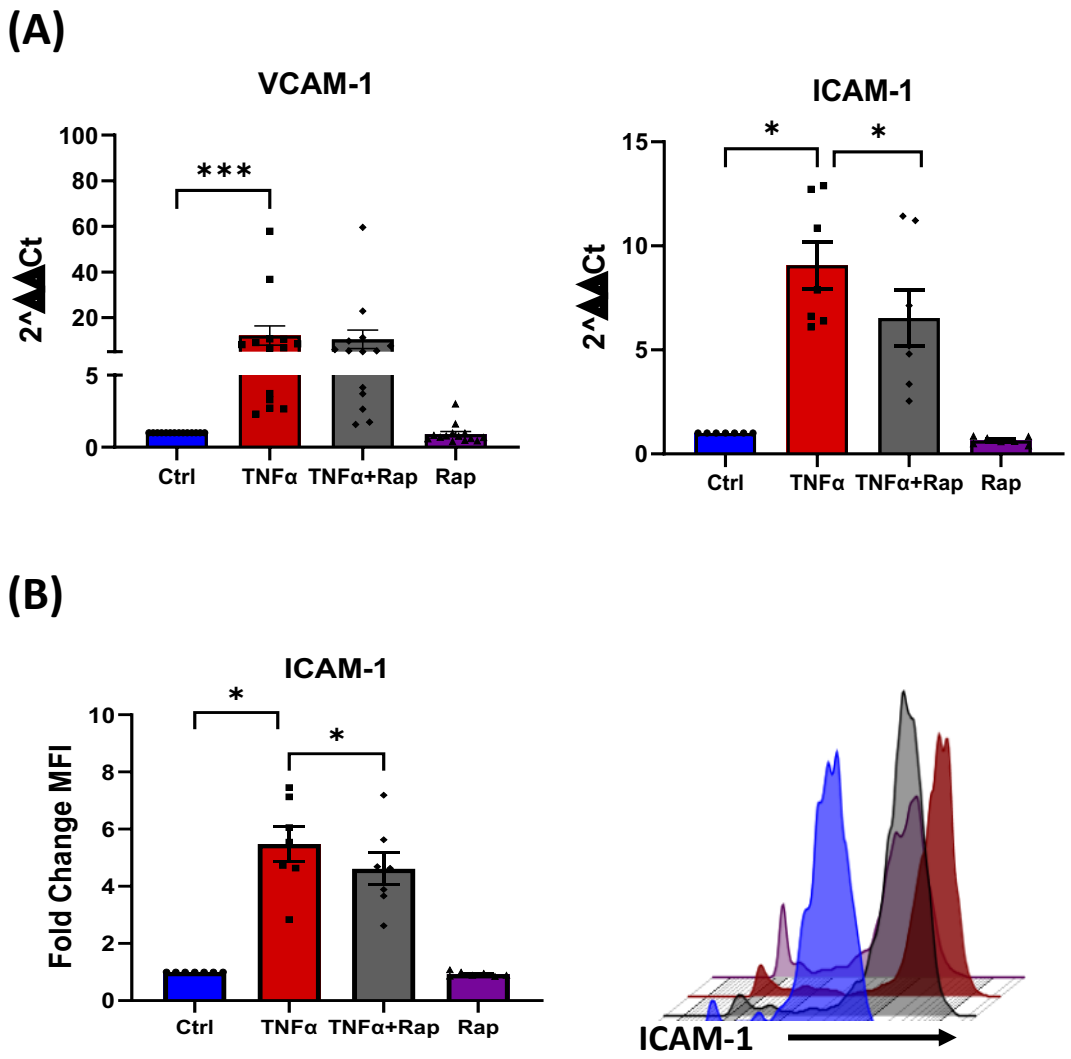

Figure 2.9: Rapamycin decreases expression of adhesion molecules in RA FLS.

(A) Bar graphs demonstrating gene expression analysis quantified using Real-time PCR of VCAM-1 and ICAM-1 on RA FLS (n= 7-14) treated with TNFα (1 ng/mL) and Rapamycin (100 nM) alone or in combination for 24 h. Fold increase compared to endogenous controls. (B) Fold change MFI expression of ICAM-1 on RA FLS (n= 7) treated with TNFα (1 ng/mL) and Rapamycin (100 nM) alone or in combination for 24 h and accompanying representative histogram. Data represented as mean ± SEM with Wilcoxon Signed-Rank test used for statistical analysis. *p<0.05, **p<0.01, ***p<0.001 statistically significant.

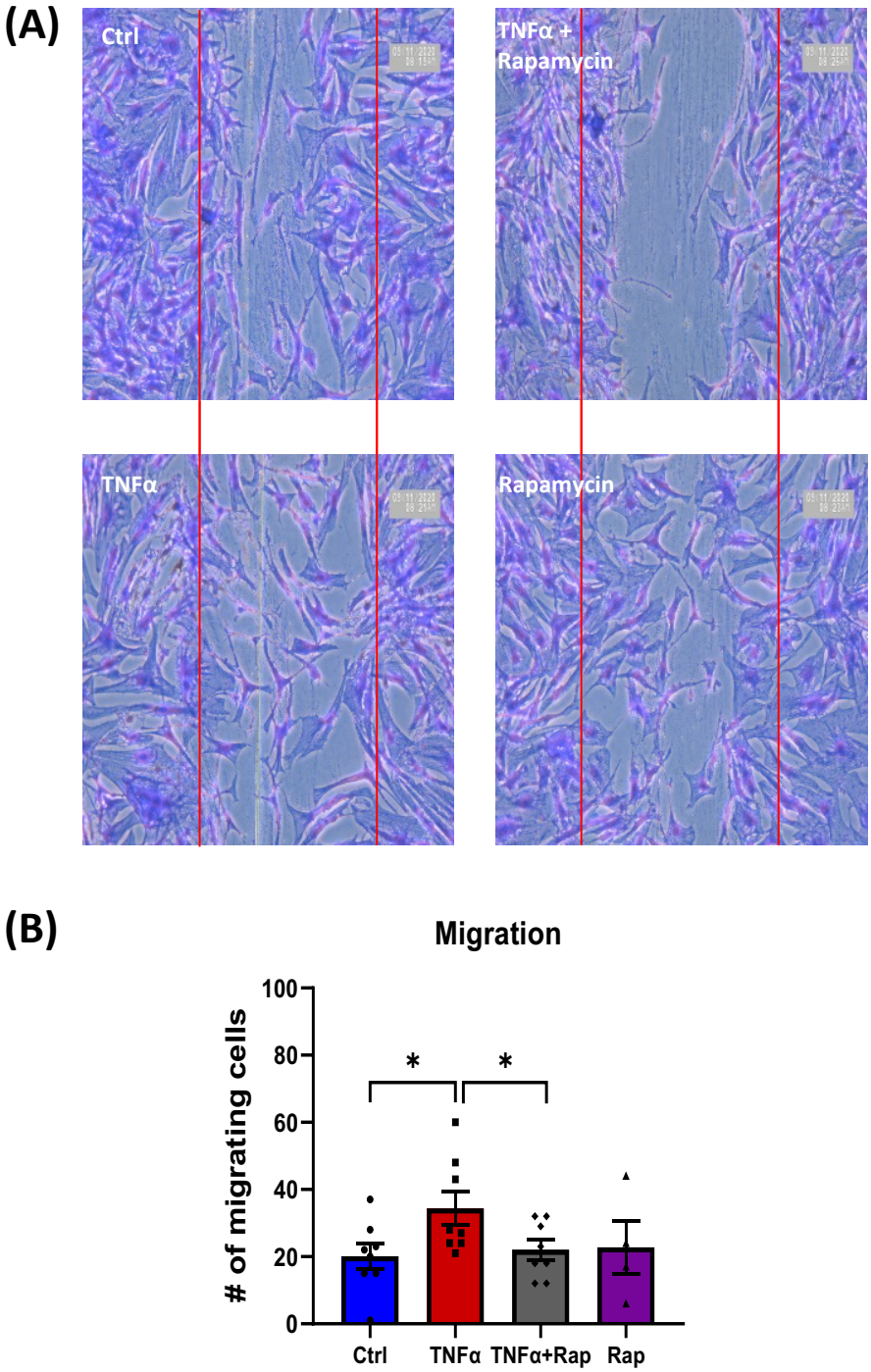

Figure 2.10: mTOR inhibition in RA FLS decreases cellular migration.

(A) Representative photomicrograph (fixed in 1% PFA and stained with 0.1% crystal violet for imaging) and (B) accompanying bar graph demonstrating cells repopulating the wound to represent migration of FLS. Images were taken of RA FLS (n=8) after being treated with TNFα (1 ng/mL) and Rapamycin (100 nM) alone or in combination for 24 h. Data represented as mean ± SEM with Wilcoxon Signed-Rank test used for statistical analysis with *p<0.05 being significant.

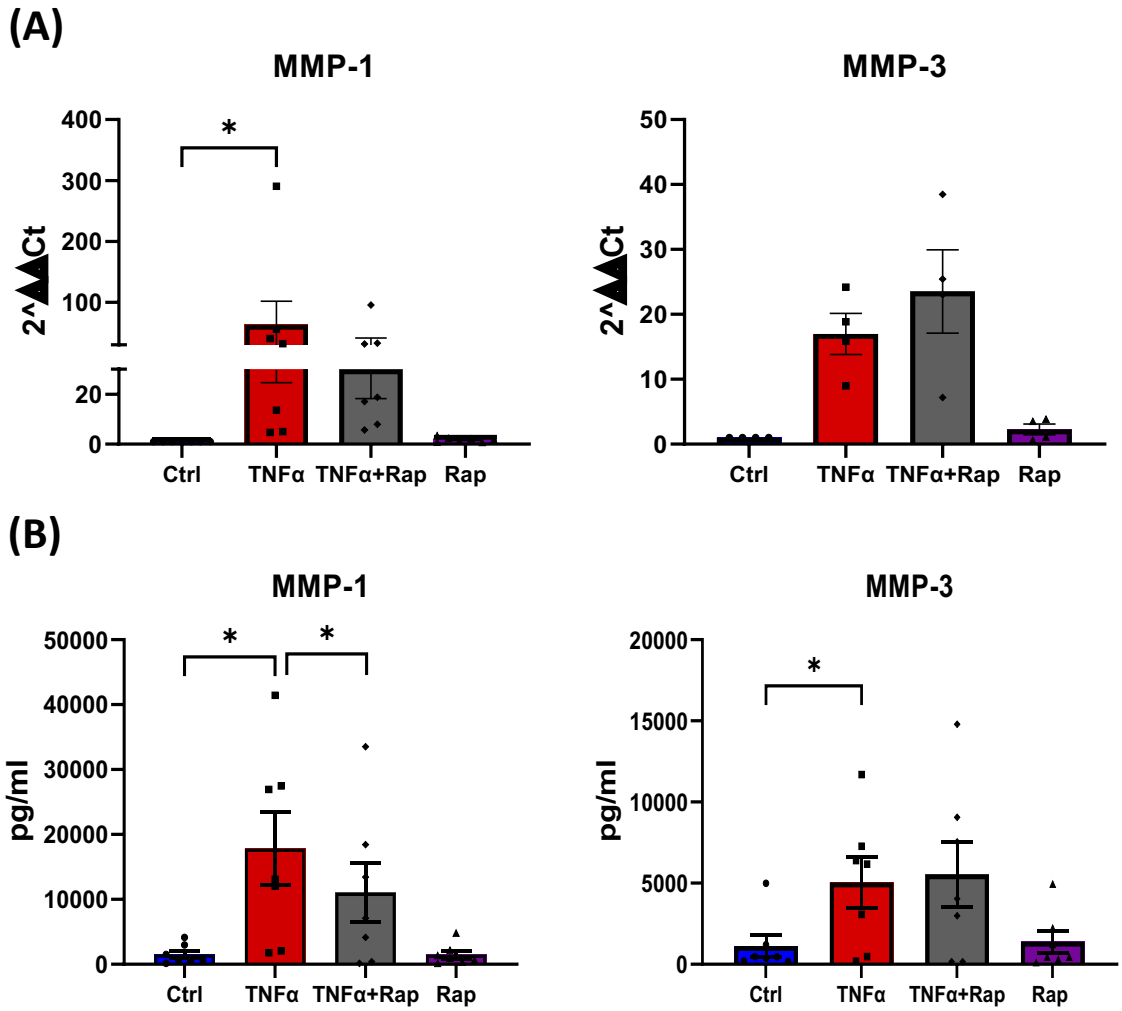

Figure 2.11: Rapamycin inhibition of mTOR alters expression of MMPs in RA FLS.

(A) Bar graphs depicting gene expression of MMP-1 and MMP-3 from RA FLS (n= 4-7) treated with TNFα (1 ng/mL) and Rapamycin (100 nM) alone or in combination for 24 h. Gene expression analysis quantified using Real-time PCR and demonstrated as fold increase compared to endogenous controls. (B) Bar graphs demonstrating measured secretion of MMP-1 and MMP-3 from RA FLS (n=7) in the presence of TNFα (1 ng/mL) and Rapamycin (100 nM) alone or in combination for 24 h. Data represented as mean ± SEM with Wilcoxon Signed-Rank test used for statistical analysis with *$p<0.05$ being significant.

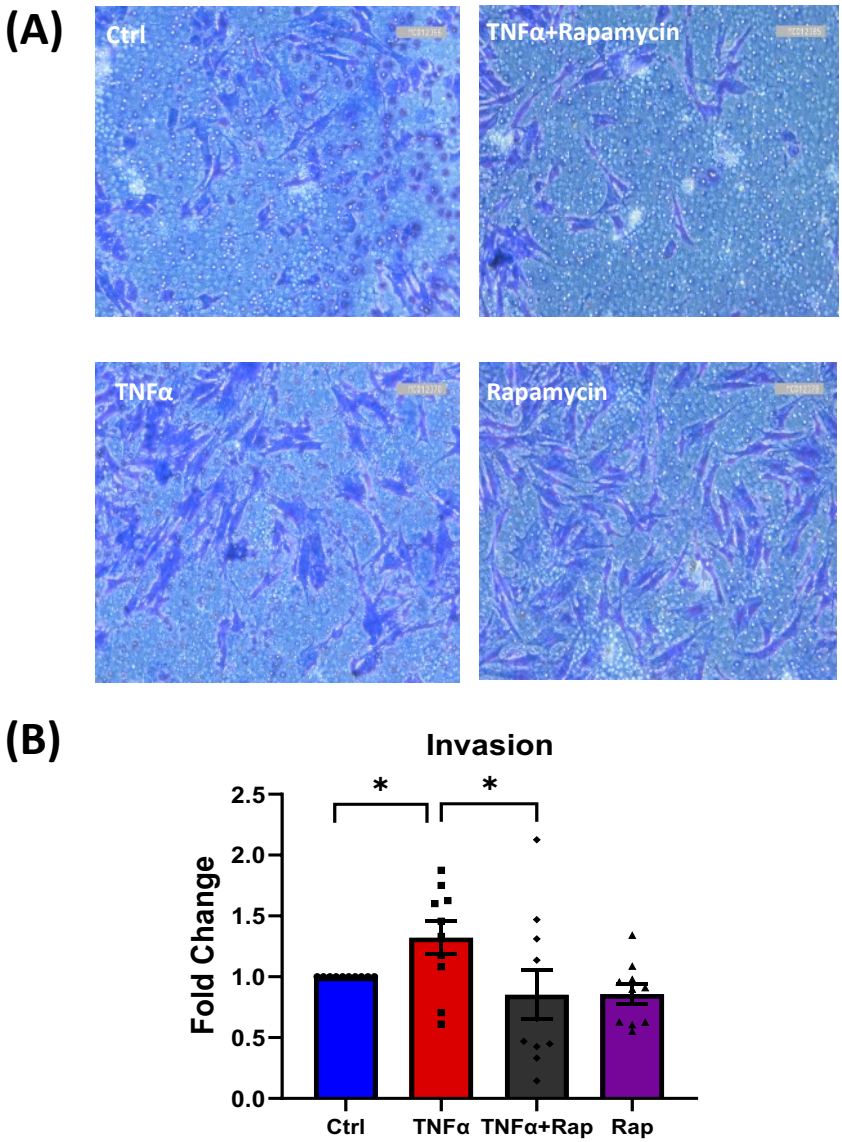

Figure 2.12: RA FLS have diminished invasive capabilities as a result of mTOR inhibition.

(A) Representative photomicrographs of RA FLS invasion with (B) accompanying bar graph quantifying invasion of RA FLS (n=10) treated with TNFα (1 ng/mL) and Rapamycin (100 nM) alone or in combination. Following 48 h stimulation, invading cells attached to lower membrane were fixed (1% PFA) and stained (0.1% crystal violet) for imaging. Data represented as mean ± SEM with Wilcoxon Signed-Rank test used for statistical analysis with *p<0.05 being significant.

2.4.5 Crosstalk between Dysregulated Hippo-YAP and mTOR Pathways Mediates RA FLS Invasion

While the mTOR pathway is known as a master regulator of cellular metabolism, its effects on cellular migration and invasion are less well known. Based on the altered functional phenotypes observed in response to Rapamycin, we next hypothesised that mTOR may interact with the Hippo-YAP pathway to mediate this RA FLS phenotype. Indeed, it is widely appreciated that the YAP pathway is a master regulator of cytoskeleton rearrangement, cell motility and cell invasion. To support this hypothesis, we identified dysregulated expression of several key genes involved in the YAP pathway in RA synovial tissue compared to HC donor synovial tissue (Figure 2.13). Specifically, increased expression of MOB1A, MOB1B, DCP2, LATS1, and STK4 (all $p<0.0001$) in RA synovial tissue with a concomitant significant decrease in LATS2 ($p<0.0001$) in RA synovial tissue compared to HC donor tissue was demonstrated (Figure 2.13 (A)). Using STRING pathway analysis, the predicted interactions of these YAP associated dysregulated proteins with those dysregulated within the mTOR pathway were demonstrated and identified that both pathways are predicted to interact and converge (Figure 2.13 (B)).

Furthermore, more extensive analysis of YAP dysregulation across RA disease initiation and progression revealed that several components of the YAP pathway are significantly dysregulated pre-disease onset in IAR (Figure 2.14). Specifically, a significant increase in MOB1A ($p< 0.0001$), MOB1B ($p<0.01$), DCP2 ($p<0.0001$) with a concomitant decrease in LATS2 ($p<0.0001$) in IAR compared to HC synovial tissue was observed (Figure 2.14). Moreover, several YAP associated genes were also upregulated in undifferentiated arthritis -MOB1A ($p<0.001$), MOB1B ($p<0.001$), DCP2 ($p<0.01$), and LATS1 ($p<0.001$), early RA - MOB1A ($p<0.0001$), MOB1B ($p<0.0001$), DCP2 ($p<0.0001$), LATS1 ($p<0.001$), and STK4 ($p<0.0001$), and established RA - MOB1A, ($p<0.0001$), MOB1B ($p<0.0001$), DCP2 ($p<0.0001$), LATS1 ($p<0.0001$), and STK4 ($p<0.0001$) (Figure 2.14). Collectively, this suggests that there is dysregulation in the YAP pathway throughout disease progression, potentially as a result of the crosstalk with the dysregulated mTOR pathway.

To further support this hypothesis, the expression of YAP in response to mTOR inhibition with Rapamycin was next investigated. Specifically, a significant decrease in protein levels of TNFα-induced YAP in response to Rapamycin ($p<0.05$) was demonstrated, evident by the representative western blot image (Figure 2.15 (A)), thus, suggesting crosstalk between the YAP and mTOR pathways in which mTOR may regulate YAP expression. Finally in the presence of a specific YAP inhibitor Verteporfin, a significant decrease in RA FLS invasion was observed (Figure 2.15 (B-C)). Specifically, a significant decrease in TNFα-induced RA FLS invasion in the presence of Verteporfin ($p<0.01$; Figure 2.15 (B)) with a concomitant decrease in TNFα-induced MMP-1 and MMP-3 secretion was demonstrated ($p<0.05$ and $p=0.0781$, respectively) (Figure 2.15 (C)). Taken

together, these data suggest that dysregulation in the mTOR pathway in RA FLS may mediate its affects via the Hippo-YAP pathway to induce RA FLS invasive mechanisms in the joint.

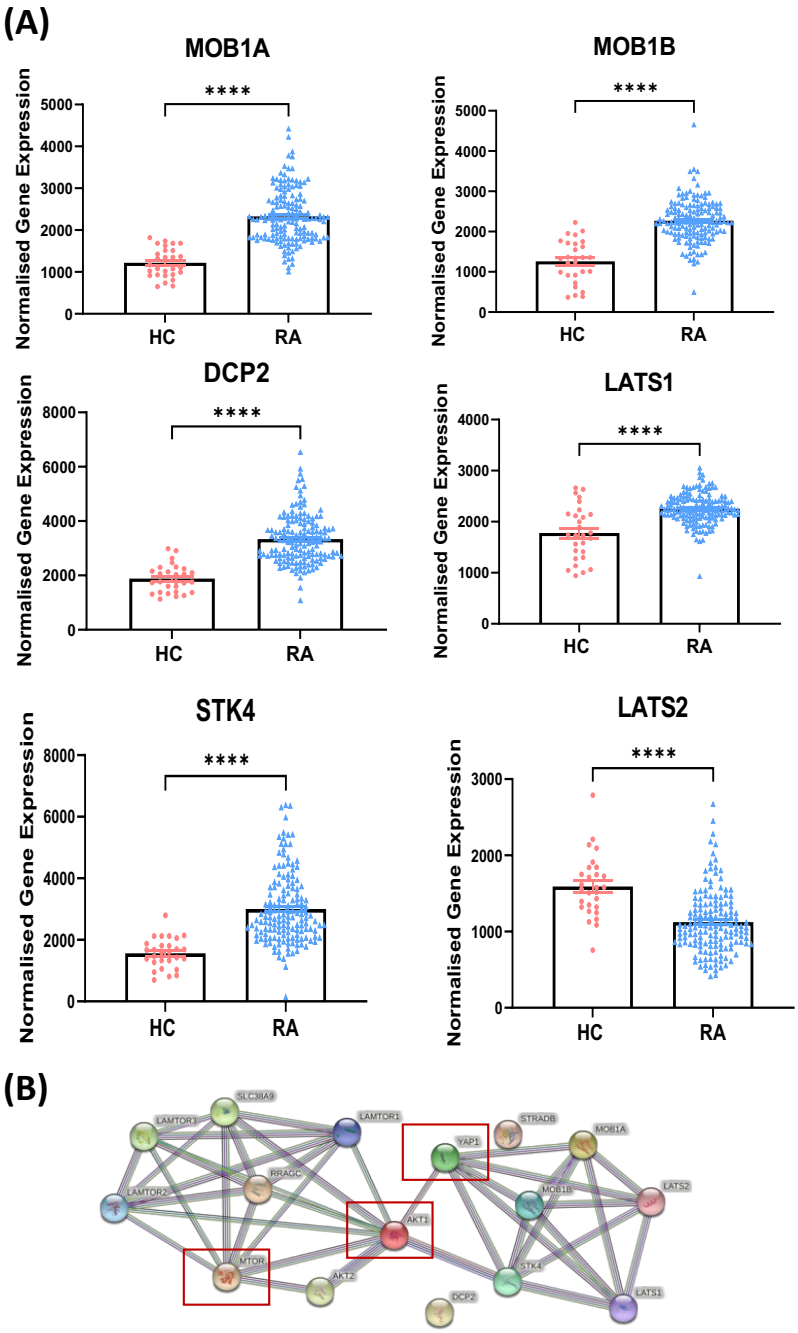

Figure 2.13: Genes involved in Hippo-YAP pathway are upregulated in RA compared to HC and may interact with mTOR.

(A) Bar graphs demonstrating normalised gene expression of MOB1A, MOB1B, DCP2, LATS1, STK4, and LATS2 in RA patients (n=152) compared to HC donors (n=28). (B) Predicted interactions of dysregulated YAP associated genes with dysregulated genes within the mTOR pathway using STRING pathway analysis. Data in graphs represented as mean ± SEM with Mann-Whitney U test used for statistical analysis with *p<0.05, **p<0.01, ***p<0.001, ****p<0.0001 being significant.

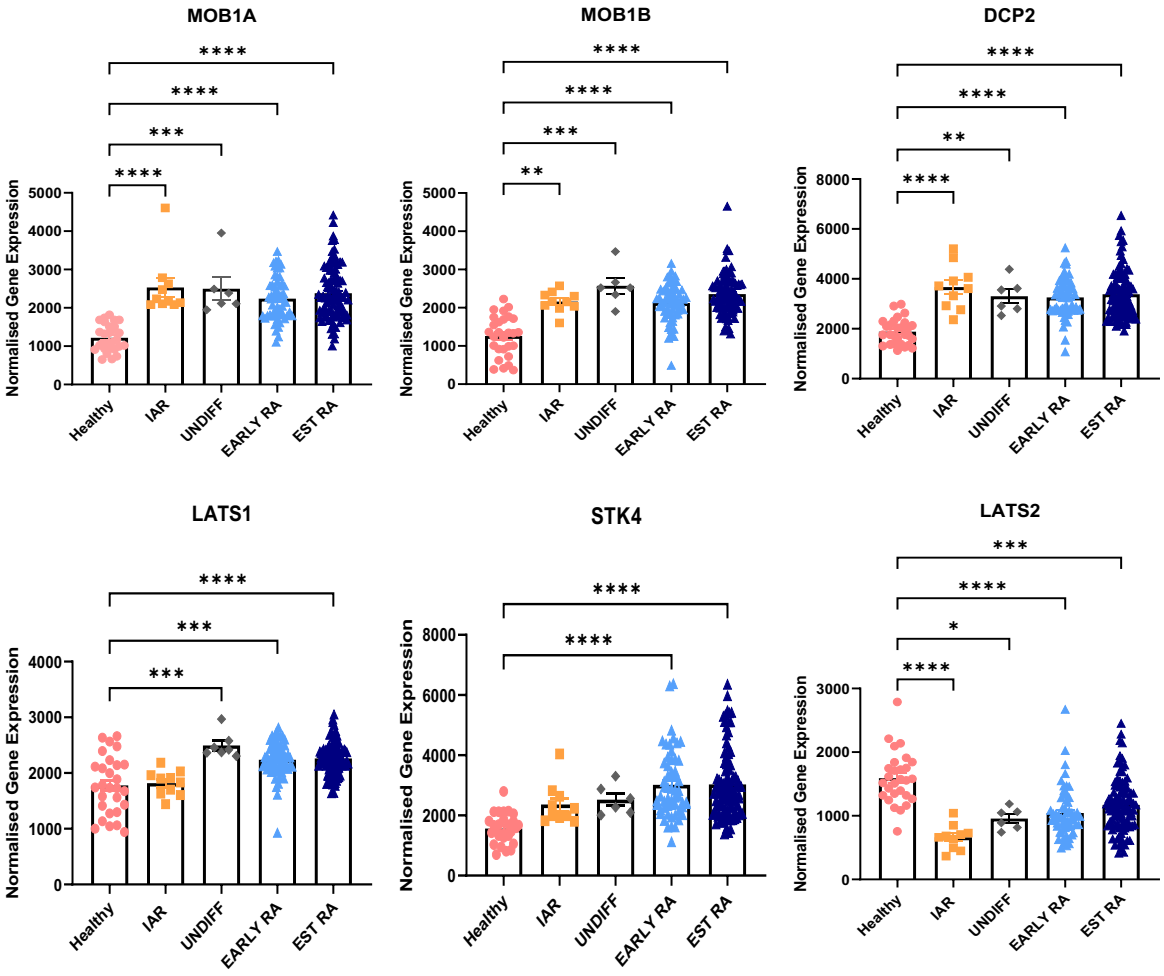

Figure 2.14: Genes involved in Hippo-YAP pathway are dysregulated prior to disease onset and throughout disease pathogenesis.

Bar graphs demonstrating normalised gene expression of key components in the YAP pathway (MOB1A, MOB1B, DCP2, LATS1, LATS2, and STK4) across disease status via transcriptomic analysis of bulk RNA-seq (GEO database GSE89408) on synovial tissue biopsies from HC donors (n=28), IAR (n=10), UA (n=6), early RA (n=57), and established RA (n=95). Data represented as mean ± SEM. Statistical analysis performed by Kruskal-Wallis ANOVA with Dunn's multiple comparisons with *p<0.05, **p<0.01, ***p<0.001, and ****p<0.0001 being statistically significant.

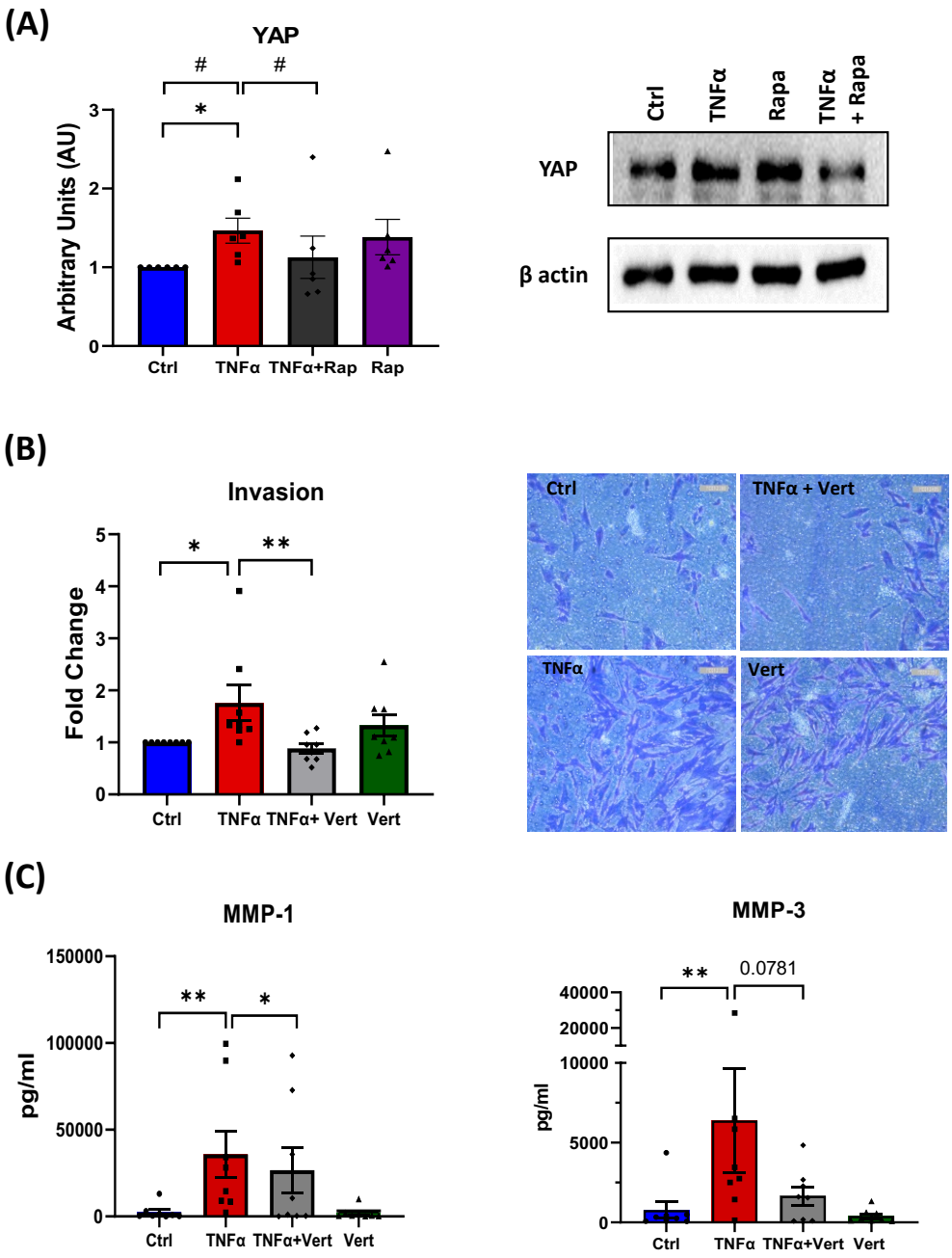

Figure 2.15: Crosstalk between dysregulated Hippo-YAP and mTOR pathways mediates RA FLS invasion.

(A) Bar graph and representative western blot image depicting total YAP expression in RA FLS (n=6) in the presence of TNFα (1 ng/mL) and Rapamycin (100 nM) alone or in combination for 24 h. β-actin was used as loading control. (B) Bar graph and accompanying representative photomicrographs demonstrating fold change of average number of invading RA FLS (n=8) treated with TNFα (1 ng/mL) and Verteporfin (50 nM) alone or in combination for 24 h. Data represented as mean ± SEM. Friedman ANOVA with Dunn's multiple comparison (#) and Wilcoxon Signed-Rank test (*) were utilised for RA FLS statistical analysis with *p<0.05, **p<0.01, #p<0.05.

2.5 Discussion:

In this chapter, a pathogenic role for the mTOR pathway in RA disease progression was identified, particularly at the site of inflammation in RA synovial tissue. Specifically, RA synovial tissue demonstrated dysregulated expression of several key components of the mTOR pathway including LAMTOR1, LAMTOR2, LAMTOR3, LAMTOR5, SLC38A9, RRAGC, STRADB, AKT1, and AKT2. Moreover, a specific increase in phosphorylated S6, the major downstream target of mTOR, in RA synovial FLS compared to HC FLS was demonstrated, an increase that was further observed in cultured primary RA FLS stimulated with TNFα which was then abrogated with the addition of Rapamycin. Rapamycin effectively altered RA FLS cellular bioenergetics by inhibiting baseline oxidative phosphorylation, overall ATP synthesis, and glycolysis along with the expression of rate-limiting glycolytic enzymes HK2, G6PD, and GLUT-1. A key role for mTOR signaling in uniquely mediating RA FLS migratory and invasive mechanisms was observed, which were significantly abrogated in the presence of Rapamycin. Finally, a significant upregulation in several genes involved in the Hippo-YAP pathway in RA synovial tissue was demonstrated, which were predicted to converge with the mTOR pathway. Crosstalk between the mTOR and YAP pathways in mediating RA FLS invasive mechanisms was identified whereby Rapamycin significantly inhibited RA invasiveness. Collectively, this chapter highlights a previously unexplored role for mTOR in RA FLS pathology via its interactions with the Hippo-YAP pathway.

A significant increase in the expression of the mTOR Ragulator complex components, LAMTOR2, LAMTOR3, and LAMTOR5 in RA synovial tissue was identified. Not only does this complex facilitate the activation of mTORC1, but previous studies have also demonstrated a role for the Ragulator complex in cell migration (Nakatani *et al.*, 2021). Moreover, an increase in the expression of SLC38A9, a lysosomal amino acid sensor that induces mTORC1 activation was demonstrated (Wang *et al.*, 2015) in RA synovial tissue. Previous studies have demonstrated that knockdown of SLC38A9 in RA FLS decreased expression of TNFα-induced TNFSF13B (also known as BAFF, a potent B cell activator) and CXCL11 (a chemokine for activated T cells) and increased expression of IL-6 and IL-8 suggesting that mTOR via SLC38A9, differentially regulates RA FLS inflammatory responses (Karonitsch *et al.*, 2018). Additionally, a significant decrease in AKT1 and AKT2 expression, known upstream regulators of mTOR, in RA synovial tissue was observed. Previous studies have demonstrated a potential role for the AKT pathway as negative regulators of inflammation. Specifically, inhibition of AKT enhances LPS-induced activation of ERK1/2, p38, JNK and NFκB in human monocytes, thus suggesting that AKT signaling may mediate inhibitory mechanisms of inflammation (Guha *et al.*, 2002). Collectively, this data suggests that dysregulation of the mTOR pathway within the RA synovium may contribute to disease pathogenesis, especially

with the observed increased expression of these genes in IAR and early RA. In support of this hypothesis, Karonitsch *et al.* (2018) demonstrated increased phosphorylated mTOR expression by histology in RA synovial tissue compared to OA tissue. Moreover, Cejka *et al.* (2010) previously reported that inhibition of mTOR reduced synovial osteoclast formation and protected against local bone erosions in TNFα-transgenic mice with inflammatory arthritis.

The inflamed RA synovium is composed of several tissue resident cells (FLS, ECs, and macrophages) and infiltrating cell subsets (T cells, B cells, monocytes, and DCs) which collectively potentiate site-specific inflammatory responses, resulting in synovial fibroblast activation, cartilage destruction, and bone erosion (McInnes and Schett, 2011). Thus, RA FLS are non-redundant pathological mediators of joint destruction. Therefore, next the mTOR pathway was examined specifically in the context of RA FLS, whereby increased expression of pS6, a marker of mTOR activation was demonstrated in RA FLS compared to HC FLS. Furthermore, RA FLS stimulated with TNFα *in vitro* recapitulated this phenotype with increased expression of pS6. This observation is in agreement with previous studies which demonstrate increased activation of pS6 in RA synovial tissue (Xu *et al.*, 2020) and in RA FLS stimulated with TNFα (Du *et al.*, 2019). The observed TNFα-induced induction of pS6 is mTOR dependent, as pS6 expression is abrogated in the presence of the mTORC1 selective inhibitor Rapamycin.

It is widely accepted that mTOR plays a critical role in cellular metabolism and, as such, is often referred to as a metabolic master regulator. While a large body of evidence now exists on the role of mTOR in regulating immune cell metabolism (Frauwirth *et al.*, 2002; Hackstein *et al.*, 2003; Thomson *et al.*, 2009; Deng *et al.*, 2017; Linke *et al.*, 2017), our understanding of the metabolic role mTOR has in stromal cells, particularly in FLS, is largely unknown. Here, for the first time a key role for mTOR signaling in RA FLS cellular bioenergetics was demonstrated. Specifically, Rapamycin inhibited both glycolysis and oxidative phosphorylation in RA FLS in addition to RA FLS ability to synthesise ATP. In parallel, inhibition of TNFα-induced HK2 and G6PD expression in the presence of Rapamycin was also observed, in contrast to a significant decrease in GLUT-1 expression. We and others have previously determined that RA FLS undergo metabolic reprogramming in the joint in response to their increased energy requirements. In response to pro-inflammatory mediators, such as TNFα, TLR signaling, hypoxia, or oxidative stress, FLS display increased glycolysis coupled with increased expression of glycolytic enzymes and glucose transporters (Biniecka *et al.*, 2016; McGarry *et al.*, 2017; Hanlon *et al.*, 2019). Moreover, previous studies have also determined a role for the JAK/STAT, HIF, and AMPK pathways (Biniecka *et al.*, 2016; Del Rey *et al.*, 2017; McGarry *et al.*, 2018; Gallagher *et al.*, 2020) in mediating RA FLS metabolic reprogramming, whereby activation of these pathways in the synovium results in a

more energetic RA FLS phenotype coupled with increased glycolysis and invasive capacity. While several pathways have been identified to date which mediate metabolic reprogramming in RA FLS, our data is the first to demonstrate a key role for mTOR signaling in RA bioenergetics.

It is now widely accepted that cellular metabolism is intrinsically linked to cellular function (Metallo and Vander Heiden, 2014). In addition to mediating metabolic reprogramming in RA FLS, a key role for mTOR in RA FLS function, specifically motility and migration was demonstrated. A significant decrease in TNFα-induced MCP-1 and RANTES secretion in response to Rapamycin was observed. This aligns with previous studies which report a decrease in LPS-induced MCP-1 and RANTES from human monocytes in response to mTOR inhibition (You-Hsien *et al.*, 2014). Interestingly, a significant increase in TNFα-induced IL-8 secretion in response to Rapamycin was shown, suggesting that mTOR may negatively regulate IL-8 production. This induction of IL-8 in response to Rapamycin was similarly observed by Karonitsch *et al.* (2018), who demonstrated an increase in IL-8 following SLC38A9 inhibition (an inducer of mTORC1).

Additionally, FLS migration is also mediated by the adhesion of fibroblasts to the extracellular matrix (ECM) via the expression of adhesion molecules such as ICAM-1 and VCAM-1 (Bartok and Firestein, 2010). While no statistically significant change in TNFα-induced VCAM-1 expression in response to Rapamycin was observed, a significant decrease in TNFα-induced ICAM-1 expression in response to Rapamycin was shown. Similarly, Sun *et al.* (2017) also reported decreased adherence of macrophages to HUVECs via decreased ICAM-1 expression in the presence of Rapamycin. This suggests that mTOR inhibition may reduce RA FLS migration in part via dysregulated chemokine production and adhesion marker expression. In support of this, a significant reduction in TNFα-induced RA FLS migration in response to Rapamycin was demonstrated. Indeed, in the cancer setting, mTOR has been shown to play a critical role in the regulation of tumour cell migration, invasion, and metastasis, while previous studies have also highlighted a key role for mTOR in EC, vascular smooth muscle cell, macrophages and granulocyte migration (Poon *et al.*, 1996; Gomez-Cambronero *et al.*, 2003; Moss *et al.*, 2010; Zhou *et al.*, 2011; Weichhart *et al.*, 2015).

TNFα-induced MMP-1 secretion and RA FLS invasion was also decreased in response to mTOR inhibition. In agreement with these findings, Laragione *et al.* (2010) reported decreased invasion of both rat and RA FLS in response to Rapamycin. This study also reported no significant change in the levels of several MMPs in response to Rapamycin, however this was performed in rat FLS and therefore is not as reflective as the invasive properties of human RA FLS. Collectively, these data suggests that mTOR specifically regulates RA FLS migratory and invasive mechanisms.

We hypothesised that mTOR may regulate this RA FLS phenotype via crosstalk with the Hippo-YAP pathway. In support of this hypothesis, increased expression of several components of the Hippo-YAP pathway in RA synovial tissue compared to HC was demonstrated, while also predicting potential protein interactions via mTOR and YAP. Moreover, previous studies have demonstrated crosstalk between the Hippo-YAP and mTOR pathways in regulating organ size during development through their combined control of cell growth and proliferation (Park *et al.*, 2016). Furthermore, YAP has been shown to upregulate mTOR activity via the upregulation of amino acid transporters (Park *et al.*, 2016), while the mTOR pathway itself has been shown to control YAP activity through various mechanisms (Collak *et al.*, 2012; Liang *et al.*, 2014; Artinian *et al.*, 2015).

Specifically, increased expression of key components of the Hippo-YAP pathway involved in cell proliferation (MOB1A; MOB1B), in addition to YAP regulation and activation (LATS1; LATS2; STK4) were demonstrated. This is consistent with previous studies which reported increased expression of YAP/TAZ target genes in RA FLS compared to osteoarthritis FLS (OA FLS) (Caire *et al.*, 2021), while YAP expression has also been shown to be increased in synovial fibroblasts from both antigen-induced arthritis mice and human RA synovium (Symons *et al.*, 2022). In addition to previously aforementioned studies which demonstrated crosstalk between mTOR and Hippo-YAP pathway, we also reported regulation of YAP expression via mTOR signaling in RA FLS. Collectively, our data in addition to previous studies suggest interactions between mTOR in mediating cell-specific effects. Indeed, blockade of YAP via Verteporfin inhibited TNFα-induced RA FLS invasion and MMP-1 and MMP-3 secretion. Caire *et al.* (2021) previously reported a significant reduction in TNFα and IL-17a induced invasion in the presence of Verteporfin in RA FLS in addition to a specific reduction in MMP-13 secretion. This suggests that inhibition of YAP and mTOR signaling can reverse the aggressive invasive synovial fibroblast phenotype present in RA.

Collectively, our data demonstrated a role for mTOR and YAP crosstalk in RA FLS pathogenicity. Given that it has previously been reported that synovial inflammation associated with a fibroblast signature (pauci-immune pathotype) is possibly linked with difficult to treat or refractory RA (Nerviani *et al.*, 2020; Rivellese *et al.*, 2022), it would be beneficial to explore these pathways in refractory RA versus those that respond to treatment. We hypothesise that due to the pathogenic role mTOR plays in RA FLS function, this pathway may be more clinically relevant in those patients with this pauci-immune, refractory disease. Indeed, while our analysis examined mTOR and YAP pathways across the evolution of RA (IAR, UA, early, and established RA), it was beyond the scope of this work to examine patients in disease remission. However, this would be

an interesting area for future investigation as it would provide more insight on the role mTOR plays in RA pathogenicity and FLS activation.

To summarise, while the metabolic and inflammatory effects of the mTOR pathway have previously been explored in both innate and adaptive immune cells, the contribution of this pathway to FLS pathogenicity has yet to be extensively studied. In this chapter, we demonstrated a significant role for mTOR in driving RA FLS metabolism and function, with a specific effect on RA FLS migration and invasion. Furthermore, we identified a potential role for mTOR:YAP crosstalk in mediating these RA FLS invasive mechanisms. Targeting the mTOR:YAP axis may prove beneficial in preventing RA FLS pathogenicity and joint destruction.

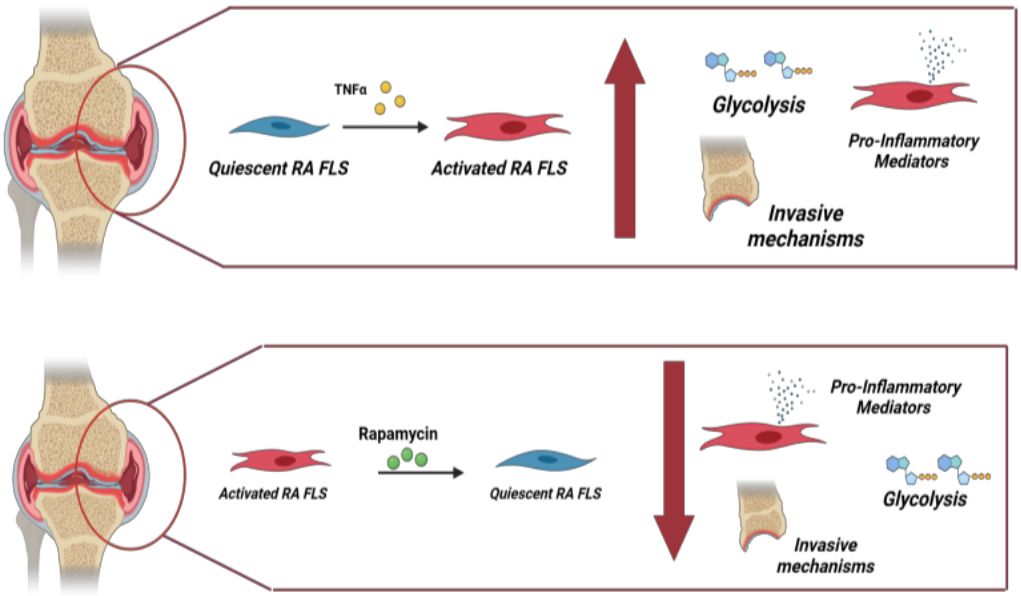

Figure 2.16: Summary of Therapeutic Effects of Rapamycin on TNFα-Stimulated RA FLS.

TNFα-induced pathogenic and metabolic phenotype of RA FLS is reversed by mTOR inhibition. These invasive mechanisms are orchestrated in part due to the crosstalk between the mTOR and YAP signaling pathways. (Image created in Biorender 2025).

CHAPTER THREE:

Identification and Characterization of PRIME Cells in the Circulation and at the Site of Inflammation in Patients with Rheumatoid Arthritis and Individuals-At-Risk

3.1 Introduction:

FLS are one of the two main resident cells found within the tissue of the healthy synovium. They are essential for maintaining normal structure and function of the joint by not only forming the lining layer of the tissue, but also providing lubrication to the joint (Jay *et al.*, 2001; Bottini and Firestein, 2013; Ospelt, 2017). In the context of RA, FLS have been shown to adopt a pathogenic phenotype through the release of pro-inflammatory cytokines, chemokines, growth factors and MMPs, in addition to the activation of pro-inflammatory signaling pathways (Xu *et al.*, 1989; Sweeney and Firestein, 2004; Grabiec *et al.*, 2015; Ospelt, 2017; Marsh *et al.*, 2021). In addition, studies have shown an inhibition of pro-apoptotic factors including PTEN, SEN-P1 and mir-34A, increased expression of pro-survival factors including FLIP, SUMO-1, and an overactivity of Ras, Myc and NFκB pathways in RA FLS, thus further supporting their survival mechanisms in disease (Korb *et al.*, 2009). RA FLS have come to be appreciated as one of main drivers of destruction within the joint due to their migratory capacity and release of MMPs capable of breaking down extracellular matrix, facilitating their invasion into the cartilage. As potent producers of RANKL, they are significant contributors to bone erosion (Kim *et al.*, 2007; Sabeh *et al.*, 2010). The migratory and invasive capacity of RA FLS and their ability to degrade cartilage is not dependent on proliferative mechanisms, but rather an altered activation of intracellular signaling pathways leading to increased expression of adhesion molecules (including VCAM-1), MMPs, and apoptotic inhibitors (Seemayer *et al.*, 2003). Their invasive phenotype is also mediated through increased β1-integrin expression and an alteration in cytoskeletal dynamics through induction of filopodia formation and activation of Rho-GTPases (McGarry *et al.*, 2015).

Recent studies have uncovered the complexity and heterogeneity of RA FLS with the identification of diverse phenotypic subsets exhibiting varied functions (Croft *et al.*, 2016; Croft *et al.*, 2019, Wei *et al.*, 2020; Lendahl *et al.*, 2022; Floudas *et al.*, 2022). FLS within the synovium can be broadly categorised into lining layer (LL) and sub-lining layer (SL) with LL FLS generally denoted as CD55+PRG4+THY-1- and SL denoted as THY-1+ (Marsh *et al.*, 2021). However, with recent technological advances such as scRNA sequencing, subsets have become more nuanced, with numerous FLS sub-types that may be defined by cell-cell gradients within the synovium and associated with a specific disease pathotype (Wei *et al.*, 2020; Kemble and Croft, 2021; Floudas *et al.*, 2022; Zhang *et al.*, 2023).

RA is often not isolated to a single joint but rather affects multiple joints in the body as the disease progresses (Aletaha *et al.*, 2010). Current speculation attributes this to humoral or cellular immune factors (Volkov *et al.*, 2019; Gao *et al.*, 2024; Salnikova *et al.*, 2024). However, Lefévre *et al.* (2009) demonstrated that human RA FLS have the capacity to migrate through the

circulation from one site of inflammation to another. Indeed, utilizing a SCID mouse model, it was shown that not only could RA FLS degrade the human cartilage it was co-implanted with, but can migrate through the circulation to cartilage contralaterally implanted without RA FLS where erosive lesions were also observed (Lefévre *et al*., 2009). This work reinforced the hypothesis that RA FLS are one of the key players in cartilage destruction and demonstrated for the first time the long-distance migratory capacity of RA FLS through the vasculature; a novel idea as FLS were thought to be tissue resident cells solely capable of migrating short distances for the purposes of wound healing. It has been proposed that the transcriptomic phenotype signature of FLS is the result of their tissue condition/state (diseased, stressed, ageing, homeostatic, regenerating), regional or anatomical heterogeneity (including developmental origin, microbiome, and tissue specific functional requirements), local heterogeneity (cell-matrix interactions, paracrine and autocrine signals, etc.), and cell phenotype (quiescent, activated, differentiating, proliferating, etc.). Indeed, multiple studies have demonstrated that the diversity and function of FLS depend on the joint type and location (positional memory) (Chang *et al.*, 2002; Frank-Bertoncelj *et al.*, 2017; Ospelt and Frank-Bertoncelj, 2017; Buckley *et al.*, 2021; Forte *et al.*, 2022). Together these studies suggest that FLS have the capacity to migrate from joint to joint, indicative of clinical disease joint spreading, and that FLS at each site are influenced by the local microenvironment.

'Pre-inflammatory mesenchymal' or PRIME cells were first identified in the circulation of RA patients by Orange *et al.* (2020). In their attempt to better understand and predict RA flares, blood samples were collected from patients at various time points. RNA-sequencing identified a cluster of genes associated with extracellular matrix organization, bone growth, and cartilage morphogenesis, not typically found in blood and indicative of mesenchymal cells. Additionally, this gene cluster contained enriched expression of sub-lining FLS genes including CD34, HLA-DR, DKK3, FAP, Cadherin11, and multiple collagens and laminins. Flow cytometry cell sorting confirmed the presence of cells expressing CD45-CD31-PDPN+ and termed PRIME cells (Orange *et al.*, 2020). Unlike fibrocytes (CD45+ cells with mesenchymal characteristics), which had already been identified in the blood, PRIME cells are CD45- (Gravellese and Robinson, 2020). Interestingly, the presence of these PRIME cells and identified gene signature were associated with disease flare, with levels of both increased prior to a flare, suggesting these cells may be migrating to the joint to mature into sub-lining FLS (Orange *et al.*, 2020). Since FLS are primarily thought of as tissue resident cells, gaining more insight on the phenotype of PRIME cells and their migratory capacity will help provide more clues on how subsets of FLS develop. Additionally, it may further elucidate the heterogeneity observed in FLS across different joints.

This chapter focuses on identifying and phenotypically characterizing circulating CD45-CD31-PDPN+ PRIME cells in patients with RA compared to healthy control (HC) and additionally determine if these cells are present and have an altered phenotype prior to disease onset in IAR. Furthermore, it aims to ascertain whether PRIME cells exhibit markers characteristic of FLS subsets, specifically sub-lining. Finally, this chapter assesses whether PRIME cells can migrate from the circulation into the joint and have the propensity to alter their phenotype further once in an inflammatory environment, by comparing the PRIME cells in circulation to CD45-CD31-PDPN+ cells identified within synovial tissue biopsies, with an objective to better understand their role in RA pathogenesis.

3.2 Specific Aims for this Chapter:

- To identify CD45-CD31-PDPN+ PRIME cells in the circulation of seropositive (RA+) and seronegative (RA-) patients and compare their frequencies to those found in HC.
- To conduct comprehensive flow cytometry characterization of PRIME cell phenotype and investigate the phenotypic differences observed between HC, RA+, and RA- samples.
- To determine whether the frequency of PRIME cells is increased prior to onset of clinical symptoms in IAR and seronegative ART individuals and elucidate whether functional profiles of these cells are altered prior to disease onset.
- To compare frequencies and phenotypes of PRIME cells from the circulation to CD45-CD31-PDPN+ cells within the site of inflammation (synovial tissue).

3.3 Materials and Methods:

3.3.1 Patient Recruitment and Sample Collection

RA patients, Individuals-at-Risk (IAR), and seronegative arthralgia (ART) individuals were recruited from the Department of Rheumatology, St. Vincent's University Hospital. All patients provided fully informed written consent for the use of biological samples and medical information approved by the St Vincent's University Hospital, Ethics and Medical Research Committee prior to inclusion. Research was performed in accordance with the guidelines and regulations of the Declaration of Helsinki. Only RA patients with an actively inflamed knee joint as well as those that fulfilled the revised ACR/EULAR criteria were included (Aletaha *et al.*, 2010). IAR were defined according to the revised ACR/EULAR criteria as having no clinical symptoms of arthritis but seropositive for RF and ACPA (Aletaha *et al.*, 2010). ART were defined as individuals presenting with general aches and pains but having no clinical symptoms of arthritis and seronegative for autoantibodies.

3.3.2 Obtaining Synovial Tissue and Blood Samples

RA patients synovial tissue biopsies were obtained from the knee at the time of key-hole video arthroscopy under local anaesthetic using a Wolf 2.7 mm arthroscope (Wolf – Germany) as previously described (Ng *et al.*, 2010). Biopsies were then viably frozen in freezing media (10% DMSO in FBS). Blood samples from RA, IAR and ART individuals were obtained at the time of arthroscopy and from rheumatology research outpatient clinics. Healthy blood, used for comparison, was also obtained from anonymous HC. Clinical information of patients with RA for synovial tissue samples (n=14) included in this study can be found in Table 3.1. Clinical information of patients with RA at time of collection of blood samples (n=39) used for peripheral blood mononuclear cell isolation (PBMC) can be found in Table 3.2.

Characteristics	Number or Average	Percent or Range
Age (years)	54.2	19-72
Female	13	92.9% (13/14)
Seropositive (ACPA+ and/or RF+)	**8**	**57.4% (8/14)**
RF positive	8	57.4% (8/14)
ACPA positive	7	50% (7/14)
Seronegative	6	42.6% (6/14)
Disease duration (years)	4.9	<1-15
DAS28 score	3.78	1.8-8.22
CRP	20.1	0-153
On DMARD	4	28.6% (4/14)
On biologic	1	7.1%
Treatment naïve	9	64.3% (9/14)

Table 3.1: **Patient demographics for RA synovial tissue biopsies used for flow cytometry analysis.** Anti-citrullinated protein antibodies (ACPA), Rheumatoid Factor (RF), Disease activity score (DAS28), Disease-modifying anti-rheumatic drug (DMARD).

Characteristics	Number or Average	Percent or Range
Age (years)	53.4	19-78
Female	30	76.9% (30/39)
Seropositive (ACPA+ and/or RF+)	**23**	**59% (23/39)**
RF positive	23	59% (23/39)
ACPA positive	20	51.3% (20/39)
Seronegative	16	41% (16/39)
Disease duration (years)	5.6	<1-22
DAS28 score	3.41	1.24-6.18
CRP	9.6	0-81.5
On DMARD	20	51.3% (20/39)
On biologic	9	23.1% (9/39)
Treatment naïve	10	25.6% (10/39)

Table 3.2: **Patient demographics for RA PBMCs used for flow cytometry analysis.**
Anti-citrullinated protein antibodies (ACPA), Rheumatoid Factor (RF), Disease activity score (DAS28), Disease-modifying anti-rheumatic drug (DMARD).

Characteristics	Number or Average	Percent or Range
Age (years)	31	23-49
Female	6	75% (6/8)

Table 3.3: Demographics for HC donor PBMCs used for flow cytometry analysis.
N=9* HC donors were included in the analysis. *Demographic information missing for one individual.

3.3.3 Synovial Tissue Digestion

The method used for synovial tissue digestion was previously described by Floudas *et al.* (2022), which optimised experimental approaches for cell yield, cellular viability, and marker stability. In brief, synovial tissue biopsies were thawed quickly in a 37°C water bath and digested enzymatically using a Tumour Dissociation Kit, human (Miltenyi Biotec, Germany) as per the manufacturer's instructions. Briefly, 50 µL Enzyme A (nuclease), 150 µL Enzyme H (protease), and 100 µL Enzyme R (protease) were diluted in 600 µL RPMI (Sigma). Biopsies were incubated in 100 µL enzyme mixture for 45 min to 1 hr at 37°C and 5% CO_2. The mixture was then passed through a 70 µM cell strainer to remove debris and undigested pieces of tissue, to yield single-cell synovial suspensions, which were then utilised for flow cytometric analysis (Section 3.3.5).

3.3.4 Peripheral Blood Mononuclear Cell Isolation

Blood was obtained from RA patients, IAR, and ART individuals either at the time of arthroscopy or from rheumatology research outpatient clinics. HC donor blood was obtained continuously from volunteers. Blood was collected in lithium heparin-containing tubes. PBMC were isolated from whole blood by Ficoll density gradient centrifugation (Lymphoprep; Stemcell Technologies, Canada). Blood was diluted in a 1:1 ratio with PBS before layering over 15 mL Lymphoprep and centrifuged at 2000 rpm for 20 min with the brake inactivated and acceleration at 1. The buffy coat PBMC layer was collected from the interface of the density gradient and washed twice with sterile PBS and centrifuged at 1800 rpm for 7 min and subsequently at 1600 rpm for 7 min. A cell count was performed and PBMC were viably frozen in freezing media (10% DMSO in FBS).

3.3.5 Flow Cytometry

Expression of cell surface markers (CD45-CD31-PDPN+) was assessed using flow cytometry to identify PRIME cells. For PBMC samples, four million cells were stained, and tissue biopsy digested samples were used in their entirety and stained. PBMCs and tissue biopsies were thawed and stained in a 96-well round bottom plate using the fluorochrome-conjugated antibodies listed in

Table 3.3. Cells were suspended in viability dye Live/Dead Zombie NIR (Biolegend) in PBS at a 1:3000 dilution (1:1000 for tissue biopsies) for 30 min in the dark at 4°C. Subsequently, cells were topped up with PBS and centrifuged at 1400 rpm for 3 min and washed a second time. Samples were resuspended and blocked in a solution 5 µL Human TruStain FcX (Biolegend) and 95 µL PBS for 10 min to eliminate nonspecific binding to the Fc-gamma receptor (FcγR). Extracellular fluorochrome-conjugated antibodies were added, and samples were vortexed and incubated for 30 min in the dark at 4°C. Samples were then washed with FACS Buffer (Dulbecco's PBS without Mg_2+ or Ca_2+ (Sigma-Aldrich), 2% heat-inactivated FBS (Biosciences) and 0.05% sodium azide (Sigma-Aldrich), 0.5 M EDTA, pH 8.0 (Ambion)) and centrifuged at 1400 rpm for 3 min. Supernatants were removed and samples washed a second time. The FoxP3/Transcription Factor Staining Buffer Set (Invitrogen, USA) was utilised for intracellular staining. After the second wash, samples were resuspended in 100 µL Fix/Perm Solution (diluted 1:4 in kit diluent) and left to incubate for 30 min in the dark at 4°C. Samples were washed with Perm Buffer, resuspended with 30 µL Perm Buffer and intracellular antibodies, and left to incubate for 30 min in the dark at 4°C. Samples were washed twice with Perm Buffer and FACS buffer, respectively and resuspended in 250 µL FACS buffer. Samples were acquired using the Aurora Flow Cytometer (Cytek Biosciences) and analysed using FlowJo software (FlowJo LLC, Oregon, USA).

Cells were gated based on forward and side scatter, and doublets and dead cells were removed. Live/Dead Zombie NIR viability dye (Biolegend) was used to eliminate dead cells. Fluorescence Minus One (FMO) controls were utilised to determine gating boundaries between markers where appropriate. To adjust for spectral overlap between laser detectors, compensation was applied via single-stained compensation beads (BD) that were prepared for each fluorochrome. Samples were spectrally unmixed directly on the Aurora Flow Cytometer before each run.

The markers analysed allowed for (i) the exclusion of other cell types included within the PBMCs, and (ii) identification of PRIME cell subsets and functional phenotype:

- Exclusion of haematopoietic cells (CD45+), ECs (CD31+), and inclusion of (PDPN+) for identification of PRIME
- PRIME immune markers (HLA-DR, CD200, CD200R1)
- PRIME proliferative and invasive markers (Ki67, PDGFRα, YAP)
- PRIME adhesive markers (VCAM-1, ICAM-1, CD44, CD61)
- PRIME metabolic markers (pAKT, pmTOR, ps6)
- PRIME FLS activation and subset markers (FAPα, Cadherin 11, CD55, CD90, CD34)

Antibody	Fluorochrome	Clone	Company
HLA-DR	BV421	L243	Biolegend
CD200	eFlour450	OX104	Invitrogen; eBioscience
VCAM-1 (CD106)	BV480	51-10C9	BD
CD34	BV510	581	Biolegend
CD31	BV605	WM59	Biolegend
Ki67*	BV650	11F6	Biolegend
CD146	BV711	P1H12	BD
CD90	BV750	5E10	BD
CD44	BV785	IM7	Biolegend
CD45	AF532	HI30	Invitrogen; eBioscience
CD61 (Integrin β3)	PerCP	VI-PL2	Biolegend
pS6 (Ser235, Ser236)*	PerCP/Cy5.5	A17020B	Biolegend
ICAM-1 (CD54)	PerCP-eFluor710	HA58	Invitrogen; eBioscience
YAP*	PE	D8H1X	Cell Signaling
pAKT*	PE-CF594	M89-61	BD
CD140α (PDGFRα)	PE/Cy5	APA5	Biolegend
CD200R1	PE/Cy5.5	OX108 (Chimeric)	NOVUS
Cadherin 11	PE/Cy7	16G5	Biolegend
CD55	APC	JS11	Biolegend
pmTOR*	AF647	O21-404	BD
FAPα	AF700	427819	Novus
Podoplanin	APC-Fire750	NC-08	Biolegend

Table 3.4: **Panel of fluorochrome antibodies used for flow cytometry analysis of PRIME cells in PBMC and synovial tissue biopsy samples.** *Indicates intracellular stains

3.3.6 Statistical Analysis

Statistical analyses were performed using GraphPad Prism 9.5.0 software. Mann Whitney U test (*) or Kruskal-Wallis ANOVA (#) were used for analysis of non-parametric data. P-values of less than 0.05 (*$p<0.05$) or (#$p<0.05$) were determined as statistically significant for Mann Whitney U test or Kruskal-Wallis ANOVA, respectively. Data were expressed as mean ± SEM.

3.4 Results:

3.4.1 Identification of PRIME Cells in the Circulation of RA Patients

RA often affects multiple joints, especially as the disease progresses, however the mechanisms by which joint spreading occurs is unclear. Previous studies have demonstrated migration of FLS from co-implantation of FLS-cartilage in one joint to cartilage alone in the contralateral joint in a SCID mouse model, suggesting FLS can migrate from site to site (Lefèvre *et al.*, 2009). This concept was further supported by the eloquent study performed by Frank-Bertoncelj *et al.* (2017), where they demonstrate positional memory of FLS is epigenetically driven leading to anatomical diversity of FLS across joints, even within the same patient. More recently, Orange *et al.* (2020) identified the presence of pre-inflammatory mesenchymal cells or 'PRIME' cells in the periphery of RA patients just before a flare, suggesting these cells may be activated by immune cells before migrating into the joint where they mature into FLS and exacerbate the inflammation seen within the tissue. In this chapter we aim to identify and phenotypically characterise PRIME cells in the circulation of RA patients compared to HC and determine whether their presence predates clinical onset. To accomplish this, bloods were obtained and PBMCs isolated from HC and patients with RA, in addition to IAR and ART individuals. PBMCs were stained using a panel of human synovial fibroblast subset associated markers (see Table 3.3) to assess the frequency and phenotype of PRIME cells.

Representative flow plots outlining the gating strategy used for detection of PRIME cells are shown in Figure 3.1. Following the exclusion of debris, cell doublets and dead cells, PRIME cells were identified based on the populations negative for CD45 (haematopoietic cells) and CD31 (EC) and positive for podoplanin (PDPN) (Figure 3.1 (A)-(F)). Further phenotyping of PRIME cells was based on the expression of markers listed in Table 3.3. PRIME cells were positively identified and had higher frequency in the peripheral blood of both seropositive (RA+) (n=23) and seronegative RA (RA-) (n=16) patients compared to HC (n=9) (Figure 3.2). The presence and frequency of PRIME cells from the periphery are demonstrated by representative flow cytometric dot plots as a percentage of live cells (Figure 3.2 (A)). Interestingly, the frequency of PRIME cells was significantly highest in RA- compared to both HC ($p<0.05$) and RA+ ($p<0.05$) (Figure 3.2 (B)).

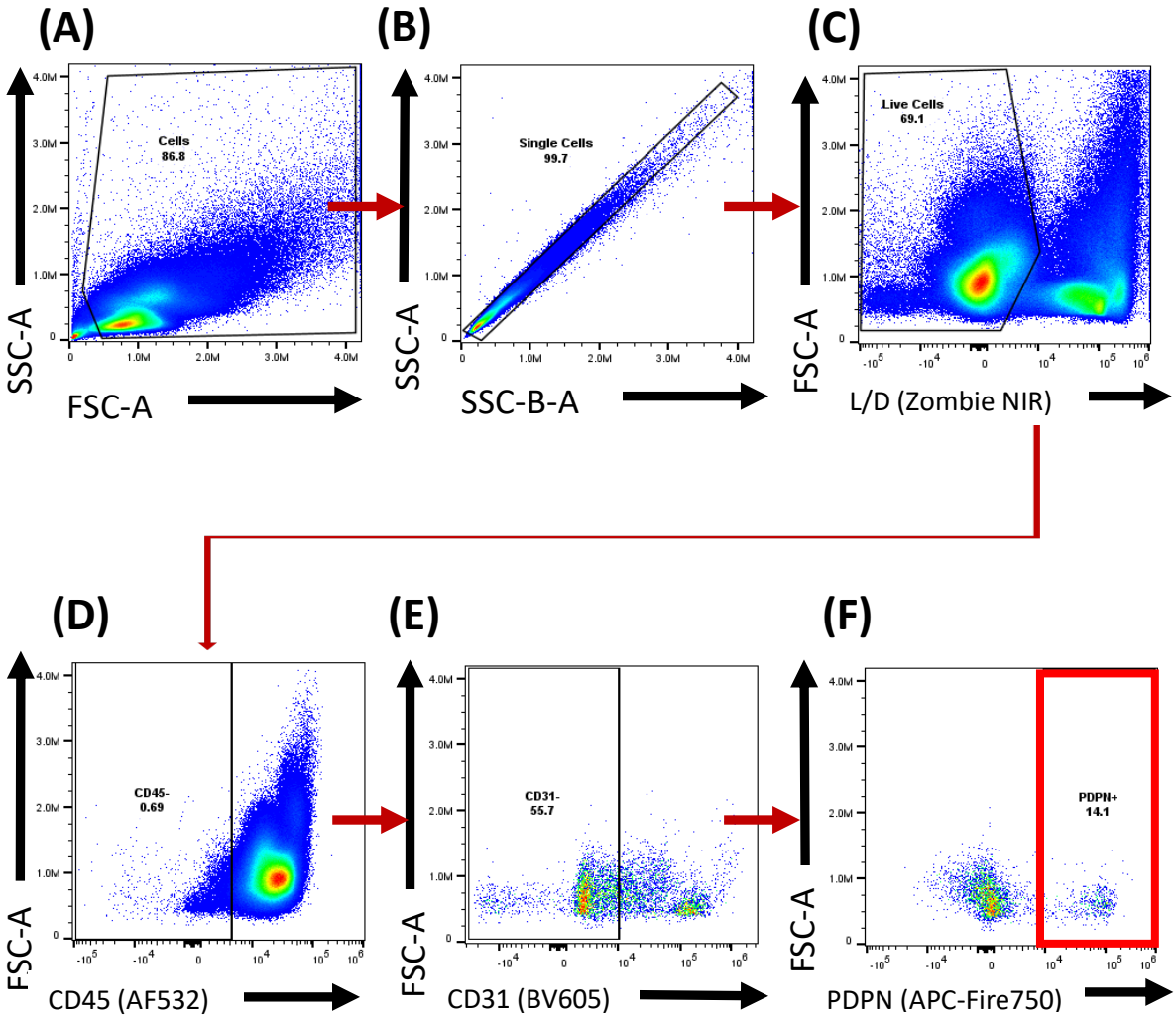

Figure 3.1: Peripheral blood PRIME cell (CD45-CD31-PDPN+) gating strategy.

Thawed PBMCs from HC donors, IAR, ART, and RA patients were stained with a panel of fluorochrome antibodies (see Table 3.3). Representative dot plots depicting the gating strategy used to identify and characterise PRIME cells from the circulation. (A-C) Forward and side scatter parameters established for cells before exclusion of doublets and dead cells. (D-F) PRIME cells were identified as CD45-CD31-PDPN+ and further characterised by expression of intracellular and extracellular markers.

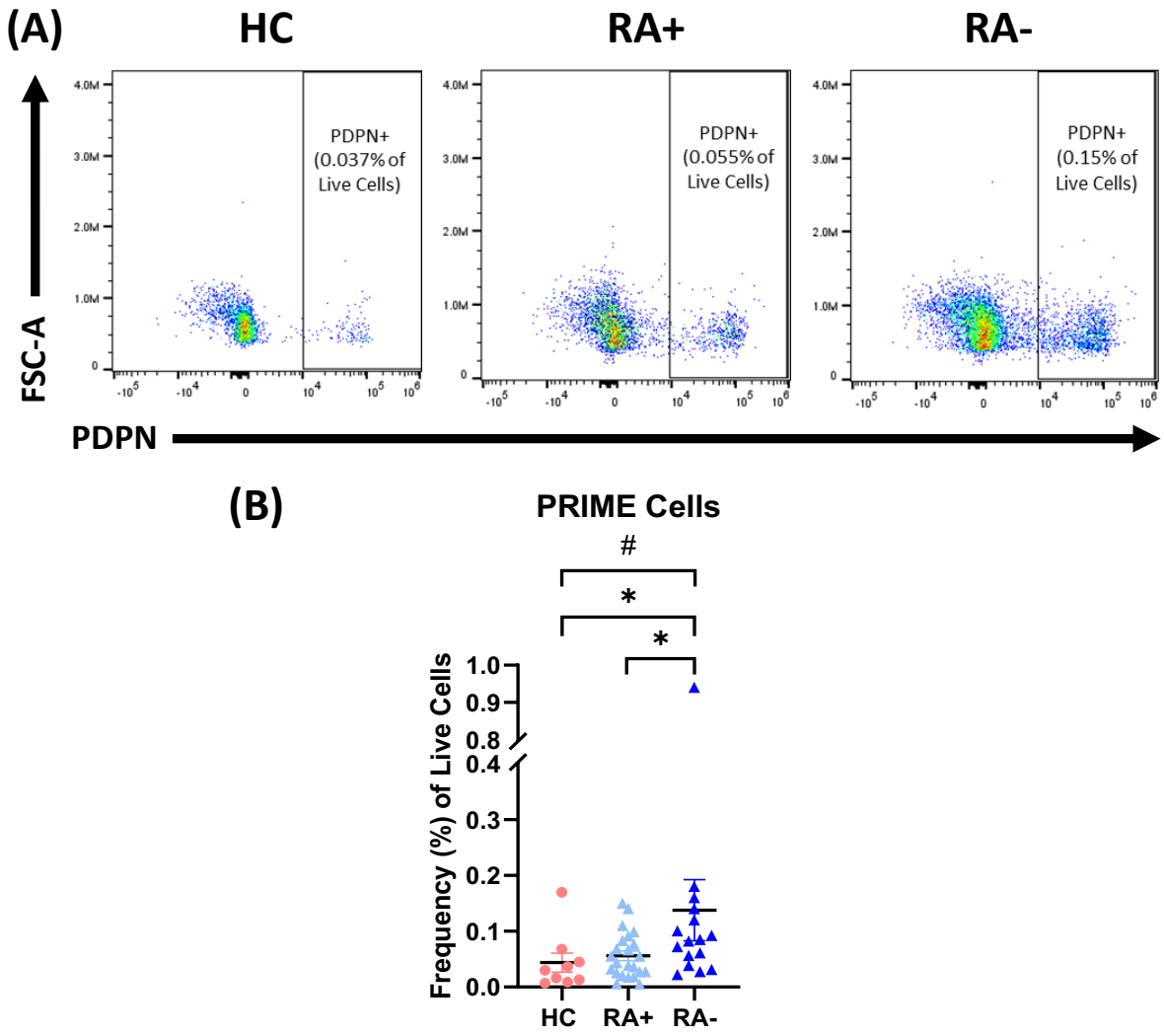

Figure 3.2: Identification of PRIME cells in the peripheral blood of HC and RA.

(A) Representative flow cytometric dot plots for the identification of CD45-CD31-PDPN+ PRIME cells in the peripheral blood of HC donors, seropositive RA (RA+), and seronegative RA (RA-) patients. (B) Dot plot demonstrating the significant increase in frequency of PRIME cells in RA- (n=16) compared to both RA+ (n=23) and HC (n=9). Data represented as mean ± SEM with each symbol representing a different sample. Statistical analysis using Mann Whitney U test (*) and Kruskal-Wallis ANOVA (#) was used to determine significance with *p<0.05 and #p<0.05 indicating significance, respectively.

3.4.2 Inflammatory Profiling of RA PRIME Cells Compared to HC

It has been previously hypothesised that PRIME cells could be activated by immune cells while in the circulation before migrating into the joint and developing into mature FLS (Orange *et al.*, 2020). To further investigate this hypothesis, we sought to phenotypically characterise PRIME cells to better understand their functional capacity. Frequency of PRIME cells expressing immunoregulatory molecules HLA-DR and CD200 was next examined, where a significantly higher frequency in RA patients compared to HC was observed (Figure 3.3 (A-C)). Specifically, HLA-DR was significantly higher on RA- PRIME cells compared to HC ($p<0.05$) with a similar increase observed for RA+ PRIME cells trending towards significance ($p=0.0762$) (Figure 3.3 (C)). No difference was observed between RA+ vs RA- HLA-DR positive PRIME cells. Additionally, CD200+ PRIME cells demonstrated a significant increase in frequency in RA+ patients compared to HC ($p<0.05$) (Figure 3.3 (C)), with a trending increase in frequency observed for RA- patients compared to HC (Figure 3.3(C)). PRIME cells also expressed the receptor CD200R1 at high frequencies, however, levels did not differ between HC, RA+, and RA- patients (Appendix Figure 7.3 (A)).

The adhesive capacity of PRIME cells was also assessed to better determine their ability to successfully migrate into the joint from the circulation. Representative flow dot plots for VCAM-1 and ICAM-1 are shown in Figure 3.4 (A) and (C). The frequency of PRIME cells positive for expression of VCAM-1 was increased in RA+ patients, but not RA- patients, compared to HC (Figure 3.4 (A-B)). Indeed, the frequency of VCAM-1+ PRIME cells was also higher in RA+ patients compared to RA- patients trending toward significance ($p=0.0522$) (Figure 3.4 (B)). Additionally, the frequency of ICAM-1 positive expressing PRIME cells was increased in RA compared to HC. A stepwise increase in the frequency of ICAM-1 positive PRIME cells was demonstrated from HC to RA+ to RA- (Figure 3.4 (C-D)). Similarly, a stepwise increase in expression of ICAM-1 on the PRIME cells, as measured by MFI, was observed from HC to RA+ to RA- (Figure 3.4 (E-F)). Representative stacked histograms demonstrating a shift in MFI across cohorts are shown for ICAM-1 expression in Figure 3.4 (F). Representative flow dot plots are shown for adhesion molecules CD61 and CD44 in Figure 3.5 (A) and (C). A stepwise increase in % frequency of PRIME cells positive for CD61, also known as integrin β3, from HC to RA+ to RA- was observed (Figure 3.5 (A-B)), however did not reach statistical significance. Likewise, a similar stepwise increase in % frequency of CD44 expressing PRIME cells was observed from HC to RA+ to RA- (Figure 3.5 (D)), with an increase in CD44 MFI expression also observed for RA PRIME cells compared to HC (Figure 3.5 (E)). Representative stacked histograms demonstrating a shift in MFI across cohorts are shown for CD44 expression in Figure 3.5 (F).

Other markers commonly expressed on FLS, such as Cadherin 11 and PDGFRα, were also analysed. No notable differences were observed in the frequency of PRIME cells positive for Cadherin 11 across HC, RA+, or RA- with a mean frequency varying between 60-75% of cells (Figure 3.6 (A)). However, the MFI of Cadherin 11 on the PRIME cells demonstrated a stepwise increase in expression from HC to RA+ to RA- (Figure 3.6 (A)), also reflected in the representative histogram demonstrating a shift in Cadherin 11 MFI. Interestingly, though all PRIME cells demonstrated a high frequency of PDGFRα, we observed a stepwise decrease in % frequency from HC to RA+ to RA-, with RA- significantly lower than HC ($p<0.05$; Figure 3.6 (B)). Similarly, there was a stepwise decrease in MFI expression of PDGFRα on PRIME cells from HC to RA+ to RA- (Figure 3.6 (B)), as demonstrated also by the shift observed in the representative stacked MFI histograms across cohorts for PDGFRα.

To determine whether the functional phenotypic differences demonstrated across the PRIME cells were a result of an altered metabolic profile, the frequency of pAKT, pmTOR, and pS6 were also examined. Approximately 10% of PRIME cells expressed pAKT and about 50% were positive for pmTOR, however, no differences were observed across disease states (Appendix Figure 7.3 (B)). pS6, a downstream marker for metabolism, was expressed at comparable % frequency between HC and RA+ PRIME cells, however, frequency of pS6 was reduced on RA- PRIME cells compared to RA+ ($p=0.0619$; Figure 3.6 (C)). This suggests that PRIME cells are metabolically active yet may differ in metabolic requirement in RA+ vs RA-. Nearly one hundred percent of PRIME cells across HC and RA were positive for the proliferation marker Ki67, with similar levels of MFI expression observed between HC and RA+, with RA- demonstrating slightly elevated expression (Appendix Figure 7.3 (C)). Additionally, similar proportions of PRIME cells across HC, RA+, and RA- expressed the cellular growth marker YAP (Appendix Figure 7.3 (C)). Collectively, these data indicate PRIME cells have the capacity for cellular growth and proliferation.

3.4.3 Differential FLS Marker Expression on RA PRIME Cells Compared to HC

It has been well established that FLS are a functionally diverse cell type and multiple FLS subsets have been previously described in RA (Croft *et al.*, 2016; Floudas *et al.*, 2022; Smith *et al.*, 2023). Therefore, we investigated whether RA PRIME cells express any FLS subset markers while still in the circulation. We focused on THY-1 and CD34 (markers associated with sub-lining FLS), CD55 (an established lining layer marker), and the FLS activation marker FAPα (Figure 3.7). Representative flow dot plots for THY-1, CD34, CD55 and FAPα are shown for HC, RA+, and RA- in Figure 3.7 (A). Indeed, RA+ and RA- PRIME cells demonstrated a higher % frequency of THY-1 expressing cells

compared to HC, with RA+ demonstrating the highest % frequency of THY-1 positive PRIME cells ($p=0.0590$; Figure 3.7 (A-B)). Similarly, RA+ and RA- PRIME cells demonstrated higher % frequency of CD34+ PRIME cells compared to HC (Figure 3.7 (A-B)). CD55 was minimally expressed on PRIME cells across all cohorts. Conversely, almost all PRIME cells were positive for FAPα with an increase in the % frequency observed for RA+ and RA-, thus implying these cells are activated (Figure 3.7 (A-B)).

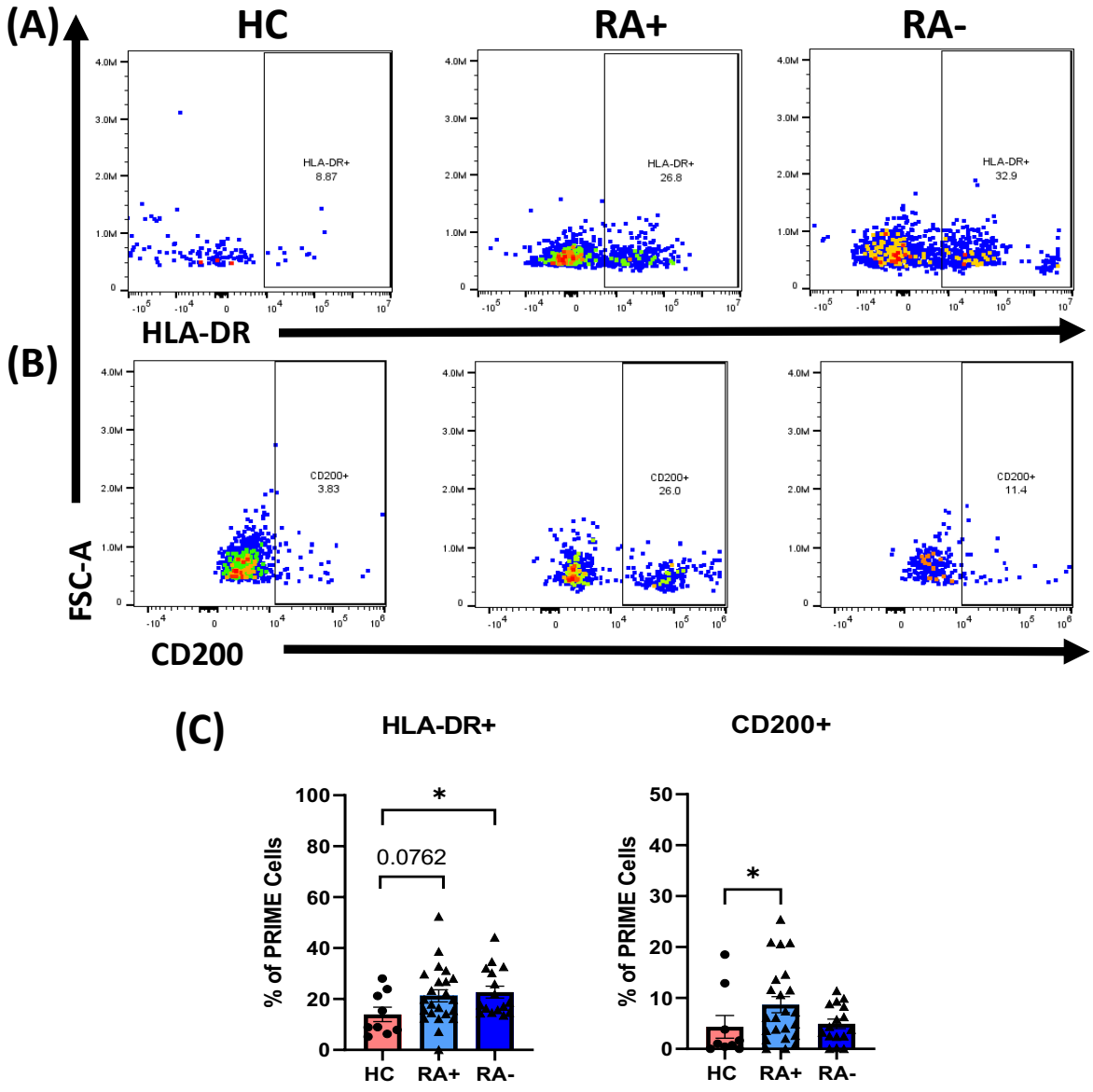

Figure 3.3: Immunoregulatory marker expression on PRIME cells in RA vs HC peripheral blood.

Representative flow cytometric dot plots of the expression of (A) HLA-DR and (B) CD200 on PRIME cells from peripheral blood of indicated disease states. (C) Accompanying dot plots depicting the frequency of HLA-DR+ and CD200+ PRIME cells in HC (n=9), RA+ (n=23), and RA- (n=16). Data represented as mean ± SEM using Mann Whitney U test (*) to determine statistical significance between disease states, with *p<0.05 being significant.

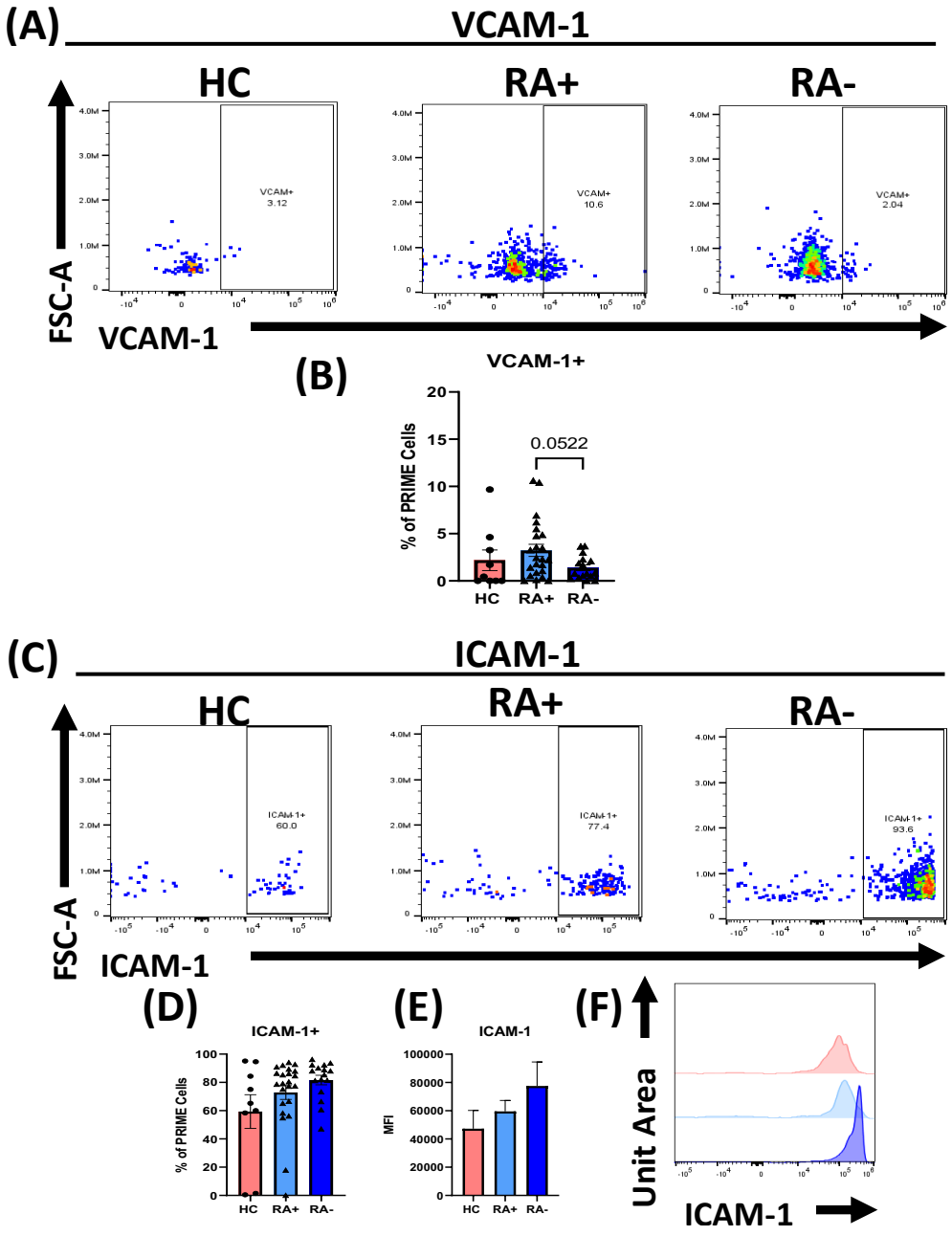

Figure 3.4: Differential expression of adhesion molecules VCAM-1 and ICAM-1 on PRIME cells.

(A) Representative flow cytometric dot plots depicting frequency of PRIME cells positive for VCAM-1 expression across the indicated disease states. (B) Dot plot comparing the differences in percentage frequency of VCAM-1+ PRIME cells in HC (n=9), RA+ (n=23), and RA- (n=16). (C) Representative flow cytometric dot plots demonstrating differences in frequency of ICAM-1 expression on PRIME cells in indicated disease states. (D) Dot plot comparing the differences in percentage frequency of ICAM-1+ PRIME cells in HC (n=9), RA+ (n=23), and RA- (n=16). (E) Bar graph depicting MFI expression of ICAM-1 on PRIME cells across indicated disease states. (F) Representative stacked histograms of ICAM-1 expression on HC, RA+, and RA- PRIME cells. Data represented as mean ± SEM using Mann Whitney U test (*) to determine statistical significance between disease states, with *p<0.05 being significant.

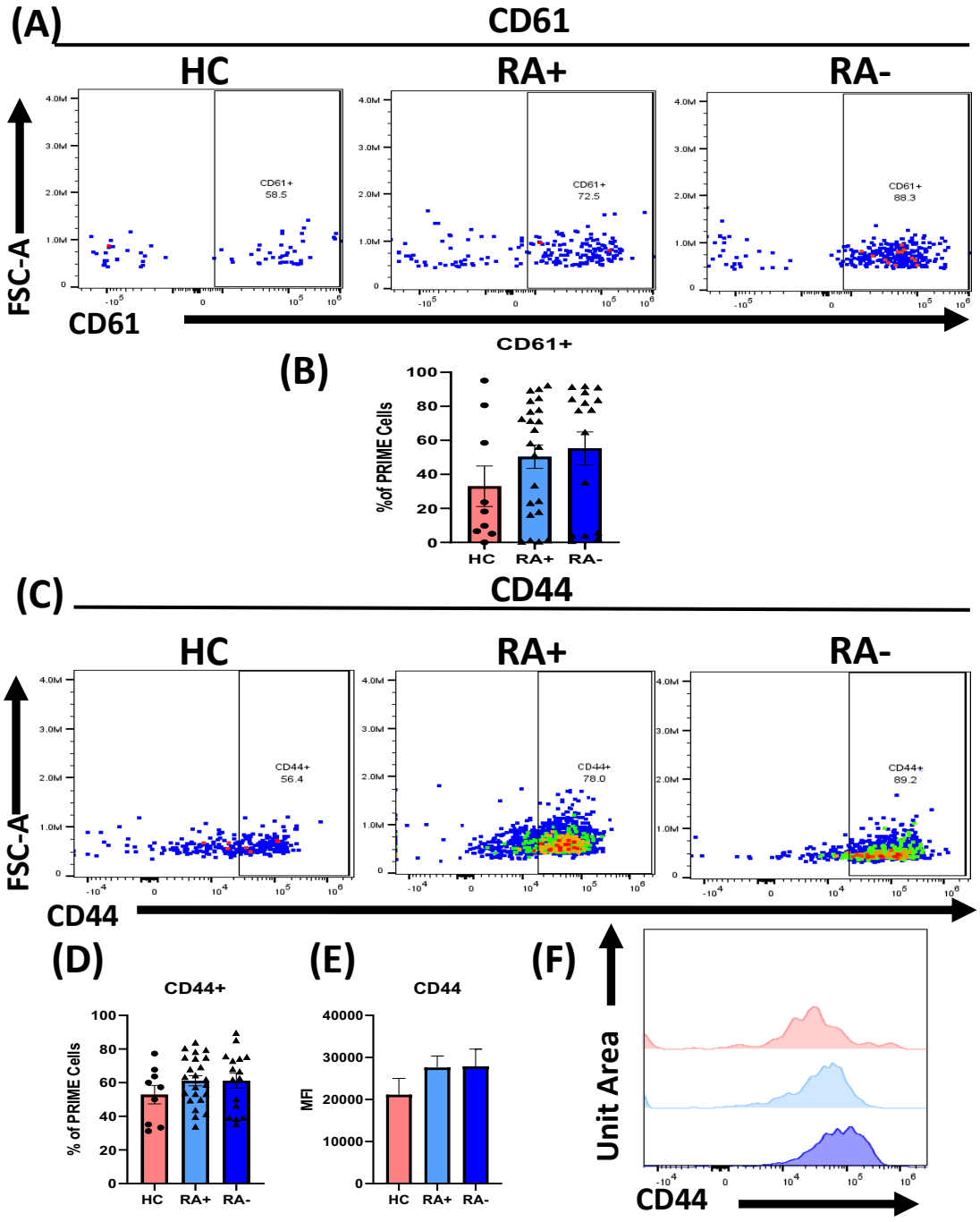

Figure 3.5: Increase in adhesion molecules CD61 and CD44 on RA PRIME cells.

(A) Representative flow cytometric dot plots depicting frequency of PRIME cells positive for CD61 expression across the indicated disease states. (B) Dot plot comparing the differences in percentage frequency of CD61+ PRIME cells in HC (n=9), RA+ (n=23), and RA- (n=16). (C) Representative flow cytometric dot plots demonstrating differences in frequency of CD44 expression on PRIME cells in indicated disease states. (D) Dot plot comparing the differences in percentage frequency of CD44+ PRIME cells in HC (n=9), RA+ (n=23), and RA- (n=16). (E) Bar graph depicting MFI expression of CD44 on PRIME cells across indicated disease states. (F) Representative stacked histograms of CD44 expression on HC, RA+, and RA- PRIME cells. Data represented as mean ± SEM.

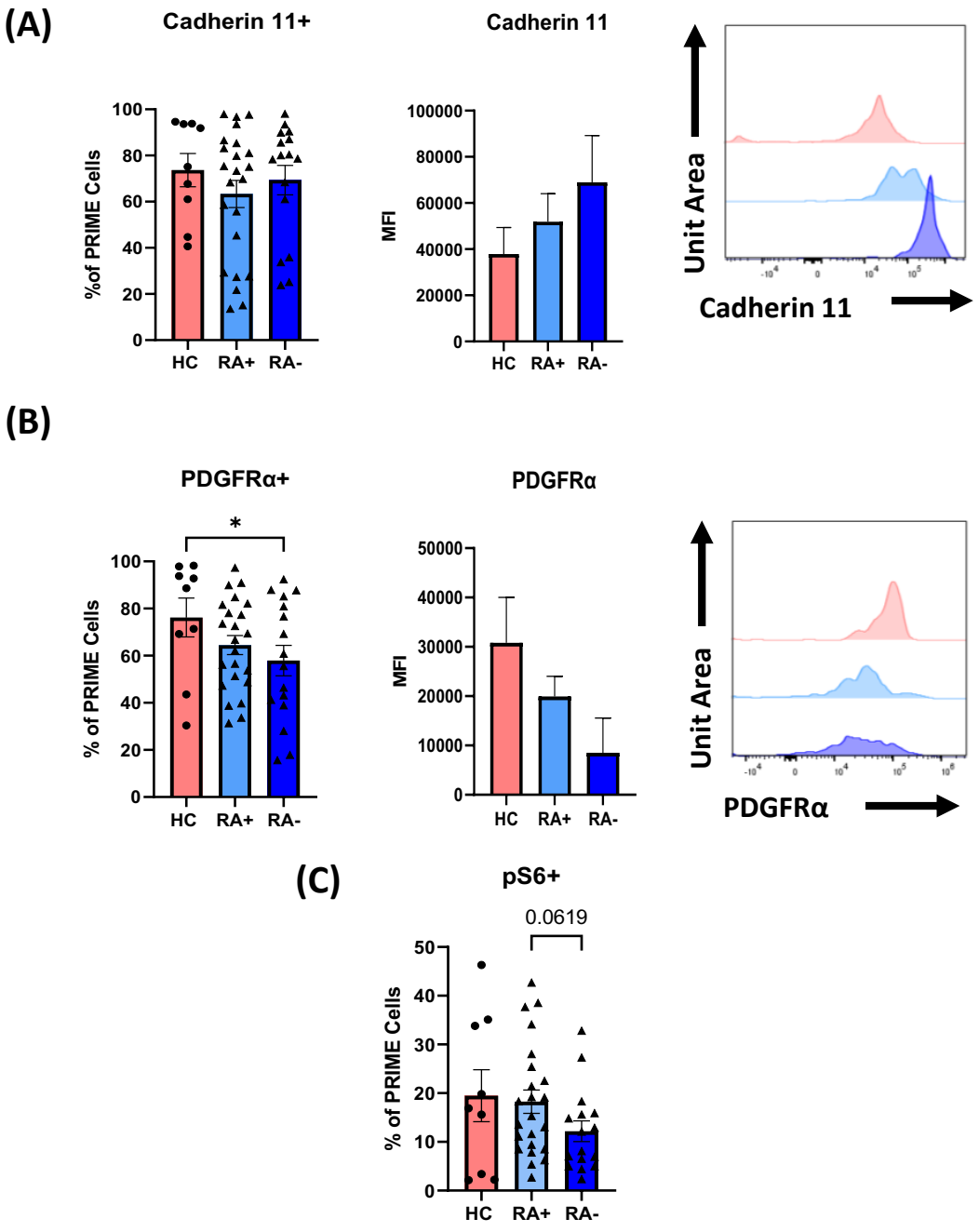

Figure 3.6: Differential expression of functional and metabolic markers on PRIME cells across disease states.

(A) Dot plot, bar graph, and representative stacked histograms demonstrating differences in percentage frequency and MFI expression of Cadherin 11 on PRIME cells in HC (n=9) compared to RA+ (n=23) and RA- (n=16) patients. (B) Dot plot, bar graph, and representative stacked histograms depicting frequency and MFI expression of PDGFRα in HC vs RA+ vs RA-. (C) Dot plot showing differences in percentage frequency of pS6+ PRIME cells in HC, RA+, and RA-. Data represented as mean ± SEM using Mann Whitney U test (*) to determine statistical significance between disease states, with *p<0.05 being significant.

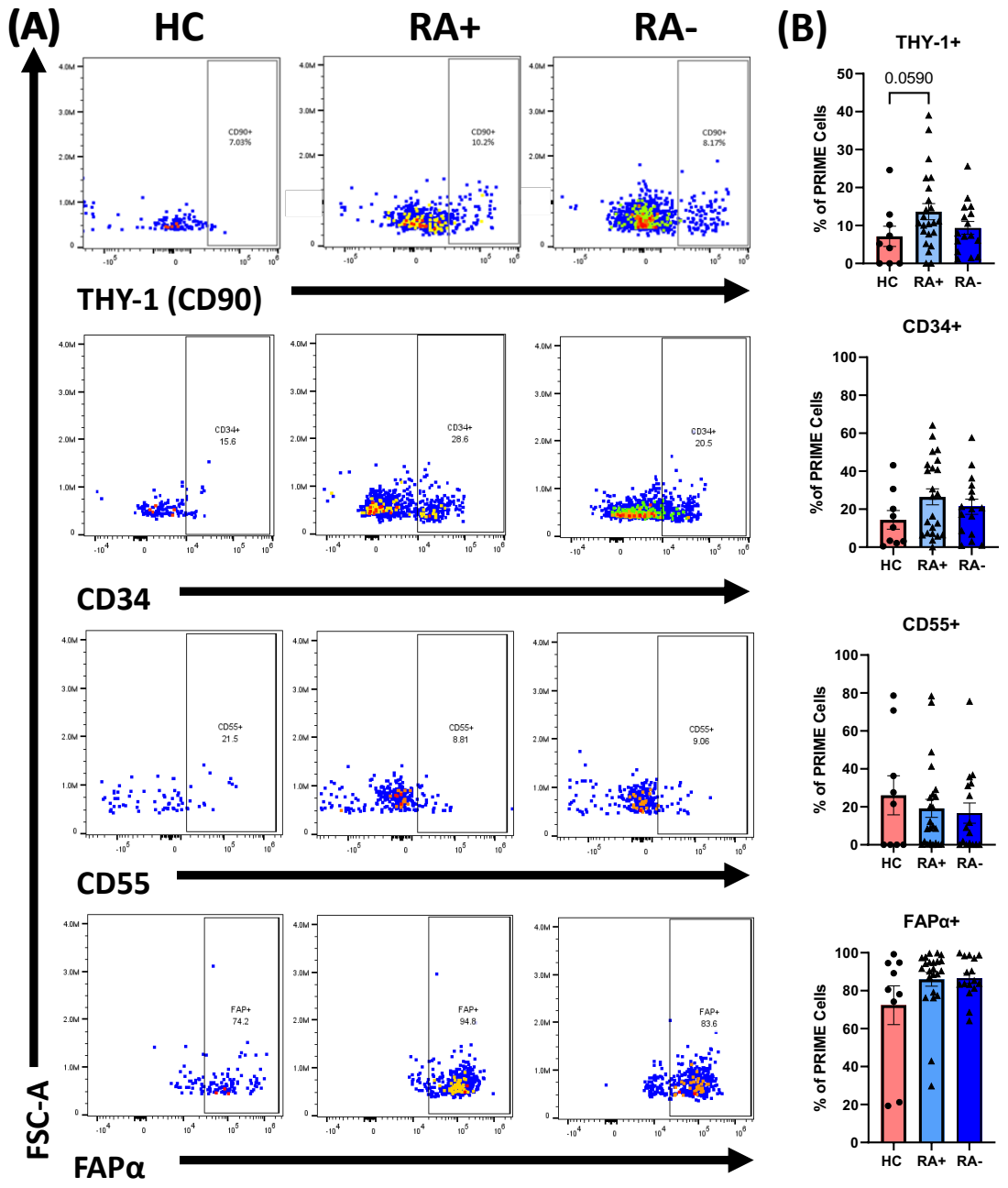

Figure 3.7: Analysis of frequency of common FLS subset markers (THY-1, CD34, CD55, FAPα) on PRIME cells across disease states.

(A) Representative dot plots depicting frequency of PRIME cells positive for THY-1, CD34, CD55, and FAPα in HC (n=9), RA (n=23), and RA- (n=16). (B) Bar graphs demonstrating differences in percentage frequency of each marker across each disease state. Data represented as mean ± SEM with each symbol denoting a separate sample, using Mann Whitney U test to determine statistical significance between disease states, with *p<0.05 being significant.

3.4.4 PRIME Cells are Present and Increased Prior to Clinical Onset of Disease and in IAR

There is growing appreciation in the necessity to investigate the immunological events that precede onset of clinical manifestations. Indeed, there has been an increasing need to understand the immunological alterations that take place in individuals-at-risk of developing RA to better determine which individuals will progress on to develop RA and those that do not. Therefore, PRIME cells were analysed in IAR (n=10) as well as ART individuals (n=5) to determine whether PRIME cells are present at increased frequencies and whether their phenotype is altered prior to disease onset. Representative flow dot plots illustrate the difference in PRIME cell frequency across all cohorts in Figure 3.8 (A). A stepwise increase was observed in the frequency of PRIME cells from HC to IAR to RA+, although not significant (Figure 3.8 (B)). Similarly, there was a significant stepwise increase in PRIME cell frequency from HC to ART to RA- (HC vs ART $p<0.05$; HC vs RA- $p<0.05$) (Figure 3.8 (B)). RA- PRIME cell frequency was also significantly higher than IAR ($p<0.05$). Furthermore, the frequency of PRIME cells was markedly different between IAR and ART with the latter demonstrating increased frequencies ($p=0.0553$) suggesting autoantibodies, or lack thereof, may play a significant role in the development of PRIME cells (Figure 3.8 (B)).

3.4.5 Pro-inflammatory Phenotype of PRIME Cells is Altered in the Pre-Clinical Stage

Even prior to clinical disease, compared to HC, PRIME cells have an increased frequency of HLA-DR in IAR ($p=0.0947$) and ART comparable to the % frequency levels observed in RA+ and RA- cohorts (Figure 3.9 (A)). Conversely, the frequency of CD200 expressing PRIME cells in IAR and ART were comparable to levels observed in HC (Figure 3.9 (A)). The frequency of VCAM-1 in IAR and ART did not differ from HC PRIME cells (Figure 3.9 (B)); however, % frequency of ICAM-1 positive cells was increased in both IAR and ART compared to HC, with similar % frequency to that of RA+ and RA- (Figure 3.9 (B)). Furthermore, MFI expression of ICAM-1 on IAR and ART PRIME cells was increased compared to HC, with ART displaying significantly higher % frequency than HC and RA+ (both $p<0.05$; Figure 3.9 (C)). The frequency of PRIME cells expressing CD61 in IAR and ART varied and did not significantly differ from HC (Figure 3.9 (B)). CD44 positive PRIME cells did not vary in % frequency between IAR and HC, but interestingly ART displayed a greater percentage of CD44+ PRIME cells compared to both HC and IAR (HC vs ART $p=0.0829$; IAR vs ART $p<0.05$) (Figure 3.9 (B)). Moreover, % frequency of CD44+ PRIME cells was increased in RA+ compared to IAR, trending towards significance ($p=0.0730$; Figure 3.9 (B)). This trend was mirrored in the MFI expression of CD44; with IAR demonstrating comparable MFI expression to HC, while ART and RA+ demonstrated increased MFI expression compared to both HC and IAR, though not significant (Figure 3.9 (C)).

ART demonstrated a decrease in % frequency of PRIME cells positive for Cadherin 11 (Figure 3.10 (A)), however, MFI expression was slightly increased (Figure 3.10 (A)). IAR had comparable % frequency levels of cells positive for Cadherin 11 to HC and RA+ (Figure 3.10 (A)) and no increase was observed in MFI expression when compared to HC (Figure 3.10 (B)). IAR demonstrated decreased % frequency of PRIME cells expressing PDGFRα compared to HC (Figure 3.10 (A)) while also exhibiting reduced MFI expression (Figure 3.10 (B)). Metabolically, ART demonstrated a similar reduction in pS6 % frequency comparable to the frequency exhibited in RA- PRIME cells (Figure 3.10 (A)). IAR, similar to what was observed with RA+, demonstrated increased % frequency of pS6+ PRIME cells compared to RA- ($p=0.0772$; Figure 3.10 (A)).

Pre-clinical PRIME cells already begin to express markers commonly found on FLS subsets (Figure 3.11). Indeed, a stepwise increase in % frequency of THY-1 positive PRIME cells was observed from HC to IAR to RA+ (Figure 3.11). This same increase was not exhibited in ART PRIME cells (Figure 3.11). Additionally, this stepwise increase was also demonstrated for CD34 frequency from HC to IAR to RA+ (Figure 3.11), while % frequency for ART was proportionate to that observed in RA- (Figure 3.11). % frequency of CD55 positive PRIME cells remained low for both IAR and ART compared to all other groups (Figure 3.11). Conversely, FAPα % frequency increased for IAR and ART PRIME cells compared to HC, with levels comparable to that of the RA cohorts (Figure 3.11), indicative of PRIME cell activation prior to onset of clinical symptoms.

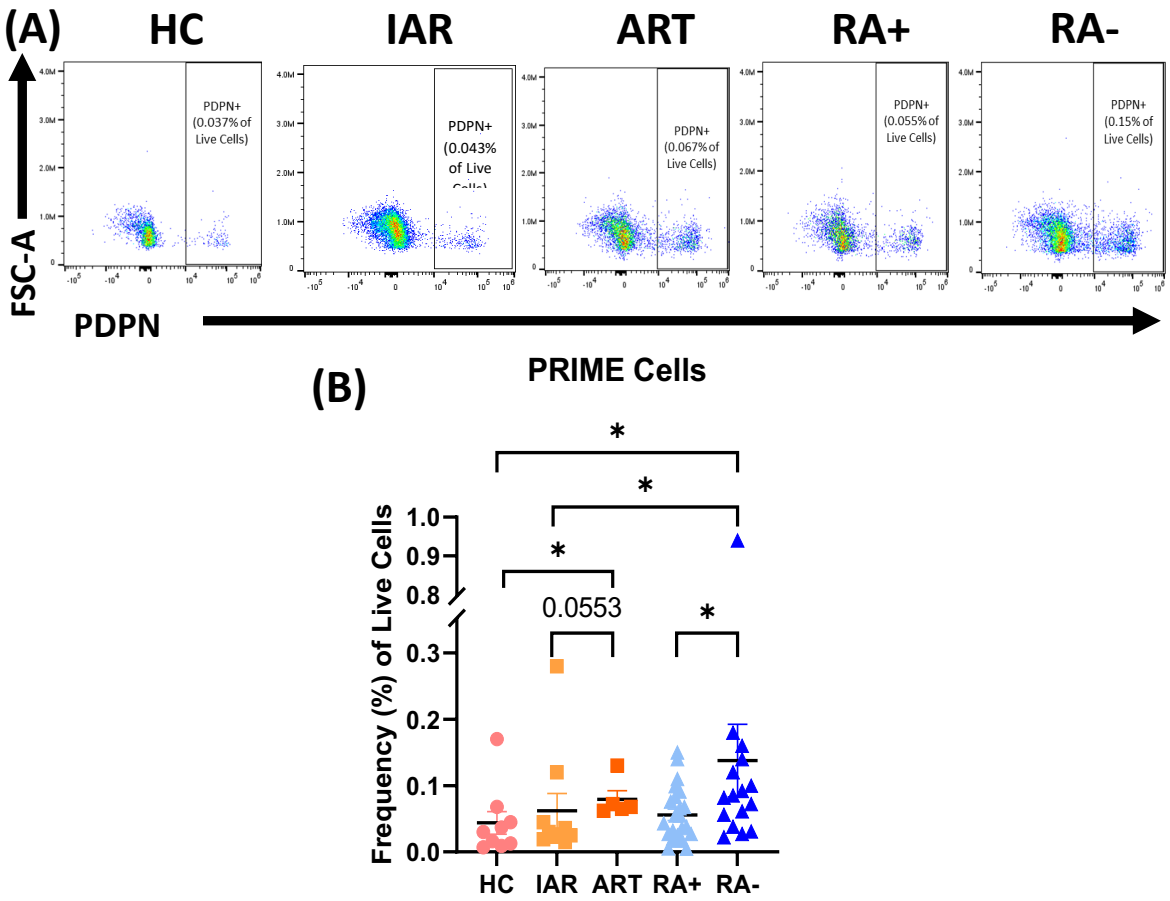

Figure 3.8: PRIME cells are present in pre-clinical disease.

(A) Representative flow cytometric dot plots for the identification of CD45-CD31-PDPN+ PRIME cells in peripheral blood of HC, IAR, ART, RA+, and RA- patients. (B) Dot plot demonstrating increased frequency of PRIME cells in IAR (n=10), ART (n=5), RA+ (n=23), and RA- (n=16) compared to HC (n=9). Data represented as mean ± SEM with each symbol representing a different sample. Statistical analysis using Mann Whitney U test (*) was used to determine significance with *p<0.05 indicating significance.

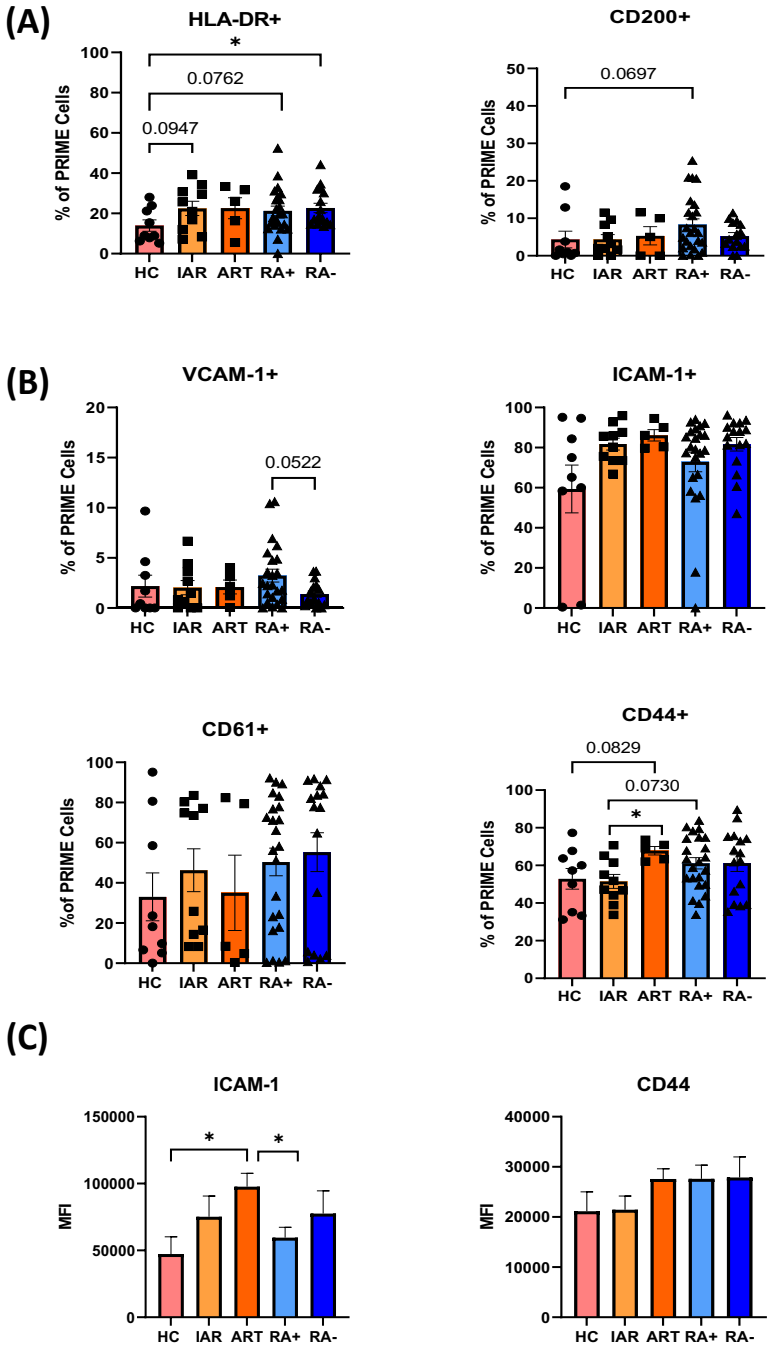

Figure 3.9: Differential frequency and expression of immunoregulatory and adhesion molecules observed prior to disease onset.

(A) Dot plots demonstrating percent frequency of PRIME cells positive for immunoregulatory markers HLA-DR and CD200 across HC (n=9), IAR (n=10), ART (n=5), RA+ (n=23), and RA- (n=16). (B) Dot plots depicting differences in frequency of PRIME cells positive for adhesion molecules VCAM-1, ICAM-1, CD61, and CD44 across pre-clinical and disease states. (C) Bar graphs of MFI expression of ICAM-1 and CD44 on pre-clinical and RA PRIME cells. Data represented as mean ± SEM with each symbol representing a different sample. Statistical analysis using Mann Whitney U test (*) was used to determine significance with *p<0.05 indicating significance.

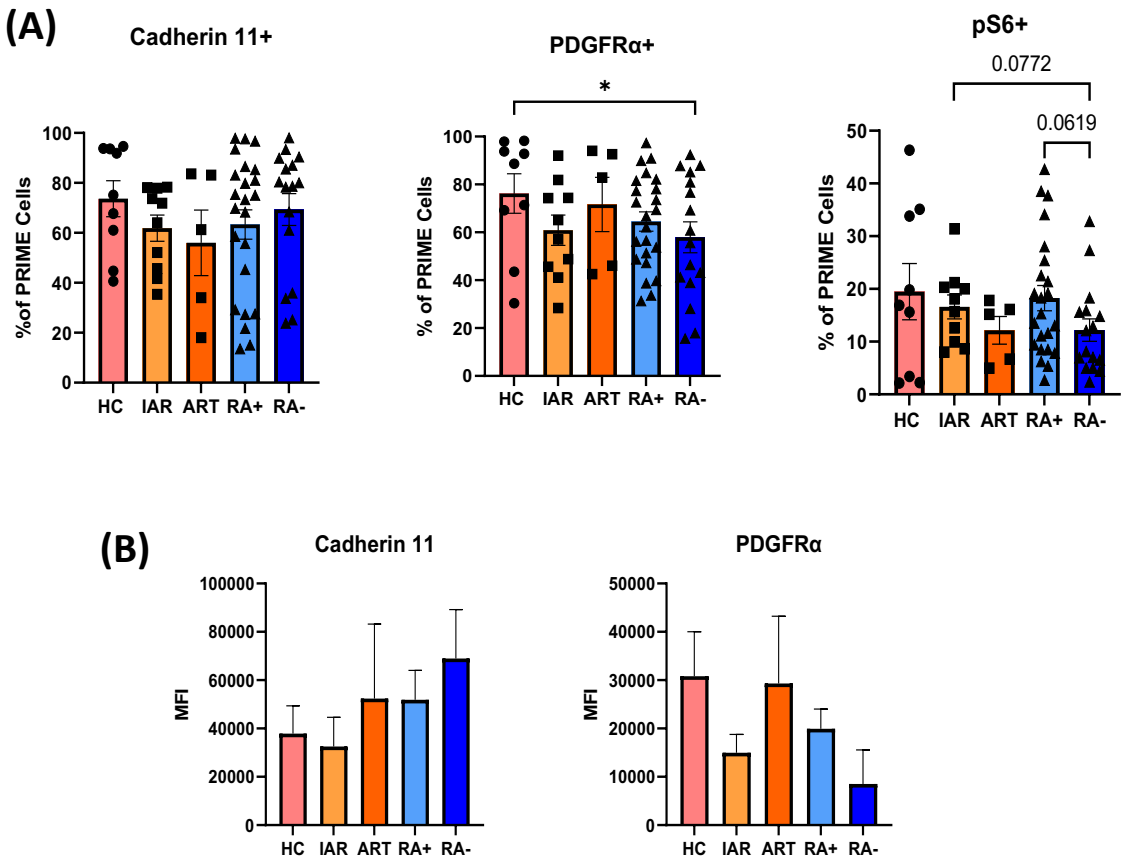

Figure 3.10: Differential expression of metabolic and functional markers in IAR and ART.

(A) Dot plots demonstrating percent frequency of PRIME cells positively expressing Cadherin 11, PDGFRα, and pS6 in HC (n=9), IAR (n=10), ART (n=5), RA+ (n=23), and RA- (n=16). (B) Bar graphs of MFI expression of Cadherin 11 and PDGFRα on HC, IAR, ART, RA+, and RA- PRIME cells. Data represented as mean ± SEM. Statistical analysis using Mann Whitney U test (*) was used to determine significance with *$p<0.05$ indicating significance.

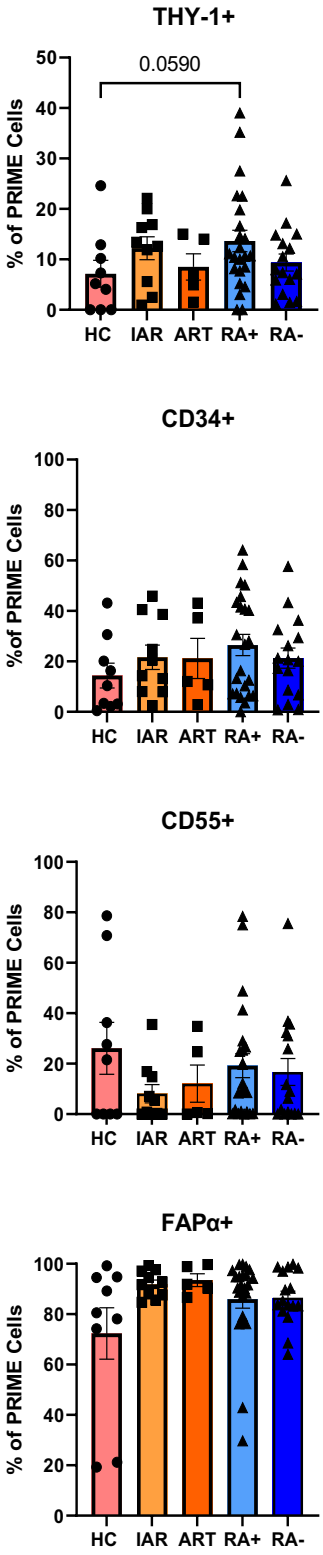

Figure 3.11: FLS subset markers present on PRIME cells prior to clinical onset.

Dot plots demonstrating frequency of PRIME cells expressing FLS subset markers THY-1, CD34, CD55, and FAPα in HC (n=9), IAR (n=10), ART (n=5), RA+ (n=23), and RA- (n=16). Data represented as mean ± SEM with each symbol representing a different sample. Statistical analysis using Mann Whitney U test (*) was used to determine significance with *p<0.05

3.4.6 Differential Frequency of CD45-CD31-PDPN+ Cells in RA Peripheral Blood and Synovial Tissue

To gain a better understanding of whether location can alter the functionality and overall phenotype of PRIME cells, we compared CD45-CD31-PDPN+ cells from the circulation to those found in the synovial tissue of RA patients. For a more reliable comparison, the same gating strategy applied to the PBMC samples to identify circulating PRIME cells was utilised for synovial tissue (Figure 3.12 (A-F)). Additionally, when comparing RA peripheral blood (PB) to synovial tissue (ST) each cohort is comprised of both RA- and RA+ patients. It is important to note that the CD45-CD31-PDPN+ cells gated in the synovial biopsy could include PRIME cells and those in the process of becoming mature FLS or FLS and therefore will be referred to as PDPN+ cells (Figure 3.12 (F)).

Representative flow cytometric dot plots of PDPN+ cells identified in the circulation and synovial tissue of the same representative donor are depicted in Figure 3.13 (A). It is evident from the dot plot of overlaying PDPN+ cells from PB and ST in Figure 3.13 (B) that differences of size and morphology of CD45-CD31-PDPN+ cells were found in circulation compared to the tissue (Figure 3.13 (B)). The % frequency of PDPN+ cells (as a proportion of all live cells) was significantly higher in ST compared to the PB ($p<0.0001$) (Figure 3.13 (C)). Indeed, the variability of PDPN+ cells observed in the tissue supports the concept that some FLS-like cells may be entering the joint from the circulation before maturing into full FLS.

3.4.7 Differential Fibroblast Marker Expression in RA Synovial Tissue Compared to Peripheral Blood

Differences were observed between the blood and tissue in the % frequency of FLS markers on the PDPN+ cells (Figure 3.14). Because we hypothesise that PDPN+ PRIME cells from the circulation migrate into the joint where they further develop to mature FLS, we next examined if there was an increase in classical FLS marker expression on PDPN+ cells in the synovial tissue compared to the blood. Indeed, % frequency of the lining layer marker CD55 was significantly increased for PDPN+ cells in the ST compared to PB ($p<0.001$) (Figure 3.14). Similarly, % frequency of PDPN+ cells positive for the sub-lining marker THY-1 was significantly higher in ST compared to PB ($p<0.0001$ (Figure 3.14)). No difference in the % frequency of CD34+ cells was observed between the two locations (Figure 3.14). Interestingly, some FLS markers demonstrated a higher % frequency on PDPN+ cells from the circulation compared to the joint. Indeed, both FAPα and Cadherin 11 exhibited a significantly increased % frequency on PDPN+ cells in the PB compared to the ST (FAPα $p<0.001$; Cadherin 11 $p<0.0001$) (Figure 3.14).

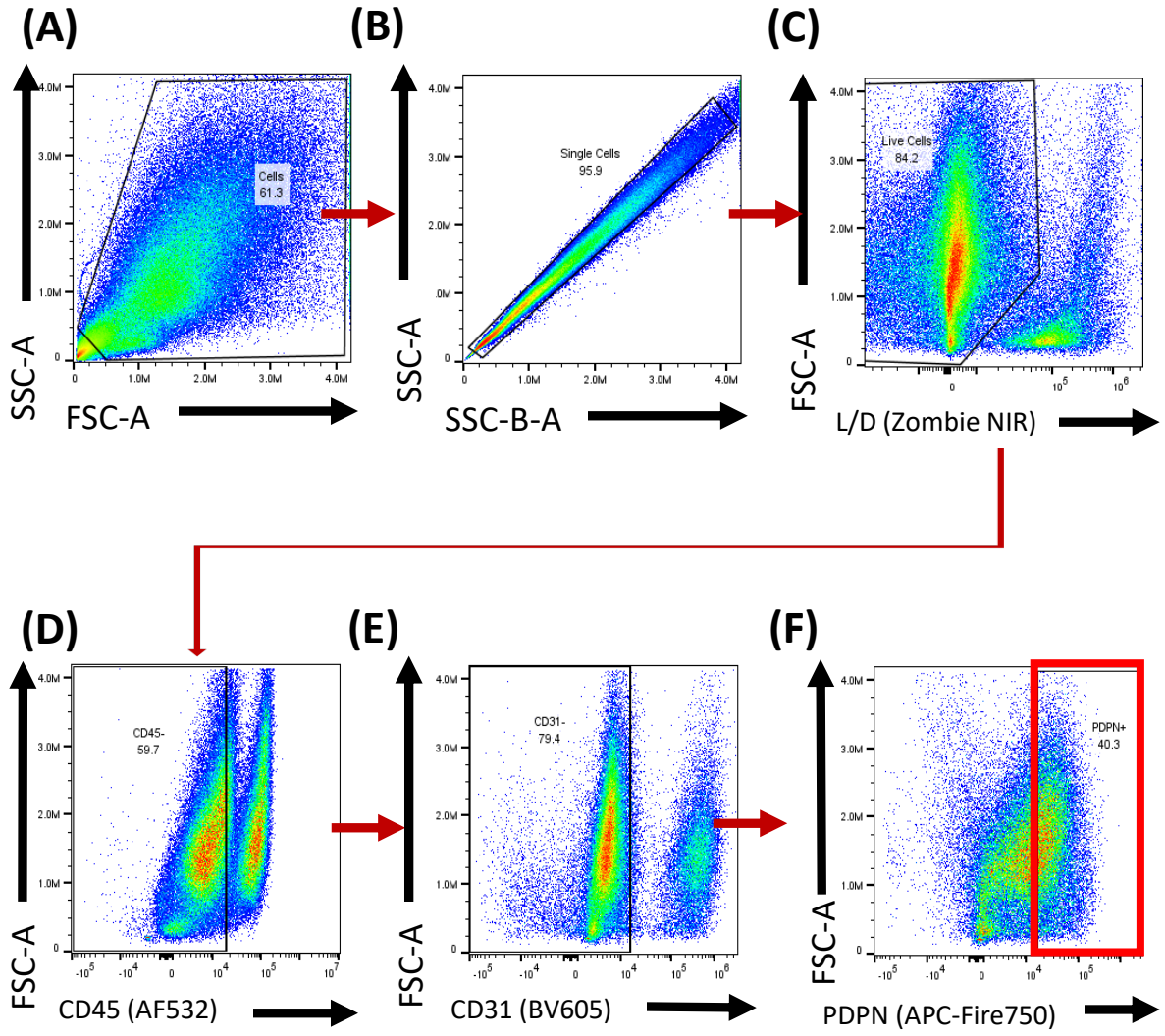

Figure 3.12: PRIME cell (CD45-CD31-PDPN+) gating strategy applied to synovial tissue.

Viably frozen synovial tissue from RA patients (n=14) were thawed, digested, and stained with a panel of fluorochrome antibodies (see Table 3.3). Representative dot plots showing the gating strategy used to identify and characterise PRIME cells in synovial tissue. (A-C) Forward and side scatter parameters of cells were set before excluding doublets and dead cells. (D-F) PRIME cells were identified as CD45-CD31-PDPN+ and further characterised by expression of intracellular and extracellular markers.

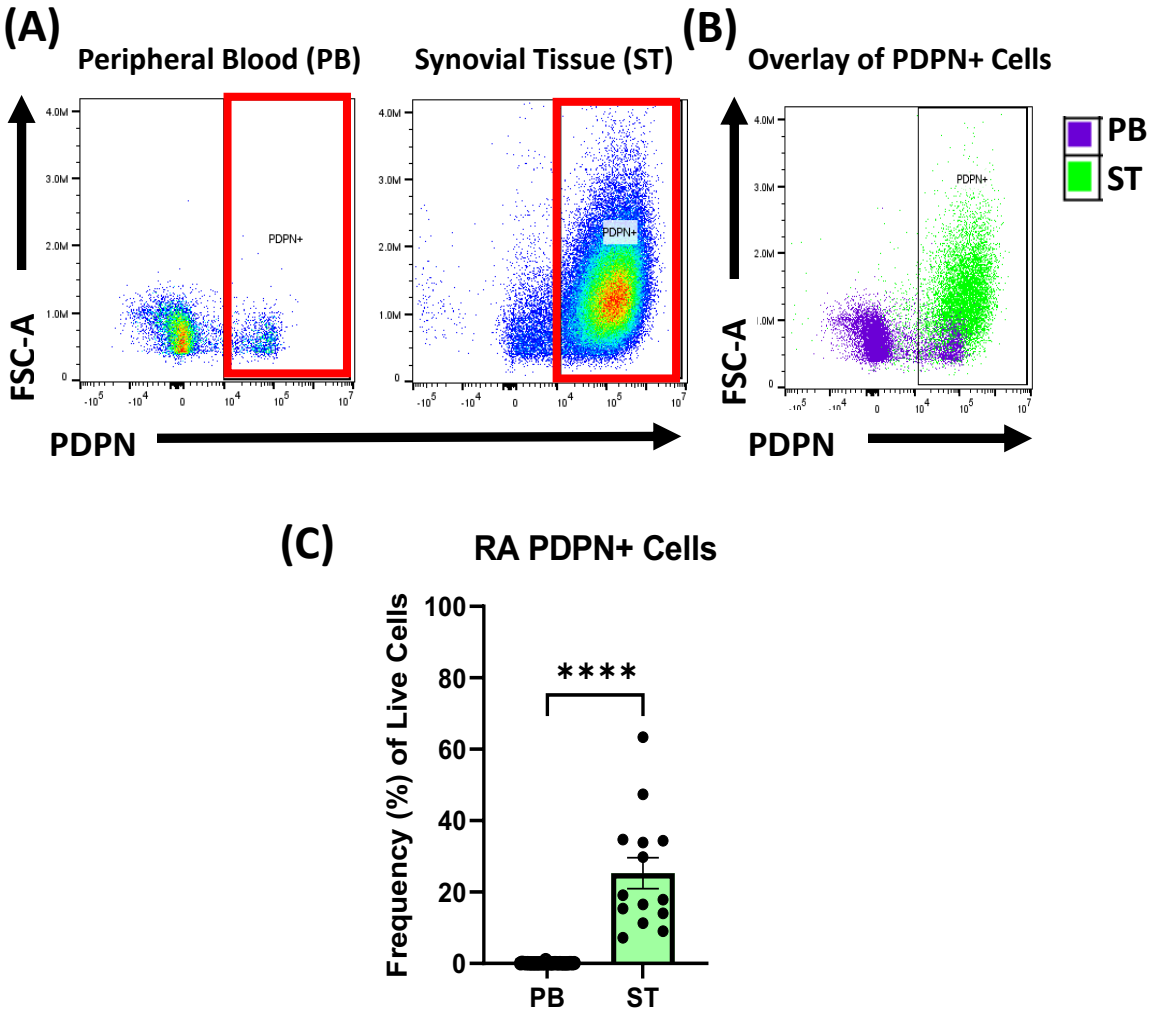

Figure 3.13: CD45-CD31-PDPN+ cells differ in frequency and size between circulation and site of inflammation.

(A) Representative flow cytometric dot plots depicting CD45-CD31-PDPN+ populations identified from the peripheral blood and synovial tissue of the same representative donor taken at time of arthroscopy. (B) Overlay of previously described flow dot plots demonstrating differences in size morphology of PDPN+ cells from the circulation and site of inflammation. (C) Dot plot bar graph representing PDPN+ cells as a frequency of live cells between all RA peripheral blood samples (n=39) and synovial tissue samples (n=14). Each cohort is comprised of RA+ and RA- samples. Data represented as mean ± SEM with each symbol representing a different sample. Statistical analysis using Mann Whitney U test (*) was used to determine significance with ****$p<0.0001$ indicating significance between PB and ST.

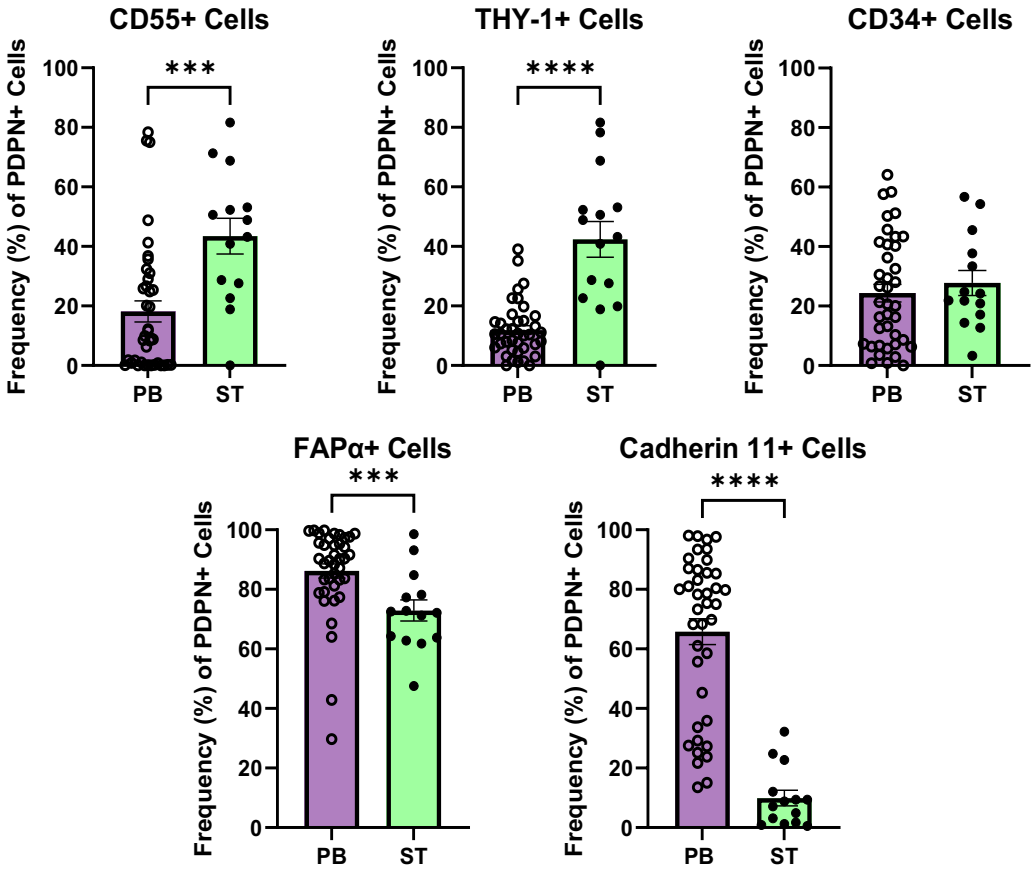

Figure 3.14: FLS marker expression differences on PDPN+ cells from RA peripheral blood compared to synovial tissue.

Dot plots demonstrating differences of percent frequency of common FLS markers CD55, THY-1, CD34, FAPα, and Cadherin 11 on PDPN+ cells found in peripheral blood (n=39) compared to synovial tissue (n=14) of RA patients. Data represented as mean ± SEM with each symbol representing a different sample. Statistical analysis using Mann Whitney U test (*) was used to determine significance with *p<0.05, **p<0.01, ****p<0.0001 indicating significance.

3.4.8 Functional and Metabolic Profiles of RA PDPN+ Cells Differ Between the Circulation and the Joint

The phenotype of RA PDPN+ cells changed depending on their location, possibly because of exposure to different environmental cues in each location or resulting from differing functional requirements. For example, PDPN+ cells preferentially expressed different adhesion molecules based on the location. A higher % frequency in CD44 positive PDPN+ cells was demonstrated in the ST compared to the blood ($p<0.01$; Figure 3.15 (A)). Conversely, a higher % frequency of PDPN+ cells expressing CD61 ($p<0.001$) and ICAM-1 ($p<0.0001$) was observed in the circulation compared to the frequency demonstrated in the tissue (Figure 3.15 (A)). VCAM-1+ cells, however, remained at a low % frequency regardless of location (Figure 3.15 (A)).

PDPN+ cells also altered their immunoregulatory profile relative to their location. The joint displayed an increased % frequency of HLA-DR expressing PDPN+ cells compared to the blood, though not significant (Figure 3.15 (B)). This was in stark contrast to the immunoregulatory receptor CD200R1 and its ligand CD200, both of which displayed an increased % frequency in the blood compared to the tissue ($p<0.01$ and $p<0.05$, respectively) (Figure 3.15 (B)).

We next examined whether these phenotypic changes were mirrored by a shift in metabolic profile for these cells. Within the joint, PDPN+ cells had a higher % frequency of pAKT expression compared to those in PB ($p=0.0767$; Figure 3.16 (A)). In contrast, metabolic markers pmTOR and pS6 had a marked increase in % frequency of PDPN+ cells in the periphery compared to ST, suggesting PDPN+ cells are at different stages in metabolic signaling in the two locations (pmTOR $p<0.0001$; pS6 $p<0.05$) (Figure 3.16 (A)). Based on our observations, there were no significant differences in the proliferation capacity or cellular growth of PDPN+ cells between the PB or ST. PDPN+ cells from each location had markedly high and comparable % frequencies for Ki67, YAP, PDGFRα (Figure 3.16 (B)).

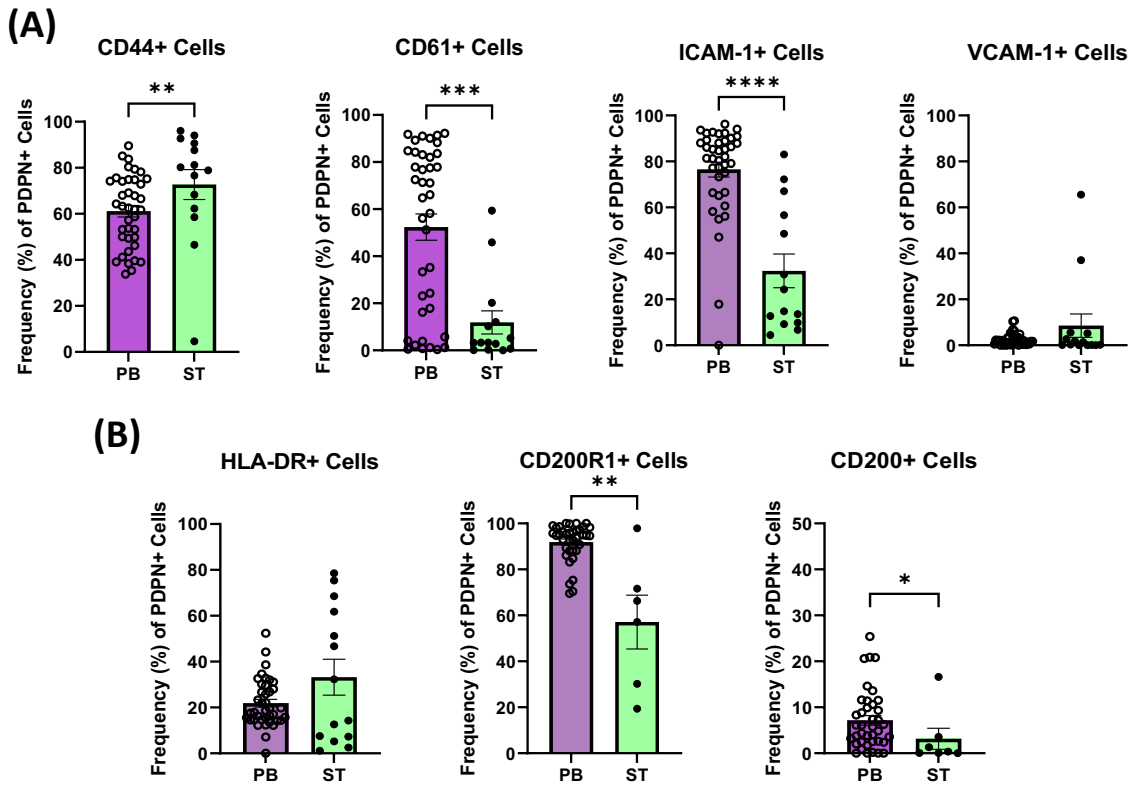

Figure 3.15: Phenotypic characterization of RA peripheral blood PDPN+ cells compared to synovial tissue.

Dot plots depicting differences in frequency of PDPN+ cells expression of (A) adhesion molecules CD44, CD61, ICAM-1, and VCAM-1 and (B) immunoregulatory markers HLA-DR, CD200R1, and CD200 between peripheral blood (n=39) and synovial tissue (n=14) of RA patients. Data represented as mean ± SEM. Statistical analysis using Mann Whitney U test (*) was used to determine significance with *p<0.05, **p<0.01, ***p<0.001, ****p<0.0001 indicating significance.

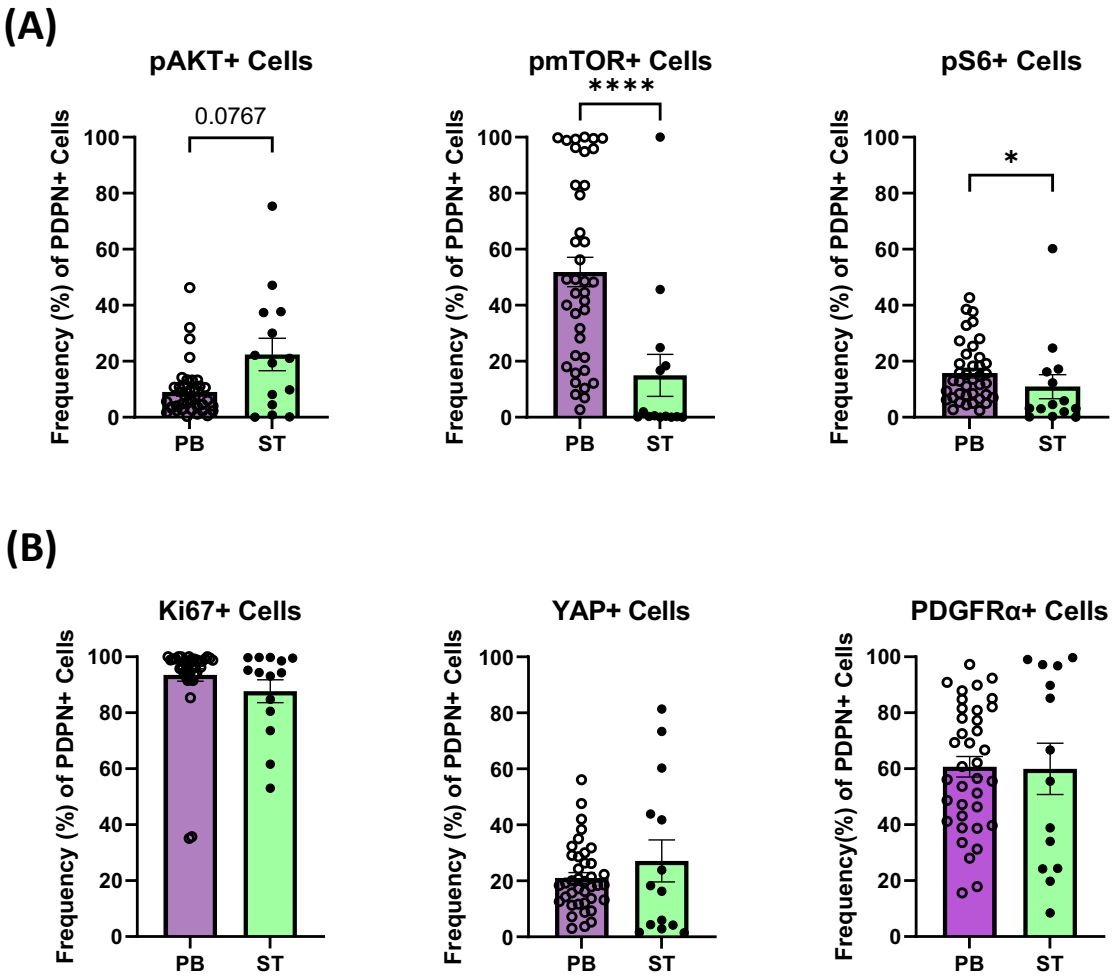

Figure 3.16: Differential metabolic profiles and cellular growth profiles of RA PDPN+ cells between peripheral blood and synovial tissue.

Dot plots demonstrating differences in frequency of PDPN+ cells positively expressing (A) metabolic markers pAKT, pmTOR, and pS6 and (B) cell growth and proliferation makers Ki67, YAP, and PDGFRα in RA peripheral blood (n=38-39) and synovial tissue (n=14). Data represented as mean ± SEM with each symbol representing a different sample. Statistical analysis using Mann Whitney U test (*) was used to determine significance with *p<0.05, ***p<0.001 indicating significance.

3.5 Discussion

In this chapter the presence of CD45-CD31-PDPN+ PRIME cells were identified in the circulation and were enriched in the blood of both seropositive and to a greater extent in seronegative RA patients compared to HC. For the first time, we have phenotypically characterised PRIME cells via flow cytometry, demonstrating phenotypic differences not only between disease and health, but also by seropositivity status. PRIME cells in both HC and RA have the capacity to proliferate, reflected by the observed high expression of Ki67 and YAP across all cohorts. Additionally, RA PRIME cells are immunomodulatory, evident by the increased frequency of HLA-DR and CD200 expression in RA compared to HC, especially in RA+ PRIME cells. Furthermore, increased frequency in the expression of key adhesion molecules, including ICAM-1, CD61, and CD44 on RA PRIME cells compared to HC, with a stepwise increase from HC<RA+<RA- was observed. Interestingly, while several studies have shown that Cadherin 11 and PDGFRα interactions drive FLS growth and provide structural support for the synovium, in this study, we observed minimal differences in Cadherin 11 across the three cohorts, while PDGFRα was significantly decreased, particularly in seronegative RA. No difference in metabolic activity between RA+ and HC was observed, however a significant decrease in pS6+ was observed for RA- compared to RA+. Analysis of markers commonly associated with sub-lining layer FLS subsets including THY-1, CD34 and FAPα were all increased in RA+, and to a lesser extent RA- compared to HC. For the first time increased frequency of PRIME cells has been identified in IAR and seronegative ART. Furthermore, the functional phenotypes of these cells have been shown to be altered prior to clinical disease onset, with the same trends as those observed for RA, including increased frequency observed for HLA-DR, ICAM-1, CD61, CD44, THY-1 and FAPα, with decreased expression of PDGFRα and pS6 demonstrated. Finally, for the first time, the frequency and phenotype of CD45-CD31-PDPN+ cells from the circulation to that of the synovial tissue has been compared and demonstrated differential frequencies of FLS subset markers, immunomodulatory and adhesion molecules, in addition to the metabolic profiles between the two locations.

The successful identification and increased frequency of CD45-CD31-PDPN+ PRIME cells in the circulation of patients with RA corroborated the initial findings by Orange *et al.*, (2020) who first identified PRIME cells from whole blood samples of seropositive RA patients. Interestingly, we demonstrated that RA- more so than RA+ had the highest frequencies of PRIME cells compared to HC. This was unexpected based on the findings of Orange *et al.*, where they identified an elevated B cell gene signature, hypothesizing that PRIME cells are activated by circulating B cells before migrating into the joint. Indeed, specific ACPAs have been shown to mediate FLS migration via the PI3K/Akt pathway resulting in actin cytoskeletal modulation (Sun *et al.*, 2019). Previous

literature, using scRNA sequencing of synovial tissue, has suggested ACPA- RA to more likely be clustered into a diffuse-myeloid (myeloid predominance and little B cells) or pauci-immune (FLS predominance with little immune cell infiltration) pathotype rather than lympho-myeloid (high B cell presence with myeloid cells) pathotype (Lewis *et al.*, 2019; Humby *et al.*, 2019; Wu *et al.*, 2021; Li *et al.*, 2022). However, other studies using single cells analysis of synovial tissue have shown similar B cell subpopulation frequency distribution between ACPA- and ACPA+ RA patients, highlighting a key role for specific B cell subsets in both disease endotypes (Floudas *et al.*, 2021). Interestingly, the synovial tissue B cells were dominated by switched and double negative memory B cells for both ACPA positive and ACPA negative, however, significant enrichment of T follicular helper (Tfh) cells were observed in the ACPA+ cohort (Floudas *et al.*, 2021), suggesting that increased Tfh cell responses in RA may drive B cell autoantibody production (Ma *et al.*, 2012; Wang *et al.*, 2019). Accumulating evidence has suggested that ACPA- RA may be a distinct disease entity from ACPA+ RA with differing underlying pathophysiology (Padyukov *et al.*, 2011; Li *et al.*, 2022). It may be that there is a higher frequency of PRIME cells in RA- due to FLS derived from this subset having a more prominent role in pathogenesis of RA- patients compared to RA+. Differential frequencies of FLS subtypes have been demonstrated between different pathotypes, including PsA vs RA (Floudas *et al.*, 2022). Furthermore, a recent eloquent study by the AMP consortium, performed an extensive deconstructive analysis of the RA synovium where they identified six different pathotypes defined by cellular abundance, and were referred to as cell-type abundance phenotypes (CTAPs) (Zhang *et al.*, 2023). FLS were most associated with two pathotypes, one was predominant for FLS (CTPA-F) and one was predominant for T cells and FLS (CTAP-TF), suggesting the FLS pathotypes associated with immune cell interactions, at least within the joint, are associated with T cell interactions (Zhang *et al.*, 2023). This study however did not stratify into ACPA+ vs ACPA- RA.

Characterization of PRIME cells demonstrated significantly increased frequency of immunoregulatory markers HLA-DR and CD200 in RA compared to HC. The concept of FLS exhibiting immune cell function has been previously demonstrated (Navarrete *et al.*, 1997; Spurrell *et al.*, 2004), with more recent studies by Zhang *et al.*, using Sc-transcriptomics identifying elevated expression of HLA-DR on the sub-lining CD45-CD31-PDPN+ FLS in synovial tissue (Zhang *et al.*, 2019). Therefore, RA PRIME and FLS cells may have a greater immunoregulatory role than previously believed. Indeed, previous studies have demonstrated the ability of RA FLS to act like innate immune cells, evident by the observed increased expression of toll-like receptors (TLR)-3 and -4 on synovial FLS, activation of which resulted in increased production of IL-6, and MMPs (Ospelt *et al.*, 2008). Moreover, TLR3 stimulation in RA FLS has been shown to induce production

of B cell-activating factor (BAFF) (Marsh *et al.*, 2021). Furthermore, it has been previously demonstrated that human FLS have the capability to present autoantigen peptides via class II MHC presentation to activated T cells in a T cell hybridoma mouse model, thus supporting their function as antigen presenting cells (Tran *et al.*, 2007). Expression of HLA-DR and interaction of co-stimulatory marker CD47 with TSP1 expressed on FLS, has been implicated as a key FLS/T cell regulatory circuit that perpetuates expansion of T cells within the inflamed joint (Vallejo *et al.*, 2003). Studies have also shown that either FLS-immune cell-cell contact or the release of soluble mediators can drive bi-directional function of FLS with T cells, macrophages, and endothelial cells within the inflamed joint (Petrasca *et al.*, 2020; Alivernini *et al.*, 2020; Fromm et al 2019; Kvacskay *et al.*, 2021; Hanlon *et al.*, 2024).

The frequency of CD200 PRIME cells was higher in RA+ compared to RA- and HC, with CD200R1 expression similar across the groups. CD200 is part of the CD200-CD200R1 immunoregulatory axis and is often associated with a dampening of an immune response, particularly in myeloid cells expressing the receptor (Vaine and Soberman, 2013). Regarding its expression on FLS, previous studies have described CD200+ FLS as having a pro-resolving phenotype, increased during periods of remission after treatment (Rauber *et al.*, 2024). However, consistent with the Rauber *et al.* (2024) study, we showed that CD200+ PRIME cells were significantly lower in the synovium compared to the circulation, as were CD200R1+ PRIME cells, suggesting within the joint environment CD200-CD200R1 engagement is lacking and consequently their immunosuppressive signaling. This divergence in expression of CD200+ PRIME cells in circulation vs synovium, may be dependent on the environmental cues at the site of inflammation, in addition to cellular interactions within the synovial extracellular matrix vs blood.

RA PRIME cells demonstrated increased frequency and expression of adhesion molecules. The increase observed in CD61 (also known as integrin β3) is consistent with findings from Lefévre *et al.* (2009), which also demonstrated increased integrin β levels on RA FLS that successfully migrated through the mouse vasculature. Additionally, ICAM-1, VCAM-1, CD44 and integrins have been well documented as being expressed on RA FLS (Firestein, 1996; Seemayer *et al.*, 2003; Bartok and Firestein, 2009; Fearon *et al.*, 2006; Koster *et al.*, 2021; Hanlon *et al.*, 2019). Not only does expression of these markers help facilitate adherence to the endothelium as a means of migrating into the joint, but this further supports the idea that circulating PRIME cells could already be or will develop into mature FLS.

The marked discrepancy between the frequencies of CD45-CD31-PDPN+ cells from the circulation and the tissue is not surprising. As expected, the tissue had a significantly greater

frequency of PDPN+ cells compared to the circulation. Due to the simplistic gating strategy, when applied to the synovial tissue, the PDPN+ gate most likely encompasses a combination of PRIME cells, mature FLS subsets, as well as FLS in varying stages of development. This becomes more evident when comparing the size and morphology of PDPN+ cells identified in each location, with those from the circulation having a smaller morphology compared to the wide range of sizes depicted in the joint.

Interestingly, expression and frequency of markers on PDPN+ cells were not unilaterally increased in synovial tissue compared to peripheral blood. Of note, most of the adhesion molecules had a higher frequency in the peripheral blood compared to synovial tissue apart from CD44. Based on the hypothesis that PRIME cells migrate into the joint from circulation, it would stand to reason that these cells would have a more prominent need to express adhesion molecules to facilitate adherence to the endothelium. However, CD44, in addition to its role in cellular adhesion, is also a receptor for hyaluronic acid (HA), osteopontin (OPN), collagens, and MMPs (Senbanjo and Chellaiah, 2017), all of which are important components of the ECM within the synovium. Interaction of CD44 with these ECM components promotes survival and migratory/invasive mechanisms (Senbanjo and Chellaiah., 2017), key phenotypic characteristics of synovial FLS.

One of the most surprising observations was the significantly increased frequency of Cadherin 11 in the circulation compared to the tissue. Cadherin 11 has become well established as playing a critical role in pathogenesis within the RA synovium, particularly on FLS function. Cadherin 11 not only plays a role in cellular adhesion, but also orchestrates tissue morphogenesis and determines the integrity and architecture of the ECM within the tissue (Valencia *et al.*, 2004). In the context of RA, it has been shown to support adhesion of FLS, mediate LL formation, contribute to pannus thickening, and influence the pro-inflammatory, invasive, and destructive response of FLS (Valencia *et al.*, 2004; Kiener and Brenner, 2004; Kiener *et al.*, 2006; Lee *et al.*, 2007; Kiener *et al.*, 2009; Chang *et al.*, 2011; Noss *et al.*, 2011). Due to the association of Cadherin 11 with lining layer FLS, the observed higher frequency on PRIME cells in the circulation is unexpected, as it is believed these PRIME cells will mature into SL FLS. Similarly, the frequency of FAPα was significantly higher in the circulation compared to the tissue, which is of interest as extensive studies have demonstrated the importance of FAPα in RA synovial pathogenesis, with THY-1+FAPα+ FLS associated with sub-lining expression (Waldele *et al.*, 2015; Croft *et al.*, 2019; Zhang *et al.*, 2019). However, the comparable or increased frequency of other FLS subset markers (CD55, THY-1, CD34) in the tissue aligns with previous studies. Croft *et al.* (2019) identified a PDPN+FAPα+THY1+ FLS population localised to the sub-lining layer that displayed immune

effector function in RA compared to OA. Consistent with this, Mizoguchi *et al.* (2018) described enrichment of THY1+CD34- FLS in RA compared to OA, while OA was more associated with THY1-CD34- FLS. Furthermore, work from our group defined differences in FLS subsets between RA and PsA, with FAP+THY-1+ dominant in RA, while FAP-THY1- are dominant in PsA (Floudas *et al.*, 2022). While outside the scope of this study, analysis of PRIME cells in PsA and OA would be of interest considering the differences in FLS subsets observed in the joint.

The differences observed between the metabolic markers pAKT (increased in the joint), pmTOR (increased in circulation), and pS6 (increased in circulation) between the circulation and the tissue suggest that PRIME cells in the circulation and PDPN+ cells within the joint have different metabolic requirements. AKT is a serine/threonine kinase that requires phosphorylation at two sites (one by PDK1 and the other by mTORC2) to attain its catalytic activity, thus becoming pAKT. Once phosphorylated, it can then phosphorylate mTORC2 creating a positive feedback loop, activate mTORC1 directly via phosphorylation, or activate mTORC1 indirectly by blocking its inhibitors TSC2 and PRAS40 (Karami Fath *et al.*, 2022). mTOR is also a serine/threonine kinase that is present in two protein complexes: mTORC1 (regulates cell growth and metabolism) and mTORC2 (controls proliferation and survival). mTORC1 in turn phosphorylates two key effectors, S6 and 4EBP (Saxton and Sabatini, 2017). As previously stated, mTORC2 phosphorylates AKT, which in addition to activating mTORC1, is important for promoting cell survival, proliferation, and growth through the phosphorylation and inhibition of other key substrates including GSK3β (metabolic regulator) and FoxO1/3a transcription factors (Saxton and Sabatini, 2017). Though these molecules are all a part of the same pathway, it is not a direct chain of events, therefore, it is possible that PRIME cells may be regulating its metabolism through the mTORC1 pathway, and the PDPN+ cells in the joint may be utilising AKT for other purposes. Indeed, metabolism is a key contributor to RA FLS pathogenicity, with FLS having the capacity to go through a metabolic switch to suit their energetic requirements (Fearon *et al.*, 2019). Previous studies have demonstrated the ability of multiple pro-inflammatory cytokines, including TNFα, Oncostatin M (OSM), and LPS, to induce a metabolic shift in FLS to a more glycolytic state (Garcia-Carbonell *et al.*, 2016; Bustamante *et al.*, 2017; Hanlon *et al.*, 2019). The mTOR pathway has gained increasing importance for its role in regulating FLS function with studies demonstrating mTORC1 mediating proliferation of RA FLS (Chen *et al.*, 2019) and TNFα co-opting the mTORC1 pathway to induce an IFN response (Karonitsch *et al.*, 2018).

Finally, we demonstrate that PRIME cells are present in IAR and ART, before clinical signs or symptoms of disease. While this is the first study to show their presence pre-disease onset, several studies have shown increased frequency and activation of other key cell types including T

cells, B cells and monocytes in IAR, in addition to cellular gene signatures within the circulation (van Baarsen *et al.*, 2010; Chalan *et al.*, 2013; Chang *et al.*, 2016; Lübbers *et al.*, 2016; Ramwadhdoebe *et al.*, 2016; van Baarsen *et al.*, 2017; Karouzakis *et al.*, 2019; Floudas *et al.*, 2021; McGarry *et al.* 2021; Cunningham *et al.*, 2021; Anang *et al.*, 2022). This increased frequency of PRIME cells prior to disease onset indicates that circulating PRIME cells in IAR/ART may display early phenotypic features of established RA PRIME cells and are preprogrammed for pro-inflammatory functions. Therefore, this study adds to our current knowledge, in addition to PRIME cells being associated with RA and predictive of disease flare, they may also be associated with disease onset.

In summary, we have corroborated previous identification of CD45-CD31-PDPN+ PRIME cells in the circulation of RA patients and have for the first time identified this population in IAR and phenotypically characterised these cells at the protein level. In addition, we have observed similar characteristics previously described by Orange *et al.* (2019) including the expression of HLA-DR, CD34, Cadherin-11, and FAPα while also expanding upon PRIME cell characterization. Further examination of the functional capabilities of these cells and the potential crosstalk between PRIME cells and other circulating immune cells will better elucidate the role of these cells in RA pathogenesis. Moreover, further investigation comparing the characteristics of circulating PRIME cells to PDPN+ cells in the joint may provide further clues as to which specific FLS subsets arise from these circulating mesenchymal precursors as opposed to a tissue resident origin. Finally, further research is needed to better understand the origins of these PRIME cells to elucidate the beginning stages of joint inflammation as well as joint spreading.

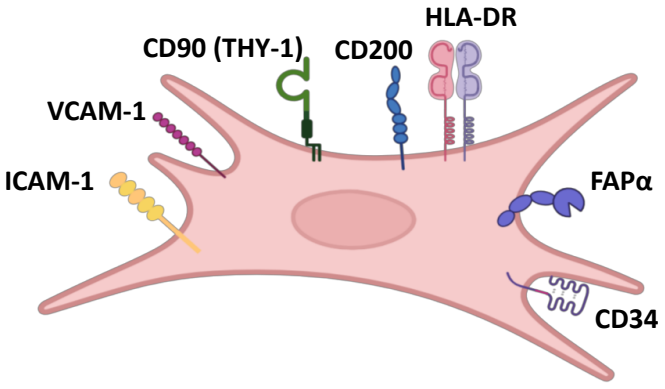

Figure 3.17: Summary of PRIME Cell Phenotype and Function.

Frequency of PRIME cells are increased in RA and demonstrate increased % frequency of immunoregulatory (HLA-DR; CD200) and adhesion (ICAM-1; VCAM-1) molecules. PRIME cells also express markers of activated SL FLS (FAPα; THY-1 (CD90); CD34). (Image created in BioRender 2025).

CHAPTER FOUR:

Distinct Homeostatic and Inflammatory FLS Signatures between RA and HC Synovial Tissue

3.1 Introduction:

The inflamed synovial joint is a very complex microenvironment, comprised of tissue-resident cells (macrophages and fibroblasts) and an influx of infiltrating immune cells from the periphery (T cells, B cells, DCs, monocytes, neutrophils, etc.) (Gravallese and Firestein, 2023). Though the functional role of each cell type and their contribution to RA pathogenesis is often studied separately, the joint is more complicated, with bidirectional cell-to-cell interactions working in tandem to activate each cell type. This activation leads to subsequent transcriptional changes and the secretion of numerous proinflammatory mediators, all of which contribute to the inflammatory response.

Extensive work has been performed in recent years to better understand mechanisms involved in shaping the synovial landscape and to gain a greater appreciation for the heterogeneous subsets of each cell type involved in synovial inflammation (Croft *et al.*, 2016; Frank-Bertoncelj *et al.*, 2017; Croft *et al.*, 2019; Aliverini *et al.*, 2020; Wei *et al.*, 2020; Floudas *et al.*, 2021; Kemble and Croft, 2021; Floudas *et al.*, 2022; Smith *et al.*, 2023; Hanlon *et al.*, 2024; Khullar *et al.*, 2024; Rauber *et al.*, 2024). Indeed, by studying tissue samples from multiple patients with RA, researchers have started to broadly categorise patients into disease pathotypes based on synovial cellular infiltrates, which may help to predict more effective treatments (Dennis *et al.*, 2014; Lewis *et al.*, 2019; Nerviani *et al.*, 2020; Zhang *et al.*, 2021; Rivellese *et al.*, 2022). An eloquent study by Rivellese *et al.* (2022), categorised patients into three subtypes based on synovial analysis, including lympho-myeloid (characterised by extensive B cell infiltration), diffuse-myeloid (presence of monocytes and macrophages, but sparse in B cells), or pauci-immune (featuring minimal immune cell infiltration, but a significant presence of FLS). This study also demonstrated that the patient's pathotype could be predictive of their response to treatments including rituximab and tocilizumab (Rivellese *et al.*, 2022). More recently, this has been expanded on by Zhang *et al.* (2023) with the additional use of scRNA sequencing and spatial transcriptomics, with six distinct pathotypes identified and referred to as cell-type abundance phenotypes (CTAPs). These categories included: endothelial, fibroblast and myeloid (CTAP-EFM); fibroblasts (CTAP-F); T cells and fibroblasts (CTAP-TF); T cells and B cells (CTAP-TB); T cells and myeloid cells (CTAP-TM); and myeloid cells (CTAP-M) (Zhang *et al.*, 2023).

It is now appreciated that immune cell-types within the inflamed joint are heterogeneous and display significant cellular plasticity depending on their environmental cues. For example, multiple subsets of macrophages have been identified in the RA synovium, with MerTK+ synovial macrophages shown to be associated with remission and disease flare (Aliverini *et al.*, 2020). More recently Hanlon *et al.* (2024) identified a CD163+CD206+CD40+ subset paralleled by a decrease in CX_3CR1+ barrier protective macrophages, associated with RA disease activity, the frequency of

which are also increased pre-disease onset in IAR. Additionally, numerous subsets of T cells have been described (Takeshita *et al.*, 2019; Argyriou *et al.*, 2022; Moon *et al.*, 2023). However, despite these advances, clinicians still face challenges in developing treatment strategies for patients who have suboptimal responses or no response. Thus, attention has now shifted to the synovial FLS and its role in the pathogenesis of RA. Indeed, a plethora of research has described this tissue-resident cell as one of the key drivers in perpetuating synovial inflammation and contributing to the irreversible and debilitating destruction of cartilage and bone observed within the joint (Müller-Ladner *et al.*, 1996; Lefévre *et al.*, 2009; Noss *et al.*, 2011; Croft *et al.*, 2019; Bai *et al.*, 2024). With the advent of technologies such as scRNA sequencing and advanced flow cytometry, researchers have started to identify and characterise the nuances of FLS subsets that reside within the inflamed joint and their roles in either promoting or resolving inflammation (Ospelt, 2017; Mizoguchi *et al.*, 2018; Wei *et al.*, 2020; Floudas *et al.*, 2022; Micheroli *et al.*, 2022; Smith *et al.*, 2023; Rauber *et al.*, 2024).

Indeed, Croft *et al.* (2016), demonstrated PDPN-expressing FLS to be significantly upregulated in the human RA synovium, the highest frequency of which resided in the lining layer, whereas CD248 expression was restricted to sub-lining perivascular FLS. These markers were further upregulated upon stimulation with various cytokines (Croft *et al.*, 2016). In their review, Kemble and Croft (2021) succinctly compiled the previous work conducted on FLS subsets to define the major FLS subsets identified to date: lining-layer defined as CD55+THY1- while also expressing CLIC5, PRG4, TSPAN15, HAS1, in addition to releasing ECM remodelling proteins. Sub-lining layers are defined by the THY-1+ (also known as CD90) cell marker and categorised into proinflammatory (expressing MHC-DR, IL-6, CXCL12, CCL2, etc.), perivascular/proinflammatory (expressing collagens, RANKL, MDK, or C3, CD34, CLEC3b), and homeostatic/pro-resolving (expressing DKK3, CADM1, OGN) (Kemble and Croft, 2021). Global transcriptomic analysis undertaken by Floudas et al. (2022) identified 11 distinct FLS subsets present in RA and PsA synovial tissue. Though all clusters were present in both diseases, the frequency of each cluster differed between disease states. Interestingly, the dominant clusters observed in RA were defined by sub-lining FLS markers. Pathway analysis of these clusters identified enrichment of pathways involved ECM receptors, focal adhesion, and collagen turnover (Floudas *et al.*, 2022). Furthermore, Wei *et al.*, demonstrated that synovial RA FLS have a positional identity, regulated by NOTCH3 signaling derived from the endothelium. This signaling played a critical role in the differentiation of THY-1+ sub-lining and perivascular FLS (Wei *et al.*, 2020).

It has also been proposed that the transcriptomic phenotype signature of FLS is the result of their tissue condition/state (diseased, stressed, ageing, homeostatic, regenerating), regional or

anatomical heterogeneity (including developmental origin, microbiome, and tissue-specific functional requirements), local heterogeneity (cell-matrix interactions, paracrine and autocrine signals, etc.), and cell phenotype (quiescent, activated, differentiating, proliferating, etc.). As a result of all these factors, scRNA sequencing has revealed the vast heterogeneity in the FLS population (Shaw and Rognoni, 2020). Multiple studies have demonstrated that the diversity and function of FLS depend on the joint type and location (positional memory) (Chang *et al.*, 2002; Frank-Bertoncelj *et al.*, 2017; Ospelt and Frank-Bertoncelj, 2017; Buckley *et al.*, 2021; Forte *et al.*, 2022;). It is believed that FLS have positional memory of their anatomical location, however their biological memory in response to transient or persistent environmental stimuli is less well understood. FLS transplantation to different anatomical locations, or even changes to their original microenvironment can influence their behaviour. However, despite this, some features are conserved, suggesting that FLS have the capacity to adapt to new environments while still retaining some memory of past stimuli (Kirk *et al.*, 2021). In addition, FLS within different organs can memorise their inflammatory, metabolic, and mechanical environment (i.e. tissue stiffness) and demonstrate distinct patterns of gene expression both within the same tissue and across different organs (Change *et al.*, 2002; Kirk *et al.*, 2021). Positional memory is an example of long-term memory and is important for maintaining tissue homeostasis, inflammation regulation, and regeneration. This positional memory has been demonstrated to be mainly driven by homeobox (HOX) gene expression (Kirk *et al.*, 2021). As highlighted in the previous chapter, it has been suggested that not all FLS subsets found in the joint are of tissue-resident origin, but rather some sub-lining FLS may arise from a pre-inflammatory mesenchymal (PRIME) precursor from the circulation, or from the process of epithelial-to-mesenchymal transition (EMT) (Orange *et al.*, 2020; Smith *et al.*, 2023). By better understanding the diverse FLS subsets within the joint, we may gain insight into their origins and additionally identify new potential targets for future treatments, especially for those patients that do not respond to current available therapies.

Therefore, in this chapter, we aim to use multiparametric flow cytometry to identify and characterise FLS subsets in the synovium of RA patients compared to IAR and HC. Furthermore, through scRNA sequencing and functional analysis, we aim to fully explore the spectrum of synovial FLS subsets residing within the RA synovium compared to HC, and determine their role in driving RA pathogenesis via the identification of upregulated pathways.

4.2 Specific Aims for this Chapter:

- Identify histological differences between HC, IAR, RA+, and RA- synovial tissue samples.
- Perform multiparametric flow cytometry analysis to identify and characterise FLS in synovial tissue biopsies from HC donors, RA+, and RA- patients.
- Determine any correlations between FLS phenotypic markers and RA disease activity.
- Compare LL and SL FLS subsets between HC, RA+, and RA- patients.
- Investigate whether frequency of FLS and subsets are altered prior to disease onset in IAR.
- Investigate whether certain functional phenotypes are preferentially expressed on certain FLS subsets.
- Utilise scRNA sequencing to identify and compare frequency of FLS clusters present between HC and RA synovial tissue and identify cell-cell interactions and key signaling pathways.

4.3 Materials and Methods:

4.3.1 Patient Recruitment and Sample Collection

RA patients, IAR, and HC undergoing anterior cruciate ligament (ACL) repair were recruited from the Department of Rheumatology, St Vincent's University Hospital and research conducted as previously outlined in Section 3.3.1, Chapter 3. Tissue biopsies from healthy individuals undergoing arthroscopy during ACL reconstruction were also included. Healthy subjects were defined as having no evidence of any form of arthritis upon examination or history and had no cartilage damage or synovitis on knee arthroscopy. RA and IAR were defined according to revised ACR/EULAR criteria as previously outlined in Section 3.3.1, Chapter 3. Two of the samples included in the IAR cohort (2/5) are ART (presented with general aches and pains, but seronegative for autoantibodies), but are included within the IAR cohort due to small sample size.

4.3.2 Obtaining Synovial Tissue Samples

HC, IAR, and RA synovial tissue biopsies were obtained from the knee at time of key-hole arthroscopy under local anaesthetic using a Wolf 2.7 mm arthroscope (Wolf – Germany) as previously described (Ng *et al.*, 2010). Biopsies were then either processed for the isolation of primary FLS or viably frozen in freezing media (10% DMSO in FBS) to be used for further downstream analysis. Biopsy processing and cellular viability were optimised in the lab and outlined by Floudas *et al.*, (2022).

4.3.3 Synovial Tissue Digestion for Flow Cytometry Analysis

Synovial tissue biopsies were thawed quickly in a 37°C water bath and digested enzymatically via the Tumour Dissociation Kit (Miltenyi Biotec, Germany) as per manufacturer's instructions. Briefly, 50 µL Enzyme A (nuclease), 150 µL Enzyme H (protease), and 100 µ Enzyme R (protease) were diluted in 600 µL RPMI (Sigma-Aldrich). Biopsies were incubated in 100 µL enzyme mixture for 45 min at 37°C and 5% CO_2. The mixture was then passed through a 70 µM cell strainer to remove debris and undigested pieces of tissue to yield a single-cell synovial cell suspension which were then utilised for flow cytometric analysis (Section 4.3.6). Clinical information of RA patients for synovial tissue samples (n=15) included in this study for flow cytometry analysis can be found in Table 4.1.

Characteristics	Number or Average	Percent or Range
Age (years)	52.4	19 - 72
Female	14	93.3% (14/15)
Seropositive (ACPA+ and/or RF+)	**9**	60% (9/15)
RF positive	9	60% (9/15)
ACPA positive	8	53.3% (8/15)
Seronegative	6	40% (6/15)
Disease Duration (years)	5	<1 - 15
DAS28 score	3.65	1.8 – 8.22
CRP	18.88	0 - 153
On DMARD	5	33.3% (5/15)
On Biologic	1	6.67% (1/15)
Treatment naïve	9	60% (9/15)

Table 4.1: **Patient demographics for RA synovial tissue biopsies used for flow cytometry analysis.** Anti-citrullinated protein antibodies (ACPA), Rheumatoid Factor (RF), Disease Activity Score (DAS), Disease Modifying Anti-Rheumatic Drugs (DMARDs).

Characteristics	Number or Average	Percent or Range
Age (years)	29.3	19-51
Female	3	25% (3/12)

Table 4.2: Patient demographics for HC synovial tissue biopsies (n=12) used for flow cytometry analysis.

4.3.4 Isolation of Primary FLS for Functional Experiments

RA synovial tissue biopsies were digested with 1 mg/mL collagenase type II (Worthington Biochemical, Freehold, NJ, USA) in RPMI-1640 (Sigma-Aldrich) and incubated for 4 h at 37°C in humidified air with 5% CO_2. Dissociated cells were grown to confluency in RPMI-1640, 10% FBS (Sigma-Aldrich), 10 mL of 1 mmol/L HEPES (Gibco), penicillin (100 units/mL; Bioscience), streptomycin (100 units/mL; Bioscience) and fungizone (0.25 µg/mL; Bioscience) before passaging. Cells were used between passages 3-8.

4.3.5 Histology Scoring

Based on the Haematoxylin and Eosin (H&E) staining, a tissue inflammatory score for each biopsy was applied. Semiquantitative analysis was performed by two independent scorers to assess the

inflammation, vascularization, and lymphoid aggregation of each biopsy. For inflammation scores, a four-scale score was utilised: 0= no to minimal inflammation, 1= mild inflammation, 2= moderate inflammation, and 3= severe inflammation. Hyperplasia of the lining layer was assessed by calculating the mean number of cells in the layer. Vascularization was measured semi quantitatively via a four-scale score: 0-1= no to minimal blood vessels, 2= moderate presence of vessels, and 3= severe number of blood vessels. Presence of lymphoid aggregates was measured on a binary scale: 0= no aggregates and 1= lymphoid aggregates present.

4.3.6 Flow Cytometry of Synovial Tissue Biopsies

Expression of cell surface markers (CD45-CD31-CD146-PDPN+) was assessed using flow cytometry to distinguish and identify FLS within the synovial tissue single-cell suspension. Tissue biopsies were thawed and digested as previously described (Section 4.3.3), to obtain a single-cell suspension which was subsequently stained and analysed. Samples were stained in a 96-well round bottom plate using the fluorochrome-conjugated antibodies listed in Table 4.2. Cells were washed with PBS and resuspended in a 1:1000 dilution of LiveDead Zombie NIR viability dye (Biolegend) diluted in PBS and left to incubate in the dark at 4°C for 30 min. Subsequently, cells were topped up with PBS and centrifuged at 1400 rpm for 3 min and washed a second time. Each sample was resuspended in a blocking solution of 5 µL Human TruStain FcX (Biolegend) and 95 µL PBS for 10 min to eliminate nonspecific binding to the FcγR. Extracellular fluorochrome-conjugated antibodies were added, samples vortexed, and incubated for 30 min in the dark at 4°C. Samples were then washed with FACS Buffer (Dulbecco's PBS without Mg^{2+} or Ca^{2+} (Sigma-Aldrich), 2% heat-inactivated FBS (Biosciences) and 0.05% sodium azide (Sigma-Aldrich), 0.5 M EDTA, pH 7.4-7.6) and centrifuged at 1400 rpm for 3 min. Supernatants were removed and samples washed a second time. The FoxP3/Transcription Factor Staining Buffer Set (Invitrogen, USA) was utilised for intracellular staining. After the second wash, samples were resuspended in 100 µL Fix/Perm Solution (diluted 1:4 in kit diluent) and left to incubate for 30 min in the dark at 4°C. Samples were washed with Perm Buffer, resuspended with 30 µL Perm Buffer and intracellular antibodies, and left to incubate for 30 min in the dark at 4°C. Samples were washed twice with Perm Buffer and FACs respectively and resuspended in 250 µL FACs. Samples were acquired using the Aurora Flow Cytometer (Cytek Biosciences) and analysed using FlowJo software (FlowJo LLC, Oregon, USA).

Cells were gated based on forward and side scatter, and doublets and dead cells were removed before downstream analysis. Live Dead Zombie NIR viability dye (Biolegend) was used to eliminate dead cells. Fluorescence Minus One (FMO) controls were utilised to determine gating boundaries between markers where appropriate. To adjust for spectral overlap between laser

detectors, compensation was applied via single-stained compensation beads (BD) that were prepared for each fluorochrome. Samples were spectrally unmixed directly on the Aurora flow cytometer before each run.

The markers analysed for (1) the exclusion of other cell types included within the whole biopsy single cell suspension and (2) the identification of FLS subsets and functional phenotype are as follows:

- Exclusion of haematopoietic cells (CD45+), ECs (CD31+), pericytes (CD146+), and inclusion of PDPN+ cells for identification of FLS.
- FLS Immune Markers (HLA-DR, CD200, CD200R1)
- FLS Proliferative and invasive markers (Ki67, PDGFRα, YAP)
- FLS Adhesive markers (VCAM-1, ICAM-1, CD44, CD61)
- FLS Metabolic markers (pAKT, pmTOR, pS6)
- FLS Activation and subset markers (FAPα, Cadherin 11, CD55, CD90 (THY-1), CD34)

Antibody	Fluorochrome	Clone	Company
HLA-DR	BV421	L243	Biolegend
CD200	eFlour450	OX104	Invitrogen; eBioscience
VCAM-1 (CD106)	BV480	51-10C9	BD
CD34	BV510	581	Biolegend
CD31	BV605	WM59	Biolegend
Ki67*	BV650	11F6	Biolegend
CD146	BV711	P1H12	BD
CD90	BV750	5E10	BD
CD44	BV785	IM7	Biolegend
CD45	AF532	HI30	Invitrogen; eBioscience
CD61 (Integrin β3)	PerCP	VI-PL2	Biolegend
pS6 (Ser235, Ser236)*	PerCP/Cy5.5	A17020B	Biolegend
ICAM-1 (CD54)	PerCP-eFluor710	HA58	Invitrogen; eBioscience
YAP*	PE	D8H1X	Cell Signaling
pAKT*	PE-CF594	M89-61	BD
CD140α (PDGFRα)	PE/Cy5	APA5	Biolegend
CD200R1	PE/Cy5.5	OX108 (Chimeric)	NOVUS
Cadherin 11	PE/Cy7	16G5	Biolegend
CD55	APC	JS11	Biolegend
pmTOR*	AF647	O21-404	BD
FAPα	AF700	427819	Novus
Podoplanin	APC-Fire750	NC-08	Biolegend

Table 4.3: **Panel of fluorochrome antibodies used for flow cytometry analysis of PRIME cells in PBMC and synovial tissue biopsy samples.** *Indicates intracellular stains.

4.3.7 TSNE Analysis of Flow Cytometry Data

Total PDPN+ FLS from the synovial tissue of one HC, one IAR, one RA+, and one RA- donor were concatenated and analysed via unbiased, unsupervised, multidimensional analysis of flow cytometric data, allowing for cell clustering to be performed by the tSNE algorithm in FlowJo. tSNE

is an unsupervised algorithm that performs dimensionality reduction of complex data by clustering cells that have similar expression profiles (Belkina *et al.*, 2019).

4.3.8 Single-Cell (sc)RNA Sequencing:

Bioinformatic analysis was carried out by Dr Conor Smith. Biological annotation and investigation of FLS clusters was performed by Brianne Barker. ScRNA-seq data were processed using Cell Ranger (v3.02) and using the 10x human transcriptome GRCh38-3.0.0 as a reference. Subsequent analysis was performed in R (v4.4.1). Cell-containing droplets were identified in each individual sample using EmptyDrops at a false discovery rate of 1% (Lun *et al.*, 2019). Droplets lacking a cell were removed from downstream analysis. For a gene to be included in subsequent downstream analysis in Seurat (v.5), it must be expressed in a minimum of 3 cells (Stuart *et al.*, 2019). Further quality control included the removal of dead and apoptotic cells using a mitochondrial content cut-off of 25%. The DoubletFinder package was used to identify and remove doublet and multiplet cells (McGinnis, Murrow, and Gartner, 2019). In order to remove any batch effects associated with the scRNA-seq data, data was integrated using the Harmony package (Korsunsky *et al.*, 2019). Data were normalised and scaled using the Seurat SCTransform pipeline. Fibroblast populations were identified by the expression of characteristic cell markers including LUM, FAP, PDPN, and THY-1. Once identified, these fibroblast clusters were isolated and the SCTransform pipeline was performed to generate a fibroblast specific dataset. Using the *FindNeighbours* and *FindClusters* functions in Seurat, 14 unique fibroblast clusters were identified. Uniform Manifold Approximation and Projection (UMAP) plots were used for dimensionality reduction and for visualization of this scRNA-seq data.

The *FindAllMarkers* function in Seurat was used to identify cluster specific markers in this fibroblast dataset. Only genes with a $Log_2FC > 0.25$, a min.pct > 0.25 and an adj.p.value < 0.05 following Bonferroni correction were included as cluster markers. Differentially expressed genes (DEGs) were identified using Wilcoxon Rank Sum test and displayed using heatmaps and volcano plots. Pathways enriched from the DEGs were identified using pathfindR (Ulgen, Ozisik and Sezerman, 2019) and pathway activity scores were calculated using the *AddModuleScore* function in Seurat. Nebulos was used to display gene expression density on the UMAP (Alquicira-Hernandez and Powell, 2021). Clinical information for RA patients (n=4) utilised for scRNA sequencing has been previously described (Hanlon *et al.*, 2024) and can be found in Table 4.3.

Characteristics	RA (n=4)
Number (M/F)	4 (1/3)
Age (years) mean, range	57.5 (39-83)
ACPA, pos/neg	3/1
RF, pos/neg	3/1
CRP, mean ± SD	14.5 ± 8.3
ESR, mean ± SD	45.6 ± 27.7
SJC28, mean ± SD	5.4 ± 7
TJC28, mean ± SD	7.8 ± 9
DAS28 score, mean ± SD	4.6 ± 1.1
Disease duration (years), mean ± SD	4.5 ± 8.3
Medications	Naïve

Table 4.4: **Patient demographics of RA synovial tissue samples used for scRNA sequencing analysis.** Anti-citrullinated protein antibodies (ACPA), Rheumatoid Factor (RF), Erythrocyte Sedimentation Rate (ESR), C-Reactive Protein (CRP), Swollen Joint Count (SJC). Tender Joint Count (TJC), Disease Activity Score (DAS), Disease Modifying Anti-Rheumatic Drugs (DMARDs).

Characteristics	HC (n=5)
Number (M/F)	(5/0)
Age (years) mean, range	22.8 (18-37)

Table 4.5: Demographics of HC synovial tissue samples used for scRNA sequencing analysis.

4.3.9 mRNA Extraction and cDNA Synthesis

Clinical information of RA patient samples (n= 9) included in this study for functional experiments can be found in Table 4.4. To assess the effects of IL-1β on genes within the NOTCH signaling pathway, RA FLS were seeded into 6-well plates at a concentration of 1 x 10^5 cells/well and allowed to grow to confluence. Cells were then incubated in serum-free (1% FBS) RPMI-1640 for 24 h and subsequently stimulated with IL-1β (1 ng/mL) for 3 hr before total RNA was collected. The γ-secretase IX inhibitor (DAPT) (565770-10MG, Millipore Corp, USA) was next used to assess its effects on the expression of NOTCH signaling and crosstalk with other pathways. Cells were plated as outlined above, then incubated in serum-free (1% FBS) RPMI-1640 for 24 h and subsequently pre-treated, where indicated, with DAPT (50 μM) or vehicle control DMSO for 2 h before stimulation with IL-1β (1 ng/mL) for 24 h. Total RNA was isolated using the miRNeasy Mini Kit (Qiagen, Germany) according to the manufacturer's instructions. The integrity of the RNA was assessed using a NanoDrop 2000 spectrophotometer. Samples with a 260:280 nm ratio of 1.8 and above were used in subsequent experiments. Isolated RNA was stored at -80°C. Total RNA (100

ng) was reverse transcribed to cDNA using a high-capacity cDNA reverse transcription kit (Applied Biosystems, Cheshire, UK) and stored at -20°C until further use.

Characteristics	Number or Average	Percent or Range
Age (years)	43.9	24-68
Female	5	55.6% (5/9)
Seropositive (ACPA+ and/or RF+)	**9**	100% (9/9)
RF positive	9	100% (9/9)
ACPA positive	7	77.8% (7/9)
Seronegative	0	0% (0/9)
Disease Duration (years)	3.2	1-6
DAS28 score	3.22	1.8-4.86
CRP	97.2	0-689
On DMARD	3*	33.3% (3/9)
On Biologic	0	0% (0/9)
Treatment naïve	6	66.7% (6/9)

Table 4.6: **Patient demographics of RA patient samples utilised for FLS functional experiments.** Anti-citrullinated protein antibodies (ACPA), Rheumatoid Factor (RF), Disease Activity Score (DAS), Disease Modifying Anti-Rheumatic Drugs (DMARDs).

4.3.10 RT-PCR analysis

Gene expression data were quantified by RT-PCR using the Quant Studio 5 Thermal Cycler (Applied Biosystems, Lewes, UK). Reaction mixtures contained 1 µL of cDNA, 10 µM of specifically designed forward and reverse primers (Table 4.5), SYBR green II Universal Master Mix (Thermo Fisher Scientific, USA) and RNase-free water. Samples lacking multiscribe reverse transcriptase acted as negative controls to ensure target-specific quantification. Data were analysed using the comparative threshold cycle (Ct) method with normalization to the expression of the housekeeping gene *RPLP0.* Reactions were performed in duplicate in a 96-well plate format. Thermal cycling conditions were applied as recommended by the manufacturer (Applied Biosystems).

Gene Name	Forward Primer	Reverse Primer
RPLPO	5’ GCGTCCTCGTGGAAGTGACATCG 3’	5’ TCAGGGATTGCCACGCAGGG 3’
NOTCH1	5’ GTCAGGGAAATCGTGCCAGCA 3’	5’ GCAGATGTAGGAGGCCTCGAA 3’
NOTCH3	5’ AGAGGAGCTACTGCGTTCCA 3’	5’ GCATTACTACCGAGCCGATC 3’
JAG1	5’ TGGCCGAGGTCCTATACGTTG 3’	5’ GGTTGAACGGTGTCATTACTG 3’
DLL4	5’ AACGGGGGACAGTGCCTGAA 3’	5’ AGTTCACAGTAGGTGCCCGTG 3’
HEY2	5’ TCGGGGCAAAGTACTAGCTCT 3’	5’ GCCTTTTCTCTATAATCCCTCTC 3’
IL-6	5’ CCCTGAGAAAGGAGACATGTAAC 3’	5’ CCTCTTTGCTGCTTTCACACATG 3’
RANTES	5’ CATCTGCCTCCCCATATTCCT 3’	5’ ATGTAGGCAAAGCAGCAGGGT 3’

Table 4.7: **Designed primer sequences used for RT-PCR analysis.**

4.3.11 Statistical Analysis

Statistical Analyses for flow cytometry and functional experiments were performed using GraphPad Prism 9.5.0 software. Wilcoxon Signed-Rank Test and paired Friedman ANOVA with Dunn’s Multiple comparisons were utilised to analyse paired nonparametric data. Mann-Whitney U test and Kruskal-Wallis ANOVA with Dunn’s Multiple comparisons were utilised to analyse unpaired nonparametric data. P-values of less than 0.05 ($p<0.05$) were determined as statistically significant. Data was expressed as mean ± SEM.

4.4 Results:

4.4.1 Histological Differences and Identification of FLS in the Synovial Tissue in HC vs RA

Synovial tissue biopsy from HC (n=5), IAR (n=4; n=2 were ART), RA+ (n=8), and RA- (n=6) were obtained at time of arthroscopy or ACL repair, and H&E sections performed and scored. As expected, the synovium of HC donors and IAR were acellular with minimal cell infiltration, a thin and defined LL, and minimal vascularization as demonstrated in the representative images in Figure 4.1 (A). Both RA+ and RA- demonstrated a significant increase in vascularity ($p<0.01$ and $p<0.05$, respectively) and cellular infiltration ($p<0.01$ and $p<0.05$, respectively) compared to HC tissue (Figure 4.1 (A-B)). Additionally, an increase LL thickness in RA+ and RA- ($p<0.01$) compared to HC was observed (Figure 4.1 (B)). Except for one RA- donor, lymphoid aggregates were only found in RA+ donors ($p<0.05$) (Figure 4.1 (B)).

In the inflamed joint microenvironment, FLS are constantly exposed to a plethora of signals and stimuli; therefore, we examined FLS phenotypes within the synovial tissue of all cohorts. Synovial tissue from HC, IAR, and RA patients were enzymatically digested to a single cell suspension and subsequently stained using a panel of human synovial FLS associated cell surface markers (see Table 4.2) to assess the phenotype and frequency of FLS. It has become more appreciated that seronegative RA patients (RA-) behave differently compared to their seropositive (RA+) counterparts. Indeed, it has been established that RA+ patients tend to present with more severe disease and have poorer prognosis, yet often respond better to current treatments compared to RA- (Carbonnell-Bobadilla *et al.*, 2022). Therefore, we stratified our analysis of FLS in the RA synovial tissue between seropositive and seronegative patients to gain a better understanding on how FLS frequency and phenotype may differ between the two cohorts.

Representative flow plots outlining the gating strategy used for identification of synovial FLS are shown in Figure 4.2. Following the exclusion of debris, cell doublets, and dead cells, FLS were identified based on the populations that were negative for CD45 (haematopoietic cells), double negative for CD146 and CD31 (pericytes and ECs) and positively expressing PDPN (Figure 4.2 (A-F)). Further phenotyping of synovial FLS was based on the expression of markers listed in Table 4.2. We first examined the frequency of CD45- cells across HC (n=12), RA+ (n=9), and RA- (n=6) (Figure 4.3). While both RA cohorts displayed an increase in number of cells compared to HC (as evidenced by the representative dot plots in Figure 4.3 (A)), RA+ demonstrated a lower frequency of CD45- cells as a percentage of total live cells (approximate mean of 48.58%) compared to HC and RA- (approximate mean of 67-69%) (Figure 4.3 (B)). This was indicative of the large proportion of immune cell infiltrates in RA+ patients. This is further emphasised in the representative flow dot plots, showing clearly that RA+ had a greater proportion of CD45+ cells

and therefore a smaller frequency of CD45- population compared to HC and RA (Figure 4.3 (A-B)). Additionally, in the context of total live cells, PDPN+ FLS increased in a stepwise manner from HC to RA+ to RA- samples (HC vs RA- p=0.0831) (Figure 4.4 (B)). Within the CD45- population, frequency of FLS were increased in both RA- and RA+, with the latter trending towards significance, compared to HC (HC vs RA+ p=0.0585) (Figure 4.4 (C)). Representative flow dot plots illustrating the differences in PDPN+ FLS frequency as a percentage of live cells are shown in Figure 4.4 (A).

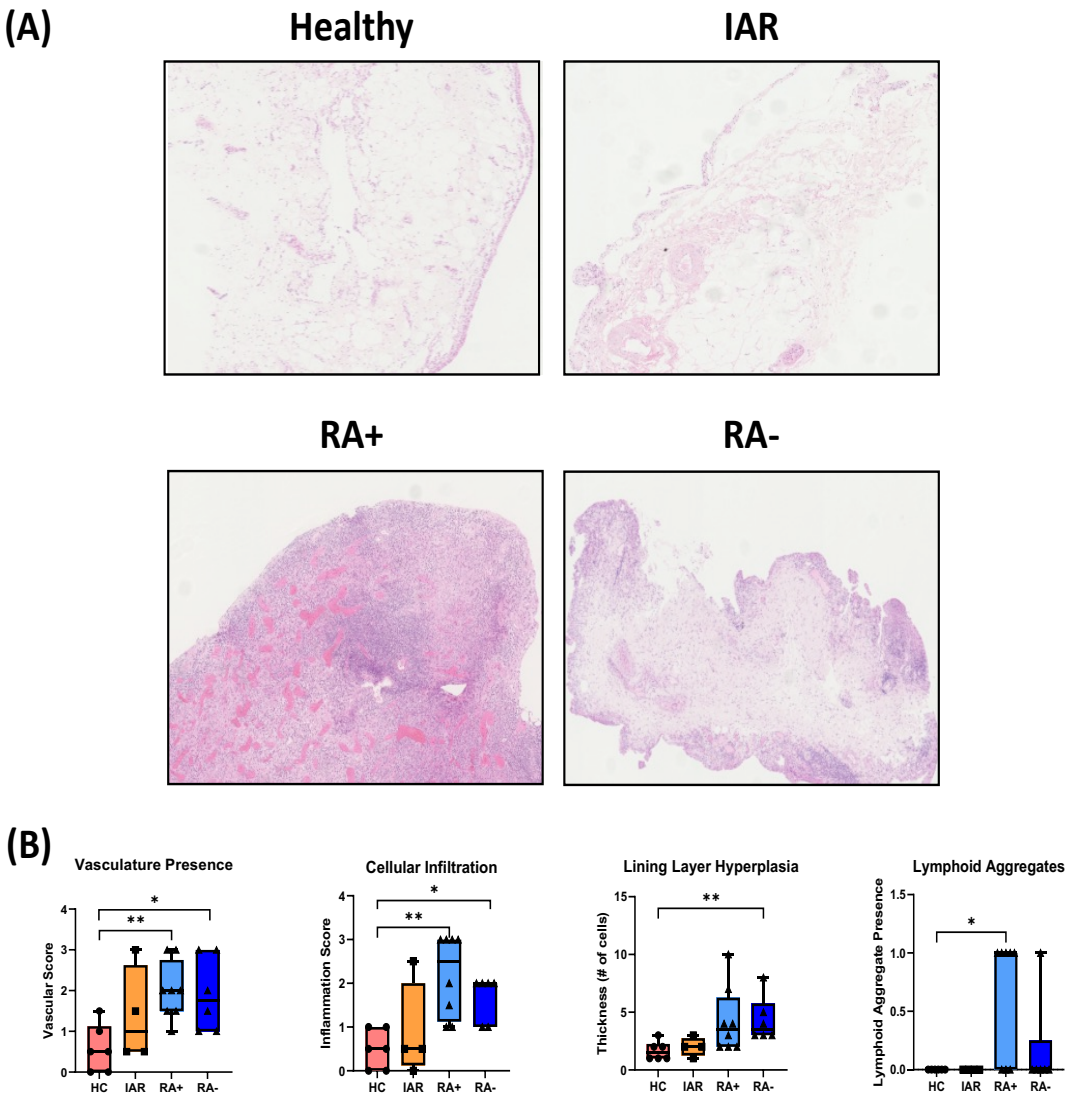

Figure 4.1: Histologic differences can be observed across disease states.

(A) Representative images of H&E histological staining of synovial tissue for HC (n=5), IAR (n=4), seropositive RA+ (n=8), and seronegative RA- (n=6) samples taken at 5x magnification. (B) Box and whisker plots of semi-quantitative scores for vascularisation (scale of 0-3), cellular infiltration (scale 0-3), lining layer hyperplasia (average number of cells), and presence of lymphoid aggregates (0=no; 1=yes). Data represented as min to max showing all points. Statistical analysis performed using the Mann-Whitney U test with *p<0.05 and **p<0.01.

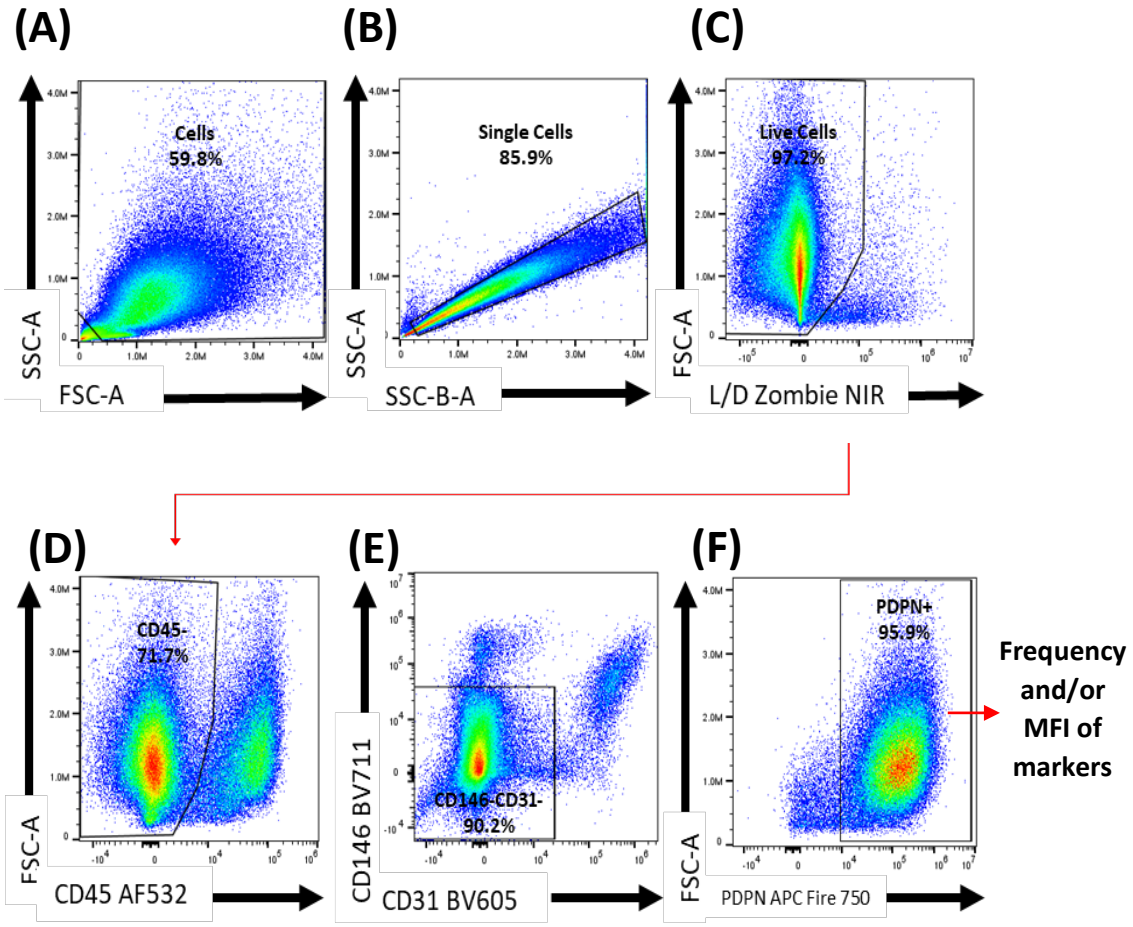

Figure 4.2: PDPN+ synovial tissue biopsy FLS gating strategy.

Whole synovial tissue biopsies from HC (n=12), IAR (n=5*), and RA (n=15) were thawed and digested down to a single cell suspension and stained with a panel consisting of 24 fluorochrome antibodies and analysed via the Cytek Aurora Cytometer. Representative dot plots depicting the gating strategy used to identify and characterise PDPN+ FLS from the tissue. (A-C) Forward and side scatter parameters established for cells before exclusion of doublets and dead cells. (D-F) FLS were identified as CD45-CD146-CD31-PDPN+ and further characterised by expression of intra- and extra-cellular markers. *Includes 2 ART.

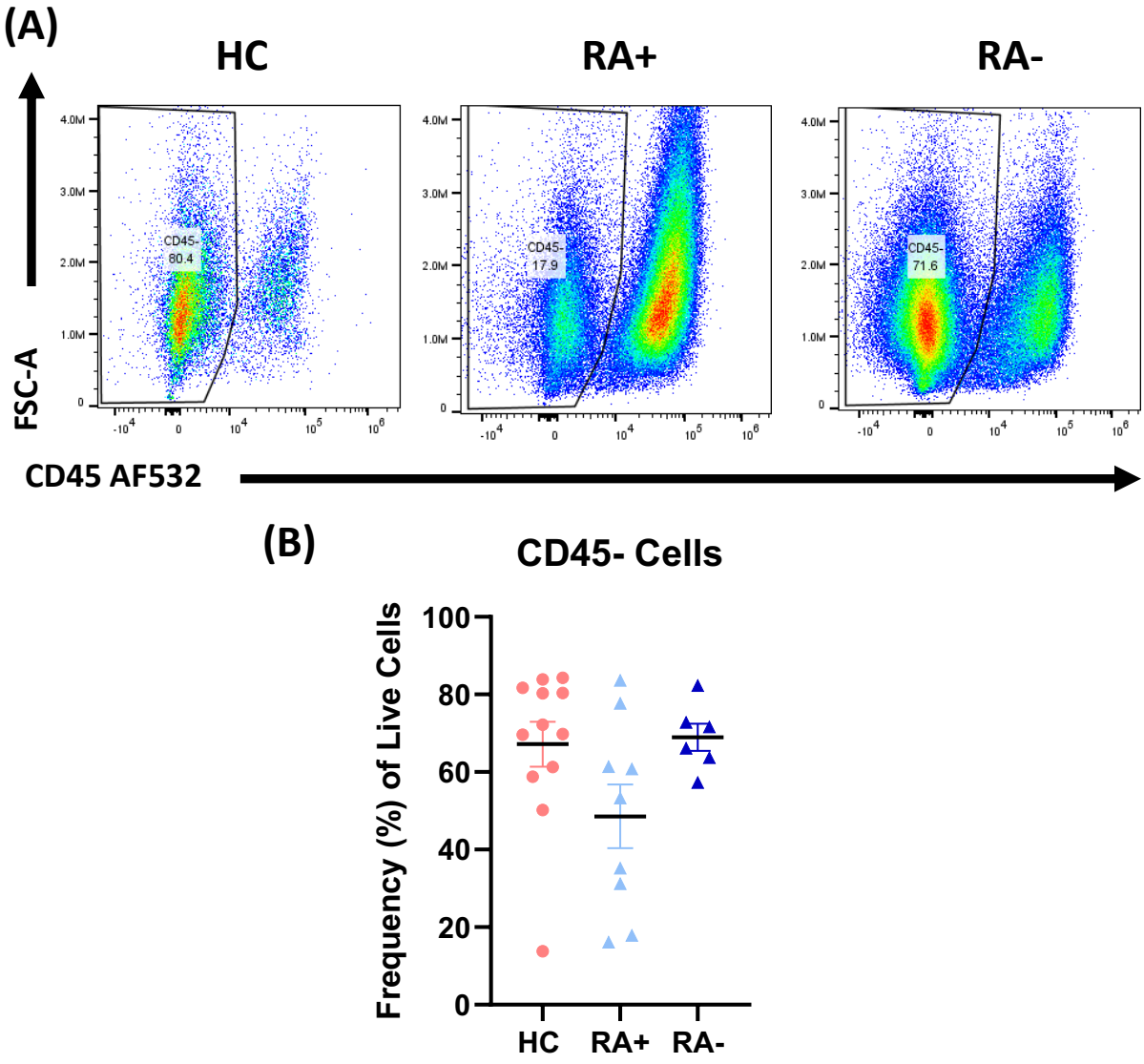

Figure 4.3: Frequency of non-immune cells (stromal cells) differ between HC and seropositive RA samples.

(A) Representative dot plots indicating differences in frequency of CD45- cells in HC, RA+, and RA- synovial tissue. (B) Dot plots demonstrating frequency of CD45- cells as a percentage of total live cells in RA+ (n=9) and RA- (n=6) synovial tissue compared to HC (n=12). Data represented as mean ± SEM.

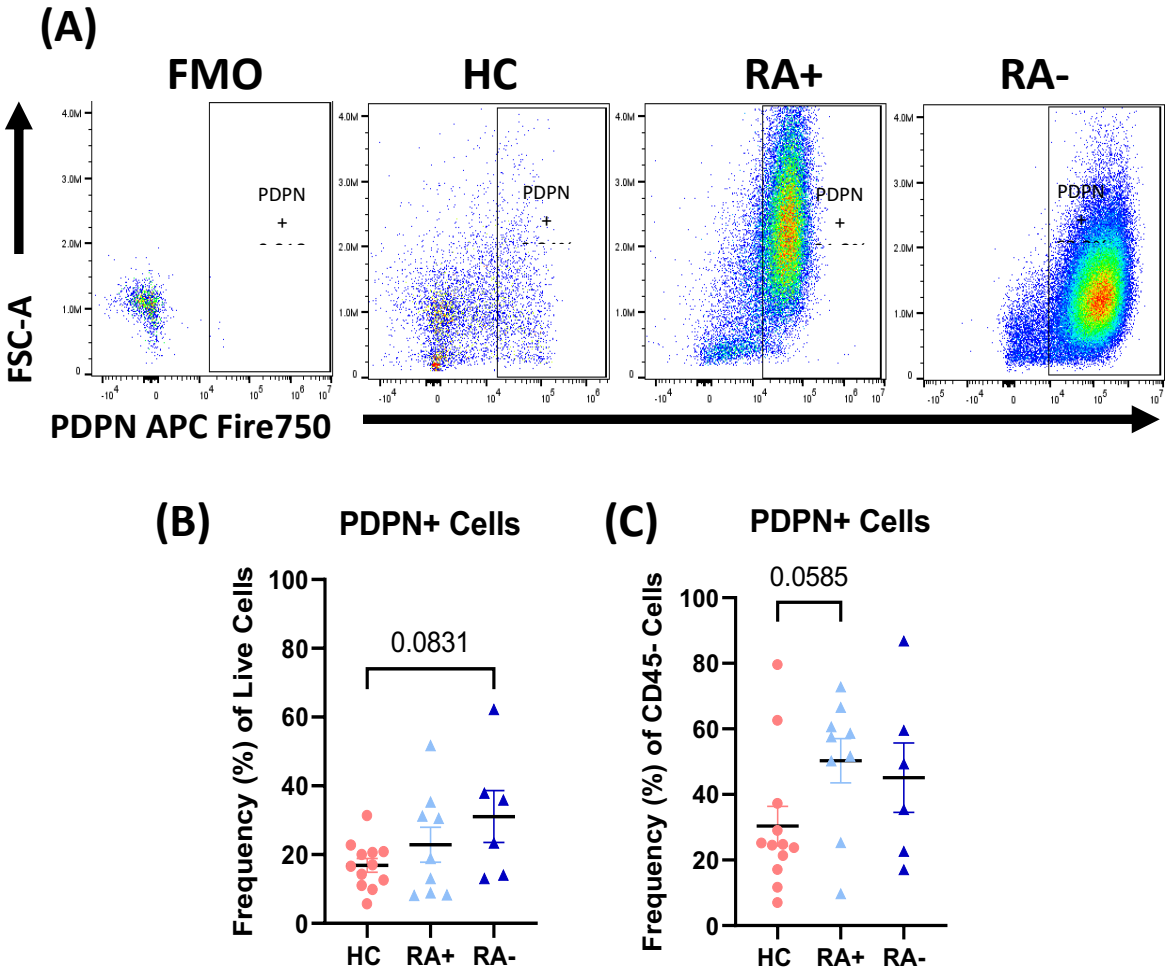

Figure 4.4: Frequency of PDPN+ FLS increased in RA synovial tissue compared to HC.

(A) Representative dot plots depicting differences in frequency of PDPN+ FLS between FMO control, HC, RA+, and RA-. (B) Scatter dot plot demonstrating differences in percentage frequency of PDPN+ FLS as a percentage of live cells in synovial tissue of HC (n=12) and between RA+ (n=9) and RA- (n=6). (C) Scatter dot plot depicting differences in PDPN+ FLS frequency as a percentage of CD45- cells. Gates were set according to FMO controls. Data expressed as mean ± SEM. Mann-Whitney U test used for statistical analysis of nonparametric data with *p<0.05 significantly different from each other.

4.4.2 Differential FLS Marker Expression on RA PDPN+ FLS Compared to HC

To further assess the diversity of FLS subsets present, we initially performed unbiased, unsupervised, multidimensional analysis of flow cytometric data from one HC, one RA+, and one RA- synovial tissue using the t-distributed stochastic neighbour embedding (tSNE) algorithm following the pre-gating of PDPN+ cells. This unsupervised algorithm performs dimensionality reduction of large, complex data by clustering cells together that share similar expression profiles, while also allowing for visualization of marker expression to help identify cell populations (Belkina *et al.*, 2018).

Total PDPN+ cells were subjected to the unsupervised clustering by tSNE algorithm following data concatenation. Data concatenation and relative expression of common FLS subset markers CD55, THY-1, CD34, and FAPα are shown in Figure 4.5. Based on this clustering, we observed the highest expression of CD55 in RA- and HC and, conversely, highest expression of THY-1 observed in RA+ (Figure 4.5 (A-B)). Though CD34 expression appeared comparable across all three patients, there was higher expression of this marker overlapping with areas of THY-1 positivity (Figure 4.5 (B)). All cells demonstrated expression of FAPα with the highest expression observed in RA+ (Figure 4.5 (B)). This analysis highlights the stark differences in FLS subsets residing within the synovial tissue of HC, RA+, and RA- patients. Therefore, we next analysed the frequency of these markers across a larger cohort of HC (n=12), RA+ (n=9), and RA- (n=6). As demonstrated in representative flow cytometric plots and accompanying dot plots, the frequency of CD55+ FLS was higher in RA- compared to both HC and RA+ ($p=0.0985$ and $p<0.05$, respectively) (Figure 4.6 (A-B)). Additionally, frequency of THY-1+ FLS was increased in RA+ compared to HC ($p=0.0955$) and RA-. Interestingly, an increase in THY-1+ FLS frequency was observed in HC when compared to RA- ($p=0.0663$) (Figure 4.6 (B)). Comparable frequencies of CD34+ FLS were observed across all cohorts (Figure 4.6 (B)). A large proportion of FLS in HC, RA+, and RA- were positive for FAPα, however, frequency was still increased in RA compared to HC (Figure 4.7 (B)). This was further demonstrated in the representative flow dot plots (Figure 4.7 (A)). Mirroring this, MFI expression (depicted in the representative stacked histogram) of FAPα was also increased on RA+ FLS compared to HC ($p=0.0574$) (Figure 4.7 (C-D)).

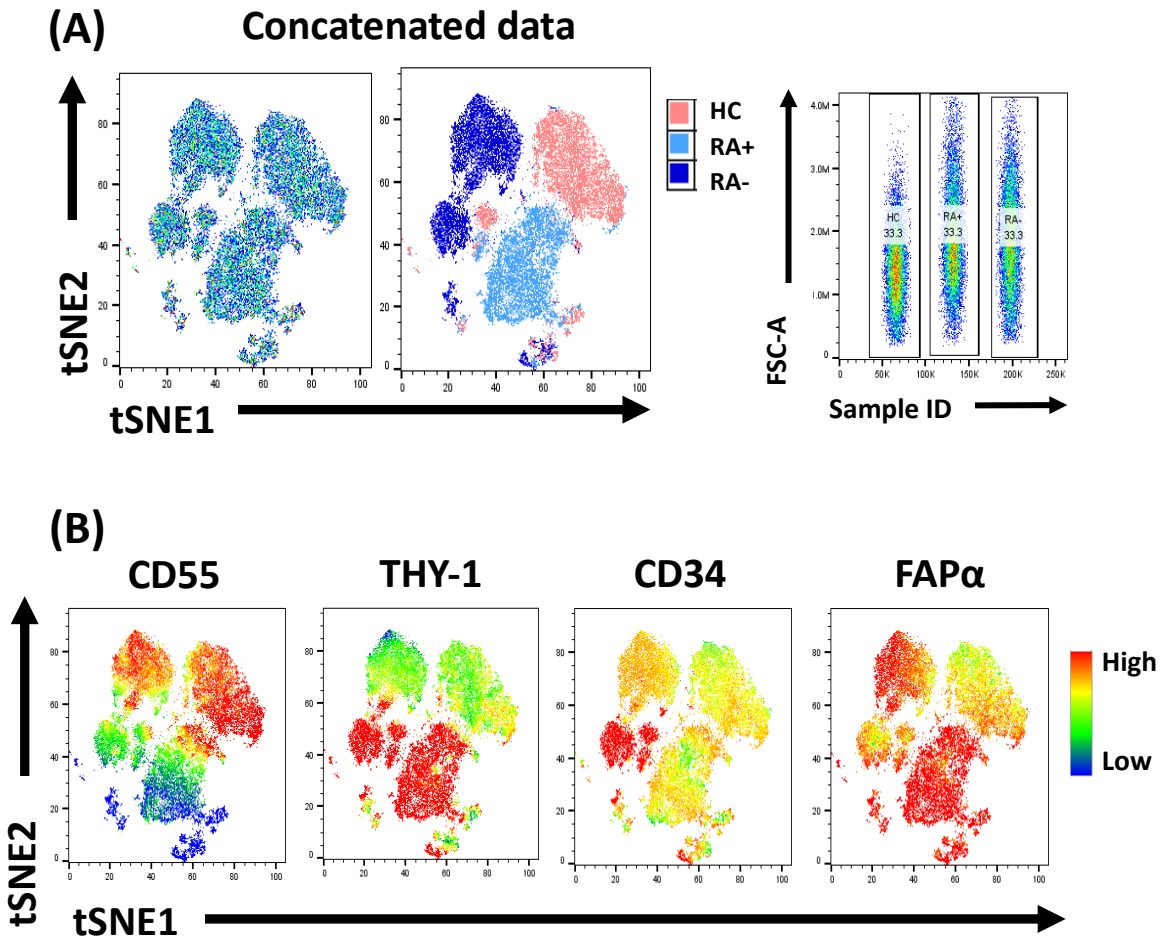

Figure 4.5: Differential FLS subset marker expression identification by unsupervised clustering.

Multiparametric flow cytometric data of total PDPN+ FLS subjected to unsupervised clustering by tSNE algorithm following data concatenation of synovial tissue from one HC, one RA+, and one RA-. (A) tSNE dot plots demonstrating data concatenation of all PDPN+ cells and overlay of HC, RA+, and RA- FLS to demonstrate how FLS cluster together. (B) tSNE plots demonstrating relative expression of FLS markers CD55, THY-1, CD34, and FAPα on concatenated PDPN+ FLS.

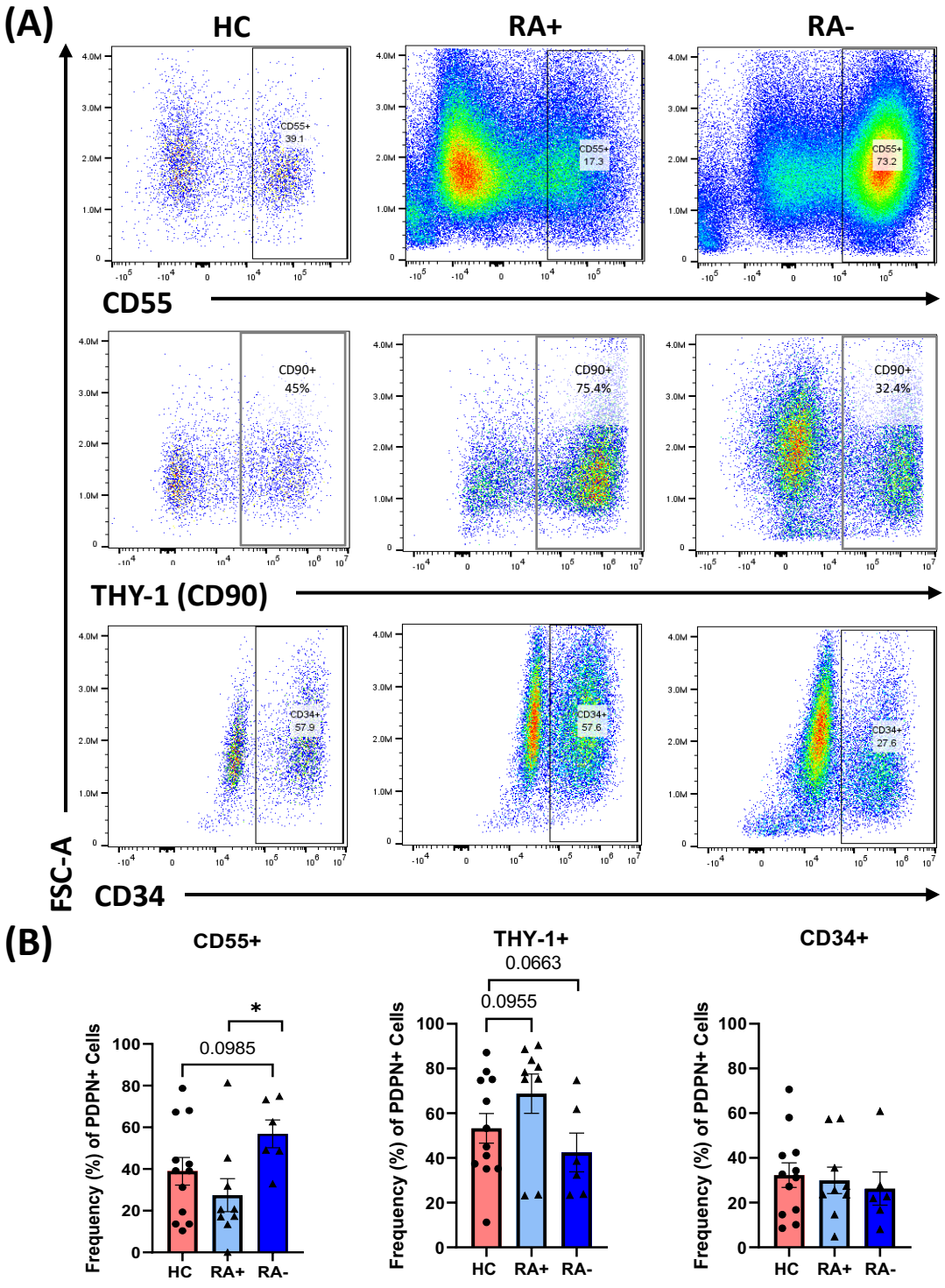

Figure 4.6: Altered frequency of classic FLS subset markers on RA FLS compared to HC.

(A) Representative flow cytometric dot plots depicting frequency of FLS positive for CD55, THY-1, and CD34 in HC (n=12), RA+ (n=9), and RA- (n=6). (B) Dot plot bar graphs demonstrating differences in percentage frequencies of each marker across HC, RA+, and RA-. Data represented as mean ± SEM. Mann-Whitney U test used for statistical analysis between disease states, with *p<0.05 significantly different from each other.

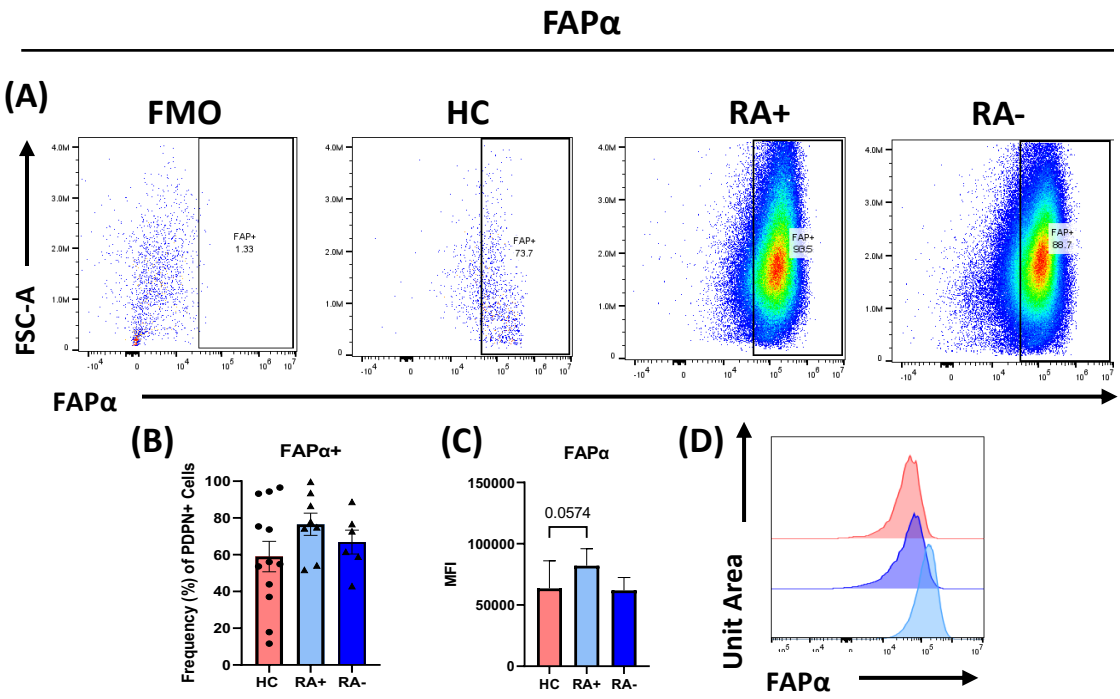

Figure 4.7: FLS in synovial tissue are activated and are increased in RA+.

(A) Representative flow dot plots demonstrating FAPα positive cells between FMO control, HC, RA+, and RA- samples. (B) Dot plot comparing percentage frequency of FAPα in HC (n=12), RA+ (n=9), and RA- (n=6). (C) Bar graph and (D) representative histogram depicting MFI expression of FAPα across HC, RA+, and RA- FLS. Data represented as mean ± SEM using Mann-Whitney U test to determine statistical significance between disease states, with *p<0.05 significantly different.

4.4.3 Inflammatory Profiling of RA FLS Compared to HC

To gain a better understanding of the phenotypic differences of FLS between HC and seropositive and seronegative RA, we first performed additional concatenated tSNE analysis as described in Section 4.4.2, and investigated the relative expression of various immunoregulatory (HLA-DR, CD200, CD200R1), adhesion (ICAM-1, VCAM-1, CD61, CD44), proliferation/invasive (Ki67, PDGFRα, YAP, Cadherin 11) and metabolic markers (pAKT, pmTOR, pS6) on the PDPN+ FLS (Figure 4.8). The unsupervised relative expression of these markers is shown in Figure 4.8 (B). Unsupervised clustering demonstrated increased expression of CD44, and Ki67 across HC, RA+, and RA- (Figure 4.8 (B)). Expression of HLA-DR and ICAM-1 demonstrated increased expression in both RA clusters, with increased ICAM-1 expression primarily in the RA+ cluster. CD200R1 expression was increased in RA+, though moderate expression was observed in the HC cluster as well (Figure 4.8 (B)). Due to initial differences observed in the tSNE plots, we next analysed the frequency of these markers across a larger cohort of HC (n=12), RA+ (n=9), and RA- (n=6).

Percent frequency and MFI expression of the MHC class II molecule HLA-DR were both significantly increased in RA+ compared to HC (both $p<0.05$) (Figure 4.9 (B-C)). A modest increase was observed in RA- compared to HC, although not significant (Figure 4.9 (B-C)). This is further evidenced by the representative dot plots and stacked MFI histogram demonstrating increased HLA-DR frequency and expression, respectively (Figure 4.9 (A) and (D)). Percent frequency of CD200 were comparable between RA+ and HC, however, decreased in RA- (Figure 4.9 (E-F)). Interestingly, MFI expression of CD200 demonstrated a stepwise decrease from HC to RA+ to RA- (Figure 4.9 (G)), further evidenced by the shift in the representative stacked MFI histogram (Figure 4.9 (H)). Similar trends in percent frequency were observed for the receptor CD200R1 (Appendix Figure 7.4).

Differential expression of adhesion molecules was also observed on synovial FLS. Percent frequency of FLS positive for ICAM-1 was significantly increased for RA+ compared to both HC and RA- ($p<0.01$ and $p<0.05$, respectively) (Figure 4.10 (B)). This was further demonstrated by the representative flow dot plots in Figure 4.10 (A). In addition, MFI expression of ICAM-1 was also significantly increased in RA+ compared to HC ($p<0.05$) and increased in RA+ compared to RA- ($p=0.0813$) (Figure 4.10 (C)). This was further depicted in the representative stacked MFI histogram showing a shift in ICAM-1 expression across the disease states (Figure 4.10 (D)). RA+ and RA- had comparable % frequency and expression of VCAM-1, and, interestingly, were lower compared to that of HC, with percent frequency trending towards significance ($p=0.0780$) (Figure 4.10 (F-G)). Representative flow dot plots and stacked histogram reinforce this (Figure 4.10 (E) and (H)). FLS positive for the integrin CD61 demonstrated a trending stepwise increase in frequency

from HC to RA+ to RA-, which could be visually observed in the representative flow dot plots (Figure 4.11 (A-B)). A large % of FLS across HC and RA positively expressed the adhesion molecule CD44 as observed in the representative flow plots (Figure 4.11 (C)) and quantification (Figure 4.11 (D)). Taken together, RA FLS within the synovium demonstrate preferential and differential expression of specific adhesion molecules.

Due to the increase in number of FLS observed in the RA tissue, we next investigated markers of proliferation and invasion. FLS across HC, RA+ and RA- demonstrated comparable high percent frequencies of FLS expressing the proliferation marker Ki67 (Figure 4.12 (A-B)), however, when examining MFI expression, HC FLS demonstrated higher expression compared to RA- and RA+ ($p<0.05$) (Figure 4.12 (C-D)). Interestingly, a stepwise decrease in YAP+ FLS was observed from HC to RA+ to RA- (Figure 4.12 (E-F)). MFI expression of YAP in RA+ and RA- FLS was also decreased compared to HC (Figure 4.12 (G-H)). A similar stepwise decrease in percent frequency was observed for PDGFRα+ and Cadherin 11+ FLS from HC to RA+ to RA- (Figure 4.13 (A-B)). To determine if the phenotypic changes in RA synovial FLS were mirrored by an alteration in cellular metabolism, we investigated the percent frequency expression of pAKT, pmTOR, and pS6 (Figure 4.13 (C)). pAKT+ and pS6+ FLS had comparable frequencies between HC and RA+, however pmTOR+ FLS demonstrated increased frequency in HC FLS compared to both RA+ and RA-.

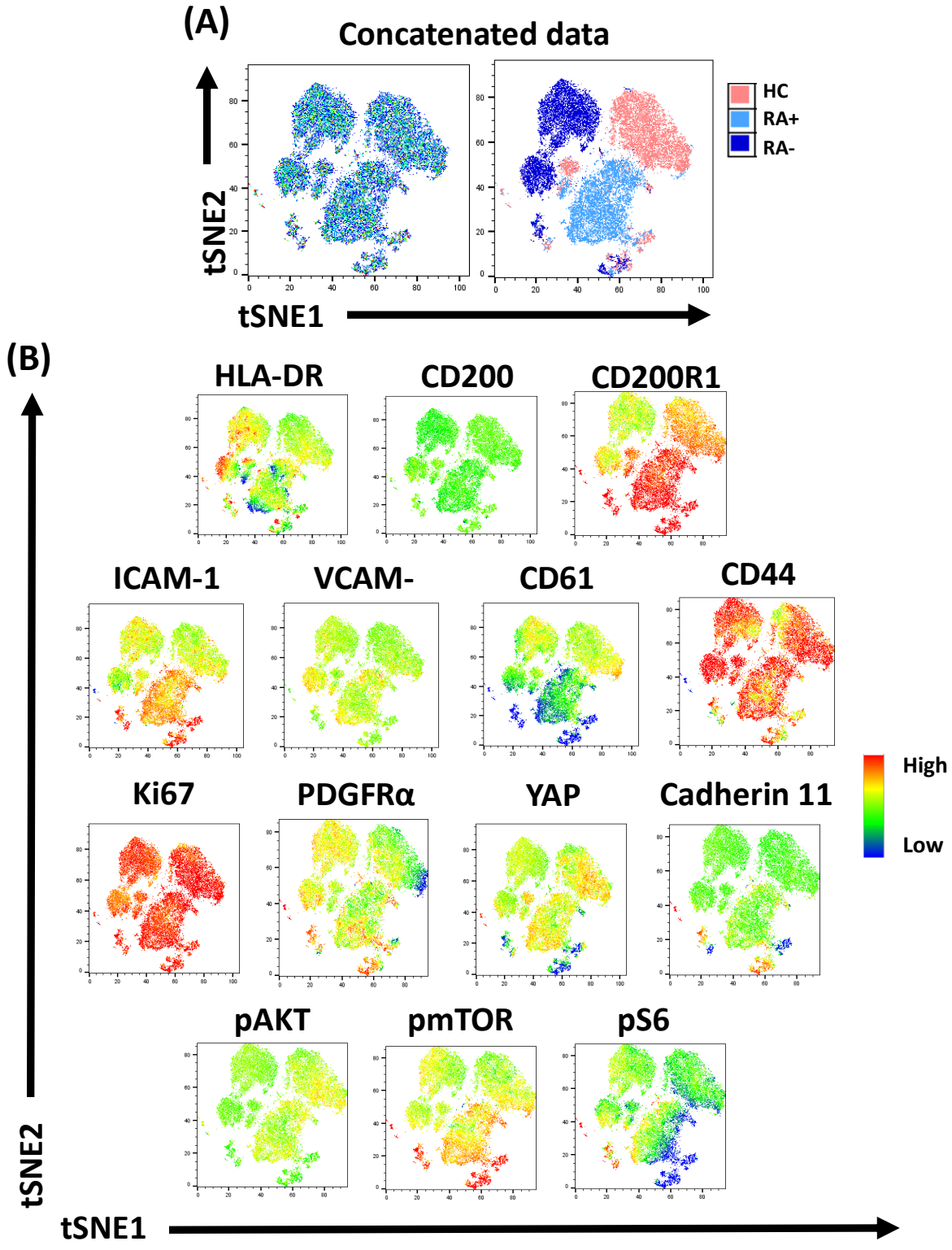

Figure 4.8: FLS phenotypic profiling by unsupervised clustering.

Multiparametric flow cytometric data of total PDPN+ FLS subjected to unsupervised clustering by tSNE algorithm following data concatenation of synovial tissue from one HC, one RA+, and one RA-. (A) tSNE dot plots demonstrating data concatenation of all PDPN+ cells and overlay of HC, RA+, and RA- FLS to demonstrate how FLS cluster together. (B) tSNE plots demonstrating relative expression of indicated markers.

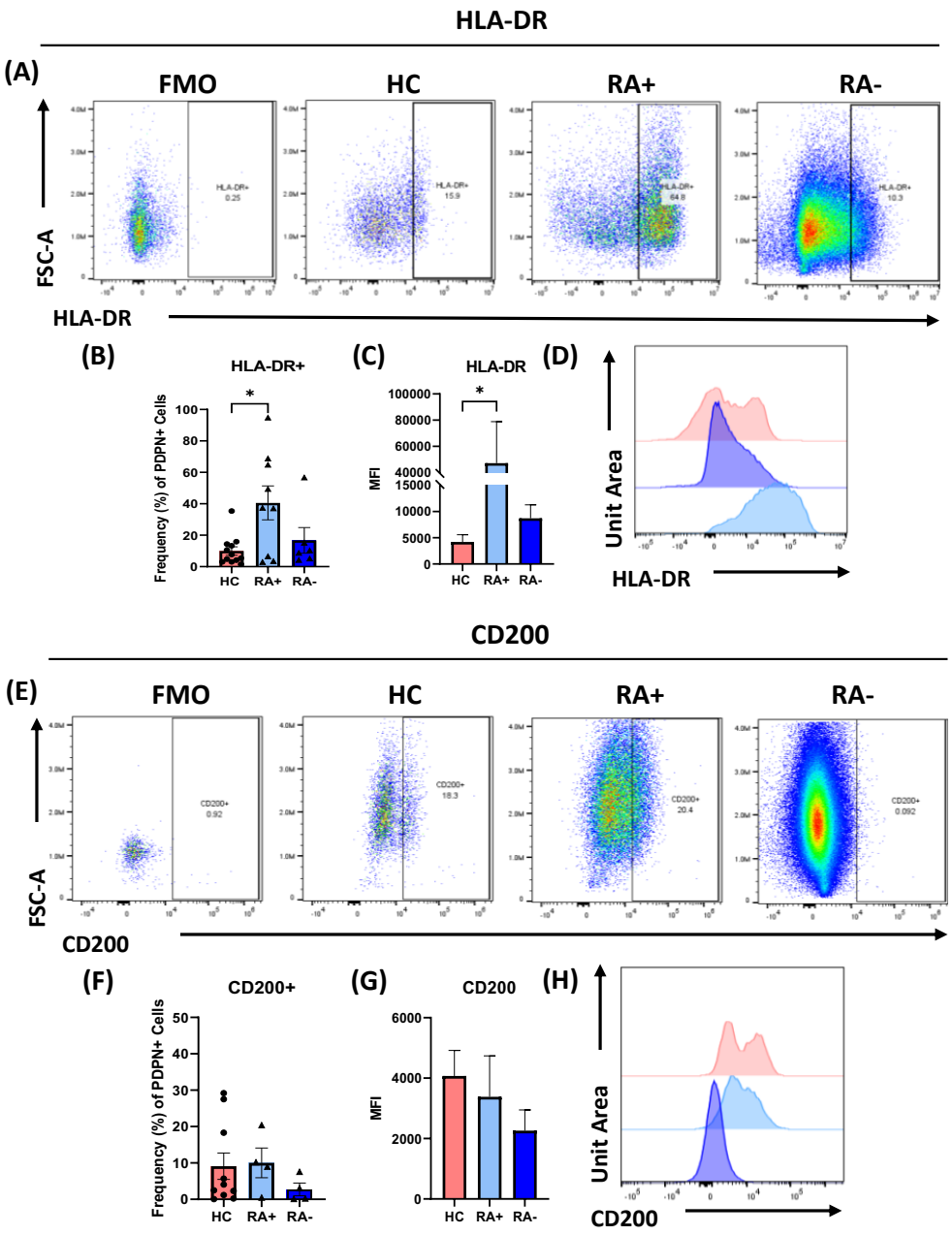

Figure 4.9: Immunoregulatory marker expression on FLS in RA vs HC synovial tissue.

(A) Representative flow cytometric dot plots of percent frequency of cells expressing HLA-DR on PDPN+ FLS from FMO control, HC, RA+, and RA-. (B) Accompanying dot plot depicting frequency of HLA-DR+ FLS in HC (n=12), RA+ (n=9), and RA- (n=6). (C) Bar graph demonstrating MFI expression of HLA-DR on FLS across indicated disease states. (D) Representative histogram of HLA-DR expression on HC, RA+, and RA- FLS. (E) Representative flow dot plots demonstrating frequency of CD200+ FLS in RA+ and RA- compared to HC and FMO control with (F) accompanying dot plot comparing percent frequency between HC (n=10), RA+ (n=4), and RA- (n=4). (G) Bar graph comparing MFI expression of CD200 across the three cohorts. (H) Representative histogram of CD200 expression between HC, RA+, and RA- FLS. Data represented as mean ± SEM using Mann-Whitney U test to determine statistical significance between disease states, with *p<0.05 significantly different.

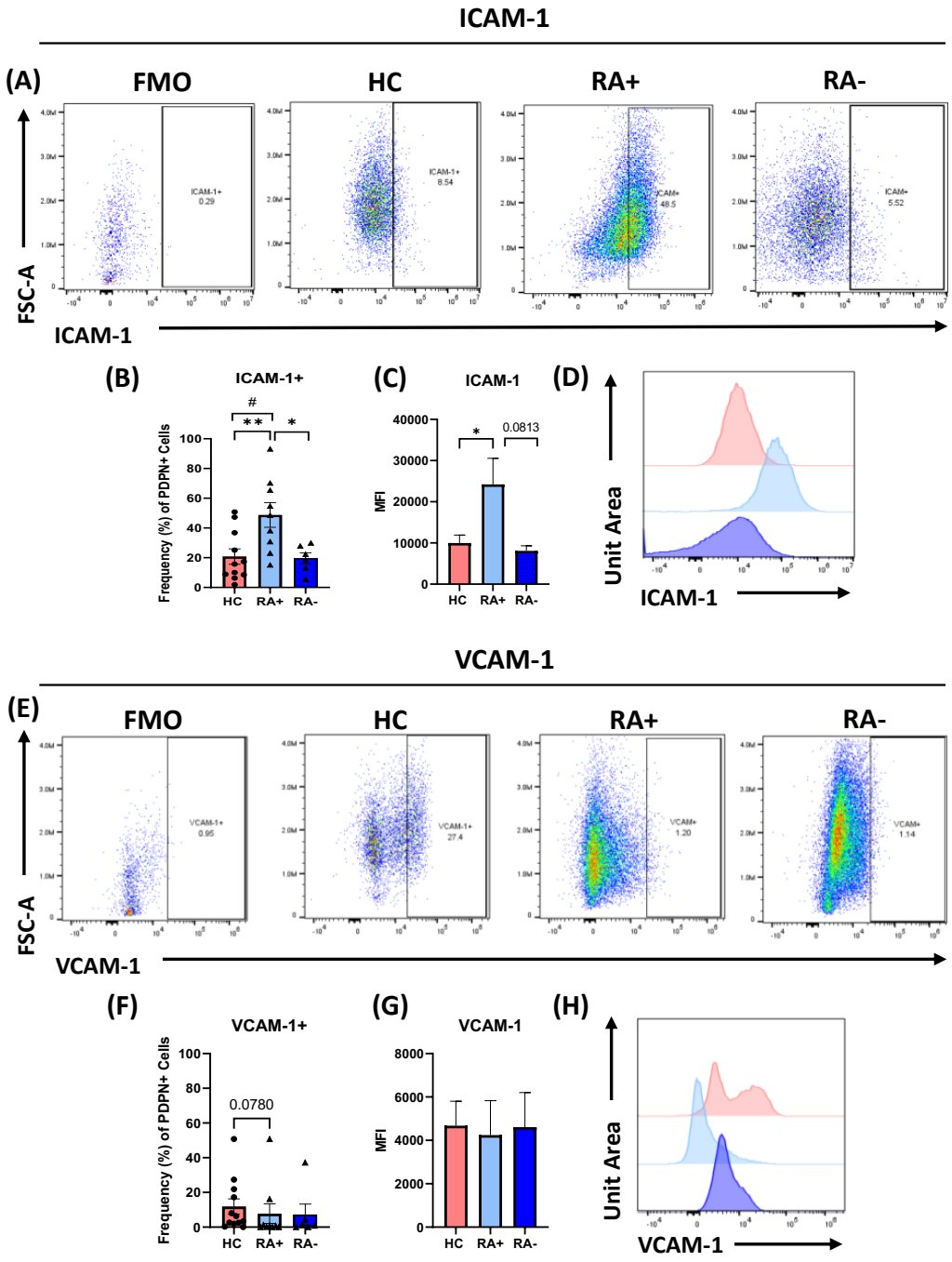

Figure 4.10: Differential expression of adhesion molecules ICAM-1 and VCAM-1 on synovial FLS.

Representative dot plots comparing percent frequencies of (A) ICAM-1 and (E) VCAM-1 expressing FLS between HC, RA+, and RA- with an FMO control. Accompanying dot plots demonstrating differences in percent frequency of (B) ICAM-1 and (F) VCAM-1 positive FLS in HC (n=11-12), RA+ (n=9), and RA- (n=6). Bar graphs demonstrating MFI expression of (C) ICAM-1 and (G) VCAM-1 across indicated disease states with accompanying representative histograms for (D) ICAM-1 expression and (H) VCAM-1 expression. Data represented as mean ± SEM. Kruskal-Wallis ANOVA (#) and Mann-Whitney U test (*) used for statistical analysis. #p<0.05; *p<0.05 and **p<0.01 statistically significant.

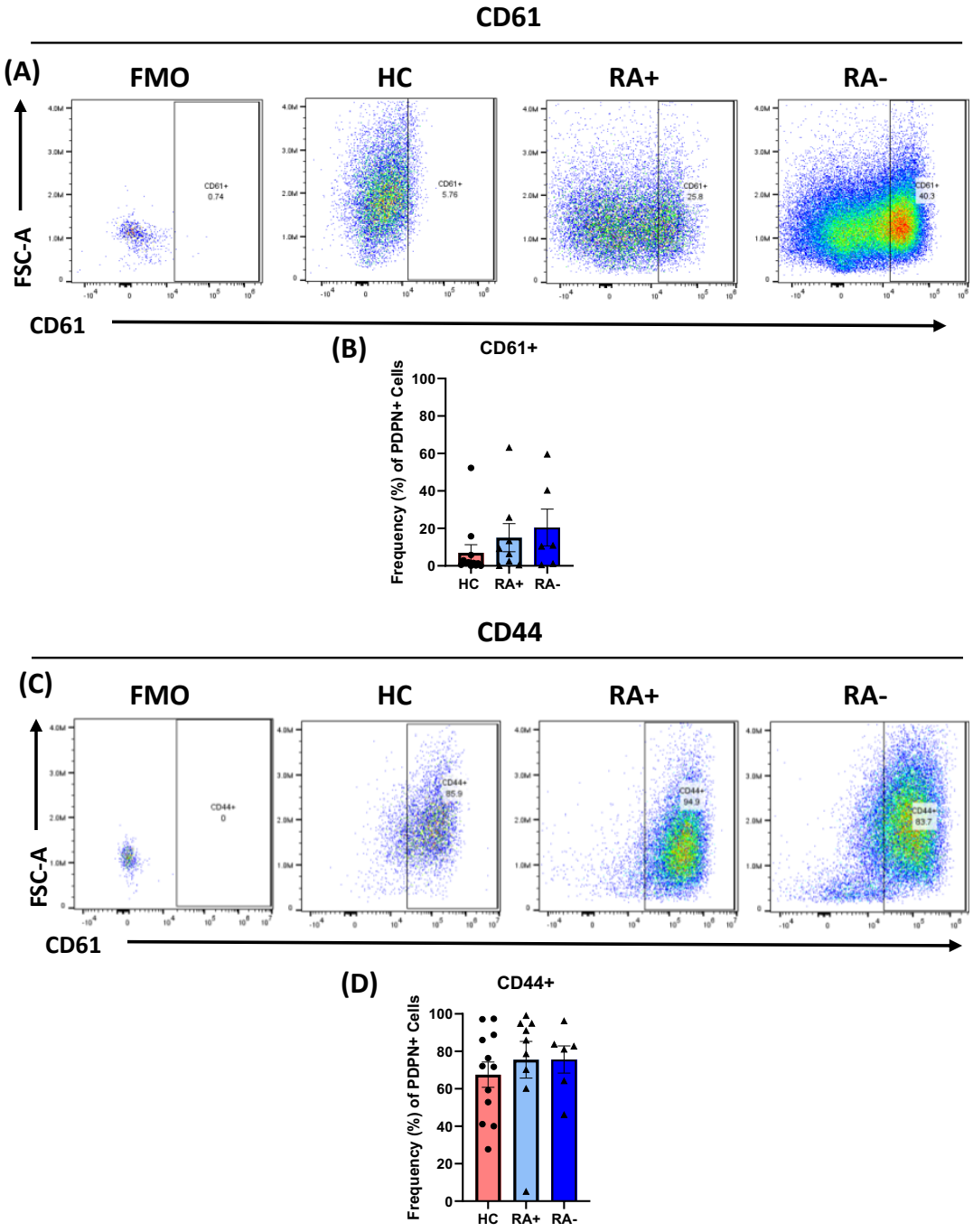

Figure 4.11: Differential frequency of FLS positive for adhesion molecules CD61 and CD44 on synovial FLS.

Representative dot plots comparing percent frequencies of (A) CD61 and (C) CD44 expressing FLS between HC, RA+, and RA- with an FMO control. Accompanying dot plots demonstrating differences in percent frequency of (B) CD61 and (D) CD44 positive FLS in HC (n=12), RA+ (n=9), and RA- (n=6). Data represented as mean ± SEM.

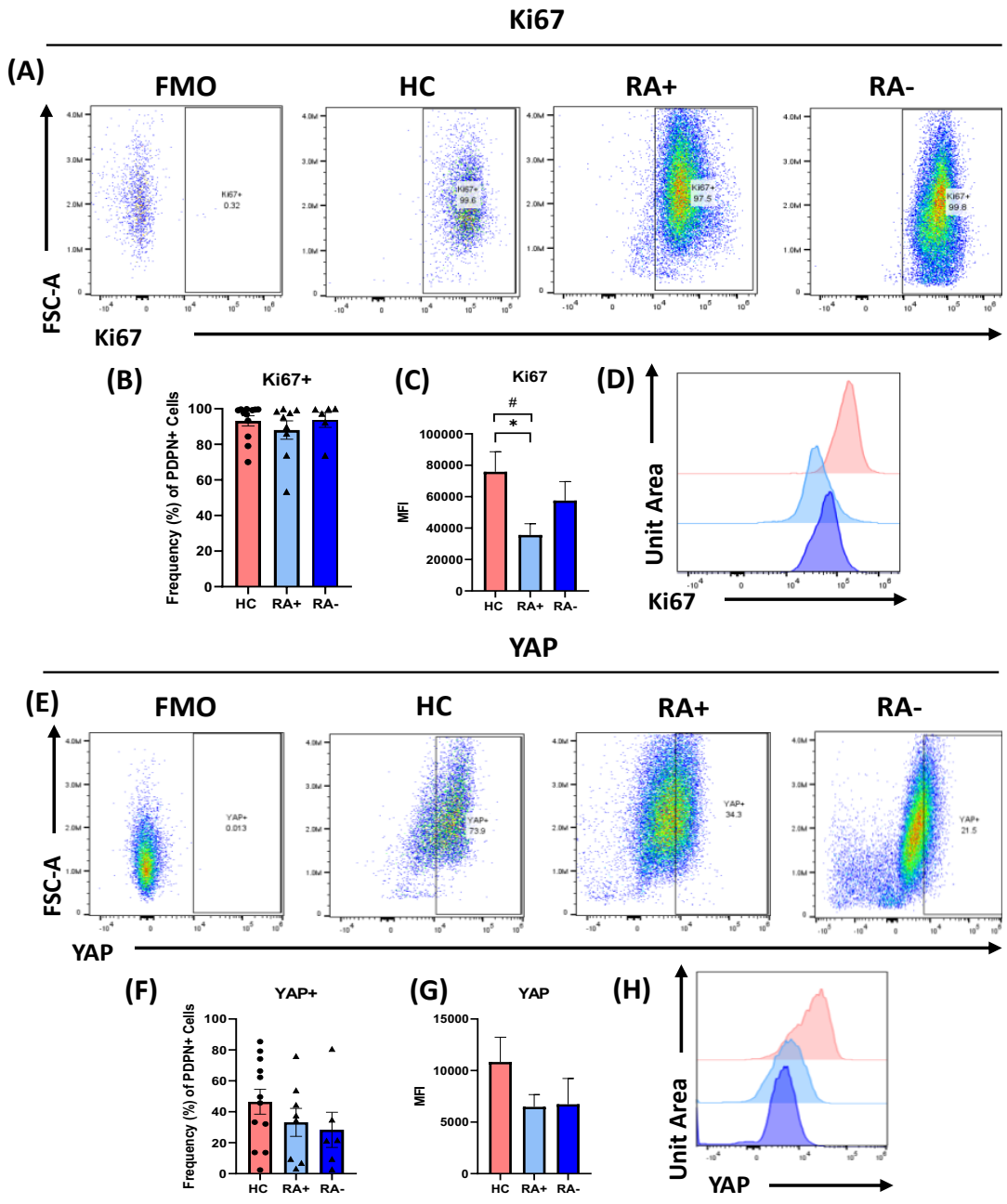

Figure 4.12: RA FLS demonstrate reduced expression for proliferation and cytoskeletal rearrangement.

Representative dot plots comparing percent frequencies of (A) Ki67 and (E) YAP expressing FLS between HC, RA+, and RA- with an FMO control. Accompanying dot plots demonstrating differences in percent frequency of (B) Ki67 and (F) YAP positive FLS in HC (n=12), RA+ (n=9), and RA- (n=6). Bar graphs demonstrating MFI expression of (C) Ki67 and (G) YAP across indicated disease states with accompanying representative histograms for (D) Ki67 expression and (H) YAP expression. Data represented as mean ± SEM. Kruskal-Wallis ANOVA (#) and Mann-Whitney U test (*) used for statistical analysis. #$p<0.05$ and *$p<0.05$ statistically significant.

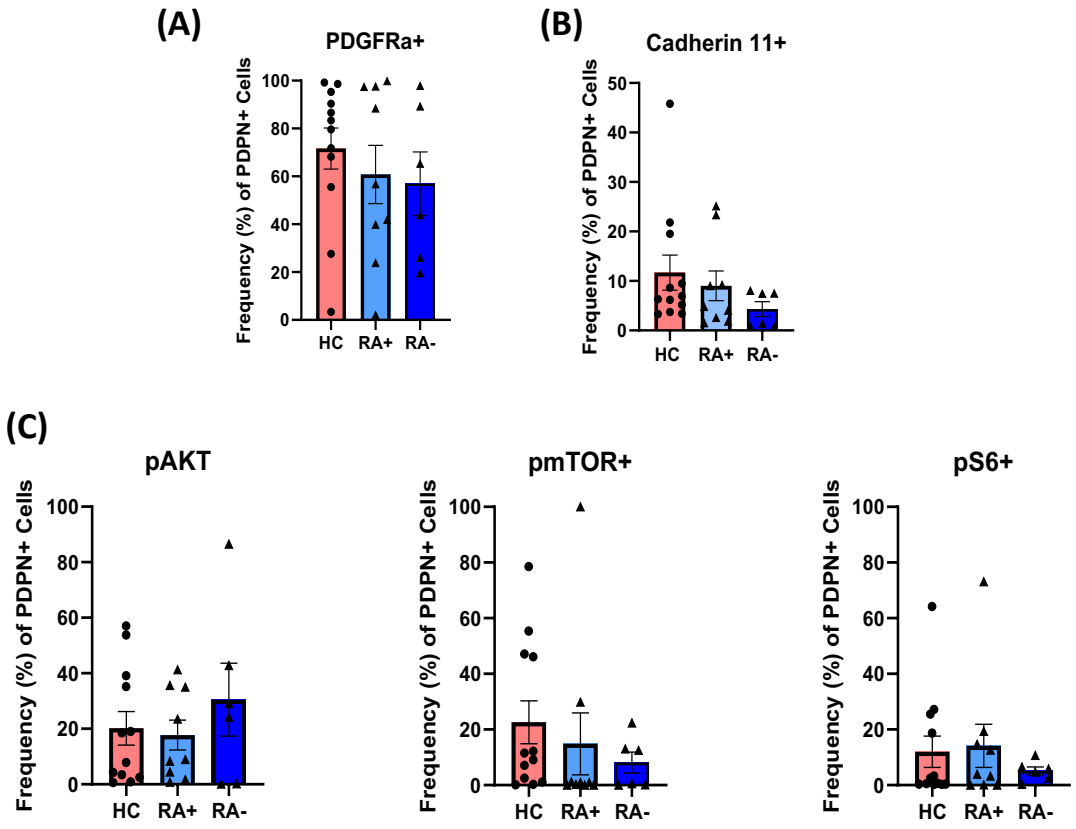

Figure 4.13: Differential expression of functional and metabolic markers on FLS across disease states.

Dot plots demonstrating differences in percent frequency expression of (A) PDGFRα, (B) Cadherin 11, and (C) metabolic markers pAKT, pmTOR, and pS6 across HC (n=12), RA+ (n=9), and RA- (n=6). Data represented as mean ± SEM.

4.4.4 Frequency of PDPN+ FLS and Their Inflammatory Profiles are Associated with High Disease Activity

Next, we stratified patient samples into high (>3.2) vs low (<3.2) RA disease activity scores (DAS28) to investigate whether FLS and their inflammatory profiles were associated with disease activity. Frequency of CD45- stromal cells as a percentage of total live cells were increased in low DAS compared to high DAS RA trending towards significance (p=0.0541) (Figure 4.14 (A)). This supports the hypothesis that greater immune cell infiltration is associated with increased inflammation and higher disease activity. To determine whether FLS frequency was associated with disease activity, we compared the frequency of PDPN+ cells as a percentage of CD45- cells so as to exclude the influence of immune cell numbers (Figure 4.14 (B)). Though not significant, high DAS RA patients demonstrated an increase in PDPN+ FLS frequency (Figure 4.14 (B)).

We next examined the expression of markers previously described to correlate with disease activity. Indeed, the adhesion molecules ICAM-1 (Figure 4.14 (C)) and CD61 (Figure 4.14 (D)) demonstrated increased % frequency in high DAS RA compared to low DAS, with CD61 expression statistically significant (p<0.01). Furthermore, it was determined that CD61+ frequency positively correlated with increasing DAS28 score (Spearman r=0.5416; p=0.0394*) (Figure 4.14 (D)). Percent frequency of the immunoregulatory marker HLA-DR was also increased for FLS of high DAS vs low DAS (Figure 4.14 (E)). Metabolism is also altered based on disease activity. Indeed, frequency of pAKT+ FLS was increased in high DAS RA compared to low DAS, with pAKT+ FLS frequency positively correlating with DAS28 score (Spearman r=0.6130; p=0.0171*) (Figure 4.14 (F)). Taken together, these data indicate a key role of FLS and their inflammatory phenotype in driving RA disease activity and severity.

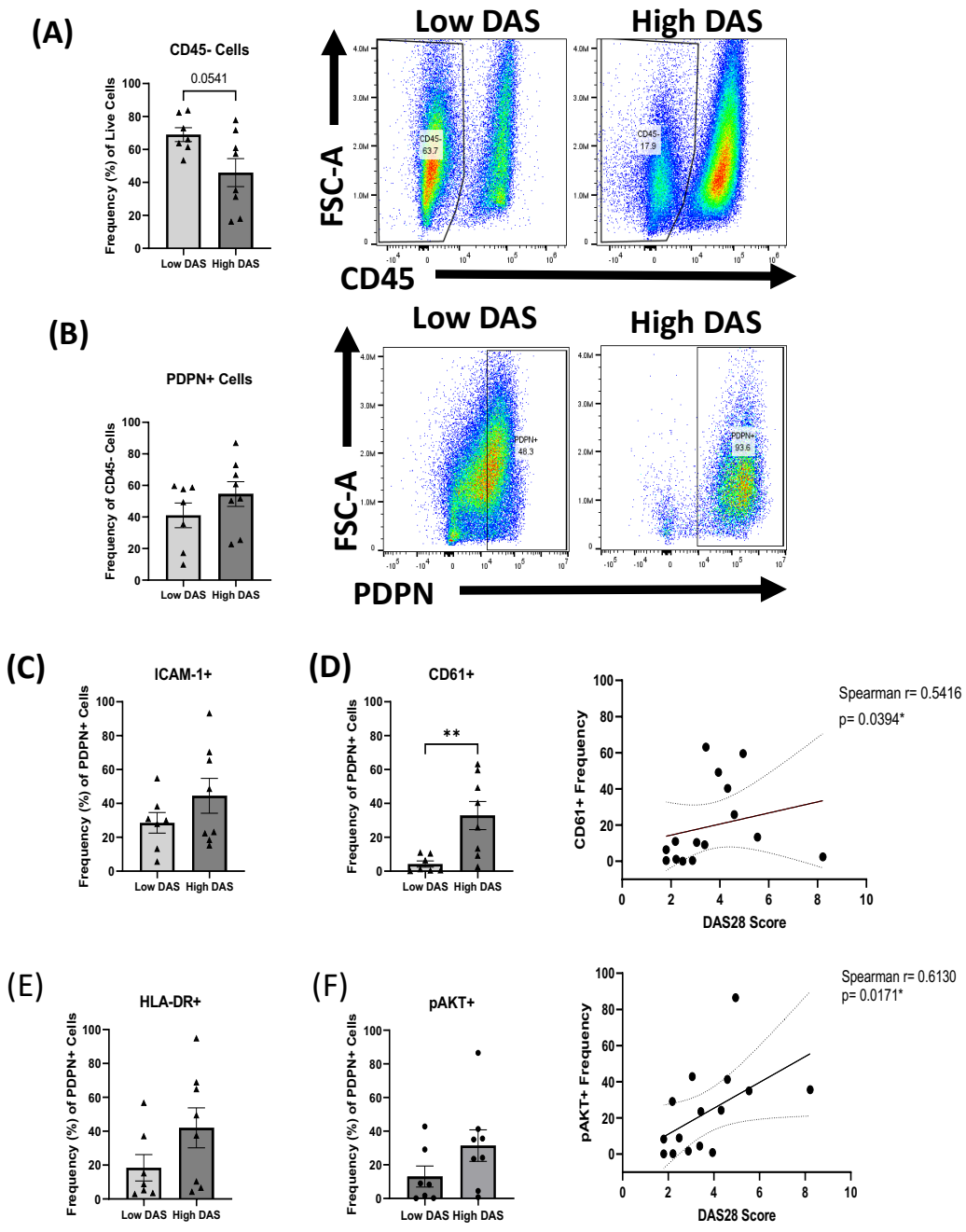

Figure 4.14: FLS frequency and functional phenotype are associated with high RA disease activity.

Low DAS indicates a RA disease activity score (DAS28) of less than 3.2 with high DAS based on scores greater than 3.2. (A) Dot plot bar graph and representative flow dot plots demonstrating differences in CD45- cells as a percentage of live cells between low and high DAS. (B) Dot plot and representative flow plots depicting frequency of PDPN+ FLS as a percentage of CD45- cells between low and high DAS. Dot plots depicting frequency of adhesion molecules (C) ICAM-1 between low and high DAS and (D) CD61 along with xy graph correlating CD61 frequency with DAS28 score. Dot plots depicting frequency of (E) HLA-DR between low and high DAS and (F)

4.4.5 Frequency of THY-1 FAPα Populations of FLS Differ Between HC, RA+, and RA-

Previous work from our group demonstrated the differential frequency of THY-1 FAPα clusters between RA and PsA synovial tissue, with RA enriched with FLS clusters double positive for THY-1 and FAPα while PsA is enriched with clusters double negative for both markers (Floudas *et al.*, 2022). Therefore, we examined THY-1 FAPα FLS subsets to determine if these differ between HC and RA, and whether differences are observed based on seropositivity. Frequencies of THY-1 FAPα subsets differed within each cohort (Figure 4.15). Representative flow dot plots illustrate the differences in FLS subset distributions across the three cohorts (Figure 4.15 (A)). Within the RA+ cohort, THY1+FAPα+ subset was the highest proportion of FLS overall and was significantly increased compared to THY1+FAPα- and THY1-FAPα- subsets (both $p<0.01$) (Figure 4.15 (B)). Additionally, within RA+ patients, frequency of THY1+FAPα- and THY1-FAPα+ subsets were both increased compared to the double negative population (the smallest proportion of FLS within this cohort) ($p<0.05$ and $p=0.0547$ respectively) (Figure 4.15 (B)). In RA- patients, the THY1-FAPα+ subset was the largest proportion of FLS, frequency of which was increased compared to THY1+FAPα- subset ($p=0.0625$) (Figure 4.15 (B)). The double positive subset constituted the second highest frequency and was increased trending towards significance compared to THY1+FAPα- ($p=0.0625$). Interestingly, the double negative subset in this cohort was comparable in frequency to THY1+FAPα- subset (Figure 4.15 (B)). The frequencies for each THY1 FAPα subsets were more comparable to one another within HC donors, however, it is important to note that the THY1+FAPα+ and THY1-FAPα+ cohorts were both increased compared to THY1+FAPα- ($p=0.0522$ and $p= 0.0884$, respectively) (Figure 4.15 (B)).

We next examined each specific cluster across disease status (Figure 4.16). Representative flow cytometric dot plots illustrate the differences in each THY1 FAPα subset frequency between HC, RA+, and RA- (Figure 4.16 (A)). When quantified, RA+ demonstrated the highest % frequency of THY1+FAPα+ compared to HC and RA- ($p<0.05$) (Figure 4.16 (B)(i)). RA- demonstrated the highest frequency of THY1-FAPα+ compared to both HC and RA+, though not significant (Figure 4.16 (B)(iii)). Frequency of THY1+FAPα- was low and comparable across HC, RA+, and RA- (Figure 4.16 (B)(ii)). The % frequency of THY1-FAPα- double negative cluster was comparable between HC and RA-, with both increased compared to RA+ (HC vs RA+ $p<0.05$; RA- vs RA+ $p=0.0531$) (Figure 4.16 (B)(iv)). This suggests that the double positive THY1+FAPα+ is specifically enriched in seropositive RA.

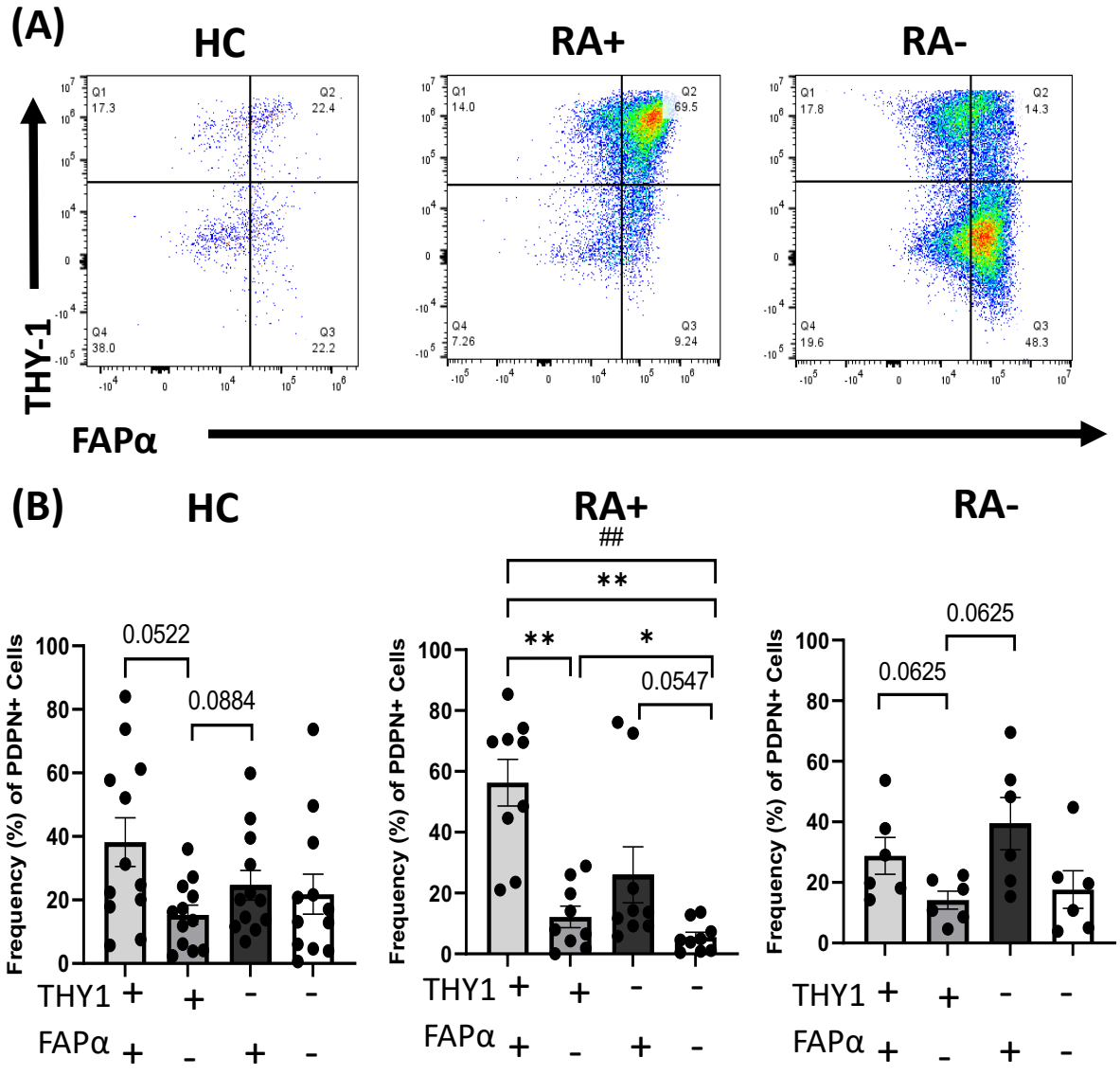

Figure 4.15: THY-1 FAPα subsets differ in proportion for HC, RA+, and RA- FLS.

(A) Representative dot plots demonstrating distribution of THY-1 FAPα subsets across HC, RA+, and RA-. (B) Accompanying dot plots demonstrating the percent frequency distribution of each subset as a percentage of total PDPN+ FLS cells within HC (n=12), RA+ (n=9), and RA- (n=6). Data represented as mean ± SEM. Friedman test with Dunn's multiple comparisons (#) and Wilcoxon signed rank test (*) utilised for statistical analysis of paired nonparametric data. #p<0.05, ##p<0.01 and *p<0.05, **p<0.01 statistically significant.

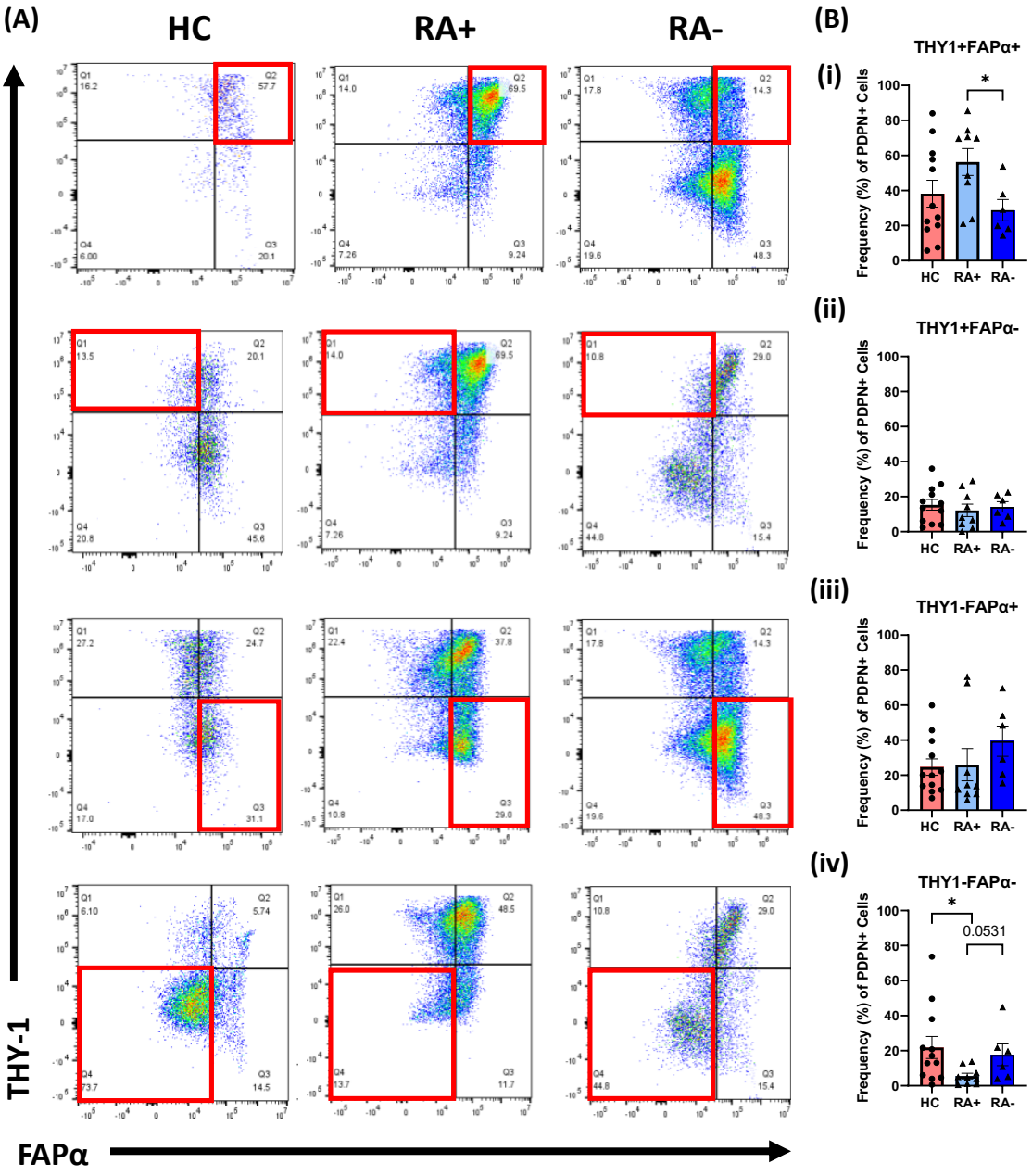

Figure 4.16: Comparison of each THY-1 FAPα subset between disease states.

(A) Representative flow cytometric dot plots of THY1+FAPα+, THY1+FAPα-, THY1-FAPα+, and THY1- FAPα- subsets across HC, RA+, and RA-. (B) Accompanying dot plot demonstrating the differences in frequency of each individual subset as a percentage of PDPN+ cells between HC (n=12), RA+ (n=9), and RA- (n=6). Data represented as mean ± SEM. Mann-Whitney U test was used to determine significance with *p<0.05 being statistically significant.

4.4.6 Identification and Comparison of Activated LL and SL FLS Subset Frequencies in HC vs RA

Next, we investigated the differences in frequencies of LL and SL FLS subsets, specifically the activated FLS. Previous observations in our lab have suggested that a majority of the FLS observed in our tissue samples are positive for FAPα, a marker that has been of particular interest in the literature in the context of pathogenic FLS within the joint (Croft *et al.*, 2019). To define the subsets of interest, we utilised the LL marker CD55, SL marker THY-1, and activation marker FAPα. Representative flow dot plots outlining the gating strategy used for identification of these FLS subsets are depicted in Figure 4.17. The initial gating strategy to identify PDPN+ FLS is outlined in Section 4.4.1. Briefly, the exclusion of debris, cell doublets, and dead cells, is followed by the exclusion of CD45+ (haematopoietic cells), exclusion of cells positive for CD146 and CD31 (pericytes and ECs), and inclusion of PDPN+ cells to gate on FLS (Figure 4.17 (A-F)). CD55 was subsequently gated against THY-1, and with the addition of FAPα, the following specific subsets were identified: CD55+THY1-FAPα+, CD55+THY1+FAPα+, CD55-THY1+FAPα+, and CD55-THY1-FAPα+ (Figure 4.17 (G-H)).

Frequencies CD55 THY-1 FAPα subsets differed within HC, RA+, and RA- cohorts (Figure 4.18). Representative flow dot plots illustrate the differences in the subset distribution across the three cohorts (Figure 4.18 (A)). Within the RA+ cohort, the CD55-THY1+FAPα+ subset were the highest proportion of FLS overall and was significantly increased compared to CD55+THY1+FAPα+ ($p<0.01$) and the CD55-THY1-FAPα+ subset ($p<0.05$), with a trending increase compared to CD55+THY1-FAPα+ ($p=0.0527$) (Figure 4.18 (B)). In RA- patients, the CD55+THY1-FAPα+ subset was the largest proportion of FLS and % frequency was increased compared to the other subsets, particularly the CD55-THY1-FAPα+ subset ($p=0.0625$) (Figure 4.18 (B)). The frequencies for each CD55 THY1 FAPα subset were more varied within HC donors, however, it is important to note that the CD55-THY1+FAPα+ and the CD55+THY1-FAPα+ subsets were both increased compared to CD55+THY1+FAPα+ ($p<0.001$ and $p=0.0923$, respectively) (Figure 4.18 (B)). Additionally, CD55-THY1+FAPα+ was also significantly increased compared to CD55-THY1-FAPα+ in the HC cohort ($p<0.05$; Figure 4.18 (B)).

We next examined each specific cluster across disease status (Figure 4.19). Representative flow cytometric dot plots illustrate the differences in frequency of each CD55 THY1 FAPα subset between HC, RA+, and RA- (Figure 4.19 (A)). Quantification demonstrated that RA+ had the highest % frequency of CD55-THY1+FAPα+ compared to HC and RA- ($p<0.05$) (Figure 4.19 (B)(iii)). RA- demonstrated the highest % frequency of CD55+THY1-FAPα+ compared to both HC and RA+ ($p=0.0791$ and $p<0.05$, respectively) (Figure 4.19 (B)(i)). Frequency of CD55+THY1+FAPα+ was low

and comparable across cohorts (Figure 4.19 (B)(ii)). Similarly, the % frequency of the CD55-THY1-FAPα+ subset was low and comparable between HC, RA+, and RA- (Figure 4.19 (B)(iv)).

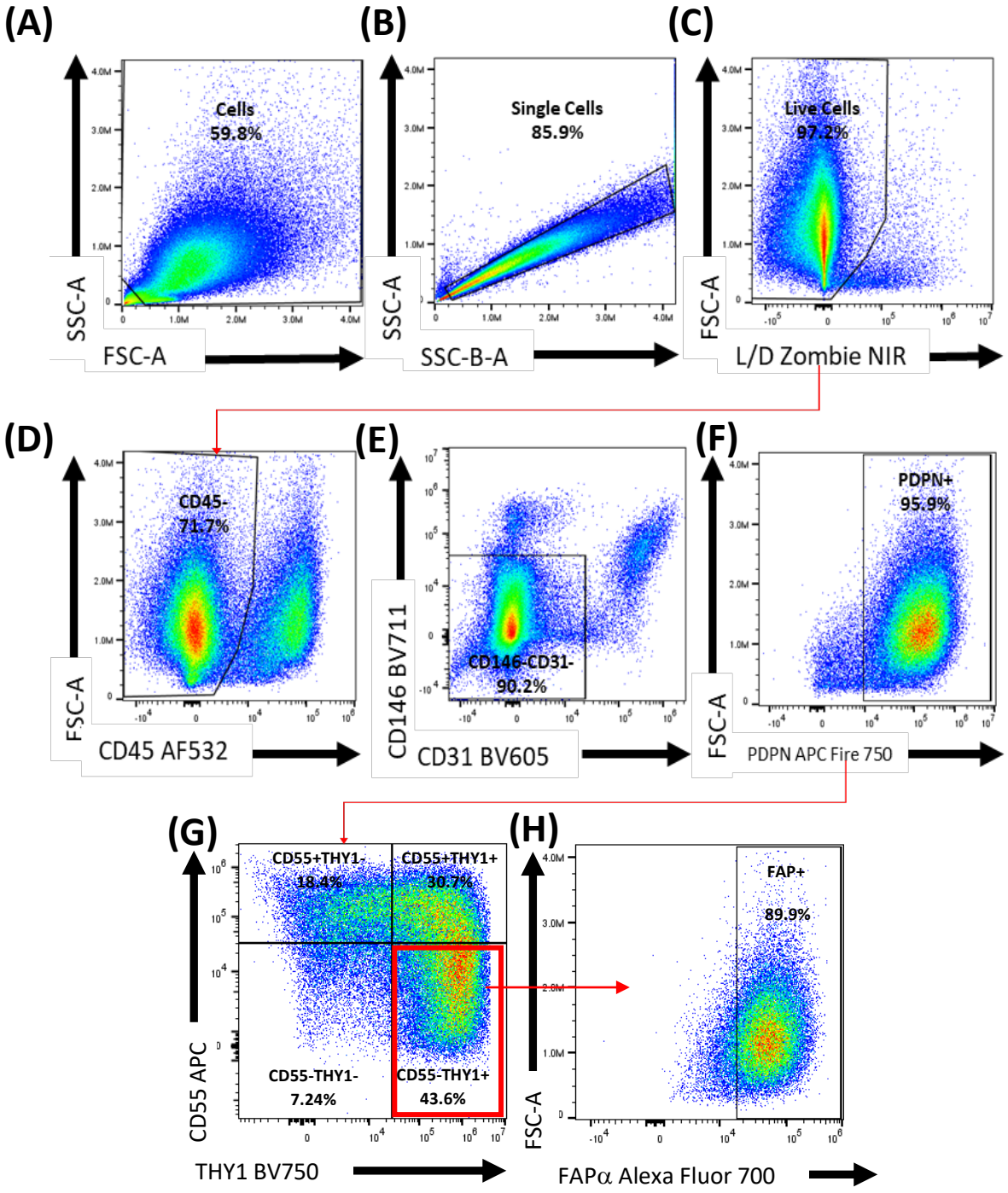

Figure 4.17: Activated LL and SL FLS subset (CD55 THY-1 FAPα) gating strategy for synovial tissue.

Representative dot plots depicting the gating strategy used to identify CD55 THY-1 FAPα FLS subsets within the (A-F) PDPN+ FLS previously described in Figure 4.2. (A-C) Forward and side scatter parameters established for cells before exclusion of doublets and dead cells. (D-F) FLS were identified as CD45-CD146-CD31-PDPN+ and further divided into (G) CD55+/- THY1+/- subsets and subsequently focused on (H) FAPα+ FLS within each of those subsets.

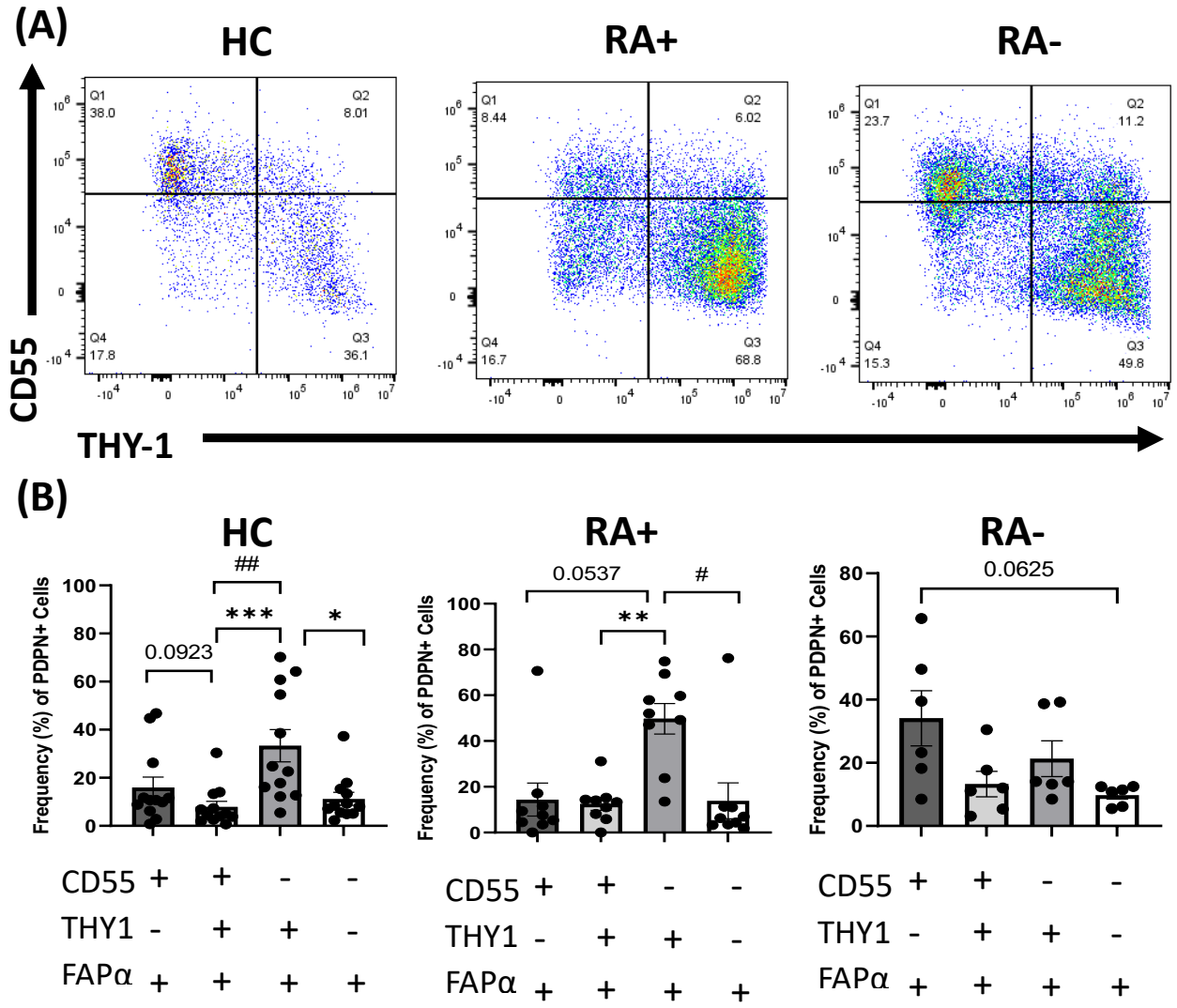

Figure 4.18: CD55 THY-1 FAPα subsets differ in proportion for HC, RA+, and RA- FLS.

(A) Representative dot plots demonstrating distribution of CD55 THY-1 FAPα subsets across HC, RA+, and RA-. (B) Accompanying dot plots demonstrating the percent frequency distribution of each subset as a percentage of total PDPN+ FLS cells within HC (n=12), RA+ (n=9), and RA- (n=6). Data represented as mean ± SEM. Friedman test with Dunn's multiple comparisons (#) and Wilcoxon signed rank test (*) utilised for statistical analysis of paired nonparametric data. #p<0.05, ##p<0.01 and *p<0.05, **p<0.01, ***p<0.001 statistically significant.

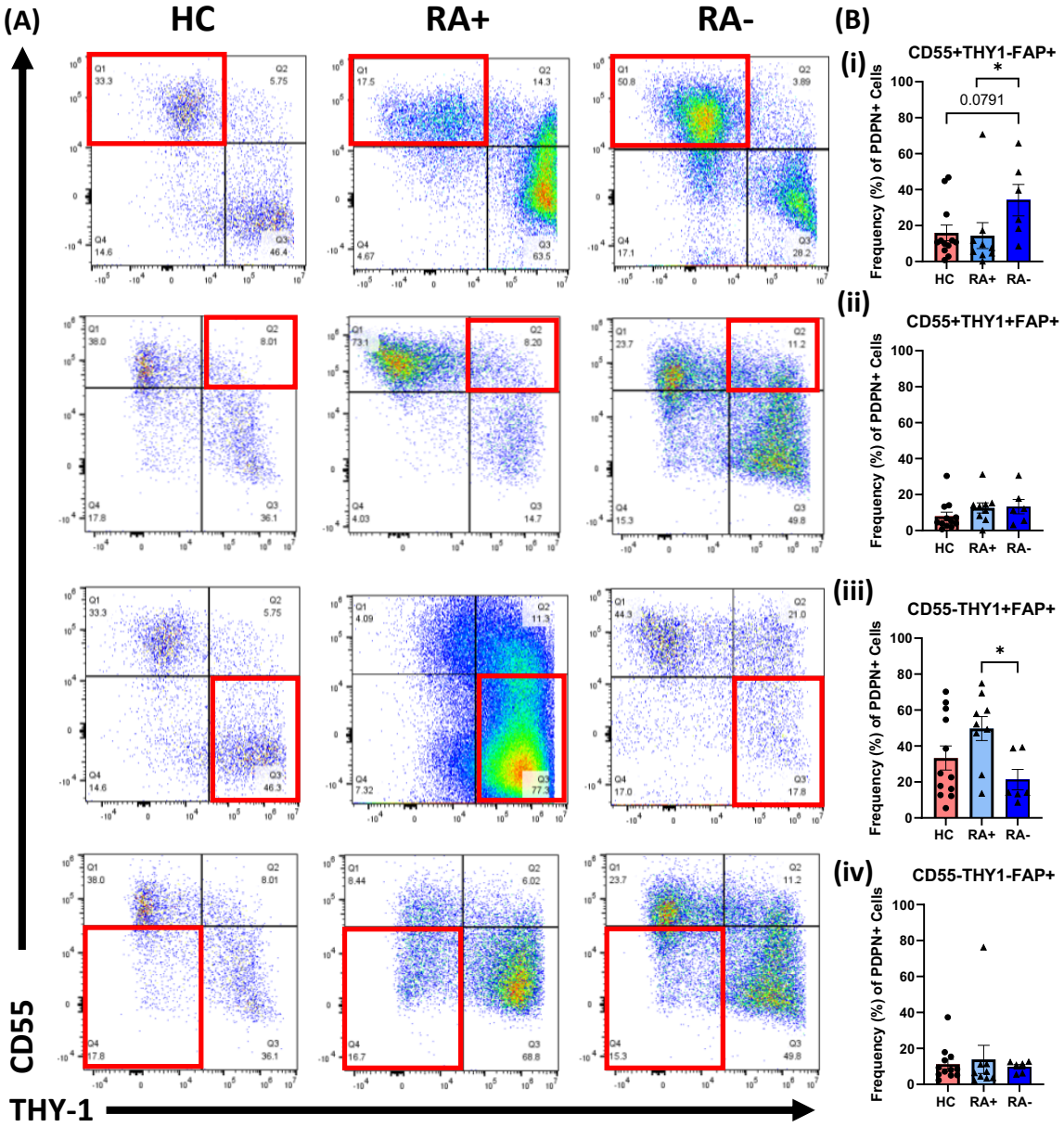

Figure 4.19: Comparison of each CD55 THY-1 FAPα subset between disease states.

(A) Representative flow cytometric dot plots of CD55+THY1-FAPα+, CD55+THY1+FAPα+, CD55-THY1+FAPα+, and CD55-THY1-FAPα+ subsets across HC, RA+, and RA-. (B) Accompanying dot plot demonstrating the differences in frequency of each individual subset as a percentage of PDPN+ cells between HC (n=12), RA+ (n=9), and RA- (n=6). Data represented as mean ± SEM. Mann-Whitney U test was used to determine significance with *p<0.05 being statistically significant.

4.4.7 Proinflammatory Profile of Synovial PDPN+ FLS is Altered Prior to Disease Onset

Individuals-at-risk for developing RA have become a particular focus in rheumatology research with the hope of identifying factors within this cohort to better predict which individuals will eventually progress on to an RA diagnosis. This would allow for earlier treatment and a reduction in debilitating disease progression. Therefore, we next investigated whether changes in FLS and their phenotype occur prior to disease onset. Due to a small sample size, in addition to the three seropositive IAR samples, we have also included two ART within this cohort. These two samples are designated accordingly within each figure. IAR demonstrated similar high frequencies of CD45- cells as a percentage of live cells compared to HC, indicating minimal immune cell infiltration (Figure 4.20 (A)). Additionally, as a proportion of total live cells, PDPN+ FLS % frequency in IAR was increased compared to HC and comparable to RA+ (Figure 4.20 (B)). Within the CD45- population, % frequency of PDPN+ cells were increased in a stepwise manner from HC to IAR to RA+ (Figure 4.20 (C)). Thus, while there is no evidence of clinical synovitis in IAR, the increased frequency of pathogenic FLS suggests early cellular changes have already occurred.

We performed unbiased, unsupervised, multidimensional analysis of flow cytometric data from one HC, one seropositive IAR, and one RA+ synovial tissue using tSNE. Data concatenation of total PDPN+ cells and relative expression of common FLS subset markers CD55, THY-1, CD34 and FAPα are shown in Figure 4.21. Interestingly, FLS from IAR clustered between RA+ and HC, and clustered more closely to the HC FLS (Figure 4.21 (A)). Relative expression from the tSNE analysis demonstrated similarities between HC and IAR in expression levels of CD55 and THY-1 (Figure 4.21 (B)). Yet for markers CD34 and FAPα, it appears that changes in expression may already be occurring pre-disease onset (Figure 4.21 (B)). We next analysed the frequency of these markers across a larger cohort: IAR (n=5) compared to the HC (n=12) and RA+ (n=9). CD55+ FLS demonstrated an increased percent frequency in IAR compared to HC and RA+, though not significant (Figure 4.21 (C)). Frequency of THY-1+ FLS was significantly lower in IAR compared to RA+ ($p<0.05$) and to HC (Figure 4.21 (C)). A similar trend was observed for frequency of CD34+ cells, where IAR was decreased compared to both HC ($p=0.0637$) and RA+ (Figure 4.21 (C)). A slight stepwise increase in FAPα frequency was demonstrated from HC to IAR to RA+ and FAPα MFI expression was increased in IAR compared to HC (Figure 4.21 (D)). Together these data suggest that there may be an increase in activated LL FLS within IAR, suggesting early signs of inflammation.

Unbiased tSNE analyses of relative expression of FLS phenotypic markers are shown in Figure 4.22 and suggest that their expression may begin to change in IAR before progressing on to disease (Figure 4.22 (B)). Specifically, % frequency and MFI expression of HLA-DR both

demonstrated a stepwise increase from HC to IAR to RA+ (Figure 4.23 (A)). However, no significant changes were observed for % frequency or MFI expression of CD200 in IAR compared to HC and RA+ (Figure 4.23 (B)). Frequency of ICAM-1+ FLS was comparable between HC and IAR with RA+ being significantly increased compared to both ($p<0.01$) (Figure 4.23 (C)). Frequency of VCAM-1+ FLS was decreased in IAR compared to HC and RA+, however, MFI expression did not change (Figure 4.23 (D)). Frequencies of CD61+ and CD44+ cells in IAR were comparable to HC and RA+ (Figure 4.23 (E-F)).

Percent frequency FLS positive for the proliferation marker Ki67 were comparable between HC, IAR, and RA+; however, MFI expression of Ki67 was significantly increased in IAR compared to RA+ ($p<0.05$) (Figure 4.24 (A)). Percent frequency of YAP was varied in IAR; however, MFI expression of YAP was increased in IAR compared to HC and RA+ (Figure 4.24 (B)). Frequencies of PDGFRα+ and Cadherin 11+ cells were comparable between HC, IAR, and RA+ (Figure 4.24 (C-D)). IAR FLS demonstrated comparable frequencies of the metabolic markers pAKT, mTOR and pS6 compared to HC and RA+ (Figure 4.24 (E)). Taken together, not all functional markers are altered in IAR FLS, however, a few select markers do begin to change in this at-risk cohort, such as HLA-DR and Ki67.

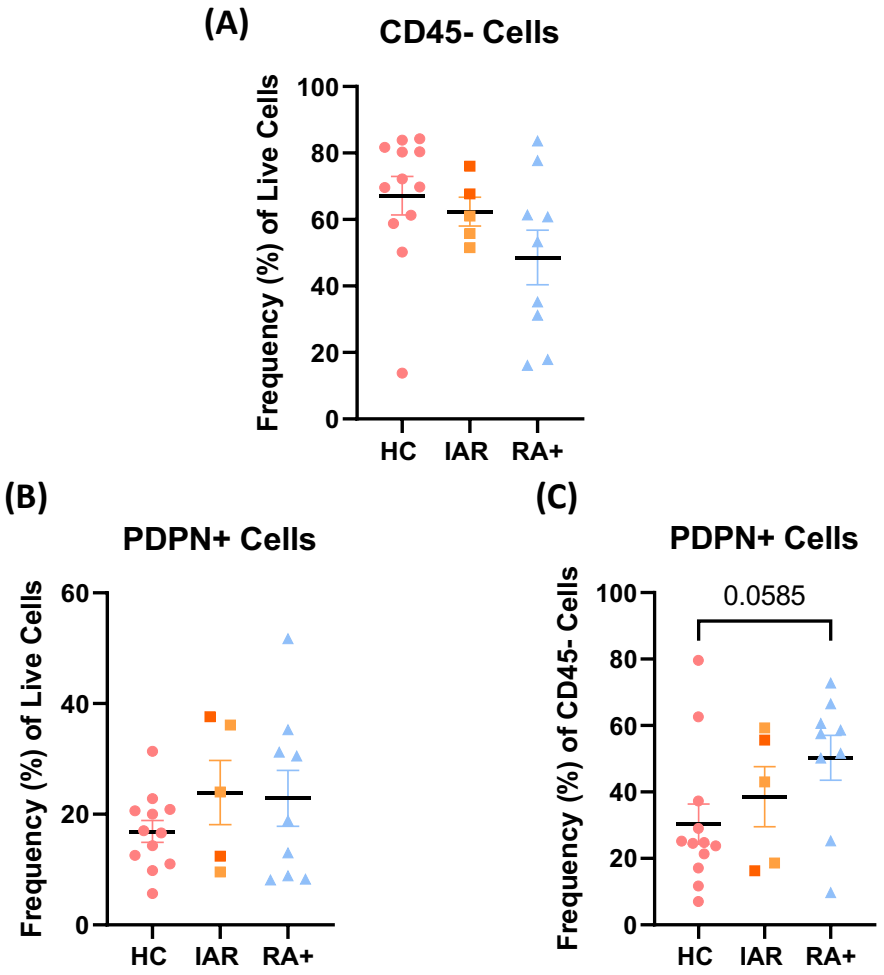

Figure 4.20: Changes in FLS frequency prior to disease onset.

(A) Dot plot demonstrating frequency of CD45- (stromal cells) as a percentage of total live cells in HC (n=12), IAR (n=5*), RA+ (n=9) synovial tissue. (B) Dot plot comparing frequency of PDPN+ FLS as a percent of total live cells between HC, IAR, and RA+. (C) Dot plot demonstrating PDPN+ frequency as a percentage of CD45- (stromal) cells between HC, IAR, and RA+. *Two donors are seronegative ART and are denoted by dark orange squares. Data represented as mean ± SEM. Statistical analysis performed using Mann-Whitney U test, with $p<0.05$ being significant.

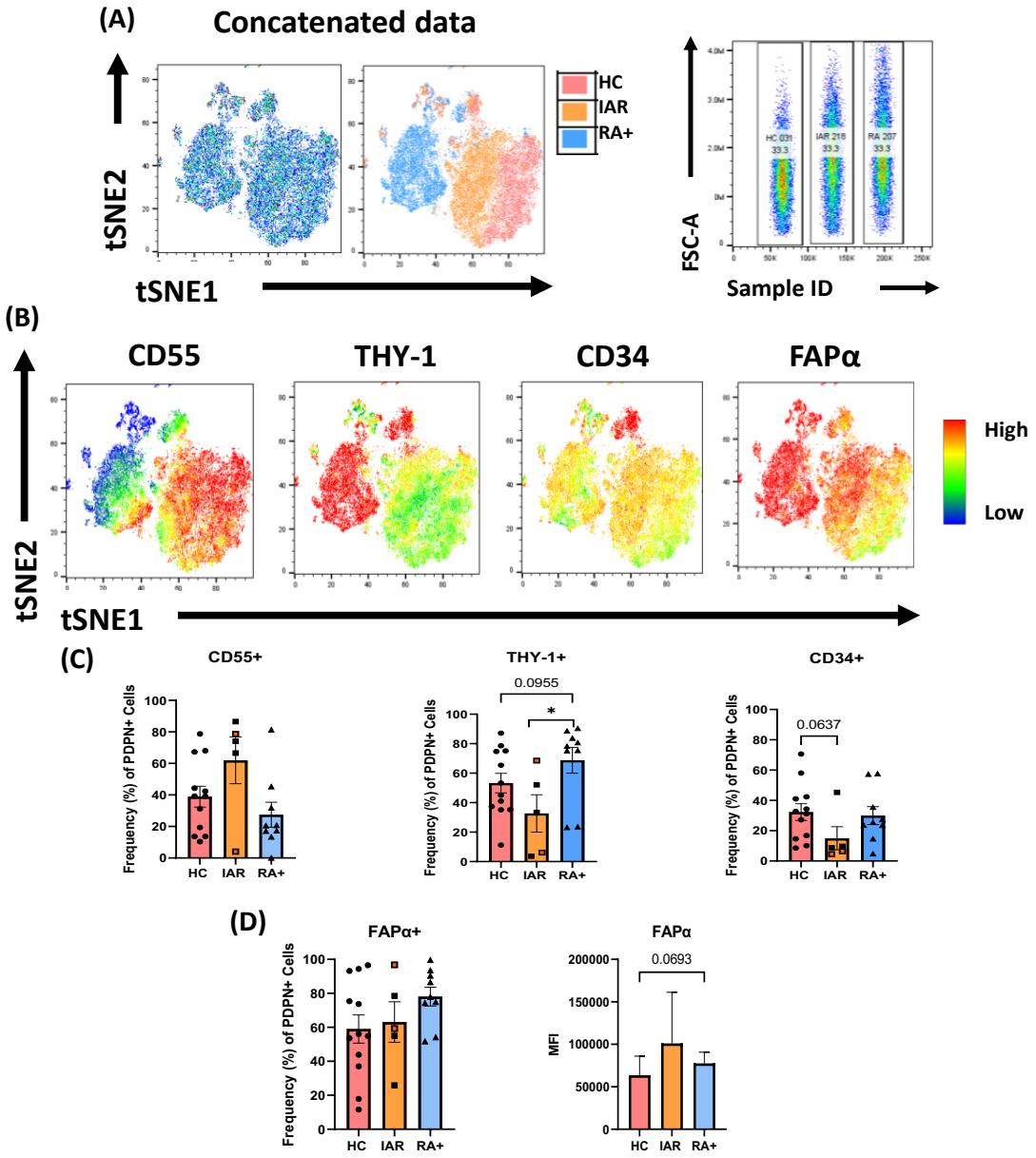

Figure 4.21: Differential FLS subset marker expression identification by unsupervised clustering between HC, IAR, and RA+.

Multiparametric flow cytometric data of total PDPN+ FLS subjected to unsupervised clustering by tSNE algorithm following data concatenation of synovial tissue from one HC, one seropositive IAR, and one RA+. (A) tSNE dot plots demonstrating data concatenation of all PDPN+ cells and overlay of HC, IAR, and RA+ FLS to demonstrate how FLS cluster together. (B) tSNE plots demonstrating relative expression of FLS markers CD55, THY-1, CD34, and FAPα on concatenated PDPN+ FLS. (C) Dot plots demonstrating differences in percentage frequencies of CD55+, THY-1+, and CD34+ cells across HC (n=12), IAR (n=5*), and RA+ (n=9). (D) Dot plot and bar graph demonstrating percent frequency and MFI expression (respectively) of FAPα across HC, IAR, and RA+. *Two donors are seronegative ART and are denoted by dark orange squares with black border. Data represented as mean ± SEM. Mann-Whitney U test used for statistical analysis between disease states, with *$p<0.05$ significantly different from each other.

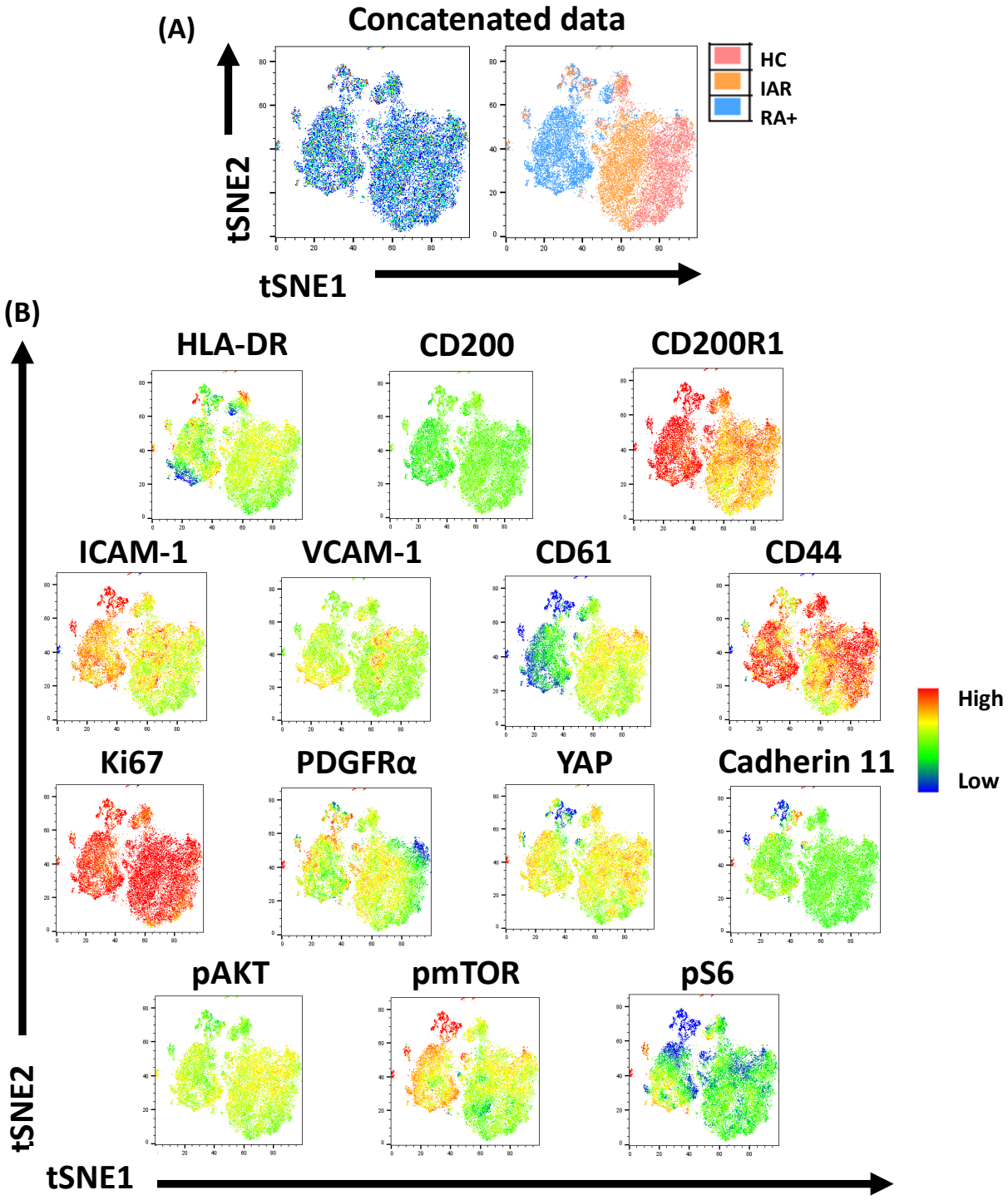

Figure 4.22: FLS phenotypic profiling by unsupervised clustering between HC, IAR, and RA+.

Multiparametric flow cytometric data of total PDPN+ FLS subjected to unsupervised clustering by tSNE algorithm following data concatenation of synovial tissue from one HC, one seropositive IAR, and one RA+. (A) tSNE dot plots demonstrating data concatenation of all PDPN+ cells and overlay of HC, IAR, and RA+ FLS to demonstrate how FLS cluster together. (B) tSNE plots demonstrating relative expression of indicated markers.

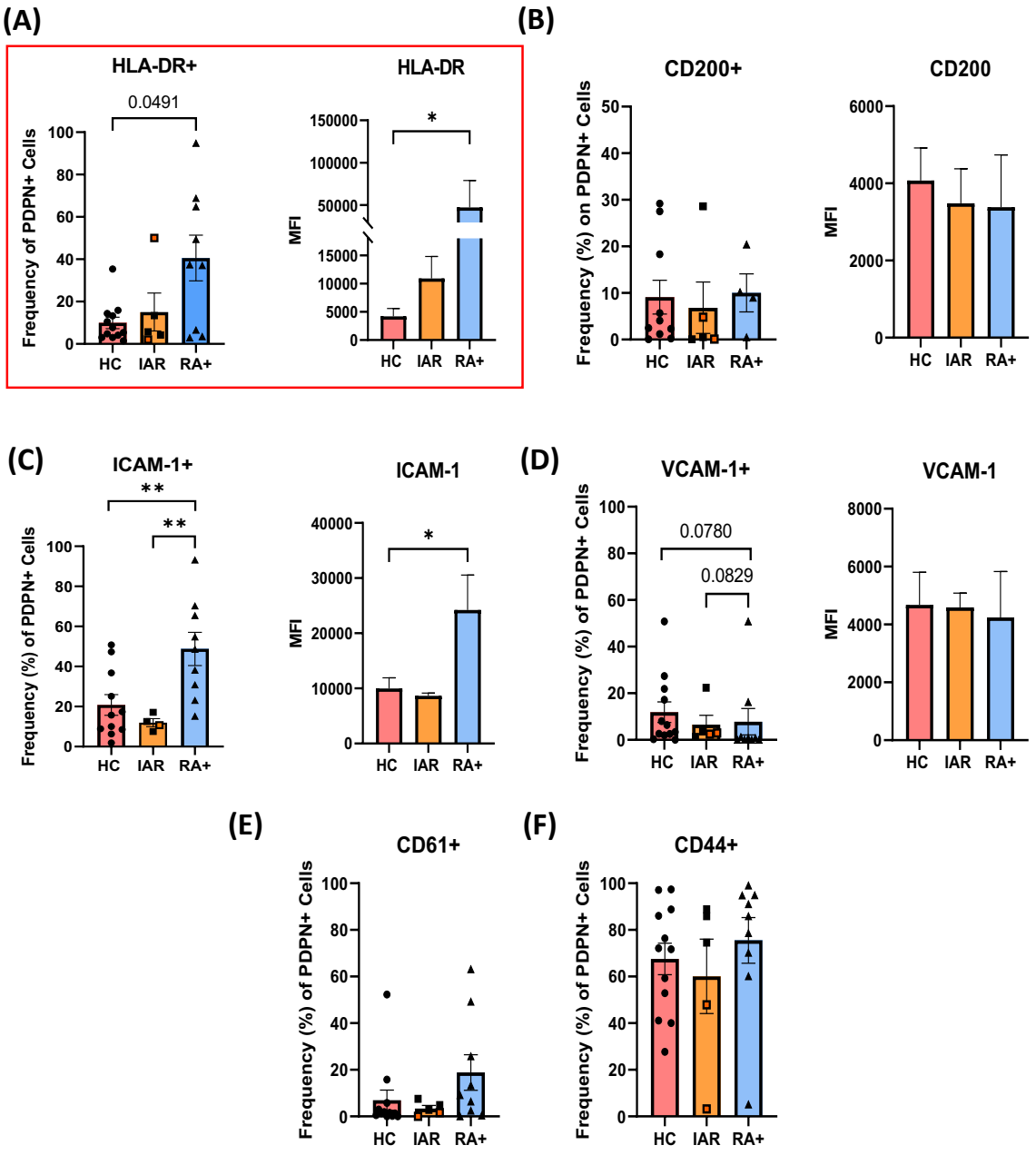

Figure 4.23: Comparison of immunoregulatory and adhesion markers across disease progression.

(A) Dot plot and bar graph demonstrating stepwise increase in percent frequency and MFI expression of HLA-DR from HC (n=12), IAR (n=5*), and RA+ (n=9). (B) Dot plot and bar graph comparing percent frequency and MFI expression of CD200 in C (n=12), IAR (n=5*), and RA+ (n=9). Dot plots and bar graphs demonstrating percent frequency and MFI expression of the adhesion molecules (C) ICAM-1 and (D) VCAM-1 across HC (n=12), IAR (n=5*), and RA+ (n=9). Dot plots demonstrating percent frequency changes of (E) CD61+ and (F) CD44+ FLS in HC (n=12), IAR (n=5*), and RA+ (n=9). *Two donors are seronegative ART and are denoted by dark orange squares with black border. Data represented as mean ± SEM. Mann-Whitney U test used for statistical analysis between disease states, with *p<0.05, **p<0.01 significantly different from each other.

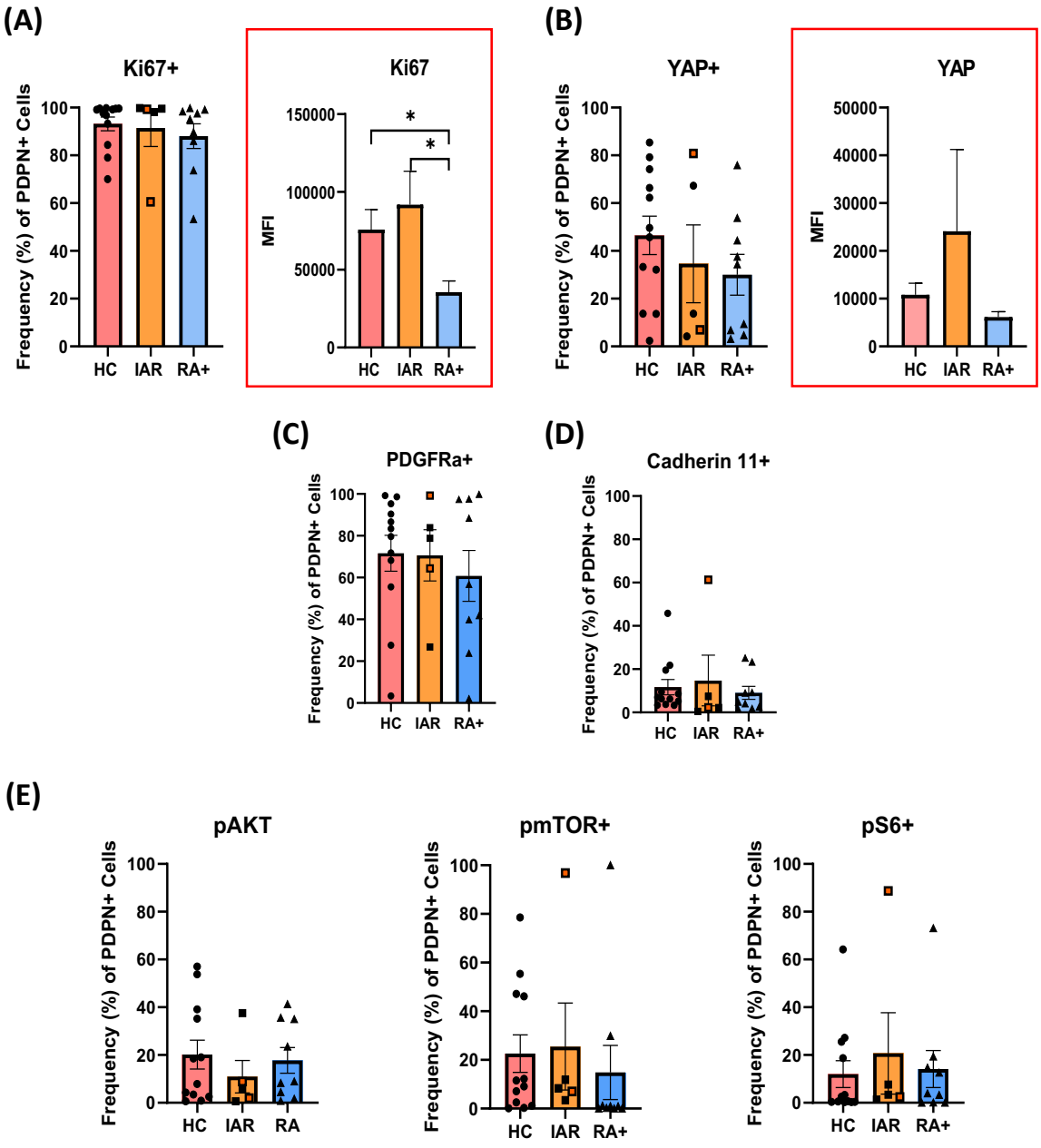

Figure 4.24: Comparison of proliferation, invasive, and metabolic markers across disease progression.

(A) Dot plot and bar graph demonstrating differences in percent frequency and MFI expression of Ki67 from HC (n=12), IAR (n=5*), and RA+ (n=9). (B) Dot plot and bar graph comparing percent frequency and MFI expression of YAP in C (n=12), IAR (n=5*), and RA+ (n=9). Dot plots demonstrating percent frequency changes of (C) PDGFRα+ and (D) Cadherin 11+ and (E) metabolic markers pAKT+, pmTOR+, and pS6+ FLS in HC (n=12), IAR (n=5*), and RA+ (n=9). *Two donors are seronegative ART and are denoted by dark orange squares with black border. Data represented as mean ± SEM. Mann-Whitney U test used for statistical analysis between disease states, with *p<0.05 significantly different from each other.

4.4.8 FLS Subset Frequencies are Altered in IAR Prior to Onset of Clinical Symptoms

Next, we sought to determine if frequencies of FLS subsets are altered prior to clinical onset of symptoms. Therefore, we first examined frequencies of THY1 FAPα FLS subsets in IAR and compared them to HC and RA+ (Figure 4.25). Within the IAR cohort, THY1-FAPα+ demonstrated the highest proportion of FLS and had an increased frequency compared to THY1+FAPα- subset (##p<0.01) (Figure 4.25 (B)). Frequencies of the double positive (THY1+FAPα+) and double negative (THY1-FAPα-) subsets were comparable to each other, and both were increased compared to THY1+FAPα- which made up the smallest proportion of FLS (both p=0.0625). This is further illustrated by the representative flow dot plots shown in Figure 4.25 (A)).

When comparing each subset across disease progression, frequency of the THY1-FAPα+ subset was increased in IAR compared to both HC and RA+ (Figure 4.26). In addition, frequency of the double negative THY1-FAPα- was significantly increased in IAR compared to RA+ (p<0.05) (Figure 4.26). However, not all subsets in IAR demonstrated increased frequency. For example, the double positive THY1+FAPα+ had decreased percent frequency compared to both RA+ and HC. Additionally, THY1+FAPα- frequency was decreased in IAR compared to RA+ and HC (HC vs IAR p=0.0637) (Figure 4.26).

Differences in CD55 THY1 FAPα subset frequencies was also demonstrated within the IAR cohort (Figure 4.27). As illustrated by the representative flow cytometric dot plots (Figure 4.27 (A)) and quantified in the accompanying bar graphs, the CD55+THY1-FAPα+ subset made up the highest proportion of PDPN+ cells in IAR, with CD55-THY1+FAPα+ making up the second largest subset (Figure 4.27 (B)). When each subset was compared to HC and RA+ individually, IAR demonstrated increased frequency of CD55+THY1-FAPα+ compared to HC and RA+ (Figure 4.28). Frequency of CD55+THY1-FAPα+ was decreased in IAR compared to both RA+ and HC. Frequencies of CD55+THY1-FAPα+ and CD55-THY1-FAPα+ did not differ between HC, IAR, and RA+.

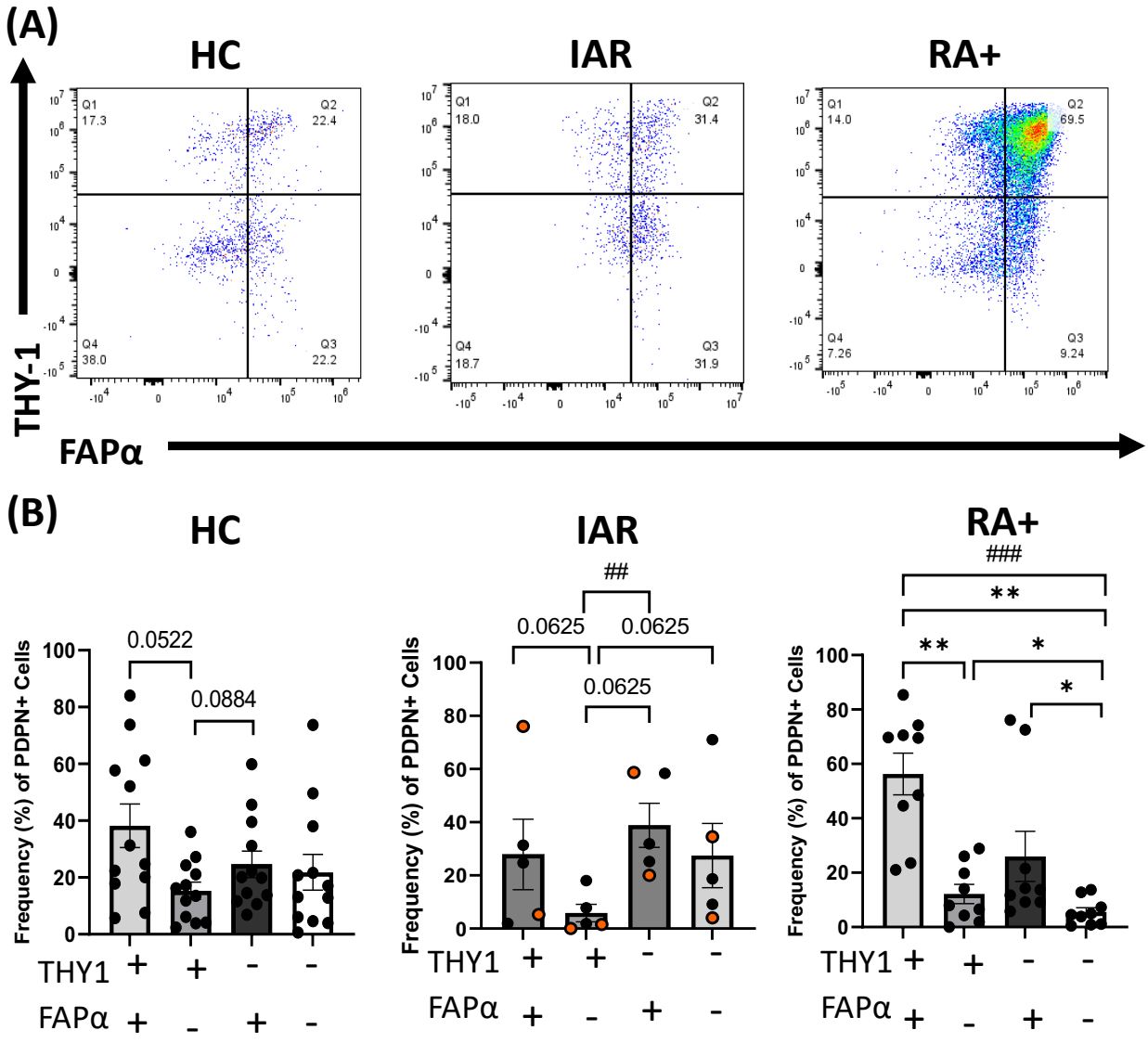

Figure 4.25: Frequency of THY-1 FAPα subsets differ in HC, IAR, and RA+ tissue.

(A) Representative dot plots demonstrating distribution of THY-1 FAPα subsets across HC, IAR, and RA+. (B) Accompanying dot plots demonstrating the percent frequency distribution of each subset as a percentage of total PDPN+ FLS cells within HC (n=12), IAR (n=5*), and RA+ (n=9). *Two donors are seronegative ART and are denoted by dark orange circles with black border. Data represented as mean ± SEM. Friedman test with Dunn's multiple comparisons (#) and Wilcoxon signed rank test (*) utilised for statistical analysis of paired nonparametric data. #p<0.05, ##p<0.01, ###p<0.001, and *p<0.05, **p<0.01 statistically significant.

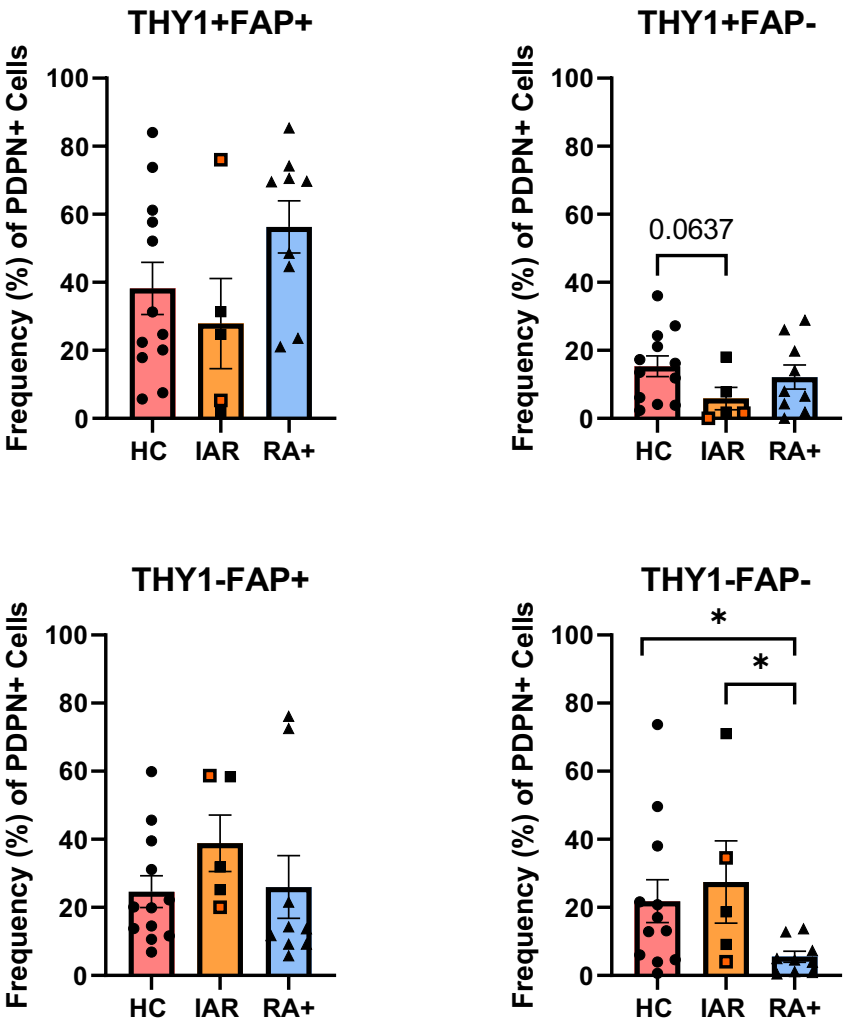

Figure 4.26: Comparison of each THY-1 FAPα subset across disease progression.

Dot plots demonstrating differences in frequency of THY1+FAPα+, THY1+FAPα-, THY1-FAPα+, and THY1- FAPα- subsets as a percentage of PDPN+ cells across HC (n=12), IAR (n=5*), and RA+ (n=9). *Two donors are seronegative ART and are denoted by dark orange squares with black border. Data represented as mean ± SEM. Mann-Whitney U test was used to determine significance with *p<0.05 being statistically significant.

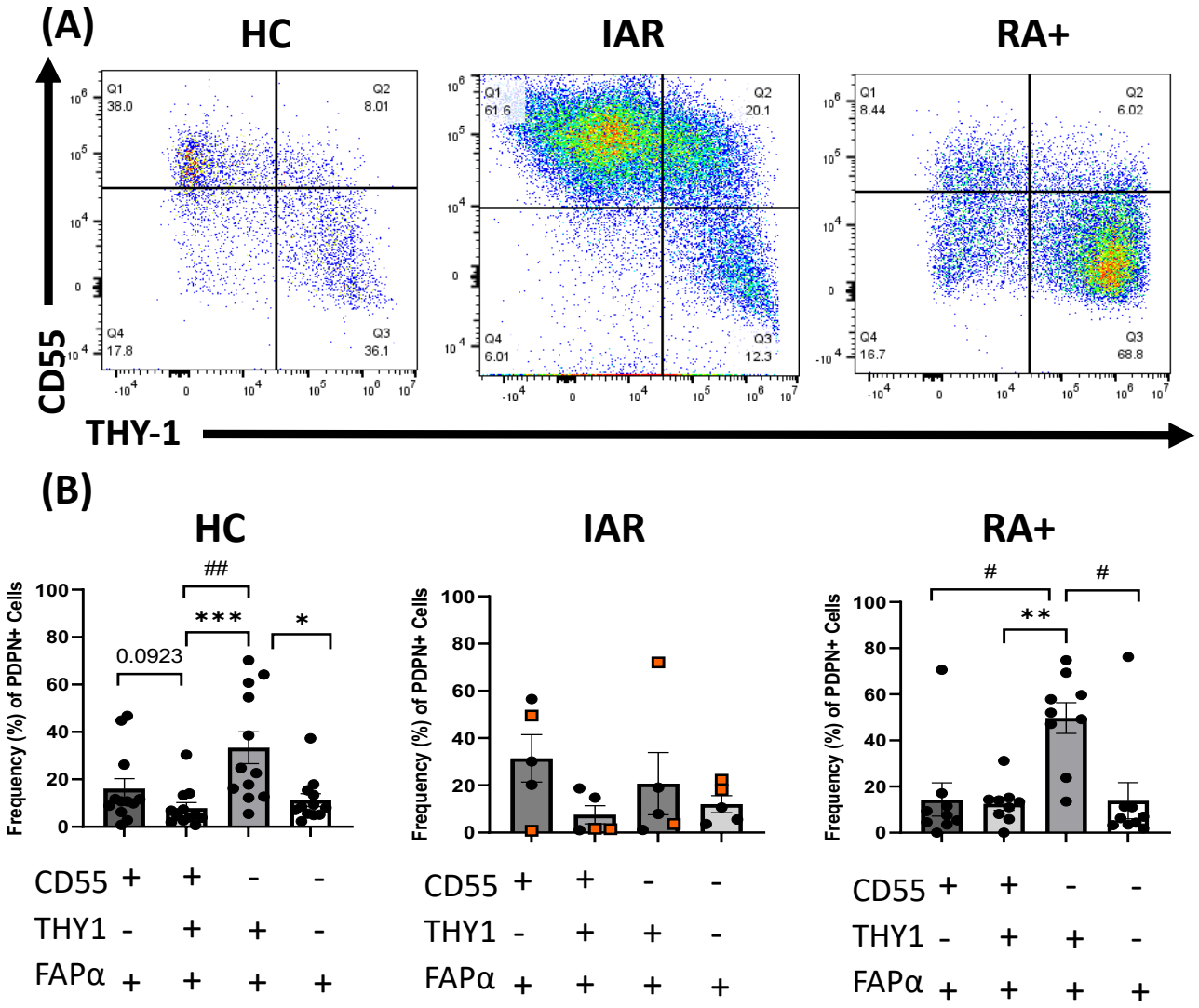

Figure 4.27: CD55 THY-1 FAPα subsets differ in proportion for HC, IAR, and RA+ FLS.

(A) Representative dot plots demonstrating distribution of CD55 THY-1 FAPα subsets across HC, IAR, and RA+. (B) Accompanying dot plots demonstrating the percent frequency distribution of each subset as a percentage of total PDPN+ FLS cells within HC (n=12), IAR (n=5*), and RA+ (n=9). *Two donors are seronegative ART and are denoted by dark orange circles with black border. Data represented as mean ± SEM. Friedman test with Dunn's multiple comparisons (#) and Wilcoxon signed rank test (*) utilised for statistical analysis of paired nonparametric data. #p<0.05, ##p<0.01 and *p<0.05, **p<0.01, ***p<0.001 statistically significant.

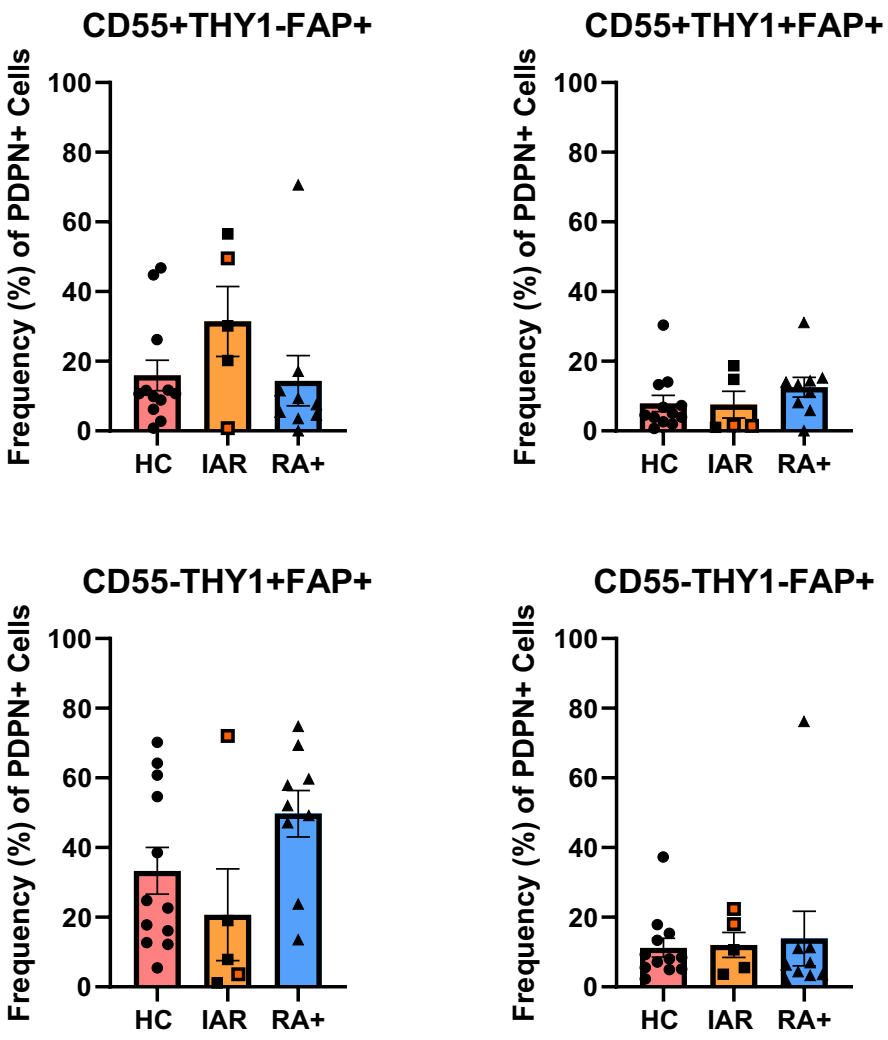

Figure 4.28: Comparison of each CD55 THY-1 FAPα subset across disease progression.

Dot plots demonstrating difference in frequencies of CD55+THY1-FAPα+, CD55+THY1+FAPα+, CD55-THY1+FAPα+, and CD55-THY1-FAPα+ subsets across HC (n=12), IAR (n=5*), and RA+ (n=9). *Two donors are seronegative ART and are denoted by dark orange squares with black border. Data represented as mean ± SEM.

4.4.9 Frequency of Proinflammatory Markers Varies Between FLS Subsets Regardless of Disease Status

So far, we have demonstrated differences in percent frequency and expression of markers on the general PDPN+ FLS population as well as differences in frequency of FLS subsets across disease state and prior to disease onset. However, whether marker expression was specific to a particular FLS subset regardless of disease status had yet to be concluded. Therefore, we next examined the percent frequency of each marker across the CD55 THY1 FAPα subsets (Figures 4.29 and 4.30).

% frequency of FLS expressing immunoregulatory (Figure 4.29 (A)) and adhesion markers (Figure 4.29 (B)) varied significantly across the CD55 THY1 FAPα subsets. SL FLS subset CD55-THY1+FAPα+ demonstrated a significant increase in HLA-DR+ and CD200+ FLS compared to LL subset CD55+THY1-FAPα+ ($p<0.0001$ and $p<0.01$, respectively; Figures 4.29 (A)(i)-(ii)). Interestingly, the double negative intermediate subset CD55-THY1-FAPα+ demonstrated the highest % frequency of CD200R1+ FLS with a significant increase observed compared to CD55+THY1-FAPα+ ($p<0.05$; Figure 4.29 (A)(iii)). SL CD55-THY1+FAPα+ and intermediate CD55-THY1-FAPα+ demonstrated significant increased % frequency of ICAM-1+ FLS compared to LL CD55+THY1-FAPα+ (both $p<0.0001$) and intermediate subset CD55+THY1+FAPα+ (both $p<0.0001$) (Figure 4.29 (B)(i)). Conversely, the intermediate CD55+THY1+FAPα+ subset demonstrated increased % frequency of VCAM-1+ FLS and CD61+ FLS compared to the other subsets, with a significant increase in VCAM-1+ compared to LL CD55+THY1-FAPα+ and in CD61+ compared to SL CD55-THY1+FAPα+ (both $p<0.05$) (Figure 4.29 (B)(ii)-(iii)). CD55+THY1+FAPα+ also demonstrated significantly increased % frequency of CD44+ FLS compared to LL CD55+THY1-FAPα+ ($p<0.05$), SL CD55-THY1+FAPα+ ($p<0.05$), and intermediate CD55-THY1-FAPα+ ($p<0.0001$) (Figure 4.29 (B)(iv)).

SL subset CD55-THY1+FAPα+ and intermediate CD55+THY1+FAPα+ demonstrated significantly increased % frequency of CD34+ FLS compared to LL CD55+THY1-FAPα+ (both $p<0.0001$) and double negative CD55-THY1-FAPα+ ($p<0.0001$ and $p<0.01$ respectively) (Figure 4.30 (A)(i)). Interestingly, SL CD55-THY1+FAPα+ demonstrated significant increased % frequency of Cadherin 11+ FLS compared to the LL and triple positive subsets (both $p<0.001$) (Figure 4.30 (A)(ii)). Additionally, the double negative intermediate subset CD55-THY1-FAPα+ demonstrated a similar increase in % frequency of Cadherin11+ FLS compared to the LL and triple positive subsets (both $p<0.0001$) (Figure 4.30 (A)(ii)). All FLS subsets demonstrated high % frequency of PDGFRα+ FLS (Figure 4.30 (B)(ii)). Similarly, all FLS subsets demonstrated high % frequency of Ki67+ FLS, however, significant increase was observed for LL CD55+THY1-FAPα+ and CD55+THY1+FAPα+ compared to the SL CD55-THY1+FAPα+ subset ($p<0.01$ and $p<0.05$, respectively) (Figure 4.30 (B)(i)). Triple positive CD55+THY1+FAPα+ had a significant increase in % frequency of YAP+ compared to CD55-THY1-FAPα+ ($p<0.05$) (Figure 4.30 (B)(iii)).

FLS subsets differed in expression of metabolic markers as well (Figure 4.30 (C)). The LL CD55+THY1-FAPα+ and intermediate CD55+THY1+FAPα+ subsets demonstrated a significant increase in % frequency of pAKT+ FLS compared to the CD55-THY1-FAPα+ intermediate subset ($p<0.01$ and $p<0.05$, respectively). A significant increase in % frequency of pAKT+ FLS was observed in CD55+THY1-FAPα+ compared to the SL CD55-THY1+FAPα+ subset ($p<0.01$) (Figure 4.30 (C)(i)). Conversely, SL CD55-THY1+FAPα+ and CD55-THY1-FAPα+ subsets demonstrated significant increased % frequencies of pmTOR+ and pS6+ FLS compared to the LL and triple positive subsets (Figure 4.30 (C)(ii)-(iii)).

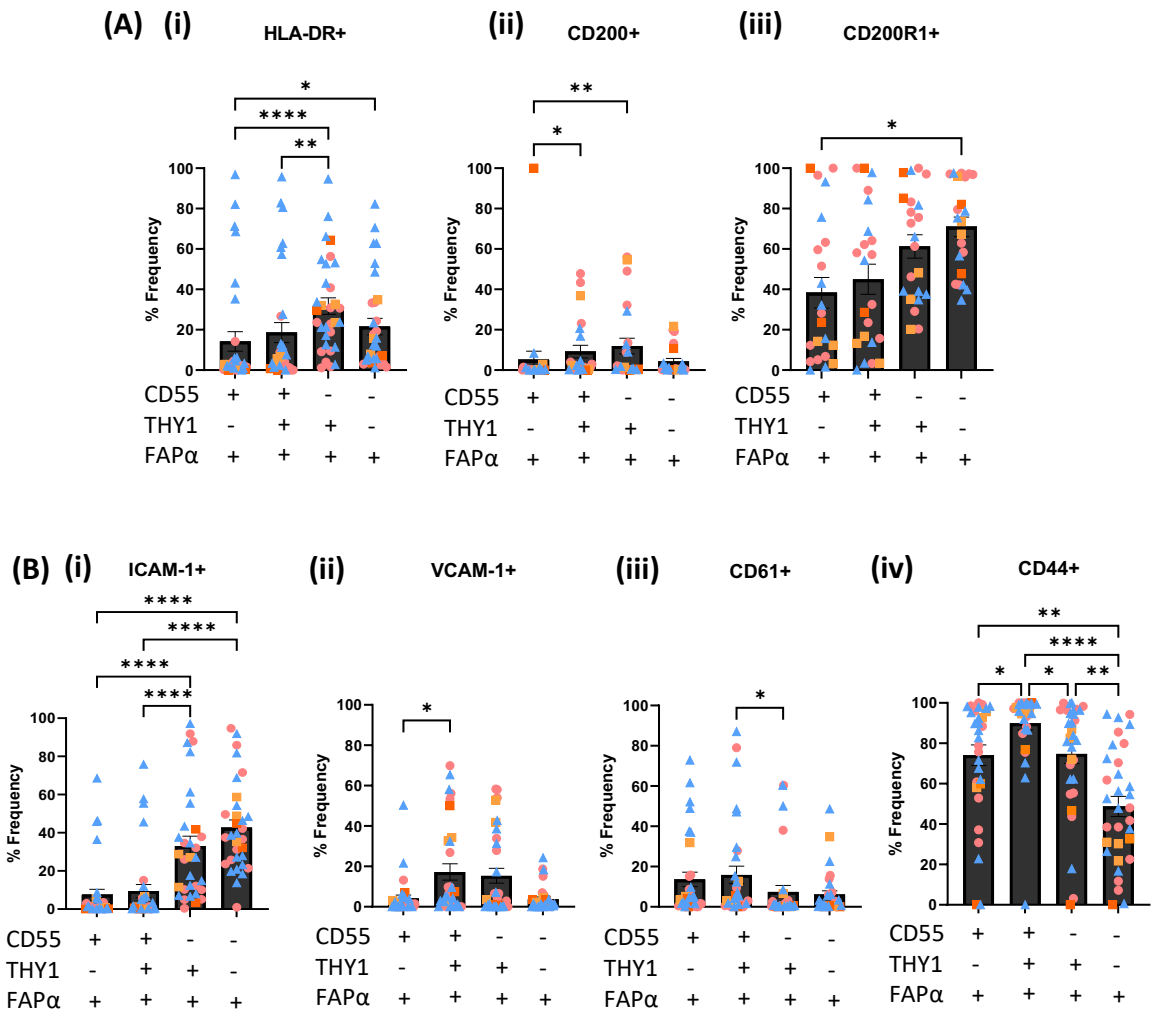

Figure 4.29: Immunoregulatory and adhesion marker expression differ between FLS subsets.

(A) Dot plots comparing frequency of (i) HLA-DR+, (ii) CD200+, and (iii) CD200R1+ cells per FLS subset regardless of disease status. (B) Dot plots comparing percent frequency of (i) ICAM-1+, (ii) VCAM-1+, (iii) CD61+, and (iv) CD44+ cells per FLS subset regardless of disease status. Data represented as mean ± SEM. Each individual shape represents an individual sample with all HC donors (n=12) represented by pink circles, IAR (n=5*) represented by orange squares, and all RA patients (n=15) (including seropositive and seronegative) represented by blue triangles. *Two donors are seronegative ART and are denoted by dark orange squares. Statistical analysis performed using Kruskal-Wallis with Dunn's multiple comparisons with *p<0.05, **p<0.01, ***p<0.001, and ****p<0.0001 being statistically significant.

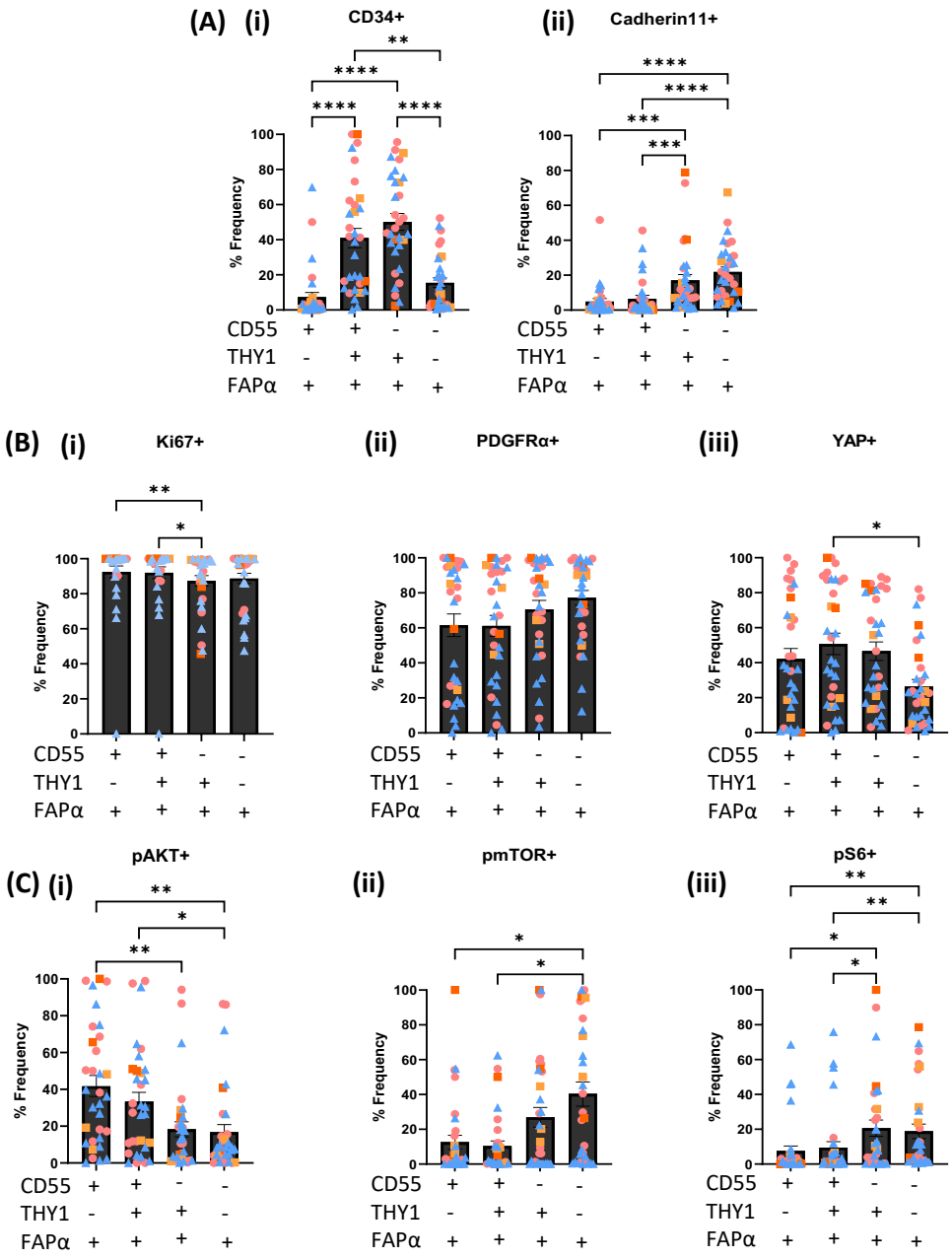

Figure 4.30: Functional markers differ across FLS subsets.

(A) Dot plots comparing frequency of (i) CD34+ and (ii) Cadherin 11+ cells per FLS subset regardless of disease status. (B) Dot plots comparing percent frequency of (i) Ki67+, (ii) PDGFRα+, and (iii) YAP+ cells per FLS subset regardless of disease status. (C) Dot plots demonstrating differences in frequency of (i) pAKT+, (ii) pmTOR+, and (iii) pS6+ across FLS subsets regardless of disease status. Data represented as mean ± SEM. Each individual shape represents an individual sample with all HC donors (n=12) represented by pink circles, IAR (n=5*) represented by orange squares, and all RA patients (n=15) (including seropositive and seronegative) represented by blue triangles. *Two donors are seronegative ART and are denoted by dark orange squares. Statistical analysis performed using Kruskal-Wallis with Dunn's multiple comparisons with *p<0.05, **p<0.01, ***p<0.001, and ****p<0.0001 being statistically significant.

4.4.10 Single-Cell Transcriptomic Analysis of Synovial Tissue FLS from Health to Disease

Single-cell transcriptomic analysis of RA synovial tissue and specifically RA FLS have recently become an area of interest. Previously, our group showed distinct synovial FLS clusters between RA and PsA (Floudas *et al.*, 2022). However, transcriptomic analysis comparing FLS clusters between RA and HC synovial tissue is limited. Therefore, we next performed scRNA-seq and transcriptomic profiling of synovial tissue from HC (n=5) and RA (n=4) to provide a unique FLS atlas from health to disease (Figures 4.31 and 4.32). scRNA-seq analysis identified 14 distinct FLS clusters depicted in the UMAP in Figure 4.31 (A) based on the top DEG cluster marker gene signatures identified for each cluster as depicted in the heatmap (Figure 4.31 (B)). Based on these genes, each cluster was annotated, functionally described and subsequently categorised into larger subpopulations based on their phenotype (Figure 4.31 (C)) and Figure 4.32). The proposed taxonomy of the FLS clusters is depicted in Figure 4.31 (D).

Cluster 0, designated VCAN+CXCL12+ (Figure 4.31 (C-D) and Figure 4.32), demonstrated enrichment of pro-inflammatory genes, such as IL-6, PDGRFα, as well as the chemokines CXCL12, CXCL2, CCL2 (MCP-1), and CXCL3 (Figure 4.31 (B) and Figure 3.2). Cluster 1, designated MMP1+MMP3+ (Figure 4.31 (C-D) and Figure 4.32), demonstrated enrichment of genes involved in motility and invasion, such as MMP-1, MMP-3, INHBA, THBS4, HTRA1, TNFAIP6, and TIMP3 (Figure 4.31 (B) and Figure 4.32). Cluster 2, designated CRTAC1+TPPP3+ (Figure 4.31 (C-D) and Figure 4.32), demonstrated enrichment of genes involved in homeostasis (DEFB1, SCARA5, MT1X) and ECM regulation (CRTAC1, TPPP3), such lubrication and hyaluronic acid synthesis (PRG4, HAS1) (Figure 4.31 (B) and Figure 4.32). Cluster 3, designated POSTN+COL3A1+ (Figure 4.31 (C-D) and Figure 4.32), demonstrated the highest expression of FAPα as well as enriched ECM reorganization genes, such as Cadherin 11, TGFBI, POSTN, COL3A1, COL1A1, COL5A1, and SPARC (Figure 4.31 (B) and Figure 4.32). Similarly, cluster 4, designated ASPN+COMP+ (Figure 4.31(C-D) and Figure 4.32) also demonstrated an enrichment of genes involved in ECM remodelling/organization (ASPN, COMP, OGN, PRELP, DCN, IGF1, MFAP5, WISP2) as well as genes involved in WNT signaling (Figure 4.31 (B) and Figure 4.32). Cluster 5, designated CXCL8+CXCL1+ (Figure 4.31 (C-D) and Figure 4.32), demonstrated enrichment of pro-inflammatory genes including but not limited to CXCL8, CXCL1, INHBA, CXCL3, EREG, VCAM1, IL6, and ITGBL1 (Figure 4.31 (B)) and Figure 4.32). Cluster 6, designated TM4SF1+VWF+ (Figure 4.31 (C-D) and Figure 4.32), was enriched in HC tissue compared to RA and interestingly expressed markers associated with ECs (VWF, PECAM1) as well as markers involved in endothelial-to-mesenchymal transition (EndoMT) and angiogenesis (ADGRL4, SELE, SPRY1, FABP5, ETS2, IGFBP7), suggesting that this cluster could be perivascular and interact with ECs within the joint (Figure 4.31 (B-C) and Figure 4.32). Cluster 7 (IER2+IRF1+)

demonstrated enrichment of genes involved in the regulation of gene expression and responses to environmental stressors, and its cluster markers were mainly comprised of transcription factors and heat-shock proteins (HES1, JUN, FOS, IER2, FOS, IRF1, DNAJB1, ATF3, EGR1, etc.) (Figure 4.31 (B-D) and Figure 4.32). Cluster 8 (APOE+APOC1+) had enrichment of genes involved in fatty acids (for example APOE, APOC1) (Figure 4.31 (C-D) and Figure 4.32). Cluster 9 (LGALS1+ENO1+) had enrichment of genes involved in homeostatic and regulatory functions such as cellular responses to heavy metal ions, zinc binding/transport, and mitochondrial function (MT1G, ENO1, MT1E, NDUFA4L2, MT1X, GAPDH) (Figure 4.31 (B-D) and Figure 4.32). Cluster 10 (MEG3+MEG8+) is a regulatory cluster with enrichment of genes involved in post-transcriptional regulation and mRNA splicing along with long non-coding RNAs (LncRNAs) and transcription factors (MEG3, MEG8, ITGB8, CLK1, EWSR1 CREB5, CCNL1, SOX5, etc.) (Figure 4.31 (B-D) and Figure 4.32). Cluster 11 (HLA-DRA+CD74+) is enriched in genes involved in immunoregulation such as HLA-DRA, CD74, HLA-DRB1, HLA-DRB5, CXCL3, CXCL8, and CCL2 (Figure 4.31 (B-D) and Figure 4.32). Cluster 12 (TAGLN+NOTCH3+) is another perivascular cluster and expresses genes found in myofibroblasts (Figure 4.31 (B-D) and Figure 4.32). Some genes enriched in this cluster include TAGLN, ACTA2, NOTCH3, HES4, MCAM, and MYL9 (Figure 4.31 (B) and Figure 4.32). Finally, cluster 13 (TNFAIP3+CXCR4+) demonstrates enrichment of immunoregulatory genes (TNFAIP3, IL7R, CXCR4, STAT4, IL32, HLA-DRB) and potentially interacts closely with macrophages due to the co-expression of PTPRC (also known as CD45) (Figure 4.31 (B-D) and Figure 4.32).

Though not significant, FLS clusters demonstrated differences in frequency between HC and RA tissue (Figure 4.31 (E-H)). For example, clusters 1, 2, and 5 were enriched in HC compared to RA while clusters 0, 3, 4, and 8 were enriched in RA (Figure 4.31 (G-H)). However, it is important to note that the inflammatory and invasive genes used to describe clusters 1 and 5 were upregulated in RA compared to HC even though frequency of those clusters were higher in HC. Of these enriched subsets, the VCAN+CXCL12+ cluster (cluster 0) and POSTN+COL3A1+ (cluster 3) were particularly enriched in RA (Figure 4.31 (H)). The intermediate clusters 7, 9 and 12 demonstrated similar frequencies between both cohorts (Figure 4.31 (H)); however, cluster 6 (TM4SF1+VWF+) was particularly enriched in HC (Figure 4.31 (F) and (H)). Frequencies of each FLS cluster varied across each individual as demonstrated in Figure 4.31 (G), demonstrating the significance of donor variability even at the single-cell level.

Clusters 1, 2, 5, 10, 11, and 13 demonstrated high expression of established LL marker PRG4 and low to no expression of established SL marker THY-1 (Figure 4.33 (A)). Conversely, clusters 0, 3, 4, and 8 demonstrated low expression of PRG4 and enriched expression for the established SL marker THY-1 (Figures 4.33 (A-C)). This is further demonstrated in the dot plot

depicting the relative expression of additional established LL and SL markers across each cluster (Figure 4.33 (B)). We next directly compared the expression of the LL marker CD55 and SL marker THY-1 to further confirm the FLS subpopulations. From this additional analysis along with closer examination of the proposed hierarchical taxonomy (Figure 3.31 (D)), we determined clusters 6, 7, 9, and 12 to be intermediate clusters, as clusters 7, 9, and 12 expressed enrichments for both CD55 and THY-1 markers while cluster 6 demonstrated low expression for both (Figure 4.33 (C)). UMAPs depicting the relative expression of CD55 and THY-1 in the FLS subsets between HC and RA demonstrate that the LL FLS cluster closely together and similarly the SL FLS cluster in a similar location, with the intermediate clusters (Figure 4.33 (D)).

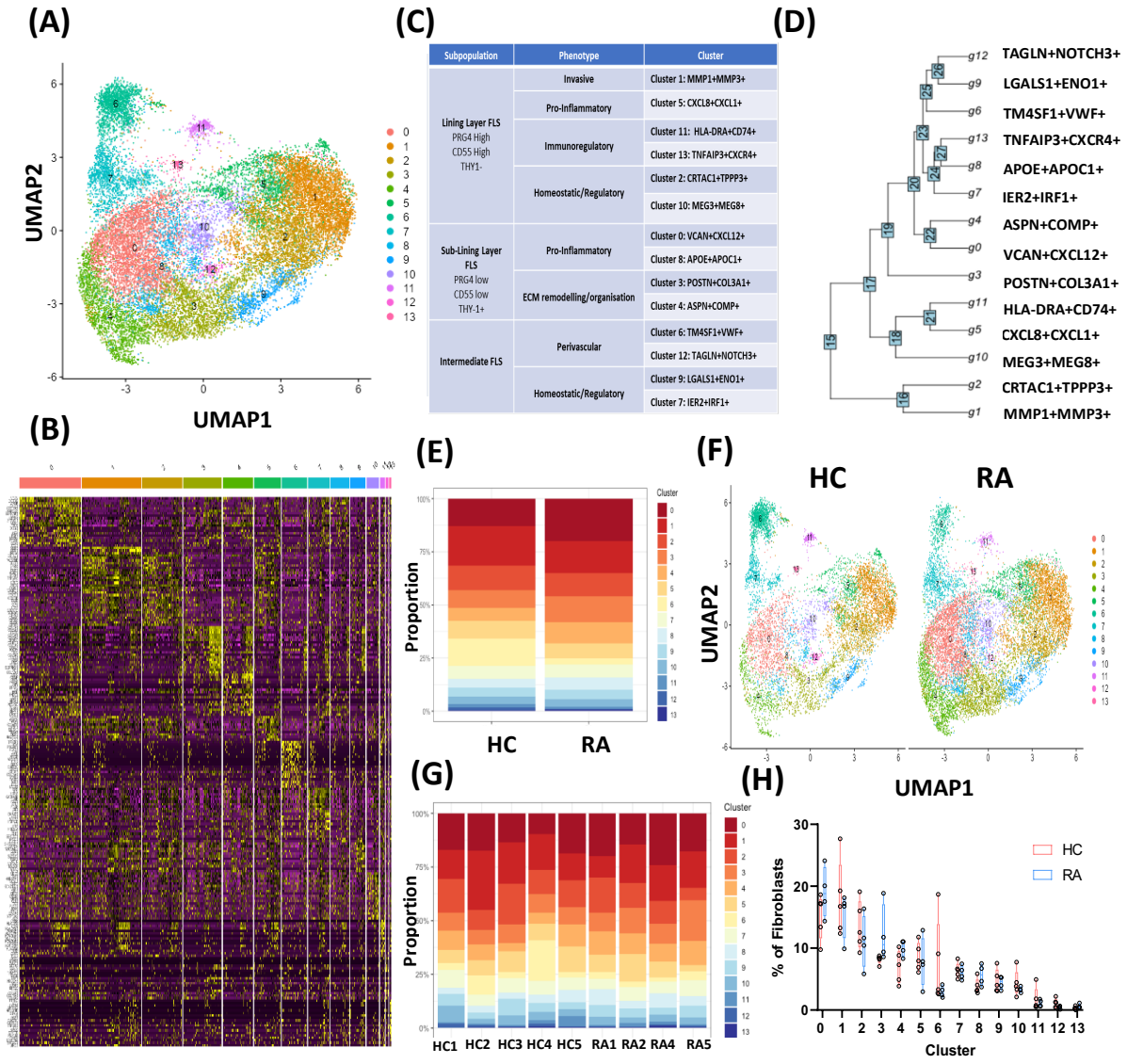

Figure 4.31: scRNA-sequencing defines synovial tissue FLS heterogeneity from health to disease.

(A) UMAP representation of 14 synovial tissue FLS clusters based on a total of 67,908 synovial tissue cells from HC (n=5) and RA (n=4) sequenced and identified by high-dimensionality scRNA-seq analysis. (B) Heatmap of the top 20 DEG cluster marker genes for each of the 14 FLS clusters. (C) Proposed classification and (D) hierarchical clustering of human synovial FLS. (E) Proportional cluster abundance between patients with RA and HC individuals. (F) UMAP depicting synovial tissue FLS cluster distribution between HC and RA synovium. (G) Proportional cluster abundance demonstrating variability per HC donor and RA patient. (H) Grouped dot plot demonstrating differential frequency of each FLS cluster as a percentage of total FLS between HC and RA with each symbol representing an individual donor/patient.

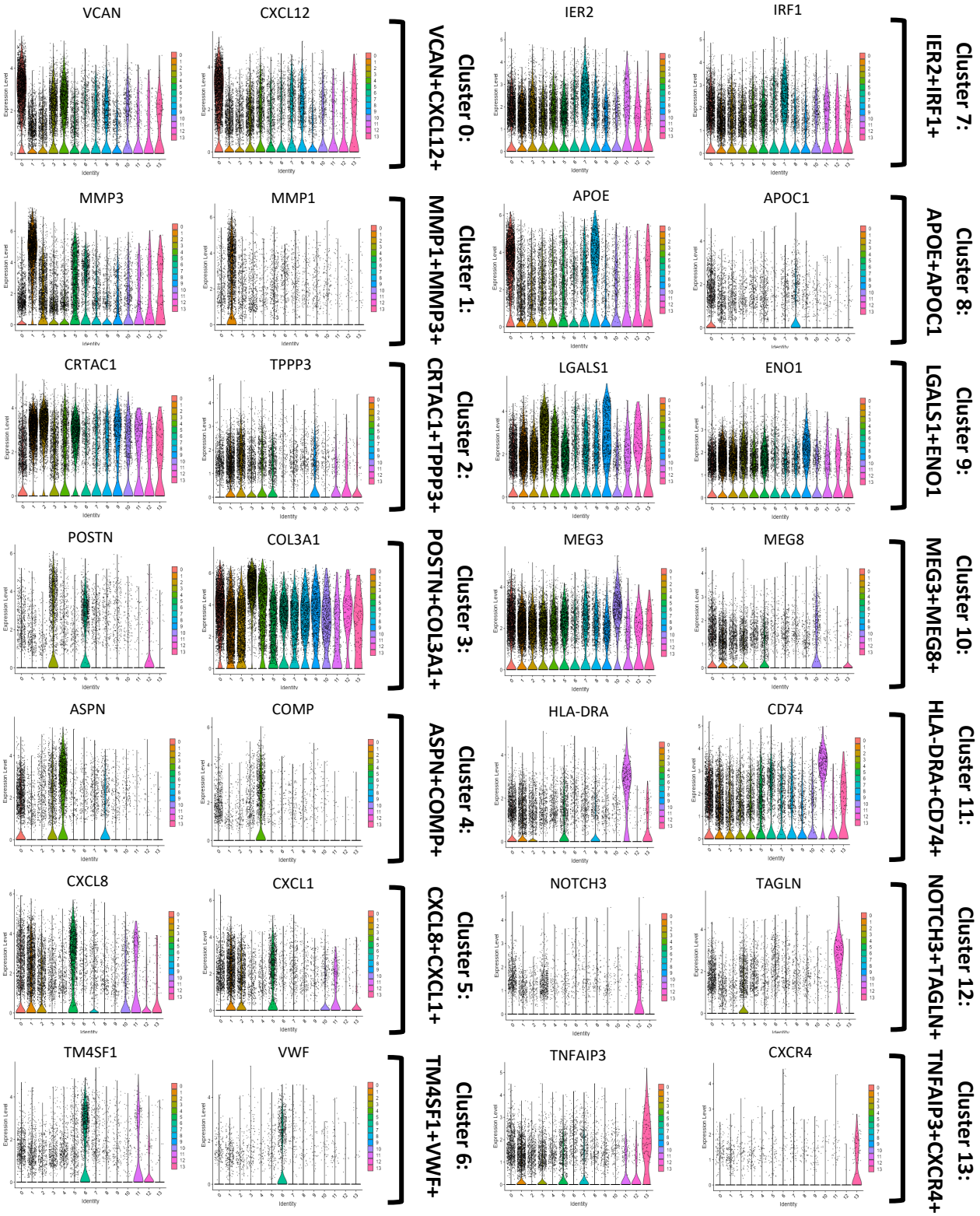

Figure 4.32: scRNA-seq transcriptional profiling of identified synovial tissue FLS clusters.

Violin plots representing log-normalised expression levels of synovial tissue FLS cluster markers used to help annotate each cluster (14 clusters in total).

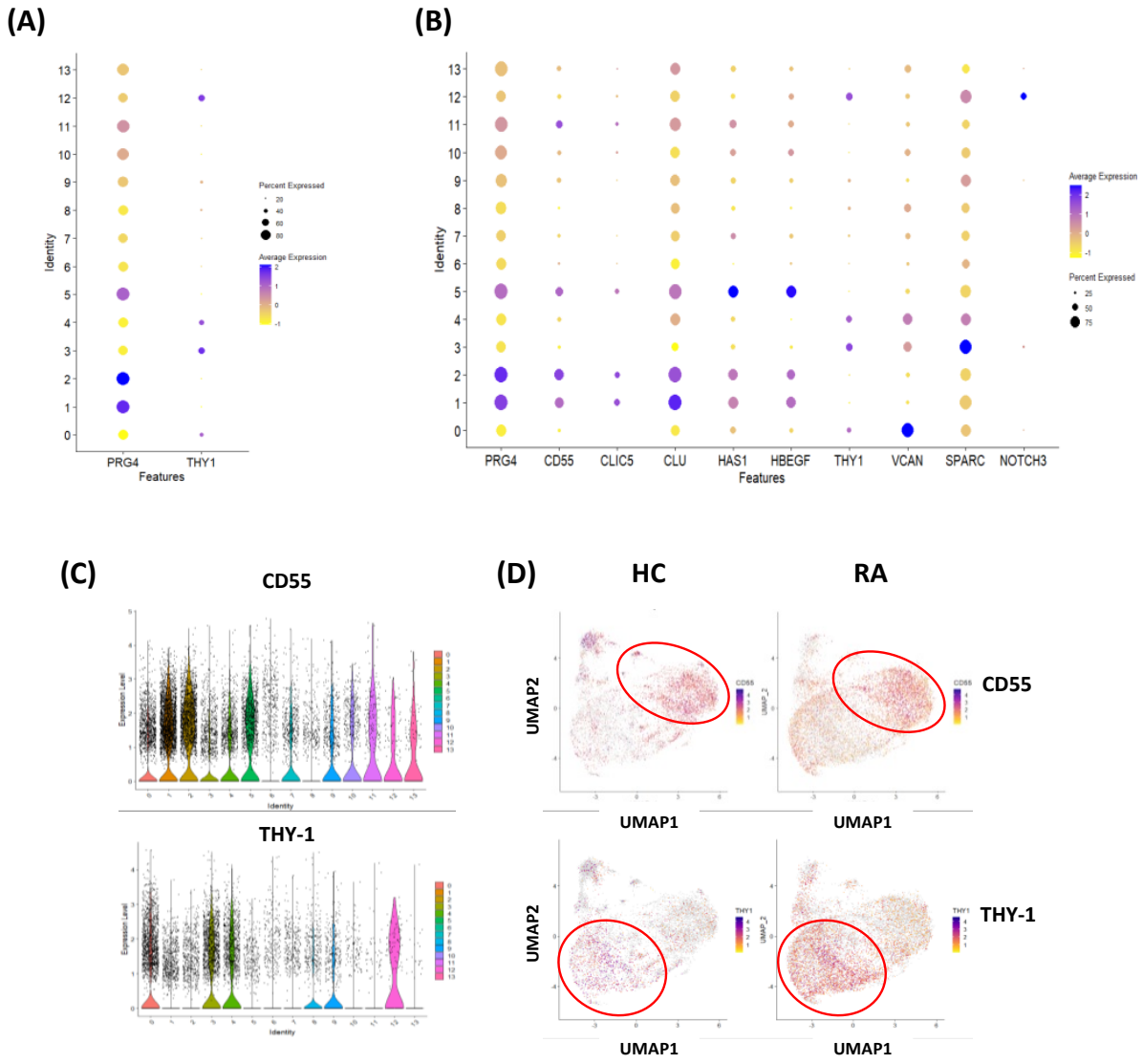

Figure 4.33: scRNA-seq transcriptional profiling of FLS clusters identified LL, SL, and intermediate subsets.

(A) Dot plot demonstrating normalised average expression of lining layer marker PRG4 and sub-lining marker THY-1 across 14 FLS subsets. (B) Dot plot of expression of established lining (PRG4, CD55, CLIC5, CLU, HAS1, HBEGF) and sub-lining FLS markers (THY-1, VCAN, SPARC, NOTCH3) established in previous literature, across 14 FLS clusters. (C) Violin plots demonstrating expression across clusters of lining layer marker, CD55, and sub-lining layer marker, THY-1, with (D) accompanying UMAPs showing the location of FLS expression of each marker between HC and RA.

4.4.11 Identification of Upregulated Signaling Pathways in FLS Clusters Enriched in RA

We next investigated which pathways were upregulated in RA FLS clusters compared to HC to gain better insight into FLS subtype phenotype. RA FLS demonstrated increased metabolic activity compared to HC with upregulated expression of both oxidative phosphorylation and glycolysis gene modules (Figure 4.34 (A) and (D)). Interestingly, expression levels of glycolysis and oxidative phosphorylation genes were differentially expressed across clusters (Figure 4.34 (B) and (E)). For example, cluster 1 (MMP1+MMP3+), cluster 3 (POSTN+COL3A1+) and cluster 9 (LGALS1+ENO1+) demonstrated highest expression of glycolysis and oxidative phosphorylation genes, with specific enrichment demonstrated in RA (Figure 4.34 (C) and (F)). This demonstrates that specific FLS clusters differ in their metabolic requirements.

As discussed in Section 4.4.10, the SL clusters VCAN+CXCL12+ (cluster 0) and POSTN+COL3A1+ (cluster 3) were particularly enriched in RA compared to HC. Therefore, we next investigated dysregulated signaling pathways within these clusters. Figure 4.35 depicts upregulated signaling pathways of interest in each cluster. The VCAN+CXCL12+ cluster demonstrated upregulation of genes involved in NF-κB, NOTCH, and TGFβ signaling in RA compared to HC as depicted in the term plots (Figure 4.35 (A)). Of note, crosstalk between the NOTCH and the TGFβ signaling pathways through the shared genes HDAC2 and EP300 was demonstrated (Figure 4.35 (A)). The POSTN+COL3A1+ cluster also demonstrated upregulation of genes involved in NF-κB and TGFβ signaling, with HDAC2 and EP300 genes dysregulated as well (Figure 4.35 (B)). Therefore, we next focused on the NOTCH signaling pathway to better understand its involvement in the FLS clusters (Figure 4.36). Analysis revealed enrichment in NOTCH signaling genes: NOTCH2, NOTCH3, RBPJ, ADAM10, HES4, NUMB, ADAM17, ADAM12, MAML2, and PSENEN in RA compared to HC as demonstrated by the stacked violin plots in Figure 4.36 (A). Individual violin plots demonstrating enrichment of some of these genes between HC and RA is shown in Figure 4.36 (B). We further investigated the expression of these genes in each FLS cluster (Figure 4.36 (C)). Expression of NOTCH3 was particularly enriched in cluster 0 (VCAN+CXCL12+), cluster 3 (POSTN+COL3A1+), and cluster 12 (TAGLN+NOTCH3+) (Figure 4.36 (C)). This was further demonstrated in the UMAP depicting the relative expression level and location of NOTCH3+ FLS (Figure 4.36 (D)). Other genes involved in downstream NOTCH signaling such as ADAM12 and HES4 were also enriched in these clusters (Figure 4.36 (C)), further demonstrated in the UMAPs in Figure 4.36 (D).

scRNA-seq revealed upregulation of genes involved in NOTCH signaling pathway in SL clusters enriched in RA compared to HC. Previous work in our lab has demonstrated that the THY+FAPα+ FLS cluster is enriched in RA compared to PsA (Floudas *et al.*, 2022). Additionally,

further work conducted in our group has demonstrated that by passage 3, cultured primary FLS are predominately THY+FAPα+ (Tynan *et al.*, (2025); unpublished). The POSTN+COL3A1+ most closely aligns to this previously described THY+FAPα+ phenotype and therefore, we specifically focused on investigating receptor-ligand interactions within this cluster to potentially identify the drivers of NOTCH signaling and further identify potential signaling pathway interactions (Figure 4.37). Some of the ligands of note on T-cells were VEGF and TGFβ (Figure 4.37 (A)). Analysis of potential downstream targets included VEGF, ADAM17, and ADAM12 (Figure 4.37 (B)). Receptor-ligand interactions with macrophages and potential downstream targets were also investigated (Figure 4.37 (C)-(D)). Notable macrophage ligands identified included TGFβ, VEGF, TNFα, and IL-1β (Figure 4.37 (C)). Analysis of predicted downstream targets revealed genes including VEGF, ADAM12, IL6 and genes involved in NF-κB signaling to name a few (Figure 4.37 (D)).

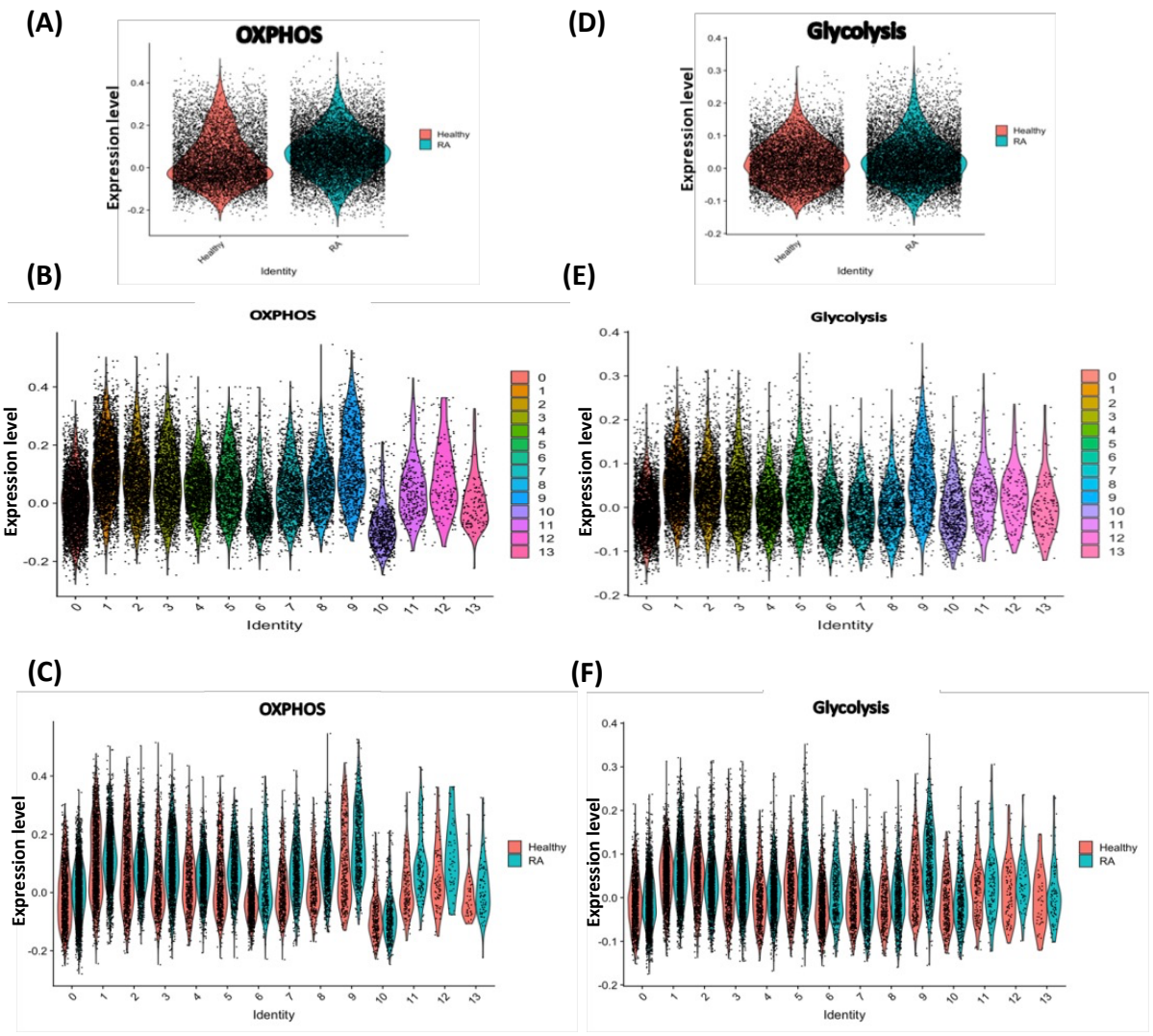

Figure 4.34: scRNA-seq analysis of metabolism associated gene modules in synovial tissue FLS.

Violin plots indicating expression levels of oxidative phosphorylation (OXPHOS) gene module in (A) HC vs RA FLS, (B) identified synovial tissue FLS clusters, and (C) FLS clusters in HC vs RA. Violin plots demonstrating expression levels of glycolysis gene module in (D) HC vs RA, (E) synovial tissue FLS clusters, and (F) FLS clusters in HC vs RA.

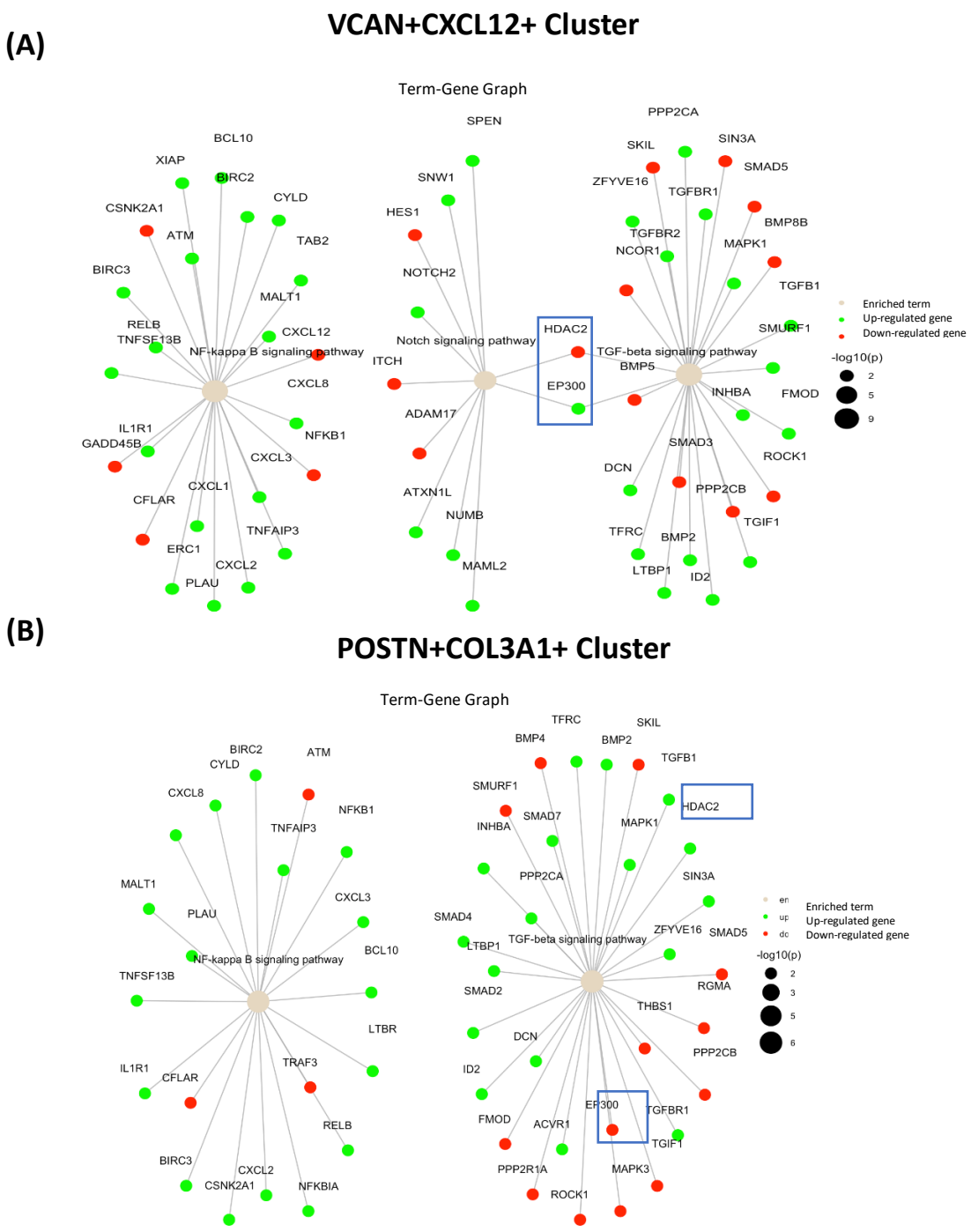

Figure 4.35: Upregulated signaling pathways in SL clusters enriched in RA suggest crosstalk.

(A) Term plots of indicated pathways (NFκB, NOTCH, TGFβ) identified in VCAN+CXCL12+ SL cluster (Cluster 0) with significant enrichment in RA compared with HC FLS. (B) Term plots of indicated pathways identified in POSTN+COL3A1+ SL cluster (Cluster 3). Colour indicates up (green) or downregulation (red) of specific genes within the pathway and dot size represents statistical significance of change.

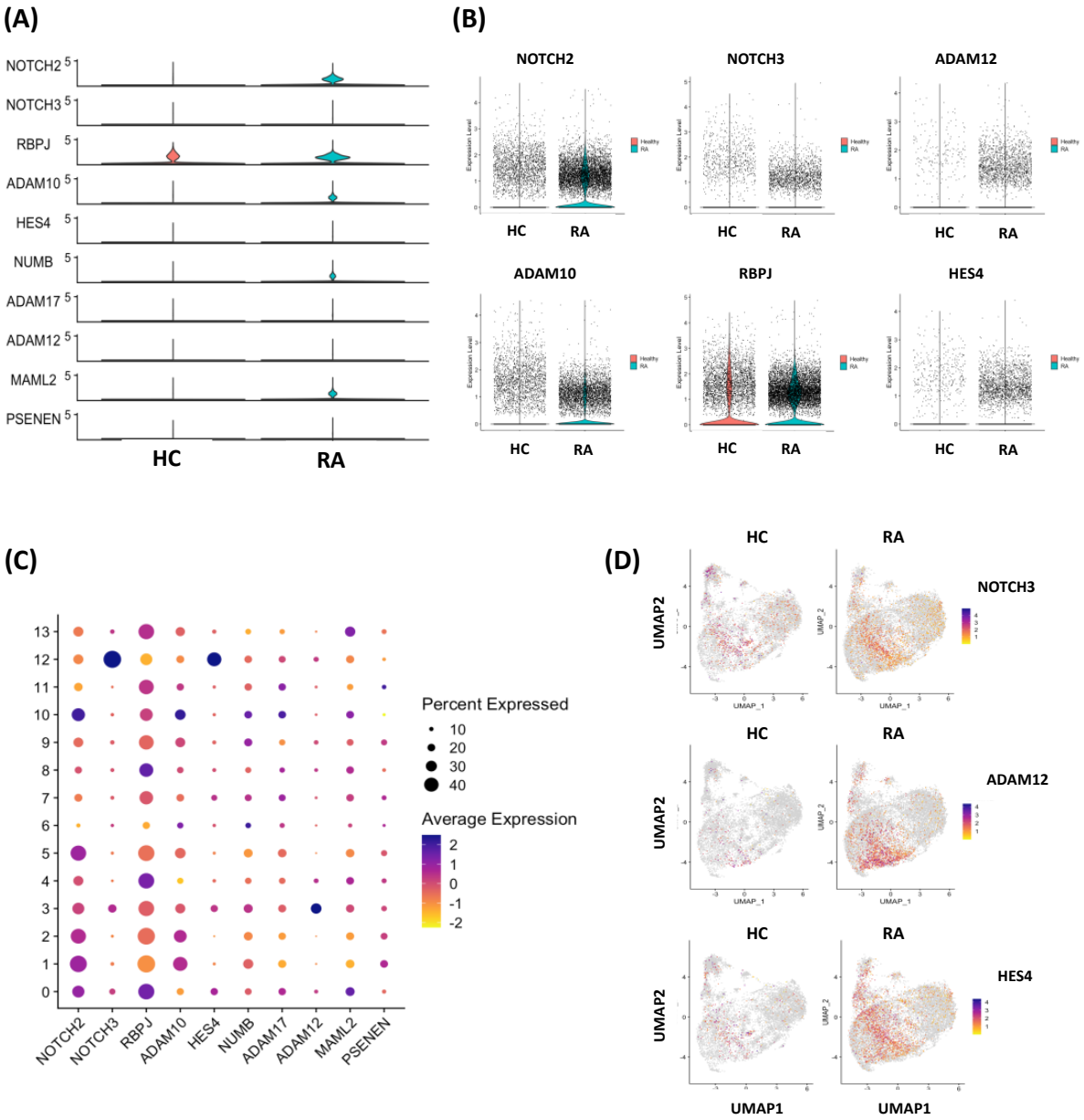

Figure 4.36: Genes within the NOTCH pathway are upregulated in RA.

(A) Stacked violin plots of expression levels of indicated genes within the NOTCH signaling pathway in HC vs RA FLS. (B) Violin plots of NOTCH2, NOTCH3, ADAM12, ADAM10, RBPJ, and HES4 gene expression in HC vs RA FLS. (C) Dot plots of indicated NOTCH genes across all FLS clusters. Colour of dots indicate level of fold change expression and size of dots indicate percentage of cells expressing each gene. (D) UMAPs demonstrating expression of NOTCH3, ADAM12, and HES4 genes and the location of FLS expressing these genes in FLS clusters in HC vs RA.

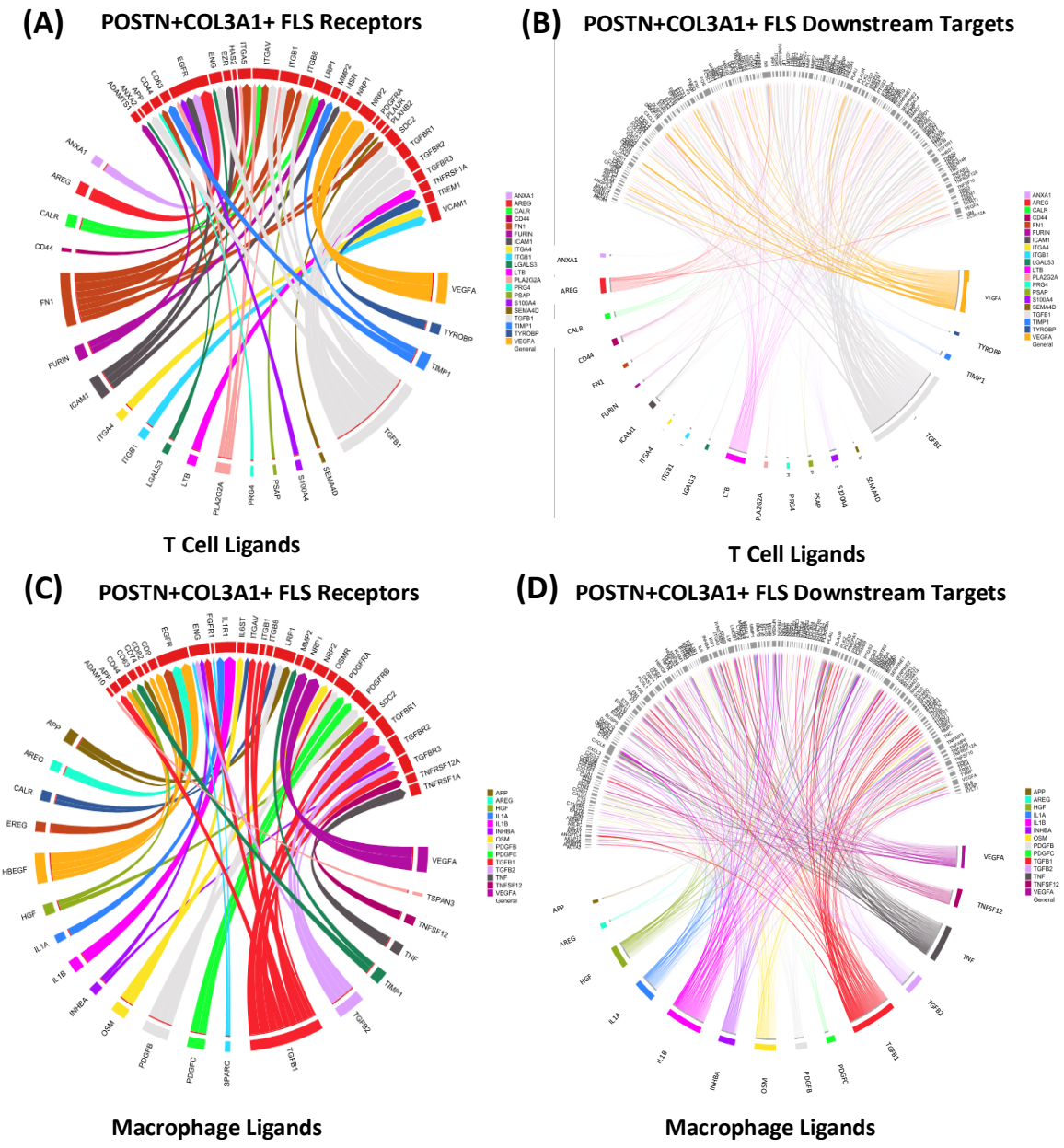

Figure 4.37: Receptor-ligand interactions and downstream targets for Cluster 3 (POSTN+COL3A1+)

Circo plots depicting the top predicted T cell ligands interacting with (A) receptors and (B) downstream targets on FLS cluster 3 (POSTN+COL3A1+). Circo plots depicting the top predicted macrophage ligands interacting with (C) receptors and (D) downstream targets on FLS cluster 3 (POSTN+COL3A1+).

4.4.12 DAPT Inhibition of NOTCH Signaling Pathway May Alleviate Pathogenic Effects of RA FLS via Crosstalk

To investigate whether NOTCH signaling contributes to the pathogenic function of RA FLS through crosstalk with other signaling pathways, and whether NOTCH inhibition can ameliorate RA FLS pathogenicity, we performed proof of concept experiments using primary cultured RA FLS. RA FLS demonstrated significantly increased gene expression of NOTCH ligands DLL4 and JAG-1 following 3 h stimulation with IL-1β (1 ng/mL) (both $p<0.05$) with no significant differences in expression observed for receptors NOTCH1 and NOTCH3 (Figure 4.38 (A)). Inhibition via the γ-secretase inhibitor (DAPT) (50 μM) after 24 h demonstrated successful inhibition of NOTCH signaling evidenced by the significantly decreased expression of downstream marker HEY2 in both IL-1β+DAPT and DAPT control conditions compared to IL-1β stimulated condition (both $p<0.05$) (Figure 4.38 (B)). Interestingly, DAPT demonstrated a significant synergistic increase in the expression of DLL4 compared to IL-1β alone ($p<0.01$) and DMSO control ($p<0.05$) (Figure 4.38 (B)), consistent with the complex lateral inhibition observed in the pathway. Finally, DAPT significantly decreased IL-β-induced expression of IL-6 ($p<0.05$); however, significantly increased expression of IL-β-induced RANTES ($p<0.01$). Taken together, preliminary experiments demonstrate the crosstalk of NOTCH and NF-κB signaling pathways and inhibition via DAPT may selectively ameliorate pro-inflammatory mechanisms in RA FLS. However, more research is required to fully understand this relationship.

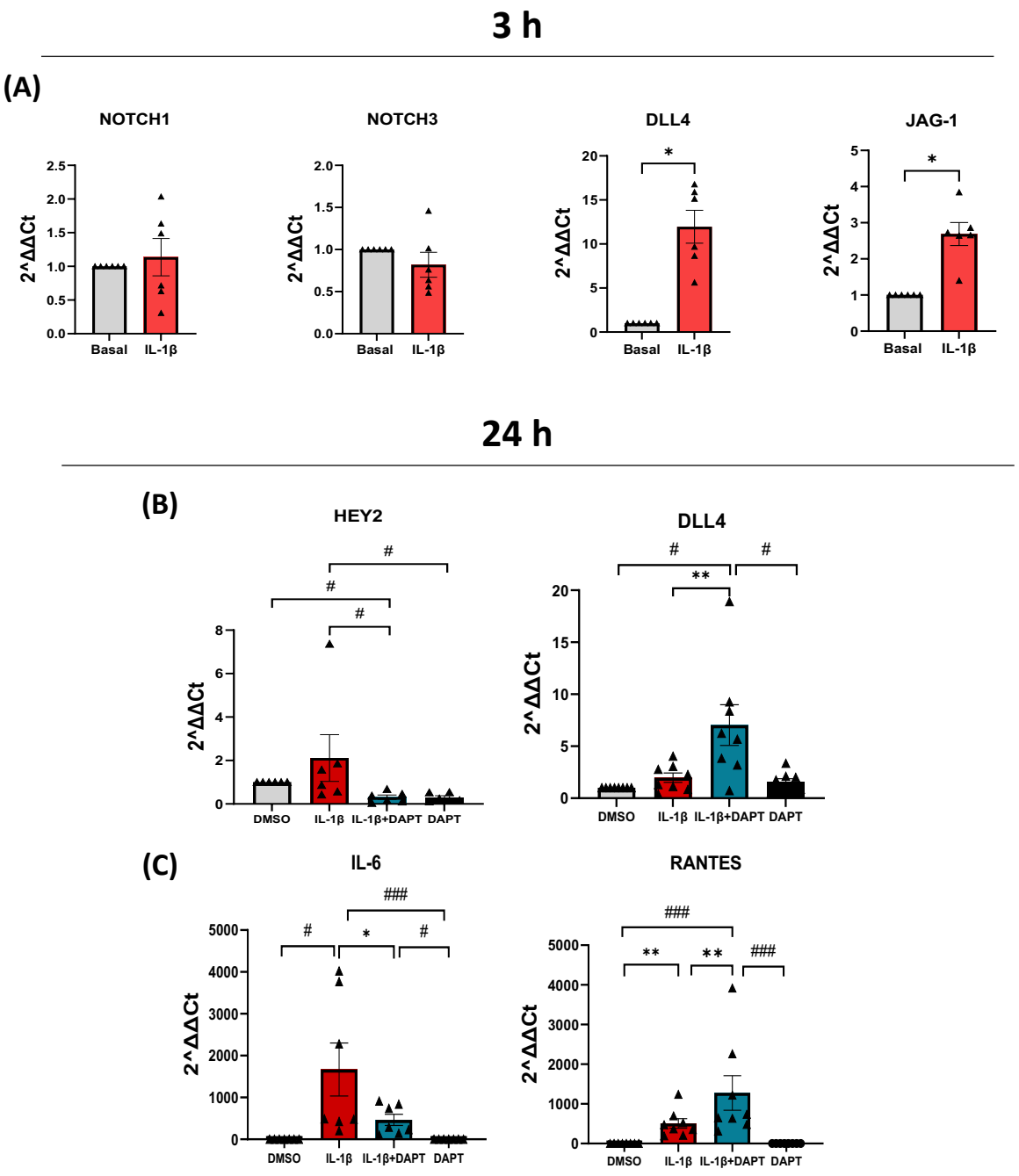

Figure 4.38: Crosstalk between dysregulated NOTCH and NFκB pathways alters FLS cytokine production.

(A) Bar graphs demonstrating gene expression of NOTCH1, NOTCH3, DLL4, and JAG-1 from FLS (n=6) treated with IL-1β (1 ng/mL) for 3 h. (B) Bar graphs demonstrating measured gene expression of HEY2, DLL4, IL-6, and RANTES from RA FLS (n= 6-8) treated with IL-1β (1 ng/mL) and DAPT (50 μM) alone or in combination for 24 h. Gene expression quantified using RT-PCR and demonstrated as fold increase compared to RPLPO endogenous control. Data represented as mean ± SEM with Wilcoxon signed rank test (*) and Friedman paired ANOVA with Dunn's multiple comparison (#) used for statistical analysis. *p<0.05, **p<0.01, #p<0.05, ##p<0.01, ###p<0.001.

4.5 Discussion:

In this chapter, differences in tissue FLS populations were identified within the synovial tissue of patients with seropositive and seronegative RA compared to HC. Furthermore, phenotypic changes in FLS subsets were also observed prior to disease onset in IAR. Histological analysis demonstrated significantly increased vascularity and cellular infiltrates in RA compared to HC, with LL cell thickness increased in RA- > RA+ compared to HC. The presence of lymphoid aggregates was exclusively identified in RA+, with no significant signs of synovitis observed for IAR. Flow cytometric analysis demonstrated increased % frequency of PDPN+ FLS in RA+ and RA- synovium compared to HC. Moreover, differences in phenotypic characterisation of PDPN+ FLS between RA and HC synovial tissue using markers for immunoregulation, adhesion, proliferation, motility/invasion, and metabolic activity was demonstrated, expression of which were also altered in relation to autoantibody status. Further stratification of FLS subtypes based on the markers CD55 (LL marker), THY-1 (SL) and FAPα+ (activation) identified enrichment in the LL subset (CD55+THY1-FAPα+) in RA- patients, while RA+ were enriched for the SL subset (CD55-THY1+FAPα+). Interestingly, analysis of these subsets demonstrated distinct functional differences associated with immune effector function, adhesion, and metabolism.

Using scRNA-seq, 14 transcriptionally distinct FLS clusters were identified between RA and HC synovial tissue. Annotation of clusters revealed 6 LL clusters demonstrating invasive, pro-inflammatory, immunoregulatory, and homeostatic/regulatory phenotypes, 4 SL clusters demonstrating pro-inflammatory and ECM remodelling/organisation phenotypes, and 4 intermediate clusters with perivascular and homeostatic/regulatory phenotypes. Frequency of clusters differed between RA and HC. Pathway analysis revealed enrichment of oxidative phosphorylation and glycolysis genes in RA vs HC. Additionally, NFκB, TGFβ, and NOTCH signaling pathways were upregulated in SL clusters enriched in RA. Receptor-ligand interaction analysis further identified ligands associated with these pathways, including IL-1β, TGFβ, and VEGF derived from T cells and/or macrophages. Proof of concept experiments in primary RA FLS demonstrated that IL-1β induced the expression of NOTCH ligands JAG-1 and DLL-4. Inhibition of NOTCH signaling significantly decreased IL-1β-induced expression of IL-6 and NOTCH downstream signaling HEY-1, yet significantly increased IL-1β-induced expression of DLL4 and RANTES.

In this chapter, differences in FLS subsets were investigated across HC, RA+, and RA- cohort. Initially, on PDPN+ FLS we observed differences in frequencies of HLA-DR+, ICAM-1+, CD61+, and pAKT+ FLS, with HLA-DR+ and ICAM-1+ enriched in RA+ and CD61+ and pAKT+ FLS enriched in RA-. Analysis of specific FLS subsets demonstrated an increase in frequency of THY1+FAPα+ FLS in RA+ compared to HC and RA-. Conversely, THY1-FAPα+ FLS were increased in

RA- compared to RA+ and HC, with the double negative THY1-FAPα- subset comparable between RA- and HC, but both were increased compared to RA+. Further stratification of the subsets demonstrated enrichment of CD55+THY1-FAPα+ in RA- compared to RA+ and HC, while CD55-THY1+FAPα+ were significantly enriched in RA+. CD55+THY1-FAPα+ displayed increased frequencies of pAKT+ FLS. This coincides with previous studies showing THY-FAPα+ were restricted to the LL, characterised by a more destructive and invasive phenotype, and associated with matrix degradation and altered metabolism (Croft *et al.*, 2019; Floudas *et al.,* 2022; Tynan *et al.,* 2023). CD55-THY1+FAPα+ were enriched in RA+ and associated with immune effector functions with increased frequencies of HLA-DR+ and ICAM-1+ FLS. This data is consistent with previous studies showing an increase in immune effector THY1+FAPα+ FLS localised to the SL in RA, that display increased HLA-DR expression, secrete elevated levels of chemokines and growth factors, and are associated with leukocyte infiltration (Mizoguchi *et al.,* 2018; Croft *et al.,* 2019; Zhang *et al.,* 2019; Alivernini *et al*., 2020; Tynan *et al*., 2023; Tynan *et al.,* 2024). This also corroborates the histological findings in this chapter, where increased vascularity and leukocyte infiltration were more closely associated with RA+ patients, whereas LL hyperplasia was more associated with RA-. Interestingly, the enriched localisation of the THY1+ FLS within the SL, and their spontaneous secretion of angiogenic growth factors, highlights their role in further promoting synovial neo-angiogenesis (Kemble and Croft, 2021; Tynan *et al.,* 2024). This bidirectional influence of synovial vessels and THY1+ FLS within the SL is further supported by eloquent studies performed by Wei *et al.* (2020) where they demonstrated SL FLS display a positional identity within the synovium that is instructed by endothelium-derived NOTCH signaling.

Interestingly, we identified differences between seropositive vs seronegative RA, suggesting that these two RA cohorts represent different pathotypes under the umbrella of RA, and phenotype and function of FLS may be influenced by autoantibody status. This is supported by studies examining PsA synovium, where THY1- FLS and CD55+ FLS were enriched in PsA, a seronegative arthropathy (Floudas *et al.,* 2022; Tynan *et al.*, 2023). Interestingly, we demonstrated comparable/reduced frequency of Cadherin11+ and PDGFRα+ FLS in RA compared to HC. Additionally, the double negative CD55-THY1-FAPα+ displayed the highest frequency of Cadherin11+ and PDGFRα+ FLS compared to LL CD55+THY1-FAPα+ subset. This contrasts with previous studies identifying increased cadherin 11 expression in the RA LL (Kiener *et al.,* 2006; Mizoguchi *et al.*, 2018). However, this observation, in addition to the reduced CD55+ FLS observed in RA+ could be the result of a breakdown in the LL protective layer in RA. Indeed, previous studies have demonstrated a depletion in LL FLS in RA compared to OA , in addition to the loss of CX_3CR1+

macrophages in RA and HC, with CX_3CR1+ critical for LL FLS and macrophage junctional interactions (Zhang *et al.,* 2023; Hanlon *et al.,* 2024).

Finally, FLS subsets were examined in IAR to gain better insights into mechanisms that might initiate inflammation within the synovium prior to disease onset. IAR demonstrated increased frequency of THY1-FAPα+ FLS compared to HC and RA+ and additionally displayed significantly increased frequency of THY1-FAP- FLS compared to RA+. Further stratification of FLS demonstrated the enrichment of the LL CD55+THY1-FAPα+ FLS in IAR. Interestingly, Hanlon *et al.* (2024) demonstrated a stepwise loss of CX_3CR1+ macrophages from HC to IAR to RA, suggesting a disruption and breakdown of the protective macrophage-LL FLS barrier prior to disease onset.

Using scRNA-seq, 14 distinct FLS clusters between RA and HC synovial tissue were identified. Of these clusters, we identified 6 LL clusters based on known LL markers previously described (Kemble and Croft, 2021; Smith *et al.,* 2023). Similarly, these LL clusters displayed increased gene expression of MMP-1 and MMP-3, consistent with their known destructive function (Mizoguchi *et al.,* 2019; Croft *et al.,* 2019). Zhang *et al.* (2023), also identified the presence of an HLA-DR+CD74+ cluster localised to the SL, which contrasts with the data observed in this chapter where the HLA-DR+CD74+ cluster was localised in the LL. The intermediate cluster LGALS1+ENO1+ had a slightly higher frequency in HC and demonstrated a homeostatic/regulatory phenotype with enrichment of MT1G, MT1X, and MT1E. This cluster aligned closely with the identified APOD+ cluster by Faust *et al.* (2024). The SL cluster VCAN+CXCL12+ enriched in RA, corresponds with other studies describing the CXCL12+ cluster as a pro-inflammatory SL cluster (Zhang *et al.,* 2019; Kemble and Croft, 2021; Smith *et al.,* 2023; Zhang *et al.*, 2023). The SL POSTN+COL3A1+ cluster enriched in RA aligns closely to POSTN+ FLS and COL3A1+ FLS identified previously, specifically with enriched expression of THY1, collagen genes, and FAPα (Marsh *et al.,* 2021; Floudas *et al.,* 2022; Micheroli *et al.*, 2022). Additionally, we identified the presence of two perivascular FLS subsets TM4SF1+VWF+ and TAGLN+NOTCH3+, the latter of which closely corresponds with previously described perivascular clusters and their association with NOTCH signaling and FLS positional identity (Wei *et al.,* 2020; Kemble and Croft, 2021; Smith *et al.,* 2023). Furthermore, Marsh *et al.* (2021) demonstrated that the SPARC3+COL3A1+ cluster, which resembles the POSTN+COL3A1+ cluster identified in this chapter, also interact with blood vessels that crosstalk via NOTCH3 signaling and TGF-β pathways.

scRNA-seq analysis also identified upregulated genes involved in the NOTCH signaling pathway, including NOTCH2, NOTCH3, ADAM10, ADAM12, and downstream targets HES4 and RBPJ in RA compared to HC, particularly enriched within the perivascular TAGLN+NOTCH3+ cluster and within RA enriched SL clusters VCAN+CXCL12+ and POSTN+COL3A1+. The NOTCH signaling

pathway is most prominently known for its role in driving angiogenesis, specifically through its regulation of tip-stalk EC differentiation (Blanco and Gerhardt, 2013). VEGF is a master regulator of angiogenesis and when bound to its receptor, VEGFR, on the tip cell, it induces expression of the NOTCH ligand DLL-4 (Roca and Adams, 2007; Gao *et al.*, 2013). In turn, DLL-4 interacts with NOTCH on a neighbouring EC, and inhibits VEGFR signaling, thus inhibiting further tip cell formation and instead promotes the stalk cell phenotype (Hellström *et al.*, 2007). Thus, this creates a lateral feedback loop that allows the leading tip cell to maintain its position as the migratory EC while the adjacent stalk cells proliferate and support sprout elongation (Hoang, Whelan, and Senger, 2004). In the context of the synovium, previous studies have demonstrated that expression of NOTCH 1IC, its ligand DLL-4, and downstream components are increased in the inflamed joint where they are localised to synovial blood vessels and regulated by hypoxia and the complimentary action of VEGF/Ang2 (Gao *et al.,* 2012; Gao *et al.,* 2013; Choe *et al.,* 2016). Wei *et al.* (2021) recently demonstrated a critical role for NOTCH3 signaling in the differentiation of perivascular and SL (THY-1+) FLS in the RA synovium. Through scRNA-seq and spatial gradients they demonstrated upregulation of NOTCH3 and NOTCH1 target genes in RA FLS and found that these signatures initiated FLS emanating from the vascular ECs (Wei *et al.,* 2021). Furthermore, NOTCH signaling is known to mediate FLS migratory and invasive functions, and induce anti-apoptotic pathways (Gao *et al.,* 2015; Biniecka *et al.,* 2016; Wei *et al.,* 2020; Chen *et al.,* 2021). Similar to the role of NOTCH signaling in EC, the lateral inhibition in FLS may also influence the guiding of the FLS gradient initiated at the endothelium, where they transition from perivascular SL THY1+ FLS, through several intermediate FLS states, to finally LL THY1- FLS (Wei *et al.*, 2020).

Receptor-ligand interactions of FLS with either T cells or macrophages demonstrated TGF-β and VEGF ligands derived from T cells and IL-1β, VEGF, and TGF-β derived from macrophages interact with receptors on FLS. Previous studies have also demonstrated the presence of TGF-β, and VEGF in the synovial membrane and synovial fluid of early RA (Fearon *et al.,* 2003). In primary RA FLS, IL-1β induced NOTCH ligands DLL-4 and JAG-1. Furthermore, NOTCH inhibition with DAPT, led to a significant reduction in downstream target HEY2, in addition to inhibition of IL-1β-induced expression of IL-6 (Fischer *et al.,* 2004). Crosstalk mechanisms between the NOTCH signaling pathway and the NF-κB pathway have been previously described (Cheng *et al.,* 2001; Moran *et al*., 2007; Osipo *et al.,* 2008; Espinosa *et al.,* 2010; Jin *et al*., 2012; Ferrandino *et al*., 2018). Indeed, identified NOTCH downstream signaling targets include several subunits of the NF-κB pathway (Cheng *et al.,* 2001). Within the synovium, complex signaling interactions between NFκB, NOTCH, JAK-STAT signaling, and metabolic pathways in RA FLS have been demonstrated (Gao *et al.,* 2013; Gao *et al.,* 2015; Biniecka *et al.,* 2016). Additionally, studies conducted in B cells demonstrated

upregulation of NOTCH ligand JAG-1 by NFκB suggesting NFκB can also modulate NOTCH signaling (Bash *et al.,* 1999).

In summary, we have identified distinct FLS subsets via flow cytometry and scRNA-seq between HC and RA. Stratification of flow cytometric analysis demonstrated phenotypic differences in RA+ and RA- FLS, with RA- FLS demonstrating similar characteristics to FLS previously described in PsA. FLS clusters identified in scRNA-seq demonstrate similar findings to that of previous studies, in addition to the similar enrichment of key signaling pathways including TGFβ, NFκB, and NOTCH3 signaling. Analysis also demonstrated early phenotypic changes of FLS in IAR, suggesting that even though clinical signs of disease are not present, FLS are already pre-programmed for a pathogenic phenotype. Better understanding of the heterogeneity of FLS subsets and the complexity of the RA synovial tissue landscape, in addition to understanding the unique pathogenic phenotypes between RA+ and RA-, will lead to better tailored treatments for patients and prediction of treatment response.

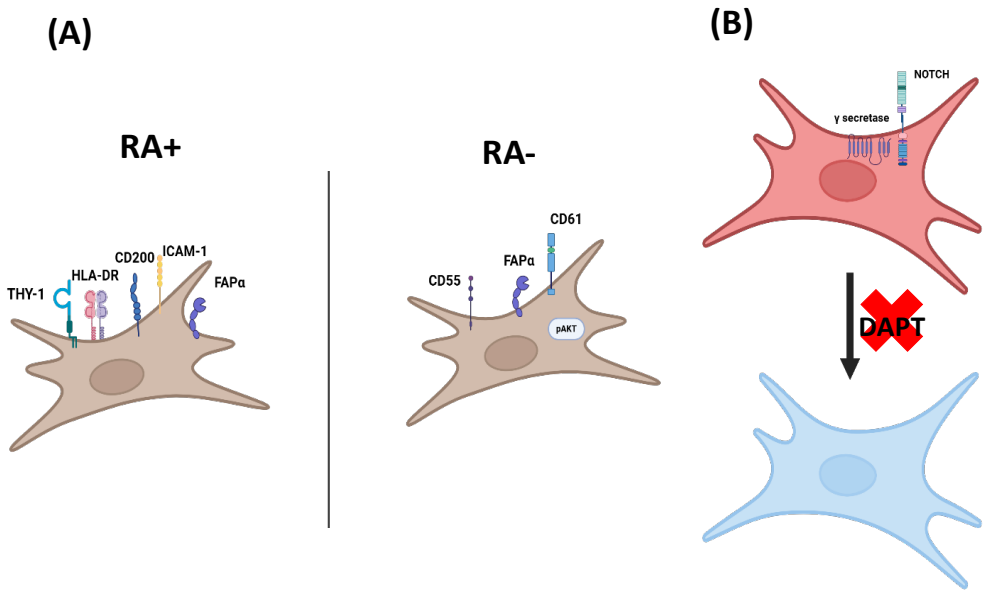

Figure 4.39: Summary of RA FLS Subsets and Therapeutic Effects of NOTCH pathway blockade.

Summary figure of (A) FLS subsets found in RA+ and RA- biopsy samples. RA+ FLS demonstrated increased % frequencies of activated SL FLS (THY-1), in addition to increased % frequencies of immunoregulatory molecules (HLA-DR; CD200) and adhesion molecule ICAM-1. RA- FLS demonstrated increased % frequencies of activated LL FLS characteristics with increased metabolic activity (pAKT) and adhesive properties (CD61). (B) Representative schematic demonstrating that DAPT, a γ secretase inhibitor, blocks NOTCH signaling in RA FLS mitigating their pathogenic effects. (Image created in BioRender 2025).

CHAPTER FIVE:

Circulating Endothelial Cells and Epithelial Progenitor Cells in the Circulation of Patients with Rheumatoid Arthritis and Individuals-At-Risk

5.1 Introduction:

Cardiovascular disease (CVD) is the most common comorbidity and cause of mortality in RA (Kłodziński and Wisłowska, 2018; DeMizio and Geraldino-Pardilla, 2020). Indeed, patients with RA have a greater risk of developing CVD compared to the general population (Fazeli *et al.*, 2021; Hansildaar *et al.*, 2021), with young seropositive RA patients at a particularly higher risk (Gkaliagkousi *et al.*, 2012). Similarly, risk of CVD is increased for active RA disease compared to those in remission (Gkaliagkousi *et al.*, 2012). Moreover, approximately 30-40% of the total mortality observed in RA can be attributed to complications of cardiovascular events, especially in patients that exhibit a high proinflammatory burden and long-standing disease (Sihvonen *et al.*, 2004; Young *et al.*, 2007; Gkaliagkousi *et al.*, 2012; Ven den Hoek, *et al.*, 2017). Due to the high prevalence of CVD amongst patients with RA, EULAR recommended that the risk value determined by the Systemic Coronary Risk Evaluation (SCORE) scoring system should be multiplied 1.5 times for patients who exhibit at least two of the following: a disease duration greater than ten years, seropositivity for RF and/or ACPA, and the presence of extraarticular manifestations (Peters *et al.*, 2010; Martin-Martinez *et al.*, 2014; Meyer *et al.*, 2018).

Under normal physiological conditions, the endothelium is responsible for modulating vascular permeability, coagulation, facilitating gas and fluid exchange, vasodilation, and is overall considered quiescent (von Zonneveld *et al.*, 2010). While new blood vessel formation at the site of inflammation 'the synovium' is a hallmark and prominent feature of RA (Akhavani, Larsen, Paleolog, 2007), systemic EC dysfunction and altered blood flow have also been implicated in RA and are early indicators of development of atherosclerosis or other CVD events (Deanfield *et al.*, 2005; Chatterjee Adhikari *et al.*, 2012; Jamil *et al.*, 2021). Studies have also shown that increased vessel stiffness, vascular remodelling, and carotid intima media thickness are associated with measures of inflammation and T-cell trafficking in RA (Liuzzo *et al.*, 2000; Umehara *et al.*, 2004; Gonzalez-Gay *et al.*, 2005; Pahor *et al.*, 2006; Hannawi *et al.*, 2007; Dumitriu *et al.*, 2012). Thus, both systemic and local synovial EC dysfunction play a role in RA pathogenesis and co-morbidities.

Dysfunctional vascular regeneration has been proposed as one of the critical mechanisms predisposing individuals with RA to CVD (van Zonneveld *et al.*, 2009). However, the concept of vascular damage having a critical role in RA pathogenesis is not a new one. In 1982, the 'vascular hypothesis' proposed that there are alterations that take place in the function and anatomy of the endothelial microvasculature due to the hypoxic state. Studies have suggested that a compromised microvasculature, in conjunction with increased metabolic needs of the synovial tissue, could potentially initiate tissue injury (via anoxia and acidosis), thus leading to vascular permeability, release of hydrolytic enzymes, and inflammatory acceleration (Rothschild, 1982).

The endothelial lining of blood vessels additionally has an important role in the pathogenesis of atherosclerosis (Akhavani, Larsen, and Paleolog, 2007). In fact, endothelial dysfunction is the rate limiting factor for atherosclerosis development (van Zonneveld *et al.*, 2009), associated not only with site of injury, but also facilitating leukocyte adhesion and migration (Akhavani, Larsen, and Paleolog, 2007).

Chronic systemic inflammation or even a moderate inflammatory stimulus can cause vascular dysfunction and increasing CVD risk. Though CVD comorbidity has been connected to multiple autoimmune rheumatic diseases, this relationship has been most extensively investigated in RA. Indeed, it has been elucidated that RA is an independent risk factor for early and accelerated atherosclerosis (Gerli *et al.*, 2004; Del Rincón *et al.*, 2007; Gkaliagkousi *et al.*, 2012; Majka *et al.*, 2017). Coronary atherosclerosis was found to be more prevalent in patients with RA compared to controls. Additionally, it was ascertained that these RA patients with atherosclerosis also had increased prevalence of hypertension, were older, and had fewer endothelial progenitor cells (EPCs) compared to those without atherosclerosis (Yiu *et al.*, 2010). In fact, there is a significant correlation between atherosclerosis (when measured as increased carotid artery intima-media thickness) and levels of acute phase response markers CRP and ESR (Del Rincón *et al.*, 2003).

Investigations focused CVD pathogenesis in RA have demonstrated increased systemic levels of proinflammatory cytokines IL-1β, IL-6, TNFα, and IFN-γ (Dessein *et al.*, 2013; Beinsberger, Heemskerk, and Cosemans, 2014; Meyer *et al.*, 2018). Additionally, increased binding of neutrophils, monocytes, and platelets to the endothelium via IL-8 and CCL2 have also been observed (Beinsberger, Heemskert, and Cosemans, 2014; Meyer *et al.*, 2018). Factors associated with EC dysfunction in RA include the shared epitope alleles: HLA-DRB1*04 and HLA-DRB1*0404, impaired NO release, high CRP levels, obesity, release of pro-fibrotic agents NO, prostaglandins, MMPs and chemokines receptors associated with T-cell trafficking (Gonzalez-Juanatey *et al.*, 2003; Dessein, Joffe, and Singh, 2005; Arosio *et al.*, 2007; Rodríguez-Rodríguez *et al.*, 2011; Petra *et al.*, 2019; Kerola, Rollefstad, and Semb, 2021). Studies have also shown that increased vessel stiffness is associated with ICAM-1 and VCAM-1 levels in RA (Dessein, Joffe, and Singh, 2005). Furthermore, vascular remodelling and carotid intima media thickness is linked to increased inflammation including raised CRP (Gonzalez-Gay *et al.*, 2004) and DAS28 (Dupont *et al.*, 2024), in addition to increased frequency of CD4+/CD28+ T lymphocytes and chemokine receptors (Liuzzo *et al.*, 2000; Pingiotti *et al.*, 2007).

Circulating endothelial cells (CECs) have become a well-established indicator of vascular damage and risk factor for CVD development (Boos, Lip, and Blann, 2006; Farinacci *et al.*, 2018).

In addition to CVD, their presence has been briefly investigated and described in autoimmune and rheumatic diseases such as vasculitis, Systemic Sclerosis (SSc), and SLE (Woywodt *et al.*, 2003; Del Papa *et al.*, 2004; Rodríguez-Carrio *et al.*, 2012; Di Martino *et al.*, 2021). Preliminary research conducted on CECs in the context of RA have demonstrated elevated frequency of these cells within the vasculature compared to controls (Foster *et al.*, 2009; Rodriguez-Carrio *et al.*, 2012; Cafaro *et al.*, 2022)).

Endothelial progenitor cells (EPCs) have the ability to mature into ECs and are believed to arise from the bone marrow (Blann and Pretorius, 2006). EPCs have been investigated more extensively in the literature with most studies reporting EPCs as having a protective role and the capacity for vascular repair (Blann and Pretorius, 2006; Akhavani *et al.*, 2007; Edwards *et al.*, 2018). EPC involvement in autoimmune diseases has also been a topic of interest (Feugray *et al.*, 2023). For example, one study observed higher numbers of EPC as well as endothelial microparticles (EMP) in patients with Sjogren's Syndrome compared to controls, however, EPCs were inversely correlated with disease duration from symptoms (Bartoloni *et al.*, 2015). The few studies that have examined EPCs in RA demonstrated a reduction of EPC numbers in RA patients compared to controls (Akhavani *et al.*, 2007; Park *et al.*, 2014; Carafo *et al.,* 2022). Additionally, it has been demonstrated that frequency of EPCs negatively correlated with high disease activity, disease duration, age, and serum CXCL12 levels (Park *et al.*, 2014).

However, to the best of our knowledge CECs, especially in the context of RA, have never been phenotypically characterised. Furthermore, to date, little is known regarding the differences in both CECs and EPCs in seropositive and seronegative patients and whether these cells are present prior to disease onset in IAR. Therefore, the aim of this chapter is to identify the presence of CECs and EPCs in patients with RA and determine if these cells are increased prior to the onset of clinical symptoms. Moreover, we aim to phenotypically characterise the CECs and determine any differences in marker expression between HC and RA. Finally, serum levels of markers associated with inflammation, vascular damage, and metabolic function will be measured to further assess the degree of vascular damage within RA and identify potential biomarkers for disease pathogenesis.

5.2 Specific Aims for this Chapter:

- To identify and compare frequencies of CECs in PBMCs of RA versus HC.
- To phenotypically characterise CECs and determine whether they exhibit a more pathogenic phenotype in RA.
- To investigate whether CECs are present prior to onset of clinical symptoms.
- To analyse soluble pro-inflammatory, vascular, and metabolic markers to potentially identify biomarkers for elevated CV risk in RA patients and IAR.

5.3 Materials and Methods:

5.3.1. Patient Recruitment and Sample Collection

RA patients, IAR, and ART were recruited and defined according to the revised ACR/EULAR criteria (Aletaha *et al.*, 2010) and as previously outlined in Section 3.3.1, Chapter 3. Healthy blood, used as comparison, was also obtained from anonymous healthy control (HC) donors. In addition, blood serum from patients with Psoriatic Arthritis (PsA) and Giant Cell Arteritis (GCA) were also obtained as disease comparators. All patient cohorts provided fully informed written consent for the use of biological samples and medical information approved by the St Vincent's University Hospital, Ethics and Medical Research Committee prior to inclusion. Research was performed in accordance with the guidelines and regulations of the Declaration of Helsinki.

5.3.2 Peripheral Blood Mononuclear Cell Isolation

Blood was obtained from RA patients, IAR, and ART either at time of arthroscopy or from rheumatology research outpatient clinics. HC donor blood was obtained continuously from volunteers. Blood was collected and PBMC isolated from all cohorts as outlined in Section 3.3.4, Chapter 3. Clinical information of patients with RA at time of collection of blood samples (n=39) used for PBMC isolation can be found in Table 5.1 and as previously described in Table 3.2 in Section 3.3.2, Chapter 3.

Characteristics	Number or Average	Percent or Range
Age (years)	53.4	19-78
Female	30	76.9% (30/39)
Seropositive (ACPA+ and/or RF+)	**23**	**59% (23/39)**
RF positive	23	59% (23/39)
ACPA positive	20	51.3% (20/39)
Seronegative	16	41% (16/39)
Disease duration (years)	5.6	<1-22
DAS28 score	3.41	1.24-6.18
CRP	9.6	0-81.5
On DMARD	20	51.3% (20/39)
On biologic	9	23.1% (9/39)
Treatment naïve	10	25.6% (10/39)

Table 5.1: **Patient demographics for RA PBMCs used for flow cytometry analysis.**
Anti-citrullinated protein antibodies (ACPA), Rheumatoid Factor (RF), Disease Activity Score (DAS), C-Reaction Protein (CRP) Disease-modifying anti-rheumatic drug (DMARD).

Characteristics	Number or Average	Percent or Range
Age (years)	31	23-49
Female	6	75% (6/8)

Table 5.2: Demographics for HC PBMCs used for flow cytometry analysis.
N=9* for HC donors analysed for CEC analysis. *Demographic information is missing for 1 donor.

5.3.3 Serum Isolation and Preparation

Separate blood samples from HC donors, IAR, ART, RA, PsA, and GCA patients at time of blood draw for PBMC collection were obtained and collected in anticoagulant-free tubes and processed within 1 h of collection as follows: samples were centrifuged at 2,000 g for 10 min at room temperature to isolate serum and subsequently aliquoted into cryovials and stored at -80°C until required for further analysis.

5.3.4 Flow Cytometry

Expression of cell surface markers (CD45-PDPN-CD146-CD31+) was assessed using flow cytometry to identify CECs. Expression of cell surface markers (PDPN-CD45dimCD34+CD133+CD31+) was assessed using flow cytometry to identify EPCs. For PBMC samples, 4 million cells were stained.

PBMCs were thawed and stained in a 96-well round bottom plate using the fluorochrome-conjugated antibodies listed in Table 5.2. Cells were suspended in viability dye of LiveDead Zombie NIR (Biolegend) in PBS at a 1:3000 dilution for 30 min in the dark at 4°C. Subsequently, cells were topped up with PBS and centrifuged at 1400 rpm for 3 min and washed a second time. Samples were resuspended and blocked in a solution of 5 µL Human TruStain FcX (Biolegend) and 95 µL PBS for 10 min to eliminate nonspecific binding to the FcγR. Extracellular fluorochrome-conjugated antibodies were added, and samples were vortexed and incubated for 30 min in the dark at 4°C. Samples were then washed with FACS Buffer (Dulbecco's PBS without Mg2+ or Ca2+ (Sigma-Aldrich), 2% heat-inactivated FBS (Biosciences) and 0.05% sodium azide (Sigma-Aldrich), 0.5 M EDTA, pH 7.4-7.6) and centrifuged at 1400 rpm for 3 min. Supernatants were removed, samples washed a second time. The FoxP3/Transcription Factor Staining Buffer Set (Invitrogen, USA) was utilised for intracellular staining. After the second wash, samples were resuspended in 100 µL Fix/Perm Solution (diluted 1:4 in kit diluent) and left to incubate for 30 mins in the dark at 4°. Samples were washed with Perm Buffer, resuspended with 30 µL Perm Buffer and intracellular antibodies, and left to incubate for 30 min in the dark at 4°C. Samples were washed twice with Perm Buffer and FACs respectively and resuspended in 250 µL FACs. Samples were acquired using the Aurora Flow Cytometer (Cytek Biosciences) and analysed using FlowJo software (FlowJo LLC, Oregon, USA).

Cells were gated based on forward and side scatter and doublets and dead cells were removed. Live/Dead Zombie NIR viability dye (Biolegend) was utilised to discern and remove dead cells. To account for spectral overlap from the detection lasers, single-stained compensation beads (BD) were prepared for each fluorochrome (cells were utilised for unstained and live/dead control) and compensation applied. Samples were spectrally unmixed directly on the Aurora flow cytometer before each run. FMO gating controls were applied to determine gating boundaries of markers when needed and where appropriate.

The markers analysed allowed for (1) the exclusion of other cell types that may be included in the sample and (2) the identification of EPC and CEC cells and their functional phenotype:

- **CEC Identification:** Exclusion of haematopoietic cells (CD45+), PRIME cells (PDPN+), pericytes (CD146+), and inclusion of CD31+ for CECs.
- **EPC Identification:** Exclusion of PRIME cells (PDPN+), immune cells (CD45+), and inclusion of precursor markers CD34+ and CD133+ and endothelial marker CD31+ for EPCs.
- **CEC subset marker (microvascular):** CD36

- **CEC adhesive markers:** VCAM-1, ICAM-1, CD44, CD61, Cadherin11
- **CEC immune markers:** HLA-DR, CD200, CD200R1, CD55
- **CEC metabolic markers:** pAKT, pmTOR, pS6
- **CEC proliferative/invasive markers:** Ki67, YAP, PDGFRα
- **CEC activation markers:** FAPα, THY-1

Antibody	Fluorochrome	Clone	Company
HLA-DR	BV421	L243	Biolegend
CD133	SuperBright436	TMP4	Bioscience (Thermo)
CD200	eFlour450	OX104	Invitrogen;eBioscience
VCAM-1 (CD106)	BV480	51-10C9	BD
CD34	BV510	581	Biolegend
CD31	BV605	WM59	Biolegend
Ki67*	BV650	11F6	Biolegend
CD146	BV711	P1H12	BD
THY-1 (CD90)	BV750	5E10	BD
CD44	BV785	IM7	Biolegend
CD36	FITC	5-271	Biolegend
CD45	AF532	HI30	Invitrogen;eBioscience
CD61 (Integrin β3)	PerCP	VI-PL2	Biolegend
pS6 (Ser235, Ser236)*	PerCP/Cy5.5	A17020B	Biolegend
ICAM-1 (CD54)	PerCP-eFluor710	HA58	Invitrogen;eBioscience
YAP*	PE	D8H1X	Cell Signaling
pAKT*	PE-CF594	M89-61	BD
CD140α (PDGFRα)	PE/Cy5	APA5	Biolegend
CD200R1	PE/Cy5.5	OX108 (Chimeric)	NOVUS
Cadherin 11	PE/Cy7	16G5	Biolegend
CD55	APC	JS11	Biolegend
pmTOR*	AF647	O21-404	BD
FAPα	AF700	427819	Novus
Podoplanin	APC-Fire750	NC-08	Biolegend

Table 5.3: **Panel of fluorochrome antibodies used for flow cytometry analysis of CEC and EPC in PBMC samples.** *Indicates intracellular stains.

5.3.5 MSD Multiplex Assay

Serums from HC donors, IAR, ART, RA, PsA, and GCA patients were thawed and spun down for 20 mins at 2000 g before sample dilution preparation to ensure no solid particulates in the serum were included. To assess the circulating levels of cytokines in patient blood compared to HC, protein concentrations of IFN-γ, IL-1β, IL-2, IL-4, IL-6, IL-8, IL-10, IL-12p70, IL-13, and TNFα were measured by multiplex cytokine panel V-PLEX Pro-Inflammatory Panel assay (Meso Scale Discovery, USA). The assay was performed following the manufacturer's instructions. To ensure cytokine measurements fell within the range of detection, all samples were prepared in a 1:2 dilution. Cytokine standards varied but ranged from 0.04-938 pg/mL.

To assess serum levels of markers for vascular damage in patients compared to HC, protein concentrations of CRP, ICAM-1, SAA, VCAM-1, and Factor VII were measured by the multiplex panel assay U-PLEX Vascular Injury Combo 1 (human) (Meso Scale Discovery, USA) according to the manufacturer's instructions. Samples were diluted 1:2000 for HC samples, 1:5000 for IAR, ART, and GCA samples, and 1:8000 for RA and PsA samples to ensure readings would fall within the detection range of the standards. The range of standards for the vascular injury markers were 0.92-2170 pg/mL (CRP), 0.11-1930 pg/mL (ICAM-1), 1.60-16,000 pg/mL (SAA), 7.78-20,500 pg/mL (VCAM-1), 0.60-6000 pg/mL (Factor VII).

To determine altered metabolic states between patients and HC, concentrations of metabolic markers, C-peptide, GLP-1 (active), GIP (active), Insulin, Glucagon, Leptin, and PP were measured by the multiplex metabolic panel V-PLEX Metabolic Combo 1 (human) assay (Meso Scale Discovery, USA) as per the manufacturer's instructions. Sample dilutions were prepared as follows: 1:2 for HC, 1:3 for IAR, ART, and GCA, and 1:5 for RA and PsA samples to levels fell within the detection range. Metabolic standards varied for each marker: 4.72-3150 pg/mL (C-peptide), 0.233-390 pg/mL (GIP active), 0.011-39 pM (GLP-1 active), 0.015-52 pM (Glucagon), 0.006-19.5 µIU/ml (Insulin), 5.78-7150 pg/mL (Leptin), 0.043-325 pg/mL (PP). Furthermore, additional metabolic markers: Clusterin, CRP, DPPIV, NGAL/LCN2, SHBG, STfR-1, ApoA1, ApoC3, Adiponectin, and RBP4 were measured by the U-PLEX Metabolic Combo 2 (human) multiplex assay (Meso Scale Discovery, USA) in accordance with the manufacturer's instructions. Sample dilutions were as follows: 1:2000 for HC, 1:5000 for IAR, ART, and GCA, and 1:8000 for RA and PsA samples. The detection range for each standard were as follows: 1.46-5000 pg/mL (Adiponectin), 4.93-25,000 pg/mL (ApoA1), 1.06-10,000 pg/mL (ApoC3), 57.7-500,000 pg/mL (Clusterin), 0.92-2170 pg/mL (CRP), 0.85-7000 pg/mL (DPPIV), 0.78-4000 pg/mL (NGAL/LCN2), 3.78-4000 pg/mL (RBP4), 3.52-25,000 pg/mL (SHBG), and 0.29-3000 pg/mL (STfR-1).

Additional markers of interest Calbindin, Clusterin, KIM-1, Osteoactivin, TFF3, and VEGF were measured in serum by the T-PLEX Kidney Injury Panel 3 (human) multiplex assay according to the manufacturer's instructions. Sample dilutions were as follows: 1:15 for HC, 1:20 for IAR, ART, and GCA, and 1:40 for RA and PsA samples to ensure values fell with the standard detection range. Detection range for each standard were 5.96-24,400 pg/mL (Calbindin), 46.88-192,000 pg/mL (Clusterin), 4.66-19,100 pg/mL (KIM-1), 9.25-37,900 pg/mL (Osteoactivin), 0.46-1890 pg/mL (TFF3), 0.57-2320 pg/mL (VEGF). Electrochemiluminescence of all markers across all assays was measured using the MSD Sector Imager 2400.

Characteristics	Number or Average	Percent or Range
Age (years)	54.9	19-78
Female	26	68.4% (26/38)
Seropositive (ACPA+ and/or RF+) **RF positive** **ACPA positive**	**22** 22 20	**57.9% (22/38)** 57.9% (22/38) 52.6% (20/38)
Seronegative	16	42.1% (16/38)
Disease duration (years)	5.1	<1-22
DAS28 score	3.35	1.24-6.18
CRP	12.54	0-81.5
On DMARD	21	55.3% (21/38)
On biologic	8	21% (8/38)
Treatment naïve	9	23.7% (9/38)

Table 5.4: Patient demographics for RA serums used for MSD analysis.
Anti-citrullinated protein antibodies (ACPA), Rheumatoid Factor (RF), Disease Activity Score (DAS), C-Reaction Protein (CRP) Disease-modifying anti-rheumatic drug (DMARD).

Characteristics	Number or Average	Percent or Range
Age (years)	40.4	23-73
Female	8	72.7% (8/11)

Table 5.5: Demographics for HC serums used for MSD analysis.
N=15* for HC donors used for MSD assay. *Demographic information missing for 4 individuals.

5.3.6 Principal component analysis (PCA), Bi-plot and String analysis.

PCA and biplots were generated using GraphPad Prism. STRING software was subsequently used to generate visual representations of the direct (physical) and indirect (functional) protein-protein interactions of the soluble markers (Szklarczyk et al., 2019).

5.3.7 Statistical Analysis

Statistical analyses were performed using GraphPad Prism 9.5.0 software. Unpaired Mann Whitney U test or Kruskal-Wallis ANOVA was used for analysis of non-parametric data. P-values of less than 0.05 (*$p<0.05$) were determined as statistically significant. Data was expressed as mean ± SEM.

5.4 Results:

5.4.1 Identification of CECs in the circulation of RA patients

There is strong evidence of a connection between RA and risk of developing CVD. It has been proposed that the chronic systemic inflammation experienced by patients with RA can exacerbate vascular damage, thus increasing risk for atherosclerosis and other CVD development. CECs have become a well-established biomarker for vascular damage and predictor for CVD, however, information regarding these cells in the context of RA is still limited. In this chapter, we aim to identify and phenotypically characterise CECs in the circulation of RA patients compared to HC donors and determine whether their presence predates clinical onset. To accomplish this, PBMCs were isolated from bloods collected from HC and patients with RA as well as from IAR and ART. PBMCs were viably frozen to allow for flow cytometry analysis in batches. PBMCs were stained using a panel of markers (see Table 5.2) to allow for the identification of CECs (while excluding other cell populations), and to assess the frequency and functional phenotype of these cells.

Following the exclusion of debris, doublets, and dead cells, CECs were identified based on the populations with negative expression of CD45 (to exclude haematopoietic cells), PDPN (PRIME/mesenchymal cells), CD146 (pericytes), and positive expression of CD31 (Figure 5.1 (A)-(G)). Additional phenotyping of CECs was based on the expression of markers for proliferation and metabolic activity (Ki67, pAKT, pmTOR), wound healing/cytoskeletal rearrangement (PDGFRα, YAP), pathogenic activation (FAPα, THY-1), immunoregulation (HLA-DR, CD200, CD200R1, CD55), and adhesion (ICAM-1, VCAM-1, CD61, cadherin 11, CD44) as outlined in Table 5.2. Analysis of CECs identified increased frequency (as a percentage of live cells) in the circulation of RA patients (n=39) compared to HC donors (n=9) as demonstrated by representative flow cytometric dot plots (Figure 5.2 (A)) and graph (Figure 5.2 (B)), however this was not statistically significant.

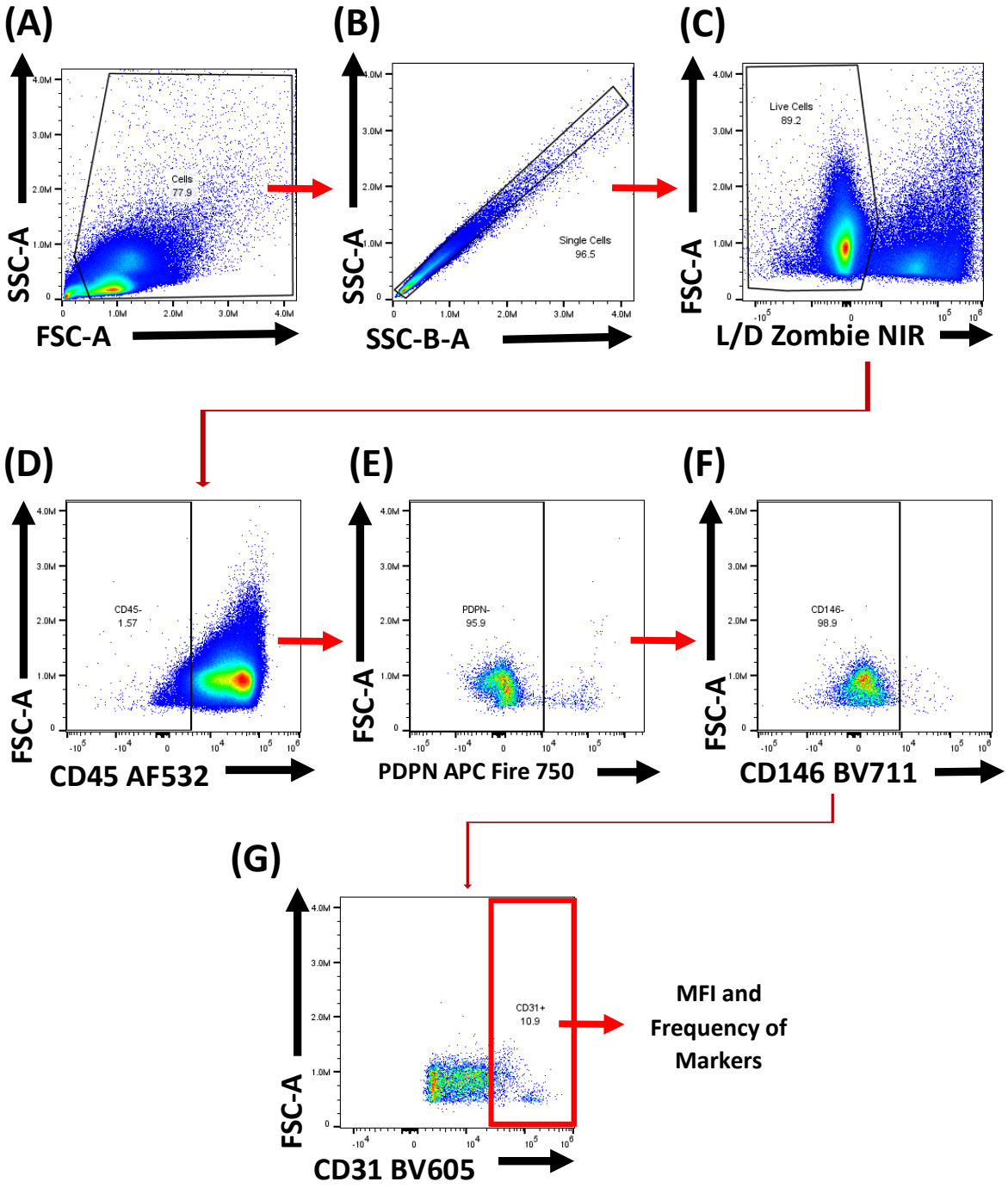

Figure 5.1: Peripheral blood Circulating Endothelial Cell (CEC) gating strategy.

Thawed PBMCs from HC donors, IAR, ART, and RA were stained with a panel of fluorochrome antibodies (see Table 5.2). Representative dot plots depicting the gating strategy used to identify and characterise CECs from the circulation. (A-C) Forward and side scatter parameters established for cells before exclusion of doublets and dead cells. (D-G) CECs were identified as CD45-PDPN-CD146-CD31+ and further characterised by expression of intracellular and extracellular markers.

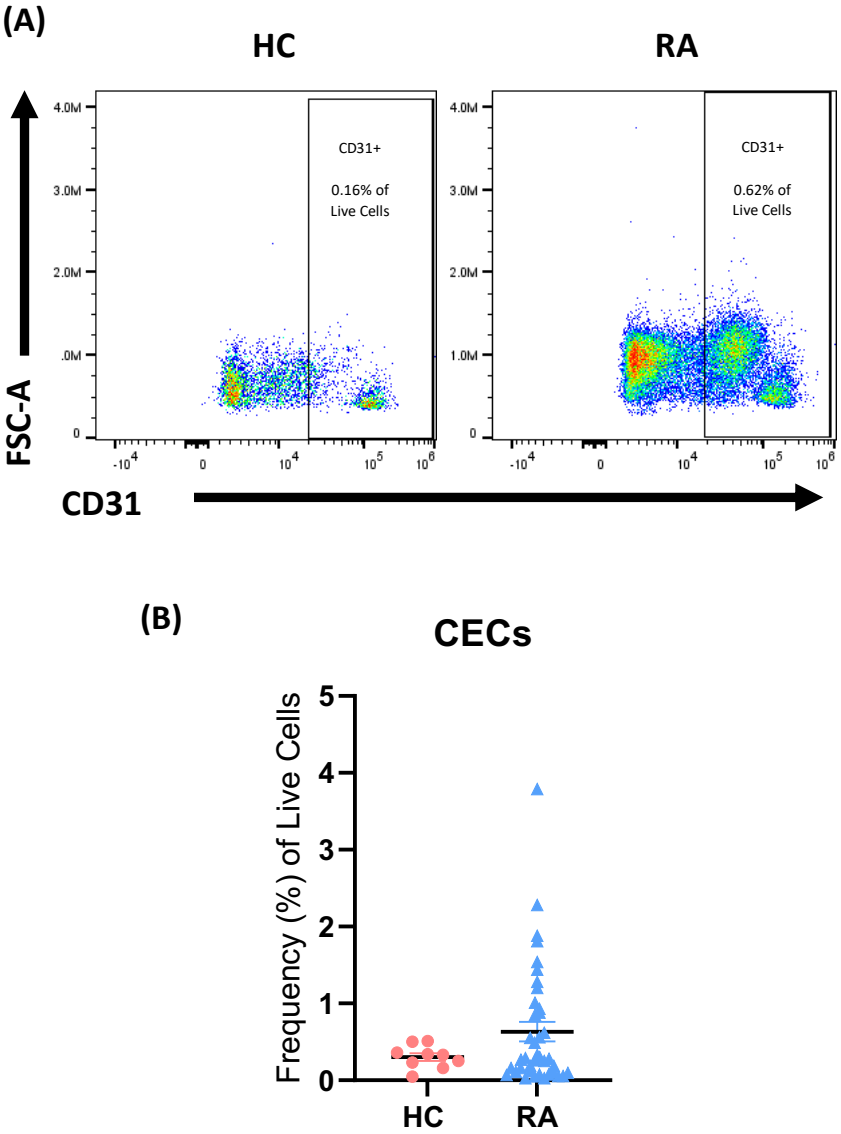

Figure 5.2: Identification of CECs in RA peripheral blood compared to HC.

(A) Representative flow cytometric dot plots for the identification of CD45-PDPN-CD146-CD31+ CECs within the PBMCs from the peripheral blood of HC donors and RA patients (includes RA+ and RA-). (B) Dot plot demonstrating the significant increase of frequency of CECs in RA (n=39) compared to HC (n=9). Data represented as mean ± SEM frequency of total live cells, with each symbol representing a different sample.

5.4.2 CECs have the capacity to proliferate further and are metabolically active

It has been questioned whether CECs are viable cells just before shedding from the endothelium and whether they remain viable afterwards, or if these cells are pre-necrotic/pre-apoptotic and are merely an indicator of damage (Blann and Pretorius, 2006). To further explore this, we sought to determine the proliferative, metabolic, and remodelling characteristics of CECs. Approximately half of HC CECs (mean 56.49±7.989) were positive for the proliferation marker Ki67 with RA demonstrating an increased % frequency for Ki67+ CECs (mean 63.03±4.245) as shown by representative dot plots and % frequency bar graph (Figure 5.3 (A-B)). Moreover, RA CECs demonstrated an elevated expression of Ki67 compared to HC ($p=0.0759$) (Figure 5.3 (C)). This increased expression is further illustrated by the shift in median fluorescence intensity (MFI) of Ki67 depicted in the representative histogram plots (Figure 5.3 (D)). In addition, a proportion of both RA and HC CECs expressed metabolic markers pAKT and pmTOR (Figure 5.4). Similar percent frequencies were observed between RA patients and HC for both markers (Figure 5.4 (A)); however, interestingly, RA CECs demonstrated a trending decrease in pAKT and pmTOR MFI (Figure 5.4 (B)).

A substantial proportion of CECs in both RA and HC were positive for PDGFRα as demonstrated by the representative dot plots (Figure 5.5 (A)) with no significant differences in frequency observed (Figure 5.5 (B)). However, PDGFRα MFI was markedly decreased on RA CECs compared to HC (Figure 5.5 (C)), further demonstrated by the representative histogram plots (Figure 5.5 (D)). A similar trend was observed for YAP, where no difference in % frequency was observed between RA and HC (Figure 5.5 (F)). A trending decrease in the expression of YAP was also demonstrated in RA CECs compared to HC (Figure 5.5 (G-H)), however, it should be noted that only a small % of CECs positively expressed YAP as depicted by the representative dot plots (Figure 5.5 (E)).

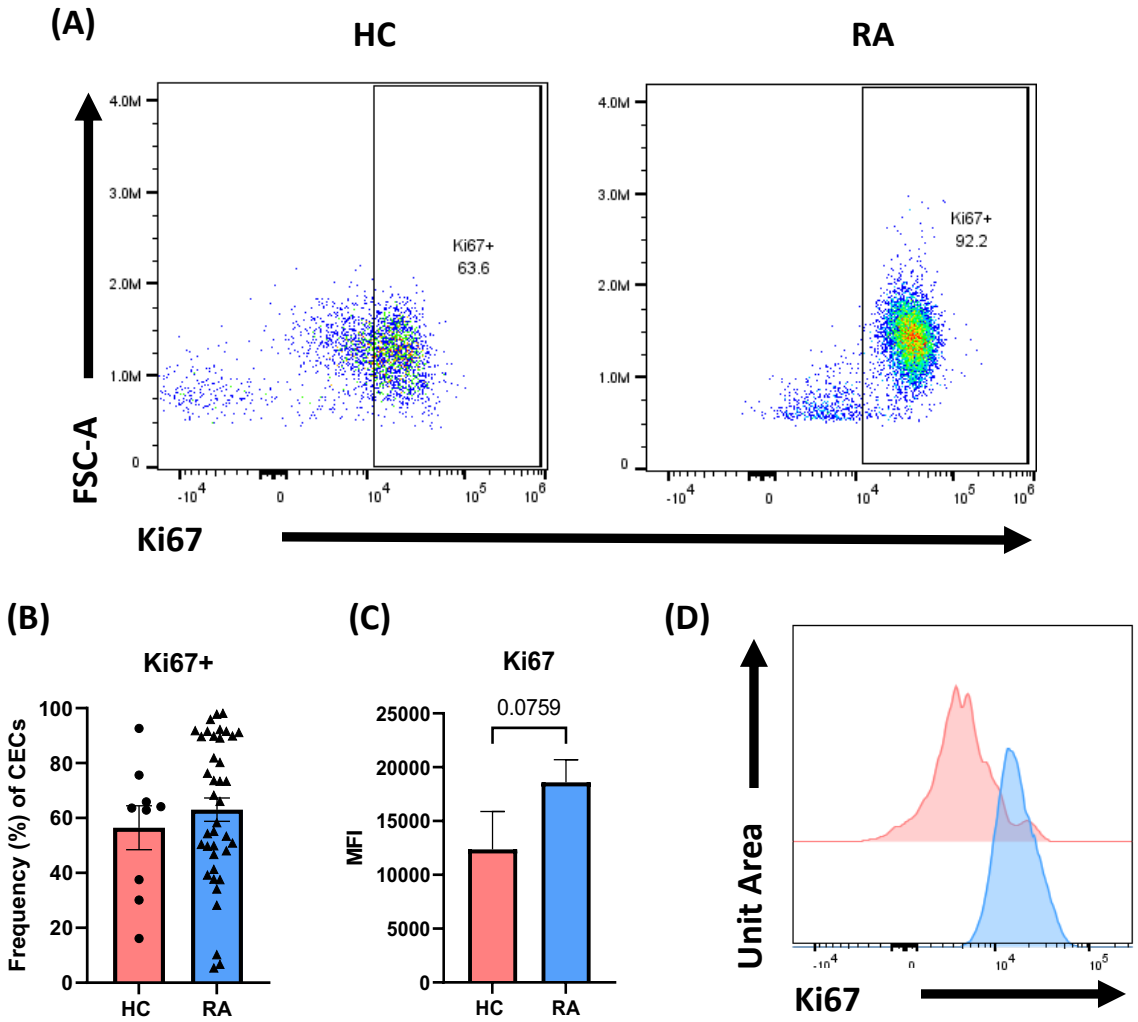

Figure 5.3: CECs retain the capacity to proliferate.

(A) Representative flow cytometric dot plots of frequency of HC and RA CECs positive for the proliferation marker Ki67. (B) Accompanying dot plot bar graph depicting the frequency of Ki67+ CECs in HC (n=9) and RA (n=39). (C-D) Bar graph displaying median fluorescence intensity (MFI) expression of Ki67 in HC and RA with accompanying representative histogram. Data represented as mean ± SEM. Statistical analysis was performed using Mann-Whitney U test. *p<0.05 significantly different from HC.

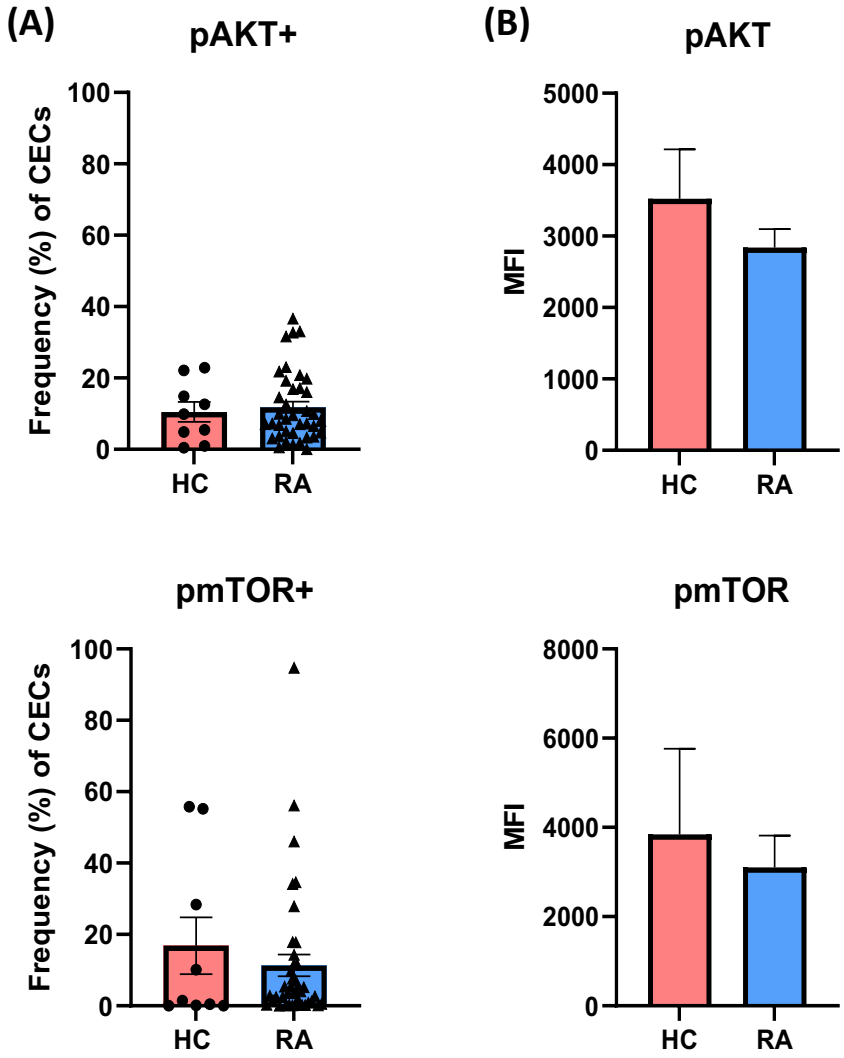

Figure 5.4: Proportion of CECs retain metabolic activity.

(A) Dot plots comparing the percentage frequency of CECs positive for metabolic markers pAKT and pmTOR in HC (n=9) and RA (n=38). (B) Bar graphs demonstrating differential MFI expression of indicated metabolic markers on CECs from HC (n=9) RA (n=39). Data represented as mean ± SEM.

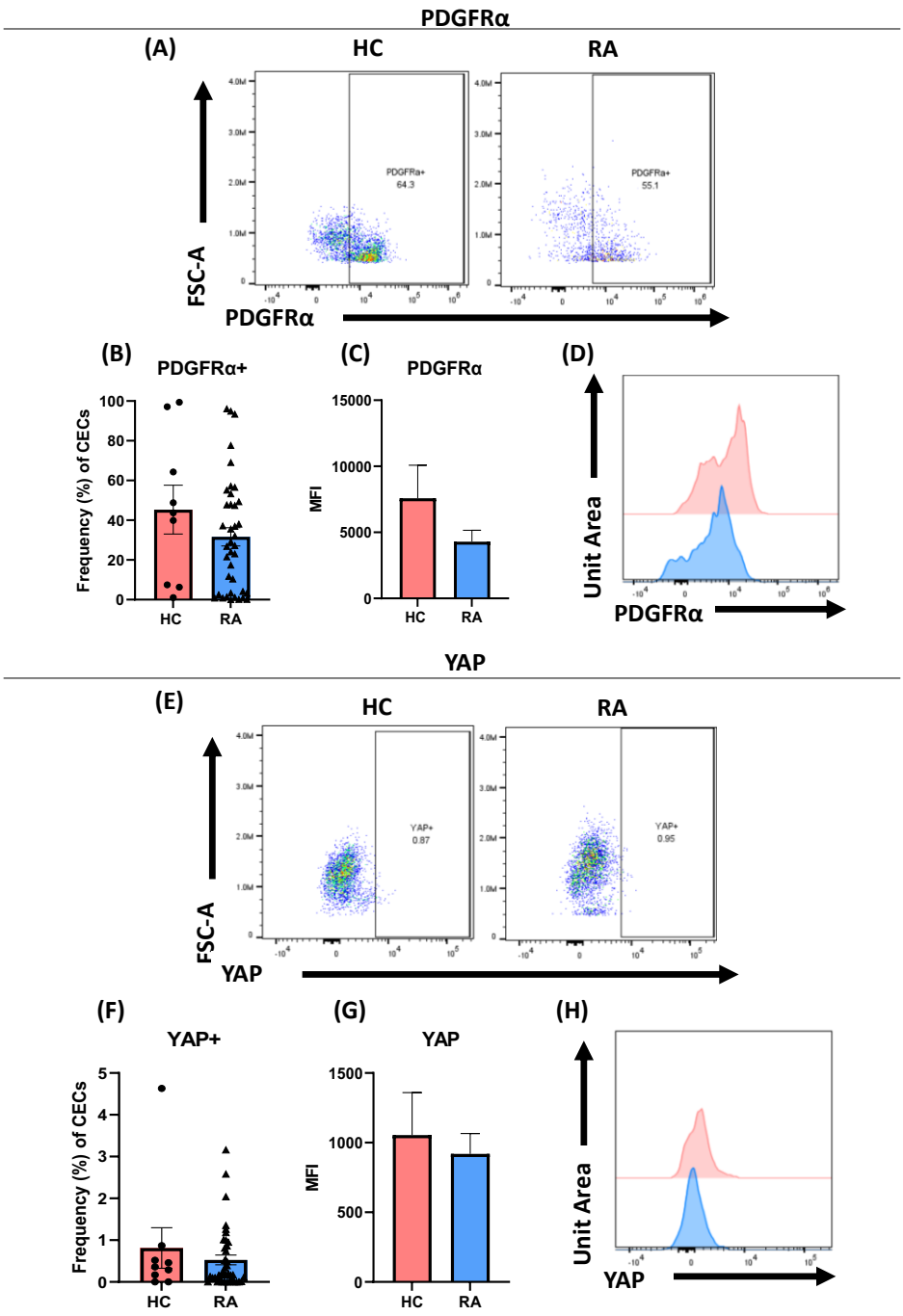

Figure 5.5: HC and RA CECs differ in their capacity for wound healing.

(A) Representative flow cytometric dot plots depicting the frequency of CECs positive for PDGFRα across HC and RA. (B) Dot plot bar graph comparing the differences in percentage frequency of PDGFRα+ CECs in HC (n=9) and RA (n=39). (C) Bar graph demonstrating MFI expression of PDGFRα on CECs between HC and RA with (D) accompanying representative histogram. (E) Representative flow cytometric dot plots depicting the frequency of CECs positive for YAP across HC and RA. (F) Dot plot bar graph comparing the differences in percentage frequency of YAP+ CECs in HC (n=9) and RA (n=39). (G) Bar graph demonstrating MFI expression of YAP on CECs between HC and RA with (D) accompanying representative histogram. Data represented as mean ± SEM.

5.4.3 RA CECs have a pathogenically activated phenotype

Most of the current literature investigating CECs, even in the context of RA, examine their frequency in relation to cardiovascular disease. However, it has yet to be elucidated whether CECs play a role in the pathogenesis of RA. To investigate this further, we sought to determine whether CECs display a pathogenic profile. Interestingly, a significantly higher % frequency of RA CECs was positive for the fibroblast activating protein FAPα compared to HC ($p<0.01$; Figure 5.6 (B)) as evidenced by the representative dot plots (Figure 5.6 (A)), that was paralleled by a trending increase in FAPα MFI compared to HC (Figure 5.6 (C-D)). Additionally, a small yet elevated % of RA CECs expressed THY-1 compared to HC , as shown by representative flow dot plots and bar graph (Figure 5.6 (E-F)), in addition a shift in the MFI expression of THY-1 for RA CECs compared to HC was observed as demonstrated in Figure 5.6 (G) and by the representative histogram plots in Figure 5.6 (H).

To further ascertain the pathogenic capabilities of CECs, the immunoregulatory capability of these CECs was investigated (Figure 5.7). RA demonstrated trending increases in the % frequency of HLA-DR+, CD200R1+, and CD200+ CECs compared to HC (Figure 5.7 (A)), as depicted in the representative flow cytometric dot plots (Figure 5.7 (B)) and by MFI bar graphs (Figure 5.7 (C)). However, these were not statistically significant.

An important component in the progression of RA disease is the ability for circulating cells to be able to adhere to the endothelium before infiltrating into the synovial tissue. Therefore, the adhesive capacity of CECs was examined. Percent frequency of ICAM-1+ CECs was slightly increased in RA compared to HC (Figure 5.8 (A-B)), with minimal change in MFI expression (Figure 5.8 (C)). Additionally, a small yet elevated % of RA CECs were positive for VCAM-1 (Figure 5.8 (A-B)); with a trending decrease in VCAM-1 MFI (Figure 5.8 (C)). MFI expression of the integrin CD61 was also markedly decreased on RA CECs compared to HC (Figure 5.8 (C)), though % frequencies were comparable between the two groups (Figure 5.8 (A-B)). Interestingly, RA CECs demonstrated a trending increase in both % frequency and MFI expression of Cadherin 11 compared to HC (Figure 5.8 (A-C)). Finally, a trending increase in % frequency and MFI expression of CD44 on RA CECs compared to HC was observed (Figure 5.8 (A-C)).

5.4.4 Identified CECs are microvasculature derived

CECs can detach from the endothelium of the microvasculature (larger vessels like arteries) or from the microvasculature (smaller veins and capillaries feeding into the tissue). To elucidate the source of the identified CECs, we investigated what proportion of CECs expressed CD36, an established subset marker for microvascular ECs (Farinacci *et al.*, 2018). As clearly illustrated by

the representative flow cytometric dot plots (Figure 5.9 (A)), almost one hundred percent of the identified CECs in both HC and RA originated from the microvasculature (Figure 5.9 (B)).

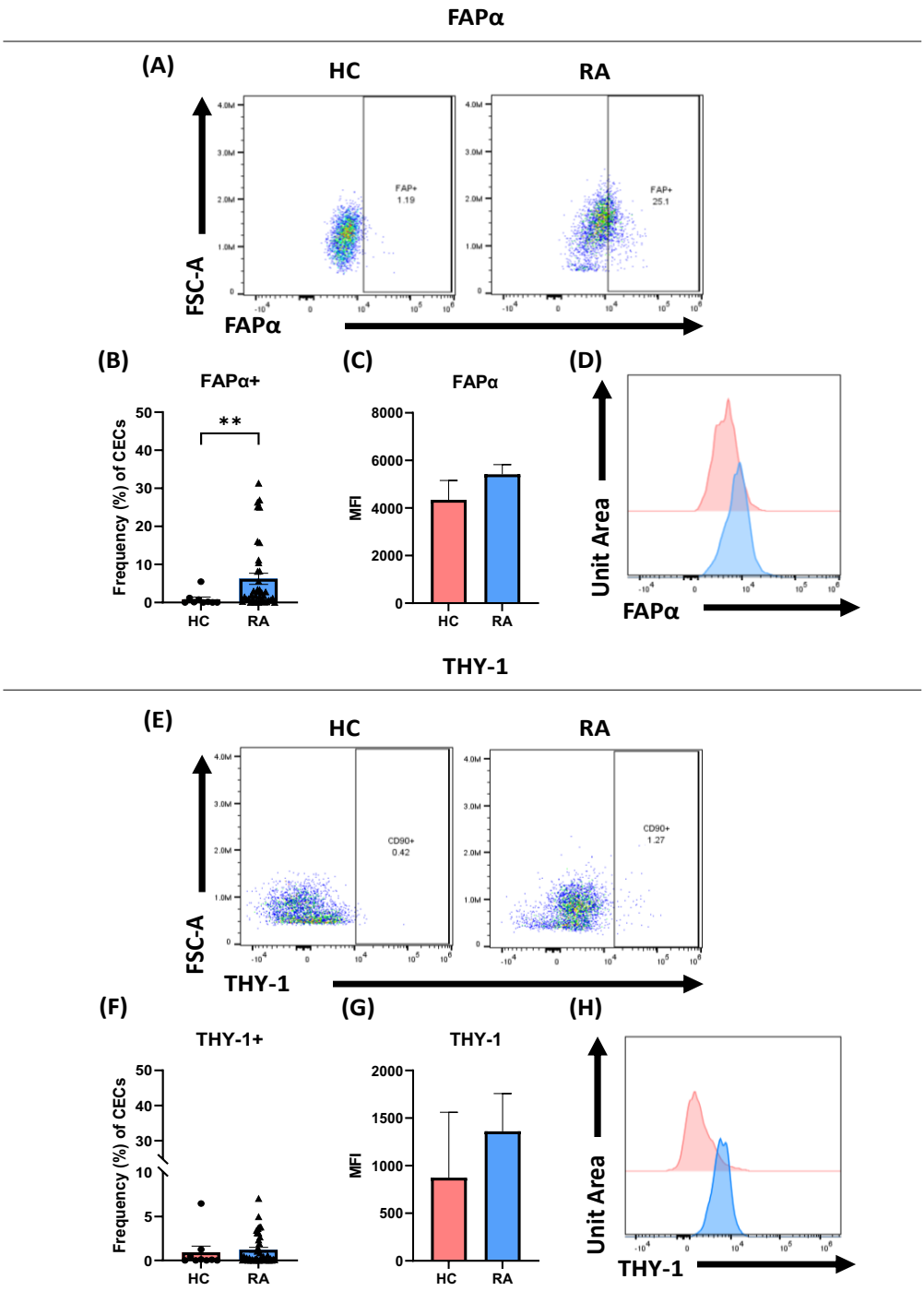

Figure 5.6: RA CECs are pathogenically activated.

(A) Representative flow dot plots illustrating differences between HC and RA in frequency of FAPα+ CECs. (B) Accompanying dot plot further demonstrating differences in FAPα+ CECs between HC (n=9) and RA (n=39). (C) Bar graph and (D) representative histogram showing differences in MFI expression between HC and RA CECs. (E) Representative flow dot plots and (F) dot plot depicting increase in frequency RA CECs positive for THY-1. (G) Bar graph and (H) representative histogram demonstrating differences in THY-1 expression on HC and RA CECs. Data represented as mean ± SEM. Statistical analysis was performed using Mann-Whitney U test. *p<0.05, **p<0.01 significantly different from HC.

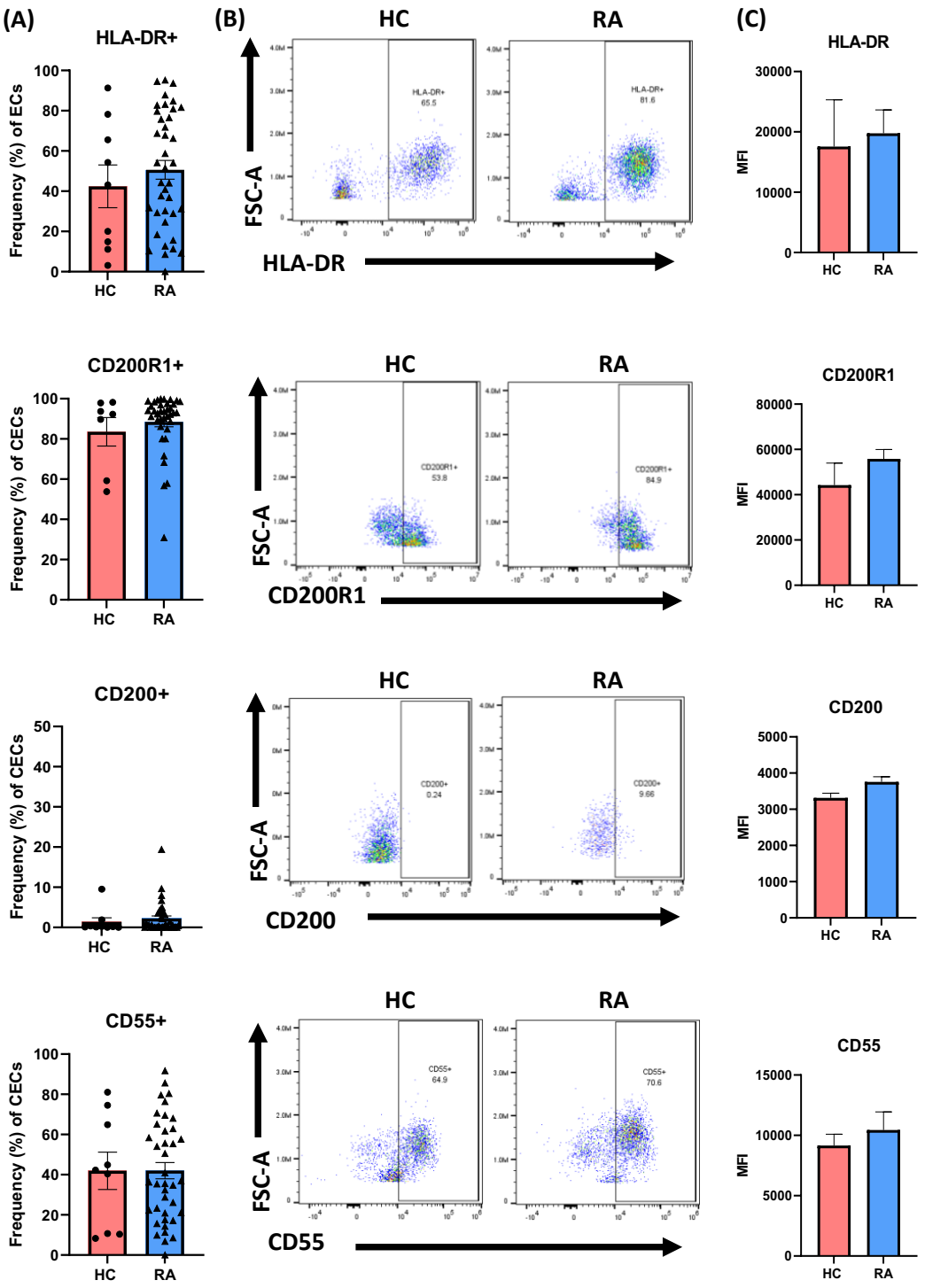

Figure 5.7: Immunoregulatory marker expression on CECs in RA vs HC PBMCs.

(A) Dot plots comparing the differences in percentage frequency of immunoregulatory markers HLA-DR, CD200R1, CD200, and CD55 expressed on the surface of HC (n=9) and RA (n=39) CECs. (B) Representative flow cytometric dot plots of CECs expressing immunoregulatory markers from HC and RA patients. (C) Bar graphs of MFI expression of indicated immunoregulatory markers on HC and RA CECs. Data represented as mean ± SEM.

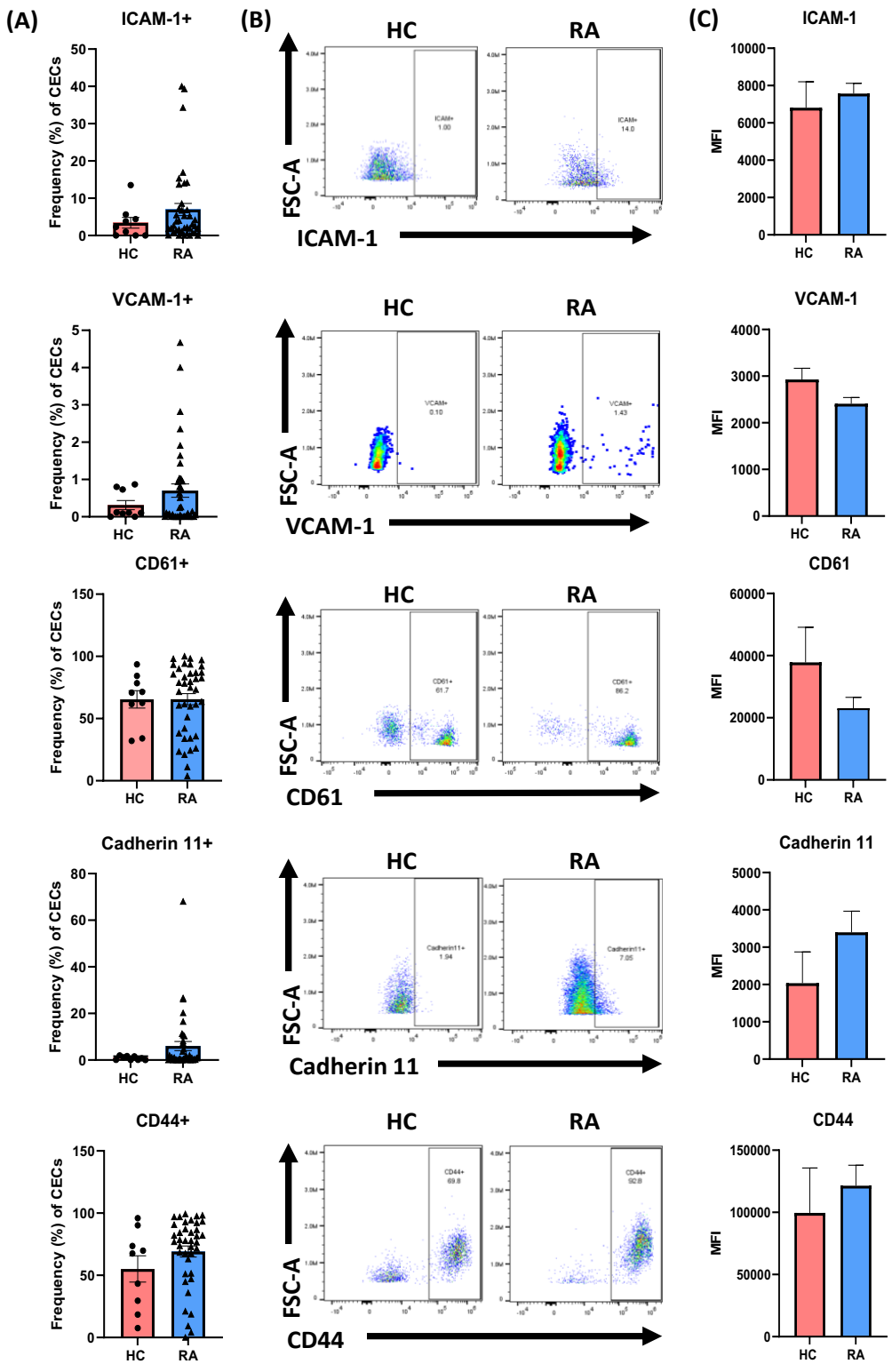

Figure 5.8: Differential expression of adhesion molecules on CECs.

(A) Dot plots comparing the differences in percentage frequency of adhesion molecules ICAM-1, VCAM-1, CD61, Cadherin 11, and CD44 expressed on the surface of HC (n=9) and RA (n=39) CECs. (B) Representative flow cytometric dot plots of expression of adhesion molecules on CECs from HC and RA patients. (C) Bar graphs of MFI expression of indicated adhesion molecules on HC and RA CECs. Data represented as mean ± SEM.

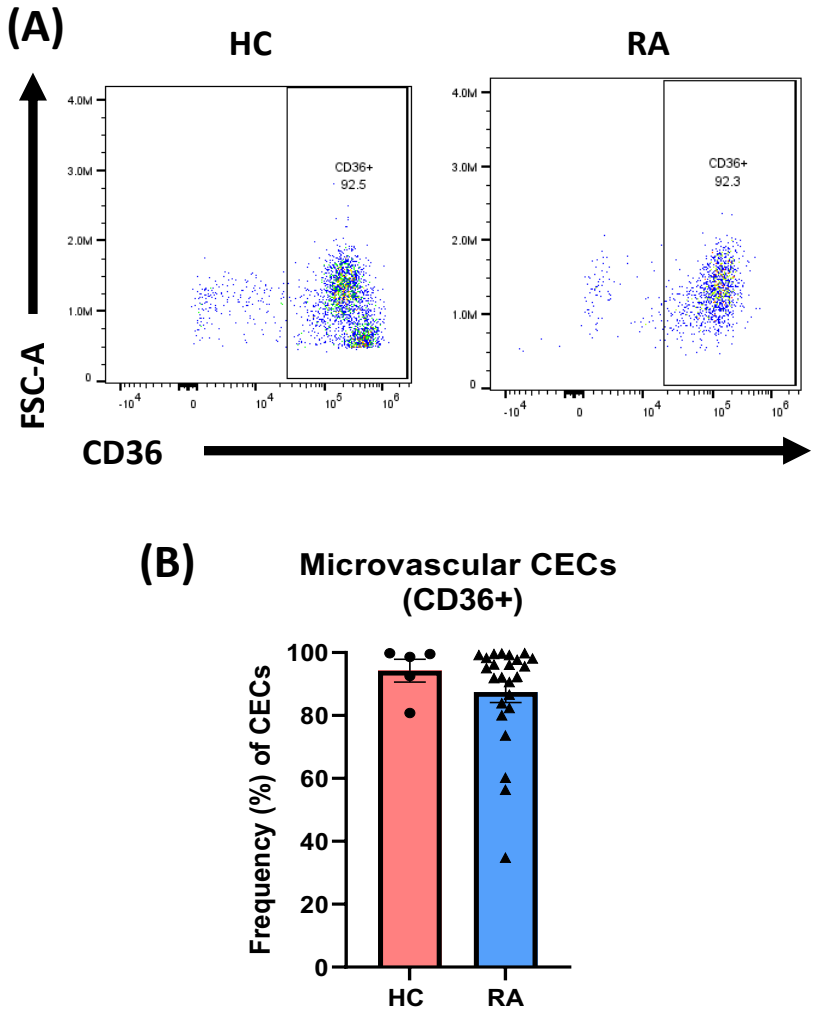

Figure 5.9: Majority of identified CECs come from the microvasculature of HC and RA individuals.

(A) Representative flow cytometric dot plots identifying CD36+ microvascular CECs in HC and RA. (B) Dot plot comparing the percentage frequency of microvascular CECs between HC (n=5) and RA (n=24). Data represented as mean ± SEM with each symbol representing a different sample.

5.4.5 Identification of EPCs from the circulation of RA patients

Current literature has identified another cell population relating to CVD, the endothelial progenitor cell (EPC). Most studies have alluded to the notion that EPCs having a protective, regenerative effect, though there have been conflicting conclusions. Therefore, to better understand what role, if any, EPC play in the context of RA, their identification and frequencies was examined in RA compared to HC. For the identification of EPCs, a similar gating strategy to the one described by Farinacci *et al.* (2018) was adopted. EPCs were defined as CD45dim, positive for the progenitor markers CD34 and CD133, and positive for the EC marker CD31 (Figure 5.10 (E-G)). An additional marker PDPN was also included to ensure exclusion of any PRIME or mesenchymal cells (Figure 5.10 (A-D)).

EPCs constituted a small % frequency of live cells, even smaller than those of CECs (Figure 5.11 (A-C)). Interestingly, a higher % frequency of EPCs was observed in RA (mean 0.08 ± 0.020) compared to HC (mean 0.05 ± 0.037) (Figure 5.11 (C)) though not significant. Size and number of EPCs can be better illustrated in the flow cytometric representative dot plots highlighting these cells in HC and RA (Figure 5.11 (A-B)).

5.4.6 RA CEC and EPC frequency differ across disease activity and can be found prior to disease onset

As CECs are associated with elevated vascular damage and increased risk for CVD, the % frequency of these CECs in RA patients was examined in relation to disease activity. A slight increase in CEC frequency in RA patients with High DAS (indicated by a DAS28 score >3.2) compared to Low DAS (Figure 5.12 (A)) was observed. Further stratification of DAS score yielded the highest frequencies of CECs in patients with a DAS28 score of <1.8 and in patients with severe disease (DAS28 score >3.2) with the latter trending towards a significant increase compared to the 1.8-2.6 cohort ($p=0.0898$) (Figure 5.12 (B)). Female patients also had a trending increase in CEC frequency compared to their male counterparts (Figure 5.12 (C)). There was no correlation between CEC frequency and patient age (data not shown).

Similarly, since it has been suggested that EPCs have a protective effect, % frequencies of EPCs across disease activity of the RA cohort was also examined. EPC frequencies exhibited no differences when patients were stratified between Low and High DAS (Figure 5.12 (D)). Interestingly, when DAS28 scores were further stratified, the 1.8-2.6 DAS28 cohort had the highest frequency of EPCs, though not statistically significant (Figure 5.12 (E)). Like CECs, EPCs were slightly increased in females compared to males (Figure 5.12 (F)), with no correlation observed between EPCs and age.

CECs could be identified with trending higher % frequencies prior to disease onset compared to HC (Figure 5.13 (A)). Indeed, CECs had a slightly elevated % frequency in both IAR and ART compared to HC, with frequencies in IAR similar to that observed in RA+ (Figure 5.13 (A)). Interestingly, RA+ demonstrated a higher frequency of CECs compared to RA- (Figure 5.13 (A)).

EPCs were also positively identified prior to disease onset (Figure 5.13 (B)). Percent frequency of EPCs were comparable between IAR and HC; however, EPC frequency was markedly increased in ART compared to HC, IAR, and RA+ though it should be noted that the sample size for ART is only n=2 (Figure 5.13 (B)). No differences in EPC % frequencies were observed between RA+ and RA- patients (Figure 5.13 (B)).

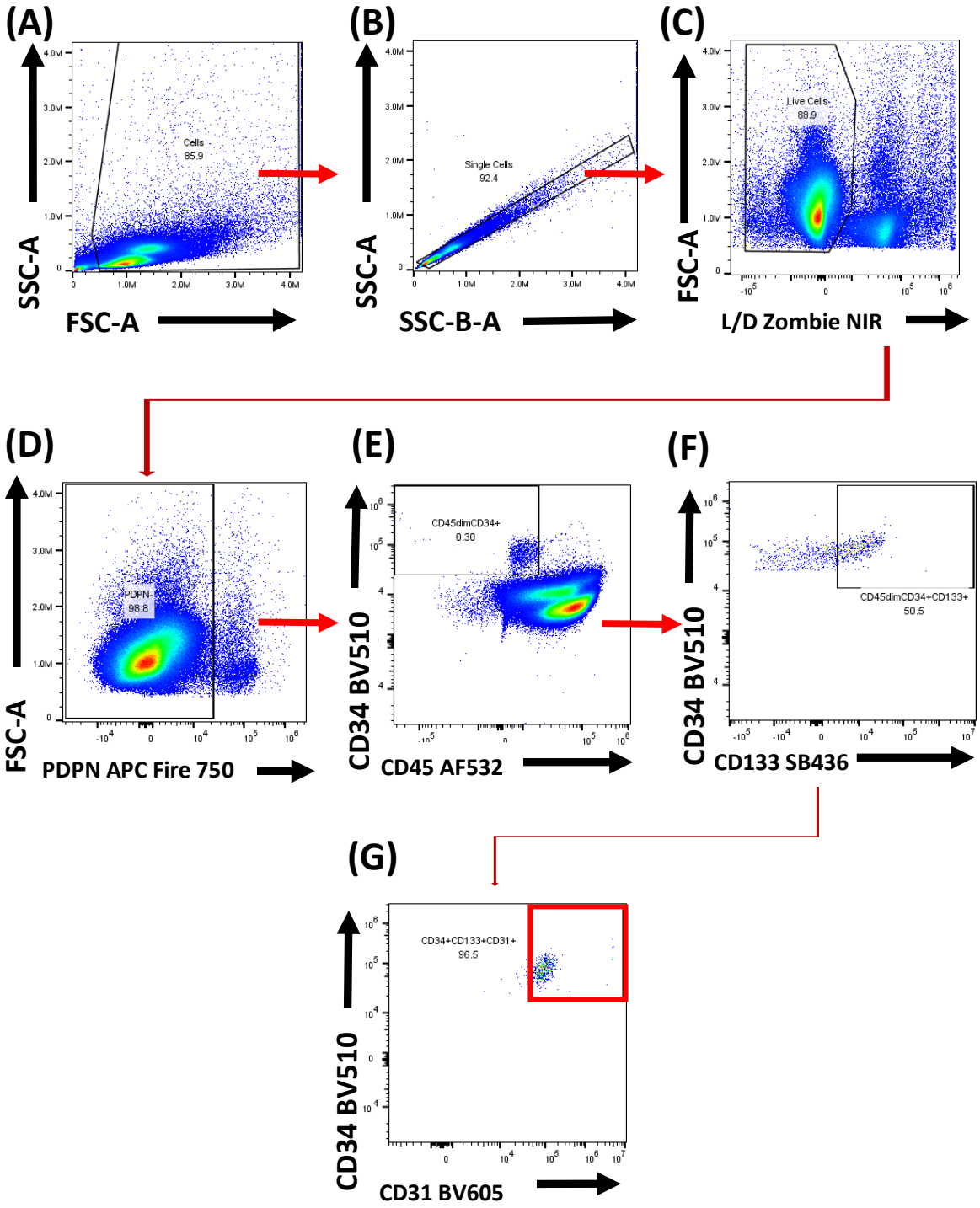

Figure 5.10: Peripheral blood endothelial progenitor cell (EPC) gating strategy.

Thawed PBMCs from HC donors, IAR, ART, and RA were stained with a panel of fluorochrome antibodies (see Table 5.1). Representative dot plots depicting the gating strategy used to identify and characterise EPCs from the circulation. (A-C) Forward and side scatter parameters established for cells before exclusion of doublets and dead cells. (D-G) Endothelial progenitor cells (EPCs) were identified as PDPN-CD45dimCD34+CD133+CD31+.

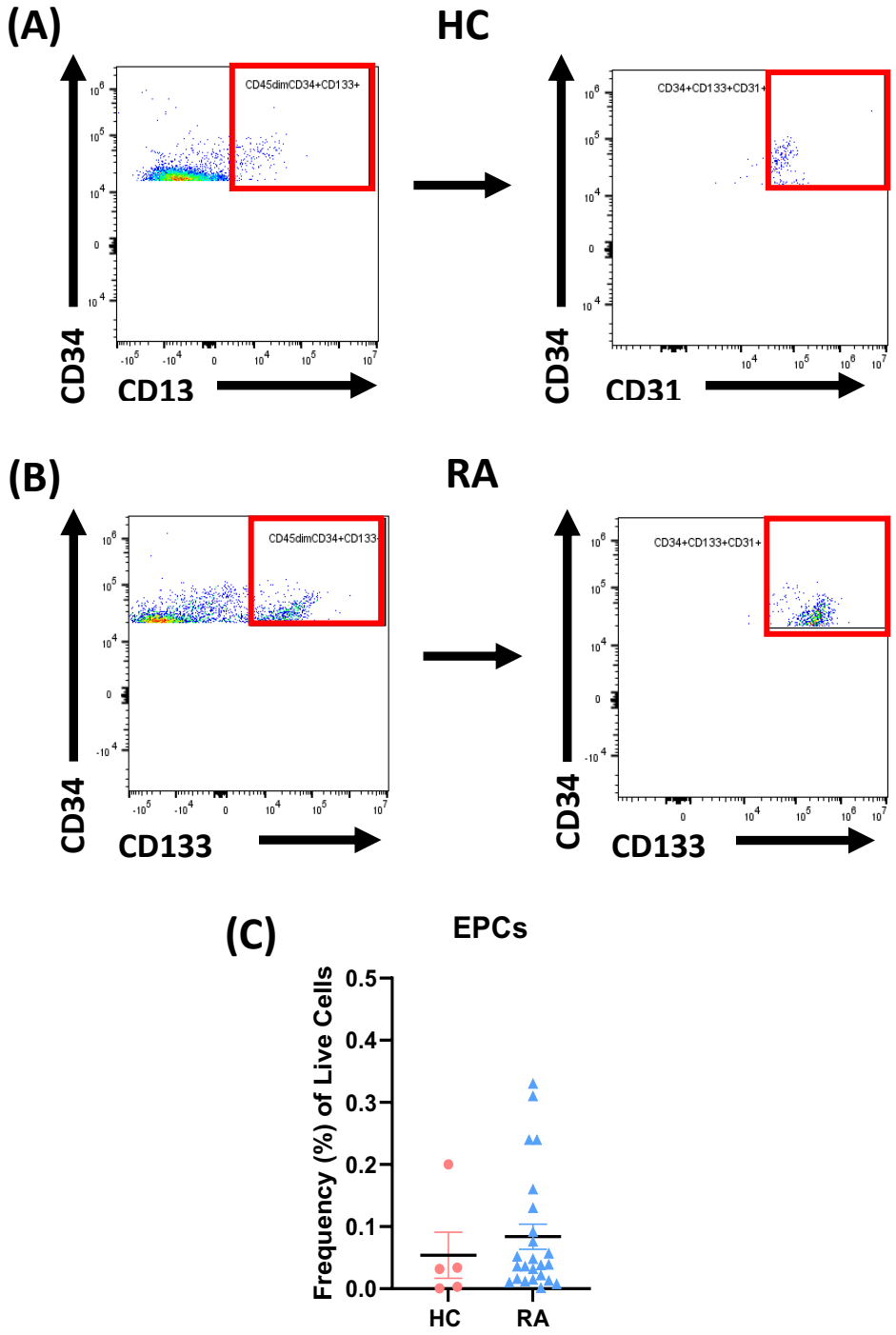

Figure 5.11: Identification of EPCs in the peripheral blood of HC and RA.

Representative flow cytometric dot plots identifying CD34+CD133+CD31+ EPCs in (A) HC donors and (B) RA patients. (C) Dot plot comparing the percentage frequency of EPCs from total live cells of HC (n=5) and RA (n=24). Data represented as mean ± SEM with each symbol representing a different sample.

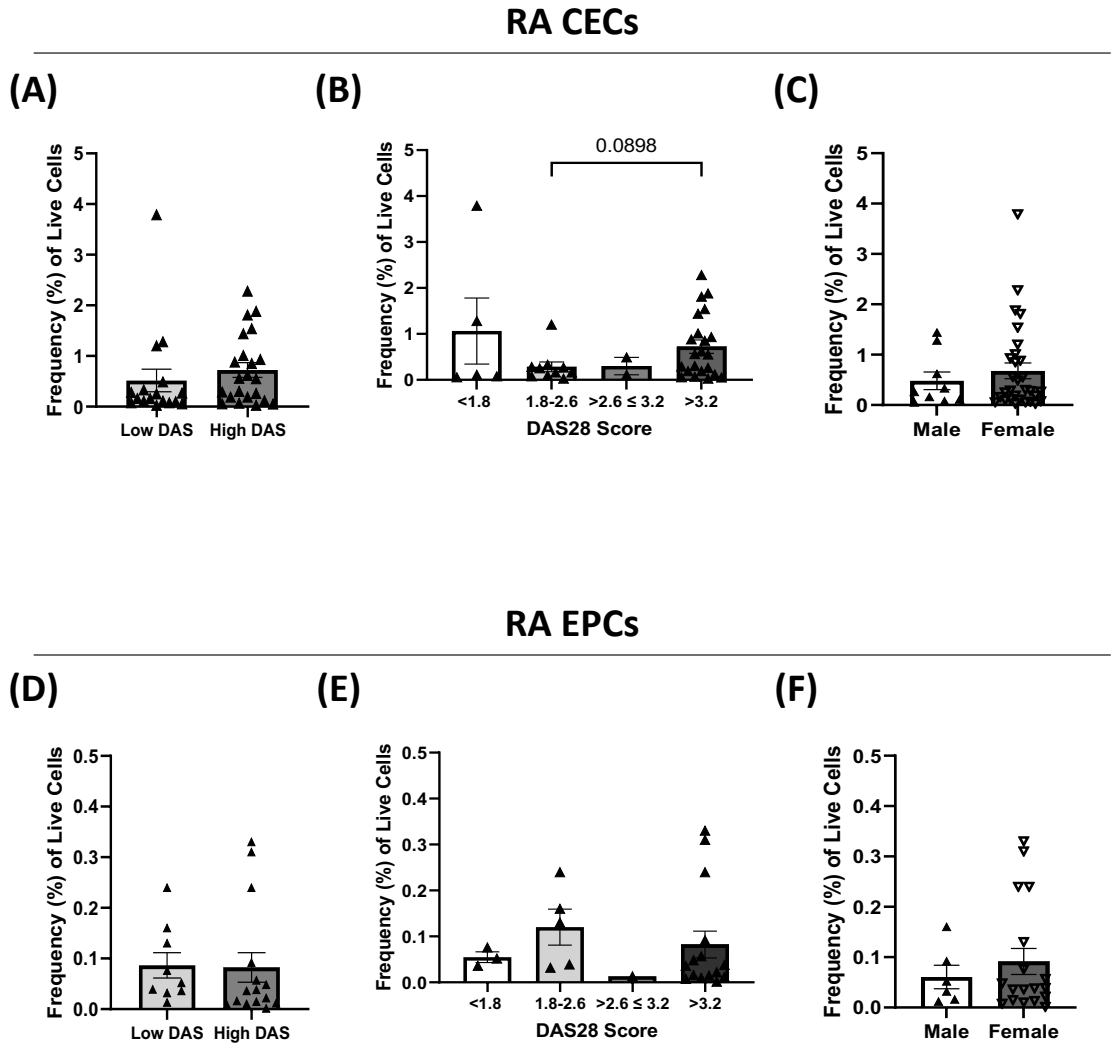

Figure 5.12: CEC and EPC frequencies differ across disease activity and between sexes.

(A) Analysis of CEC frequency based on RA disease activity scores. Low DAS (n=17) indicates a DAS28 score less than 3.2 with high DAS (n=22) based on scores of greater than 3.6. (B) RA CEC frequency stratified by DAS28 score. (C) Dot plot depicting differences in RA CEC frequency between males and females. (D) Analysis of EPC frequency based on RA disease activity scores. Low DAS (n=9) indicates a DAS28 score less than 3.2 with high DAS (n=15) based on scores of greater than 3.6. Dot plots demonstrating differences in EPC frequency across (E) DAS28 scores and (F) between males and females. Data represented as mean ± SEM with each symbol representing a different sample. Statistical analysis was performed using Mann-Whitney U test with *p<0.05 being statistically significant.

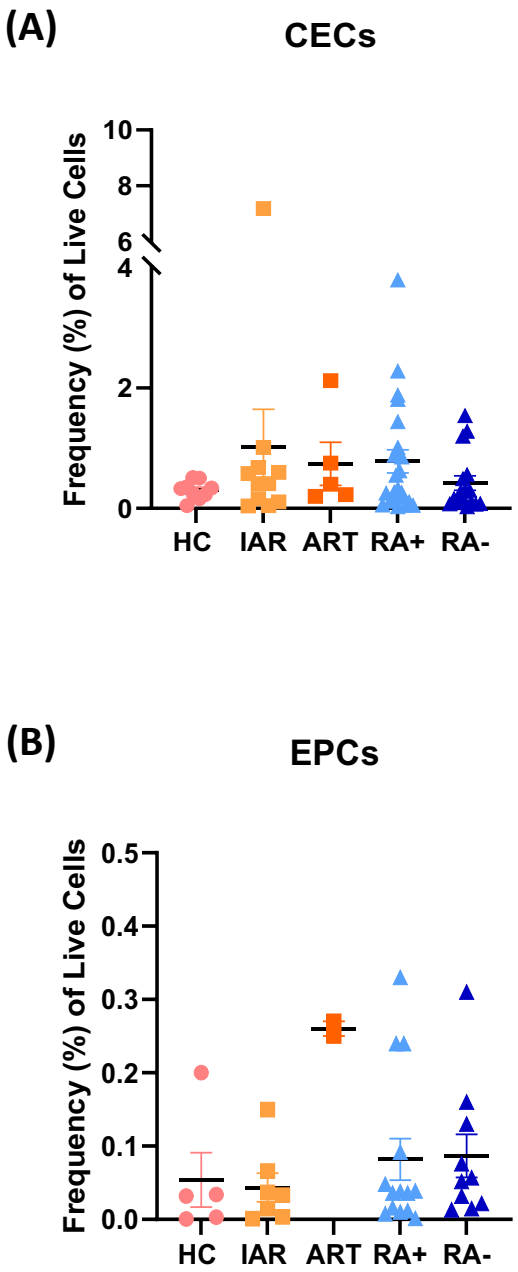

Figure 5.13: CECs and EPCs are present in altered numbers in circulation prior to clinical onset of disease.

Dot plots demonstrating differential frequency of CECs and EPCs in HC donors, seropositive individuals-at-risk (IAR), seronegative arthralgia (ART), and RA patients. RA patients have been stratified between seropositive (RA+) and seronegative (RA-). (A) Frequencies of CECs in IAR (n=11), ART (n=5), RA+ (n=23), and RA- (n=16) compared to HC (n=9). (B) Dot plot depicting differences in EPC frequency across HC (n=5), IAR (n=7), ART (n=2), RA+ (n=14), and RA- (n=10). Data represented as mean ± SEM with each symbol representing a different sample. Statistical analysis was performed using Mann-Whitney U test with *p<0.05 being statistically significant.

5.4.7. Hierarchical clustering analysis and protein-protein interactions of CEC cellular markers

Next correlation, PCA, and biplot analysis was performed to further confirm the relationship of the CEC markers to each other. Correlation matrix for all markers for HC CEC and RA CEC are shown in Figure 5.14 (A-B). Blue defines positive correlations and red defines negative correlations. As demonstrated in the correlation matrix, the majority of marker correlations in RA are positive (Figure 5.14 (A)), in contrast to HC (Figure 5.14 (B)), where a mixture of positive and negative correlations are observed. This data suggests that in disease these markers become activated and together contribute to the pathogenic phenotype of CECs. To further examine the relationship of the markers in RA, PCA and bi-plot analysis was performed. After defining the PCs, the scores for each PC were calculated using the linear combination which define the PC. PCA and bi-plot analysis in RA patients identified four separate clusters (Figure 5.15 (A)). Within each cluster, these markers are most strongly correlated together. Cluster one included Ki67 and HLA-DR (red), Cluster two included VCAM-1, CD200R1, CD200, Cadherin-11 (green) and Cluster three ICAM-1 and FAPα (blue). Interestingly, CD55 appeared to not be associated with any markers. These clusters align with the correlations shown in Figure 5.15 (A). Interestingly these clusters are not correlated in HC, further confirming the different regulation of these markers in health and disease.

The STRING software tool was next used to create a visual representation of the protein-protein interactions. The protein clustering demonstrates that all markers were associated with each other (Figure 5.15 (B)). Interestingly, ICAM-1 and CD200 are focal points (red arrows) of these interactions, both of which activate EC and induce the adhesive capacity of EC for leukocytes, with studies suggesting CD200 is selective for T cell adhesion. Furthermore, associated gene interaction protein tyrosine phosphatase receptor C was also a focal point, function of which in cell growth and differentiation.

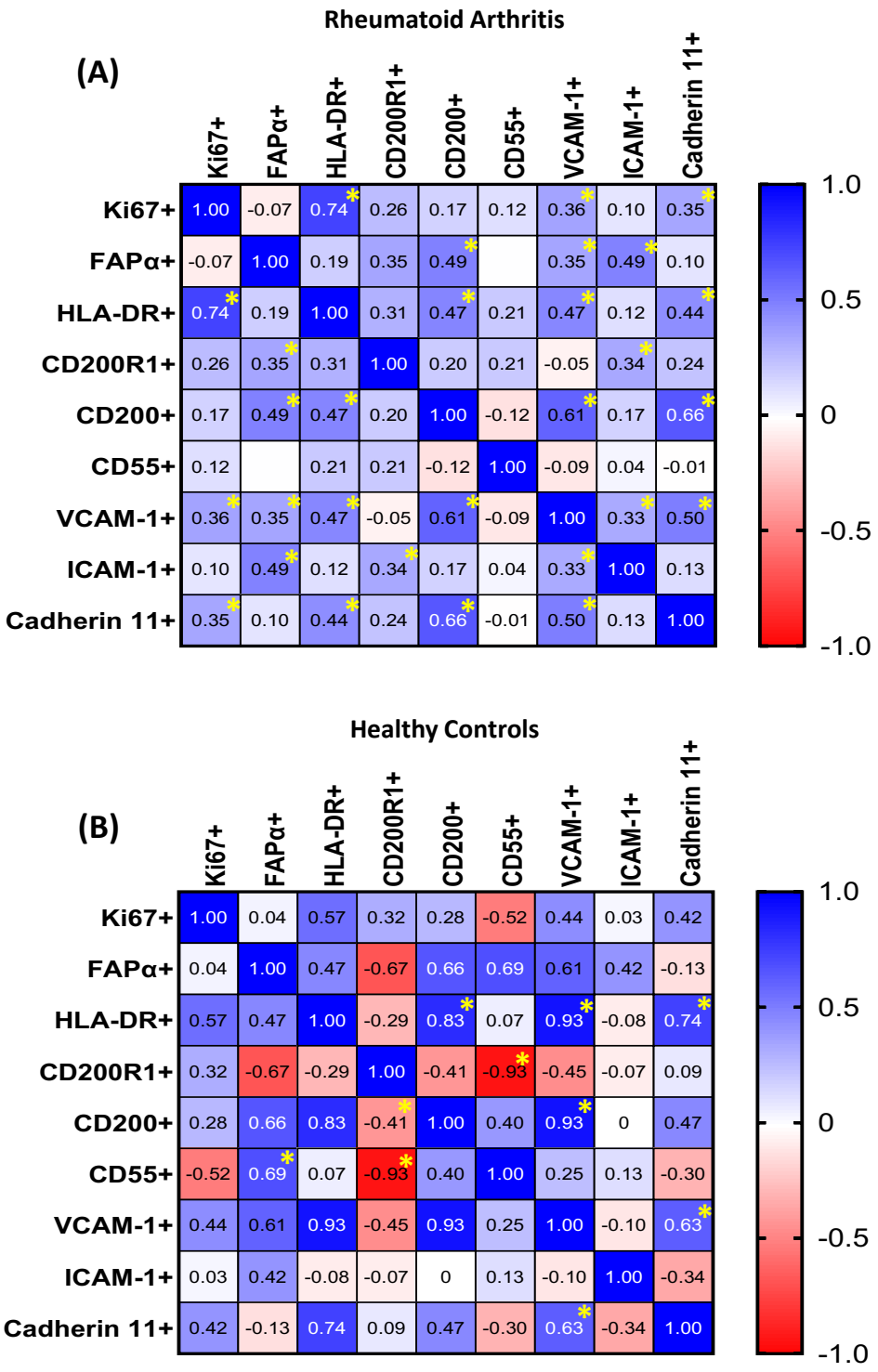

Figure 5.14: Correlation of Marker Expression on CECs varies between RA and HC.

Correlation Matrix of CEC markers for (A) RA+ (n=39) and (B) HC (n=9). Positive correlations denoted by blue and negative correlations denoted by red. Numbers displayed in each box represent correlation co-efficient. * $p<0.05$ statistically significant.

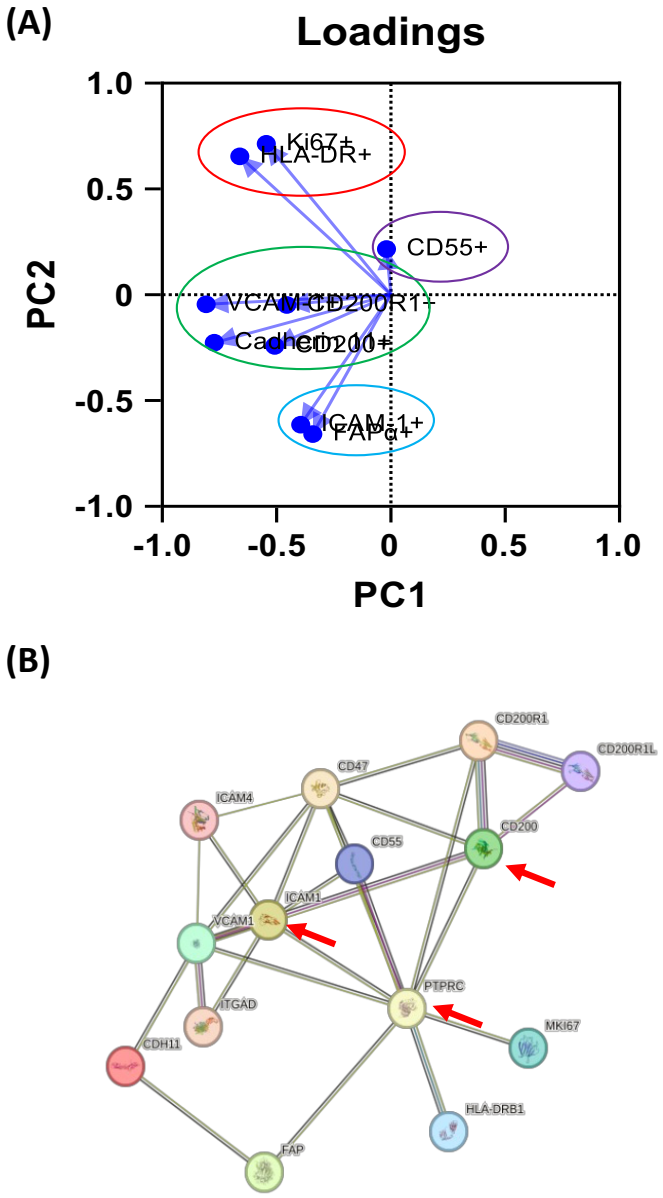

Figure 5.15: CECs form distinct clusters based on phenotypic marker expression.

(A) Principal Component Analysis (PCA) demonstrating three main clusters in the CEC markers, with CD55 displayed independently in RA (n=39). Red=cluster 1, Green=cluster 2, Blue=cluster 3, Purple=CD55. (B) Potential protein-protein biomarker interactions using the STRING software; Ki67, FAPα, HLA-DR, CD200R1, CD200, CD55, VCAM-1, ICAM-1 and Cadherin-11, with associated markers CD47, PTPRC, ITGAD.

5.4.8. Serum profiling across disease states

To further identify possible circulating biomarkers for RA and elevated CVD risk, the serums of RA+, RA-, IAR, and ART compared to HC donors were analysed. Firstly, the following soluble pro-inflammatory cytokine levels were measured: TNFα, IL-1β, IL-6, IFN-γ, IL-8, IL-4, IL-13, IL-10, IL12p70, and IL-2 (Figure 5.16). Consistent with previous studies low levels were observed across all disease states for TNFα, IL-1β, and IL-6 (Figure 5.16). Increased IFN- γ levels in IAR compared to the other disease states was observed, although not significant (Figure 5.16). Interestingly, IL-8 and IL-4 ($p=0.0836$ HC vs RA-; $p=0.0632$ RA+ vs RA-) demonstrated a stepwise decrease from HC to IAR to RA+ with little to no expression observed in ART or RA- for either (Figure 5.16). Similarly, levels of IL-13 and IL-10 were highest in HC compared to disease states and no significant differences were observed in expression for IL12p70 and IL-2 (Figure 5.16).

Previous work performed on CECs also examined soluble markers of vascular damage. Therefore, levels of CRP, ICAM-1, VCAM-1, VEGF, Serum Amyloid A (SAA), and Factor VIII in the serums of RA+, RA-, IAR, ART, and HC were analysed (Figure 5.17). Additional cohorts as disease comparators were analysed including PsA patients and GCA as increased vascular dysfunction is associated with both diseases. As expected, soluble CRP levels were significantly increased in RA+ ($p<0.0001$), RA- ($p<0.01$), and PsA ($p<0.05$) compared to HC (Figure 5.17). Additionally, RA+ was significantly increased compared to IAR ($p<0.01$) (Figure 5.17). ICAM-1 demonstrated a stepwise increase from HC to IAR to RA+ with RA+ being significantly increased ($p<0.0001$). A similar stepwise increase was observed from HC to ART to RA- with RA- significantly increased ($p<0.001$) (Figure 5.17). Similar stepwise increases were observed for VCAM-1 and VEGF from HC to IAR to RA+ (VCAM-1 $p<0.001$; VEGF $p<0.05$). Both markers were also significantly elevated in RA-patients compared to HC (VCAM-1 $p<0.01$; VEGF $p<0.05$) (Figure 5.17). Interestingly, A-SAA levels were significantly increased only in RA+ compared to IAR and HC ($p<0.01$ for each) (Figure 5.17). Factor VIII levels were also elevated in RA+ compared to HC ($p=0.0587$).

Often utilised as markers for kidney injury, TFF3, Calbindin, Osteoactivin, and KIM-1 have also been implicated as predictors of other diseases and indicators of tissue damage, therefore these markers were investigated next. TFF3 demonstrated a significant stepwise increase in serum levels from HC to IAR ($p<0.05$) to RA+ ($p<0.05$). Levels were also significantly increased for RA- compared to HC ($p<0.05$) (Figure 5.18). Calbindin demonstrated significantly increased levels for RA- ($p<0.0001$), PsA ($p<0.05$), RA+ ($p<0.0001$), and IAR ($p<0.05$) compared to HC (Figure 5.18). Serum levels were significantly increased for Osteoactivin in ART ($p=0.0610$), RA- ($p<0.05$), and PsA ($p=0.0924$) compared to HC (Figure 5.18). KIM-1 was significantly increased for IAR compared to HC ($p<0.05$) (Figure 5.18).

Soluble metabolic markers were also investigated across the disease states to identify any significant alterations. Serum levels were measured for Clusterin, RBP4, SHBG, NGAL/LNC2, ApoC3, Adiponectin, DPPIV, and STfR-1 (Figure 5.19). Of note, stepwise increases were observed for HC to IAR to RA+ for RBP4 ($p<0.0001$), ApoC3 ($p<0.05$), and Adiponectin (Figure 5.19). Additionally, RBP4 was significantly elevated in RA- ($p<0.0001$) and PsA ($p<0.001$) serums compared to HC (Figure 5.19). Clusterin was significantly higher in RA+ compared to IAR ($p<0.001$) and HC ($p<0.01$) and a similar increase was observed for STfR-1 (IAR vs RA+ $p<0.001$; HC vs RA $p<0.0001$) (Figure 5.19). RA+ also demonstrated significantly higher levels of DPPIV compared to HC ($p<0.05$) (Figure 5.19).

No significant differences were observed in soluble insulin levels, C-peptide levels, glucagon, or pancreatic polypeptide (PP) across disease states compared to HC (Figure 5.20). GCA for most of the soluble markers measured, consistently demonstrated lower levels compared to the other disease states and HC. However, active GIP and active GLP-1 were significantly elevated in GCA serum compared to HC ($p<0.05$ for each) (Figure 5.20). In addition, RA+ and RA- also demonstrated significantly raised levels of active GIP compared to HC (RA+ $p<0.001$; RA- $p<0.05$) (Figure 5.20).

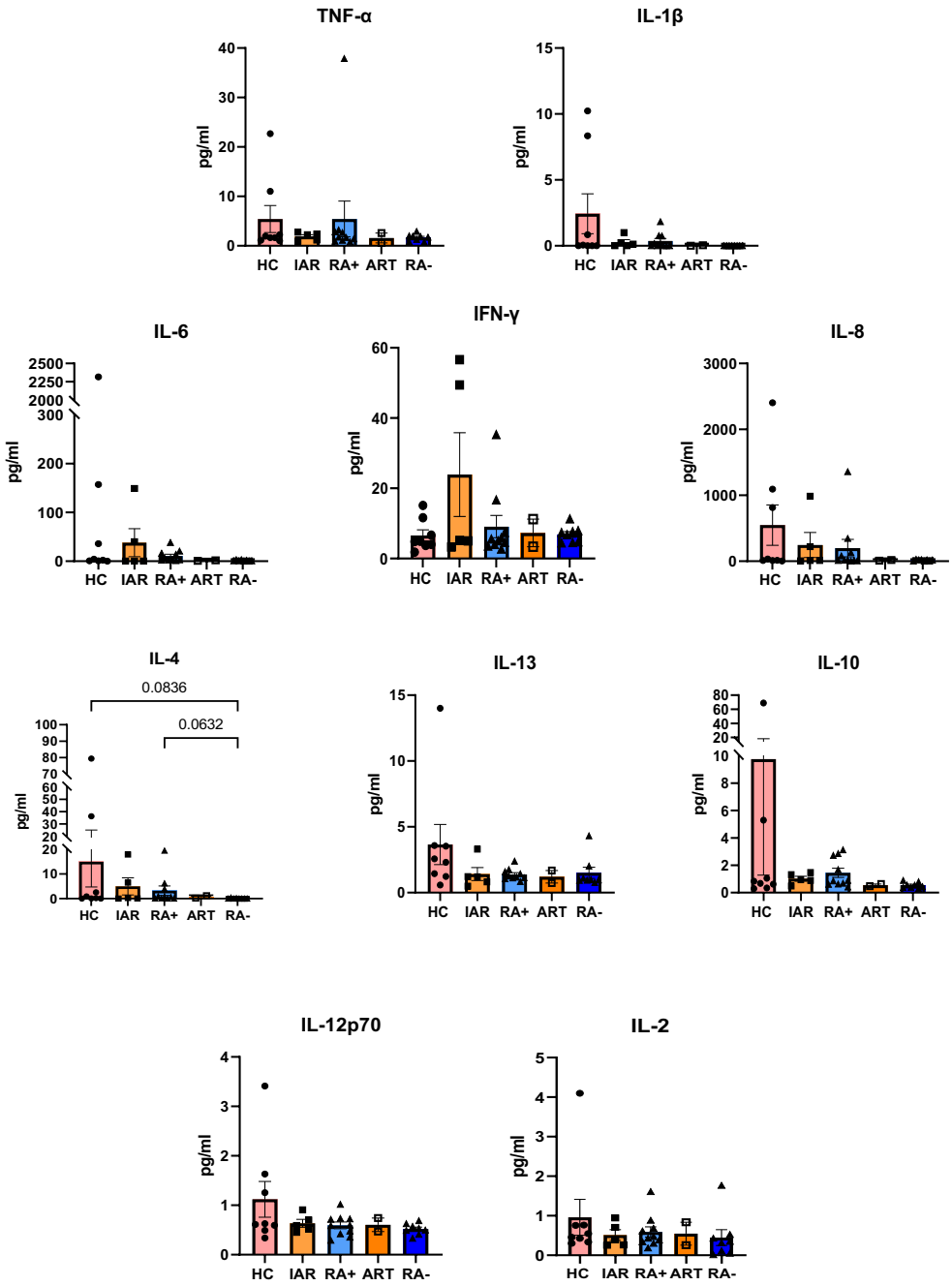

Figure 5.16: Minimal levels of pro-inflammatory cytokines expressed in serums from HC, pre-disease, and RA patients.

Dot plot bar graphs depicting differences in concentration of soluble pro-inflammatory cytokines TNFα, IL-1β, IL-6, IFN-γ, IL-8, IL-4, IL-13, IL-10, IL-12p70, and IL-2 measured from the serums of HC (n=8), IAR (n=5), ART (n=2), RA+ (n=10), and RA- (n=8). Data represented as mean ± SEM. Statistical analysis was performed using Kruskal-Wallis unpaired, nonparametric ANOVA with $p<0.05$ being statistically significant.

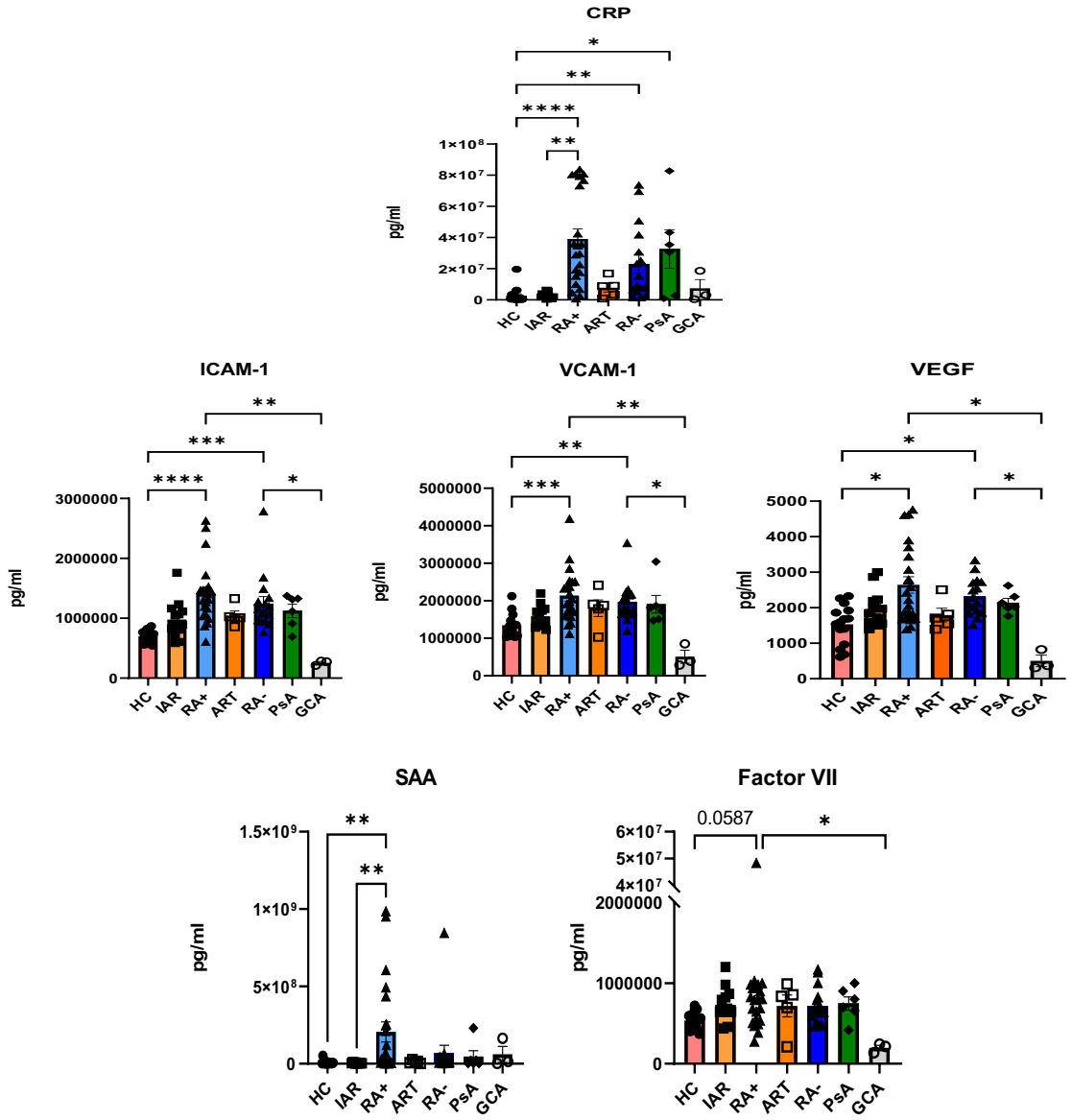

Figure 5.17: Elevated levels of soluble adhesion molecules and markers of vascular injury across disease states.

Dot plot bar graphs demonstrating elevated serum levels of soluble markers of vascular injury and adhesion molecules CRP, ICAM-1, VCAM-1, VEGF, SAA, and Factor VII across HC (n=15), IAR (n=13), ART (n=5), RA+ (n=22), RA- (n=16), PsA (n=6), and GCA (n=3). Data represented as mean ± SEM. Statistical analysis was performed using Kruskal-Wallis unpaired, nonparametric ANOVA with *p<0.05, **p<0.01, ***p<0.001, ****p<0.0001 being statistically significant.

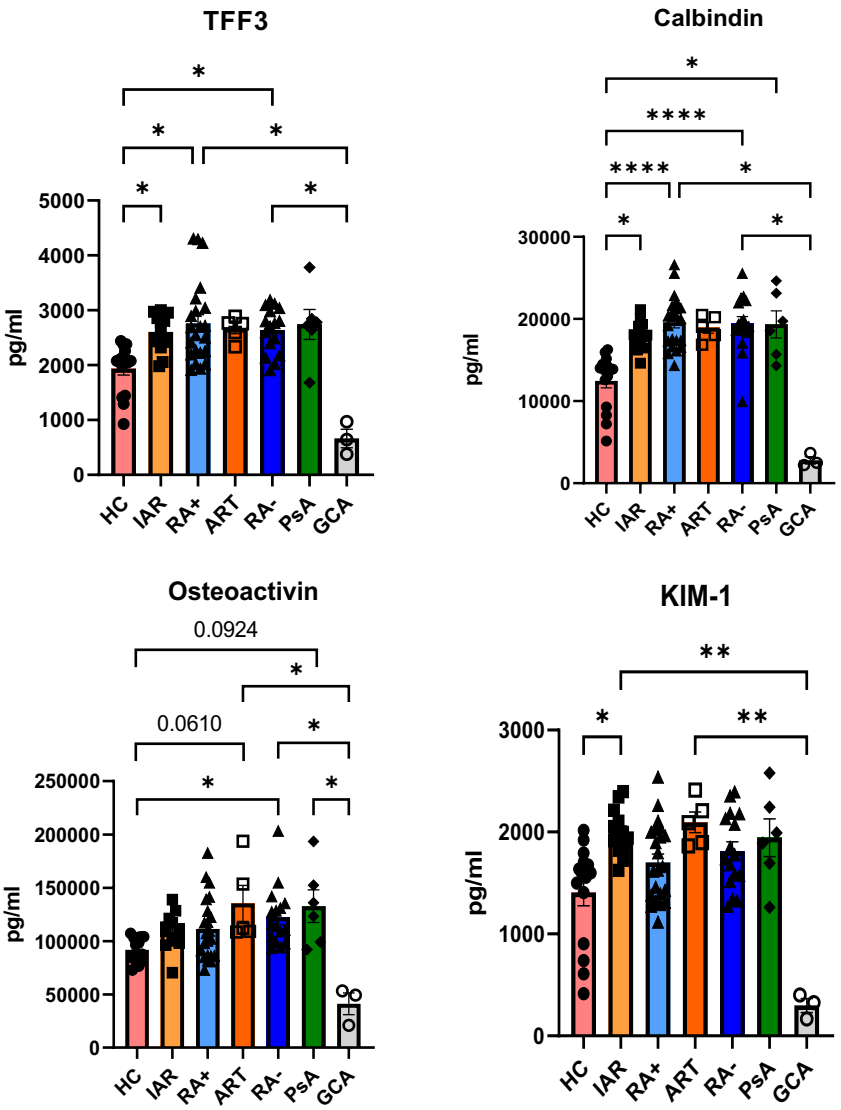

Figure 5.18: Elevated levels of soluble markers for tissue injury observed in serums across disease states.

Dot plot bar graphs demonstrating the differential serum level concentrations of TFF3, Calbindin, Osteoactivin, and KIM-1 from HC (n=15), IAR (n=13), ART (n=5), RA+ (n=22), RA- (n=16), PsA (n=6), and GCA (n=3). Data represented as mean ± SEM Statistical analysis was performed using Kruskal-Wallis unpaired, nonparametric ANOVA with *p<0.05, **p<0.01, ***p<0.001, ****p<0.0001 being statistically significant.

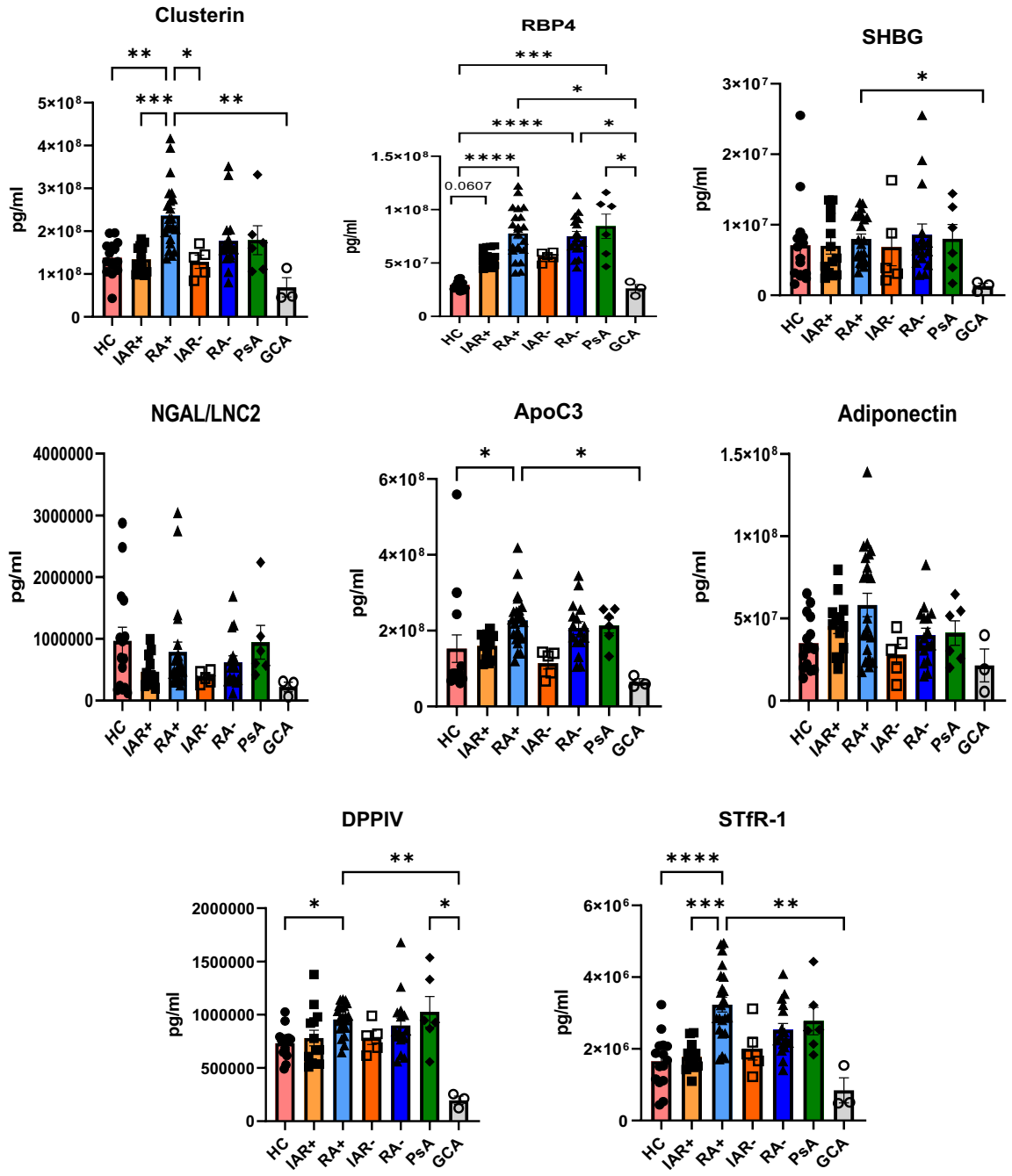

Figure 5.19: Differential expression of soluble metabolic markers in serum across disease states.

Dot plot bar graphs demonstrating the differential serum level concentrations of soluble metabolic markers Clusterin, RBP4, SHBG, NGAL(LNC2), ApoC3, Adiponectin, DPPIV, and StfR-1 from HC (n=15), IAR (n=13), ART (n=5), RA+ (n=22), RA- (n=16), PsA (n=6), and GCA (n=3). Data represented as mean ± SEM Statistical analysis was performed using Kruskal-Wallis unpaired, nonparametric ANOVA with *p<0.05, **p<0.01, ***p<0.001, ****p<0.0001 being statistically significant.

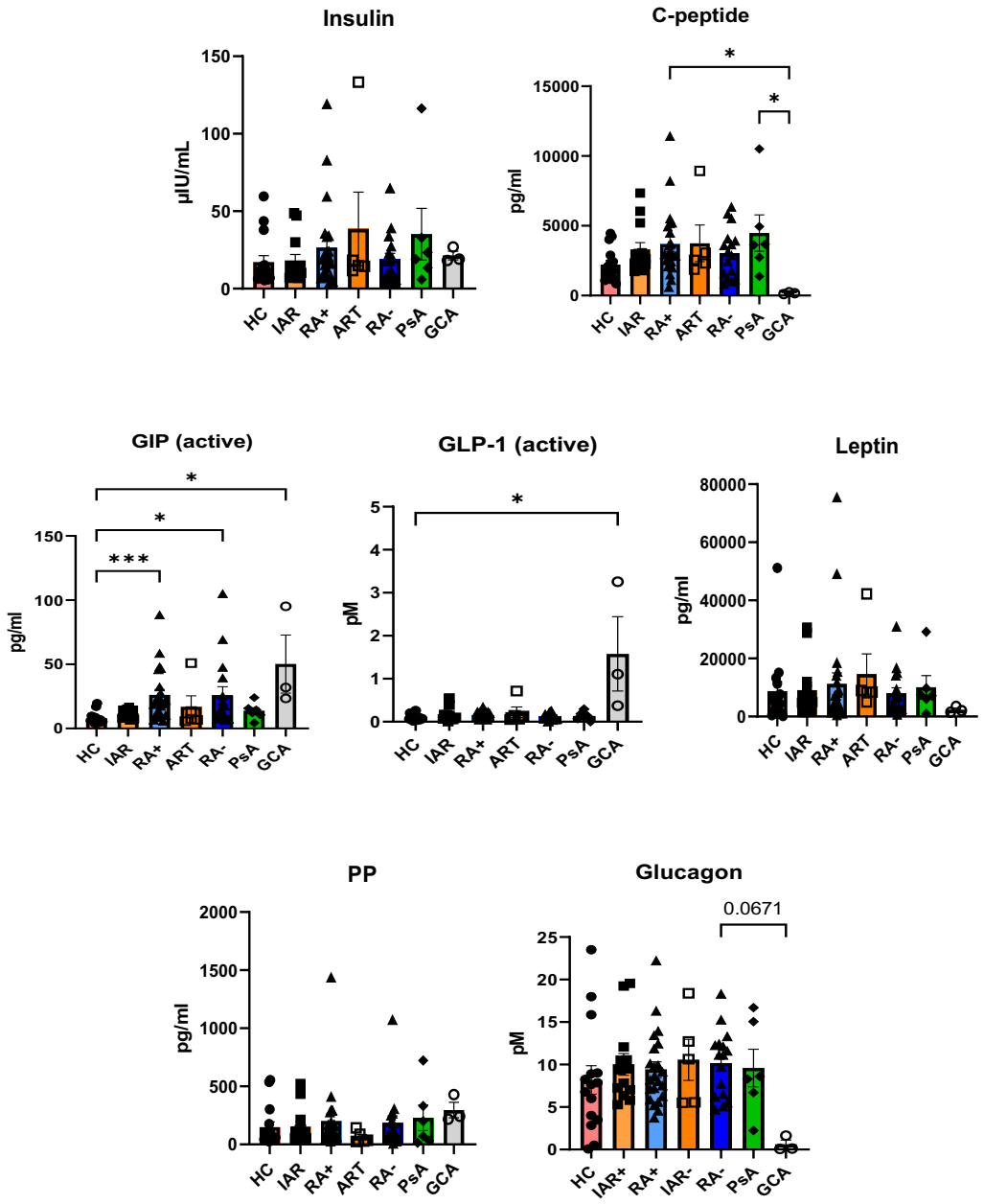

Figure 5.20: Expression of soluble metabolic markers in serum across disease states.

Dot plot bar graphs demonstrating the differential serum level concentrations of soluble metabolic markers Insulin, C-peptide, active GIP, active GLP-1, Leptin, Pancreatic polypeptide (PP), and Glucagon from HC (n=15), IAR (n=13), ART (n=5), RA+ (n=22), RA- (n=16), PsA (n=6), and GCA (n=3). Data represented as mean ± SEM Statistical analysis was performed using Kruskal-Wallis unpaired, nonparametric ANOVA with *p<0.05, **p<0.01, ***p<0.001, being statistically significant.

5.4.9. Hierarchical clustering analysis and protein-protein interactions of serum markers

PCA, biplot, and string analysis was performed to further confirm the relationship of serum biomarkers with each other. As these markers were consistently elevated in the RA+ patients, analysis was focused on this cohort. PCA analysis in RA+ patients identified five separate clusters (Figure 5.21 (A)). Within each cluster, these markers are most strongly correlated together. Cluster one includes DPPV, ApoC3 and RBP4 (red), Cluster two includes Adiponectin and Factor VIII (green), Cluster three includes VCAM-1, ICAM-1, A-SAA, and CRP (blue), Cluster four includes Clusterin, STfR-1 and VEGF (yellow) and Cluster five includes TFF3, Osteoactivin, Calbindin and KIM3 (purple). Cluster four (yellow) crossed both bottom quadrants and is associated with the inflammatory marker cluster (blue) and tissue injury cluster (purple). Cluster three includes VEGF, Clusterin and STfR-1 thus both growth factor and metabolic markers. Together, this data highlights the association between inflammation, tissue injury factors and metabolic factors. Finally, STRING software tool was used to examine protein-protein interactions (Figure 5.21(B)), which demonstrated numerous key focal points (red arrows) demonstrating crosstalk between proteins involved in EC activation, injury and metabolism.

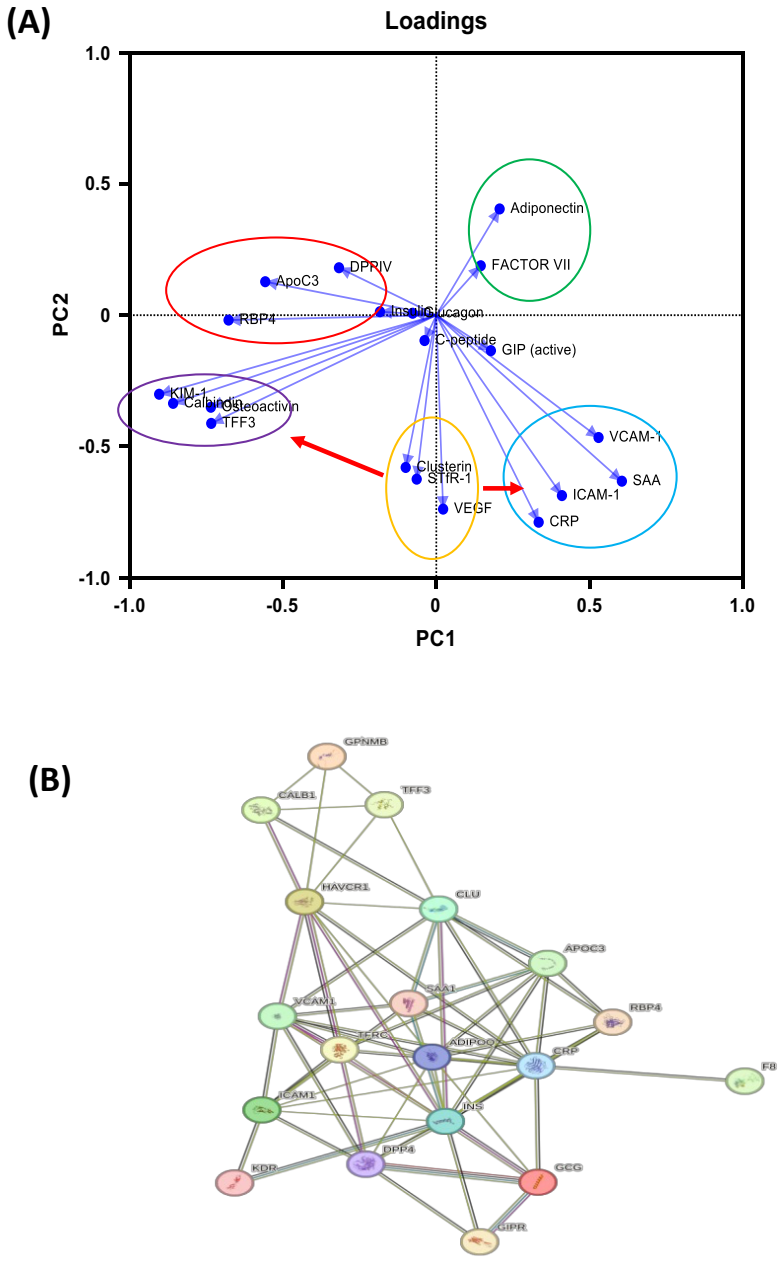

Figure 5.21: Soluble marker expression forms distinct serum cluster profiles for RA+ patients.

(A) Principal Component Analysis (PCA) demonstrating five clusters amongst serum biomarkers in RA+ (n=10-22). (Red=cluster 1, green=cluster 2, blue=cluster 3, yellow=cluster 4, and purple =cluster 5). Red arrows denote that cluster 4 (yellow) overlaps the two bottom quadrants, with markers associated with cluster 2 (blue) or cluster 5 (purple). (B) Potential protein biomarker interactions using the STRING software; CRP, ICAM-1, VCAM-1, VEGF, A-SAA, FACTOR VIII, TFF3, CaLbindin, Osteoactivin, KIM-1, Clusterin, RBP4, ApoC3, Adiponectin, DPPIV, STfR-1, GIP(Active), Insulin, C-peptide, Glucagon.

5.5 Discussion:

In this chapter CD45-PDPN-CD146-CD31+ CECs were identified in the circulation and enriched in the blood of RA patients compared to HC. The majority of the identified CECs were derived from the microvasculature for both cohorts. Frequency of RA CECs demonstrated trending increases for females and patients with high DAS28 score (> 3.2). For the first time, phenotypic characterisation of CECs was performed, demonstrating differences between disease and health. CECs in both HC and RA have the capacity to proliferate, reflected by the observed high frequency of CECs positive for Ki67 with increased expression observed in RA patients. However, RA CECs may be metabolically impaired, with reduced expression observed for the metabolic markers pAKT and pmTOR compared to HC. RA CECs demonstrate reduced ability for wound healing reflected by the observed decrease in expression for PDGFRα and YAP compared to HC. RA CECs demonstrate a pathogenically activated phenotype with a significant increase observed for FAPα+ CECs, and to a lesser extent THY-1+ CECs. Increased frequency and expression were also observed for immunoregulatory markers including HLA-DR and adhesion molecules ICAM-1, VCAM-1, Cadherin 11, and CD44, with minimal differences observed for integrin CD61. The presence of PDPN-CD45dimCD34+CD133+CD31+ EPCs were also identified in the circulation with a trending increase in RA patients compared to HC donors. Frequency of RA EPCs demonstrated a slight increase in females compared to males and no significant changes between high and low DAS28, however EPC levels were highest in the remission group with a DAS28 (1.8-2.8). Furthermore, the presence of both CECs and EPCs were identified in IAR and ART, in addition to differences between RA+ and RA- patients. Finally, this chapter investigated serum soluble markers of inflammation, vascular/tissue injury and metabolic activity across healthy, pre-disease, RA, PsA and GCA for disease comparators. Stepwise increases from HC to IAR to RA+ were observed for several markers of key vascular damage and metabolic activity. Furthermore, while cytokine levels were low (as expected) a decrease in anti-inflammatory cytokines in disease cohorts was observed including IL-4, IL-10 and IL-13.

The increased frequency of CECs in the circulation of patients with RA is consistent with previous studies demonstrating increased numbers in patients with RA and SLE compared to controls (Foster *et al.,* 2009; Rodriguez-Carrio *et al.,* 2012; Cafaro *et al.,* 2022). The majority of the CECs identified in this study were derived from the microvasculature, with microvascular endothelial dysfunction implicated in RA and associated CVD development (Bordy *et al.,* 2018). Increased frequency and/or expression of FAPα, THY-1, HLA-DR, ICAM-1, VCAM-1, CD44, and Cadherin 11 were demonstrated in RA compared to HC, suggesting CECs are more activated in RA. While this is the first study to demonstrate HLA-DR expression on CECs in RA, previous studies

have shown HLA-DR expression on stromal cells in the synovium, including synovial EC and FLS (Barkley *et al*., 1989; Navarrete Santos *et al*., 1997; Spurrell *et al*., 2004; Køster *et al*., 2021), suggesting it may play an important role in antigen presentation and disease chronicity in RA. Furthermore, the HLA-DRB1 shared epitope alleles have been implicated in vascular endothelial injury and endothelial dysfunction in RA, thus potentially having a direct effect on EC function (Gonzalez-Gay, Gonzalez-Juanatey, and Ollier, 2004). The FAPα and THY-1 markers are normally associated with FLS phenotype and function (Croft *et al.,* 2019; Floudas *et al.,* 2022). While little is known about FAPα expression on ECs in RA, studies have demonstrated increased expression of FAPα on ECs in glioblastoma compared to normal tissue (Ebert *et al*., 2020). FAPα expression on ECs has also been identified in other cancers including melanoma and ovarian cancer, with its functional role associated with promoting angiogenesis and invasive mechanisms (Ghersi *et al.*, 2006; Ghilardi *et al*., 2008). Similarly, expression of THY-1 has been demonstrated on activated microvascular ECs, where it mediates leukocyte adhesion via interaction with CD11b (Wetzel *et al.,* 2004). Furthermore, VEGF and TNFα can induce the expression of THY-1 expression on microvascular ECs, with THY-1+ ECs associated with melanoma metastasis (Schubert *et al.*, 2013). In the context of FLS, co-expression of these two markers (THY-1+FAP+) is associated with an activated immunomodulatory function in RA, suggesting that their role on EC may include both immune cell engagement and the migratory/invasive functional capacity of EC (Floudas *et al*., 2022). The observed trending increases in ICAM-1, VCAM-1, CD44, and Cadherin 11 on CECs, again suggests activation and enhanced migration/adhesive function. Specifically ICAM-1 and VCAM-1 are induced on synovial microvascular endothelial cells in response to pro-inflammatory mediators, is increased on synovial vascular EC, with one of its main roles to facilitate lymphocyte infiltration and retention in the joint (Carlos *et al.,* 1990; Abbot *et al*., 1992; Muller-Ladner *et al.,* 1996; Mulherin *et al*., 1996; Klimiuk *et al.*, 2002; Klint *et al*., 2005; Mullan *et al.*, 2006; Fearon *et al.*, 2006; Petrasca *et al*., 2020). Additionally, synovial FLS can enhance EC expression of ICAM-1 and VCAM-1 in co-culture models, an effect that also induces leukocyte adhesion (Fromm *et al.,* 2019). Little is known about the function of CD44 and Cadherin-11 in the context of CEC, but increased CD44 is associated with corneal EC differentiation and activation, while studies have shown that Cadherin-11 induces vascular remodelling through modulation of cardiomyocytes via IL-6 secretion (Fang *et al.,* 2023; Zou *et al.,* 2024). Together, the observed increase in the expression of HLA-DR, FAPα, THY-1, ICAM-1, VCAM-1, CD44, and Cadherin-11 on RA CEC, suggest at the systemic levels circulatory EC are pathologically activated, with implication for the development of CVD.

Increased frequency of EPCs in patients with RA compared to HC was also demonstrated in this chapter. This contrasts with previous studies reporting that levels of EPCs are decreased in RA compared to HC (Akhavani *et al*., 2007; Park *et al*., 2014; Cafaro *et al*., 2022). Increases in EPC frequency in inactive RA compared to HC, paralleled by decreased frequencies in active RA have also been observed (Grisar *et al*., 2005). Furthermore, Yiu *et a*l, 2010, demonstrated an inverse correlation between EPC levels and prevalence of RA patients with atherosclerosis, concluding that the depletion of EPCs potentially contributes to the development of atherosclerosis in RA patients (Yiu *et al.,* 2010). In contrast, Rodríguez-Carrio *et al.* (2012) demonstrated no differences in RA EPC frequency compared to HC, however showed an increase in SLE. Furthermore, de Villeroche *et al.,* 2010, demonstrated elevated numbers of EPCs in active RA compared to remission, levels of which correlated with disease activity. However, de Villeroché *et al.* (2010) also demonstrated no correlation between EPC numbers and serum markers of inflammation, EC injury, or synovitis, so whether these cells are contributing to or compensating for disease activity is unclear. Based on these conflicting studies it is still unclear if EPCs act as a beneficial, reparative cell, or negatively contribute to pathogenic mechanisms.

Circulating levels of CRP were significantly increased in RA+, RA-, and PsA. This aligns with the fact that CRP is utilised as part of the routine blood analysis for RA diagnosis, but also with studies demonstrating elevated CRP levels in patients with RA and CVD (Pope *et al.,* 2021). We also demonstrate increased serum levels of SAA specifically in RA+ patients, which is consistent with previous studies that identified SAA as a potential biomarker of disease specifically for RA, compared to other forms of arthritis (Cunnane *et al.*, 2000; Connolly *et al.,* 2012). Studies have also shown SAA responds differentially to treatment with better responses observed for RA patients on anti-TNFα therapies compared conventional DMARDs (Connolly *et al.,* 2012; Hwang *et al.*, 2016). Interestingly, Hwang *et al*, also demonstrated that A-SAA is a potentially better biomarker of RA disease activity and response compared to CRP. Furthermore, recent studies have shown that A-SAA is a strong potential biomarker of vascular inflammation in RA (Cabay *et al.,* 2020; Giles *et al.,* 2024).

In this chapter increased serum levels of ICAM-1, VCAM-1, VEGF, and Factor VIII were also demonstrated in RA compared to HC, particularly for RA+ patients. These findings corroborate previous literature demonstrating high levels of ICAM-1 and VEGF in the systemic circulation of RA patients, levels of which are also associated with RA disease activity (Grisar *et al*., 2005; Akhavani *et al.,* 2007; Klimiuk *et al.,* 2007; Foster *et al*., 2009; Lee and Bae, 2018; Boldeanu *et a*l., 2023). Strong correlations between circulatory levels of ICAM-1, VCAM-1, SAA, and VEGF have been shown in cardiovascular disease, further implying an association between RA systemic

inflammation and CVD (Jenny *et al*., 2006; Wada *et al.,* 2020; Troncoso *et al.*, 2021). Interestingly, studies have shown that SAA can induce ICAM-1, VCAM-1 and angiogenic factor expression in both EC and FLS, suggesting SAA can act as a biomarker but also induce pathogenic mechanisms which contribute to both systemic and joint inflammation (O'Hara *et al*., 2004; Mullan *et al*., 2006; Mullan *et al*., 2010; Connolly *et al.*, 2010).

Stepwise increases from HC to IAR to RA+ were observed for serum levels of TFF3, Calbindin, and Osteoactivin. Increased levels were also observed for KIM-1 with significantly higher levels observed in IAR. TFF3 is a small molecular peptide secreted by goblet and epithelial cells that has been implicated in cancer with its involvement in proliferation, invasion, resistance to apoptosis, and angiogenesis of cancer cells (Yang et al., 2022). Previous studies have identified increased expression of TFF3 in the RA synovial membrane compared to OA and HC (Popp, et al., 2019). Similarly, TFF3 has been implicated as a biomarker in CVD with increased levels observed in those with peripheral artery disease as well as chronic heart failure (Eidizadeh *et al.,* 2023; Pesau *et al.,* 2024). Calbindin is a calcium-binding protein that regulates intracellular calcium levels and though its serum levels have not been investigated in RA or CVD, circulating calcium has been identified as a risk factor for vascular disease (Lee *et al.*, 2006; Reid, Birstow, and Bolland, 2017). Osteoactivin, also known as GPNMB, is a glycoprotein. Serum levels have not been investigated in RA; however, studies have shown it can upregulate the expression of MMP-3 and MMP-9 in FLS in mice and plays an important functional role in the regulation of mouse osteoclast formation/activity possibly via RANKL-dependent fusion (Ogawa *et al.,* 2005; Sheng *et al*., 2008). KIM-1 is a phosphatidylserine receptor that recognises apoptotic cells and directs them to lysosomes (Bonventre, 2014). In an acute setting, it has been described as having protective and anti-inflammatory properties, however, chronic overexpression has been associated with inflammation (Brilland *et al.,* 2023). Studies have linked KIM-1 to coronary atherosclerosis and have implicated it as a promising new biomarker for early diagnosis and prediction of clinical outcomes for CVD (Medić *et al*., 2015; Lin *et al.,* 2024).

Changes in soluble markers for metabolic activity were also observed in the serums of at risk and disease cohorts compared to HC. Indeed, Clusterin, RBP4, ApoC3, Adiponectin, STfR-1, DPPIV, and active GIP demonstrated increased serum levels in RA+, RA-, and PsA. Increased levels of circulating metabolites have been implicated in vascular damage and CVD (dos Santos *et al.,* 2013; Wang *et al.,* 2015; Codoñer-Franch *et al.*, 2016; Bradley *et al*., 2019; Wilson *et al.,* 2020; Zhu *et al.*, 2022). The relationship between adipose tissue and IA is still not clearly understood; however, studies have demonstrated increased levels of circulating adipokines such as adiponectin in RA patients (Otero *et al.*, 2006; Yoshino *et al.,* 2011). Interestingly, GCA

demonstrated low expression for all measured serum markers with the exception of active GIP and GLP-1. These two hormonal peptides have been implicated in the management of obesity and prevention of CVD (Wilson *et al.,* 2020; Pirro *et al.,* 2022; Liu *et al.*, 2024).

Understanding how markers of vascular damage and tissue injury present themselves in RA and prior to clinical disease could not only help predict those who will be more at risk for CVD complications but may also provide a better benchmark to compare the effects of treatments to in their ability to reduce CVD risk in RA patients. For example, studies have shown methotrexate reduced soluble adhesion markers in RA patients and consequently, methotrexate has been associated with reduced CVD risk in RA patients with a reduction of up to 21% (Klimiuk *et al.*, 2007; Westlake *et al.,* 2010; Micha *et al.*, 2011). Conversely, high doses of glucocorticoids are associated with CVD risk and have been shown to have unfavourable, adverse effects on the metabolic profile of patients (Wei, MacDonald, Walker, 2004; Gkaliagkousi *et al.,* 2012).

The contrary findings of EPCs and CECs in the literature could, in part, be the consequence of inconsistent use of markers to identify each cell type; however, one cannot discount donor variability as well. This highlights the need for additional studies to be performed on larger cohorts of patients. Due to this being a preliminary study, it would be beneficial to increase our cohort numbers to not only provide more insight into the association of systemic inflammation in RA and development of CVD, but also provide us with the opportunity to increase numbers for stratification across patient cohorts.

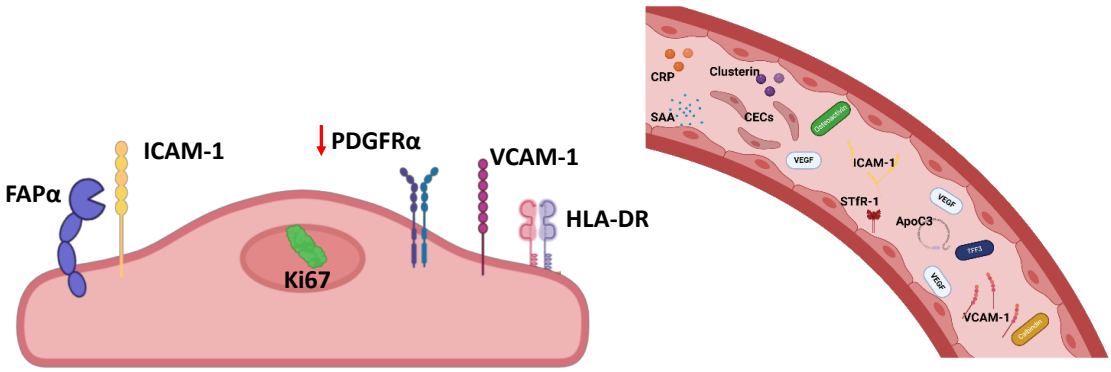

Figure 5.22: Summary of CEC phenotype and function in RA.

Frequencies of CECs and EPCs are in increased in RA compared to HC. RA CECs demonstrated a pathogenically activated phenotype with increased % frequency of FAPα, adhesion molecules (ICAM-1 and VCAM-1), and immunoregulatory molecule HLA-DR. CECs have the capacity to proliferate further evident by the increased expression of Ki67. Alterations in CEC and EPC frequencies are observed prior to disease onset. Soluble markers for vascular and tissue injury and metabolic changes were increased in and prior to disease. (Image created in BioRender 2025).

CHAPTER SIX:

General Discussion and Future Directions

6.1 General Discussion:

RA is a common chronic autoimmune disease responsible for tissue destruction within the joint, leading to functional disability and, ultimately, premature mortality. It is a common cause of pain in the general population, especially for young females, and therefore may have profound impacts on entire family units and society. In addition, RA reduces mobility, increases social isolation, and is significantly associated with other co-morbidities including obesity, diabetes and cardiovascular disease. It is estimated that approximately 40,000 people (1/100) currently have RA in Ireland with an estimated cost of €20,000 per patient per year and overall cost of about €544 million (Arthritis Ireland, 2018).

Targeted biotherapeutics have major effects on the outcome of RA, however, as highlighted throughout this thesis, patients may experience serious adverse events, sub-optimal responses, or no response at all. RA provides an ideal 'model' for a systems approach to personalised medicine; however, better understanding is needed regarding the mechanisms of disease before treat-to-target approaches are feasible. There is currently an array of biologic therapies available directed against molecules, cells, or signaling pathways to treat patients with RA. Currently, when individuals are diagnosed with RA, they are grouped together under the umbrella diagnosis of RA and further subcategorised as either seropositive or seronegative. So, for all RA patients (despite any possible genetic, molecular, or cellular differences they may have) the first drug of choice is the DMARD MTX. In the event a patient fails MTX, they are then eligible for anti-TNF therapy. Those who do not respond to anti-TNF therapy can switch to B-cell depleting therapy (rituximab), T-cell co-stimulation blockade (abatacept), IL-6R blockade (tocilizumab), and if all these fail, small molecule targeted inhibitors (JAKi) are utilised. Thus, patients can cycle through numerous drugs before finding one they respond well to, at which point they may have already developed irreversible bone and cartilage damage.

A significant non–response rate of 2 years is well established for many of these therapeutic agents including MTX (45%), anti-TNF (30%) and RTX (40%), thus forcing patients to move to alternate therapies. Studies have demonstrated that, if introduced early, the right treatment consistently produced better long-term outcomes including reduced joint damage, reduced disability, and employment. However, it is impossible to predict who will develop severe, erosive disease or whether a patient will respond to a particular treatment**.** This **'**trial-and-error' approach is not a cost-effective strategy and can negatively impact a patient's outcome. Unfortunately, as there is currently no cure for RA, patients require lifelong treatment.

The identification of individuals 'at-risk' (IAR) has emerged as a major focus in the field, with studies searching for clues in understanding the evolution of RA and identifying biomarkers

to better predict disease onset. One potential corollary in studying this cohort is the promise of developing a cure for RA, where the initial break in self-tolerance can be identified and targeted therapeutically. While the presence of autoantibodies might precede disease onset by a decade or more, studies have still found it difficult to predict who will go on to develop RA. Fortunately, this has slowly been improving with enhanced imaging techniques that can identify evidence of subclinical synovitis in combination with ACPA positivity (Nam *et al.*, 2016; van Steenbergen *et al.*, 2016). Many studies have demonstrated alterations in molecular and cellular profiles in these individuals at both the systemic level and at the site of inflammation (Chang *et al.*, 2016; Lübbers *et al.*, 2016; Guo *et al.*, 2017; Cole *et al.*, 2018; McGarry *et al.*, 2021; Anang *et al.*, 2022; de Jong *et al.*, 2022), suggesting they have had an initial 'first hit' immune response, and any subsequent insult may induce the development of RA. Additionally, studies have also focused on other tissue sites for evidence of RA development, including the lymph nodes, mouth, gut and lungs (Lerner and Matthias, 2015; Catrina *et al.*, 2016; Jiménez-Martínez *et al.*, 2024). A recent study demonstrated that a single dose of RTX along with methylprednisolone did not improve patient reported outcomes at two years in IAR (Frazzei *et al.*, 2024). In contrast, recently an eloquent study by Cope *et al.* (2024) demonstrated that IAR treated with abatacept for 12 months significantly reduced progression to RA.

Numerous studies have performed genome-wide association, transcriptomic, proteomic, epigenetic, and metabolomic studies in RA patients; however, in the clinic, serological status is still the only biomarker used for RA patient stratification. This is largely due to the lack of validated biomarkers at the systemic level that can accurately inform clinicians of the correct treatment decisions within the clinical setting. The synovium is the main tissue targeted in RA; therefore, it is critical to better understand the complexity of this microenvironment. Recent advances in single-cell technologies have allowed for in-depth analyses of the synovial tissue and the cell populations that constitute it. These advanced technologies are emerging as methodologic approaches that may have clinical significance for real stratification of patients, leading to better therapeutic strategies as well as new therapeutic targets and biomarkers. These technologies, along with spatial anatomical analysis and with improved methods of synovial tissue analysis (both arthroscopic biopsy and ultrasound-guided synovial biopsies), are already enabling significant progress in this field. This detailed profiling of synovial tissue along with paired analysis of blood, may lead to the development of a blood correlate that will define specific synovial pathotypes in RA, and this information could be then utilised in the clinic to predict the right treatment option for patients from the outset of disease.

This thesis explored the role stromal cells play in regulating the balance between inflammation and homeostasis in the synovial joint as well as their role in RA progression. Specifically, we examined the metabolic pathway alterations within the RA synovium and their impact on RA FLS pathogenicity via crosstalk with other signaling pathways. Furthermore, we identified and examined the functional phenotype of circulating PRIME cells in RA+ and RA- patients, as well as prior to disease onset in IAR, to better understand the role these cells play in initiating synovial inflammation and joint spreading. Moreover, we performed an in-depth investigation, by flow cytometry and scRNA-seq, on the heterogeneity of FLS subsets present within the RA synovium compared to HC, identifying both homeostatic and pathogenic populations. Finally, we examined the role of circulating CECs and EPCs in RA pathogenesis and potential soluble biomarkers to determine patients' risk for developing CVD. Given the crucial role FLS play in perpetuating inflammation in the joint, understanding the molecular mechanisms that shape FLS phenotypes may enable better identification of IAR who may progress on to RA, better patient selection for targeted therapies, improved monitoring of treatment efficacy, and, finally, allow for more specific stratification of patients with inherently more progressive disease and those who may be refractory to treatment.

Chapter 2 examined the role of the mTOR pathway in mediating RA FLS metabolism and activation and determined its interaction with the Hippo-YAP pathway, a key signaling pathway involved in cellular survival and invasive mechanisms. Transcriptomic analysis of HC and RA synovial tissue revealed dysregulated expression of several key components of the mTOR pathway in RA. Moreover, the expression of pS6, the major downstream target of mTOR, is increased in RA FLS compared to HC. In the presence of TNF, RA FLS display heightened phosphorylation of S6 and are responsive to mTOR inhibition via Rapamycin. Rapamycin effectively alters RA FLS cellular bioenergetics by inhibiting glycolysis and the expression of rate limiting glycolytic enzymes. Furthermore, mTOR signaling mediated RA FLS migratory and invasive mechanisms, which were significantly abrogated in the presence of Rapamycin. Finally, we reported a significant upregulation in several genes involved in the Hippo-YAP pathway in RA synovial tissue, which are predicted to converge with the mTOR pathway. To confirm this, we demonstrated crosstalk between the mTOR and YAP pathways in mediating RA FLS function whereby Rapamycin significantly abrogated YAP expression, and in turn YAP inhibition significantly inhibited RA FLS invasiveness. Therefore, in this chapter we demonstrated that mTOR drives key pathogenic mechanisms in RA FLS, an effect which is in part mediated via crosstalk with the Hippo-YAP pathway. Furthermore, we showed that these pathways were not only altered in established RA,

but also pre-disease onset in IAR, thus suggesting it is an early metabolic signature that shapes the RA joint microenvironment and represents a potential therapeutic strategy early in disease.

In Chapter 3 we investigated 'pre-inflammatory mesenchymal' (PRIME) cells in the circulation of patients with RA. While very few studies have focused on these cells, one eloquent study by Orange *et al.* (2020) demonstrated that their gene signature in the blood is a predictor of flare in patients with RA. However, little is known regarding the functional capacity of 'PRIME' cells, therefore in this chapter we aimed to characterise PRIME cells in patients with RA compared to HC and to determine if these cells are altered prior to disease onset. Additionally, we aimed to identify differences in PRIME cells between the circulation and the site of inflammation (synovial tissue). The frequency of PRIME cells (CD45-CD31-PDPN+) was increased in RA+ and RA- compared to HC, with the greatest increase observed for RA-. An increase in the frequency of RA+ PRIME cells positive for immunoregulatory markers CD200+ and HLA-DR+ was observed compared to HC. Similarly, RA- patients also demonstrated a significant increased frequency of HLA-DR+ PRIME cells compared to HC. The adhesive capacity of PRIME cells was increased in disease vs HC, evident by increased expression of ICAM-1+, CD44+, VCAM-1+ and CD61+. This may facilitate their adhesion and trans-endothelial cell migration into, as well as subsequent retention in, the inflamed joint. Interestingly, we demonstrated an unexpected inverse relationship between Cadherin 11 and PDGFRα expression on PRIME cells. Previous studies have demonstrated that Cadherin 11 engagement activates RA FLS, promoting inflammatory and degradative function (Lee *et al.*, 2007; Noss *et al.*, 2011). Similarly, PDGFRα activation induces a pro-destructive invadosome-forming phenotype in RA FLS, promoting their migratory and invasive nature (Charbonneau *et al.*, 2016). Furthermore, interaction between Cadherin 11 and PDGFRα induces RA FLS proliferative capacity and ECM degradative enzymes, an effect mediated through PI3K/Akt signaling. However, PDGFRα activation of RA FLS can be Cadherin 11 dependent or independent (McLachlan and Yap, 2007; Bhanupriya *et al.*, 2019). Dependent interactions co-regulate cell adhesion and cell growth, while PDGFRα-independent Cadherin 11 pathways induce more inflammatory RA FLS phenotypes (Madarampalli *et al.*, 2019). Whether the phenotype of circulatory 'PRIME cells' is more immunoregulatory and adhesive rather than invasive is unclear, however, these cells may influence joint spreading, which is a feature of RA, with studies in animal models demonstrating that joint spreading may be mediated through circulatory FLS (Lefèvre *et al.*, 2009).

Next, we examined the established FLS subset/SL markers THY1, CD34 and FAPα, and demonstrated increased frequency in RA>IAR>ART>HC PRIME cells, suggesting that these cells may be pre-determined to become SL FLS once they have entered the joint. The increased expression of HLA-DR+ and ICAM-1+ was also observed in IAR and/or ART, indicating these

phenotypic changes occur prior to disease onset. Finally, in this chapter we demonstrated enrichment of PDPN+ cells in the synovial tissue compared to HC. Differential expression of functional markers was observed between the two sites, with CD61+, ICAM-1+, CD200R1+, CD200+, Cadherin 11+, pmTOR+ and pS6+ enriched in the circulation, in contrast to CD44+, HLA-DR+ and pAKT+ enriched in the joint. Thus, these cells display phenotypic features that are site specific and most likely influenced by environmental cues. Further examination of the functional capability of these cells and their potential crosstalk with other circulating immune cells could better elucidate the role that these cells play in RA pathogenesis. Moreover, further investigation comparing the characteristics of circulating PRIME cells to PDPN+ cells in the joint may provide clues as to which specific FLS subsets arise from these circulating mesenchymal precursors as opposed to a tissue resident origin. Finally, further research is required to better understand the origins of PRIME cells to elucidate the beginning stages of joint inflammation as well as joint spreading.

Recent literature has demonstrated the complexity of the inflamed synovium and identified multiple FLS populations within the RA synovium with distinct inflammatory and functional profiles (Croft *et al.,* 2019; Floudas *et al*., 2022; Zhang *et al.*, 2024). Despite current advances in classifying the heterogeneity of FLS subsets, understanding of the FLS landscape in RA compared to HC and IAR is limited. Therefore, building on this previous work, in Chapter 4, we aimed to fully explore the spectrum of synovial FLS subsets residing within the RA synovium. Initially, we demonstrated an increase in PDPN+ cells in the RA+ and RA- synovium compared to HC. Flow analysis enabled us to identify populations (THY-1, CD55, CD34 and FAP) and examine their functional capacity based on an array of cellular surface markers. Differential expression of CD55 (LL), THY-1 (SL) and FAPα+ (activation) FLS were observed between RA+ and RA- when compared to HC. RA+ demonstrated significantly increased frequencies of HLA-DR+ and ICAM-1+ cells compared to HC, while RA- demonstrated an increased frequency of CD61+ FLS. Furthermore, frequencies of ICAM-1+, CD61+, HLA-DR+ and pAKT+ FLS were associated with a high DAS28.

With further stratification of FLS subtypes, we identified that RA+ displayed the highest proportion of THY1+FAPα+, while THY1-FAPα+ was highest in RA-. Furthermore, RA- were enriched for the LL subset (CD55+THY1-FAPα+), while RA+ were enriched for the SL subset (CD55-THY1+FAPα+). The enrichment of CD55-THY1+FAPα+ is supported by the histological analysis, which showed significantly greater immune cell infiltration and lymphoid aggregates in RA+ compared to RA- and HC. A similar LL thickness was observed between both RA+ vs RA- donors, with cell layer thickness increased compared to HC, evidence of significant LL hyperplasia in RA. Interestingly, the differences in RA+ vs RA- FLS subtypes underpin the hypothesis that seropositive

vs seronegative RA are different diseases. The enrichment of the SL population in RA+ and of the LL subset in RA-, is supported by recent scRNSeq data comparing RA and PsA, with the latter also being seronegative (Floudas *et al.*, 2022). Indeed, the FLS phenotype of the RA- patients in this study more closely align with the dominant FLS population identified in PsA, with this subset displaying enhanced expression of ECM degrading enzymes, emphasising its role in invasion and destruction of adjacent cartilage and bone (Floudas *et al.*, 2022). The decreased frequency of LL FLS subtypes in RA+ patients is corroborated by some recent eloquent studies, which have shown breakdown of the protective LL barrier in RA compared to HC (Culemann *et al.*, 2019; Huang *et al.*, 2021; Hanlon *et al.*, 2024). These studies demonstrated a lack of CX_3CR1+ macrophages in LL of RA. These macrophages form a tight junction-mediated shield with LL FLS to protect the joint from insult. In contrast, the observed enrichment of the SL CD55-THY1+FAPα+ in RA+ is consistent with Croft *et al.* (2019), where they identified FAPα+THY1+ immune effector subtypes localised to the SL, with adoptive transfer of these in a mouse model resulting in a more severe and persistent inflammatory arthritis.

scRNA-seq identified 14 FLS clusters between HC and RA synovial tissue, which were displayed at different frequencies across the two cohorts. Clusters 1, 2, 5, 10, 11, and 13 demonstrated increased expression of LL markers, while clusters 0, 3, 4, and 8 displayed markers associated with SL FLS and were more associated with RA. Clusters 6, 7, 9, and 12 were characterised as intermediate or transitionary FLS as they either displayed characteristics of both LL and SL, or neither. Cluster 3 (POSTN+COL3A1+), identified as a SL cluster, was increased in RA compared to HC, enriched with genes relating to collagen and ECM reorganisation, and demonstrated the highest expression of FAPα+. Further, receptor-ligand interaction analysis between macrophages, T cells and FLS for this cluster, identified key ligands, including IL-1β, VEGF, and TGF-β, that interacted with receptors on FLS. Some notable upregulated pathways within the POSTN+COL3A1+ cluster included NF-κB, TGF-β, and NOTCH signaling pathways. Functional assays demonstrated IL-1β-induced expression of NOTCH ligand DLL4 and JAG-1, with inhibition of NOTCH altering downstream signaling and pro-inflammatory cytokines. The NOTCH signaling pathway is upregulated in the RA synovium (Gao *et al.*, 2013; Gao *et al.*, 2015) and plays a pivotal role in tip-stalk development during the process of angiogenesis (Gao *et al.*, 2013). However, its important role in FLS phenotype/function was demonstrated by Wei *et al.* (2020), where NOTCH signaling was shown to drive spatial gradients starting from synovial vascular EC outwards to FLS influencing the adaptation of the SL phenotype of FLS.

RA is known to be associated with an increased risk of CVD, which is characterised by endothelial dysfunction resulting in CECs within the vasculature. In Chapter 5, we demonstrated

an increased frequency of CECs in RA patients compared to HC, with a similar increase observed in IAR. Most CECs identified for both HC and RA originated from the microvasculature with the majority positive for CD36 expression. RA CECs demonstrated an activated phenotype and increased immune and adhesive functions, with an impaired capacity for wound healing. In parallel, increased serum levels of markers associated with inflammation, cardiovascular, and metabolic dysfunction were observed in RA compared to HC. Collectively, this chapter demonstrates changes to the vasculature in RA, with the potential for CECs and circulating serum markers to act as potential biomarkers in IAR and RA patients for disease onset and progression. This may also have implications for those at greater risk of developing a cardiovascular comorbidity, further contributing to disease pathogenesis.

In summary, the data presented in Chapters 2-5 of this thesis provided a comprehensive analysis of circulatory and synovial FLS at the cellular and molecular level, as well as their contribution to inflammation in RA. Furthermore, we provided insight into the role of FLS in different disease pathotypes, but also identified that FLS pathogenic alterations occur prior to disease onset. We identified that circulatory FLS are primed for inflammation and may act as a biomarker of disease-activity, pathotype, and indeed disease onset. We have characterised distinct FLS subtypes within the joint that are transcriptionally distinct and display differential immune-stromal cell interactions, which may drive specific FLS cluster function. We demonstrated that FLS function may be regulated through key signaling pathways including NOTCH and mTOR signaling, blockade of which abrogates pro-inflammatory responses. Finally, RA is characterised by both systemic and joint-specific inflammation, with Chapter 5 demonstrating the potential risk for development of CVD in RA patients.

6.2 Future Directions:

This thesis provides evidence for the crucial role of FLS in driving pathogenic mechanisms involved in synovial inflammation in RA, in addition to determining the potential plasticity of FLS within the joint and their role in homeostasis vs inflammation. Analysis of cultured primary RA FLS demonstrated that RA FLS activation and invasive mechanisms in-part are mediated through metabolic pathways, particularly the mTOR pathway. Within the joint, however, RA FLS do not act alone but rather interact with numerous immune cells including T cells, B cells, macrophages, and DC. Indeed, numerous studies have demonstrated that the metabolic pathways utilised by different cell types differ and can be influenced by nutrient competition within the inflamed microenvironment (Biniecka *et al.*, 2016; Garcia-Carbonell *et al.*, 2016; Bustamante *et al.*, 2017; Van den Bossche and O'Neill, 2017; McGarry *et al.*, 2018; Gallagher *et al.*, 2020; Petrasca *et al.*,

2020; Qui et al, 2021; Fearon et al, 2022). Therefore, it is critical to understand the role of the mTOR pathway (in addition to other master metabolic regulators) in the context of cellular competition models. Thus, further experimental approaches will aim to analyse pro-inflammatory responses in co-culture models of FLS/T cells and FLS/macrophages, in addition to whole synovial tissue explant *ex vivo* models as previously described (Gao *et al.*, 2016; McGarry *et al.*, 2018). These models more closely reflect the *in vivo* joint microenvironment, where cell-cell contacts and architecture of the joint remain intact. Further models being developed include 3D culture models, using an ECM scaffold to examine the dynamic interactions between FLS, T cells and monocytes. In addition, another model in development is a joint-on-chip platform, where individual tissue chips (FLS-, cartilage-, bone-on-chip) are physically connected to allow tissue-tissue communication. Therefore, the use of more complex competitive models along with analysis of alternative metabolic pathways will give significantly more insight into the role of metabolism and potential targets in rheumatic diseases.

Chapters 3 and 4 of this thesis focused on circulatory 'PRIME' cells and joint specific FLS. These chapters have significantly advanced our understanding of the complex phenotypes of FLS within the joint, but also the potential to monitor PRIME cells within the systemic circulation. To develop the work conducted on PRIME cells, further stratification and their correlation with joint inflammation and pathotype are required. As highlighted throughout this thesis, RA should not be seen as one disease, but rather as numerous subtypes defined by a specific predominance of certain cell types within the joint. The few studies that have analysed this have shown stratification based on ACPA+ and ACPA- (Orr *et al.*, 2017), lympho-myeloid, diffuse-myeloid, and pauci-immune pathotypes (Lewis, *et al.*, 2019; Nerviani *et al.*, 2020; Rivellese *et al.*, 2022) with the more recent eloquent work performed by Zhang *et al.* (2023), demonstrating six pathotypes referred to as CTAPs. Therefore, analysis of PRIME cells in relation to pathotype is an important potential approach. Our data also demonstrated that circulating PRIME cells from 'at risk' individuals display functional abnormalities prior to disease onset. Indeed, we identified a stepwise increase in the expression of many pro-inflammatory mediators from HC to IAR to RA on PRIME cells. Therefore, future studies would include a time-course analysis, where PRIME cells are isolated from IAR patients at 3, 6, and 12 months to investigate whether cell phenotypes change in parallel with RA disease progression. Another area of particular interest would be to analyse PRIME cells from IAR in relation to non-convertors vs convertors to RA. One difficult question to answer is, do these PRIME cells successfully migrate into the joint and if so, what is their function?

This is the first study to compare RA to HC synovium at the single cell level by scRNA-seq and flow analysis, and indeed, ACPA+ vs ACPA-. Therefore, similar to the PRIME cells, expanding

on this work across disease pathotypes and other forms of arthritis, including PsA, AnkSpon and OA, would give a complete picture of the role FLS play within the joint. Furthermore, analysis of synovial FLS pre- and post-therapy, and particularly in patients who do not respond to any current therapies, could give insight into whether refractory patients are indeed associated with FLS dominant synovial phenotypes. Analysis of FLS in non-responsive patients could identify key molecular signatures that may lead to new therapeutic approaches in these difficult-to-treat patients.

All the results in Chapter 4 were performed on synovial tissue cell suspensions, with functional analysis by flow cytometry. To fully understand the differential functions of the FLS subsets identified, additional approaches, including the sorting of these cells for *in vitro* culture, would be of interest. Cell sorting would enable analysis of specific secreted proteins by the distinct FLS subsets, which would give better insight into their functional role. Analysis of the FLS subset-specific markers would also give an improved understanding of whether primary RA FLS retain their *in vivo* phenotype *in vitro*, even at passage 0. Validation of this would facilitate the identification of potential targets in scRNA-seq, whereby subsequent blockade could induce resolution of inflammation. The potential role of NOTCH signaling pathways in FLS function was studied in Chapter 4, and targeting these pathways in co-culture and *ex vivo* models would enhance elucidation of its contribution to RA disease.

In Chapter 5 we investigated the presence of CECs and their potential role in RA pathogenesis. Additionally, cellular and soluble biomarkers were examined as potential markers of EC dysfunction. To validate this data, further studies in larger cohorts across disease stages are required. Furthermore, in addition to disease activity scores associated with RA, sub-analysis of patients who have associated CVD may further focus this panel of biomarkers, to identify a more definitive signature.

Finally, as highlighted in the main introduction, RA occurs more frequently in women than in men (the ratio is between 2:1 and 3:1). It is also clear that RA disease peak prevalence occurs in the 3rd-4th decade, when reproduction is most likely. Therefore, RA presents specific problems for women, not only in relation to their personal health, but that of their children and the family. Numerous factors have been implicated in the over-representation of women in RA including hormonal, genetic and environmental factors (Oliver and Silman, 2009). The role of sex hormones in the disease course of RA is further emphasised by the observation that female patients may experience remission during their pregnancy. Several studies have identified that gender and sex chromosomes may have significant influences on the course of disease, response to treatment and outcomes (Kvien *et al.,* 2006; Forslind *et al.,* 2007). Indeed, poorer outcomes in female

patients in response to bDMARDs have been observed (Saber *et al.,* 2010; Murray *et al.,* 2019). Patients with PsA (which skews slightly towards males) show consistently better responses to bDMARDs, however it is not clear if this represents a gender or a disease pathogenetic effect (Saber *et al.,* 2010). The reasons for this are unclear, however differences may lie in the hormonal milieu, different biometrics and metabolic profiles, there may also be differences in the distribution and processing of the medications that impact on efficacy. These variations in gender, namely in terms of susceptibility, disease severity, response to therapy, and knowledge of their disease, are important to be considered in future work. The data would be analysed across the whole study cohort and would also compare gender sub-groups and gender specific risk-factors.

Bibliography:

Abbot, S.E., Kaul, A., Stevens, C.R. and Blake, D.R., 1992. Isolation and culture of synovial microvascular endothelial cells. Characterization and assessment of adhesion molecule expression. *Arthritis & Rheumatism: Official Journal of the American College of Rheumatology*, *35*(4), pp.401-406.

Agbanoma, G., Li, C., Ennis, D., Palfreeman, A.C., Williams, L.M. and Brennan, F.M., 2012. Production of TNF-α in macrophages activated by T cells, compared with lipopolysaccharide, uses distinct IL-10–dependent regulatory mechanism. *The Journal of Immunology*, *188*(3), pp.1307-1317.

Aghakhani, S., Zerrouk, N. and Niarakis, A., 2020. Metabolic reprogramming of fibroblasts as therapeutic target in rheumatoid arthritis and cancer: deciphering key mechanisms using computational systems biology approaches. *Cancers*, *13*(1), p.35.

Ahmed, S., Mahony, C.B., Torres, A., Murillo-Saich, J., Kemble, S., Cedeno, M., John, P., Bhatti, A., Croft, A.P. and Guma, M., 2023. Dual inhibition of glycolysis and glutaminolysis for synergistic therapy of rheumatoid arthritis. *Arthritis Research & Therapy*, *25*(1), p.176.

Ahn, J.K., Kim, S., Hwang, J., Kim, J., Kim, K.H. and Cha, H.S., 2016. GC/TOF-MS-based metabolomic profiling in cultured fibroblast-like synoviocytes from rheumatoid arthritis. *Joint Bone Spine*, *83*(6), pp.707-713.

Ahn, J.K., Koh, E.M., Cha, H.S., Lee, Y.S., Kim, J., Bae, E.K. and Ahn, K.S., 2008. Role of hypoxia-inducible factor-1α in hypoxia-induced expressions of IL-8, MMP-1 and MMP-3 in rheumatoid fibroblast-like synoviocytes. *Rheumatology*, *47*(6), pp.834-839.

Aho, K., Koskenvuo, M., Tuominen, J. and Kaprio, J., 1986. Occurrence of rheumatoid arthritis in a nationwide series of twins. *The Journal of rheumatology*, *13*(5), pp.899-902.

Ajeganova, S., Andersson, M.L., Hafström, I. and BARFOT Study Group, 2013. Association of obesity with worse disease severity in rheumatoid arthritis as well as with comorbidities: A long-term followup from disease onset. *Arthritis care & research*, *65*(1), pp.78-87.

Ajeganova, S., Andersson, M.L., Frostegård, J. and Hafström, I., 2013. Disease factors in early rheumatoid arthritis are associated with differential risks for cardiovascular events and mortality depending on age at onset: a 10-year observational cohort study. *The Journal of rheumatology*, *40*(12), pp.1958-1966.

Ajeganova, S., Humphreys, J.H., Verheul, M.K., Van Steenbergen, H.W., van Nies, J.A.B., Hafström, I., Svensson, B., Huizinga, T.W.J., Trouw, L.A., Verstappen, S.M.M. and van der Helm-van Mil, A.H.M., 2016. Anticitrullinated protein antibodies and rheumatoid factor are associated with increased mortality but with different causes of death in patients with rheumatoid arthritis: a longitudinal study in three European cohorts. *Annals of the rheumatic diseases*, *75*(11), pp.1924-1932.

Akhavani, M.A., Larsen, H. and Paleolog, E., 2007. Circulating endothelial progenitor cells as a link between synovial vascularity and cardiovascular mortality in rheumatoid arthritis. *Scandinavian journal of rheumatology*, *36*(2), pp.83-90.

Albani, S., Tuckwell, J.E., Esparza, L., Carson, D.A. and Roudier, J., 1992. The susceptibility sequence to rheumatoid arthritis is a cross-reactive B cell epitope shared by the Escherichia coli heat shock protein dnaJ and the histocompatibility leukocyte antigen DRB10401 molecule. *The Journal of clinical investigation*, *89*(1), pp.327-331.

Aldridge, J., Lundell, A.C., Andersson, K., Mark, L., Østergaard, M., Uhlig, T., Haavardsholm, E.A., Nurmohamed, M., Lampa, J., Nordström, D. and Hørslev-Petersen, K., 2021. Blood chemokine levels are markers of disease activity but not predictors of remission in early rheumatoid arthritis. *Clinical and experimental rheumatology*, *40*(7), pp.1393-1402.

Aletaha, D., Breedveld, F.C. and Smolen, J.S., 2005. The need for new classification criteria for rheumatoid arthritis. *Arthritis & Rheumatism*, *52*(11), pp.3333-3336.

Aletaha, D., Neogi, T., Silman, A.J., Funovits, J., Felson, D.T., Bingham III, C.O., Birnbaum, N.S., Burmester, G.R., Bykerk, V.P., Cohen, M.D. and Combe, B., 2010. 2010 rheumatoid arthritis classification criteria: an American College of Rheumatology/European League Against Rheumatism collaborative initiative. *Arthritis & rheumatism*, *62*(9), pp.2569-2581.

Alivernini, S., Firestein, G.S. and McInnes, I.B., 2022. The pathogenesis of rheumatoid arthritis. *Immunity*, *55*(12), pp.2255-2270.

Alivernini, S., Galeazzi, M., Peleg, H., Tolusso, B., Gremese, E., Ferraccioli, G. and Naparstek, Y., 2017. Is ACPA positivity the main driver for rheumatoid arthritis treatment? Pros and cons. *Autoimmunity reviews*, *16*(11), pp.1096-1102.

Alivernini, S., MacDonald, L., Elmesmari, A., Finlay, S., Tolusso, B., Gigante, M.R., Petricca, L., Di Mario, C., Bui, L., Perniola, S. and Attar, M., 2020. Distinct synovial tissue macrophage subsets regulate inflammation and remission in rheumatoid arthritis. *Nature medicine*, *26*(8), pp.1295-1306.

Almutairi, K., Nossent, J., Preen, D., Keen, H. and Inderjeeth, C., 2021. The global prevalence of rheumatoid arthritis: a meta-analysis based on a systematic review. *Rheumatology international*, *41*(5), pp.863-877.

Alquicira-Hernandez, J. and Powell, J.E., 2021. Nebulosa recovers single-cell gene expression signals by kernel density estimation. *Bioinformatics*, *37*(16), pp.2485-2487.

Al-Shakarchi, I., Gullick, N.J. and Scott, D.L., 2013. Current perspectives on tocilizumab for the treatment of rheumatoid arthritis: a review. *Patient preference and adherence*, pp.653-666.

Alspaugh, M.A., Jensen, F.C., Rabin, H. and Tan, E.M., 1978. Lymphocytes transformed by Epstein-Barr virus. Induction of nuclear antigen reactive with antibody in rheumatoid arthritis. *Journal of Experimental Medicine*, *147*(4), pp.1018-1027.

Alunno, A., Carubbi, F., Giacomelli, R. and Gerli, R., 2017. Cytokines in the pathogenesis of rheumatoid arthritis: new players and therapeutic targets. *BMC rheumatology*, *1*, pp.1-13.

Amara K, Steen J, Murray F, Morbach H, Fernandez-Rodriguez BM, Joshua V, Engström M, Snir O, Israelsson L, Catrina AI, Wardemann H, Corti D, Meffre E, Klareskog L, Malmström V. Monoclonal IgG antibodies generated from joint-derived B cells of RA patients have a strong bias toward citrullinated autoantigen recognition. *J Exp Med.* 2013;210:445–55.

Anang, D.C., Ramwadhdoebe, T.H., Hähnlein, J.S., van Kuijk, B., Smits, N., van Lienden, K.P., Maas, M., Gerlag, D.M., Tak, P.P., de Vries, N. and van Baarsen, L.G., 2022. Increased frequency of Cd4+ follicular helper T and Cd8+ follicular T cells in human lymph node biopsies during the earliest stages of rheumatoid arthritis. *Cells*, *11*(7), p.1104.

Anderson, A.E., Pratt, A.G., Sedhom, M.A., Doran, J.P., Routledge, C., Hargreaves, B., Brown, P.M., Lê Cao, K.A., Isaacs, J.D. and Thomas, R., 2016. IL-6-driven STAT signaling in circulating CD4+ lymphocytes is a marker for early anticitrullinated peptide antibody-negative rheumatoid arthritis. *Annals of the rheumatic diseases*, *75*(2), pp.466-473.

Anyfanti, P., Ainatzoglou, A., Angeloudi, E., Michailou, O., Defteraiou, K., Bekiari, E., Kitas, G.D. and Dimitroulas, T., 2024. Cardiovascular Risk in Rheumatoid Arthritis: Considerations on Assessment and Management. *Mediterranean Journal of Rheumatology*, *35*(3), p.402.

Araujo, L., Khim, P., Mkhikian, H., Mortales, C.L. and Demetriou, M., 2017. Glycolysis and glutaminolysis cooperatively control T cell function by limiting metabolite supply to N-glycosylation. *elife*, *6*, p.e21330.

Argyriou, A., Wadsworth, M.H., Lendvai, A., Christensen, S.M., Hensvold, A.H., Gerstner, C., van Vollenhoven, A., Kravarik, K., Winkler, A., Malmström, V. and Chemin, K., 2022. Single cell sequencing identifies clonally expanded synovial CD4+ TPH cells expressing GPR56 in rheumatoid arthritis. *Nature communications*, *13*(1), p.4046.

Armstrong, D.J., McCausland, E.M., Quinn, A.D. and Wright, G.D., 2006. Obesity and cardiovascular risk factors in rheumatoid arthritis. *Rheumatology*, *45*(6), pp.782-782.

Arnett, F.C., Edworthy, S.M., Bloch, D.A., Mcshane, D.J., Fries, J.F., Cooper, N.S., Healey, L.A., Kaplan, S.R., Liang, M.H., Luthra, H.S. and Medsger Jr, T.A., 1988. The American Rheumatism Association 1987 revised criteria for the classification of rheumatoid arthritis. *Arthritis & Rheumatism: Official Journal of the American College of Rheumatology*, *31*(3), pp.315-324.

Arosio E, De MS, Rigoni A et al (2007) Forearm haemodynamics, arterial stiffness and microcirculatory reactivity in rheumatoid arthritis. J Hypertens 25:1273–1278

Arthritis in Ireland. The Centre for Arthritis and Rheumatic Diseases. (2018, October 2).

Arthritis Ireland. (2023). *Living with Rheumatoid Arthritis*. Dublin. Retrieved October 2024.

Artinian, N., Cloninger, C., Holmes, B., Benavides-Serrato, A., Bashir, T. and Gera, J., 2015. Phosphorylation of the Hippo pathway component AMOTL2 by the mTORC2 kinase promotes YAP signaling, resulting in enhanced glioblastoma growth and invasiveness. *Journal of Biological Chemistry*, *290*(32), pp.19387-19401.

Aubart, F et al. 2011. "High Levels of Anti-Cyclic Citrullinated Peptide Autoantibodies Are Associated with Co-Occurrence of Pulmonary Diseases with Rheumatoid Arthritis." *J Rheumatol* 38(6): 979–82.

Auger, I. and Roudier, J., 1997. A function for the QKRAA amino acid motif: mediating binding of DnaJ to DnaK. Implications for the association of rheumatoid arthritis with HLA-DR4. *The Journal of clinical investigation*, *99*(8), pp.1818-1822.

Aulak, K.S., Mavarakis, L., Tian, L., Paul, D., Comhair, S.A., Dweik, R.A. and Tonelli, A.R., 2024. Characteristic disease defects in circulating endothelial cells isolated from patients with pulmonary arterial hypertension. *Plos one*, *19*(10), p.e0312535.

Avina-Zubieta, J.A., Thomas, J., Sadatsafavi, M., Lehman, A.J. and Lacaille, D., 2012. Risk of incident cardiovascular events in patients with rheumatoid arthritis: a meta-analysis of observational studies. *Annals of the rheumatic diseases*, *71*(9), pp.1524-1529.

Ayala Herrera JL, Apreza Patrón L, Martínez Martínez RE, Domínguez Pérez RA, Abud Mendoza C, Hernández Castro B. Filifactor alocis and Dialister pneumosintes in a Mexican population affected by periodontitis and rheumatoid arthritis: An exploratory study. Microbiol Immunol. 2019 Sep;63(9):392-395. doi: 10.1111/1348-0421.12727. Epub 2019 Aug 12.

Bacon, K. *et al.* (2002) 'Chemokine/Chemokine Receptor Nomenclature', *Journal of Interferon & Cytokine Research*, 22(10), pp. 1067–1068.

Baecklund, E., Iliadou, A., Askling, J., Ekbom, A., Backlin, C., Granath, F., Catrina, A.I., Rosenquist, R., Feltelius, N., Sundström, C. and Klareskog, L. (2006), Association of chronic inflammation, not its treatment, with increased lymphoma risk in rheumatoid arthritis. Arthritis & Rheumatism, 54: 692-701.

Baeten, D., Kruithof, E., De Rycke, L., Boots, A.M., Mielants, H., Veys, E.M. and De Keyser, F., 2005. Infiltration of the synovial membrane with macrophage subsets and polymorphonuclear cells reflects global disease activity in spondyloarthropathy. *Arthritis Res Ther*, *7*, pp.1-11..

Bai, Z., Bartelo, N., Aslam, M., Murphy, E.A., Hale, C.R., Blachere, N.E., Parveen, S., Spolaore, E., DiCarlo, E., Gravallese, E.M. and Smith, M.H., 2024. Synovial fibroblast gene expression is associated with sensory nerve growth and pain in rheumatoid arthritis. *Science Translational Medicine*, *16*(742), p.eadk3506.

Balogh, E., Biniecka, M., Fearon, U., Veale, D.J. and Szekanecz, Z., 2019. Angiogenesis in Inflammatory Arthritis. *The Israel Medical Association Journal: IMAJ*, *21*(5), pp.345-352.

Balogh, E., Veale, D.J., McGarry, T., Orr, C., Szekanecz, Z., Ng, C.T., Fearon, U. and Biniecka, M., 2018. Oxidative stress impairs energy metabolism in primary cells and synovial tissue of patients with rheumatoid arthritis. *Arthritis research & therapy*, *20*, pp.1-15.

Barkley, D., Allard, S., Feldmann, M. and Maini, R.N., 1989. Increased expression Of HLA—DQ antigens by interstitial cells and endothelium in the synovial membrane of rheumatoid arthritis patients compared with reactive arthritis patients. *Arthritis & Rheumatism: Official Journal of the American College of Rheumatology*, *32*(8), pp.955-963.

Bartok, B. and Firestein, G.S., 2010. Fibroblast-like synoviocytes: key effector cells in rheumatoid arthritis. *Immunological reviews*, *233*(1), pp.233-255.

Bartoloni, E., Alunno, A., Bistoni, O., Caterbi, S., Luccioli, F., Santoboni, G., Mirabelli, G., Cannarile, F. and Gerli, R., 2015. Characterization of circulating endothelial microparticles and endothelial progenitor cells in primary Sjögren's syndrome: new markers of chronic endothelial damage?. *Rheumatology*, *54*(3), pp.536-544.

Barton A, Thomson W, Ke X, Eyre S, Hinks A, Bowes J, Plant D, Gibbons LJ; Wellcome Trust Case Control Consortium; YEAR Consortium; BIRAC Consortium; Wilson AG, Bax DE, Morgan AW, Emery P, Steer S, Hocking L, Reid DM, Wordsworth P, Harrison P, Worthington J. Rheumatoid arthritis susceptibility loci at chromosomes 10p15, 12q13 and 22q13. Nat Genet. 2008 Oct;40(10):1156-9.

Basdeo, S.A., Cluxton, D., Sulaimani, J., Moran, B., Canavan, M., Orr, C., Veale, D.J., Fearon, U. and Fletcher, J.M., 2017. Ex-Th17 (nonclassical Th1) cells are functionally distinct from classical Th1 and Th17 cells and are not constrained by regulatory T cells. *The Journal of Immunology*, *198*(6), pp.2249-2259.

Basdeo, S.A., Moran, B., Cluxton, D., Canavan, M., McCormick, J., Connolly, M., Orr, C., Mills, K.H., Veale, D.J., Fearon, U. and Fletcher, J.M., 2015. Polyfunctional, pathogenic CD161+ Th17 lineage cells are resistant to regulatory T cell–mediated suppression in the context of autoimmunity. *The Journal of Immunology*, *195*(2), pp.528-540.

Bash, J., Zong, W.X., Banga, S., Rivera, A., Ballard, D.W., Ron, Y. and Gélinas, C., 1999. Rel/NF-κB can trigger the Notch signaling pathway by inducing the expression of Jagged1, a ligand for Notch receptors. *The EMBO journal*.

Bechman, K., Dalrymple, A., Southey-Bassols, C., Cope, A.P. and Galloway, J.B., 2020. A systematic review of CXCL13 as a biomarker of disease and treatment response in rheumatoid arthritis. *BMC rheumatology*, *4*, pp.1-9.

Beerepoot, L.V., Mehra, N., Vermaat, J.S.P., Zonnenberg, B.A., Gebbink, M.F.G.B. and Voest, E.E., 2004. Increased levels of viable circulating endothelial cells are an indicator of progressive disease in cancer patients. *Annals of oncology*, *15*(1), pp.139-145.

Begovich, A.B., Carlton, V.E., Honigberg, L.A., Schrodi, S.J., Chokkalingam, A.P., Alexander, H.C., Ardlie, K.G., Huang, Q., Smith, A.M., Spoerke, J.M. and Conn, M.T., 2004. A missense single-nucleotide polymorphism in a gene encoding a protein tyrosine phosphatase (PTPN22) is associated with rheumatoid arthritis. *The American Journal of Human Genetics*, *75*(2), pp.330-337.

Beinsberger, J., Heemskerk, J.W. and Cosemans, J.M., 2014, December. Chronic arthritis and cardiovascular disease: altered blood parameters give rise to a prothrombotic propensity. In *Seminars in arthritis and rheumatism* (Vol. 44, No. 3, pp. 345-352). WB Saunders.

Belkina, A.C., Ciccolella, C.O., Anno, R., Halpert, R., Spidlen, J. and Snyder-Cappione, J.E., 2018. AUTOMATED OPTIMAL PARAMETERS FOR T-DISTRIBUTED STOCHASTIC NEIGHBOR EMBEDDING IMPROVE VISUALIZATION AND ALLOW ANALYSIS OF LARGE DATASETS.

Bergers, G. and Song, S., 2005. The role of pericytes in blood-vessel formation and maintenance. *Neuro-oncology*, *7*(4), pp.452-464.

Bergman, G.J., Hochberg, M.C., Boers, M., Wintfeld, N., Kielhorn, A. and Jansen, J.P., 2010, June. Indirect comparison of tocilizumab and other biologic agents in patients with rheumatoid arthritis and inadequate response to disease-modifying antirheumatic drugs. In *Seminars in arthritis and rheumatism* (Vol. 39, No. 6, pp. 425-441). WB Saunders.

Bernardoni, B.L., D'Agostino, I., La Motta, C. and Angeli, A., 2024. An insight into the last 5-year patents on Porphyromonas gingivalis and Streptococcus mutans, the pivotal pathogens in the oral cavity. *Expert Opinion on Therapeutic Patents*, *34*(6), pp.433-463.

Betts, J. G., Young, K. A., Wise, J. A., Johnson, E., Poe, B., Kruse, Dean H. , Korol, O., Johnson, J. E., Womble, M., Womble, M., & DeSaix, P. (2013). Chapter 9.4 Synovial Joints. In *Anatomy and Physiology*. OpenStax.

Biniecka, M., Connolly, M., Gao, W., Ng, C.T., Balogh, E., Gogarty, M., Santos, L., Murphy, E., Brayden, D., Veale, D.J. and Fearon, U., 2014. Redox-mediated angiogenesis in the hypoxic joint of inflammatory arthritis. *Arthritis & rheumatology*, *66*(12), pp.3300-3310.

Biniecka, M., Canavan, M., McGarry, T., Gao, W., McCormick, J., Cregan, S., Gallagher, L., Smith, T., Phelan, J.J., Ryan, J. and O'Sullivan, J., 2016. Dysregulated bioenergetics: a key regulator of joint inflammation. *Annals of the rheumatic diseases*, *75*(12), pp.2192-2200.

Biniecka, M., Fox, E., Gao, W., Ng, C.T., Veale, D.J., Fearon, U. and O'Sullivan, J., 2011. Hypoxia induces mitochondrial mutagenesis and dysfunction in inflammatory arthritis. *Arthritis & Rheumatism*, *63*(8), pp.2172-2182.

Biniecka, M., Kennedy, A., Fearon, U., Ng, C.T., Veale, D.J. and O'Sullivan, J.N., 2010. Oxidative damage in synovial tissue is associated with in vivo hypoxic status in the arthritic joint. *Annals of the rheumatic diseases*, *69*(6), pp.1172-1178.

Biniecka, M., Kennedy, A., Ng, C.T., Chang, T.C., Balogh, E., Fox, E., Veale, D.J., Fearon, U. and O'Sullivan, J.N., 2011. Successful tumour necrosis factor (TNF) blocking therapy suppresses oxidative stress and hypoxia-induced mitochondrial mutagenesis in inflammatory arthritis. *Arthritis research & therapy*, *13*, pp.1-9.

Birnbaum, H., Pike, C., Kaufman, R., Maynchenko, M., Kidolezi, Y. and Cifaldi, M., 2010. Societal cost of rheumatoid arthritis patients in the US. *Current medical research and opinion*, *26*(1), pp.77-90.

Black, R.J., Cross, M., Haile, L.M., Culbreth, G.T., Steinmetz, J.D., Hagins, H., Kopec, J.A., Brooks, P.M., Woolf, A.D., Ong, K.L. and Kopansky-Giles, D.R., 2023. Global, regional, and national burden of rheumatoid arthritis, 1990–2020, and projections to 2050: a systematic analysis of the Global Burden of Disease Study 2021. *The Lancet Rheumatology*, *5*(10), pp.e594-e610.

Blanco, R. and Gerhardt, H., 2013. VEGF and Notch in tip and stalk cell selection. *Cold Spring Harbor perspectives in medicine*, *3*(1), p.a006569.

Blann, A.D. and Pretorius, A., 2006. Circulating endothelial cells and endothelial progenitor cells: two sides of the same coin, or two different coins?. *Atherosclerosis*, *188*(1), pp.12-18.

Blann, A.D., Woywodt, A., Bertolini, F., Bull, T.M., Buyon, J.P., Clancy, R.M., Haubitz, M., Hebbel, R.P., Lip, G.Y., Mancuso, P. and Sampol, J., 2005. Circulating endothelial cells. *Thrombosis and haemostasis*, *93*(02), pp.228-235.

Blaschke, S., Schwarz, G., Moneke, D., Binder, L., Müller, G. and Reuss-Borst, M., 2000. Epstein-Barr virus infection in peripheral blood mononuclear cells, synovial fluid cells, and synovial membranes of patients with rheumatoid arthritis. *The Journal of rheumatology*, *27*(4), pp.866-873.

Boldeanu, M.V., Boldeanu, L., Cristea, O.M., Ciobanu, D.A., Poenariu, S.I., Dijmărescu, A.L., Bărbulescu, A.L., Pădureanu, V., Sas, T.N., Dinescu, Ș.C. and Vreju, F.A., 2023. MMP-13, VEGF, and disease activity in a cohort of rheumatoid arthritis patients. *Diagnostics*, *13*(9), p.1653.

Bonelli, M. and Scheinecker, C., 2018. How does abatacept really work in rheumatoid arthritis?. *Current opinion in rheumatology*, *30*(3), pp.295-300.

Bonventre, J.V., 2014. Kidney injury molecule-1: a translational journey. *Transactions of the American Clinical and Climatological Association*, *125*, p.293.

Boonen, A. and Mau, W., 2009. The economic burden of disease: comparison between rheumatoid arthritis and ankylosing spondylitis. *Clinical & Experimental Rheumatology*, *27*(4), p.S112.

Boonen, A. and Severens, J.L., 2011. The burden of illness of rheumatoid arthritis. *Clinical rheumatology*, *30*, pp.3-8.

Boos CJ, Lip GY, Blann AD. Circulating endothelial cells in cardiovascular disease. J Am Coll Cardiol. 2006 Oct 17;48(8):1538-47. doi: 10.1016/j.jacc.2006.02.078. Epub 2006 Sep 26. PMID: 17045885.

Bordy, R., Totoson, P., Prati, C., Marie, C., Wendling, D. and Demougeot, C., 2018. Microvascular endothelial dysfunction in rheumatoid arthritis. *Nature Reviews Rheumatology*, *14*(7), pp.404-420.

Bottini, A., Wu, D.J., Ai, R., Le Roux, M., Bartok, B., Bombardieri, M., Doody, K.M., Zhang, V., Sacchetti, C., Zoccheddu, M. and Lonic, A., 2019. PTPN14 phosphatase and YAP promote TGFβ signaling in rheumatoid synoviocytes. *Annals of the rheumatic diseases*, *78*(5), pp.600-609.

Bottini, N. and Firestein, G.S., 2013. Duality of fibroblast-like synoviocytes in RA: passive responders and imprinted aggressors. *Nature Reviews Rheumatology*, *9*(1), pp.24-33.

Bourdely, P., Anselmi, G., Vaivode, K., Ramos, R.N., Missolo-Koussou, Y., Hidalgo, S., Tosselo, J., Nuñez, N., Richer, W., Vincent-Salomon, A. and Saxena, A., 2020. Transcriptional and functional analysis of CD1c+ human dendritic cells identifies a CD163+ subset priming CD8+ CD103+ T cells. *Immunity*, *53*(2), pp.335-352.

Boyette, L.B., Macedo, C., Hadi, K., Elinoff, B.D., Walters, J.T., Ramaswami, B., Chalasani, G., Taboas, J.M., Lakkis, F.G. and Metes, D.M., 2017. Phenotype, function, and differentiation potential of human monocyte subsets. *PloS one*, *12*(4), p.e0176460.

Bradfield, P.F., Amft, N., Vernon-Wilson, E., Exley, A.E., Parsonage, G., Rainger, G.E., Nash, G.B., Thomas, A.M., Simmons, D.L., Salmon, M. and Buckley, C.D., 2003. Rheumatoid fibroblast-like synoviocytes overexpress the chemokine stromal cell–derived factor 1 (CXCL12), which supports distinct patterns and rates of CD4+ and CD8+ T cell migration within synovial tissue. *Arthritis & Rheumatism: Official Journal of the American College of Rheumatology*, *48*(9), pp.2472-2482.

Bradley, D., Blaszczak, A., Yin, Z., Liu, J., Joseph, J.J., Wright, V., Anandani, K., Needleman, B., Noria, S., Renton, D. and Yearsley, M., 2019. Clusterin impairs hepatic insulin sensitivity and adipocyte clusterin associates with cardiometabolic risk. *Diabetes care*, *42*(3), pp.466-475.

Brennan FM, Zachariae CO, Chantry D, Larsen CG, Turner M, Maini RN, et al. Detection of interleukin 8 biological activity in synovial fluids from patients with rheumatoid arthritis and production of interleukin 8 mRNA by isolated synovial cells. Eur J Immunol. 1990;20:2141–4.

Brennan, F., Jackson, A., Chantry, D., Maini, R. and Feldmann, M., 1989. Inhibitory effect of TNFα antibodies on synovial cell interleukin-1 production in rheumatoid arthritis. *The Lancet*, *334*(8657), pp.244-247.

Bresnihan, B., Gerlag, D.M., Rooney, T., Smeets, T.J., Wijbrandts, C.A., Boyle, D., Fitzgerald, O., Kirkham, B.W., McInnes, I.B., Smith, M. and Ulfgren, A.K., 2007. Synovial macrophages as a biomarker of response to therapeutic intervention in rheumatoid arthritis: standardization and consistency across centers. *The Journal of Rheumatology*, *34*(3), pp.620-622.

Bresnihan, B., Pontifex, E., Thurlings, R.M., Vinkenoog, M., El-Gabalawy, H., Fearon, U., Fitzgerald, O., Gerlag, D.M., Rooney, T., van de SANDE, M.G. and Veale, D., 2009. Synovial tissue sublining CD68 expression is a biomarker of therapeutic response in rheumatoid arthritis clinical trials: consistency across centers. *The Journal of rheumatology*, *36*(8), pp.1800-1802.

Breton, G., Zheng, S., Valieris, R., Tojal da Silva, I., Satija, R. and Nussenzweig, M.C., 2016. Human dendritic cells (DCs) are derived from distinct circulating precursors that are precommitted to become CD1c+ or CD141+ DCs. *Journal of Experimental Medicine*, *213*(13), pp.2861-2870.

Brilland, B., Boud'hors, C., Wacrenier, S., Blanchard, S., Cayon, J., Blanchet, O., Piccoli, G.B., Henry, N., Djema, A., Coindre, J.P. and Jeannin, P., 2023. Kidney injury molecule 1 (KIM-1): A potential biomarker of acute kidney injury and tubulointerstitial injury in patients with ANCA-glomerulonephritis. *Clinical Kidney Journal*, *16*(9), pp.1521-1533.

Brouwer, E., Gouw, A.S.H., Posthumus, M.D., Van Leeuwen, M.A., Boerboom, A.L., Bijzet, J., Limburg, P.C., Kallenberg, C.G.M., Westra, J. and Bos, R., 2009. Hypoxia inducible factor-1-alpha (HIF-1 alpha) is related to both angiogenesis and inflammation in rheumatoid arthritis. *Clinical and experimental rheumatology*, *27*(6), pp.945-951.

Buch, M.H., Vital, E.M. and Emery, P., 2008. Abatacept in the treatment of rheumatoid arthritis. *Arthritis research & therapy*, *10*, pp.1-10.

Buchakjian, M.R. and Kornbluth, S., 2010. The engine driving the ship: metabolic steering of cell proliferation and death. *Nature reviews Molecular cell biology*, *11*(10), pp.715-727.

Buckley, C.D., Ospelt, C., Gay, S. and Midwood, K.S., 2021. Location, location, location: how the tissue microenvironment affects inflammation in RA. *Nature Reviews Rheumatology*, *17*(4), pp.195-212.

Bugatti, S., Vitolo, B., Caporali, R., Montecucco, C. and Manzo, A., 2014. B cells in rheumatoid arthritis: from pathogenic players to disease biomarkers. *BioMed research international*, *2014*(1), p.681678.

Burman, A., Haworth, O., Bradfield, P., Parsonage, G., Filer, A., Thomas, A.M., Amft, N., Salmon, M. and Buckley, C.D., 2005. The role of leukocyte-stromal interactions in chronic inflammatory joint disease. *Joint Bone Spine*, *72*(1), pp.10-16.

Bustamante, M.F., Garcia-Carbonell, R., Whisenant, K.D. and Guma, M., 2017. Fibroblast-like synoviocyte metabolism in the pathogenesis of rheumatoid arthritis. *Arthritis research & therapy*, *19*, pp.1-12.

Chang, M.F., Oliveira, P.G., Garcia-Carbonell, R., Croft, A.P., Smith, J.M., Serrano, R.L., Sanchez-Lopez, E., Liu, X., Kisseleva, T., Hay, N. and Buckley, C.D., 2018. Hexokinase 2 as a novel selective metabolic target for rheumatoid arthritis. *Annals of the rheumatic diseases*, *77*(11), pp.1636-1643.

Cafaro, G., Petito, E., Bistoni, O., Falcinelli, E., Cipriani, S., Borghi, M.C., Bonifacio, A.F., Giglio, E., Alunno, A., Perricone, C. and Gerli, R., 2022. Methotrexate improves endothelial function in early rheumatoid arthritis patients after 3 months of treatment. *Arthritis Research & Therapy*, *24*(1), p.236.

Caire, R., Audoux, E., Courbon, G., Michaud, E., Petit, C., Dalix, E., Chafchafi, M., Thomas, M., Vanden-Bossche, A., Navarro, L. and Linossier, M.T., 2021. YAP/TAZ: key players for rheumatoid arthritis severity by driving fibroblast like synoviocytes phenotype and fibro-inflammatory response. *Frontiers in immunology*, *12*, p.791907.

Cambier, S., Gouwy, M. & Proost, P. The chemokines CXCL8 and CXCL12: molecular and functional properties, role in disease and efforts towards pharmacological intervention. *Cell Mol Immunol* 20, 217–251 (2023).

Canavan, M., Marzaioli, V., Bhargava, V., Nagpal, S., Gallagher, P., Hurson, C., Mullan, R., Veale, D.J. and Fearon, U., 2021. Functionally mature CD1c+ dendritic cells preferentially accumulate in the inflammatory arthritis synovium. *Frontiers in Immunology*, *12*, p.745226.

Canavan, M., Walsh, A.M., Bhargava, V., Wade, S.M., McGarry, T., Marzaioli, V., Moran, B., Biniecka, M., Convery, H., Wade, S. and Orr, C., 2018. Enriched Cd141+ DCs in the joint are transcriptionally distinct, activated, and contribute to joint pathogenesis. *JCI insight*, *3*(23), p.e95228.

Canavan, M., Marzaioli, V., McGarry, T., Bhargava, V., Nagpal, S., Veale, D.J. and Fearon, U., 2020. Rheumatoid arthritis synovial microenvironment induces metabolic and functional adaptations in dendritic cells. *Clinical & Experimental Immunology*, *202*(2), pp.226-238.

Canete, J.D., Celis, R., Moll, C., Izquierdo, E., Marsal, S., Sanmarti, R., Palacín, A., Lora, D., De La Cruz, J. and Pablos, J.L., 2009. Clinical significance of synovial lymphoid neogenesis and its reversal after anti-tumour necrosis factor α therapy in rheumatoid arthritis. *Annals of the rheumatic diseases*, *68*(5), pp.751-756.

Carbonell-Bobadilla, N., Soto-Fajardo, C., Amezcua-Guerra, L.M., Batres-Marroquín, A.B., Vargas, T., Hernández-Diazcouder, A., Jiménez-Rojas, V., Medina-García, A.C., Pineda, C. and Silveira, L.H., 2022. Patients with seronegative rheumatoid arthritis have a different phenotype than seropositive patients: A clinical and ultrasound study. *Frontiers in Medicine*, *9*, p.978351.

Carlos, T.M., Schwartz, B.R., Kovach, N.L., Yee, E., Rosa, M., Osborn, L., Chi-Rosso, G., Newman, B., Lobb, R. and Rosso M $[corrected to Rosa, M., 1990. Vascular cell adhesion molecule-1 mediates lymphocyte adherence to cytokine-activated cultured human endothelial cells [published erratum appears in Blood 1990 Dec 1; 76 (11): 2420].

Carmeliet, P., De Smet, F., Loges, S. and Mazzone, M., 2009. Branching morphogenesis and antiangiogenesis candidates: tip cells lead the way. *Nature reviews Clinical oncology*, *6*(6), pp.315-326.

Caslin, H.L., Abebayehu, D., Pinette, J.A. and Ryan, J.J., 2021. Lactate is a metabolic mediator that shapes immune cell fate and function. *Frontiers in Physiology*, *12*, p.688485.

Catrina, A.I., Svensson, C.I., Malmström, V., Schett, G. and Klareskog, L., 2017. Mechanisms leading from systemic autoimmunity to joint-specific disease in rheumatoid arthritis. *Nature Reviews Rheumatology*, *13*(2), pp.79-86.

Catrina, A.I., Joshua, V., Klareskog, L. and Malmström, V., 2016. Mechanisms involved in triggering rheumatoid arthritis. *Immunological reviews*, *269*(1), pp.162-174.

Cejka, D., Hayer, S., Niederreiter, B., Sieghart, W., Fuereder, T., Zwerina, J. and Schett, G., 2010. Mammalian target of rapamycin signaling is crucial for joint destruction in experimental arthritis and is activated in osteoclasts from patients with rheumatoid arthritis. *Arthritis & Rheumatism*, *62*(8), pp.2294-2302.

Cha, H.S., Ahn, K.S., Jeon, C.H., Kim, J., Song, Y.W. and Koh, E.M., 2003. Influence of hypoxia on the expression of matrix metalloproteinase-1,-3 and tissue inhibitor of metalloproteinase-1 in rheumatoid synovial fibroblasts. *Clinical and experimental rheumatology*, *21*(5), pp.593-598.

Chaban, Y., Boekema, E.J. and Dudkina, N.V., 2014. Structures of mitochondrial oxidative phosphorylation supercomplexes and mechanisms for their stabilisation. *Biochimica et Biophysica Acta (BBA)-Bioenergetics*, *1837*(4), pp.418-426.

Chabaud, M., Durand, J.M., Buchs, N., Fossiez, F., Page, G., Frappart, L. and Miossec, P., 1999. Human interleukin-17: AT cell–derived proinflammatory cytokine produced by the rheumatoid synovium. *Arthritis & Rheumatism: Official Journal of the American College of Rheumatology*, *42*(5), pp.963-970.

Chalan, P., Kroesen, B.J., van der Geest, K.S., Huitema, M.G., Abdulahad, W.H., Bijzet, J., Brouwer, E. and Boots, A.M., 2013. Circulating CD4+ CD161+ T lymphocytes are increased in seropositive arthralgia patients but decreased in patients with newly diagnosed rheumatoid arthritis. *PloS one*, *8*(11), p.e79370.

Chan, E.S. and Cronstein, B.N., 2010. Methotrexate—how does it really work?. *Nature Reviews Rheumatology*, *6*(3), pp.175-178.

Chang, H.H., Liu, G.Y., Dwivedi, N., Sun, B., Okamoto, Y., Kinslow, J.D., Deane, K.D., Demoruelle, M.K., Norris, J.M., Thompson, P.R. and Sparks, J.A., 2016. A molecular signature of preclinical rheumatoid arthritis triggered by dysregulated PTPN22. *JCI insight*, *1*(17), p.e90045.

Chang, H.Y., Chi, J.T., Dudoit, S., Bondre, C., Van De Rijn, M., Botstein, D. and Brown, P.O., 2002. Diversity, topographic differentiation, and positional memory in human fibroblasts. *Proceedings of the National Academy of Sciences*, *99*(20), pp.12877-12882.

Chang, S.K., Noss, E.H., Chen, M., Gu, Z., Townsend, K., Grenha, R., Leon, L., Lee, S.Y., Lee, D.M. and Brenner, M.B., 2011. Cadherin-11 regulates fibroblast inflammation. *Proceedings of the National Academy of Sciences*, *108*(20), pp.8402-8407.

Charbonneau, M., Harper, K., Grondin, F., Pelmus, M., McDonald, P.P. and Dubois, C.M., 2007. Hypoxia-inducible factor mediates hypoxic and tumor necrosis factor α-induced increases in tumor necrosis factor-α converting enzyme/ADAM17 expression by synovial cells. *Journal of Biological Chemistry*, *282*(46), pp.33714-33724.

Charbonneau, M., Lavoie, R.R., Lauzier, A., Harper, K., McDonald, P.P. and Dubois, C.M., 2016. Platelet-derived growth factor receptor activation promotes the prodestructive invadosome-forming phenotype of synoviocytes from patients with rheumatoid arthritis. *The Journal of Immunology*, *196*(8), pp.3264-3275.

Chatterjee Adhikari M, Guin A, Chakraborty S et al (2012) Subclinical atherosclerosis and endothelial dysfunction in patients with early rheumatoid arthritis as evidenced by measurement of carotid intima-media thickness and flow-mediated vasodilatation: an observational study. Semin Arthritis Rheum 41:669–675. 10.1016

Chaudhari, K., Rizvi, S. and Syed, B.A., 2016. Rheumatoid arthritis: current and future trends. *Nature reviews Drug discovery*, *15*(5), pp.305-306.

Chen B, Zhao Y, Li S, Yang L, Wang H, Wang T, Bin Shi, Gai Z, Heng X, Zhang C, Yang J, Zhang L. Variations in oral microbiome profiles in rheumatoid arthritis and osteoarthritis with potential biomarkers for arthritis screening. Sci Rep. 2018 Nov 20;8(1):17126. doi: 10.1038/s41598-018-35473-6. PMID: 30459400; PMCID: PMC6244360.

Chen, J., Cheng, W., Li, J., Wang, Y., Chen, J., Shen, X., Su, A., Gan, D., Ke, L., Liu, G. and Lin, J., 2021. Notch-1 and Notch-3 mediate hypoxia-induced activation of synovial fibroblasts in rheumatoid arthritis. *Arthritis & Rheumatology*, *73*(10), pp.1810-1819.

Chen, K., Lin, Z.W., He, S.M., Wang, C.Q., Yang, J.C., Lu, Y., Xie, X.B. and Li, Q., 2019. Metformin inhibits the proliferation of rheumatoid arthritis fibroblast-like synoviocytes through IGF-IR/PI3K/AKT/m-TOR pathway. *Biomedicine & Pharmacotherapy*, *115*, p.108875.

Chen, Y.M., Chen, H.H., Huang, W.N., Liao, T.L., Chen, J.P., Chao, W.C., Lin, C.T., Hung, W.T., Hsieh, C.W., Hsieh, T.Y. and Chen, Y.H., 2017. Tocilizumab potentially prevents bone loss in patients with anticitrullinated protein antibody-positive rheumatoid arthritis. *PLoS One*, *12*(11), p.e0188454.

Chen, X., Oppenheim, J. J. and Howard, O. M. Z. (2004) 'Chemokines and chemokine receptors as novel therapeutic targets in rheumatoid arthritis (RA): inhibitory effects of traditional Chinese medicinal components.', *Cellular & molecular immunology*, 1(5), pp. 336–42.

Cheng, P., Zlobin, A., Volgina, V., Gottipati, S., Osborne, B., Simel, E.J., Miele, L. and Gabrilovich, D.I., 2001. Notch-1 regulates NF-κB activity in hemopoietic progenitor cells. *The Journal of Immunology*, *167*(8), pp.4458-4467.

Chervonsky, A.V., 2010. Influence of microbial environment on autoimmunity. *Nature immunology*, *11*(1), pp.28-35.

Chi, H., 2022. Immunometabolism at the intersection of metabolic signaling, cell fate, and systems immunology. *Cellular & molecular immunology*, *19*(3), pp.299-302.

Cho, I. and Blaser, M.J., 2012. The human microbiome: at the interface of health and disease. *Nature Reviews Genetics*, *13*(4), pp.260-270.

Choe, J.Y., Hun Kim, J., Park, K.Y., Choi, C.H. and Kim, S.K., 2016. Activation of dickkopf-1 and focal adhesion kinase pathway by tumour necrosis factor α induces enhanced migration of fibroblast-like synoviocytes in rheumatoid arthritis. *Rheumatology*, *55*(5), pp.928-938.

Choy, E.H. and Panayi, G.S., 2001. Cytokine pathways and joint inflammation in rheumatoid arthritis. *New England Journal of Medicine*, *344*(12), pp.907-916.

Choy, E.H., Pitzalis, C., Cauli, A., Bijl, J.A., Schantz, A., Woody, J., Kingsley, G.H. and Panayi, G.S., 1996. Percentage of anti-CD4 monoclonal antibody-coated lymphocytes in the rheumatoid joint is associated with clinical improvement. Implications for the development of immunotherapeutic dosing regimens. *Arthritis & Rheumatism: Official Journal of the American College of Rheumatology*, *39*(1), pp.52-56.

Codoñer-Franch, P., Carrasco-Luna, J., Allepuz, P., Codoñer-Alejos, A. and Guillem, V., 2016. Association of RBP4 genetic variants with childhood obesity and cardiovascular risk factors. *Pediatric diabetes*, *17*(8), pp.576-583.

Cohen, S.B., Emery, P., Greenwald, M.W., Dougados, M., Furie, R.A., Genovese, M.C., Keystone, E.C., Loveless, J.E., Burmester, G.R., Cravets, M.W. and Hessey, E.W., 2006. Rituximab for rheumatoid arthritis refractory to anti–tumor necrosis factor therapy: results of a multicenter, randomised, double-blind,

placebo-controlled, phase III trial evaluating primary efficacy and safety at twenty-four weeks. *Arthritis & Rheumatism*, *54*(9), pp.2793-2806.

Cole, S., Walsh, A., Yin, X., Wechalekar, M.D., Smith, M.D., Proudman, S.M., Veale, D.J., Fearon, U., Pitzalis, C., Humby, F. and Bombardieri, M., 2018. Integrative analysis reveals CD38 as a therapeutic target for plasma cell-rich pre-disease and established rheumatoid arthritis and systemic lupus erythematosus. *Arthritis research & therapy*, *20*, pp.1-14.

Collak, F.K., Yagiz, K., Luthringer, D.J., Erkaya, B. and Cinar, B., 2012. Threonine-120 phosphorylation regulated by phosphoinositide-3-kinase/Akt and mammalian target of rapamycin pathway signaling limits the antitumor activity of mammalian sterile 20-like kinase 1. *Journal of Biological Chemistry*, *287*(28), pp.23698-23709.

Collin, M. and Bigley, V., 2018. Human dendritic cell subsets: an update. *Immunology*, *154*(1), pp.3-20.

Conaghan, P.G., Peterfy, C., Olech, E., Kaine, J., Ridley, D., DiCarlo, J., Friedman, J., Devenport, J. and Troum, O., 2014. The effects of tocilizumab on osteitis, synovitis and erosion progression in rheumatoid arthritis: results from the ACT-RAY MRI substudy. *Annals of the Rheumatic Diseases*, *73*(5), pp.810-816.

Connolly, M., Marrelli, A., Blades, M., McCormick, J., Maderna, P., Godson, C., Mullan, R., FitzGerald, O., Bresnihan, B., Pitzalis, C. and Veale, D.J., 2010. Acute serum amyloid A induces migration, angiogenesis, and inflammation in synovial cells in vitro and in a human rheumatoid arthritis/SCID mouse chimera model. *The Journal of Immunology*, *184*(11), pp.6427-6437.

Connolly, M., Mullan, R.H., McCormick, J., Matthews, C., Sullivan, O., Kennedy, A., FitzGerald, O., Poole, A.R., Bresnihan, B., Veale, D.J. and Fearon, U., 2012. Acute-phase serum amyloid A regulates tumor necrosis factor α and matrix turnover and predicts disease progression in patients with inflammatory arthritis before and after biologic therapy. *Arthritis & Rheumatism*, *64*(4), pp.1035-1045.

Constans, J. and Conri, C., 2006. Circulating markers of endothelial function in cardiovascular disease. *Clinica chimica acta*, *368*(1-2), pp.33-47.

Cooles, F.A., Anderson, A.E., Skelton, A., Pratt, A.G., Kurowska-Stolarska, M.S., McInnes, I., Hilkens, C.M. and Isaacs, J.D., 2018. Phenotypic and transcriptomic analysis of peripheral blood plasmacytoid and conventional dendritic cells in early drug naïve rheumatoid arthritis. *Frontiers in immunology*, *9*, p.755.

Cooper, N.J., 2000. Economic burden of rheumatoid arthritis: a systematic review. *Rheumatology*, *39*(1), pp.28-33.

Cope, A.P., Jasenecova, M., Vasconcelos, J.C., Filer, A., Raza, K., Qureshi, S., D'Agostino, M.A., McInnes, I.B., Isaacs, J.D., Pratt, A.G. and Fisher, B.A., 2024. Abatacept in individuals at high risk of rheumatoid arthritis (APIPPRA): a randomised, double-blind, multicentre, parallel, placebo-controlled, phase 2b clinical trial. *The Lancet*, *403*(10429), pp.838-849.

Copeman, W.S.C., 1971. Historical notes on rheumatology. *Rheumatology*, *11*(4), pp.145-155.

Corsiero, E., Bombardieri, M., Manzo, A., Bugatti, S., Uguccioni, M. and Pitzalis, C., 2012. Role of lymphoid chemokines in the development of functional ectopic lymphoid structures in rheumatic autoimmune diseases. *Immunology letters*, *145*(1-2), pp.62-67.

Costello, P., Bresnihan, B., O'Farrelly, C. and FitzGerald, O., 1999. Predominance of CD8+ T lymphocytes in psoriatic arthritis. *The Journal of rheumatology*, *26*(5), pp.1117-1124.

Coultas, L., Chawengsaksophak, K. and Rossant, J., 2005. Endothelial cells and VEGF in vascular development. *Nature*, *438*(7070), pp.937-945. Coultas, L., Chawengsaksophak, K. and Rossant, J., 2005. Endothelial cells and VEGF in vascular development. *Nature*, *438*(7070), pp.937-945.

Coulthard, L.R., Geiler, J., Mathews, R.J., Church, L.D., Dickie, L.J., Cooper, D.L., Wong, C., Savic, S., Bryer, D., Buch, M.H. and Emery, P., 2012. Differential effects of infliximab on absolute circulating blood leucocyte counts of innate immune cells in early and late rheumatoid arthritis patients. *Clinical & Experimental Immunology*, *170*(1), pp.36-46.

Courvoisier, D.S., Chatzidionysiou, K., Mongin, D., Lauper, K., Mariette, X., Morel, J., Gottenberg, J.E., Bergstra, S.A., Suarez, M.P., Codreanu, C. and Kvien, T.K., 2021. The impact of seropositivity on the effectiveness of biologic anti-rheumatic agents: results from a collaboration of 16 registries. *Rheumatology*, *60*(2), pp.820-828.

Creamer, D., Allen, M.H., Sousa, A., Poston, R. and Barker, J.N.W.N., 1997. Localization of endothelial proliferation and microvascular expansion in active plaque psoriasis. British Journal of Dermatology, 136(6), pp.859-865.

Croft, A.P., Campos, J., Jansen, K., Turner, J.D., Marshall, J., Attar, M., Savary, L., Wehmeyer, C., Naylor, A.J., Kemble, S. and Begum, J., 2019. Distinct fibroblast subsets drive inflammation and damage in arthritis. *Nature*, *570*(7760), pp.246-251.

Croft, A.P., Campos, J., Jansen, K., Turner, J.D., Marshall, J., Attar, M., Savary, L., Wehmeyer, C.,

Croft, A.P., Naylor, A.J., Marshall, J.L., Hardie, D.L., Zimmermann, B., Turner, J., Desanti, G., Adams, H., Yemm, A.I., Müller-Ladner, U. and Dayer, J.M., 2016. Rheumatoid synovial fibroblasts differentiate into distinct subsets in the presence of cytokines and cartilage. *Arthritis research & therapy*, *18*, pp.1-11.

Cross, M., Smith, E., Hoy, D., Carmona, L., Wolfe, F., Vos, T., Williams, B., Gabriel, S., Lassere, M., Johns, N. and Buchbinder, R., 2014. The global burden of rheumatoid arthritis: estimates from the global burden of disease 2010 study. *Annals of the rheumatic diseases*, *73*(7), pp.1316-1322.

Crowson, C.S., Liao, K.P., Davis III, J.M., Solomon, D.H., Matteson, E.L., Knutson, K.L., Hlatky, M.A. and Gabriel, S.E., 2013. Rheumatoid arthritis and cardiovascular disease. *American heart journal*, *166*(4), pp.622-628.

Crowson, C.S., Matteson, E.L., Myasoedova, E., Michet, C.J., Ernste, F.C., Warrington, K.J., Davis III, J.M., Hunder, G.G., Therneau, T.M. and Gabriel, S.E., 2011. The lifetime risk of adult-onset rheumatoid arthritis and other inflammatory autoimmune rheumatic diseases. *Arthritis & Rheumatism*, *63*(3), pp.633-639.

Cruys, B., Wong, B., Kuchnio, A. *et al.* Glycolytic regulation of cell rearrangement in angiogenesis. *Nat Commun* **7**, 12240 (2016).

Cuesta-López L, Escudero-Contreras A, Hanaee Y, Pérez-Sánchez C, Ruiz-Ponce M, Martínez-Moreno Cuesta-López, L., Escudero-Contreras, A., Hanaee, Y., Pérez-Sánchez, C., Ruiz-Ponce, M., Martínez-Moreno, J.M., Pérez-Pampin, E., González, A., Plasencia-Rodriguez, C., Martínez-Feito, A. and Balsa, A., 2024. Exploring candidate biomarkers for rheumatoid arthritis through cardiovascular and cardiometabolic serum proteome profiling. *Frontiers in Immunology*, *15*, p.1333995.

Culemann, S., Grüneboom, A., Nicolás-Ávila, J.Á., Weidner, D., Lämmle, K.F., Rothe, T., Quintana, J.A., Kirchner, P., Krljanac, B., Eberhardt, M. and Ferrazzi, F., 2019. Locally renewing resident synovial macrophages provide a protective barrier for the joint. *Nature*, *572*(7771), pp.670-675.

Cunnane, G., Grehan, S., Geoghegan, S., McCormack, C., Shields, D., Whitehead, A.S., Bresnihan, B. and Fitzgerald, O., 2000. Serum amyloid A in the assessment of early inflammatory arthritis. *The Journal of rheumatology*, *27*(1), pp.58-63.

Cunningham, C.C., Wade, S., Floudas, A., Orr, C., McGarry, T., Wade, S., Cregan, S., Fearon, U. and Veale, D.J., 2021. Serum miRNA signature in rheumatoid arthritis and "at-risk individuals". *Frontiers in immunology*, *12*, p.633201.

Curtis, J.R. and Singh, J.A., 2011. Use of biologics in rheumatoid arthritis: current and emerging paradigms of care. *Clinical therapeutics*, *33*(6), pp.679-707.

Dai, Q., Zhou, D., Xu, L. and Song, X., 2018. Curcumin alleviates rheumatoid arthritis-induced inflammation and synovial hyperplasia by targeting mTOR pathway in rats. *Drug design, development and therapy*, pp.4095-4105.

Dalén, J., Luttropp, K., Svedbom, A., Black, C.M. and Kachroo, S., 2020. Healthcare-Related Costs Associated with Switching Subcutaneous Tumor Necrosis Factor-α Inhibitor in the Treatment of Inflammatory Arthritis: a Retrospective Study. *Advances in Therapy*, *37*, pp.3746-3760.

Dalod, M., Chelbi, R., Malissen, B. and Lawrence, T., 2014. Dendritic cell maturation: functional specialization through signaling specificity and transcriptional programming. *The EMBO journal*, *33*(10), pp.1104-1116.

Darrieutort-Laffite, C., Boutet, M.A., Chatelais, M., Brion, R., Blanchard, F., Heymann, D. and Le Goff, B., 2014. IL-1β and TNFα Promote Monocyte Viability through the Induction of GM-CSF Expression by Rheumatoid Arthritis Synovial Fibroblasts. *Mediators of inflammation*, *2014*(1), p.241840.

Davis JM 3rd. Rheumatoid Arthritis: A Severe Disease That Preventive Approaches Would Greatly Benefit. Clin Ther. 2019 Jul;41(7):1240-1245. doi: 10.1016/j.clinthera.2019.04.026. Epub 2019 Jun 10. PMID: 31196648.

De Bock, K., Georgiadou, M., Schoors, S., Kuchnio, A., Wong, B.W., Cantelmo, A.R., Quaegebeur, A., Ghesquiere, B., Cauwenberghs, S., Eelen, G. and Phng, L.K., 2013. Role of PFKFB3-driven glycolysis in vessel sprouting. *Cell*, *154*(3), pp.651-663.

De Cock, D. and Hyrich, K., 2018. Malignancy and rheumatoid arthritis: epidemiology, risk factors and management. *Best Practice & Research Clinical Rheumatology*, *32*(6), pp.869-886.

de Hair, M.J., Leclerc, P., Newsum, E.C., Maijer, K.I., van de Sande, M.G., Ramwadhdoebe, T.H., van Schaardenburg, D., van Baarsen, L.G., Korotkova, M., Gerlag, D.M. and Tak, P.P., 2015. Expression of prostaglandin E2 enzymes in the synovium of arthralgia patients at risk of developing rheumatoid arthritis and in early arthritis patients. *PLoS One*, *10*(7), p.e0133669.

De Hair, M.J.H., Van De Sande, M.G.H., Ramwadhdoebe, T.H., Hansson, M., Landewé, R., Van Der Leij, C., Maas, M., Serre, G., Van Schaardenburg, D., Klareskog, L. and Gerlag, D.M., 2014. Features of the synovium of individuals at risk of developing rheumatoid arthritis: implications for understanding preclinical rheumatoid arthritis. *Arthritis & rheumatology*, *66*(3), pp.513-522.

de Jong, T.A., de Hair, M.J., van de Sande, M.G., Semmelink, J.F., Choi, I.Y., Gerlag, D.M., Tak, P.P. and van Baarsen, L.G., 2022. Synovial gene signatures associated with the development of rheumatoid arthritis in at risk individuals: A prospective study. *Journal of autoimmunity*, *133*, p.102923.

De Oliveira, P.G., Farinon, M., Sanchez-Lopez, E., Miyamoto, S. and Guma, M., 2019. Fibroblast-like synoviocytes glucose metabolism as a therapeutic target in rheumatoid arthritis. *Frontiers in Immunology*, *10*, p.1743.

de Smit, M.J., Westra, J., Brouwer, E., Janssen, K.M.J., Vissink, A. and van Winkelhoff, A.J. (2015), Commentary: Periodontitis and Rheumatoid Arthritis: What Do We Know?. Journal of Periodontology, 86: 1013-1019.

de Villeroché, V.J., Avouac, J., Ponceau, A., Ruiz, B., Kahan, A., Boileau, C., Uzan, G. and Allanore, Y., 2010. Research article Enhanced late-outgrowth circulating endothelial progenitor cell levels in rheumatoid arthritis and correlation with disease activity.

De Wilde, K., Martens, A., Lambrecht, S., Jacques, P., Drennan, M.B., Debusschere, K., Govindarajan, S., Coudenys, J., Verheugen, E., Windels, F. and Catrysse, L., 2017. A20 inhibition of STAT1 expression in myeloid cells: a novel endogenous regulatory mechanism preventing development of enthesitis. *Annals of the rheumatic diseases*, *76*(3), pp.585-592.

Deane, K.D., Demoruelle, M.K., Kelmenson, L.B., Kuhn, K.A., Norris, J.M. and Holers, V.M., 2017. Genetic and environmental risk factors for rheumatoid arthritis. *Best practice & research Clinical rheumatology*, *31*(1), pp.3-18.

Deanfield, J., Donald, A., Ferri, C., Giannattasio, C., Halcox, J., Halligan, S., Lerman, A., Mancia, G., Oliver, J.J., Pessina, A.C. and Rizzoni, D., 2005. Endothelial function and dysfunction. Part I: Methodological issues for

assessment in the different vascular beds: a statement by the Working Group on Endothelin and Endothelial Factors of the European Society of Hypertension. *Journal of hypertension*, *23*(1), pp.7-17.

DeBerardinis, R.J. and Thompson, C.B., 2012. Cellular metabolism and disease: what do metabolic outliers teach us?. *Cell*, *148*(6), pp.1132-1144..

Dedmon, L.E., 2020. The genetics of rheumatoid arthritis. *Rheumatology*, *59*(10), pp.2661-2670.

Del Papa, N., Colombo, G., Fracchiolla, N., Moronetti, L.M., Ingegnoli, F., Maglione, W., Comina, D.P., Vitali, C., Fantini, F. and Cortelezzi, A., 2004. Circulating endothelial cells as a marker of ongoing vascular disease in systemic sclerosis. *Arthritis & Rheumatism: Official Journal of the American College of Rheumatology*, *50*(4), pp.1296-1304.

Del Rey, M.J., Valín, Á., Usategui, A., García-Herrero, C.M., Sánchez-Aragó, M., Cuezva, J.M., Galindo, M., Bravo, B., Cañete, J.D., Blanco, F.J. and Criado, G., 2017. Hif-1α knockdown reduces glycolytic metabolism and induces cell death of human synovial fibroblasts under normoxic conditions. *Scientific reports*, *7*(1), p.3644.

Del Rincón, I., Williams, K., Stern, M.P., Freeman, G.L., O'Leary, D.H. and Escalante, A., 2003. Association between carotid atherosclerosis and markers of inflammation in rheumatoid arthritis patients and healthy subjects. *Arthritis & Rheumatism: Official Journal of the American College of Rheumatology*, *48*(7), pp.1833-1840.

Del Rincón, I., O'Leary, D.H., Freeman, G.L. and Escalante, A., 2007. Acceleration of atherosclerosis during the course of rheumatoid arthritis. *Atherosclerosis*, *195*(2), pp.354-360.

DeMizio, D.J. and Geraldino-Pardilla, L.B., 2020. Autoimmunity and inflammation link to cardiovascular disease risk in rheumatoid arthritis. *Rheumatology and therapy*, *7*(1), pp.19-33.

Demoruelle, M.K. and Deane, K.D., 2012. Treatment strategies in early rheumatoid arthritis and prevention of rheumatoid arthritis. *Current rheumatology reports*, *14*, pp.472-480.

Deng, W., Yang, J., Lin, X., Shin, J., Gao, J. and Zhong, X.P., 2017. Essential role of mTORC1 in self-renewal of murine alveolar macrophages. *The Journal of Immunology*, *198*(1), pp.492-504.

Dennis, G., Holweg, C.T., Kummerfeld, S.K., Choy, D.F., Setiadi, A.F., Hackney, J.A., Haverty, P.M., Gilbert, H., Lin, W.Y., Diehl, L. and Fischer, S., 2014. Synovial phenotypes in rheumatoid arthritis correlate with response to biologic therapeutics. *Arthritis research & therapy*, *16*, pp.1-18.

Deon D, Ahmed S, Tai K, Scaletta N, Herrero C, Lee IH, Krause A, Ivashkiv LB. Cross-talk between IL-1 and IL-6 signaling pathways in rheumatoid arthritis synovial fibroblasts. J Immunol. 2001 Nov 1;167(9):5395-403. doi: 10.4049/jimmunol.167.9.5395. PMID: 11673558.

Deshmane, S.L., Kremlev, S., Amini, S. and Sawaya, B.E., 2009. Monocyte chemoattractant protein-1 (MCP-1): an overview. *Journal of interferon & cytokine research*, *29*(6), pp.313-326.

Dessein, P.H., Joffe, B.I. and Singh, S., 2005. Biomarkers of endothelial dysfunction, cardiovascular risk factors and atherosclerosis in rheumatoid arthritis. *Arthritis research & therapy*, *7*, pp.1-10.

Dessein, P.H., Solomon, A., Woodiwiss, A.J., Norton, G.R., Tsang, L. and Gonzalez-Gay, M.A., 2013. Marked Independent Relationship between Circulating Interleukin-6 Concentrations and Endothelial Activation in Rheumatoid Arthritis. *Mediators of Inflammation*, *2013*(1), p.510243.

Detert, J., Pischon, N., Burmester, G.R. and Buttgereit, F., 2010. The association between rheumatoid arthritis and periodontal disease. *Arthritis research & therapy*, *12*, pp.1-7.

Di Gaetano, N., Cittera, E., Nota, R., Vecchi, A., Grieco, V., Scanziani, E., Botto, M., Introna, M. and Golay, J., 2003. Complement activation determines the therapeutic activity of rituximab in vivo. *The Journal of Immunology*, *171*(3), pp.1581-1587.

Di Giuseppe, D., Wallin, A., Bottai, M., Askling, J. and Wolk, A., 2014. Long-term intake of dietary long-chain n-3 polyunsaturated fatty acids and risk of rheumatoid arthritis: a prospective cohort study of women. *Annals of the rheumatic diseases*, *73*(11), pp.1949-1953.

Di Martino, M.L., Frau, A., Losa, F., Muggianu, E., Mura, M.N., Rotta, G., Scotti, L. and Marongiu, F., 2021. Role of circulating endothelial cells in assessing the severity of systemic sclerosis and predicting its clinical worsening. *Scientific Reports*, *11*(1), p.2681.

Diller, M., Hasseli, R., Hülser, M.L., Aykara, I., Frommer, K., Rehart, S., Müller-Ladner, U. and Neumann, E., 2019. Targeting activated synovial fibroblasts in rheumatoid arthritis by peficitinib. *Frontiers in immunology*, *10*, p.541.

Din, F.V., Theodoratou, E., Farrington, S.M., Tenesa, A., Barnetson, R.A., Cetnarskyj, R., Stark, L., Porteous, M.E., Campbell, H. and Dunlop, M.G., 2010. Effect of aspirin and NSAIDs on risk and survival from colorectal cancer. *Gut*, *59*(12), pp.1670-1679.

Dinarello, C.A., 2009. Immunological and inflammatory functions of the interleukin-1 family. *Annual review of immunology*, *27*(1), pp.519-550.

Dobin, A., Davis, C.A., Schlesinger, F., Drenkow, J., Zaleski, C., Jha, S., Batut, P., Chaisson, M. and Gingeras, T.R., 2013. STAR: ultrafast universal RNA-seq aligner. *Bioinformatics*, *29*(1), pp.15-21.

Doherty, E. and O'neill, C., 2014. Estimating the health-care usage associated with osteoarthritis and rheumatoid arthritis in an older adult population in Ireland. *Journal of Public Health*, *36*(3), pp.504-510.

Dorrell, M.I., Aguilar, E. and Friedlander, M., 2002. Retinal vascular development is mediated by endothelial filopodia, a preexisting astrocytic template and specific R-cadherin adhesion. *Investigative ophthalmology & visual science*, *43*(11), pp.3500-3510..

dos Santos, L., Salles, T.A., Arruda-Junior, D.F., Campos, L.C., Pereira, A.C., Barreto, A.L.T., Antonio, E.L., Mansur, A.J., Tucci, P.J., Krieger, J.E. and Girardi, A.C., 2013. Circulating dipeptidyl peptidase IV activity correlates with cardiac dysfunction in human and experimental heart failure. *Circulation: Heart Failure*, *6*(5), pp.1029-1038.

Drexler, S.K., Kong, P.L., Wales, J. and Foxwell, B.M., 2008. Cell signaling in macrophages, the principal innate immune effector cells of rheumatoid arthritis. *Arthritis research & therapy*, *10*, pp.1-12.

Du, H., Zhang, X., Zeng, Y., Huang, X., Chen, H., Wang, S., Wu, J., Li, Q., Zhu, W., Li, H. and Liu, T., 2019. A novel phytochemical, DIM, inhibits proliferation, migration, invasion and TNF-α induced inflammatory cytokine production of synovial fibroblasts from rheumatoid arthritis patients by targeting MAPK and AKT/mTOR signal pathway. *Frontiers in immunology*, *10*, p.1620.

Duke, O., Panayi, G.S., Janossy, G. and Poulter, L.W., 1982. An immunohistological analysis of lymphocyte subpopulations and their microenvironment in the synovial membranes of patients with rheumatoid arthritis using monoclonal antibodies. *Clinical and experimental immunology*, *49*(1), p.22.

Dumitriu, I.E., Baruah, P., Finlayson, C.J., Loftus, I.M., Antunes, R.F., Lim, P., Bunce, N. and Carlos Kaski, J., 2012. High levels of costimulatory receptors OX40 and 4-1BB characterise CD4+ CD28null T cells in patients with acute coronary syndrome. *Circulation research*, *110*(6), pp.857-869.

Dupont, A., Constantin, A., Soubrier, M., Rincheval, N. and Avouac, J., 2024. DAS28-γGT for the prediction of major cardiovascular events in rheumatoid arthritis: results from the ESPOIR cohort. *Rheumatology*, *63*(3), pp.665-671.

Ebert, L.M., Yu, W., Gargett, T., Toubia, J., Kollis, P.M., Tea, M.N., Ebert, B.W., Bardy, C., van den Hurk, M., Bonder, C.S. and Manavis, J., 2020. Endothelial, pericyte and tumor cell expression in glioblastoma identifies fibroblast activation protein (FAP) as an excellent target for immunotherapy. *Clinical & Translational Immunology*, *9*(10), p.e1191.

Ebrahimi, M., Nourbakhsh, E., Hazara, A.Z., Mirzaei, A., Shafieyari, S., Salehi, A., Hoseinzadeh, M., Payandeh, Z. and Barati, G., 2022. PI3K/Akt/mTOR signaling pathway in cancer stem cells. *Pathology-Research and Practice*, *237*, p.154010.

Edwards, J.C.W., Leandro, M.J. and Cambridge, G., 2004. B lymphocyte depletion therapy with rituximab in rheumatoid arthritis. *Rheumatic Disease Clinics*, *30*(2), pp.393-403.

Edwards, N., Langford-Smith, A.W., Wilkinson, F.L. and Alexander, M.Y., 2018. Endothelial progenitor cells: new targets for therapeutics for inflammatory conditions with high cardiovascular risk. *Frontiers in medicine*, *5*, p.200.

Eelen, G., Cruys, B., Welti, J., De Bock, K. and Carmeliet, P., 2013. Control of vessel sprouting by genetic and metabolic determinants. *Trends in Endocrinology & Metabolism*, *24*(12), pp.589-596.

Eelen, G., de Zeeuw, P., Treps, L., Harjes, U., Wong, B.W. and Carmeliet, P., 2018. Endothelial cell metabolism. *Physiological reviews*, *98*(1), pp.3-58.

Eidizadeh, A., Schnelle, M., Leha, A., Edelmann, F., Nolte, K., Werhahn, S.M., Binder, L. and Wachter, R., 2023. Biomarker profiles in heart failure with preserved vs. reduced ejection fraction: results from the DIAST-CHF study. *ESC Heart Failure*, *10*(1), pp.200-210.

Emery, P. and Seto, Y., 2003. Role of biologics in early arthritis. *Clinical and experimental rheumatology*, *21*(5; SUPP 31), pp.S191-S194.

Emery, P., 2006. Treatment of rheumatoid arthritis. *Bmj*, *332*(7534), pp.152-155.

Emery, P., Keystone, E., Tony, H.P., Cantagrel, A., Van Vollenhoven, R., Sanchez, A., Alecock, E., Lee, J. and Kremer, J., 2008. IL-6 receptor inhibition with tocilizumab improves treatment outcomes in patients with rheumatoid arthritis refractory to anti-tumour necrosis factor biologicals: results from a 24-week multicentre randomised placebo-controlled trial. *Annals of the rheumatic diseases*, *67*(11), pp.1516-1523.

Endres, M., Andreas, K., Kalwitz, G., Freymann, U., Neumann, K., Ringe, J., Sittinger, M., Häupl, T. and Kaps, C., 2010. Chemokine profile of synovial fluid from normal, osteoarthritis and rheumatoid arthritis patients: CCL25, CXCL10 and XCL1 recruit human subchondral mesenchymal progenitor cells. *Osteoarthritis and cartilage*, *18*(11), pp.1458-1466.

Entezami, P., Fox, D.A., Clapham, P.J. and Chung, K.C., 2011. Historical perspective on the etiology of rheumatoid arthritis. *Hand clinics*, *27*(1), pp.1-10.

Epitope, Differential et al. 1997. "Anti-A2 / RA33 Autoantibodies Are Directed to the RNA Binding Region of the A2 Protein of the Heterogeneous Nuclear Ribonucleoprotein Complex." *Society* 2: 127–35.

Erdbruegger, U., Haubitz, M. and Woywodt, A., 2006. Circulating endothelial cells: a novel marker of endothelial damage. *Clinica chimica acta*, *373*(1-2), pp.17-26.

Espinosa, L., Cathelin, S., D'Altri, T., Trimarchi, T., Statnikov, A., Guiu, J., Rodilla, V., Inglés-Esteve, J., Nomdedeu, J., Bellosillo, B. and Besses, C., 2010. The Notch/Hes1 pathway sustains NF-κB activation through CYLD repression in T cell leukemia. *Cancer cell*, *18*(3), pp.268-281.

Fakhri, M., Azadeh, H., Jokar, A., Moosazadeh, M., Fakheri, H. and Ramezanpour, M., 2023. The relationship between fish consumption and rheumatoid arthritis; a systematic review and meta-analysis. *Immunopathologia Persa*, *10*(1), pp.e36452-e36452.

Fang, G., Li, Y., Yuan, J., Cao, W., Song, S., Chen, L., Wang, Y. and Wang, Q., 2023. Cadherin-11-interleukin-6 signaling between cardiac fibroblast and cardiomyocyte promotes ventricular remodeling in a mouse pressure overload-induced heart failure model. *International Journal of Molecular Sciences*, *24*(7), p.6549.

Fantuzzi, G., 2008. Adiponectin and inflammation: consensus and controversy. *Journal of Allergy and Clinical Immunology*, *121*(2), pp.326-330.

Farinacci, M., Krahn, T., Dinh, W., Volk, H.D., Düngen, H.D., Wagner, J., Konen, T. and von Ahsen, O., 2019. Circulating endothelial cells as biomarker for cardiovascular diseases. *Research and Practice in Thrombosis and Haemostasis*, *3*(1), pp.49-58.

Fassbender HG, Simmling-Annefeld M. The potential aggressiveness of synovial tissue in rheumatoid arthritis. J Pathol. 1983;139:399–406. doi: 10.1002/path.1711390314.

Faust, H.J., Cheng, T.Y., Korsunsky, I., Watts, G.F., Gal-Oz, S.T., Trim, W.V., Kongthong, S., Jonsson, A.H., Simmons, D.P., Zhang, F. and Padera, R., 2024. Adipocyte associated glucocorticoid signaling regulates normal fibroblast function which is lost in inflammatory arthritis. *Nature Communications*, *15*(1), p.9859.

Fazeli, M.S., Khaychuk, V., Wittstock, K., Breznen, B., Crocket, G., Pourrahmat, M.M. and Ferri, L., 2021. Cardiovascular disease in rheumatoid arthritis: risk factors, autoantibodies, and the effect of antirheumatic therapies. *Clinical Medicine Insights: Arthritis and Musculoskeletal Disorders*, *14*, p.11795441211028751.

Fearon, U., Canavan, M., Biniecka, M. and Veale, D.J., 2016. Hypoxia, mitochondrial dysfunction and synovial invasiveness in rheumatoid arthritis. *Nature Reviews Rheumatology*, *12*(7), pp.385-397.

Fearon, U., Griosios, K., Fraser, A., Reece, R., Emery, P., Jones, P.F. and Veale, D.J., 2003. Angiopoietins, growth factors, and vascular morphology in early arthritis. *The Journal of Rheumatology*, *30*(2), pp.260-268.

Fearon, U., Hanlon, M.M., Floudas, A. and Veale, D.J., 2022. Cellular metabolic adaptations in rheumatoid arthritis and their therapeutic implications. *Nature Reviews Rheumatology*, *18*(7), pp.398-414.

Fearon, U., Hanlon, M.M., Wade, S.M. and Fletcher, J.M., 2019. Altered metabolic pathways regulate synovial inflammation in rheumatoid arthritis. *Clinical & Experimental Immunology*, *197*(2), pp.170-180.

Fearon, U., Mullan, R., Markham, T., Connolly, M., Sullivan, S., Poole, A.R., FitzGerald, O., Bresnihan, B. and Veale, D.J., 2006. Oncostatin M induces angiogenesis and cartilage degradation in rheumatoid arthritis synovial tissue and human cartilage cocultures. *Arthritis & Rheumatism: Official Journal of the American College of Rheumatology*, *54*(10), pp.3152-3162.

Fearon, U., Reece, R., Smith, J., Emery, P. and Veale, D.J., 1999. Synovial cytokine and growth factor regulation of MMPs/TIMPs: implications for erosions and angiogenesis in early rheumatoid and psoriatic arthritis patients. *Annals of the New York Academy of Sciences*, *878*(1), pp.619-621.

Fearon U, Szekanecz Z, V. D. (2020) 'Angiogenesis', in *Firestein's and Kelley's Textbook for Rheumatology*.

Feldmann M, Brennan FM, Maini RN. Role of cytokines in rheumatoid arthritis. Annu Rev Immunol. 1996;14:397-440. doi: 10.1146/annurev.immunol.14.1.397. PMID: 8717520.

Feldmann M, Brennan FM, Paleolog E, Cope A, Taylor P, Williams R, Woody J, Maini RN. Anti-TNFalpha therapy of rheumatoid arthritis: what can we learn about chronic disease? Novartis Found Symp. 2004;256:53-69; discussion 69-73, 106-11, 266-9. PMID: 15027483.

Ferrandino, F., Grazioli, P., Bellavia, D., Campese, A.F., Screpanti, I. and Felli, M.P., 2018. Notch and NF-κB: coach and players of regulatory T-cell response in cancer. *Frontiers in Immunology*, *9*, p.2165.

Feugray, G., Miranda, S., Le Cam Duchez, V., Bellien, J. and Billoir, P., 2023. Endothelial progenitor cells in autoimmune disorders. *Stem Cell Reviews and Reports*, *19*(8), pp.2597-2611.

Filer, A., 2013. The fibroblast as a therapeutic target in rheumatoid arthritis. *Current opinion in pharmacology*, *13*(3), pp.413-419.

Finckh, A., Gilbert, B., Hodkinson, B., Bae, S.C., Thomas, R., Deane, K.D., Alpizar-Rodriguez, D. and Lauper, K., 2022. Global epidemiology of rheumatoid arthritis. *Nature Reviews Rheumatology*, *18*(10), pp.591-602.

Fink, A.M., Cauza, E., Hassfeld, W., Dunky, A., Bayer, P.M., Jurecka, W. and Steiner, A., 2007. Vascular endothelial growth factor in patients with psoriatic arthritis. *Clinical and experimental rheumatology*, *25*(2), p.305.

Fiocco U, Cozzi L, Chieco-Bianchi F, Rigon C, Vezzù M, Favero E, Ferro F, Sfriso P, Rubaltelli L, Nardacchione R, Todesco S. Vascular changes in psoriatic knee joint synovitis. J Rheumatol. 2001 Nov;28(11):2480-6. PMID: 11708422.

Fiocco, U., Accordi, B., Martini, V., Oliviero, F., Facco, M., Cabrelle, A., Piva, L., Molena, B., Caso, F., Costa, L. and Scanu, A., 2014. JAK/STAT/PKCδ molecular pathways in synovial fluid T lymphocytes reflect the in vivo T helper-17 expansion in psoriatic arthritis. *Immunologic research*, *58*, pp.61-69.

Firestein, G.S. and McInnes, I.B., 2017. Immunopathogenesis of rheumatoid arthritis. *Immunity*, *46*(2), pp.183-196.

Firestein, G.S., 1996. Invasive fibroblast-like synoviocytes in rheumatoid arthritis. Passive responders or transformed aggressors?. *Arthritis & Rheumatism*, *39*(11), pp.1781-1790.

Firestein, G.S., Budd, R.C., Gabriel, S.E., McInnes, I.B. and O'Dell, J.R., 2016. *Kelley and Firestein's textbook of rheumatology*. Elsevier Health Sciences.

Firestein, G.S., Xu, W.D., Townsend, K., Broide, D.A.V.I.D., Alvaro-Gracia, J.O.S.E., Glasebrook, A.N.D.R.E.W. and Zvaifler, N.J., 1988. Cytokines in chronic inflammatory arthritis. I. Failure to detect T cell lymphokines (interleukin 2 and interleukin 3) and presence of macrophage colony-stimulating factor (CSF-1) and a novel mast cell growth factor in rheumatoid synovitis. *Journal of Experimental Medicine*, *168*(5), pp.1573-1586.

Fischer, A., Schumacher, N., Maier, M., Sendtner, M. and Gessler, M., 2004. The Notch target genes Hey1 and Hey2 are required for embryonic vascular development. *Genes & development*, *18*(8), pp.901-911.

Floudas, A., Canavan, M., McGarry, T., Mullan, R., Nagpal, S., Veale, D.J. and Fearon, U., 2021. ACPA status correlates with differential immune profile in patients with rheumatoid arthritis. *Cells*, *10*(3), p.647.

Floudas, A., Gorman, A., Neto, N., Monaghan, M.G., Elliott, Z., Fearon, U. and Marzaioli, V., 2022. Inside the joint of inflammatory arthritis patients: handling and processing of synovial tissue biopsies for high throughput analysis. *Frontiers in Medicine*, *9*, p.830998.

Floudas, A., Neto, N., Orr, C., Canavan, M., Gallagher, P., Hurson, C., Monaghan, M.G., Nagpar, S., Mullan, R.H., Veale, D.J. and Fearon, U., 2022. Loss of balance between protective and pro-inflammatory synovial tissue T-cell polyfunctionality predates clinical onset of rheumatoid arthritis. *Annals of the rheumatic diseases*, *81*(2), pp.193-205.

Floudas, A., Smith, C.M., Tynan, O., Neto, N., Krishna, V., Wade, S.M., Hanlon, M., Cunningham, C., Marzaioli, V., Canavan, M. and Fletcher, J.M., 2022. Distinct stromal and immune cell interactions shape the pathogenesis of rheumatoid and psoriatic arthritis. *Annals of the rheumatic diseases*, *81*(9), pp.1224-1242.

Folkman J, Watson K, Ingber D, Hanahan D. Induction of angiogenesis during the transition from hyperplasia to neoplasia. Nature. 1989 May 4;339(6219):58-61. doi: 10.1038/339058a0. PMID: 2469964.

Fontana, A., Hengartner, H., Weber, E., Fehr, K., Grob, P.J. and Cohen, G., 1982. Interleukin 1 activity in the synovial fluid of patients with rheumatoid arthritis. *Rheumatology international*, *2*, pp.49-53.

Forslind, K., Hafström, I., Ahlmen, M. and Svensson, B., 2007. Sex: a major predictor of remission in early rheumatoid arthritis?. *Annals of the rheumatic diseases*, *66*(1), pp.46-52.

Forte, E., Ramialison, M., Nim, H.T., Mara, M., Li, J.Y., Cohn, R., Daigle, S.L., Boyd, S., Stanley, E.G., Elefanty, A.G. and Hinson, J.T., 2022. Adult mouse fibroblasts retain organ-specific transcriptomic identity. *Elife*, *11*, p.e71008.

Foster, W., Shantsila, E., Carruthers, D., Lip, G.Y. and Blann, A.D., 2009. Circulating endothelial cells and rheumatoid arthritis: relationship with plasma markers of endothelial damage/dysfunction. *Rheumatology*, *48*(3), pp.285-288.

Fragoulis, G.E., McInnes, I.B. and Siebert, S., 2019. JAK-inhibitors. New players in the field of immune-mediated diseases, beyond rheumatoid arthritis. *Rheumatology*, *58*(Supplement_1), pp.i43-i54.

Frank-Bertoncelj, M., Trenkmann, M., Klein, K., Karouzakis, E., Rehrauer, H., Bratus, A., Kolling, C., Armaka, M., Filer, A., Michel, B.A. and Gay, R.E., 2017. Epigenetically-driven anatomical diversity of synovial fibroblasts guides joint-specific fibroblast functions. *Nature communications*, *8*(1), p.14852.

Fraser, A., Fearon, U., Reece, R., Emery, P. and Veale, D.J., 2001. Matrix metalloproteinase 9, apoptosis, and vascular morphology in early arthritis. *Arthritis & Rheumatism: Official Journal of the American College of Rheumatology*, *44*(9), pp.2024-2028.

Frauwirth, K.A., Riley, J.L., Harris, M.H., Parry, R.V., Rathmell, J.C., Plas, D.R., Elstrom, R.L., June, C.H. and Thompson, C.B., 2002. The CD28 signaling pathway regulates glucose metabolism. *Immunity*, *16*(6), pp.769-777.

Frazzei, G., Cramer, S.H., Landewé, R.B., Maijer, K.I., Gerlag, D.M., Tak, P.P., de Vries, N., van Baarsen, L.G., van Vollenhoven, R.F. and Tas, S.W., 2024. The effect of rituximab on patient reported outcomes in the preclinical phase of rheumatoid arthritis: 2 year data from the PRAIRI study. *RMD open*, *10*(4), p.e004622.

Frisell, T., Saevarsdottir, S. & Askling, J. Family history of rheumatoid arthritis: an old concept with new developments. *Nat Rev Rheumatol* **12**, 335–343 (2016). https://doi.org/10.1038/nrrheum.2016.52

Fromm, S., Cunningham, C.C., Dunne, M.R., Veale, D.J., Fearon, U. and Wade, S.M., 2019. Enhanced angiogenic function in response to fibroblasts from psoriatic arthritis synovium compared to rheumatoid arthritis. *Arthritis research & therapy*, *21*, pp.1-11.

Fujii, W., Kawahito, Y., Nagahara, H., Kukida, Y., Seno, T., Yamamoto, A., Kohno, M., Oda, R., Taniguchi, D., Fujiwara, H. and Ejima, A., 2015. Monocarboxylate transporter 4, associated with the acidification of synovial fluid, is a novel therapeutic target for inflammatory arthritis. *Arthritis & rheumatology*, *67*(11), pp.2888-2896.

Gabay, C., 2006. Interleukin-6 and chronic inflammation. *Arthritis research & therapy*, *8*, pp.1-6.

Gabay, C., Burmester, G.R., Strand, V., Msihid, J., Zilberstein, M., Kimura, T., van Hoogstraten, H., Boklage, S.H., Sadeh, J., Graham, N.M. and Boyapati, A., 2020. Sarilumab and adalimumab differential effects on bone remodelling and cardiovascular risk biomarkers, and predictions of treatment outcomes. *Arthritis research & therapy*, *22*, pp.1-11.

Gallagher, L., Cregan, S., Biniecka, M., Cunningham, C., Veale, D.J., Kane, D.J., Fearon, U. and Mullan, R.H., 2020. Insulin-resistant pathways are associated with disease activity in rheumatoid arthritis and are subject to disease modification through metabolic reprogramming: a potential novel therapeutic approach. *Arthritis & Rheumatology*, *72*(6), pp.896-902.

Gan, R. W. *et al.* (2015) 'Anti-carbamylated protein antibodies are present prior to rheumatoid arthritis and are associated with its future diagnosis', *Journal of Rheumatology*. Journal of Rheumatology, 42(4), pp. 572–579. doi: 10.3899/jrheum.140767.

Ganeshan, K. and Chawla, A., 2014. Metabolic regulation of immune responses. *Annual review of immunology*, *32*(1), pp.609-634.

Gao, W., McCormick, J., Connolly, M., Balogh, E., Veale, D.J. and Fearon, U., 2015. Hypoxia and STAT3 signaling interactions regulate pro-inflammatory pathways in rheumatoid arthritis. *Annals of the rheumatic diseases*, *74*(6), pp.1275-1283..

Gao, W., McGarry, T., Orr, C., McCormick, J., Veale, D.J. and Fearon, U., 2016. Tofacitinib regulates synovial inflammation in psoriatic arthritis, inhibiting STAT activation and induction of negative feedback inhibitors. *Annals of the rheumatic diseases*, *75*(1), pp.311-315.

Gao, W., Sweeney, C., Connolly, M., Kennedy, A., Ng, C.T., McCormick, J., Veale, D.J. and Fearon, U., 2012. Notch-1 mediates hypoxia-induced angiogenesis in rheumatoid arthritis. *Arthritis & Rheumatism*, *64*(7), pp.2104-2113.

Gao, W., Sweeney, C., Walsh, C., Rooney, P., McCormick, J., Veale, D.J. and Fearon, U., 2013. Notch signaling pathways mediate synovial angiogenesis in response to vascular endothelial growth factor and angiopoietin 2. *Annals of the rheumatic diseases*, *72*(6), pp.1080-1088.

Gao, Y., Zhang, Y. and Liu, X., 2024. Rheumatoid arthritis: pathogenesis and therapeutic advances. *MedComm*, *5*(3), p.e509.

Garcia-Carbonell, R., Divakaruni, A.S., Lodi, A., Vicente-Suarez, I., Saha, A., Cheroutre, H., Boss, G.R., Tiziani, S., Murphy, A.N. and Guma, M., 2016. Critical role of glucose metabolism in rheumatoid arthritis fibroblast-like synoviocytes. *Arthritis & rheumatology*, *68*(7), pp.1614-1626.

García-Domínguez, E., Carretero, A., Viña-Almunia, A., Domenech-Fernandez, J., Olaso-Gonzalez, G., Viña, J. and Gomez-Cabrera, M.C., 2022. Glucose 6-P dehydrogenase—an antioxidant enzyme with regulatory functions in skeletal muscle during exercise. *Cells*, *11*(19), p.3041.

Garrod, A.E., 1890. *A treatise on rheumatism and rheumatoid arthritis*. Griffin.

Genestier, L., Paillot, R., Fournel, S., Ferraro, C., Miossec, P. and Revillard, J.P., 1998. Immunosuppressive properties of methotrexate: apoptosis and clonal deletion of activated peripheral T cells. *The Journal of clinical investigation*, *102*(2), pp.322-328.

Genovese, M.C., Schiff, M., Luggen, M., Le Bars, M., Aranda, R., Elegbe, A. and Dougados, M., 2012. Longterm safety and efficacy of abatacept through 5 years of treatment in patients with rheumatoid arthritis and an inadequate response to tumor necrosis factor inhibitor therapy. *The Journal of rheumatology*, *39*(8), pp.1546-1554.

Gerhardt, H. and Betsholtz, C., 2005. How do endothelial cells orientate?. *Mechanisms of angiogenesis*, pp.3-15.

Gerhardt, H. and Semb, H., 2008. Pericytes: gatekeepers in tumour cell metastasis?. *Journal of molecular medicine*, *86*, pp.135-144.

Gerhardt, H., Golding, M., Fruttiger, M., Ruhrberg, C., Lundkvist, A., Abramsson, A., Jeltsch, M., Mitchell, C., Alitalo, K., Shima, D. and Betsholtz, C., 2003. VEGF guides angiogenic sprouting utilizing endothelial tip cell filopodia. *Journal of Cell Biology*, *161*(6), pp.1163-1177.

Gerlag, D.M., Raza, K., Van Baarsen, L.G., Brouwer, E., Buckley, C.D., Burmester, G.R., Gabay, C., Catrina, A.I., Cope, A.P., Cornelis, F. and Dahlqvist, S.R., 2012. EULAR recommendations for terminology and research in individuals at risk of rheumatoid arthritis: report from the Study Group for Risk Factors for Rheumatoid Arthritis. *Annals of the rheumatic diseases*, *71*(5), pp.638-641.

Gerli, R., Schillaci, G., Giordano, A., Bocci, E.B., Bistoni, O., Vaudo, G., Marchesi, S., Pirro, M., Ragni, F., Shoenfeld, Y. and Mannarino, E., 2004. CD4+ CD28− T lymphocytes contribute to early atherosclerotic damage in rheumatoid arthritis patients. *Circulation*, *109*(22), pp.2744-2748.

Geudens, I. and Gerhardt, H., 2011. Coordinating cell behaviour during blood vessel formation. *Development*, *138*(21), pp.4569-4583.

Geusens, P., Wouters, C., Nijs, J., Jiang, Y. and Dequeker, J., 1994. Long-term effect of omega-3 fatty acid supplementation in active rheumatoid arthritis. *Arthritis & Rheumatism: Official Journal of the American College of Rheumatology*, *37*(6), pp.824-829.

Ghersi, G., Zhao, Q., Salamone, M., Yeh, Y., Zucker, S. and Chen, W.T., 2006. The protease complex consisting of dipeptidyl peptidase IV and seprase plays a role in the migration and invasion of human endothelial cells in collagenous matrices. *Cancer research*, *66*(9), pp.4652-4661.

Ghilardi, C., Chiorino, G., Dossi, R., Nagy, Z., Giavazzi, R. and Bani, M., 2008. Identification of novel vascular markers through gene expression profiling of tumor-derived endothelium. *BMC genomics*, *9*, pp.1-18.

Giatromanolaki, A., Sivridis, E., Maltezos, E., Athanassou, N., Papazoglou, D., Gatter, K.C., Harris, A.L. and Koukourakis, M.I., 2003. Upregulated hypoxia inducible factor-1α and-2α pathway in rheumatoid arthritis and osteoarthritis. *Arthritis Res Ther*, *5*, pp.1-9.

Gierut, A., Perlman, H. and Pope, R.M., 2010. Innate immunity and rheumatoid arthritis. *Rheumatic diseases clinics of North America*, *36*(2), p.271.

Giles, J.T., Solomon, D.H., Liao, K.P., Rist, P.M., Fayad, Z.A., Tawakol, A. and Bathon, J.M., 2024. Association of the multi-biomarker disease activity score with arterial 18-fluorodeoxyglucose uptake in rheumatoid arthritis. *Rheumatology*, p.keae242.

Gioia, C., Lucchino, B., Tarsitano, M.G., Iannuccelli, C. and Di Franco, M., 2020. Dietary habits and nutrition in rheumatoid arthritis: can diet influence disease development and clinical manifestations?. *Nutrients*, *12*(5), p.1456.

Gkaliagkousi, E., Gavriilaki, E., Doumas, M., Petidis, K., Aslanidis, S. and Stella, D., 2012. Cardiovascular risk in rheumatoid arthritis: pathogenesis, diagnosis, and management. *JCR: Journal of Clinical Rheumatology*, *18*(8), pp.422-430.

Goldring, S.R., 2003. Pathogenesis of bone and cartilage destruction in rheumatoid arthritis. *Rheumatology*, *42*(suppl_2), pp.ii11-ii16.

Gomez-Cambronero, J., 2003. Rapamycin inhibits GM-CSF-induced neutrophil migration. *FEBS letters*, *550*(1-3), pp.94-100.

Gómez-Puerta, J.A., Celis, R., Hernández, M.V., Ruiz-Esquide, V., Ramírez, J., Haro, I., Cañete, J.D. and Sanmartí, R., 2013. Differences in synovial fluid cytokine levels but not in synovial tissue cell infiltrate between anti-citrullinated peptide/protein antibody-positive and–negative rheumatoid arthritis patients. *Arthritis research & therapy*, *15*, pp.1-9.

Gonzalez-Gay MA, Gonzalez-Juanatey C, Piñeiro A et al (2005) High-grade C-reactive protein elevation correlates with accelerated atherogenesis in patients with rheumatoid arthritis. J Rheumatol 32:1219–1223

Gonzalez-Gay, M.A., Gonzalez-Juanatey, C. and Ollier, W.E., 2004. Endothelial dysfunction in rheumatoid arthritis: influence of HLA-DRB1 alleles. *Autoimmunity reviews*, *3*(4), pp.301-304.

Gonzalez-Juanatey, C., Testa, A., Garcia-Castelo, A., Garcia-Porrua, C., Llorca, J., Vidan, J., Hajeer, A.H., Ollier, W.E., Mattey, D.L. and Gonzalez-Gay, M.A., 2003. HLA-DRB1 status affects endothelial function in treated patients with rheumatoid arthritis. *The American journal of medicine*, *114*(8), pp.647-652.

Goon, P.K., Boos, C.J. and Lip, G.Y., 2005. Circulating endothelial cells: markers of vascular dysfunction. *Clinical laboratory*, *51*(9-10), pp.531-538.

Gorman, J. D. *et al.* (2004) 'Particular HLA-DRB1 shared epitope genotypes are strongly associated with rheumatoid vasculitis', *Arthritis and Rheumatism*, 50(11), pp. 3476–3484. doi: 10.1002/art.20588.

Gossec, L., Baraliakos, X., Kerschbaumer, A., de Wit, M., McInnes, I., Dougados, M., Primdahl, J., McGonagle, D.G., Aletaha, D., Balanescu, A. and Balint, P.V., 2020. EULAR recommendations for the management of psoriatic arthritis with pharmacological therapies: 2019 update. *Annals of the rheumatic diseases*, *79*(6), pp.700-712.

Grabiec, A.M., Angiolilli, C., Hartkamp, L.M., van Baarsen, L.G., Tak, P.P. and Reedquist, K.A., 2015. JNK-dependent downregulation of FoxO1 is required to promote the survival of fibroblast-like synoviocytes in rheumatoid arthritis. *Annals of the Rheumatic Diseases*, *74*(9), pp.1763-1771.

Gravallese, E.M. and Firestein, G.S., 2023. Rheumatoid arthritis—common origins, divergent mechanisms. *New England Journal of Medicine*, *388*(6), pp.529-542.

Gravallese, E.M. and Robinson, W.H., 2020. PRIME time in rheumatoid arthritis. *New England Journal of Medicine*, *383*(3), pp.278-279

Gravallese, E.M., Manning, C., Tsay, A., Naito, A., Pan, C., Amento, E. and Goldring, S.R., 2000. Synovial tissue in rheumatoid arthritis is a source of osteoclast differentiation factor. *Arthritis & Rheumatism: Official Journal of the American College of Rheumatology*, *43*(2), pp.250-258.

Gregersen, P.K., Silver, J. and Winchester, R.J., 1987. The shared epitope hypothesis. An approach to understanding the molecular genetics of susceptibility to rheumatoid arthritis. *Arthritis & Rheumatism*, *30*(11), pp.1205-1213.

Gremese E, Carletto A, Padovan M, Atzeni F, Raffeiner B, Giardina AR, Favalli EG, Erre GL, Gorla R, Galeazzi M, Foti R, Cantini F, Salvarani C, Olivieri I, Lapadula G, Ferraccioli G; Gruppo Italiano di Studio sulle Early Arthritis (GISEA). Obesity and reduction of the response rate to anti-tumor necrosis factor α in rheumatoid arthritis: an approach to a personalised medicine. Arthritis Care Res (Hoboken). 2013 Jan;65(1):94-100. doi: 10.1002/acr.21768. PMID: 22730143.

Grisar, J., Aletaha, D., Steiner, C.W., Kapral, T., Steiner, S., Seidinger, D., Weigel, G., Schwarzinger, I., Wolozcszuk, W., Steiner, G. and Smolen, J.S., 2005. Depletion of endothelial progenitor cells in the peripheral blood of patients with rheumatoid arthritis. *Circulation*, *111*(2), pp.204-211.

Guan, C.M. and Beg, S., 2023. Diet as a risk factor for rheumatoid arthritis. *Cureus*, *15*(5).

Guła, Z., Łosińska, K., Kuszmiersz, P., Strach, M., Nowakowski, J., Biedroń, G., Zimba, O., Dyczek, Ł., Haugeberg, G. and Korkosz, M., 2024. A comparison of comorbidities and their risk factors prevalence across rheumatoid arthritis, psoriatic arthritis and axial spondyloarthritis with focus on cardiovascular diseases: data from a single center real-world cohort. *Rheumatology International*, *44*(12), pp.2817-2828.

Guma, M., Sanchez-Lopez, E., Lodi, A., Garcia-Carbonell, R., Tiziani, S., Karin, M., Lacal, J.C. and Firestein, G.S., 2015. Choline kinase inhibition in rheumatoid arthritis. *Annals of the rheumatic diseases*, *74*(7), pp.1399-1407.

Guo, X. and Chen, G., 2020. Hypoxia-inducible factor is critical for pathogenesis and regulation of immune cell functions in rheumatoid arthritis. *Frontiers in Immunology*, *11*, p.1668.

Guo, J., Zhang, H., Xia, J., Hou, J., Wang, Y., Yang, T. ... Wu, X. (2018). Interleukin-1β induces intercellular adhesion molecule-1 expression, thus enhancing the adhesion between mesenchymal stem cells and endothelial progenitor cells via the p38 MAPK signaling pathway. International Journal of Molecular Medicine, 41, 1976-1982.

Guo, Y., Walsh, A.M., Fearon, U., Smith, M.D., Wechalekar, M.D., Yin, X., Cole, S., Orr, C., McGarry, T., Canavan, M. and Kelly, S., 2017. CD40L-dependent pathway is active at various stages of rheumatoid arthritis disease progression. *The Journal of Immunology*, *198*(11), pp.4490-4501.

Gutiérrez B. et al. Recommendations for the management of cardiovascular risk in patients with rheumatoid arthritis: scientific evidence and expert opinion. 2014;44(1):1–8. doi: 10.1016/j.semarthrit.2014.01.002

Haas, R., Smith, J., Rocher-Ros, V., Nadkarni, S., Montero-Melendez, T., D'acquisto, F., Bland, E.J., Bombardieri, M., Pitzalis, C., Perretti, M. and Marelli-Berg, F.M., 2015. Lactate regulates metabolic and pro-inflammatory circuits in control of T cell migration and effector functions. *PLoS biology*, *13*(7), p.e1002202.

Hackstein, H., Taner, T., Zahorchak, A.F., Morelli, A.E., Logar, A.J., Gessner, A. and Thomson, A.W., 2003. Rapamycin inhibits IL-4—induced dendritic cell maturation in vitro and dendritic cell mobilization and function in vivo. *Blood*, *101*(11), pp.4457-4463.

Hamel, K., Doodes, P., Cao, Y., Wang, Y., Martinson, J., Dunn, R., Kehry, M.R., Farkas, B. and Finnegan, A., 2008. Suppression of proteoglycan-induced arthritis by anti-CD20 B Cell depletion therapy is mediated by reduction in autoantibodies and CD4+ T cell reactivity. *The journal of immunology*, *180*(7), pp.4994-5003.
Hammad, D.B., Hider, S.L., Liyanapathirana, V.C. and Tonge, D.P., 2020. Molecular characterization of circulating microbiome signatures in rheumatoid arthritis. *Frontiers in Cellular and Infection Microbiology*, *9*, p.440.

Hamoya, T., Fujii, G., Miyamoto, S., Takahashi, M., Totsuka, Y., Wakabayashi, K., Toshima, J. and Mutoh, M., 2016. Effects of NSAIDs on the risk factors of colorectal cancer: a mini review. *Genes and Environment*, *38*, pp.1-7.

Han, C., Robinson, D.W., Hackett, M.V., Paramore, L.C., Fraeman, K.H. and Bala, M.V., 2006. Cardiovascular disease and risk factors in patients with rheumatoid arthritis, psoriatic arthritis, and ankylosing spondylitis. *The Journal of rheumatology*, *33*(11), pp.2167-2172.

Hanlon, M.M., McGarry, T., Marzaioli, V., Amaechi, S., Song, Q., Nagpal, S., Veale, D.J. and Fearon, U., 2023. Rheumatoid arthritis macrophages are primed for inflammation and display bioenergetic and functional alterations. *Rheumatology*, *62*(7), pp.2611-2620.

Hanlon, M.M., Canavan, M., Barker, B.E. and Fearon, U., 2022. Metabolites as drivers and targets in rheumatoid arthritis. *Clinical and experimental immunology*, *208*(2), pp.167-180.

Hanlon, M.M., Rakovich, T., Cunningham, C.C., Ansboro, S., Veale, D.J., Fearon, U. and McGarry, T., 2019. STAT3 mediates the differential effects of oncostatin M and TNFα on RA synovial fibroblast and endothelial cell function. *Frontiers in immunology*, *10*, p.2056.

Hanlon, M.M., Smith, C.M., Canavan, M., Neto, N.G., Song, Q., Lewis, M.J., O'Rourke, A.M., Tynan, O., Barker, B.E., Gallagher, P. and Mullan, R., 2024. Loss of synovial tissue macrophage homeostasis precedes rheumatoid arthritis clinical onset. *Science advances*, *10*(39), p.eadj1252.

Hannawi, S., Haluska, B., Marwick, T.H. and Thomas, R., 2007. Atherosclerotic disease is increased in recent-onset rheumatoid arthritis: a critical role for inflammation. *Arthritis research & therapy*, *9*, pp.1-9.

Hannemann, N., Apparailly, F. and Courties, G., 2021. Synovial macrophages: from ordinary eaters to extraordinary multitaskers. *Trends in immunology*, *42*(5), pp.368-371.

Hansen, C.G., Ng, Y.L.D., Lam, W.L.M., Plouffe, S.W. and Guan, K.L., 2015. The Hippo pathway effectors YAP and TAZ promote cell growth by modulating amino acid signaling to mTORC1. *Cell research*, *25*(12), pp.1299-1313.

Hansildaar, R., Vedder, D., Baniaamam, M., Tausche, A.K., Gerritsen, M. and Nurmohamed, M.T., 2021. Cardiovascular risk in inflammatory arthritis: rheumatoid arthritis and gout. *The Lancet Rheumatology*, *3*(1), pp.e58-e70.

Haringman, J.J., Gerlag, D.M., Zwinderman, A.H., Smeets, T.J., Kraan, M.C., Baeten, D., McInnes, I.B., Bresnihan, B. and Tak, P.P., 2004. Synovial tissue macrophages: highly sensitive biomarkers for response to treatment in rheumatoid arthritis patients. *Annals of the Rheumatic Diseases*.

Harrison, B.J., Symmons, D.P., Barrett, E.M. and Silman, A.J., 1998. The performance of the 1987 ARA classification criteria for rheumatoid arthritis in a population-based cohort of patients with early inflammatory polyarthritis. American Rheumatism Association. *The Journal of rheumatology*, *25*(12), pp.2324-2330.

Harrold, L.R., Bryson, J., Lehman, T., Zhuo, J., Gao, S., Han, X., Schrader, A., Rebello, S., Pappas, D.A., Sommers, T. and Kremer, J.M., 2021. Association between baseline anti-cyclic citrullinated peptide antibodies and 6-month clinical response following abatacept or TNF inhibitor treatment: a real-world analysis of biologic-experienced patients with RA. *Rheumatology and Therapy*, *8*(2), pp.937-953.

Hassfeld, W et al. 1989. "Demonstration of a New Antinuclear Antibody (Anti-RA33) That Is Highly Specific for Rheumatoid Arthritis." *Arthritis and rheumatism* 32(12): 1515–20.

Helfrich, I. and Schadendorf, D., 2011. Blood vessel maturation, vascular phenotype and angiogenic potential in malignant melanoma: one step forward for overcoming anti-angiogenic drug resistance?. *Molecular oncology*, *5*(2), pp.137-149.

Hellström, M., Phng, L.K., Hofmann, J.J., Wallgard, E., Coultas, L., Lindblom, P., Alva, J., Nilsson, A.K., Karlsson, L., Gaiano, N. and Yoon, K., 2007. Dll4 signaling through Notch1 regulates formation of tip cells during angiogenesis. *Nature*, *445*(7129), pp.776-780.

Hemminki K, Li X, Sundquist J, Sundquist K. Familial associations of rheumatoid arthritis with autoimmune diseases and related conditions. Arthritis & Rheumatism: Official Journal of the American College of Rheumatology. 2009 Mar;60(3):661-8.

Hill, J.A., Southwood, S., Sette, A., Jevnikar, A.M., Bell, D.A. and Cairns, E., 2003. Cutting edge: the conversion of arginine to citrulline allows for a high-affinity peptide interaction with the rheumatoid arthritis-associated HLA-DRB1* 0401 MHC class II molecule. *The Journal of Immunology*, *171*(2), pp.538-541.

Hitchon, C., Wong, K., Ma, G., Reed, J., Lyttle, D. and El-Gabalawy, H., 2002. Hypoxia-induced production of stromal cell–derived factor 1 (CXCL12) and vascular endothelial growth factor by synovial fibroblasts. *Arthritis & Rheumatism*, *46*(10), pp.2587-2597.

Hitchon CA, et al. Antibodies to Porphyromonas gingivalis are associated with anticitrullinated protein antibodies in patients with rheumatoid arthritis and their relatives. J. Rheumatol. 2010;37:1105–1112. doi: 10.3899/jrheum.091323.

Hoang, M.V., Whelan, M.C. and Senger, D.R., 2004. Rho activity critically and selectively regulates endothelial cell organization during angiogenesis. *Proceedings of the National Academy of Sciences*, *101*(7), pp.1874-1879.

Hobl, E.L., Mader, R.M., Erlacher, L., Duhm, B., Mustak, M., Bröll, H., Högger, P., Kalipciyan, M. and Jilma, B., 2011. The influence of methotrexate on the gene expression of the pro-inflammatory cytokine IL-12A in the therapy of rheumatoid arthritis. *Clinical and Experimental Rheumatology-Incl Supplements*, *29*(6), p.963.

Holoshitz, J., 2010. The rheumatoid arthritis HLA–DRB1 shared epitope. *Current opinion in rheumatology*, *22*(3), pp.293-298.

Honorati, M.C., Cattini, L. and Facchini, A., 2004. IL-17, IL-1β and TNF-α stimulate VEGF production by dedifferentiated chondrocytes. *Osteoarthritis and cartilage*, *12*(9), pp.683-691.

Hopkins, S.J. and Meager, A., 1988. Cytokines in synovial fluid: II. The presence of tumour necrosis factor and interferon. *Clinical and experimental immunology*, *73*(1), p.88.

Hosaka, S. *et al.* (1994) 'Expression of the chemokine superfamily in rheumatoid arthritis.', *Clinical and experimental immunology*, 97(3), pp. 451–7. doi: 10.1111/j.1365-2249.1994.tb06109.x.

Hot, A., Zrioual, S., Lenief, V. and Miossec, P., 2012. IL-17 and tumour necrosis factor α combination induces a HIF-1α-dependent invasive phenotype in synoviocytes. *Annals of the rheumatic diseases*, *71*(8), pp.1393-1401.

Hou, SM., Chen, PC., Lin, CM. *et al.* CXCL1 contributes to IL-6 expression in osteoarthritis and rheumatoid arthritis synovial fibroblasts by CXCR2, c-Raf, MAPK, and AP-1 pathway. *Arthritis Res Ther* **22**, 251 (2020).

Hu, F., Mu, R., Zhu, J., Shi, L., Li, Y., Liu, X., Shao, W., Li, G., Li, M., Su, Y. and Cohen, P.L., 2014. Hypoxia and hypoxia-inducible factor-1α provoke toll-like receptor signaling-induced inflammation in rheumatoid arthritis. *Annals of the rheumatic diseases*, *73*(5), pp.928-936.

Hu, T., Liu, CH., Lei, M. *et al.* Metabolic regulation of the immune system in health and diseases: mechanisms and interventions. *Sig Transduct Target Ther* **9**, 268 (2024).

Huang, Q.Q., Doyle, R., Chen, S.Y., Sheng, Q., Misharin, A.V., Mao, Q., Winter, D.R. and Pope, R.M., 2021. Critical role of synovial tissue–resident macrophage niche in joint homeostasis and suppression of chronic inflammation. *Science Advances*, *7*(2), p.eabd0515.

Huang, Y., Zheng, S., Wang, R., Tang, C., Zhu, J. and Li, J., 2019. CCL5 and related genes might be the potential diagnostic biomarkers for the therapeutic strategies of rheumatoid arthritis. *Clinical Rheumatology*, *38*, pp.2629-2635.

Humby, F., Bombardieri, M., Manzo, A., Kelly, S., Blades, M.C., Kirkham, B., Spencer, J. and Pitzalis, C., 2009. Ectopic lymphoid structures support ongoing production of class-switched autoantibodies in rheumatoid synovium. *PLoS medicine*, *6*(1), p.e1.

Humby, F., Durez, P., Buch, M.H., Lewis, M.J., Rizvi, H., Rivellese, F., Nerviani, A., Giorli, G., Mahto, A., Montecucco, C. and Lauwerys, B., 2021. Rituximab versus tocilizumab in anti-TNF inadequate responder patients with rheumatoid arthritis (R4RA): 16-week outcomes of a stratified, biopsy-driven, multicentre, open-label, phase 4 randomised controlled trial. *The Lancet*, *397*(10271), pp.305-317.

Humby, F., Lewis, M., Ramamoorthi, N., Hackney, J.A., Barnes, M.R., Bombardieri, M., Setiadi, A.F., Kelly, S., Bene, F., DiCicco, M. and Riahi, S., 2019. Synovial cellular and molecular signatures stratify clinical response

to csDMARD therapy and predict radiographic progression in early rheumatoid arthritis patients. *Annals of the rheumatic diseases*, *78*(6), pp.761-772.

Hunt, L., Hensor, E.M., Nam, J., Burska, A.N., Parmar, R., Emery, P. and Ponchel, F., 2016. T cell subsets: an immunological biomarker to predict progression to clinical arthritis in ACPA-positive individuals. *Annals of the Rheumatic Diseases*, *75*(10), pp.1884-1889.

Hunter, W., 1900. Oral sepsis as a cause of disease. *British medical journal*, *2*(2065), p.215.

Hwang, Y.G., Balasubramani, G.K., Metes, I.D., Levesque, M.C., Bridges, S.L. and Moreland, L.W., 2016. Differential response of serum amyloid A to different therapies in early rheumatoid arthritis and its potential value as a disease activity biomarker. *Arthritis research & therapy*, *18*, pp.1-8.

Hyndman, I.J., 2017. Rheumatoid arthritis: past, present and future approaches to treating the disease. *International journal of rheumatic diseases*, *20*(4), pp.417-419.

Iguchi, T. and Ziff, M., 1986. Electron microscopic study of rheumatoid synovial vasculature. Intimate relationship between tall endothelium and lymphoid aggregation. *The Journal of clinical investigation*, *77*(2), pp.355-361.

Ioan-Facsinay, A., Willemze, A., Robinson, D.B., Peschken, C.A., Markland, J., van der Woude, D., Elias, B., Ménard, H.A., Newkirk, M., Fritzler, M.J. and Toes, R.E., 2008. Marked differences in fine specificity and isotype usage of the anti–citrullinated protein antibody in health and disease. *Arthritis & Rheumatism: Official Journal of the American College of Rheumatology*, *58*(10), pp.3000-3008.

Isaacs, J.D., Cohen, S.B., Emery, P., Tak, P.P., Wang, J., Lei, G., Williams, S., Lal, P. and Read, S.J., 2013. Effect of baseline rheumatoid factor and anticitrullinated peptide antibody serotype on rituximab clinical response: a meta-analysis. *Annals of the rheumatic diseases*, *72*(3), pp.329-336.

Italiani, P. and Boraschi, D., 2014. From monocytes to M1/M2 macrophages: phenotypical vs. functional differentiation. *Frontiers in immunology*, *5*, p.514.

Ivanov, I.I., Atarashi, K., Manel, N., Brodie, E.L., Shima, T., Karaoz, U., Wei, D., Goldfarb, K.C., Santee, C.A., Lynch, S.V. and Tanoue, T., 2009. Induction of intestinal Th17 cells by segmented filamentous bacteria. *Cell*, *139*(3), pp.485-498.

IWANAGA, T., Shikichi, M., KITAMURA, H., YANASE, H. and NOZAWA-INOUE, K., 2000. Morphology and functional roles of synoviocytes in the joint. *Archives of histology and cytology*, *63*(1), pp.17-31.

Izquierdo, E., Canete, J.D., Celis, R., Santiago, B., Usategui, A., Sanmartí, R., Del Rey, M.J. and Pablos, J.L., 2009. Immature blood vessels in rheumatoid synovium are selectively depleted in response to anti-TNF therapy. *PLoS One*, *4*(12), p.e8131.

James, M.J., Cleland, L.G. and Rofe, A.M., 1992. Determinants of synovial fluid lactate concentration. *The Journal of Rheumatology*, *19*(7), pp.1107-1110.

Jamil M, Aslam R, Patel A et al (2021) Prevalence and extent of subclinical atherosclerosis and associated cardiovascular risk factors in adult patients with psoriatic arthritis: a systematic review. Cureus. 10.7759/cureus.16853 10.7759/cureus.16853

Jansen, L M et al. 2003. "The Predictive Value of Anti-Cyclic Citrullinated Peptide Antibodies in Early Arthritis." *J Rheumatol* 30(8): 1691–95.

Jay, G.D., Tantravahi, U., Britt, D.E., Barrach, H.J. and Cha, C.J., 2001. Homology of lubricin and superficial zone protein (SZP): products of megakaryocyte stimulating factor (MSF) gene expression by human synovial fibroblasts and articular chondrocytes localised to chromosome 1q25. *Journal of Orthopaedic Research*, *19*(4), pp.677-687.

Jenny, N.S., Arnold, A.M., Kuller, L.H., Sharrett, A.R., Fried, L.P., Psaty, B.M. and Tracy, R.P., 2006. Soluble intracellular adhesion molecule-1 is associated with cardiovascular disease risk and mortality in older adults. *Journal of thrombosis and haemostasis*, *4*(1), pp.107-113.

Jiang, X., Trouw, L.A., van Wesemael, T.J., Shi, J., Bengtsson, C., Källberg, H., Malmström, V., Israelsson, L., Hreggvidsdottir, H., Verduijn, W. and Klareskog, L., 2014. Anti-CarP antibodies in two large cohorts of patients with rheumatoid arthritis and their relationship to genetic risk factors, cigarette smoking and other autoantibodies. *Annals of the rheumatic diseases*, *73*(10), pp.1761-1768.

Jiménez-Martínez, M., Dankers, W. and van Baarsen, L.G., 2024. The key role of the lymph node niche in the development of rheumatoid arthritis. *Joint bone spine*, *91*(2), p.105661.

Jin, S., Mutvei, A.P., Chivukula, I.V., Andersson, E.R., Ramsköld, D., Sandberg, R., Lee, K.L., Kronqvist, P., Mamaeva, V., Östling, P. and Mpindi, J.P., 2013. Non-canonical Notch signaling activates IL-6/JAK/STAT signaling in breast tumor cells and is controlled by p53 and IKKα/IKKβ. *Oncogene*, *32*(41), pp.4892-4902.

Johnson, M.O., Wolf, M.M., Madden, M.Z., Andrejeva, G., Sugiura, A., Contreras, D.C., Maseda, D., Liberti, M.V., Paz, K., Kishton, R.J. and Johnson, M.E., 2018. Distinct regulation of Th17 and Th1 cell differentiation by glutaminase-dependent metabolism. *Cell*, *175*(7), pp.1780-1795.

Johnson, R. and Halder, G., 2014. The two faces of Hippo: targeting the Hippo pathway for regenerative medicine and cancer treatment. *Nature reviews Drug discovery*, *13*(1), pp.63-79.

Jongbloed, S.L., Lebre, M.C., Fraser, A.R., Gracie, J.A., Sturrock, R.D., Tak, P.P. and McInnes, I.B., 2005. Enumeration and phenotypical analysis of distinct dendritic cell subsets in psoriatic arthritis and rheumatoid arthritis. *Arthritis research & therapy*, *8*, pp.1-13.

Judge A, Dodd MS. Metabolism. Essays Biochem. 2020 Oct 8;64(4):607-647.

Jutley, G. S., Latif, Z. P., & Raza, K. (2017). Symptoms in individuals at risk of rheumatoid arthritis. *Best Practice & Research Clinical Rheumatology*, *31*(1), 59-70.

Källberg, H., Ding, B., Padyukov, L., Bengtsson, C., Rönnelid, J., Klareskog, L., Alfredsson, L. and EIRA Study Group, 2011. Smoking is a major preventable risk factor for rheumatoid arthritis: estimations of risks after various exposures to cigarette smoke. *Annals of the rheumatic diseases*, *70*(3), pp.508-511.

Källberg, H., Jacobsen, S., Bengtsson, C., Pedersen, M., Padyukov, L., Garred, P., Frisch, M., Karlson, E.W., Klareskog, L. and Alfredsson, L., 2009. Alcohol consumption is associated with decreased risk of rheumatoid arthritis: results from two Scandinavian case–control studies. *Annals of the rheumatic diseases*, *68*(2), pp.222-227.

Kaly, L. and Rosner, I., 2012. Tocilizumab–a novel therapy for non-organ-specific autoimmune diseases. *Best practice & research Clinical rheumatology*, *26*(1), pp.157-165.

Kanagawa, H et al. 2015. "Mycobacterium Tuberculosis Promotes Arthritis Development through Toll-like Receptor 2." *J Bone Miner Metab* 33(2): 135–41.

Kapellos, T.S., Bonaguro, L., Gemünd, I., Reusch, N., Saglam, A., Hinkley, E.R. and Schultze, J.L., 2019. Human monocyte subsets and phenotypes in major chronic inflammatory diseases. *Frontiers in immunology*, *10*, p.2035.

Karami, J., Aslani, S., Jamshidi, A., Garshasbi, M. and Mahmoudi, M., 2019. Genetic implications in the pathogenesis of rheumatoid arthritis; an updated review. *Gene*, *702*, pp.8-16.

Karonitsch, T., Kandasamy, R.K., Kartnig, F., Herdy, B., Dalwigk, K., Niederreiter, B., Holinka, J., Sevelda, F., Windhager, R., Bilban, M. and Weichhart, T., 2018. mTOR senses environmental cues to shape the fibroblast-like synoviocyte response to inflammation. *Cell Reports*, *23*(7), pp.2157-2167.

Karouzakis, E., Hähnlein, J., Grasso, C., Semmelink, J.F., Tak, P.P., Gerlag, D.M., Gay, S., Ospelt, C. and van Baarsen, L.G., 2019. Molecular characterization of human lymph node stromal cells during the earliest phases of rheumatoid arthritis. *Frontiers in immunology*, *10*, p.1863.

Kauppi M, Pukkala E, Isomäki H. Low incidence of colorectal cancer in patients with rheumatoid arthritis. Clin Exp Rheumatol. 1996 Sep-Oct;14(5):551-3. PMID: 8913658.

Kavanaugh, A., Rosengren, S., Lee, S.J., Hammaker, D., Firestein, G.S., Kalunian, K., Wei, N. and Boyle, D.L., 2008. Assessment of rituximab's immunomodulatory synovial effects (ARISE trial). 1: clinical and synovial biomarker results. *Annals of the rheumatic diseases*, *67*(3), pp.402-408.

Kay J, Calabrese L. The role of interleukin-1 in the pathogenesis of rheumatoid arthritis. Rheumatology (Oxford). 2004 Jun;43 Suppl 3:iii2-iii9. doi: 10.1093/rheumatology/keh201. PMID: 15150426.

Kelleher, D., Barry, L., McGowan, B., Doherty, E., Carey, J.J. and Kane, D., 2020. Budget impact analysis of an early identification and referral model for diagnosing patients with suspected rheumatoid arthritis in Ireland. *Rheumatology Advances in Practice*, *4*(2), p.rkaa059.

Kemble, S. and Croft, A.P., 2021. Critical role of synovial tissue–resident macrophage and fibroblast subsets in the persistence of joint inflammation. *Frontiers in immunology*, *12*, p.715894.

Kennedy, A., Ng, C.T., Chang, T.C., Biniecka, M., O'Sullivan, J.N., Heffernan, E., Fearon, U. and Veale, D.J., 2011. Tumor necrosis factor blocking therapy alters joint inflammation and hypoxia. *Arthritis & Rheumatism*, *63*(4), pp.923-932.

Kennedy, A., Ng, C.T., Biniecka, M., Saber, T., Taylor, C., O'Sullivan, J., Veale, D.J. and Fearon, U., 2010. Angiogenesis and blood vessel stability in inflammatory arthritis. *Arthritis & Rheumatism*, *62*(3), pp.711-721.

Kerola, A.M.; Rollefstad, S.; Semb, A.G. Atherosclerotic cardiovascular disease in rheumatoid arthritis: Impact of inflammation and antirheumatic treatment. Eur. Cardiol. 2021, 16, e18

Khosrow-Khavar, F., Desai, R.J., Lee, H., Lee, S.B. and Kim, S.C., 2022. Tofacitinib and risk of malignancy: results from the safety of tofacitinib in routine care patients with rheumatoid arthritis (STAR-RA) study. *Arthritis & Rheumatology*, *74*(10), pp.1648-1659.

Khullar, A., Dhir, V., Saikia, B., Yadav, A.K., Leishangthem, B., Prasad, C.B., Jayaprakash, S., Jain, S., Naidu, G.S.R.S.N.K., Sharma, S.K. and Sharma, A., 2024. Rheumatoid arthritis synovial fluid shows enrichment of T-cells producing GMCSF which are polyfunctional for TNFα and IFNγ. *Clin Exp Rheumatol*.

Kiener, H.P. and Brenner, M.B., 2005. Building the synovium: cadherin-11 mediates fibroblast-like synoviocyte cell-to-cell adhesion. *Arthritis Res Ther*, *7*, pp.1-6.

Kiener, H.P., Lee, D.M., Agarwal, S.K. and Brenner, M.B., 2006. Cadherin-11 induces rheumatoid arthritis fibroblast-like synoviocytes to form lining layers in vitro. *The American journal of pathology*, *168*(5), pp.1486-1499.

Kiener, H.P., Niederreiter, B., Lee, D.M., Jimenez-Boj, E., Smolen, J.S. and Brenner, M.B., 2009. Cadherin 11 promotes invasive behavior of fibroblast-like synoviocytes. *Arthritis & Rheumatism*, *60*(5), pp.1305-1310.

Kim, B., Kim, H.Y., Yoon, B.R., Yeo, J., In Jung, J., Yu, K.S., Kim, H.C., Yoo, S.J., Park, J.K., Kang, S.W. and Lee, W.W., 2022. Cytoplasmic zinc promotes IL-1β production by monocytes and macrophages through mTORC1-induced glycolysis in rheumatoid arthritis. *Science Signaling*, *15*(716), p.eabi7400.

Kim, H.R., Kim, K.W., Kim, B.M., Cho, M.L. and Lee, S.H., 2015. The effect of vascular endothelial growth factor on osteoclastogenesis in rheumatoid arthritis. *PloS one*, *10*(4), p.e0124909.

Kim, S., Hwang, J., Xuan, J., Jung, Y.H., Cha, H.S. and Kim, K.H., 2014. Global metabolite profiling of synovial fluid for the specific diagnosis of rheumatoid arthritis from other inflammatory arthritis. *PloS one*, *9*(6), p.e97501.

Kim, S.C., Pawar, A., Desai, R.J., Solomon, D.H., Gale, S., Bao, M., Sarsour, K. and Schneeweiss, S., 2019, October. Risk of malignancy associated with use of tocilizumab versus other biologics in patients with rheumatoid arthritis: a multi-database cohort study. In *Seminars in arthritis and rheumatism* (Vol. 49, No. 2, pp. 222-228). WB Saunders.

Kim, K.W., Cho, M.L., Lee, S.H., Oh, H.J., Kang, C.M., Ju, J.H., Min, S.Y., Cho, Y.G., Park, S.H. and Kim, H.Y., 2007. Human rheumatoid synovial fibroblasts promote osteoclastogenic activity by activating RANKL via TLR-2 and TLR-4 activation. *Immunology letters*, *110*(1), pp.54-64.

Kirk, T., Ahmed, A. and Rognoni, E., 2021. Fibroblast memory in development, homeostasis and disease. *Cells*, *10*(11), p.2840.

Kjeldsen-Kragh J. Rheumatoid arthritis treated with vegetarian diets. Am J Clin Nutr. 1999 Sep;70(3 Suppl):594S-600S. doi: 10.1093/ajcn/70.3.594s. PMID: 10479237.

Klareskog, L., Stolt, P., Lundberg, K., Källberg, H., Bengtsson, C., Grunewald, J., Rönnelid, J., Erlandsson Harris, H., Ulfgren, A.K., Rantapää-Dahlqvist, S. and Eklund, A., 2006. A new model for an etiology of rheumatoid arthritis: smoking may trigger HLA–DR (shared epitope)–restricted immune reactions to autoantigens modified by citrullination. *Arthritis & Rheumatism: Official Journal of the American College of Rheumatology*, *54*(1), pp.38-46.

Klimek, E., Mikołajczyk, T., Sulicka, J., Kwaśny-Krochin, B., Korkosz, M., Osmenda, G., Wizner, B., Surdacki, A., Guzik, T., Grodzicki, T.K. and Skalska, A., 2014. Blood monocyte subsets and selected cardiovascular risk markers in rheumatoid arthritis of short duration in relation to disease activity. *BioMed research international*, *2014*(1), p.736853.

Klimiuk, P.A., Sierakowski, S., Domyslawska, I. and Chwiecko, J., 2009. Effect of etanercept on serum levels of soluble cell adhesion molecules (sICAM-1, sVCAM-1, and sE-selectin) and vascular endothelial growth factor in patients with rheumatoid arthritis. *Scandinavian journal of rheumatology*, *38*(6), pp.439-444.

Klimiuk, P., Sierakowski, S., Latosiewicz, R., Cylwik, J.P., Cylwik, B., Skowronski, J. and Chwiecko, J., 2002. Soluble adhesion molecules (ICAM-1, VCAM-1, and E-selectin) and vascular endothelial growth factor (VEGF) in patients with distinct variants of rheumatoid synovitis. *Annals of the rheumatic diseases*, *61*(9), pp.804-809.

Klimiuk, P.A., Fiedorczyk, M., Sierakowski, S. and Chwiecko, J., 2007. Soluble cell adhesion molecules (sICAM-1, sVCAM-1, and sE-selectin) in patients with early rheumatoid arthritis. *Scandinavian journal of rheumatology*, *36*(5), pp.345-350.

Klimiuk, P.A., Sierakowski, S., Latosiewicz, R., Cylwik, J.P., Cylwik, B., Skowronski, J. and Chwiecko, J., 2003. Circulating tumour necrosis factor α and soluble tumour necrosis factor receptors in patients with different patterns of rheumatoid synovitis. *Annals of the rheumatic diseases*, *62*(5), pp.472-475.

Klint, E.A., Grundtman, C., Engström, M., Catrina, A.I., Makrygiannakis, D., Klareskog, L., Andersson, U. and Ulfgren, A.K., 2005. Intraarticular glucocorticoid treatment reduces inflammation in synovial cell infiltrations more efficiently than in synovial blood vessels. *Arthritis & Rheumatism*, *52*(12), pp.3880-3889.

Kłodziński Ł, Wisłowska M. Comorbidities in rheumatic arthritis. Reumatologia. 2018;56(4):228-233. doi: 10.5114/reum.2018.77974. Epub 2018 Aug 31. PMID: 30237627; PMCID: PMC6142024.

Klysz, D., Tai, X., Robert, P.A., Craveiro, M., Cretenet, G., Oburoglu, L., Mongellaz, C., Floess, S., Fritz, V., Matias, M.I. and Yong, C., 2015. Glutamine-dependent α-ketoglutarate production regulates the balance between T helper 1 cell and regulatory T cell generation. *Science signaling*, *8*(396), pp.ra97-ra97.

Kobayashi T, Bartold PM. Periodontitis and periodontopathic bacteria as risk factors for rheumatoid arthritis: a review of the last 10 years. Japanese Dental Sci Rev. 2023;59:263–72.

Koch AE, Kunkel SL, Burrows JC, Evanoff HL, Haines GK, Pope RM, Strieter RM. Synovial tissue macrophage as a source of the chemotactic cytokine IL-8. J Immunol. 1991 Oct 1;147(7):2187-95. PMID: 1918955.

Koch, A.E., 2003. Angiogenesis as a target in rheumatoid arthritis. *Annals of the rheumatic diseases*, *62*(suppl 2), pp.ii60-ii67.

Koedderitzsch, K., Zezina, E., Li, L., Herrmann, M. and Biesemann, N., 2021. TNF induces glycolytic shift in fibroblast like synoviocytes via GLUT1 and HIF1A. *Scientific reports*, *11*(1), p.19385.

Kolarz, B. and Majdan, M., 2017, June. Epigenetic aspects of rheumatoid arthritis: contribution of non-coding RNAs. In *Seminars in arthritis and rheumatism* (Vol. 46, No. 6, pp. 724-731). WB Saunders.

Komano, Y., Nanki, T., Hayashida, K., Taniguchi, K. and Miyasaka, N., 2006. Identification of a human peripheral blood monocyte subset that differentiates into osteoclasts. *Arthritis research & therapy*, *8*, pp.1-14.

Konig, M.F., Abusleme, L., Reinholdt, J., Palmer, R.J., Teles, R.P., Sampson, K., Rosen, A., Nigrovic, P.A., Sokolove, J., Giles, J.T. and Moutsopoulos, N.M., 2016. Aggregatibacter actinomycetemcomitans–induced hypercitrullination links periodontal infection to autoimmunity in rheumatoid arthritis. *Science translational medicine*, *8*(369), pp.369ra176-369ra176.

Korb, A., Pavenstädt, H. and Pap, T., 2009. Cell death in rheumatoid arthritis. *Apoptosis*, *14*, pp.447-454.

Korsunsky, I., Millard, N., Fan, J., Slowikowski, K., Zhang, F., Wei, K., Baglaenko, Y., Brenner, M., Loh, P.R. and Raychaudhuri, S., 2019. Fast, sensitive and accurate integration of single-cell data with Harmony. *Nature methods*, *16*(12), pp.1289-1296.

Korsunsky, I., Wei, K., Pohin, M., Kim, E.Y., Barone, F., Major, T., Taylor, E., Ravindran, R., Kemble, S., Watts, G.F. and Jonsson, A.H., 2022. Cross-tissue, single-cell stromal atlas identifies shared pathological fibroblast phenotypes in four chronic inflammatory diseases. *Med*, *3*(7), pp.481-518.

Køster, D., Egedal, J.H., Hvid, M., Jakobsen, M.R., Mueller-Ladner, U., Deleuran, B., Kragstrup, T.W., Neumann, E. and Nielsen, M.A., 2020. Phenotypic and functional characterization of synovial fluid-derived fibroblast-like synoviocytes in rheumatoid arthritis. *Annals of the Rheumatic Diseases*, *79*(Suppl. 1), p.1345.

Kouri, T., Petersen, J., Rhodes, G., Aho, K., Palosuo, T., Heliövaara, M., Isomäki, H., von Essen, R. and Vaughan, J.H., 1990. Antibodies to synthetic peptides from Epstein-Barr nuclear antigen-1 in sera of patients with early rheumatoid arthritis and in preillness sera. *The Journal of rheumatology*, *17*(11), pp.1442-1449.

Kraan, M.C., Patel, D.D., Haringman, J.J., Smith, M.D., Weedon, H., Ahern, M.J., Breedveld, F.C. and Tak, P.P., 2000. The development of clinical signs of rheumatoid synovial inflammation is associated with increased synthesis of the chemokine CXCL8 (interleukin-8). *Arthritis Research & Therapy*, *3*, pp.1-7.

Krawczyk, C.M., Holowka, T., Sun, J., Blagih, J., Amiel, E., DeBerardinis, R.J., Cross, J.R., Jung, E., Thompson, C.B., Jones, R.G. and Pearce, E.J., 2010. Toll-like receptor–induced changes in glycolytic metabolism regulate dendritic cell activation. *Blood, The Journal of the American Society of Hematology*, *115*(23), pp.4742-4749.

Krishnamurthy, A., Joshua, V., Hensvold, A.H., Jin, T., Sun, M., Vivar, N., Ytterberg, A.J., Engström, M., Fernandes-Cerqueira, C., Amara, K. and Magnusson, M., 2016. Identification of a novel chemokine-dependent molecular mechanism underlying rheumatoid arthritis-associated autoantibody-mediated bone loss. *Annals of the rheumatic diseases*, *75*(4), pp.721-729.

Kroot, E J et al. 2000. "The Prognostic Value of Anti-Cyclic Citrullinated Peptide Antibody in Patients with Recent-Onset Rheumatoid Arthritis." *Arthritis Rheum* 43(8): 1831–35

Kuan, W.P., Tam, L.S., Wong, C.K., Ko, F.W., Li, T., Zhu, T. and Li, E.K., 2010. CXCL 9 and CXCL 10 as Sensitive markers of disease activity in patients with rheumatoid arthritis. *The Journal of rheumatology*, *37*(2), pp.257-264.

Kuang L, Wu J, Su N, Qi H, Chen H, Zhou S, et al. FGFR3 deficiency enhances CXCL12-dependent chemotaxis of macrophages via upregulating CXCR7 and aggravates joint destruction in mice. Ann Rheum Dis. 2020;79:112–22.

Kubo, Satoshi, Kunihiro Yamaoka, Masahiro Kondo, Kaoru Yamagata, Jidong Zhao, Shigeru Iwata, and Yoshiya Tanaka. "The JAK inhibitor, tofacitinib, reduces the T cell stimulatory capacity of human monocyte-derived dendritic cells." *Annals of the rheumatic diseases* 73, no. 12 (2014): 2192-2198.

Kular, J.K., Basu, S. and Sharma, R.I., 2014. The extracellular matrix: Structure, composition, age-related differences, tools for analysis and applications for tissue engineering. *Journal of tissue engineering*, *5*, p.2041731414557112.

Kuo, D., Ding, J., Cohn, I.S., Zhang, F., Wei, K., Rao, D.A., Rozo, C., Sokhi, U.K., Shanaj, S., Oliver, D.J. and Echeverria, A.P., 2019. HBEGF+ macrophages in rheumatoid arthritis induce fibroblast invasiveness. *Science translational medicine*, *11*(491), p.eaau8587.

Kurowska-Stolarska, M. and Alivernini, S., 2017. Synovial tissue macrophages: friend or foe?. *RMD open*, *3*(2), p.e000527.

Kvacskay, P., Yao, N., Schnotz, J.H., Scarpone, R., Carvalho, R.D.A., Klika, K.D., Merkt, W., Tretter, T., Lorenz, H.M. and Tykocinski, L.O., 2021. Increase of aerobic glycolysis mediated by activated T helper cells drives synovial fibroblasts towards an inflammatory phenotype: new targets for therapy?. *Arthritis research & therapy*, *23*, pp.1-15.

Kvien, T.K., Uhlig, T., Ødegård, S. and Heiberg, M.S., 2006. Epidemiological aspects of rheumatoid arthritis: the sex ratio. *Annals of the New York academy of Sciences*, *1069*(1), pp.212-222.

L'homme, L. *et al.* (2013) 'Unsaturated fatty acids prevent activation of NLRP3 inflammasome in human monocytes/macrophages.', *Journal of lipid research*, 54(11), pp. 2998–3008. doi: 10.1194/jlr.M037861.

Lampropoulou, V., Sergushichev, A., Bambouskova, M., Nair, S., Vincent, E.E., Loginicheva, E., Cervantes-Barragan, L., Ma, X., Huang, S.C.C., Griss, T. and Weinheimer, C.J., 2016. Itaconate links inhibition of succinate dehydrogenase with macrophage metabolic remodeling and regulation of inflammation. *Cell metabolism*, *24*(1), pp.158-166.

Landewé, R.B., Boers, M., Verhoeven, A.C., Westhovens, R., van de Laar, M.A., Markusse, H.M., van Denderen, J.C., Westedt, M.L., Peeters, A.J., Dijkmans, B.A. and Jacobs, P., 2002. COBRA combination therapy in patients with early rheumatoid arthritis: long-term structural benefits of a brief intervention. *Arthritis & Rheumatism*, *46*(2), pp.347-356.

Landré-Beauvais, A.J., 2001. The first description of rheumatoid arthritis. Unabridged text of the doctoral dissertation presented in 1800. *Joint bone spine*, *68*(2), pp.130-143.

Laragione, T. and Gulko, P.S., 2010. mTOR regulates the invasive properties of synovial fibroblasts in rheumatoid arthritis. *Molecular Medicine*, *16*, pp.352-358.

Lee, C.K., Lee, E.Y., Chung, S.M., Mun, S.H., Yoo, B. and Moon, H.B., 2004. Effects of disease-modifying antirheumatic drugs and antiinflammatory cytokines on human osteoclastogenesis through interaction with receptor activator of nuclear factor κB, osteoprotegerin, and receptor activator of nuclear factor κB ligand. *Arthritis & rheumatism*, *50*(12), pp.3831-3843.

Lee, D.M., Phillips, R., Hagan, E.M., Chibnik, L.B., Costenbader, K.H. and Schur, P.H., 2008. Quantifying Anti-CCP titer: clinical utility and association with tobacco exposure in patients with rheumatoid arthritis. *Annals of the Rheumatic Diseases*.

Lee, E.B., Fleischmann, R., Hall, S., Wilkinson, B., Bradley, J.D., Gruben, D., Koncz, T., Krishnaswami, S., Wallenstein, G.V., Zang, C. and Zwillich, S.H., 2014. Tofacitinib versus methotrexate in rheumatoid arthritis. *New England Journal of Medicine*, *370*(25), pp.2377-2386.

Lee, Y.H. and Bae, S.C., 2016. Comparative efficacy and safety of tocilizumab, rituximab, abatacept and tofacitinib in patients with active rheumatoid arthritis that inadequately responds to tumor necrosis factor inhibitors: a Bayesian network meta-analysis of randomised controlled trials. *International journal of rheumatic diseases*, *19*(11), pp.1103-1111.

Lee, D., Obukhov, A.G., Shen, Q., Liu, Y., Dhawan, P., Nowycky, M.C. and Christakos, S., 2006. Calbindin-D28k decreases L-type calcium channel activity and modulates intracellular calcium homeostasis in response to K+ depolarization in a rat beta cell line RINr1046-38. *Cell calcium*, *39*(6), pp.475-485.

Lee, D.M., Kiener, H.P., Agarwal, S.K., Noss, E.H., Watts, G.F., Chisaka, O., Takeichi, M. and Brenner, M.B., 2007. Cadherin-11 in synovial lining formation and pathology in arthritis. *Science*, *315*(5814), pp.1006-1010.

Lee, Y.A., Choi, H.M., Lee, S.H., Hong, S.J., Yang, H.I., Yoo, M.C. and Kim, K.S., 2012. Hypoxia differentially affects IL-1β-stimulated MMP-1 and MMP-13 expression of fibroblast-like synoviocytes in an HIF-1α-dependent manner. *Rheumatology*, *51*(3), pp.443-450.

Lee, Y.H. and Bae, S.C., 2018. Correlation between circulating VEGF levels and disease activity in rheumatoid arthritis: a meta-analysis. *Zeitschrift fur Rheumatologie*, *77*(3), pp.240-248.

Lefèvre, S., Knedla, A., Tennie, C., Kampmann, A., Wunrau, C., Dinser, R., Korb, A., Schnäker, E.M., Tarner, I.H., Robbins, P.D. and Evans, C.H., 2009. Synovial fibroblasts spread rheumatoid arthritis to unaffected joints. *Nature medicine*, *15*(12), pp.1414-1420.

Lei, Q., Yang, J., Li, L., Zhao, N., Lu, C., Lu, A. and He, X., 2023. Lipid metabolism and rheumatoid arthritis. *Frontiers in immunology*, *14*, p.1190607.

Lendahl, U., Muhl, L. and Betsholtz, C., 2022. Identification, discrimination and heterogeneity of fibroblasts. *Nature communications*, *13*(1), p.3409.

Levin, R.W., Park, J., Ostrov, B., Reginato, A., Baker, D.G., Bomalaski, J.S., Borofsky, M., Gardiner, M., Leventhal, L., Louthrenoo, W. and Von Feldt, J., 1996. Clinical assessment of the 1987 American College of Rheumatology criteria for rheumatoid arthritis. *Scandinavian journal of rheumatology*, *25*(5), pp.277-281.

Levings, M.K. and Schrader, J.W., 1999. IL-4 inhibits the production of TNF-α and IL-12 by STAT6-dependent and-independent mechanisms. *The Journal of Immunology*, *162*(9), pp.5224-5229.

Lewis, M.J., Barnes, M.R., Blighe, K., Goldmann, K., Rana, S., Hackney, J.A., Ramamoorthi, N., John, C.R., Watson, D.S., Kummerfeld, S.K. and Hands, R., 2019. Molecular portraits of early rheumatoid arthritis identify clinical and treatment response phenotypes. *Cell reports*, *28*(9), pp.2455-2470.

Li, Q., Zhou, L., Xia, D. and Wang, J., 2024. Rheumatoid arthritis reduces the risk of colorectal cancer through immune inflammation mediation. *Journal of Cellular and Molecular Medicine*, *28*(13), p.e18515.

Li, X., Sun, H., Li, H., Li, D., Cai, Z., Xu, J. and Ma, R., 2023. A single-cell RNA-sequencing analysis of distinct subsets of synovial macrophages in rheumatoid arthritis. *DNA and Cell Biology*, *42*(4), pp.212-222.

Li, Y., Liu, Y., Wang, C., Xia, W.R., Zheng, J.Y., Yang, J., Liu, B., Liu, J.Q. and Liu, L.F., 2018. Succinate induces synovial angiogenesis in rheumatoid arthritis through metabolic remodeling and HIF-1α/VEGF axis. *Free Radical Biology and Medicine*, *126*, pp.1-14.

Li, Y., Zheng, J.Y., Liu, J.Q., Yang, J., Liu, Y., Wang, C., Ma, X.N., Liu, B.L., Xin, G.Z. and Liu, L.F., 2016. Succinate/NLRP3 inflammasome induces synovial fibroblast activation: therapeutical effects of clematichinenoside AR on arthritis. *Frontiers in immunology*, *7*, p.532.

Li, K., Wang, M., Zhao, L., Liu, Y. and Zhang, X., 2022. ACPA-negative rheumatoid arthritis: From immune mechanisms to clinical translation. *EBioMedicine*, *83*.

Liang, N., Zhang, C., Dill, P., Panasyuk, G., Pion, D., Koka, V., Gallazzini, M., Olson, E.N., Lam, H., Henske, E.P. and Dong, Z., 2014. Regulation of YAP by mTOR and autophagy reveals a therapeutic target of tuberous sclerosis complex. *Journal of Experimental Medicine*, *211*(11), pp.2249-2263.

Liao, K.P., Batra, K.L., Chibnik, L., Schur, P.H. and Costenbader, K.H., 2008. Anti-cyclic citrullinated peptide revised criteria for the classification of rheumatoid arthritis. *Annals of the rheumatic diseases*, *67*(11), pp.1557-1561.

Lin, H.Y.H., Chang, K.T., Hung, C.C., Kuo, C.H., Hwang, S.J., Chen, H.C., Hung, C.H. and Lin, S.F., 2014. Effects of the mTOR inhibitor rapamycin on monocyte-secreted chemokines. *BMC immunology*, *15*, pp.1-9.

Lin, Y.T., Wuopio, J., Larsson, A., Malinovschi, A., Feldreich, T., Engström, G., Fall, T. and Ärnlöv, J., 2024. The association between novel urinary kidney damage biomarkers and coronary atherosclerosis in an apparently healthy population. *Scientific Reports*, *14*(1), p.29215.

Lindblom, P., Gerhardt, H., Liebner, S., Abramsson, A., Enge, M., Hellström, M., Bäckström, G., Fredriksson, S., Landegren, U., Nyström, H.C. and Bergström, G., 2003. Endothelial PDGF-B retention is required for proper investment of pericytes in the microvessel wall. *Genes & development*, *17*(15), pp.1835-1840.

Linke, M., Fritsch, S.D., Sukhbaatar, N., Hengstschläger, M. and Weichhart, T., 2017. mTORC 1 and mTORC 2 as regulators of cell metabolism in immunity. *FEBS letters*, *591*(19), pp.3089-3103.

Liossis, S.N.C. and Sfikakis, P.P., 2008. Rituximab-induced B cell depletion in autoimmune diseases: potential effects on T cells. *Clinical immunology*, *127*(3), pp.280-285.

Liu, Y., Aryee, M.J., Padyukov, L., Fallin, M.D., Hesselberg, E., Runarsson, A., Reinius, L., Acevedo, N., Taub, M., Ronninger, M. and Shchetynsky, K., 2013. Epigenome-wide association data implicate DNA methylation as an intermediary of genetic risk in rheumatoid arthritis. *Nature biotechnology*, *31*(2), pp.142-147.

Liu, Q.K., 2024. Mechanisms of action and therapeutic applications of GLP-1 and dual GIP/GLP-1 receptor agonists. *Frontiers in Endocrinology*, *15*, p.1431292.

Liuzzo, G., Goronzy, J.J., Yang, H., Kopecky, S.L., Holmes, D.R., Frye, R.L. and Weyand, C.M., 2000. Monoclonal T-cell proliferation and plaque instability in acute coronary syndromes. *Circulation*, *101*(25), pp.2883-2888.

Lliso-Ribera, G., Humby, F., Lewis, M., Nerviani, A., Mauro, D., Rivellese, F., Kelly, S., Hands, R., Bene, F., Ramamoorthi, N. and Hackney, J.A., 2019. Synovial tissue signatures enhance clinical classification and prognostic/treatment response algorithms in early inflammatory arthritis and predict requirement for subsequent biological therapy: results from the pathobiology of early arthritis cohort (PEAC). *Annals of the rheumatic diseases*, *78*(12), pp.1642-1652.

López-Bravo, M., de la Escalera, M.M., Domínguez, P.M., González-Cintado, L., del Fresno, C., Martín, P., del Hoyo, G.M. and Ardavín, C., 2013. IL-4 blocks TH1-polarizing/inflammatory cytokine gene expression during monocyte-derived dendritic cell differentiation through histone hypoacetylation. *Journal of allergy and clinical immunology*, *132*(6), pp.1409-1419.

Lopez-Longo, F J, S Sanchez-Ramon, and L Carreno. 2009. "The Value of Anti-Cyclic Citrullinated Peptide Antibodies in Rheumatoid Arthritis: Do They Imply New Risk Factors?" *Drug News Perspect* 22(9): 543–48.

Lopez-Oliva, I., Paropkari, A.D., Saraswat, S., Serban, S., Yonel, Z., Sharma, P., de Pablo, P., Raza, K., Filer, A., Chapple, I. and Dietrich, T., 2018. Dysbiotic subgingival microbial communities in periodontally healthy patients with rheumatoid arthritis. *Arthritis & Rheumatology*, *70*(7), pp.1008-1013.

Low, A.S., Symmons, D.P., Lunt, M., Mercer, L.K., Gale, C.P., Watson, K.D., Dixon, W.G. and Hyrich, K.L., 2017. Relationship between exposure to tumour necrosis factor inhibitor therapy and incidence and severity of myocardial infarction in patients with rheumatoid arthritis. *Annals of the rheumatic diseases*, *76*(4), pp.654-660.

Lu, B., Rho, Y.H., Cui, J., Iannaccone, C.K., Frits, M.L., Karlson, E.W. and Shadick, N.A., 2014. Associations of smoking and alcohol consumption with disease activity and functional status in rheumatoid arthritis. *The Journal of rheumatology*, *41*(1), pp.24-30.

Lu, B., Solomon, D.H., Costenbader, K.H. and Karlson, E.W., 2014. Alcohol consumption and risk of incident rheumatoid arthritis in women: a prospective study. *Arthritis & rheumatology*, *66*(8), pp.1998-2005.

Lübbers, J., van Beers-Tas, M.H., Vosslamber, S., Turk, S.A., de Ridder, S., Mantel, E., Wesseling, J.G., Reijm, M., van Hoogstraten, I.M., Bijlsma, J.W. and van Schaardenburg, D., 2016. Changes in peripheral blood lymphocyte subsets during arthritis development in arthralgia patients. *Arthritis research & therapy*, *18*, pp.1-10.

Lubberts, E., Koenders, M.I. and van den Berg, W.B., 2004. The role of T cell interleukin-17 in conducting destructive arthritis: lessons from animal models. *Arthritis Res Ther*, *7*, pp.1-9.

Lubberts, E. and van den Berg, W.B., 2013. Cytokines in the pathogenesis of rheumatoid arthritis and collagen-induced arthritis. *Madame Curie Bioscience Database [Internet]*.

Lun, A.T., Riesenfeld, S., Andrews, T., Dao, T.P., Gomes, T., Participants in the 1st Human Cell Atlas Jamboree and Marioni, J.C., 2019. EmptyDrops: distinguishing cells from empty droplets in droplet-based single-cell RNA sequencing data. *Genome biology*, *20*, pp.1-9.

Lundkvist J, Kastäng F, Kobelt G. The burden of rheumatoid arthritis and access to treatment: health burden and costs. Eur J Health Econ. 2008 Jan;8 Suppl 2:S49-60. doi: 10.1007/s10198-007-0088-8. PMID: 18157732.

Luo, Q., Xiao, P., Li, X., Deng, Z., Qing, C., Su, R., Xu, J., Guo, Y., Huang, Z. and Li, J., 2018. Overexpression of CD64 on CD14++ CD16-and CD14++ CD16+ monocytes of rheumatoid arthritis patients correlates with disease activity. *Experimental and therapeutic medicine*, *16*(3), pp.2703-2711.

Ma, X. and Xu, S., 2013. TNF inhibitor therapy for rheumatoid arthritis. *Biomedical reports*, *1*(2), pp.177-184.

Ma, J., Zhu, C., Ma, B., Tian, J., Baidoo, S.E., Mao, C., Wu, W., Chen, J., Tong, J., Yang, M. and Jiao, Z., 2012. Increased frequency of circulating follicular helper T cells in patients with rheumatoid arthritis. *Journal of Immunology Research*, *2012*(1), p.827480.

MacGregor, A.J., Snieder, H., Rigby, A.S., Koskenvuo, M., Kaprio, J., Aho, K. and Silman, A.J., 2000. Characterizing the quantitative genetic contribution to rheumatoid arthritis using data from twins. *Arthritis & Rheumatism: Official Journal of the American College of Rheumatology*, *43*(1), pp.30-37.

Machold, K.P., Stamm, T.A., Nell, V.P.K., Pflugbeil, S., Aletaha, D., Steiner, G., Uffmann, M. and Smolen, J.S., 2007. Very recent onset rheumatoid arthritis: clinical and serological patient characteristics associated with radiographic progression over the first years of disease. *Rheumatology*, *46*(2), pp.342-349.

Madarampalli, B., Watts, G.F., Panipinto, P.M., Nguygen, H.N., Brenner, M.B. and Noss, E.H., 2019. Interactions between cadherin-11 and platelet-derived growth factor receptor-alpha signaling link cell adhesion and proliferation. *Biochimica et Biophysica Acta (BBA)-Molecular Basis of Disease*, *1865*(6), pp.1516-1524.

Majka, D.S., Vu, T.H.T., Pope, R.M., Teodorescu, M., Karlson, E.W., Liu, K. and Chang, R.W., 2017. Association of rheumatoid factors with subclinical and clinical atherosclerosis in African American women: the multiethnic study of atherosclerosis. *Arthritis Care & Research*, *69*(2), pp.166-174.

Maracle, C.X., Kucharzewska, P., Helder, B., van der Horst, C., Correa de Sampaio, P., Noort, A.R., van Zoest, K., Griffioen, A.W., Olsson, H. and Tas, S.W., 2017. Targeting non-canonical nuclear factor-κB signaling attenuates neovascularization in a novel 3D model of rheumatoid arthritis synovial angiogenesis. *Rheumatology*, *56*(2), pp.294-302.

Maradit-Kremers, H., Nicola, P.J., Crowson, C.S., Ballman, K.V. and Gabriel, S.E. (2005), Cardiovascular death in rheumatoid arthritis: A population-based study. Arthritis & Rheumatism, 52: 722-732.

Marie, J.C., Letterio, J.J., Gavin, M. and Rudensky, A.Y., 2005. TGF-β1 maintains suppressor function and Foxp3 expression in CD4+ CD25+ regulatory T cells. *The Journal of experimental medicine*, *201*(7), pp.1061-1067.

Markham, T., Mullan, R., Golden-Mason, L., Rogers, S., Bresnihan, B., FitzGerald, O., Fearon, U. and Veale, D.J., 2006. Resolution of endothelial activation and down-regulation of Tie2 receptor in psoriatic skin after infliximab therapy. *Journal of the American Academy of Dermatology*, *54*(6), pp.1003-1012.

Marsh, L.J., Kemble, S., Reis Nisa, P., Singh, R. and Croft, A.P., 2021. Fibroblast pathology in inflammatory joint disease. *Immunological reviews*, *302*(1), pp.163-183.

Martel-Pelletier, J., Boileau, C., Pelletier, J.P. and Roughley, P.J., 2008. Cartilage in normal and osteoarthritis conditions. *Best practice & research Clinical rheumatology*, *22*(2), pp.351-384.

Marzaioli, V., Canavan, M., Floudas, A., Flynn, K., Mullan, R., Veale, D.J. and Fearon, U., 2022. CD209/CD14+ dendritic cells characterization in rheumatoid and psoriatic arthritis patients: activation, synovial infiltration, and therapeutic targeting. *Frontiers in Immunology*, *12*, p.722349.

Marzaioli, V., Hurtado-Nedelec, M., Pintard, C., Tlili, A., Marie, J.C., Monteiro, R.C., Gougerot-Pocidalo, M.A., Dang, P.M.C. and El-Benna, J., 2017. NOX5 and p22phox are 2 novel regulators of human monocytic differentiation into dendritic cells. *Blood, The Journal of the American Society of Hematology*, *130*(15), pp.1734-1745.

Marzaioli, V., Canavan, M., Floudas, A., Wade, S.C., Low, C., Veale, D.J. and Fearon, U., 2020. Monocyte-derived dendritic cell differentiation in inflammatory arthritis is regulated by the JAK/STAT axis via NADPH oxidase regulation. *Frontiers in Immunology*, *11*, p.1406.

Masdottir, B., Jonsson, T., Manfreðsdóttir, V., Víkingsson, A., Brekkan, Á. and Valdimarsson, H., 2000. Smoking, rheumatoid factor isotypes and severity of rheumatoid arthritis. *Rheumatology*, *39*(11), pp.1202-1205.

Mason, U., Aldrich, J., Breedveld, F., Davis, C.B., Elliott, M., Jackson, M., Jorgensen, C., Keystone, E., Levy, R., Tesser, J. and Totoritis, M., 2002. CD4 coating, but not CD4 depletion, is a predictor of efficacy with primatised monoclonal anti-CD4 treatment of active rheumatoid arthritis. *The Journal of Rheumatology*, *29*(2), pp.220-229.

Masopust, D. and Soerens, A.G., 2019. Tissue-resident T cells and other resident leukocytes. *Annual review of immunology*, *37*(1), pp.521-546.

Mathis, D. and Shoelson, S.E., 2011. Immunometabolism: an emerging frontier. *Nature Reviews. Immunology*, *11*(2), p.81.

Maxwell, J.R., Gowers, I.R., Moore, D.J. and Wilson, A.G., 2010. Alcohol consumption is inversely associated with risk and severity of rheumatoid arthritis. *Rheumatology*, *49*(11), pp.2140-2146.

McGarry, T. and Fearon, U., 2019. Cell metabolism as a potentially targetable pathway in RA. *Nature Reviews Rheumatology*, *15*(2), pp.70-72.

McGarry, T., Biniecka, M., Gao, W., Cluxton, D., Canavan, M., Wade, S., Wade, S., Gallagher, L., Orr, C., Veale, D.J. and Fearon, U., 2017. Resolution of TLR2-induced inflammation through manipulation of metabolic pathways in rheumatoid arthritis. *Scientific reports*, *7*(1), p.43165.

McGarry, T., Biniecka, M., Veale, D.J. and Fearon, U., 2018. Hypoxia, oxidative stress and inflammation. *Free Radical Biology and Medicine*, *125*, pp.15-24.

McGarry, T., Hanlon, M.M., Marzaioli, V., Cunningham, C.C., Krishna, V., Murray, K., Hurson, C., Gallagher, P., Nagpal, S., Veale, D.J. and Fearon, U., 2021. Rheumatoid arthritis CD14+ monocytes display metabolic and inflammatory dysfunction, a phenotype that precedes clinical manifestation of disease. *Clinical & translational immunology*, *10*(1), p.e1237.

McGarry, T., Orr, C., Wade, S., Biniecka, M., Wade, S., Gallagher, L., Low, C., Veale, D.J. and Fearon, U., 2018. JAK/STAT blockade alters synovial bioenergetics, mitochondrial function, and proinflammatory mediators in rheumatoid arthritis. *Arthritis & Rheumatology*, *70*(12), pp.1959-1970.

McGarry, T., Veale, D.J., Gao, W., Orr, C., Fearon, U. and Connolly, M., 2015. Toll-like receptor 2 (TLR2) induces migration and invasive mechanisms in rheumatoid arthritis. *Arthritis research & therapy*, *17*, pp.1-14.

McGettrick, A.F. and O'Neill, L.A., 2013. How metabolism generates signals during innate immunity and inflammation. *Journal of Biological Chemistry*, *288*(32), pp.22893-22898.

McGinnis, C.S., Murrow, L.M. and Gartner, Z.J., 2019. DoubletFinder: doublet detection in single-cell RNA sequencing data using artificial nearest neighbors. *Cell systems*, *8*(4), pp.329-337.

McInnes, I.B. and Schett, G., 2007. Cytokines in the pathogenesis of rheumatoid arthritis. *Nature Reviews Immunology*, *7*(6), pp.429-442.

McInnes, I.B. and Schett, G., 2011. The pathogenesis of rheumatoid arthritis. *New England Journal of Medicine*, *365*(23), pp.2205-2219.

McInnes, I.B., Buckley, C.D. and Isaacs, J.D., 2016. Cytokines in rheumatoid arthritis—shaping the immunological landscape. *Nature Reviews Rheumatology*, *12*(1), pp.63-68.

McKellar, G. *et al.* (2007) 'A pilot study of a Mediterranean-type diet intervention in female patients with rheumatoid arthritis living in areas of social deprivation in Glasgow', *Annals of the Rheumatic Diseases*, 66(9), pp. 1239–1243. doi: 10.1136/ard.2006.065151.

McKinney, C., Merriman, M.E., Chapman, P.T., Gow, P.J., Harrison, A.A., Highton, J., Jones, P.B., McLean, L., O'Donnell, J.L., Pokorny, V. and Spellerberg, M., 2008. Evidence for an influence of chemokine ligand 3-like 1 (CCL3L1) gene copy number on susceptibility to rheumatoid arthritis. *Annals of the rheumatic diseases*, *67*(3), pp.409-413.

McLachlan, R.W. and Yap, A.S., 2007. Not so simple: the complexity of phosphotyrosine signaling at cadherin adhesive contacts. *Journal of Molecular Medicine*, *85*, pp.545-554.

Medić, B., Rovčanin, B., Basta Jovanović, G., Radojević-Škodrić, S. and Prostran, M., 2015. Kidney injury molecule-1 and cardiovascular diseases: from basic science to clinical practice. *BioMed Research International*, *2015*(1), p.854070.

Metallo, C.M. and Vander Heiden, M.G., 2013. Understanding metabolic regulation and its influence on cell physiology. *Molecular cell*, *49*(3), pp.388-398.

Meyer, P.W., Anderson, R., Ker, J.A. and Ally, M.T., 2018. Rheumatoid arthritis and risk of cardiovascular disease. *Cardiovascular journal of Africa*, *29*(5), pp.317-321.

Meyer, O., Labarre, C., Dougados, M., Goupille, P., Cantagrel, A., Dubois, A., Nicaise-Roland, P., Sibilia, J. and Combe, B., 2003. Anticitrullinated protein/peptide antibody assays in early rheumatoid arthritis for predicting five year radiographic damage. *Annals of the rheumatic diseases*, *62*(2), pp.120-126.

Meyer, P.W., Anderson, R., Ker, J.A. and Ally, M.T., 2018. Rheumatoid arthritis and risk of cardiovascular disease. *Cardiovascular journal of Africa*, *29*(5), pp.317-321.

Micha, R., Imamura, F., von Ballmoos, M.W., Solomon, D.H., Hernán, M.A., Ridker, P.M. and Mozaffarian, D., 2011. Systematic review and meta-analysis of methotrexate use and risk of cardiovascular disease. *The American journal of cardiology*, *108*(9), pp.1362-1370.

Michaud, K., Messer, J., Choi, H.K. and Wolfe, F., 2003. Direct medical costs and their predictors in patients with rheumatoid arthritis: a three-year study of 7,527 patients. *Arthritis & Rheumatism*, *48*(10), pp.2750-2762.

Michaud, K. and Wolfe, F., 2007. Comorbidities in rheumatoid arthritis. *Best practice & research Clinical rheumatology*, *21*(5), pp.885-906.

Micheroli, R., Elhai, M., Edalat, S., Frank-Bertoncelj, M., Bürki, K., Ciurea, A., MacDonald, L., Kurowska-Stolarska, M., Lewis, M.J., Goldmann, K. and Cubuk, C., 2022. Role of synovial fibroblast subsets across synovial pathotypes in rheumatoid arthritis: a deconvolution analysis. *RMD open*, *8*(1), p.e001949.

Michopoulos, F., Karagianni, N., Whalley, N.M., Firth, M.A., Nikolaou, C., Wilson, I.D., Critchlow, S.E., Kollias, G. and Theodoridis, G.A., 2016. Targeted metabolic profiling of the Tg197 mouse model reveals itaconic acid as a marker of rheumatoid arthritis. *Journal of proteome research*, *15*(12), pp.4579-4590.

Middleton, J., Neil, S., Wintle, J., Clark-Lewis, I., Moore, H., Lam, C., Auer, M., Hub, E. and Rot, A., 1997. Transcytosis and surface presentation of IL-8 by venular endothelial cells. *Cell*, *91*(3), pp.385-395.

Mihara, M., Ohsugi, Y. and Kishimoto, T., 2011. Tocilizumab, a humanised anti-interleukin-6 receptor antibody, for treatment of rheumatoid arthritis. *Open access rheumatology: research and reviews*, pp.19-29.

Miller, H., Neovius, M., Askling, J. and Bruze, G., 2024. Impact of incident rheumatoid arthritis on earnings: a nationwide sibling comparison study. *Rheumatology*, p.keae535.

Mills, E.L., Kelly, B., Logan, A., Costa, A.S., Varma, M., Bryant, C.E., Tourlomousis, P., Däbritz, J.H.M., Gottlieb, E., Latorre, I. and Corr, S.C., 2016. Succinate dehydrogenase supports metabolic repurposing of mitochondria to drive inflammatory macrophages. *Cell*, *167*(2), pp.457-470.

Mills, E.L., Ryan, D.G., Prag, H.A., Dikovskaya, D., Menon, D., Zaslona, Z., Jedrychowski, M.P., Costa, A.S., Higgins, M., Hams, E. and Szpyt, J., 2018. Itaconate is an anti-inflammatory metabolite that activates Nrf2 via alkylation of KEAP1. *Nature*, *556*(7699), pp.113-117.

Miossec, P., Korn, T. and Kuchroo, V.K., 2009. Interleukin-17 and type 17 helper T cells. *New England Journal of Medicine*, *361*(9), pp.888-898.

Miranda, L.C., Santos, H., Ferreira, J., Coelho, P., Silva, C. and Saraiva-Ribeiro, J., 2012. Finding rheumatoid arthritis impact on life (frail study): economic burden. *Acta Reumatol Port*, *37*(2), pp.134-42.

Misharin, A.V., Cuda, C.M., Saber, R., Turner, J.D., Gierut, A.K., Haines, G.K., Berdnikovs, S., Filer, A., Clark, A.R., Buckley, C.D. and Mutlu, G.M., 2014. Nonclassical Ly6C− monocytes drive the development of inflammatory arthritis in mice. *Cell reports*, *9*(2), pp.591-604.

Misra, S., Bagchi, A., Sarkar, A., Niyogi, S., Bhattacharjee, D., Chatterjee, S., Mondal, S., Chattopadhyay, A., Saha, A., Chatterjee, S. and Sinhamahapatra, P., 2021. Methotrexate and theaflavin-3, 3′-digallate synergistically restore the balance between apoptosis and autophagy in synovial fibroblast of RA: an ex vivo approach with cultured human RA FLS. *Inflammopharmacology*, *29*, pp.1427-1442.

Mitchell, D.M. and Fries, J.F., 1982. An analysis of the American Rheumatism Association criteria for rheumatoid arthritis. *Arthritis & Rheumatism: Official Journal of the American College of Rheumatology*, *25*(5), pp.481-487.

Mizoguchi, F., Slowikowski, K., Wei, K., Marshall, J.L., Rao, D.A., Chang, S.K., Nguyen, H.N., Noss, E.H., Turner, J.D., Earp, B.E. and Blazar, P.E., 2018. Functionally distinct disease-associated fibroblast subsets in rheumatoid arthritis. *Nature communications*, *9*(1), p.789.

Mok, C.C., 2014. Rituximab for the treatment of rheumatoid arthritis: an update. *Drug design, development and therapy*, pp.87-100.

Moon, J.S., Younis, S., Ramadoss, N.S., Iyer, R., Sheth, K., Sharpe, O., Rao, N.L., Becart, S., Carman, J.A., James, E.A. and Buckner, J.H., 2023. Cytotoxic CD8+ T cells target citrullinated antigens in rheumatoid arthritis. *Nature communications*, *14*(1), p.319.

Mor, A., Abramson, S.B. and Pillinger, M.H., 2005. The fibroblast-like synovial cell in rheumatoid arthritis: a key player in inflammation and joint destruction. *Clinical immunology*, *115*(2), pp.118-128.

Morales-Ducret J, Wayner E, Elices MJ, Alvaro-Gracia JM, Zvaifler NJ, Firestein GS. Alpha 4/beta 1 integrin (VLA-4) ligands in arthritis. Vascular cell adhesion molecule-1 expression in synovium and on fibroblast-like synoviocytes. J Immunol. 1992 Aug 15;149(4):1424-31. PMID: 1380043.

Moran, S.T., Cariappa, A., Liu, H., Muir, B., Sgroi, D., Boboila, C. and Pillai, S., 2007. Synergism between NF-κB1/p50 and Notch2 during the development of marginal zone B lymphocytes. *The Journal of Immunology*, *179*(1), pp.195-200.

Moret, F.M., Hack, C.E., van der Wurff-Jacobs, K.M., de Jager, W., Radstake, T.R., Lafeber, F.P. and van Roon, J.A., 2013. Intra-articular CD1c-expressing myeloid dendritic cells from rheumatoid arthritis patients express a unique set of T cell-attracting chemokines and spontaneously induce Th1, Th17 and Th2 cell activity. *Arthritis research & therapy*, *15*, pp.1-10.

Moss, S.C., Lightell, D.J., Marx, S.O., Marks, A.R. and Woods, T.C., 2010. Rapamycin regulates endothelial cell migration through regulation of the cyclin-dependent kinase inhibitor p27Kip1. *Journal of Biological Chemistry*, *285*(16), pp.11991-11997.

Mulherin, D., Fitzgerald, O. and Bresnihan, B., 1996. Synovial tissue macrophage populations and articular damage in rheumatoid arthritis. *Arthritis & Rheumatism: Official Journal of the American College of Rheumatology*, *39*(1), pp.115-124.

Mulherin, D.M., Veale, D.J., Belch, J.J.F., Bresnihan, B. and Fitzgerald, O., 1996. Adhesion molecule in untreated inflammatory arthritis. *QJM: An International Journal of Medicine*, *89*(3), pp.195-204.

Mullan, R.H., Matthews, C., Bresnihan, B., FitzGerald, O., King, L., Poole, A.R., Fearon, U. and Veale, D.J., 2007. Early changes in serum type II collagen biomarkers predict radiographic progression at one year in inflammatory arthritis patients after biologic therapy. *Arthritis & Rheumatism: Official Journal of the American College of Rheumatology*, *56*(9), pp.2919-2928.

Mullan, R.H., Bresnihan, B., Golden-Mason, L., Markham, T., O'Hara, R., FitzGerald, O., Veale, D.J. and Fearon, U., 2006. Acute-phase serum amyloid A stimulation of angiogenesis, leukocyte recruitment, and matrix degradation in rheumatoid arthritis through an NF-κB–dependent signal transduction pathway. *Arthritis & Rheumatism: Official Journal of the American College of Rheumatology*, *54*(1), pp.105-114.

Mullan, R.H., McCormick, J., Connolly, M., Bresnihan, B., Veale, D.J. and Fearon, U., 2010. A role for the high-density lipoprotein receptor SR-B1 in synovial inflammation via serum amyloid-A. *The American journal of pathology*, *176*(4), pp.1999-2008.

Müller-Ladner, U., Kriegsmann, J., Franklin, B.N., Matsumoto, S., Geiler, T., Gay, R.E. and Gay, S., 1996. Synovial fibroblasts of patients with rheumatoid arthritis attach to and invade normal human cartilage when engrafted into SCID mice. *The American journal of pathology*, *149*(5), p.1607.

Murayama, M.A., Shimizu, J., Miyabe, C., Yudo, K. and Miyabe, Y., 2023. Chemokines and chemokine receptors as promising targets in rheumatoid arthritis. *Frontiers in Immunology*, *14*, p.1100869.

Murray, K., Moore, L., McAuliffe, F. and Veale, D.J., 2019. Reproductive health outcomes in women with psoriatic arthritis. *Annals of the Rheumatic Diseases*, *78*(6), pp.850-852.

Murray, K., Turk, M., Alammari, Y., Young, F., Gallagher, P., Saber, T., Fearon, U. and Veale, D.J., 2021. Long-term remission and biologic persistence rates: 12-year real-world data. *Arthritis research & therapy*, *23*, pp.1-10.

Mutunga, M., Fulton, B., Bullock, R., Batchelor, A., Gascoigne, A., Gillespie, J.I. and Baudouin, S.V., 2001. Circulating endothelial cells in patients with septic shock. *American journal of respiratory and critical care medicine*, *163*(1), pp.195-200.

Nakatani, T., Tsujimoto, K., Park, J., Jo, T., Kimura, T., Hayama, Y., Konaka, H., Morita, T., Kato, Y., Nishide, M. and Koyama, S., 2021. The lysosomal Ragulator complex plays an essential role in leukocyte trafficking by activating myosin II. *Nature communications*, *12*(1), p.3333.

Nam, J.L., Hensor, E.M., Hunt, L., Conaghan, P.G., Wakefield, R.J. and Emery, P., 2016. Ultrasound findings predict progression to inflammatory arthritis in anti-CCP antibody-positive patients without clinical synovitis. *Annals of the rheumatic diseases*, *75*(12), pp.2060-2067.

Nam JL, Ramiro S, Gaujoux-Viala C, Takase K, Leon-Garcia M, Emery P, Gossec L, Landewe R, Smolen JS, Buch MH. Efficacy of biological disease-modifying antirheumatic drugs: a systematic literature review informing the 2013 update of the EULAR recommendations for the management of rheumatoid arthritis. Ann Rheum Dis. 2014 Mar;73(3):516-28. doi: 10.1136/annrheumdis-2013-204577.

Nanki, T., Nagasaka, K., Hayashida, K., Saita, Y. and Miyasaka, N., 2001. Chemokines regulate IL-6 and IL-8 production by fibroblast-like synoviocytes from patients with rheumatoid arthritis. *The Journal of Immunology*, *167*(9), pp.5381-5385.

Naranjo, A., Sokka, T., Descalzo, M.A., Calvo-Alén, J., Hørslev-Petersen, K., Luukkainen, R.K., Combe, B., Burmester, G.R., Devlin, J., Ferraccioli, G. and Morelli, A., 2008. Cardiovascular disease in patients with rheumatoid arthritis: results from the QUEST-RA study. *Arthritis research & therapy*, *10*, pp.1-10.

Nash, P., Coates, L.C., Kivitz, A.J., Mease, P.J., Gladman, D.D., Covarrubias-Cobos, J.A., FitzGerald, O., Fleishaker, D., Wang, C., Wu, J. and Hsu, M.A., 2020. Safety and efficacy of tofacitinib in patients with active psoriatic arthritis: interim analysis of OPAL balance, an open-label, long-term extension study. *Rheumatology and therapy*, *7*, pp.553-580.

Naughton, D., Whelan, M., Smith, E.C., Williams, R., Blake, D.R. and Grootveld, M., 1993. An investigation of the abnormal metabolic status of synovial fluid from patients with rheumatoid arthritis by high field proton nuclear magnetic resonance spectroscopy. *FEBS letters*, *317*(1-2), pp.135-138.

Nell, V.P.K., Machold, K.P., Eberl, G., Stamm, T.A., Uffmann, M. and Smolen, J.S., 2004. Benefit of very early referral and very early therapy with disease-modifying anti-rheumatic drugs in patients with early rheumatoid arthritis. *Rheumatology*, *43*(7), pp.906-914.

Nepom, G.T., Hansen, J.A. and Nepom, B.S., 1987. The molecular basis for HLA class II associations with rheumatoid arthritis. *Journal of clinical immunology*, *7*, pp.1-7.

Nerviani, A., Di Cicco, M., Mahto, A., Lliso-Ribera, G., Rivellese, F., Thorborn, G., Hands, R., Bellan, M., Mauro, D., Boutet, M.A. and Giorli, G., 2020. A pauci-immune synovial pathotype predicts inadequate response to TNFα-blockade in rheumatoid arthritis patients. *Frontiers in immunology*, *11*, p.845.

Newkirk, M.M., Goldbach-Mansky, R., Senior, B.W., Klippel, J., Schumacher Jr, H.R. and El-Gabalawy, H.S., 2005. Elevated levels of IgM and IgA antibodies to Proteus mirabilis and IgM antibodies to Escherichia coli are associated with early rheumatoid factor (RF)-positive rheumatoid arthritis. *Rheumatology*, *44*(11), pp.1433-1441.

Ng, C.T., Biniecka, M., Kennedy, A., McCormick, J., Fitzgerald, O., Bresnihan, B., Buggy, D., Taylor, C.T., O'sullivan, J., Fearon, U. and Veale, D.J., 2010. Synovial tissue hypoxia and inflammation in vivo. *Annals of the rheumatic diseases*, *69*(7), pp.1389-1395.

Nielen, Markus M J et al. 2004. "Specific Autoantibodies Precede the Symptoms of Rheumatoid Arthritis: A Study of Serial Measurements in Blood Donors." *Arthritis & Rheumatism* 50(2): 380–86.

Nikiphorou, E., Negoescu, A., Fitzpatrick, J.D., Goudie, C.T., Badcock, A., Östör, A.J. and Malaviya, A.P., 2014. Indispensable or intolerable? Methotrexate in patients with rheumatoid and psoriatic arthritis: a retrospective review of discontinuation rates from a large UK cohort. *Clinical rheumatology*, *33*, pp.609-614.

Nishimura, K et al. 2007. "Meta-Analysis: Diagnostic Accuracy of Anti-Cyclic Citrullinated Peptide Antibody and Rheumatoid Factor for Rheumatoid Arthritis." *Ann Intern Med* 146(11): 797–808.

Noss, E.H., Chang, S.K., Watts, G.F. and Brenner, M.B., 2011. Cadherin-11 engagement modulates matrix metalloproteinase production by rheumatoid arthritis synovial fibroblasts. *Arthritis and rheumatism*, *63*(12), p.3768.

O'Brien, A., Hanlon, M.M., Marzaioli, V., Wade, S.C., Flynn, K., Fearon, U. and Veale, D.J., 2021. Targeting JAK-STAT signaling alters PsA synovial fibroblast pro-inflammatory and metabolic function. *Frontiers in Immunology*, *12*, p.672461.

O'Connor, P.A.T.R.I.C.I.A., Orford, C.R. and Gardner, D.L., 1988. Differential response to compressive loads of zones of canine hyaline articular cartilage: micromechanical, light and electron microscopic studies. *Annals of the rheumatic diseases*, *47*(5), pp.414-420.

Ogawa, T., Nikawa, T., Furochi, H., Kosyoji, M., Hirasaka, K., Suzue, N., Sairyo, K., Nakano, S., Yamaoka, T., Itakura, M. and Kishi, K., 2005. Osteoactivin upregulates expression of MMP-3 and MMP-9 in fibroblasts infiltrated into denervated skeletal muscle in mice. *American Journal of Physiology-Cell Physiology*, *289*(3), pp.C697-C707.

Ogrendik, M., 2009. Rheumatoid arthritis is linked to oral bacteria: etiological association. *Modern rheumatology*, *19*(5), pp.453-456.

O'Hara, R., Murphy, E.P., Whitehead, A.S., FitzGerald, O. and Bresnihan, B., 2004. Local expression of the serum amyloid A and formyl peptide receptor–like 1 genes in synovial tissue is associated with matrix metalloproteinase production in patients with inflammatory arthritis. *Arthritis & Rheumatism: Official Journal of the American College of Rheumatology*, *50*(6), pp.1788-1799.

Oliver, J.E. and Silman, A.J., 2009. Why are women predisposed to autoimmune rheumatic diseases?. *Arthritis research & therapy*, *11*, pp.1-9.

Onderdijk, A.J., Baerveldt, E.M., Kurek, D., Kant, M., Florencia, E.F., Debets, R. and Prens, E.P., 2015. IL-4 downregulates IL-1β and IL-6 and induces GATA3 in psoriatic epidermal cells: route of action of a Th2 cytokine. *The Journal of Immunology*, *195*(4), pp.1744-1752.

O'Neill, L.A., Kishton, R.J. and Rathmell, J., 2016. A guide to immunometabolism for immunologists. *Nature reviews immunology*, *16*(9), pp.553-565.

Orange, D.E., Yao, V., Sawicka, K., Fak, J., Frank, M.O., Parveen, S., Blachere, N.E., Hale, C., Zhang, F., Raychaudhuri, S. and Troyanskaya, O.G., 2020. RNA identification of PRIME cells predicting rheumatoid arthritis flares. *New England Journal of Medicine*, *383*(3), pp.218-228.

Orr, C. *et al.* (2017) 'Synovial tissue research: A state-of-the-art review', *Nature Reviews Rheumatology*. Nature Publishing Group, 13(8), pp. 463–475. doi: 10.1038/nrrheum.2017.115.

Orr, C., Najm, A., Biniecka, M., McGarry, T., Ng, C.T., Young, F., Fearon, U. and Veale, D.J., 2017. Synovial immunophenotype and anti–citrullinated peptide antibodies in rheumatoid arthritis patients: relationship to treatment response and radiologic prognosis. *Arthritis & Rheumatology*, *69*(11), pp.2114-2123.

O'shea, J.J., Laurence, A. and McInnes, I.B., 2013. Back to the future: oral targeted therapy for RA and other autoimmune diseases. *Nature Reviews Rheumatology*, *9*(3), pp.173-182.

Osipo, C., Golde, T.E., Osborne, B.A. and Miele, L.A., 2008. Off the beaten pathway: the complex cross talk between Notch and NF-κB. *Laboratory investigation*, *88*(1), pp.11-17.

Ospelt, C., Neidhart, M., Gay, R.E. and Gay, S., 2004. Synovial activation in rheumatoid arthritis. *Front Biosci*, *9*(2323), p.34.

Ospelt, C. and Frank-Bertoncelj, M., 2017. Why location matters—site-specific factors in rheumatic diseases. *Nature reviews Rheumatology*, *13*(7), pp.433-442.

Ospelt, C., 2017. Synovial fibroblasts in 2017. *RMD open*, *3*(2), p.e000471.

Ospelt, C., Brentano, F., Rengel, Y., Stanczyk, J., Kolling, C., Tak, P.P., Gay, R.E., Gay, S. and Kyburz, D., 2008. Overexpression of toll-like receptors 3 and 4 in synovial tissue from patients with early rheumatoid arthritis: toll-like receptor expression in early and longstanding arthritis. *Arthritis & Rheumatism: Official Journal of the American College of Rheumatology*, *58*(12), pp.3684-3692.

Otero, M., Lago, R., Gomez, R., Lago, F., Dieguez, C., Gomez-Reino, J.J. and Gualillo, O., 2006. Changes in plasma levels of fat-derived hormones adiponectin, leptin, resistin and visfatin in patients with rheumatoid arthritis. *Annals of the rheumatic diseases*, *65*(9), pp.1198-1201.

Padyukov, L., Seielstad, M., Ong, R.T., Ding, B., Rönnelid, J., Seddighzadeh, M., Alfredsson, L., Klareskog, L. and Epidemiological Investigation of Rheumatoid Arthritis (EIRA) study group, 2011. A genome-wide association study suggests contrasting associations in ACPA-positive versus ACPA-negative rheumatoid arthritis. *Annals of the rheumatic diseases*, *70*(2), pp.259-265.

Pahor, A., Hojs, R., Gorenjak, M. and Rozman, B., 2006. Accelerated atherosclerosis in pre-menopausal female patients with rheumatoid arthritis. *Rheumatology international*, *27*, pp.119-123.

Palsson-McDermott, E.M. and O'neill, L.A., 2013. The Warburg effect then and now: from cancer to inflammatory diseases. *Bioessays*, *35*(11), pp.965-973.

Panchagnula, R., Rajiv, S.R., Prakash, J., Chandrashekara, S. and Suresh, K.P., 2006. Role of anticyclic citrullinated peptide in the diagnosis of early rheumatoid factor-negative suspected rheumatoid arthritis: is it worthwhile to order the test?. *JCR: Journal of Clinical Rheumatology*, *12*(4), pp.172-175.

Pandya, J.M., Lundell, A.C., Andersson, K., Nordström, I., Theander, E. and Rudin, A., 2017. Blood chemokine profile in untreated early rheumatoid arthritis: CXCL10 as a disease activity marker. *Arthritis research & therapy*, *19*, pp.1-12.

Pap, T. *et al.* (2000) 'Fibroblast biology. Role of synovial fibroblasts in the pathogenesis of rheumatoid arthritis.', *Arthritis research*, 2(5), pp. 361–7. doi: 10.1186/ar113.

Park, Y.J., Kim, J.Y., Park, J., Choi, J.J., Kim, W.U. and Cho, C.S., 2014. Bone erosion is associated with reduction of circulating endothelial progenitor cells and endothelial dysfunction in rheumatoid arthritis. *Arthritis & Rheumatology*, *66*(6), pp.1450-1460.

Park, Y.Y., Sohn, B.H., Johnson, R.L., Kang, M.H., Kim, S.B., Shim, J.J., Mangala, L.S., Kim, J.H., Yoo, J.E., Rodriguez-Aguayo, C. and Pradeep, S., 2016. Yes-associated protein 1 and transcriptional coactivator with PDZ-binding motif activate the mammalian target of rapamycin complex 1 pathway by regulating amino acid transporters in hepatocellular carcinoma. *Hepatology*, *63*(1), pp.159-172.

Pattison, D.J., Symmons, D.P.M., Lunt, M., Welch, A., Luben, R., Bingham, S.A., Khaw, K.-T., Day, N.E. and Silman, A.J. (2004), Dietary risk factors for the development of inflammatory polyarthritis: Evidence for a role of high level of red meat consumption. Arthritis & Rheumatism, 50: 3804-3812.

Paulissen, S.M., van Hamburg, J.P., Davelaar, N., Vroman, H., Hazes, J.M., de Jong, P.H. and Lubberts, E., 2015. CCR6+ Th cell populations distinguish ACPA positive from ACPA negative rheumatoid arthritis. *Arthritis research & therapy*, *17*, pp.1-9.

Goldbergova, M.P., Lipkova, J., Pavek, N., Gatterova, J., Vasku, A., Soucek, M. and Nemec, P., 2012. RANTES, MCP-1 chemokines and factors describing rheumatoid arthritis. *Molecular Immunology*, *52*(3-4), pp.273-278.

Pesau, G., Zierfuss, B., Hoebaus, C., Koppensteiner, R. and Schernthaner, G.H., 2024. Serum trefoil factor-3 predicts survival in peripheral artery disease. *Angiology*, p.00033197241230973.

Pessentheiner, A.R., Pelzmann, H.J., Walenta, E., Schweiger, M., Groschner, L.N., Graier, W.F., Kolb, D., Uno, K., Miyazaki, T., Nitta, A. and Rieder, D., 2013. NAT8L (N-acetyltransferase 8-like) accelerates lipid turnover and increases energy expenditure in brown adipocytes. *Journal of Biological Chemistry*, *288*(50), pp.36040-36051.

Peters, M.J.L., Symmons, D.P.M., McCarey, D., Dijkmans, B.A.C., Nicola, P.J.M.Z., Kvien, T.K., McInnes, I.B., Haentzschel, H., Gonzalez-Gay, M.A., Provan, S. and Semb, A., 2010. EULAR evidence-based recommendations for cardiovascular risk management in patients with rheumatoid arthritis and other forms of inflammatory arthritis. *Annals of the rheumatic diseases*, *69*(2), pp.325-331.

Petra CV, Albu A, Pamfil C et al (2019) The relationship between epicardial adipose tissue and arterial stiffness in patients with rheumatoid arthritis. Med Ultrason 21:427–434.

Petrasca, A., Phelan, J.J., Ansboro, S., Veale, D.J., Fearon, U. and Fletcher, J.M., 2020. Targeting bioenergetics prevents CD4 T cell–mediated activation of synovial fibroblasts in rheumatoid arthritis. *Rheumatology*, *59*(10), pp.2816-2828.

Pieper, J., Dubnovitsky, A., Gerstner, C., James, E.A., Rieck, M., Kozhukh, G., Tandre, K., Pellegrino, S., Gebe, J.A., Rönnblom, L. and Sandalova, T., 2018. Memory T cells specific to citrullinated α-enolase are enriched in the rheumatic joint. *Journal of autoimmunity*, *92*, pp.47-56.

Pierreisnard, A., Issa, N., Barnetche, T., Richez, C. and Schaeverbeke, T., 2013. Meta-analysis of clinical and radiological efficacy of biologics in rheumatoid arthritis patients naive or inadequately responsive to methotrexate. *Joint Bone Spine*, *80*(4), pp.386-392.

Pikwer, M., Bergström, U., Nilsson, J.Å., Jacobsson, L. and Turesson, C., 2012. Early menopause is an independent predictor of rheumatoid arthritis. *Annals of the rheumatic diseases*, *71*(3), pp.378-381.

Pillinger, M.H. and Abramson, S.B., 1995. The neutrophil in rheumatoid arthritis. *Rheumatic Disease Clinics of North America*, *21*(3), pp.691-714.

Pingiotti, E., Cipriani, P., Marrelli, A., Liakouli, V., Fratini, S., Penco, M. and Giacomelli, R., 2007. Surface expression of fractalkine receptor (CX3CR1) on CD4+/CD28− T cells in RA patients and correlation with atherosclerotic damage. *Annals of the New York Academy of Sciences*, *1107*(1), pp.32-41.

Pirro, V., Roth, K.D., Lin, Y., Willency, J.A., Milligan, P.L., Wilson, J.M., Ruotolo, G., Haupt, A., Newgard, C.B. and Duffin, K.L., 2022. Effects of tirzepatide, a dual GIP and GLP-1 RA, on lipid and metabolite profiles in subjects with type 2 diabetes. *The Journal of Clinical Endocrinology & Metabolism*, *107*(2), pp.363-378.

Plenge, R.M., Seielstad, M., Padyukov, L., Lee, A.T., Remmers, E.F., Ding, B., Liew, A., Khalili, H., Chandrasekaran, A., Davies, L.R. and Li, W., 2007. TRAF1–C5 as a risk locus for rheumatoid arthritis—a genomewide study. *New England Journal of Medicine*, *357*(12), pp.1199-1209.

Ponchel, F., Burska, A.N., Hunt, L., Gul, H., Rabin, T., Parmar, R., Buch, M.H., Conaghan, P.G. and Emery, P., 2020. T-cell subset abnormalities predict progression along the Inflammatory Arthritis disease continuum: implications for management. *Scientific reports*, *10*(1), p.3669.

Poon, M., Marx, S.O., Gallo, R., Badimon, J.J., Taubman, M.B. and Marks, A.R., 1996. Rapamycin inhibits vascular smooth muscle cell migration. *The Journal of clinical investigation*, *98*(10), pp.2277-2283.

Pope, J.E. and Choy, E.H., 2021, February. C-reactive protein and implications in rheumatoid arthritis and associated comorbidities. In *Seminars in arthritis and rheumatism* (Vol. 51, No. 1, pp. 219-229).

Popp, J., Schicht, M., Garreis, F., Klinger, P., Gelse, K., Sesselmann, S., Tsokos, M., Etzold, S., Stiller, D., Claassen, H. and Paulsen, F., 2019. Human synovia contains trefoil factor family (TFF) peptides 1–3 although synovial membrane only produces TFF3: Implications in osteoarthritis and rheumatoid arthritis. *International journal of molecular sciences*, *20*(23), p.6105.

Potempa, J., Mydel, P. and Koziel, J., 2017. The case for periodontitis in the pathogenesis of rheumatoid arthritis. *Nature Reviews Rheumatology*, *13*(10), pp.606-620.

Potente, M., Gerhardt, H. and Carmeliet, P., 2011. Basic and therapeutic aspects of angiogenesis. *Cell*, *146*(6), pp.873-887.

Potlabathini, T., Pothacamuri, M.A., Bandi, V.V., Anjum, M., Shah, P., Molina, M., Dutta, N., Adzhymuratov, O., Mathew, M., Sadu, V. and Zahid, S.A., 2024. FDA-approved janus kinase-signal transducer and activator of transcription (JAK-STAT) inhibitors for managing rheumatoid arthritis: a narrative review of the literature. *Cureus*, *16*(5).

Povoleri, G.A., Durham, L.E., Gray, E.H., Lalnunhlimi, S., Kannambath, S., Pitcher, M.J., Dhami, P., Leeuw, T., Ryan, S.E., Steel, K.J. and Kirkham, B.W., 2023. Psoriatic and rheumatoid arthritis joints differ in the composition of CD8+ tissue-resident memory T cell subsets. *Cell reports*, *42*(5).

Powell, J.D., Pollizzi, K.N., Heikamp, E.B. and Horton, M.R., 2012. Regulation of immune responses by mTOR. *Annual review of immunology*, *30*(1), pp.39-68.

Power, D., Codd, M., Ivers, L., Sant, S. and Barry, M., 1999. Prevalence of rheumatoid arthritis in Dublin, Ireland: a population-based survey. *Irish journal of medical science*, *168*, pp.197-200.

Premer, C., Kanelidis, A.J., Hare, J.M. and Schulman, I.H., 2019. Rethinking endothelial dysfunction as a crucial target in fighting heart failure. *Mayo Clinic Proceedings: Innovations, Quality & Outcomes*, *3*(1), pp.1-13.

Proudman SM, Cleland LG, Mayrhofer G. Effects of tumor necrosis factor-, interleukin-1, and activated peripheral blood mononuclear cells on the expression of adhesion molecules and recruitment of leukocytes in rheumatoid synovial xenografts in SCID mice. J Rheumatol 1999;26:1877–89.

Pucino, V., Nefla, M., Gauthier, V., Alsaleh, G., Clayton, S.A., Marshall, J., Filer, A., Clark, A.R., Raza, K. and Buckley, C.D., 2023. Differential effect of lactate on synovial fibroblast and macrophage effector functions. *Frontiers in immunology*, *14*, p.1183825.

Pugh, C.W. and Ratcliffe, P.J., 2003. Regulation of angiogenesis by hypoxia: role of the HIF system. *Nature medicine*, *9*(6), pp.677-684.

Purcell, W.T. and Ettinger, D.S., 2003. Novel antifolate drugs. *Current oncology reports*, *5*, pp.114-125.

Qiao, Y., Chen, J., Lim, Y.B., Finch-Edmondson, M.L., Seshachalam, V.P., Qin, L., Jiang, T., Low, B.C., Singh, H., Lim, C.T. and Sudol, M., 2017. YAP regulates actin dynamics through ARHGAP29 and promotes metastasis. *Cell reports*, *19*(8), pp.1495-1502.

Qiu, J., Wu, B., Goodman, S.B., Berry, G.J., Goronzy, J.J. and Weyand, C.M., 2021. Metabolic control of autoimmunity and tissue inflammation in rheumatoid arthritis. *Frontiers in immunology*, *12*, p.652771.

Qu, Z., Garcia, C.H., O'Rourke, L.M., Planck, S.R., Kohli, M. and Rosenbaum, J.T., 1994. Local proliferation of fibroblast-like synoviocytes contributes to synovial hyperplasia. *Arthritis & Rheumatism: Official Journal of the American College of Rheumatology*, *37*(2), pp.212-220.

Quinn, M.A., Conaghan, P.G., O'Connor, P.J., Karim, Z., Greenstein, A., Brown, A., Brown, C., Fraser, A., Jarret, S. and Emery, P., 2005. Very early treatment with infliximab in addition to methotrexate in early, poor-prognosis rheumatoid arthritis reduces magnetic resonance imaging evidence of synovitis and damage, with sustained benefit after infliximab withdrawal: results from a twelve-month randomised, double-blind, placebo-controlled trial. *Arthritis & Rheumatism: Official Journal of the American College of Rheumatology*, *52*(1), pp.27-35.

Quinn, M.A. and Cox, S., 2005. The evidence for early intervention. *Rheumatic Disease Clinics*, *31*(4), pp.575-589.

Quinn, M.A. and Emery, P., 2003. Window of opportunity in early rheumatoid arthritis: possibility of altering the disease process with early intervention. *Clinical and experimental rheumatology*, *21*(5; SUPP 31), pp.S154-S157.

Raine, C. and Giles, I., 2022. What is the impact of sex hormones on the pathogenesis of rheumatoid arthritis?. *Frontiers in Medicine*, *9*, p.909879.

Raingeaud, J. and Pierre, J., 2005. Interleukin-4 downregulates TNFα-induced IL-8 production in keratinocytes. *FEBS letters*, *579*(18), pp.3953-3959.

Rajagopalan, S., Somers, E.C., Brook, R.D., Kehrer, C., Pfenninger, D., Lewis, E., Chakrabarti, A., Richardson, B.C., Shelden, E., McCune, W.J. and Kaplan, M.J., 2004. Endothelial cell apoptosis in systemic lupus erythematosus: a common pathway for abnormal vascular function and thrombosis propensity. *Blood*, *103*(10), pp.3677-3683.

Ramwadhdoebe, T.H., van Baarsen, L.G., Boumans, M.J., Bruijnen, S.T., Safy, M., Berger, F.H., Semmelink, J.F., van der Laken, C.J., Gerlag, D.M., Thurlings, R.M. and Tak, P.P., 2019. Effect of rituximab treatment on T and B cell subsets in lymph node biopsies of patients with rheumatoid arthritis. *Rheumatology*, *58*(6), pp.1075-1085.

Ramwadhdoebe, T.H., Hähnlein, J., Maijer, K.I., van Boven, L.J., Gerlag, D.M., Tak, P.P. and van Baarsen, L.G., 2016. Lymph node biopsy analysis reveals an altered immunoregulatory balance already during the at-risk phase of autoantibody positive rheumatoid arthritis. *European journal of immunology*, *46*(12), pp.2812-2821.

Rana, A.K., Li, Y., Dang, Q. and Yang, F., 2018. Monocytes in rheumatoid arthritis: Circulating precursors of macrophages and osteoclasts and, their heterogeneity and plasticity role in RA pathogenesis. *International immunopharmacology*, *65*, pp.348-359.

Rantapaa-Dahlqvist, S et al. 2003. “Antibodies against Cyclic Citrullinated Peptide and IgA Rheumatoid Factor Predict the Development of Rheumatoid Arthritis.” *Arthritis Rheum* 48(10): 2741–49.

Rao, D.A., Gurish, M.F., Marshall, J.L., Slowikowski, K., Fonseka, C.Y., Liu, Y., Donlin, L.T., Henderson, L.A., Wei, K., Mizoguchi, F. and Teslovich, N.C., 2017. Pathologically expanded peripheral T helper cell subset drives B cells in rheumatoid arthritis. *Nature*, *542*(7639), pp.110-114.

Rauber, S., Mohammadian, H., Schmidkonz, C., Atzinger, A., Soare, A., Treutlein, C., Kemble, S., Mahony, C.B., Geisthoff, M., Angeli, M.R. and Raimondo, M.G., 2024. CD200+ fibroblasts form a pro-resolving mesenchymal network in arthritis. *Nature Immunology*, *25*(4), pp.682-692.

Raychaudhuri, S.P., Raychaudhuri, S.K. and Genovese, M.C., 2012. IL-17 receptor and its functional significance in psoriatic arthritis. *Molecular and cellular biochemistry*, *359*, pp.419-429.

Raychaudhuri, S., Sandor, C., Stahl, E.A., Freudenberg, J., Lee, H.S., Jia, X., Alfredsson, L., Padyukov, L., Klareskog, L., Worthington, J. and Siminovitch, K.A., 2012. Five amino acids in three HLA proteins explain most of the association between MHC and seropositive rheumatoid arthritis. *Nature genetics*, *44*(3), pp.291-296.

Raza, K., 2010. The Michael Mason prize: early rheumatoid arthritis—the window narrows. *Rheumatology*, *49*(3), pp.406-410.

Raza, K., Scheel-Toellner, D., Lee, CY. *et al.* Synovial fluid leukocyte apoptosis is inhibited in patients with very early rheumatoid arthritis. *Arthritis Res Ther* **8**, R120 (2006).

Reece, R.J., Canete, J.D., Parsons, W.J., Emery, P. and Veale, D.J., 1999. Distinct vascular patterns of early synovitis in psoriatic, reactive, and rheumatoid arthritis. *Arthritis & Rheumatism: Official Journal of the American College of Rheumatology*, *42*(7), pp.1481-1484.

Reichert, S., Haffner, M., Keyßer, G., Schäfer, C., Stein, J.M., Schaller, H.G., Wienke, A., Strauss, H., Heide, S. and Schulz, S., 2013. Detection of oral bacterial DNA in synovial fluid. *Journal of clinical periodontology*, *40*(6), pp.591-598.

Reid, I.R., Birstow, S.M. and Bolland, M.J., 2017. Calcium and cardiovascular disease. *Endocrinology and Metabolism*, *32*(3), p.339.

Remmers, E.F., Plenge, R.M., Lee, A.T., Graham, R.R., Hom, G., Behrens, T.W., De Bakker, P.I., Le, J.M., Lee, H.S., Batliwalla, F. and Li, W., 2007. STAT4 and the risk of rheumatoid arthritis and systemic lupus erythematosus. *New England Journal of Medicine*, *357*(10), pp.977-986.

Rengel, Y., Ospelt, C. and Gay, S., 2007. Proteinases in the joint: clinical relevance of proteinases in joint destruction. *Arthritis research & therapy*, *9*, pp.1-10.

Rhodes, J.W., Tong, O., Harman, A.N. and Turville, S.G., 2019. Human dendritic cell subsets, ontogeny, and impact on HIV infection. *Frontiers in immunology*, *10*, p.1088.

Rinaldi, N., Schwarz-Eywill, M., Weis, D., Leppelmann-Jansen, P., Lukoschek, M., Keilholz, U. and Barth, T.F.E., 1997. Increased expression of integrins on fibroblast-like synoviocytes from rheumatoid arthritis in vitro correlates with enhanced binding to extracellular matrix proteins. *Annals of the rheumatic diseases*, *56*(1), pp.45-51.

Rivellese, F., Humby, F., Bugatti, S., Fossati-Jimack, L., Rizvi, H., Lucchesi, D., Lliso-Ribera, G., Nerviani, A., Hands, R.E., Giorli, G. and Frias, B., 2020. B cell synovitis and clinical phenotypes in rheumatoid arthritis: relationship to disease stages and drug exposure. *Arthritis & Rheumatology*, *72*(5), pp.714-725.

Rivellese, F., Surace, A.E., Goldmann, K., Sciacca, E., Çubuk, C., Giorli, G., John, C.R., Nerviani, A., Fossati-Jimack, L., Thorborn, G. and Ahmed, M., 2022. Rituximab versus tocilizumab in rheumatoid arthritis: synovial biopsy-based biomarker analysis of the phase 4 R4RA randomised trial. *Nature medicine*, *28*(6), pp.1256-1268.

Robertson, J. et al. (2013) 'Changes in lipid levels with inflammation and therapy in RA: a maturing paradigm', Nature Reviews Rheumatology, 9(9), pp. 513–523. doi: 10.1038/nrrheum.2013.91.

Roca, C. and Adams, R.H., 2007. Regulation of vascular morphogenesis by Notch signaling. *Genes & development*, *21*(20), pp.2511-2524.

Rodríguez-Carrio, J., Prado, C., De Paz, B., Lopez, P., Gomez, J., Alperi-Lopez, M., Ballina-García, F.J. and Suarez, A., 2012. Circulating endothelial cells and their progenitors in systemic lupus erythematosus and early rheumatoid arthritis patients. *Rheumatology*, *51*(10), pp.1775-1784.

Rodríguez-Carrio, J., Hähnlein, J.S., Ramwadhdoebe, T.H., Semmelink, J.F., Choi, I.Y., van Lienden, K.P., Maas, M., Gerlag, D.M., Tak, P.P., Geijtenbeek, T.B. and van Baarsen, L.G., 2017. Brief report: altered innate lymphoid cell subsets in human lymph node biopsy specimens obtained during the at-risk and earliest phases of rheumatoid arthritis. *Arthritis & Rheumatology*, *69*(1), pp.70-76.

Rodríguez-Rodríguez L, González-Juanatey C, García-Bermúdez M et al (2011) CCR5Δ32 variant and cardiovascular disease in patients with rheumatoid arthritis: a cohort study. Arthritis Res Ther 13:R133. 10.1186/ar3444 10.1186/ar3444

Romão, V.C., Vital, E.M., Fonseca, J.E. and Buch, M.H., 2017. Right drug, right patient, right time: aspiration or future promise for biologics in rheumatoid arthritis?. *Arthritis research & therapy*, *19*, pp.1-13.

Roodenrijs, N.M., Welsing, P.M., van Roon, J., Schoneveld, J.L., van der Goes, M.C., Nagy, G., Townsend, M.J. and van Laar, J.M., 2022. Mechanisms underlying DMARD inefficacy in difficult-to-treat rheumatoid arthritis: a narrative review with systematic literature search. *Rheumatology*, *61*(9), pp.3552-3566.

Rosengren, S., Corr, M., Firestein, G.S. and Boyle, D.L., 2012. The JAK inhibitor CP-690,550 (tofacitinib) inhibits TNF-induced chemokine expression in fibroblast-like synoviocytes: autocrine role of type I interferon. *Annals of the rheumatic diseases*, *71*(3), pp.440-447.

Rosenstein, E.D., Greenwald, R.A., Kushner, L.J. and Weissmann, G., 2004. Hypothesis: the humoral immune response to oral bacteria provides a stimulus for the development of rheumatoid arthritis. *Inflammation*, *28*(6), pp.311-318.

Rossi, D., Modena, V., Sciascia, S. and Roccatello, D., 2015. Rheumatoid arthritis: biological therapy other than anti-TNF. *International immunopharmacology*, *27*(2), pp.185-188.

Rossol, M., Kraus, S., Pierer, M., Baerwald, C. and Wagner, U., 2012. The CD14brightCD16+ monocyte subset is expanded in rheumatoid arthritis and promotes expansion of the Th17 cell population. *Arthritis & Rheumatism*, *64*(3), pp.671-677.

Rothschild, B.M. and Masi, A.T., 1982, August. Pathogenesis of rheumatoid arthritis: a vascular hypothesis. In *Seminars in arthritis and rheumatism* (Vol. 12, No. 1, pp. 11-31). WB Saunders.

Rudan, I., Sidhu, S., Papana, A., Meng, S.J., Xin–Wei, Y., Wang, W., Campbell–Page, R.M., Demaio, A.R., Nair, H., Sridhar, D. and Theodoratou, E., 2015. Prevalence of rheumatoid arthritis in low–and middle–income countries: A systematic review and analysis. *Journal of global health*, *5*(1), p.010409.

Ruiz-Limón, P., Ortega, R., de la Rosa, I.A., Del Carmen Abalos-Aguilera, M., Perez-Sanchez, C., Jimenez-Gomez, Y., Peralbo-Santaella, E., Font, P., Ruiz-Vilches, D., Ferrin, G. and Collantes-Estevez, E., 2017. Tocilizumab improves the proatherothrombotic profile of rheumatoid arthritis patients modulating endothelial dysfunction, NETosis, and inflammation. *Translational Research*, *183*, pp.87-103.

Ruschen, S., Lemm, G. and Warnatz, H., 1989. Spontaneous and LPS-stimulated production of intracellular IL-1 beta by synovial macrophages in rheumatoid arthritis is inhibited by IFN-gamma. *Clinical and experimental immunology*, *76*(2), p.246.

Russell MD, Stovin C, Alveyn E, et alJAK inhibitors and the risk of malignancy: a meta-analysis across disease indicationsAnnals of the Rheumatic Diseases 2023;82:1059-1067.

Ryu, S., Lee, J.H. and Kim, S.I., 2006. IL-17 increased the production of vascular endothelial growth factor in rheumatoid arthritis synoviocytes. *Clinical rheumatology*, *25*, pp.16-20.

Saag, K.G., Cerhan, J.R., Kolluri, S., Ohashi, K., Hunninghake, G.W. and Schwartz, D.A., 1997. Cigarette smoking and rheumatoid arthritis severity. *Annals of the rheumatic diseases*, *56*(8), pp.463-469.

Sabeh, F., Fox, D. and Weiss, S.J., 2010. Membrane-type I matrix metalloproteinase-dependent regulation of rheumatoid arthritis synoviocyte function. *The Journal of Immunology*, *184*(11), pp.6396-6406.

Saber, T.P., Ng, C.T., Renard, G., Lynch, B.M., Pontifex, E., Walsh, C.A., Grier, A., Molloy, M., Bresnihan, B., FitzGerald, O. and Fearon, U., 2010. Remission in psoriatic arthritis: is it possible and how can it be predicted?. *Arthritis research & therapy*, *12*, pp.1-6.

Safiri, S., Kolahi, A.A., Hoy, D., Smith, E., Bettampadi, D., Mansournia, M.A., Almasi-Hashiani, A., Ashrafi-Asgarabad, A., Moradi-Lakeh, M., Qorbani, M. and Collins, G., 2019. Global, regional and national burden of rheumatoid arthritis 1990–2017: a systematic analysis of the Global Burden of Disease study 2017. *Annals of the rheumatic diseases*, *78*(11), pp.1463-1471.

Saini, R., Marawar, P.P., Shete, S. and Saini, S., 2009. Periodontitis, a true infection. *Journal of global infectious diseases*, *1*(2), pp.149-150.

Sakurada, S., Kato, T. and Okamoto, T., 1996. Induction of cytokines and ICAM-1 by proinflammatory cytokines in primary rheumatoid synovial fibroblasts and inhibition by N-acetyl-L-cysteine and aspirin. *International immunology*, *8*(10), pp.1483-1493.

Salgado, E. and Gómez-Reino, J. J. (2011) 'The risk of tuberculosis in patients treated with TNF antagonists', *Expert Review of Clinical Immunology*, 7(3), pp. 329–340. doi: 10.1586/eci.11.6.

Salnikova, D.I., Nikiforov, N.G., Postnov, A.Y. and Orekhov, A.N., 2024. Target Role of Monocytes as Key Cells of Innate Immunity in Rheumatoid Arthritis. *Diseases*, *12*(5), p.81.

Samuvel, D.J., Sundararaj, K.P., Nareika, A., Lopes-Virella, M.F. and Huang, Y., 2009. Lactate boosts TLR4 signaling and NF-κB pathway-mediated gene transcription in macrophages via monocarboxylate transporters and MD-2 up-regulation. *The Journal of Immunology*, *182*(4), pp.2476-2484.

Sandberg, M.E., Bengtsson, C., Källberg, H., Wesley, A., Klareskog, L., Alfredsson, L. and Saevarsdottir, S., 2014. Overweight decreases the chance of achieving good response and low disease activity in early rheumatoid arthritis. *Annals of the rheumatic diseases*, *73*(11), pp.2029-2033.

Santos, A.N., Riemann, D., Thiele, K., Kehlen, A., Santos, A.N. and Langner, J., 1997. Constitutive expression of HLA class II mRNA in synovial fibroblast-like cells from patients with rheumatoid arthritis. *Immunology letters*, *58*(1), pp.53-58.

Saraux, A., Berthelot, J.M., Chalès, G., Le Henaff, C., Thorel, J.B., Hoang, S., Valls, I., Devauchelle, V., Martin, A., Baron, D. and Pennec, Y., 2001. Ability of the American College of Rheumatology 1987 criteria to predict rheumatoid arthritis in patients with early arthritis and classification of these patients two years later. *Arthritis & Rheumatism*, *44*(11), pp.2485-2491.

Saxton, R.A. and Sabatini, D.M., 2017. mTOR signaling in growth, metabolism, and disease. *Cell*, *168*(6), pp.960-976.

Schellekens, G A et al. 2000. "The Diagnostic Properties of Rheumatoid Arthritis Antibodies Recognizing a Cyclic Citrullinated Peptide." *Arthritis Rheum* 43(1): 155–63.

Scher, J.U. and Abramson, S.B., 2011. The microbiome and rheumatoid arthritis. *Nature reviews rheumatology*, *7*(10), pp.569-578.

Schiff, M., Keiserman, M., Codding, C., Songcharoen, S., Berman, A., Nayiager, S., Saldate, C., Aranda, R., Becker, J.C., Nys, M. and Le Bars, M., 2011. Clinical response and tolerability to abatacept in patients with rheumatoid arthritis previously treated with infliximab or abatacept: open-label extension of the ATTEST Study. *Annals of the rheumatic diseases*, *70*(11), pp.2003-2007.

Schnoor, M., Alcaide, P., Voisin, M.B. and van Buul, J.D., 2015. Crossing the vascular wall: common and unique mechanisms exploited by different leukocyte subsets during extravasation. *Mediators of inflammation*, *2015*(1), p.946509.

Schönenberger, K.A., Schüpfer, A.C., Gloy, V.L., Hasler, P., Stanga, Z., Kaegi-Braun, N. and Reber, E., 2021. Effect of anti-inflammatory diets on pain in rheumatoid arthritis: a systematic review and meta-analysis. *Nutrients*, *13*(12), p.4221.

Schubert, K., Gutknecht, D., Köberle, M., Anderegg, U. and Saalbach, A., 2013. Melanoma cells use Thy-1 (CD90) on endothelial cells for metastasis formation. *The American journal of pathology*, *182*(1), pp.266-276.

Seemayer, C.A., Kuchen, S., Kuenzler, P., Řihošková, V., Rethage, J., Aicher, W.K., Michel, B.A., Gay, R.E., Kyburz, D., Neidhart, M. and Gay, S., 2003. Cartilage destruction mediated by synovial fibroblasts does not depend on proliferation in rheumatoid arthritis. *The American journal of pathology*, *162*(5), pp.1549-1557.

Segura, E., Touzot, M., Bohineust, A., Cappuccio, A., Chiocchia, G., Hosmalin, A., Dalod, M., Soumelis, V. and Amigorena, S., 2013. Human inflammatory dendritic cells induce Th17 cell differentiation. *Immunity*, *38*(2), pp.336-348.

Sellam, J., Hendel-Chavez, H., Rouanet, S., Abbed, K., Combe, B., Le Loët, X., Tebib, J., Sibilia, J., Taoufik, Y., Dougados, M. and Mariette, X., 2011. B cell activation biomarkers as predictive factors for the response to rituximab in rheumatoid arthritis: a six-month, national, multicenter, open-label study. *Arthritis & Rheumatism*, *63*(4), pp.933-938.

Senbanjo, L.T. and Chellaiah, M.A., 2017. CD44: a multifunctional cell surface adhesion receptor is a regulator of progression and metastasis of cancer cells. *Frontiers in cell and developmental biology*, *5*, p.18.

Senior, B.W., McBride, P.D.P., Morley, K.D. and Kerr, M.A., 1995. The detection of raised levels of IgM to Proteus mirabilis in sera from patients with rheumatoid arthritis. *Journal of medical microbiology*, *43*(3), pp.176-184.

Senyilmaz, D. and Teleman, A.A., 2015. Chicken or the egg: Warburg effect and mitochondrial dysfunction. *F1000prime reports*, *7*, p.41.

Sepriano, A., Kerschbaumer, A., Bergstra, S.A., Smolen, J.S., Van Der Heijde, D., Caporali, R., Edwards, C.J., Verschueren, P., De Souza, S., Pope, J. and Takeuchi, T., 2023. Safety of synthetic and biological DMARDs: a systematic literature review informing the 2022 update of the EULAR recommendations for the management of rheumatoid arthritis. *Annals of the rheumatic diseases*, *82*(1), pp.107-118.

Shao, P., Ma, L., Ren, Y. and Liu, H., 2017. Modulation of the immune response in rheumatoid arthritis with strategically released rapamycin. *Molecular medicine reports*, *16*(4), pp.5257-5262.

Shaw, T.J. and Rognoni, E., 2020. Dissecting fibroblast heterogeneity in health and fibrotic disease. *Current rheumatology reports*, *22*, pp.1-10.

Sheng, M.H.C., Wergedal, J.E., Mohan, S. and Lau, K.H.W., 2008. Osteoactivin is a novel osteoclastic protein and plays a key role in osteoclast differentiation and activity. *FEBS letters*, *582*(10), pp.1451-1458.

Sherri, N., Assaf, R., Bitar, E.R., Znait, S., Borghol, A.H., Kassem, A. and Rahal, E.A., 2024. Epstein–Barr Virus DNA Exacerbates Arthritis in a Mouse Model via Toll-like Receptor 9. *International Journal of Molecular Sciences*, *25*(9), p.4661.

Shervington, L., Darekar, A., Shaikh, M., Mathews, R. and Shervington, A., 2018. Identifying reliable diagnostic/predictive biomarkers for rheumatoid arthritis. *Biomarker insights*, *13*, p.1177271918801005.

Shi, G., Liao, X., Lin, Z., Liu, W., Luo, X., Zhan, H. and Cai, X., 2023. Estimation of the global prevalence, incidence, years lived with disability of rheumatoid arthritis in 2019 and forecasted incidence in 2040: results from the Global Burden of Disease Study 2019. *Clinical Rheumatology*, *42*(9), pp.2297-2309.

Shi, J. *et al.* (2013) 'Anti-carbamylated protein antibodies are present in arthralgia patients and predict the development of rheumatoid arthritis', *Arthritis and Rheumatism*, 65(4), pp. 911–915. doi: 10.1002/art.37830.

Shi, Jing et al. 2011. "Autoantibodies Recognizing Carbamylated Proteins Are Present in Sera of Patients with Rheumatoid Arthritis and Predict Joint Damage." *Proceedings of the National Academy of Sciences of the United States of America* 108(42): 17372–77.

Shiel Jr., W C, and M Jason. 1989. "The Diagnostic Associations of Patients with Antinuclear Antibodies Referred to a Community Rheumatologist." *J Rheumatol* 16(6): 782–85.

Shime, H., Yabu, M., Akazawa, T., Kodama, K., Matsumoto, M., Seya, T. and Inoue, N., 2008. Tumor-secreted lactic acid promotes IL-23/IL-17 proinflammatory pathway. *The Journal of Immunology*, *180*(11), pp.7175-7183.

Short, C.L., 1974. The antiquity of rheumatoid arthritis. *Arthritis & Rheumatism: Official Journal of the American College of Rheumatology*, *17*(3), pp.193-205.

Shortman, K. and Liu, Y.J., 2002. Mouse and human dendritic cell subtypes. *Nature Reviews Immunology*, *2*(3), pp.151-161.

Sihvonen, S., Korpela, M., Laippala, P., Mustonen, J. and Pasternack, A., 2004. Death rates and causes of death in patients with rheumatoid arthritis: a population-based study. *Scandinavian journal of rheumatology*, *33*(4), pp.221-227.

Silman, A.J., MacGregor, A.J., Thomson, W., Holligan, S., Carthy, D., Farhan, A. and Ollier, W.E.R., 1993. Twin concordance rates for rheumatoid arthritis: results from a nationwide study. *Rheumatology*, *32*(10), pp.903-907.

Silman, A.J. and Pearson, J.E., 2002. Epidemiology and genetics of rheumatoid arthritis. *Arthritis research & therapy*, *4*, pp.1-8.

Silva-Fernández, L., Macía-Villa, C., Seoane-Mato, D., Cortés-Verdú, R., Romero-Pérez, A., Quevedo-Vila, V., Fábregas-Canales, D., Antón-Pagés, F., Añez, G., Brandy, A. and Martínez-Dubois, C., 2020. The prevalence of rheumatoid arthritis in Spain. *Scientific reports*, *10*(1), p.21551.

Simmons, D.P., Nguyen, H.N., Gomez-Rivas, E., Jeong, Y., Jonsson, A.H., Chen, A.F., Lange, J.K., Dyer, G.S., Blazar, P., Earp, B.E. and Coblyn, J.S., 2022. SLAMF7 engagement superactivates macrophages in acute and chronic inflammation. *Science immunology*, *7*(68), p.eabf2846.

Simon, T.A., Thompson, A., Gandhi, K.K., Hochberg, M.C. and Suissa, S., 2015. Incidence of malignancy in adult patients with rheumatoid arthritis: a meta-analysis. *Arthritis research & therapy*, *17*, pp.1-10.

Sköldstam, L., Hagfors, L. and Johansson, G. (2003) 'An experimental study of a Mediterranean diet intervention for patients with rheumatoid arthritis', *Annals of the Rheumatic Diseases*, 62(3), pp. 208–214. doi: 10.1136/ard.62.3.208.

Slater, C.A., Davis, R.B. and Shmerling, R.H., 1996. Antinuclear antibody testing: a study of clinical utility. *Archives of Internal Medicine*, *156*(13), pp.1421-1425.

Smith, M.D., 2011. The normal synovium. *The open rheumatology journal*, *5*, p.100.

Smith, M.H., Gao, V.R., Periyakoil, P.K., Kochen, A., DiCarlo, E.F., Goodman, S.M., Norman, T.M., Donlin, L.T., Leslie, C.S. and Rudensky, A.Y., 2023. Drivers of heterogeneity in synovial fibroblasts in rheumatoid arthritis. *Nature Immunology*, *24*(7), pp.1200-1210.

Smolen JS, Aletaha D, McInnes IB. Rheumatoid arthritis. Lancet. 2016 Oct 22;388(10055):2023-2038. doi: 10.1016/S0140-6736(16)30173-8. Epub 2016 May 3. Erratum in: Lancet. 2016 Oct 22;388(10055):1984. doi: 10.1016/S0140-6736(16)30794-2. PMID: 27156434.

Smolen, J.O.S.E.F., Landewé, R.B., Mease, P.H.I.L.I.P., Brzezicki, J., Mason, D., Luijtens, K., van Vollenhoven, R.F., Kavanaugh, A., Schiff, M., Burmester, G.R. and Strand, V., 2009. Efficacy and safety of certolizumab pegol plus methotrexate in active rheumatoid arthritis: the RAPID 2 study. A randomised controlled trial. *Annals of the rheumatic diseases*, *68*(6), pp.797-804.

Smolen, J.S., Aletaha, D., Barton, A., Burmester, G.R., Emery, P., Firestein, G.S., Kavanaugh, A., McInnes, I.B., Solomon, D.H., Strand, V. and Yamamoto, K., 2018. *Rheumatoid arthritis Nat Rev Dis Primers 4: 18001* [online].

Smolen, J.S., Landewé, R., Breedveld, F.C., Dougados, M., Emery, P., Gaujoux-Viala, C., Gorter, S., Knevel, R., Nam, J., Schoels, M. and Aletaha, D., 2010. EULAR recommendations for the management of rheumatoid arthritis with synthetic and biological disease-modifying antirheumatic drugs. *Annals of the rheumatic diseases*, *69*(6), pp.964-975.

Smolen, J.S., Landewé, R.B., Bergstra, S.A., Kerschbaumer, A., Sepriano, A., Aletaha, D., Caporali, R., Edwards, C.J., Hyrich, K.L., Pope, J.E. and De Souza, S., 2023. EULAR recommendations for the management of rheumatoid arthritis with synthetic and biological disease-modifying antirheumatic drugs: 2022 update. *Annals of the rheumatic diseases*, *82*(1), pp.3-18.

Smolen, J.S. and Steiner, G., 2003. Therapeutic strategies for rheumatoid arthritis. *Nature reviews Drug discovery*, *2*(6), pp.473-488.

Sokolove, J., Schiff, M., Fleischmann, R., Weinblatt, M.E., Connolly, S.E., Johnsen, A., Zhu, J., Maldonado, M.A., Patel, S. and Robinson, W.H., 2016. Impact of baseline anti-cyclic citrullinated peptide-2 antibody concentration on efficacy outcomes following treatment with subcutaneous abatacept or adalimumab: 2-year results from the AMPLE trial. *Annals of the rheumatic diseases*, *75*(4), pp.709-714.

Song, S.N.J., Iwahashi, M., Tomosugi, N., Uno, K., Yamana, J., Yamana, S., Isobe, T., Ito, H., Kawabata, H. and Yoshizaki, K., 2013. Comparative evaluation of the effects of treatment with tocilizumab and TNF-α inhibitors on serum hepcidin, anemia response and disease activity in rheumatoid arthritis patients. *Arthritis Research & Therapy*, *15*, pp.1-10.

Sorensen, J., Valentelyte, G., Birgisdóttir, U. R., Hammond, L., Kinneavy, C., O'Sullivan, T., Boyd, P., Regan, T., O'Leary, G., & RCSI University of Medicine and Health Sciences. (2024). Financial and personal burden of arthritis: Results from the 2024 Arthritis Ireland Cost Survey 2024. In *https://www.arthritisireland.ie/counting-the-cost-of-arthritis*. Arthritis Ireland.

Spurrell, D.R., Oldford, S.A., Frost, T., Larsen, B., Codner, D., Edgecombe, A. and Drover, S., 2004. Discordant expression of HLA class II-associated co-chaperones and HLA-DRB alleles in cultured fibroblast-like synoviocytes. *Human immunology*, *65*(12), pp.1516-1529.

Srirangan, S. and Choy, E.H., 2010. The role of interleukin 6 in the pathophysiology of rheumatoid arthritis. *Therapeutic advances in musculoskeletal disease*, *2*(5), pp.247-256.

Stahl, E.A., Wegmann, D., Trynka, G., Gutierrez-Achury, J., Do, R., Voight, B.F., Kraft, P., Chen, R., Kallberg, H.J., Kurreeman, F.A. and Diabetes Genetics Replication and Meta-analysis Consortium, 2012. Bayesian inference analyses of the polygenic architecture of rheumatoid arthritis. *Nature genetics*, *44*(5), pp.483-489.

Strand, V., Lee, E.B., Fleischmann, R., Alten, R.E., Koncz, T., Zwillich, S.H., Gruben, D., Wilkinson, B., Krishnaswami, S. and Wallenstein, G., 2016. Tofacitinib versus methotrexate in rheumatoid arthritis: patient-reported outcomes from the randomised phase III ORAL Start trial. *RMD open*, *2*(2), p.e000308.

Stuart, T., Butler, A., Hoffman, P., Hafemeister, C., Papalexi, E., Mauck, W.M., Hao, Y., Stoeckius, M., Smibert, P. and Satija, R., 2019. Comprehensive integration of single-cell data. *cell*, *177*(7), pp.1888-1902.

Sudoł-Szopińska, I., Kontny, E., Maśliński, W., Prochorec-Sobieszek, M., Kwiatkowska, B., Zaniewicz-Kaniewska, K. and Warczyńska, A., 2012. The pathogenesis of rheumatoid arthritis in radiological studies. Part I: Formation of inflammatory infiltrates within the synovial membrane. *Journal of ultrasonography*, *12*(49), p.202.

Sugimoto, H., Takeda, A. and Hyodoh, K., 2000. Early-stage rheumatoid arthritis: prospective study of the effectiveness of MR imaging for diagnosis. *Radiology*, *216*(2), pp.569-575.

Sugiyama D, Nishimura K, Tamaki K, et al Impact of smoking as a risk factor for developing rheumatoid arthritis: a meta-analysis of observational studies Annals of the Rheumatic Diseases 2010;69:70-81.

Sun, J.J., Yin, X.W., Liu, H.H., Du, W.X., Shi, L.Y., Huang, Y.B., Wang, F., Liu, C.F., Cao, Y.J. and Zhang, Y.L., 2018. Rapamycin inhibits ox-LDL-induced inflammation in human endothelial cells in vitro by inhibiting the mTORC2/PKC/c-Fos pathway. *Acta Pharmacologica Sinica*, *39*(3), pp.336-344.

Sun, M., Rethi, B., Krishnamurthy, A., Joshua, V., Circiumaru, A., Hensvold, A.H., Ossipova, E., Grönwall, C., Liu, Y., Engstrom, M. and Catrina, S.B., 2019. Anticitrullinated protein antibodies facilitate migration of synovial tissue-derived fibroblasts. *Annals of the rheumatic diseases*, *78*(12), pp.1621-1631.

Suto, T. and Karonitsch, T., 2020. The immunobiology of mTOR in autoimmunity. *Journal of autoimmunity*, *110*, p.102373.

Suzuki, A., Yamada, R., Chang, X., Tokuhiro, S., Sawada, T., Suzuki, M., Nagasaki, M., Nakayama-Hamada, M., Kawaida, R., Ono, M. and Ohtsuki, M., 2003. Functional haplotypes of PADI4, encoding citrullinating enzyme peptidylarginine deiminase 4, are associated with rheumatoid arthritis. *Nature genetics*, *34*(4), pp.395-402.

Sweeney, S.E. and Firestein, G.S., 2004. Rheumatoid arthritis: regulation of synovial inflammation. *The international journal of biochemistry & cell biology*, *36*(3), pp.372-378.

Symmons, D. and Harrison, B., 2000. Early inflammatory polyarthritis: results from the Norfolk Arthritis Register with a review of the literature. I. Risk factors for the development of inflammatory polyarthritis and rheumatoid arthritis. *Rheumatology*, *39*(8), pp.835-843.

Symons, R.A., Colella, F., Collins, F.L., Rafipay, A.J., Kania, K., McClure, J.J., White, N., Cunningham, I., Ashraf, S., Hay, E. and Mackenzie, K.S., 2022. Targeting the IL-6–Yap–Snail signaling axis in synovial fibroblasts ameliorates inflammatory arthritis. *Annals of the rheumatic diseases*, *81*(2), pp.214-224.

Syversen, S.W., Gaarder, P.I., Goll, G.L., Ødegård, S., Haavardsholm, E.A., Mowinckel, P., Van Der Heijde, D., Landewé, R. and Kvien, T.K., 2008. High anti-cyclic citrullinated peptide levels and an algorithm of four variables predict radiographic progression in patients with rheumatoid arthritis: results from a 10-year longitudinal study. *Annals of the rheumatic diseases*, *67*(2), pp.212-217.

Szekanecz, Z., Besenyei, T., Szentpétery, Á. and Koch, A.E., 2010. Angiogenesis and vasculogenesis in rheumatoid arthritis. *Current opinion in rheumatology*, *22*(3), pp.299-306.

Szekanecz, Z. and Koch, A.E., 2007. Macrophages and their products in rheumatoid arthritis. *Current opinion in rheumatology*, *19*(3), pp.289-295.

Szekanecz, Z. and Koch, A.E., 2016. Successes and failures of chemokine-pathway targeting in rheumatoid arthritis. *Nature Reviews Rheumatology*, *12*(1), pp.5-13.

Szekanecz, Z., Vegvari, A., Szabo, Z. and Koch, A.E., 2010. Chemokines and chemokine receptors in arthritis. *Frontiers in bioscience (Scholar edition)*, *2*, p.153.

Taheri, M., Eghtedarian, R., Dinger, M.E. and Ghafouri-Fard, S., 2020. Dysregulation of non-coding RNAs in rheumatoid arthritis. *Biomedicine & Pharmacotherapy*, *130*, p.110617.

Tak, P.P. and Bresnihan, B., 2000. The pathogenesis and prevention of joint damage in rheumatoid arthritis: advances from synovial biopsy and tissue analysis. *Arthritis & Rheumatism*, *43*(12), pp.2619-2633.

Tak, P.P. and Kalden, J.R., 2011. Advances in rheumatology: new targeted therapeutics. *Arthritis research & therapy*, *13*, pp.1-14.

Tak, P.P., 2012. A personalized medicine approach to biologic treatment of rheumatoid arthritis: a preliminary treatment algorithm. *Rheumatology*, *51*(4), pp.600-609.

Takahashi, S., Saegusa, J., Sendo, S., Okano, T., Akashi, K., Irino, Y. and Morinobu, A., 2017. Glutaminase 1 plays a key role in the cell growth of fibroblast-like synoviocytes in rheumatoid arthritis. *Arthritis research & therapy*, *19*, pp.1-10.

Takemura, S., Klimiuk, P.A., Braun, A., Goronzy, J.J. and Weyand, C.M., 2001. T cell activation in rheumatoid synovium is B cell dependent. *The Journal of Immunology*, *167*(8), pp.4710-4718.

Takeshita, M., Suzuki, K., Kondo, Y., Morita, R., Okuzono, Y., Koga, K., Kassai, Y., Gamo, K., Takiguchi, M., Kurisu, R. and Mototani, H., 2019. Multi-dimensional analysis identified rheumatoid arthritis-driving pathway in human T cell. *Annals of the rheumatic diseases*, *78*(10), pp.1346-1356.

Tamer, T.M., 2013. Hyaluronan and synovial joint: function, distribution and healing. *Interdisciplinary toxicology*, *6*(3), p.111.

Tanaka, Y., Takeuchi, T., Amano, K., Saito, K., Hanami, K., Nawata, M., Fukuyo, S., Kameda, H., Kaneko, Y., Kurasawa, T. and Nagasawa, H., 2014. Effect of interleukin-6 receptor inhibitor, tocilizumab, in preventing joint destruction in patients with rheumatoid arthritis showing inadequate response to TNF inhibitors. *Modern rheumatology*, *24*(3), pp.399-404.

Tannahill, G.M., Curtis, A.M., Adamik, J., Palsson-McDermott, E.M., McGettrick, A.F., Goel, G., Frezza, C., Bernard, N.J., Kelly, B., Foley, N.H. and Zheng, L., 2013. Succinate is an inflammatory signal that induces IL-1β through HIF-1α. *Nature*, *496*(7444), pp.238-242.

Tas, S.W., Maracle, C.X., Balogh, E. and Szekanecz, Z., 2016. Targeting of proangiogenic signaling pathways in chronic inflammation. *Nature Reviews Rheumatology*, *12*(2), pp.111-122.

Tedeschi, S.K. and Costenbader, K.H., 2016. Is there a role for diet in the therapy of rheumatoid arthritis?. *Current rheumatology reports*, *18*, pp.1-9.

Teng, Y.O., Levarht, E.N., Hashemi, M., Bajema, I.M., Toes, R.E., Huizinga, T.W. and van Laar, J.M., 2007. Immunohistochemical analysis as a means to predict responsiveness to rituximab treatment. *Arthritis & Rheumatism: Official Journal of the American College of Rheumatology*, *56*(12), pp.3909-3918.

Thomas, G., Tacke, R., Hedrick, C.C. and Hanna, R.N., 2015. Nonclassical patrolling monocyte function in the vasculature. *Arteriosclerosis, thrombosis, and vascular biology*, *35*(6), pp.1306-1316.

Thomson, A.W., Turnquist, H.R. and Raimondi, G., 2009. Immunoregulatory functions of mTOR inhibition. *Nature Reviews Immunology*, *9*(5), pp.324-337.

Thurlings, R.M., Vos, K., Wijbrandts, C.A., Zwinderman, A.H., Gerlag, D.M. and Tak, P.P., 2008. Synovial tissue response to rituximab: mechanism of action and identification of biomarkers of response. *Annals of the rheumatic diseases*, *67*(7), pp.917-925.

Tolboom, T.C.A., Pieterman, E., Van der Laan, W.H., Toes, R.E.M., Huidekoper, A.L., Nelissen, R.G.H.H., Breedveld, F.C. and Huizinga, T.W.J., 2002. Invasive properties of fibroblast-like synoviocytes: correlation with growth characteristics and expression of MMP-1, MMP-3, and MMP-10. *Annals of the rheumatic diseases*, *61*(11), pp.975-980.

Toussirot, E. and Wendling, D., 2005. Late-onset ankylosing spondylitis and related spondylarthropathies: clinical and radiological characteristics and pharmacological treatment options. *Drugs & aging*, *22*, pp.451-469.

Tran, C.N., Davis, M.J., Tesmer, L.A., Endres, J.L., Motyl, C.D., Smuda, C., Somers, E.C., Chung, K.C., Urquhart, A.G., Lundy, S.K. and Kovats, S., 2007. Presentation of arthritogenic peptide to antigen-specific T cells by fibroblast-like synoviocytes. *Arthritis & Rheumatism*, *56*(5), pp.1497-1506.

Treuhaft, P.S. and McCarty, D.J., 1971. Synovial fluid pH, lactate, oxygen and carbon dioxide partial pressure in various joint diseases. *Arthritis & Rheumatism: Official Journal of the American College of Rheumatology*, *14*(4), pp.475-484.

Trompette, A., Gollwitzer, E.S., Yadava, K., Sichelstiel, A.K., Sprenger, N., Ngom-Bru, C., Blanchard, C., Junt, T., Nicod, L.P., Harris, N.L. and Marsland, B.J., 2014. Gut microbiota metabolism of dietary fiber influences allergic airway disease and hematopoiesis. *Nature medicine*, *20*(2), pp.159-166.

Troncoso, M.F., Ortiz-Quintero, J., Garrido-Moreno, V., Sanhueza-Olivares, F., Guerrero-Moncayo, A., Chiong, M., Castro, P.F., García, L., Gabrielli, L., Corbalán, R. and Garrido-Olivares, L., 2021. VCAM-1 as a predictor biomarker in cardiovascular disease. *Biochimica et Biophysica Acta (BBA)-Molecular Basis of Disease*, *1867*(9), p.166170.

Troughton, P.R., Platt, R., Bird, H., El-Manzalawi, E., Bassiouni, M. and Wright, V., 1996. Synovial fluid interleukin-8 and neutrophil function in rheumatoid arthritis and seronegative polyarthritis. *Rheumatology*, *35*(12), pp.1244-1251.

Trowell, H.C., 1982. Ants distinguish diabetes mellitus from diabetes insipidus. *British Medical Journal (Clinical research ed.)*, *285*(6336), p.217.

Trowell, H.C., 1975. Dietary-fiber hypothesis of the etiology of diabetes mellitus. *Diabetes*, *24*(8), pp.762-765.

Tsukamoto, M., Seta, N., Yoshimoto, K., Suzuki, K., Yamaoka, K. and Takeuchi, T., 2017. CD14 bright CD16+ intermediate monocytes are induced by interleukin-10 and positively correlate with disease activity in rheumatoid arthritis. *Arthritis research & therapy*, *19*, pp.1-10.

Tu, J., Hong, W., Zhang, P., Wang, X., Körner, H. and Wei, W., 2018. Ontology and function of fibroblast-like and macrophage-like synoviocytes: how do they talk to each other, and can they be targeted for rheumatoid arthritis therapy?. *Frontiers in immunology*, *9*, p.1467.

Tynan, Ó. (2025) *Differential pathogenic mechanisms driving stromal cell inflammatory pathways in Rheumatoid arthritis and Psoriatic arthritis*. PhD Thesis, Trinity College Dublin.

Tynan Ó, Canavan M, Floudas A, Smith C, O' Rourke A, Anton D, Orr C, Veale D, Fearon U. Synovial Tissue Single-Cell Analysis Demonstrates Differential Fibroblast Populations Between RA and PsA Which Display Distinct Function [abstract]. *Arthritis Rheumatol.* 2023; 75 (suppl 9). https://acrabstracts.org/abstract/synovial-tissue-single-cell-analysis-demonstrates-differential-fibroblast-populations-between-ra-and-psa-which-display-distinct-function/.

Tynan, Ó., Smith, C., Floudas, A., Canavan , M., Neto, N., O'Rourke, A., Anton, D., Orr, C., Veale, D. and Fearon, U. (2024). DISTINCT FLS POPULATIONS WITH UNIQUE FUNCTIONAL PROPERTIES AND REGULATORS DEFINE RHEUMATOID AND PSORIATIC ARTHRITIS PATHOTYPES. [abstract] in: 43rd European Workshop for Rheumatology Research. 43rd European Workshop for Rheumatology Research.

Ulgen, E., Ozisik, O. and Sezerman, O.U., 2019. pathfindR: an R package for comprehensive identification of enriched pathways in omics data through active subnetworks. *Frontiers in genetics*, *10*, p.858.

Umehara, H., Bloom, E.T., Okazaki, T., Nagano, Y., Yoshie, O. and Imai, T., 2004. Fractalkine in vascular biology: from basic research to clinical disease. *Arteriosclerosis, thrombosis, and vascular biology*, *24*(1), pp.34-40.

Vaahtovuo, J., Munukka, E., Korkeamäki, M., Luukkainen, R. and Toivanen, P., 2008. Fecal microbiota in early rheumatoid arthritis. *The Journal of rheumatology*, *35*(8), pp.1500-1505.

Vaine, C.A. and Soberman, R.J., 2014. The CD200–CD200R1 inhibitory signaling pathway: immune regulation and host–pathogen interactions. *Advances in immunology*, *121*, pp.191-211.

Valencia, X., Higgins, J.M., Kiener, H.P., Lee, D.M., Podrebarac, T.A., Dascher, C.C., Watts, G.F., Mizoguchi, E., Simmons, B., Patel, D.D. and Bhan, A.K., 2004. Cadherin-11 provides specific cellular adhesion between fibroblast-like synoviocytes. *The Journal of experimental medicine*, *200*(12), pp.1673-1679.

Vallejo, A.N., Yang, H., Klimiuk, P.A., Weyand, C.M. and Goronzy, J.J., 2003. Synoviocyte-mediated expansion of inflammatory T cells in rheumatoid synovitis is dependent on CD47-thrombospondin 1 interaction. *The Journal of Immunology*, *171*(4), pp.1732-1740.

van Baarsen, L.G., Bos, W.H., Rustenburg, F., van der Pouw Kraan, T.C., Wolbink, G.J.J., Dijkmans, B.A., van Schaardenburg, D. and Verweij, C.L., 2010. Gene expression profiling in autoantibody-positive patients with arthralgia predicts development of arthritis. *Arthritis & Rheumatism*, *62*(3), pp.694-704.

van Baarsen, L.G., Lebre, M.C., van der Coelen, D., Aarrass, S., Tang, M.W., Ramwadhdoebe, T.H., Gerlag, D.M. and Tak, P.P., 2014. Heterogeneous expression pattern of interleukin 17A (IL-17A), IL-17F and their receptors in synovium of rheumatoid arthritis, psoriatic arthritis and osteoarthritis: possible explanation for nonresponse to anti-IL-17 therapy?. *Arthritis research & therapy*, *16*, pp.1-10.chooy

van Boheemen, L., & van Schaardenburg, D. (2019). Predicting rheumatoid arthritis in at-risk individuals. *Clinical therapeutics*, *41*(7), 1286-1298.

van de Sande, M G, M J de Hair, et al. 2011. "Different Stages of Rheumatoid Arthritis: Features of the Synovium in the Preclinical Phase." *Ann Rheum Dis* 70(5): 772–77.

Van den Bossche, J., O'Neill, L.A. and Menon, D., 2017. Macrophage immunometabolism: where are we (going)?. *Trends in immunology*, *38*(6), pp.395-406.

Van den Hoek, J., Boshuizen, H.C., Roorda, L.D., Tijhuis, G.J., Nurmohamed, M.T., Van den Bos, G.A.M. and Dekker, J., 2017. Mortality in patients with rheumatoid arthritis: a 15-year prospective cohort study. Rheumatology international, 37, pp.487-493.

van der Heide, A., Jacobs, J.W., Bijlsma, J.W., Heurkens, A.H., van Booma-Frankfort, C., van der Veen, M.J., Haanen, H.C. and Hofman, D.M., 1996. The effectiveness of early treatment with "second-line" antirheumatic drugs: a randomized, controlled trial. *Annals of internal medicine*, *124*(8), pp.699-707.

Van der Heijde, D.M., 1996. Plain X-rays in rheumatoid arthritis: overview of scoring methods, their reliability and applicability. *Bailliere's clinical rheumatology*, *10*(3), pp.435-453.

Van der Heijde, D.M., 2000. Radiographic imaging: the'gold standard'for assessment of disease progression in rheumatoid arthritis. *Rheumatology (Oxford, England)*, *39*, pp.9-16.

van der Helm-van Mil, A.H., Verpoort, K.N., Breedveld, F.C., Toes, R.E. and Huizinga, T.W., 2005. Antibodies to citrullinated proteins and differences in clinical progression of rheumatoid arthritis. *Arthritis research & therapy*, *7*, pp.1-10.

Van Der Linden, M.P., Le Cessie, S., Raza, K., Van Der Woude, D., Knevel, R., Huizinga, T.W. and van der Helm-van Mil, A.H., 2010. Long-term impact of delay in assessment of patients with early arthritis. *Arthritis & Rheumatism*, *62*(12), pp.3537-3546.

Van der Linden, M.P.M., Knevel, R., Huizinga, T.W.J. and van der Helm-van Mil, A.M., 2011. Classification of rheumatoid arthritis: comparison of the 1987 American College of Rheumatology criteria and the 2010 American College of Rheumatology/European League Against Rheumatism criteria. *Arthritis & Rheumatism*, *63*(1), pp.37-42.

van der Woude, D. and van der Helm-van, A.H., 2018. Update on the epidemiology, risk factors, and disease outcomes of rheumatoid arthritis. *Best practice & research Clinical rheumatology*, *32*(2), pp.174-187.

Van Jaarsveld, C.H.M., Jacobs, J.W.G., Van Der Veen, M.J., Blaauw, A.A.M., Kruize, A.A., Hofman, D.M., Brus, H.L.M., van Albada-Kuipers, G.A., Heurkens, A.H.M., Ter Borg, E.J. and Haanen, H.C.M., 2000. Aggressive treatment in early rheumatoid arthritis: a randomised controlled trial. *Annals of the Rheumatic Diseases*, *59*(6), pp.468-477.

Van Oosterhout, M., Bajema, I., Levarht, E.W.N., Toes, R.E.M., Huizinga, T.W.J. and Van Laar, J.M., 2008. Differences in synovial tissue infiltrates between anti–cyclic citrullinated peptide–positive rheumatoid arthritis and anti–cyclic citrullinated peptide–negative rheumatoid arthritis. *Arthritis & Rheumatism*, *58*(1), pp.53-60.

Van Steenbergen, H. W., Da Silva, J. A. P., Huizinga, T. W., & van der Helm-van Mil, A. H. (2018). Preventing progression from arthralgia to arthritis: targeting the right patients. *Nature Reviews Rheumatology*, *14*(1), 32-41.

van Steenbergen, H.W., Mangnus, L., Reijnierse, M., Huizinga, T.W. and van der Helm-van, A.H., 2016. Clinical factors, anticitrullinated peptide antibodies and MRI-detected subclinical inflammation in relation to progression from clinically suspect arthralgia to arthritis. *Annals of the rheumatic diseases*, *75*(10), pp.1824-1830.

Van Zonneveld, A.J., De Boer, H.C., Van Der Veer, E.P. and Rabelink, T.J., 2010. Inflammation, vascular injury and repair in rheumatoid arthritis. *Annals of the Rheumatic Diseases*, *69*, pp.i57-i60.

Vandanmagsar, B., Youm, Y.H., Ravussin, A., Galgani, J.E., Stadler, K., Mynatt, R.L., Ravussin, E., Stephens, J.M. and Dixit, V.D., 2011. The NLRP3 inflammasome instigates obesity-induced inflammation and insulin resistance. *Nature medicine*, *17*(2), pp.179-188.

Veale, D. J., & Firestein, G. S. (2024). Chapter 2 Synovium. In *Kelley's and Firestein's Textbook of Rheumatology: Vol. Volume 1* (Twelfth Edition, pp. 20–33). Elsevier.

Veale, D., Yanni, G., Rogers, S., Barnes, L., Bresnihan, B. and Fitzgerald, O., 1993. Reduced synovial membrane macrophage numbers, ELAM-1 expression, and lining layer hyperplasia in psoriatic arthritis as compared with rheumatoid arthritis. *Arthritis & Rheumatism: Official Journal of the American College of Rheumatology*, *36*(7), pp.893-900.

Veale, D.J. and Fearon, U., 2006. Inhibition of angiogenic pathways in rheumatoid arthritis: potential for therapeutic targeting. *Best Practice & Research Clinical Rheumatology*, *20*(5), pp.941-947.

Veale, D.J. and Fearon, U., 2015. What makes psoriatic and rheumatoid arthritis so different?. *RMD open*, *1*(1), p.e000025.

Veale, D.J., Reece, R.J., Parsons, W., Radjenovic, A., O'Connor, P.J., Orgles, C.S., Berry, E., Ridgway, J.P., Mason, U., Boylston, A.W. and Gibbon, W., 1999. Intra-articular primatised anti-CD4: efficacy in resistant rheumatoid knees. A study of combined arthroscopy, magnetic resonance imaging, and histology. *Annals of the rheumatic diseases*, *58*(6), pp.342-349.

Verpoort, K.N., Papendrecht-van der Voort, E.A.M., van der Helm-van Mil, A.H.M., Jol-van der Zijde, C.M., Van Tol, M.J.D., Drijfhout, J.W., Breedveld, F.C., De Vries, R.R.P., Huizinga, T.W.J. and Toes, R.E.M., 2007. Association of smoking with the constitution of the anti–cyclic citrullinated peptide response in the absence of HLA–DRB1 shared epitope alleles. *Arthritis & Rheumatism: Official Journal of the American College of Rheumatology*, *56*(9), pp.2913-2918.

Verstappen, S.M.M., Bijlsma, J.W.J., Verkleij, H., Buskens, E., Blaauw, A.A.M., Ter Borg, E.J., Jacobs, J.W.G. and Utrecht Rheumatoid Arthritis Cohort Study Group, 2004. Overview of work disability in rheumatoid arthritis patients as observed in cross-sectional and longitudinal surveys. *Arthritis Care & Research*, *51*(3), pp.488-497.

Voigt, L.F., Koepsell, T.D., Nelson, J.L., Dugowson, C.E. and Daling, J.R., 1994. Smoking, obesity, alcohol consumption, and the risk of rheumatoid arthritis. *Epidemiology*, *5*(5), pp.525-532.

Volin, M.V. and Koch, A.E., 2011. Interleukin-18: a mediator of inflammation and angiogenesis in rheumatoid arthritis. *Journal of Interferon & Cytokine Research*, *31*(10), pp.745-751.

Volker, D., Fitzgerald, P., Major, G. and Garg, M., 2000. Efficacy of fish oil concentrate in the treatment of rheumatoid arthritis. *The Journal of rheumatology*, *27*(10), pp.2343-2346.

Volkov, M., van Schie, K.A. and van der Woude, D., 2020. Autoantibodies and B Cells: The ABC of rheumatoid arthritis pathophysiology. *Immunological reviews*, *294*(1), pp.148-163.

Vossenaar, E.R., Zendman, A.J. and Van Venrooij, W.J., 2003. Citrullination, a possible functional link between susceptibility genes and rheumatoid arthritis. *Arthritis Res Ther*, *6*, pp.1-5.

Vossenaar, E R, S Nijenhuis, et al. 2003. "Citrullination of Synovial Proteins in Murine Models of Rheumatoid Arthritis." *Arthritis Rheum* 48(9): 2489–2500.

Waaler, Erik. 2007. "On the Occurrence of a Factor in Human Serum Activating the Specific Agglutintion of Sheep Blood Corpuscles. 1939." *APMIS : acta pathologica, microbiologica, et immunologica Scandinavica* 115(5): 422–38; discussion 439.

Wada, H., Suzuki, M., Matsuda, M., Ajiro, Y., Shinozaki, T., Sakagami, S., Yonezawa, K., Shimizu, M., Funada, J., Takenaka, T. and Morita, Y., 2020. Distinct characteristics of VEGF-D and VEGF-C to predict mortality in patients with suspected or known coronary artery disease. *Journal of the American Heart Association*, *9*(9), p.e015761.

Wade, S.M., Ohnesorge, N., McLoughlin, H., Biniecka, M., Carter, S.P., Trenkman, M., Cunningham, C.C., McGarry, T., Canavan, M., Kennedy, B.N. and Veale, D.J., 2019. Dysregulated miR-125a promotes angiogenesis through enhanced glycolysis. *EBioMedicine*, *47*, pp.402-413.

Wäldele, S., Koers-Wunrau, C., Beckmann, D., Korb-Pap, A., Wehmeyer, C., Pap, T. and Dankbar, B., 2015. Deficiency of fibroblast activation protein alpha ameliorates cartilage destruction in inflammatory destructive arthritis. *Arthritis research & therapy*, *17*, pp.1-7.

Wallenstein, G.V., Kanik, K.S., Wilkinson, B., Cohen, S., Cutolo, M., Fleischmann, R.M., Genovese, M.C., Gomez Reino, J., Gruben, D., Kremer, J. and Krishnaswami, S., 2016. Effects of the oral Janus kinase inhibitor tofacitinib on patient-reported outcomes in patients with active rheumatoid arthritis: results of two Phase 2 randomised controlled trials. *Clin Exp Rheumatol*, *34*(3), pp.430-42.

Walsh, D.A. and Pearson, C.I., 2001. Angiogenesis in the pathogenesis of inflammatory joint and lung diseases. *Arthritis Research & Therapy*, *3*, pp.1-7.

Walsh, C.A.E., Fearon, U., FitzGerald, O., Veale, D.J. and Bresnihan, B., 2008. Decreased CD20 expression in rheumatoid arthritis synovium following 8 weeks of rituximab therapy. *Clinical & Experimental Rheumatology*, *26*(4), p.656.

Wang, Y. and Patti, G.J., 2023. The Warburg effect: a signature of mitochondrial overload. *Trends in cell biology*, *33*(12), pp.1014-1020.

Wang, Z., Huang, J., Xie, D., He, D., Lu, A. and Liang, C., 2021. Toward overcoming treatment failure in rheumatoid arthritis. *Frontiers in immunology*, *12*, p.755844.

Wang, J., Chen, H., Liu, Y., Zhou, W., Sun, R. and Xia, M., 2015. Retinol binding protein 4 induces mitochondrial dysfunction and vascular oxidative damage. *Atherosclerosis*, *240*(2), pp.335-344.

Wang, S., Tsun, Z.Y., Wolfson, R., Shen, K., Wyant, G.A., Plovanich, M.E., Yuan, E.D., Jones, T.D., Chantranupong, L., Comb, W. and Wang, T., 2015. The amino acid transporter SLC38A9 is a key component of a lysosomal membrane complex that signals arginine sufficiency to mTORC1. *Science (New York, NY)*, *347*(6218), p.188.

Wang, X., Yang, C., Xu, F., Qi, L., Wang, J. and Yang, P., 2019. Imbalance of circulating Tfr/Tfh ratio in patients with rheumatoid arthritis. *Clinical and experimental medicine*, *19*, pp.55-64.

Warburg, O., 1956. On the origin of cancer cells. *Science*, *123*(3191), pp.309-314.

Watson, D.J., Rhodes, T. and Guess, H.A., 2003. All-cause mortality and vascular events among patients with rheumatoid arthritis, osteoarthritis, or no arthritis in the UK General Practice Research Database. *The Journal of rheumatology*, *30*(6), pp.1196-1202.

Weber, B.N., Giles, J.T. and Liao, K.P., 2023. Shared inflammatory pathways of rheumatoid arthritis and atherosclerotic cardiovascular disease. *Nature Reviews Rheumatology*, *19*(7), pp.417-428.

Wegner, N., Wait, R., Sroka, A., Eick, S., Nguyen, K.A., Lundberg, K., Kinloch, A., Culshaw, S., Potempa, J. and Venables, P.J., 2010. Peptidylarginine deiminase from Porphyromonas gingivalis citrullinates human fibrinogen and α-enolase: Implications for autoimmunity in rheumatoid arthritis. *Arthritis & Rheumatism*, *62*(9), pp.2662-2672..

Wei, K., Korsunsky, I., Marshall, J.L., Gao, A., Watts, G.F., Major, T., Croft, A.P., Watts, J., Blazar, P.E., Lange, J.K. and Thornhill, T.S., 2020. Notch signaling drives synovial fibroblast identity and arthritis pathology. *Nature*, *582*(7811), pp.259-264.

Weichhart, T., Hengstschläger, M. and Linke, M., 2015. Regulation of innate immune cell function by mTOR. *Nature Reviews Immunology*, *15*(10), pp.599-614.

Westlake, S.L., Colebatch, A.N., Baird, J., Kiely, P., Quinn, M., Choy, E., Ostor, A.J. and Edwards, C.J., 2010. The effect of methotrexate on cardiovascular disease in patients with rheumatoid arthritis: a systematic literature review. *Rheumatology*, *49*(2), pp.295-307.

Wetzel, A., Chavakis, T., Preissner, K.T., Sticherling, M., Haustein, U.F., Anderegg, U. and Saalbach, A., 2004. Human Thy-1 (CD90) on activated endothelial cells is a counterreceptor for the leukocyte integrin Mac-1 (CD11b/CD18). *The Journal of Immunology*, *172*(6), pp.3850-3859.

Williams, R.O., Feldmann, M. and Maini, R.N., 1992. Anti-tumor necrosis factor ameliorates joint disease in murine collagen-induced arthritis. *Proceedings of the National Academy of Sciences*, *89*(20), pp.9784-9788.

Wilson, J.M., Nikooienejad, A., Robins, D.A., Roell, W.C., Riesmeyer, J.S., Haupt, A., Duffin, K.L., Taskinen, M.R. and Ruotolo, G., 2020. The dual glucose-dependent insulinotropic peptide and glucagon-like peptide-1 receptor agonist, tirzepatide, improves lipoprotein biomarkers associated with insulin resistance and cardiovascular risk in patients with type 2 diabetes. *Diabetes, obesity and metabolism*, *22*(12), pp.2451-2459.

Winthrop, K. L. (2006) 'Risk and prevention of tuberculosis and other serious opportunistic infections associated with the inhibition of tumor necrosis factor', *Nature Clinical Practice Rheumatology*, 2(11), pp. 602–610. doi: 10.1038/ncprheum0336.

Wise, D.R. and Thompson, C.B., 2010. Glutamine addiction: a new therapeutic target in cancer. *Trends in biochemical sciences*, *35*(8), pp.427-433.

Witkin, S.S., Alvi, S., Bongiovanni, A.M., Linhares, I.M. and Ledger, W.J., 2011. Lactic acid stimulates interleukin-23 production by peripheral blood mononuclear cells exposed to bacterial lipopolysaccharide. *FEMS Immunology & Medical Microbiology*, *61*(2), pp.153-158.

Wong, L.E., Huang, W.T., Pope, J.E., Haraoui, B., Boire, G., Thorne, J.C., Hitchon, C.A., Tin, D., Keystone, E.C., Bykerk, V.P. and Canadian Early Arthritis Cohort Investigators, 2015. Effect of age at menopause on disease presentation in early rheumatoid arthritis: results from the Canadian Early Arthritis Cohort. *Arthritis care & research*, *67*(5), pp.616-623.

Wood, N.C., Symons, J.A., Dickens, E. and Duff, G.W., 1992. In situ hybridization of IL-6 in rheumatoid arthritis. *Clinical & Experimental Immunology*, *87*(2), pp.183-189.

Woywodt, A., Streiber, F., de Groot, K., Regelsberger, H., Haller, H. and Haubitz, M., 2003. Circulating endothelial cells as markers for ANCA-associated small-vessel vasculitis. *The Lancet*, *361*(9353), pp.206-210.

Wu, H., Chen, H. and Hu, P.C., 2007. Circulating endothelial cells and endothelial progenitors as surrogate biomarkers in vascular dysfunction. *Clinical Laboratory*, *53*(5-6), pp.285-296.

Wu, X., Liu, Y., Jin, S., Wang, M., Jiao, Y., Yang, B., Lu, X., Ji, X., Fei, Y., Yang, H. and Zhao, L., 2021. Single-cell sequencing of immune cells from anticitrullinated peptide antibody positive and negative rheumatoid arthritis. *Nature communications*, *12*(1), p.4977.

Xian, X., Håkansson, J., Ståhlberg, A., Lindblom, P., Betsholtz, C., Gerhardt, H. and Semb, H., 2006. Pericytes limit tumor cell metastasis. *The Journal of clinical investigation*, *116*(3), pp.642-651.

Xu, T., Stewart, K.M., Wang, X., Liu, K., Xie, M., Ryu, J.K., Li, K., Ma, T., Wang, H., Ni, L. and Zhu, S., 2017. Metabolic control of TH17 and induced Treg cell balance by an epigenetic mechanism. *Nature*, *548*(7666), pp.228-233.

Xu, J., Jiang, C., Cai, Y., Guo, Y., Wang, X., Zhang, J., Xu, J., Xu, K., Zhu, W., Wang, S. and Zhang, F., 2020. Intervening upregulated SLC7A5 could mitigate inflammatory mediator by mTOR-P70S6K signal in rheumatoid arthritis synoviocytes. *Arthritis research & therapy*, *22*, pp.1-13.

Xu, W.D., Firestein, G.S., Taetle, R., Kaushansky, K. and Zvaifler, N.J., 1989. Cytokines in chronic inflammatory arthritis. II. Granulocyte-macrophage colony-stimulating factor in rheumatoid synovial effusions. *The Journal of clinical investigation*, *83*(3), pp.876-882.

Xue, J., Xu, L., Zhu, H., Bai, M., Li, X., Zhao, Z., Zhong, H., Cheng, G., Li, X., Hu, F. and Su, Y., 2020. CD14+ CD16− monocytes are the main precursors of osteoclasts in rheumatoid arthritis via expressing Tyro3TK. *Arthritis Research & Therapy*, *22*, pp.1-11.

Yang R, Yao Y, Wang P. Hypoxia-induced the upregulation of stromal cell-derived factor 1 in fibroblast-like synoviocytes contributes to migration of monocytes into synovium tissue in rheumatoid arthritis. Cell Biosci. 2018;8:11.

Yang, D.H., Huang, J.Y., Chiou, J.Y. and Wei, J.C.C., 2018. Analysis of socioeconomic status in the patients with rheumatoid arthritis. *International journal of environmental research and public health*, *15*(6), p.1194.

Yang, J., Zhang, L., Yu, C., Yang, X.F. and Wang, H., 2014. Monocyte and macrophage differentiation: circulation inflammatory monocyte as biomarker for inflammatory diseases. *Biomarker research*, *2*, pp.1-9.

Yang, Y., Lin, Z., Lin, Q., Bei, W. and Guo, J., 2022. Pathological and therapeutic roles of bioactive peptide trefoil factor 3 in diverse diseases: recent progress and perspective. *Cell death & disease*, *13*(1), p.62.

Yeoh, N., Burton, J.P., Suppiah, P., Reid, G. and Stebbings, S., 2013. The role of the microbiome in rheumatic diseases. *Current rheumatology reports*, *15*, pp.1-11.

Yiu, K.H., Wang, S., Mok, M.Y., Ooi, G.C., Khong, P.L., Lau, C.P., Lai, W.H., Wong, L.Y., Lam, K.F., Lau, C.S. and Tse, H.F., 2010. Role of circulating endothelial progenitor cells in patients with rheumatoid arthritis with coronary calcification. *The Journal of rheumatology*, *37*(3), pp.529-535.

Yoshino, T., Kusunoki, N., Tanaka, N., Kaneko, K., Kusunoki, Y., Endo, H., Hasunuma, T. and Kawai, S., 2011. Elevated serum levels of resistin, leptin, and adiponectin are associated with C-reactive protein and also other clinical conditions in rheumatoid arthritis. Internal Medicine, 50(4), pp.269-275

Young, A., Koduri, G., Batley, M., Kulinskaya, E., Gough, A., Norton, S. and Dixey, J., 2007. Mortality in rheumatoid arthritis. Increased in the early course of disease, in ischaemic heart disease and in pulmonary fibrosis. *Rheumatology*, *46*(2), pp.350-357.

Zack SR, Alzoubi O, Satoeya N, Singh KP, Deen S, Nijim W, Lewis MJ, Pitzalis C, Sweiss N, Ivashkiv LB, Shahrara S. Another Notch in the Belt of Rheumatoid Arthritis. Arthritis Rheumatol. 2024 Oct;76(10):1475-1478. doi: 10.1002/art.42937. Epub 2024 Aug 9. PMID: 38961731; PMCID: PMC11421962.

Zeisbrich, M., Yanes, R.E., Zhang, H., Watanabe, R., Li, Y., Brosig, L., Hong, J., Wallis, B.B., Giacomini, J.C., Assimes, T.L. and Goronzy, J.J., 2018. Hypermetabolic macrophages in rheumatoid arthritis and coronary artery disease due to glycogen synthase kinase 3b inactivation. *Annals of the rheumatic diseases*, *77*(7), pp.1053-1062.

Zhang, F., Jonsson, A.H., Nathan, A., Millard, N., Curtis, M., Xiao, Q., Gutierrez-Arcelus, M., Apruzzese, W., Watts, G.F., Weisenfeld, D. and Nayar, S., 2023. Deconstruction of rheumatoid arthritis synovium defines inflammatory subtypes. *Nature*, *623*(7987), pp.616-624.

Zhang, F., Wei, K., Slowikowski, K., Fonseka, C.Y., Rao, D.A., Kelly, S., Goodman, S.M., Tabechian, D., Hughes, L.B., Salomon-Escoto, K. and Watts, G.F., 2019. Defining inflammatory cell states in rheumatoid arthritis joint synovial tissues by integrating single-cell transcriptomics and mass cytometry. *Nature immunology*, *20*(7), pp.928-942.

Zhang, X.P., Ma, J.D., Mo, Y.Q., Jing, J., Zheng, D.H., Chen, L.F., Wu, T., Chen, C.T., Zhang, Q., Zou, Y.Y. and Lin, J.Z., 2021. Addition of fibroblast-stromal cell markers to immune synovium pathotypes better predicts radiographic progression at 1 year in active rheumatoid arthritis. *Frontiers in Immunology*, *12*, p.778480.

Zhang, Y., Dong, J., He, P., Li, W., Zhang, Q., Li, N. and Sun, T., 2012. Genistein inhibit cytokines or growth factor-induced proliferation and transformation phenotype in fibroblast-like synoviocytes of rheumatoid arthritis. *Inflammation*, *35*, pp.377-387.

Zhou, H. and Huang, S., 2011. Role of mTOR signaling in tumor cell motility, invasion and metastasis. *Current Protein and Peptide Science*, *12*(1), pp.30-42.

Zhou, J., Dai, Y., Lin, Y. and Chen, K., 2022, February. Association between serum amyloid A and rheumatoid arthritis: A systematic review and meta-analysis. In *Seminars in Arthritis and Rheumatism* (Vol. 52, p. 151943). WB Saunders.

Zhou, W., Shen, Q., Wang, H., Yang, J., Zhang, C., Deng, Z., Wu, K., Zhou, Y., Zeng, J., Zhang, Y. and Shen, W., 2020. Knockdown of YAP/TAZ inhibits the migration and invasion of fibroblast synovial cells in rheumatoid arthritis by regulating autophagy. *Journal of immunology research*, *2020*(1), p.9510594.

Zhu, J. and Thompson, C.B., 2019. Metabolic regulation of cell growth and proliferation. *Nature reviews Molecular cell biology*, *20*(7), pp.436-450.

Zhu, S., Liu, C., Zhao, C., Chen, G., Meng, S., Hong, M., Xiang, M. and Xie, Y., 2022. Increased serum soluble transferrin receptor levels were associated with high prevalence of cardiovascular diseases: insights from the National Health and Nutrition Examination Survey 2017–2018. *Frontiers in Cell and Developmental Biology*, *10*, p.874846.

Zou, D., Wang, T., Li, W., Wang, X., Ma, B., Hu, X., Zhou, Q., Li, Z., Shi, W. and Duan, H., 2024. Nicotinamide promotes the differentiation of functional corneal endothelial cells from human embryonic stem cells. *Experimental Eye Research*, *242*, p.109883.

Zou, Y., Zeng, S., Huang, M., Qiu, Q., Xiao, Y., Shi, M., Zhan, Z., Liang, L., Yang, X. and Xu, H., 2017. Inhibition of 6-phosphofructo-2-kinase suppresses fibroblast-like synoviocytes-mediated synovial inflammation and joint destruction in rheumatoid arthritis. *British journal of pharmacology*, *174*(9), pp.893-908.

Appendix

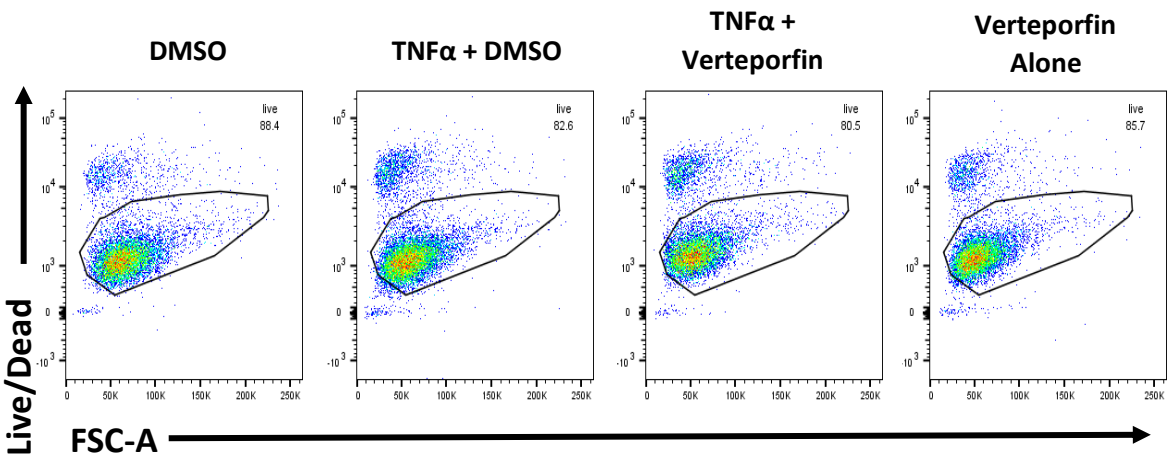

Figure 7.1: Verteporfin Did Not Affect FLS viability.

Representative flow cytometric dots demonstrating percent frequency of live cells for cultured FLS stimulated with DMSO (50 µM), TNFα (1ng/ml) + DMSO (50 µM), TNFα (1ng/ml) + Verteporfin (50 µM), and Verteporfin (50 µM) alone.

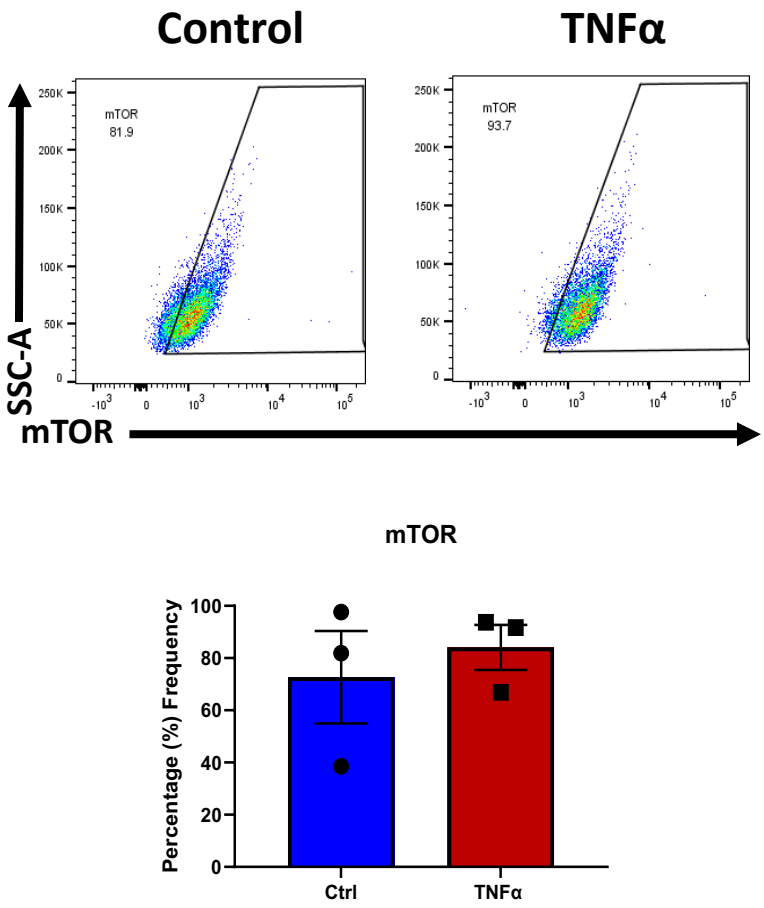

Figure 7.2: Effects of TNFα on % Frequency of mTOR in Cultured FLS.

Representative flow cytometric dots and accompanying graph demonstrating percent frequency of mTOR expressed by cultured RA FLS (n=3) stimulated with or without TNFα (1ng/ml). Data represented as mean ± SEM.

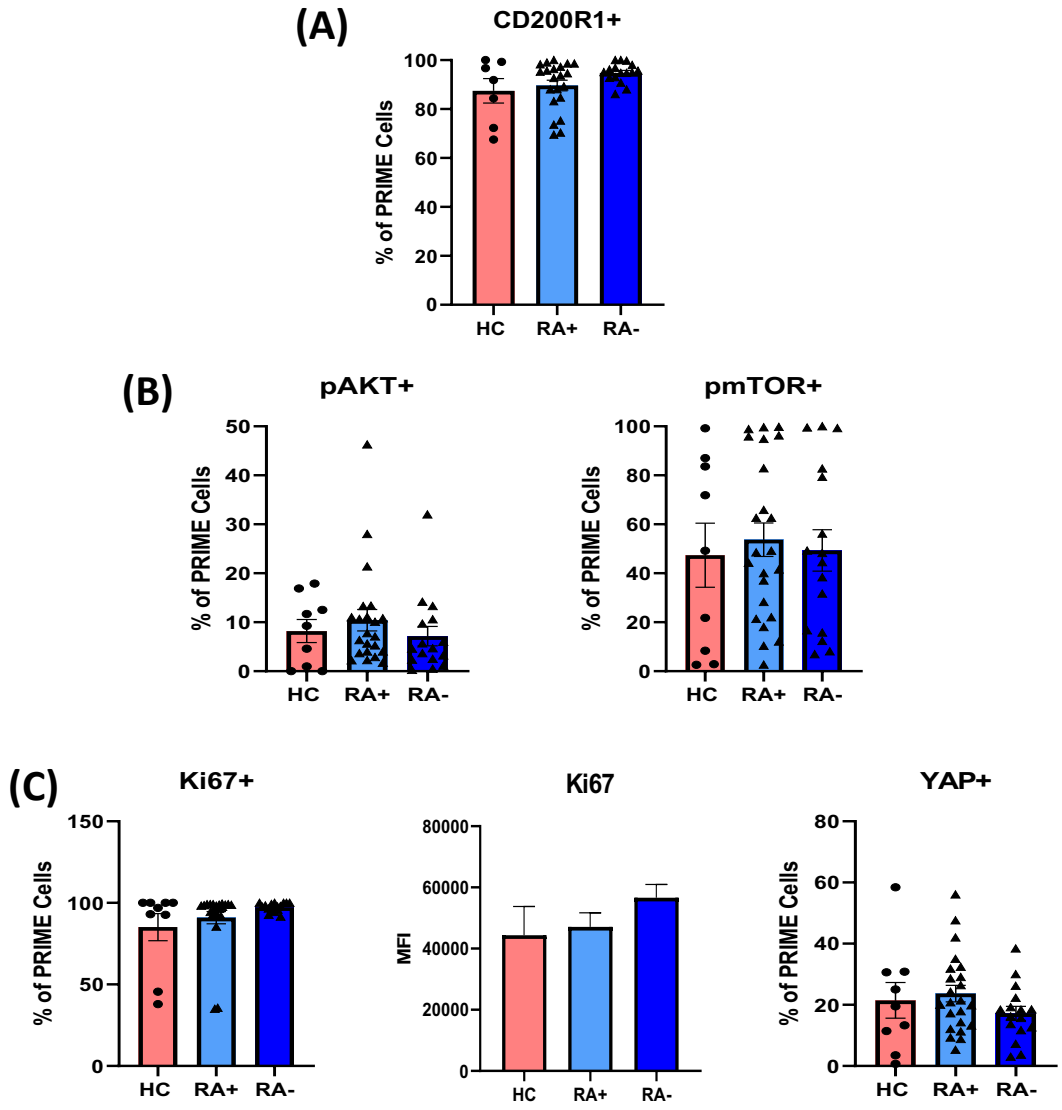

Figure 7.3: Additional Markers Analysed on PRIME Cells.

(A) Dot plot bar graphs demonstrating percent frequency of PRIME cells positive for CD200R1 in HC (n=9), RA+ (n=23), and RA- (n=23). (B) Dot plots depicting frequency of PRIME cells positive for expression of metabolic markers pAKT and pmTOR in HC (n=9), RA+ (n=38-39), and RA- (n=16). (C) Dot plots demonstrating percent frequency of Ki67+ and YAP+ PRIME cells and bar graph showing MFI expression of Ki67 across HC (n=9), RA+ (n=39), and RA- (n=16). Data represented as mean ± SEM.

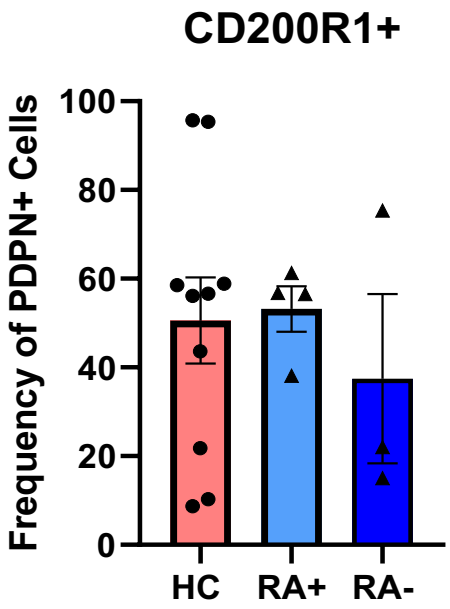

Figure 7.4: Frequency of CD200R1+ FLS in HC, RA+, and RA-.

Dot plot bar graphs demonstrating percent frequency of PRIME cells positive for CD200R1 in HC (n=10), RA+ (n=4), and RA- (n=3). Data represented as mean ± SEM.